Synthesis and pharmacological characterization of bivalent and fluorescent ligands to detect receptor dimerization for the D_2-H_3 heteromer

Dissertation

zur Erlangung des Doktorgrades der Naturwissenschaften (Dr. rer. nat.)

an der Fakultät für Chemie und Pharmazie

der Universität Regensburg

vorgelegt von

Martin Nagl

aus Falkenberg

2022

Die vorliegende Arbeit entstand in der Zeit von Januar 2019 bis November 2022 unter der Leitung von Herrn Dr. Steffen Pockes am Institut für Pharmazie der Fakultät für Chemie und Pharmazie der Universität Regensburg.

Das Promotionsgesuch wurde eingereicht im November 2022

Tag der mündlichen Prüfung:

Vorsitzender des Prüfungsausschusses:	Prof. Dr. Achim Göpferich
Erstgutachter:	Dr. Steffen Pockes
Zweitgutachter:	Prof. Dr. Sigurd Elz
Drittprüfer:	Prof. Dr. Jörg Heilmann

Acknowledgments and declaration of collaborations

An dieser Stelle möchte ich mich ganz herzlich bei allen bedanken, die zum Gelingen dieser Arbeit maßgeblich beigetragen und mich über die letzten vier Jahre begleitet haben. Besonders bedanken möchte ich mich:

An erster Stelle bei meinem Doktorvater Herrn Dr. Steffen Pockes für die Möglichkeit und das Vertrauen, dieses interessante und herausfordernde Projekt unter seiner Leitung zu bearbeiten. Seine konstruktive Kritik und fachlichen Hilfestellungen waren neben seiner freundschaftlichen Betreuung und seinen aufmunternden Worten in Zeiten ausbleibenden Erfolgs essenziell für diese Arbeit;

Bei Herrn Professor Dr. Sigurd Elz für das Erstellen des Zweitgutachtens sowie für die Bereitstellung sämtlicher Räumlichkeiten und Gerätschaften, die zur Bearbeitung dieses Projekts nötig waren;

Bei Herrn Professor Dr. Jörg Heilmann für seine Bereitschaft, das Amt des Drittprüfers zu übernehmen und für die Zurverfügungstellung der Zellkultur;

Bei Herrn Professor Dr. Achim Göpferich für die Teilnahme als Vorsitzender an der mündlichen Prüfung;

Bei Frau Professor Dr. Gemma Navarro und Herrn Professor Dr. Rafael Franco und ihrer Arbeitsgruppe für ihre herzliche Aufnahme in ihrem Arbeitskreis. Mit ihrer freundlichen und hilfsbereiten Art standen sie mir immer mit Rat und Tat zur Seite und haben die vier Monate in Barcelona trotz einiger Misserfolge zu einer unvergesslichen Zeit gemacht, an die ich mich sehr gerne zurückerinnere;

Beim Graduiertenkolleg „Elitenetzwerk Bayern“ für die Aufnahme als assoziiertes Mitglied. Mithilfe der fachlichen und finanziellen Unterstützung seitens des Kollegs hatte ich die Möglichkeit an zahlreichen Workshops und Konferenzen teilzunehmen, was für das Verfassen dieser Arbeit äußerst förderlich war;

Bei Herrn PD Dr. Max Keller für das Bereitstellen von etlichen Gerätschaften und seine Hilfestellungen rund um Probleme der HPLC-Anlagen und des Harvesters im Radioaktivlabor;

Bei Frau Vivien Czipper für ihre engagierte Mitarbeit bei synthetischen Aufgaben und in der Zellkultur;

Bei Frau Uta Hasselmann für ihre tatkräftige Unterstützung bei organisatorischen Problemen aller Art und für ihr sonniges Gemüt;

Bei Herrn Peter Richthammer für die zahlreichen netten Gespräche und für seine stete Hilfsbereitschaft und Kompetenz bei allen technischen Herausforderungen;

Bei Herrn Dr. Herwig Pongratz und Frau Julia Blüml für ihr offenes Ohr bei synthetischen Fragestellungen und wunderbare Kochabende;

Bei Herrn Niklas Rosier für vier gemeinsame Jahre im Labor. Mit seiner stets positiven, lustigen und hilfsbereiten Art hat er es immer geschafft, mich in Zeiten des Misserfolgs wieder aufzubauen und weiter zu motivieren. Gleichzeitig war er auch immer verfügbar, wenn es darum ging, Erfolge mit einem Feierabendbier zu feiern. Die vier gemeinsamen Monate in Barcelona hat er aufgrund seiner Dolmetscherfähigkeiten enorm erleichtert und für die ein oder andere lustige Geschichte gesorgt. So wurde spätestens zu dieser Zeit aus einem Kollegen ein wahrer Freund;

Bei Herrn Lukas Wirth für die gemeinsame Zeit im Arbeitskreis. Auch er war mit seinem sonnigen Gemüt enorm wichtig, in schwierigen Zeiten die Freude an der Arbeit nicht zu verlieren. Einzig sein unverdientes Glück und seine unerklärlich guten Kicker-Manager Ergebnisse werden mir negativ in Erinnerung bleiben;

Bei Herrn Sebastian Pitzl, Herrn Alexander Hubmann, Herrn Jonas Daschner, Herrn Merlin Bresinsky, Herrn Simon Scheuerer und Frau Denise Mönnich für die gemeinsame Zeit am Arbeitskreis und die vielen unvergesslichen Momente bei außeruniversitären Veranstaltungen;

Bei Herrn Sebastian Schmid und dem Team der easyApotheke in Eggenfelden, die mir bei den regelmäßigen Wochenenddiensten immer wieder bewusst gemacht haben, dass es auch ein Arbeitsleben außerhalb des Labors gibt;

Bei meiner Familie rund um meine Eltern Anna und Jakob, meinem Bruder Bernhard und meiner Schwester Julia sowie deren Familien, die immer und jederzeit ein offenes Ohr hatten und mich in jeder Lebenslage unterstützen;

Zu guter Letzt und vor allem bei meiner Freundin Sophie. Ohne ihre Geduld, ihr Verständnis und ihren bedingungslosen Rückhalt wäre das Entstehen dieser Arbeit nicht möglich gewesen.

Publications, presentations and professional training

Peer-reviewed journal articles

(1) Niklas Rosier, Lukas Grätz, Hannes Schihada, Jan Möller, Ali Işbilir, Laura J. Humphrys, Martin Nagl, Ulla Seibel, Martin J. Lohse, and Steffen Pockes, A Versatile Sub-Nanomolar Fluorescent Ligand Enables NanoBRET Binding Studies and Single-Molecule Microscopy at the Histamine H_3 Receptor, *J. Med. Chem* 64 (2021).

(2) Katarzyna Szczepańska. Steffen Pockes, Sabina Podlewska, Carina Höring, Kamil Mika, Gniewomir Latacz, Marek Bednarski, Agata Siwek, Tadeusz Karcz, Martin Nagl, Merlin Bresinsky, Denise Mönnich, Ulla Seibel, Kamil J. Kuder, Magdalena Kotańska, Holger Stark, Sigurd Elz, Katarzyna Kieć-Kononowicz, Structural modifications in the distal, regulatory region of histamine H_3 receptor antagonists leading to the identification of a potent anti-obesity agent, *Europ. J. Med. Chem* 213 (2021).

Poster presentations (only contributions as presenting author are listed)

Nagl M., Rosier N., Grätz L., Schihada H., Franco R., Pockes S., Synthesis and Pharmacological Characterization of Bivalent Ligands for the D_2-H_3-Receptor Heteromer, *DPhG Annual Meeting, September 2019, Heidelberg, Germany*.

Nagl M., Rosier N., Grätz L., Schihada H., Franco R., Pockes S., Synthesis and Pharmacological Characterization of Bivalent Ligands for the D_2-H_3-Receptor Heteromer, *DPhG Annual Meeting, September 2021, Leipzig, Germany, digital*.

Nagl M., Mönnich D., Rosier N., Navarro G., Gomez M., Pardo L., Franco R., Pockes S., Targeting the D_2H_3 Heteromer with Bivalent Ligands, *ADPD Annual Meeting, March 2022, Barcelona, Spain*.

Nagl M., Mönnich D., Rosier N., Navarro G., Gomez M., Pardo L., Franco R., Pockes S., Synthesis and biological evaluation of bivalent ligands targeting D_2-H_3-Receptor heteromer, *4GPCRnet, September 2022, Leipzig, Germany*.

Professional training

07/2019 - 09/2022:	assoziiertes Mitglied im Graduiertenkolleg “Elitenetzwerk Bayern (ENB)”
11/2020 – 04/2021:	Teilnahme an der Veranstaltung „Radioanalytische Arbeitsmethoden für Pharmazeuten“
08/2019 - 12/2022:	Fachapotheker für pharmazeutische Analytik und Technologie, Landesapothekerkammer Bayern

Contents

List of abbreviations ..... **X**

1. Introduction **1**

1.1 G protein-coupled receptors (GPCRs) **1**

1.1.1 Structure and classification 1

1.1.2 GPCR activation 3

1.1.3 G protein signaling cascade 5

1.2 Dopamine **7**

1.2.1 Dopamine as a neurotransmitter and its receptors 7

1.2.2 Dopamine D_2 receptor 8

1.3 Histamine **10**

1.3.1 Histamine as a neurotransmitter and its receptors 10

1.3.2 Histamine H_3 receptor 11

1.4 Receptor dimerization **13**

1.4.1 Bivalent ligands 15

1.4.2 D_2-H_3 heteroreceptor dimer 16

1.5 Fluorescent ligands **17**

1.6 Parkinson`s Disease **19**

2. Scope and objectives **23**

2.1 Bivalent ligands **23**

2.2 Fluorescent ligands **27**

3. Bivalent ligands targeting the D_2-H_3 receptor dimer **31**

3.1 Synthesis **31**

3.1.1 Precursors for the D_2R 31

3.1.1 L-471,626 31

3.1.1.2 1,4-DAP 32

3.1.1.3 5-OH-DPAT 33

3.1.1.4 *N*-propylaminoindane 34

3.1.1.5 Spiperone 35

3.1.2 Precursors for the H_3R 36

3.1.3 Linker structures 38

3.1.4 Precursor for endcapped ligands 39

3.1.5 Final bivalent compounds 40

3.2 Biological evaluation 44

3.2.1 Radioligand binding assay to determine binding affinities 44

3.2.2 cAMP assay to determine pharmacological mode of action 50

3.2.2.1 Monoexpressing systems 51

3.2.2.2 Co-expressing systems 53

3.3 Conclusion 54

4. Fluorescent ligands 57

4.1 Synthesis 57

4.2 Biological evaluation 59

4.2.1 Binding affinities 59

4.2.2 Functional characterization 60

4.3 Fluorescence properties 61

4.4 Development of NanoBRET assays for D_2-like receptors 63

4.5 Conclusion 65

5. Bivalent fluorescent ligands 67

5.1 Synthesis 67

5.2 Biological evaluation 69

5.3 Fluorescence properties 70

5.4 Conclusion 71

6. Summary **73**

7. Experimental section **77**

7.1 General chemical procedures **77**

7.2 Synthetic procedures and analytical data **79**

7.3 Fluorescence properties **170**

7.4 Radioligand binding assays **171**

7.4.1 Dopamine receptors 171

7.4.2 Histamine receptors 171

7.5 Functional assays **172**

8. References **174**

9. Appendix **203**

Eidesstattliche Erklärung **247**

List of abbreviations

AADC	aromatic amino acid decarboxylase
AC	adenylyl cyclase
AMP	adenosine 5`-monophosphate
aq	aqueous
ATP	adenosine 5`-triphosphate
BBB	blood-brain barrier
B_{max}	maximal specific binding of a ligand
Boc	*tert*-butoxycarbonyl
BRET	bioluminescence resonance energy transfer
bs	broad singlet
BSA	bovine serum albumin
cAMP	cyclic adenosine 3`,5`-monophosphate
cGMP	cyclic guanosine 3`,5`-monophosphate
Celite	Celite 535®
CI	chemical ionization
CNS	central nervous system
CREB	cAMP response element binding protein
CTCM	cubic ternary complex model
d	doublet
DAG	1,2-diacylglycerol
DCM	dichloromethane
DEPT	Distortionless Enhancement by Polarization Transfer

DIPEA	diisopropylethylamine
DMEM	Dulbecco`s Modified Eagle Medium
DMF	*N,N*-dimethylformamide
DMSO	dimethyl sulfoxide
EC_{50}	concentration of agonist producing 50% of the maximal effect
ECL	extracellular loop of a G protein-coupled receptor
EDC	1-Ethyl-3-(3-dimethylaminopropyl)carbodiimide
EI	electron (impact) ionization
eq	equivalent(s)
ESI	electrospray ionization
ERK	extracellular signal-regulated kinase
etc.	et cetera
ETCM	extended ternary complex model
Et_2O	diethyl ether
EtOAc	ethyl acetate
EtOH	ethanol
Et_3N	triethylamine
FRET	fluorescence resonance energy transfer
GC	guanylyl cyclase
GDP	guanosine 5`-diphosphate
GMP	guanosine 5`-monophosphate
GPCR	G protein-coupled receptor
GRK	G protein-coupled receptor kinase

GTP	guanosine 5`-triphosphate
$G\alpha_i$	α-subunit of G proteins that inhibits certain isoforms of adenylyl cyclase
$G\alpha_q$	α-subunit of G proteins that stimulates phospholipase C
$G\alpha_s$	α-subunit of G proteins that stimulates adenylyl cyclase
$G_{\beta\gamma}$	βγ-subunits of a heterotrimeric G protein
h	hour(s)
H_1R, H_2R, H_3R, H_4R	histamine receptor subtypes
HATU	1-[Bis(dimethylamino)methylene]-1H-1,2,3-triazolo[4,5-b]pyridinium 3-oxide hexafluorophosphate
HEK cells	human embryonic kidney cells
HIS	histamine
HOBt	hydroxybenzotriazole
HPLC	high performance liquid chromatography
HRMS	high resolution mass spectrometry
IC_{50}	concentration of inhibitor producing 50% of inhibition
ICL	intracellular loop of a G protein-coupled receptor
IP_3	inositol-1,4,5-trisphosphate
J	NMR coupling constant
k	retention factor
K_d	dissociation constant of a radioligand/fluorescent ligand
K_i	dissociation constant of a competitive inhibitor and a receptor
λ	wavelength

M	mol/L
m	multiplet
MAPK	mitogen-acitivated protein kinase
MeCN	acetonitrile
MeOH	methanol
min	minute(s)
n.d.	not determined
NMR	nuclear magnetic resonance
NO	nitric oxide
PBS	phosphate buffered saline
PDE	phosphodiesterase
Pd/C	palladium on carbon
pEC_{50}	-log of the EC_{50} value
PEG	polyethylene glycole
PEI	polyethyleneimine
P_i	inorganic phosphate
PI3K	phosphatidylinositol-3-kinase
pIC_{50}	-log of the IC_{50} value
PIP2	phosphatidylinositol-4,5-bisphosphate
PKA	protein kinase A
PKC	protein kinase C
pK_d	-log of the K_d value
pK_i	-log of the K_i value
PLA2	phospholipase A2

PLC	phospholipase C
q	quartet
R	inactive state of a G protein-coupled receptor
R*	active state of a G protein-coupled receptor
RGS	regulator of G protein signaling
Rho-GEFs	Ras homology guanine nucleotide exchange factors
RP-HPLC	reversed phase high-performance liquid chromatography
RT	room temperature
SARs	structure-activity relationships
s	singlet
t_0	HPLC dead time
t_R	HPLC retention time
TBAB	tetrabutylammonium bromide
TCM	ternary complex model
TFA	trifluoroacetic acid
THF	tetrahydrofurane
TM	transmembrane domain of a G protein-coupled receptor
TLC	thin-layer chromatography

Chapter 1: Introduction

1. Introduction

1.1 G protein-coupled receptors (GPCRs)

G protein-coupled receptors (GPCRs), a superfamily of biological receptors, represent the largest group of proteins in the human genome.[1] These membrane-bound receptors transmit extracellular stimuli to the interior of the cell by interacting with guanosinetriphosphate-binding proteins (G proteins).[2] Until now approximately 800 different GPCRs have been identified which are divided into to two different groups.[3] Chemosensory GPCRs (csGPCRs) react to signals of external origins, such as odors, tastes, or pheromones, while endoGPCRs respond to endogenous ligands like lipids, peptides or neurotransmitters.[4] Despite intense research and remarkable progress concerning GPCR research in recent years the endogenous ligands for roughly 120 GPCRs have not been identified yet which is why these receptors are referred to as “orphan receptors”.[5] Since GPCRs are involved in numerous physiological and pathophysiological processes GPCR based drug research plays a crucial role concerning indications like psychiatric, neurodegenerative, metabolic, oncologic, and cardiovascular diseases.[6] The importance of GPCRs for modern medicine and drug development is highlighted by the fact that about 34 % of FDA approved drugs target 108 GPCRs and generate a global sales volume worth 180 billion US dollars.[7] Especially orphan receptors have attracted a great deal of attention and are currently taking center stage concerning research and development of drugs for rare diseases.[8,9]

1.1.1 Structure and classification

All GPCRs exhibit a common structure. They feature seven alpha-helical transmembrane helices (TM 1 – TM 7) consisting of 25-30 amino acids each.[10] These helices are connected by three intracellular (IL 1-3) and three extracellular loops (EL 1-3), which vary greatly in size.[11,12] Furthermore, all GPCRs possess an extracellular N-terminus as well as an intracellular C-terminal domain.[13] There are two main possibilities for ligands to target their desired GPCR. While some ligands address an extracellular binding site around the N-terminus others head for a binding pocket formed by the transmembrane helices within the lipidlayer.[14] The C-terminal region is responsible for the transmission of the signal as this part of the receptor as well as IL 2,3 represent binding sites for the G proteins.[15] Recent publications have also described novel binding pockets within the intracellular domain of certain GPCRs such as the

chemokine receptors CCR2 and CCR9.[16,17] These lately discovered binding sites represent highly interesting targets for further GPCR research in the future.[18] After the exact structure of GPCRs had remained unclear for a long time the year 2000 marked a milestone in GPCR research when the X-ray structure of a GPCR (bovine rhodopsine) was published.[19] For the very first time scientists from all over the world got better insight into the three dimensional structure of GPCRs. Seven years later the first structure of a human GPCR was discovered (β_2)[20], followed by the publication of the β_1 receptor in 2008.[21] The importance and impact of research on crystal structures of GPCRs was highly appreciated when Brian K. Kobilka and Robert Lefkowitz were awarded the nobel price of chemistry in 2012.[22] To this date more than 100 structures of 25 class A GPCRs have been published.[23] Their discovery has streamlined the research and development of GPCR targeting drugs. Based on modern techniques like “Molecular Modeling” promising lead structures can be identified more easily which rationalizes the early stages of drug development.[24]

Several systems have been established to classify GPCRs.[25] One conventional classification ranks GPCRs of vertebrate and invertebrate according to their functional characteristics in families from A to F.[26] Classes A (rhodopsin like), B (secretin like), and C (glutamate like) characterize vertebrate GPCRs while Classes D (fungal pheromone receptors), E (cAMP receptors in Nematodes), and F (olfactory receptors of insects) mainly apply to invertebrate species.[27] In contrast the most commonly used method is the “GRAFS-System” which categorizes mammalian GPCRs based on their phylogenetic and structural differences into the following five families: **g**lutamate, **r**hodopsine, **a**dhesion, **f**rizzled/taste2, and **s**ecretin.[28] The rhodopsine-family represents by far the majority with 701 members and is again subdivided into subgroups α, β, γ, δ.[25,28] Additionally, this group can also be classified in olfactory and non-olfactory receptors.[25,29] The frizzled/taste2 family is formed by 11 frizzled and 25 taste2 receptors. This family is mainly involved in sensing bitter taste and furthering cell development.[30,31] The adhesion family is named after the fact that its giant N-termini play a crucial role concerning cell-adhesion.[32] These N-termini vary largely in size and consist of 200 to 3000 amino acids.[33] The glutamate family is known for its characteristic binding mechanism which is also referred to as “venus flytrap module” according to the insect eating plant.[14] The N-terminus forms two distinct lobes that are separated by a cavity in which glutamate binds. As soon as the binding happens the lobes close around the ligand in a comparable manner to the aforementioned plant.[34,35] The secretin family includes 50

members and binds primarily hormones and neuropeptides such as corticotropin-releasing factor (CRF), glucagon-like peptide (GLP), and calcitonin gene-related peptide (CGRP).[36]

1.1.2 GPCR activation

In recent years several models have been established to characterize ligand-receptor interaction and to explain the following cascade of signal transduction. One of the first commonly accepted models was the ternary complex model (TCM) established by De Lean et al. in 1980 (cf. **Figure 1.1, A**).[37] According to their approach binding of an agonist to the receptor induces interaction with transducer proteins, later identified as G proteins.[37,38] However, it was soon found that several GPCRs display a certain amount of activity in the absence of agonists. This phenomenon is described as constitutive activity.[39] Thereupon, the "extended ternary complex model" (ETCM) (cf. **Figure 1.1, B**) was established according to

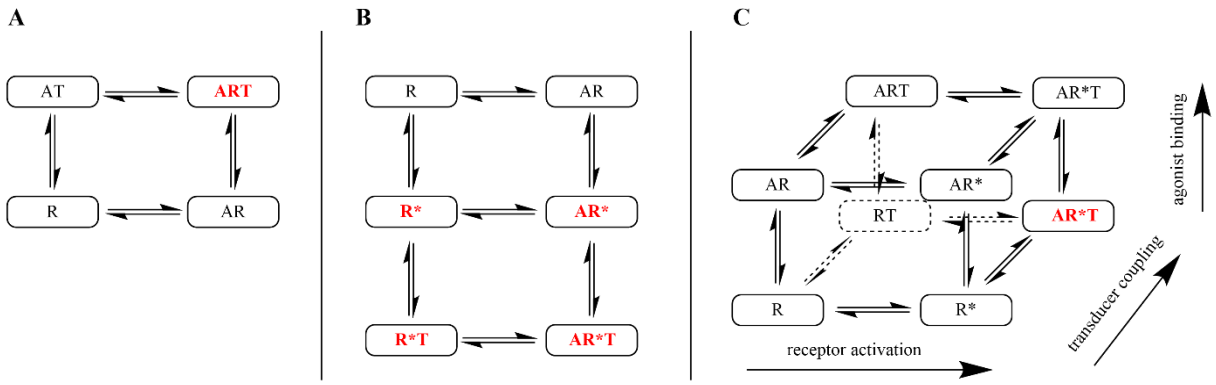

Figure 1.1: Different models of GPCR signaling: **A**: ternary complex model (TCM); **B**: extended ternary complex model (ETCM); **C**: cubic ternary complex model (CTCM); (adapted from [40]).

which the receptor exists in an inactive conformation (R) and an active conformation (R*) which couples to transducer proteins and sets the signaling cascade in motion.[38,41] Both conformations can isomerize into their corresponding counterpart without the presence of ligands which explains the aforementioned phenomenon of constitutive activity.[42] The "cubic ternary complex model" (CTCM) (cf. **Figure 1.1, C**) represents an advancement to the ETCM because it also includes interactions between the inactive receptor and the transducer protein which raises the number of possible conformations.[43] Accordingly, ligands can be subclassified based on their pharmacological profile (cf. **Figure 1.2**). A full agonist shifts the equilibrium entirely towards the active conformation (R*).[44] Partial agonists also favor R* but are not able to display full level of activity.[45] Full inverse agonists shift the equilibrium towards the inactive state (R) and reduce the constitutive activity of the receptor entirely.[46] A partial inverse agonist also diminishes the constitutive activity but not to that extent of a full

inverse agonist.[46] Antagonists have no impact on the equilibrium at all and therefore do not influence the constitutive activity. By simply blocking the orthosteric binding site they prevent agonists or inverse agonists from shifting the equilibrium.[47] Yet, recent studies have indicated

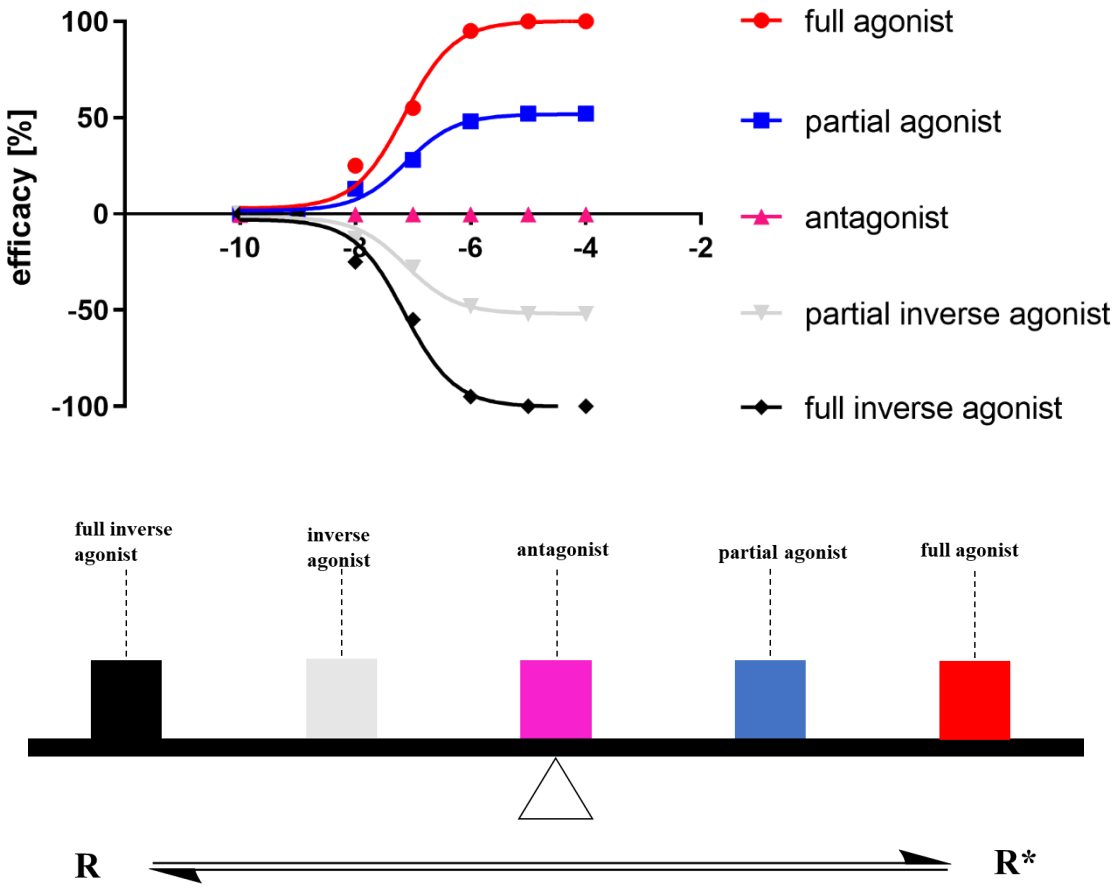

Figure 1.2: Ligand classification based on their influence on the equilibrium between both active and inactive receptor state and functional activity upon binding (adapted from [48]).

that this model also strongly simplifies actual mechanisms in the receptor.[45] The three-state model portrays GPCRs as switches that are either turned on or off but neglects the fact these receptors are also able to process external stimuli resulting in different signaling cascades. Information can be passed on through receptor activity modifying proteins (RAMPs), arrestines, and G proteins.[49,50] These findings support the theory that there are way more receptor conformations than the above-quoted models suggest.[51] In this context so called "biased ligands" have gained more and more importance in recent years.[52] They are defined as ligands that selectively trigger certain signaling cascades leading to a phenomenon called "functional selectivity".[53,54] Taking advantage of this functional selectivity is believed to lead to the development of more effective drugs with less side effects.[52,54]

1.1.3 G protein signaling cascade

After an agonist binds to the receptor the signal is transported to the interior of the cell. This leads to a change of conformation in the intracellular compartment (cf. **Figure 1.3**).[15] Heterotrimeric G proteins consisting of a G_{α}-unit, a $G_{\beta\gamma}$-unit and GDP can now bind to the C-terminus or the IL domains and form a ternary complex together with the agonist and the receptor.[55] This process is immediately followed by the dissociation of GDP which is replaced by GTP. GTP then induces a cleavage of the G protein which splits into the βγ-unit and the α-unit/GTP complex.[56] Both aggregates are able to interact with effector proteins such as adenylylcylase C (AC) and phospholipase C (PLC) (especially α-unit/GTP complex) or ion channels and G protein-coupled receptor kinases (GRKs; especially βγ-unit) to induce a cellular response.[57,58] Simultaneously the cleavage of the G protein causes a change conformation which reduces the affinity of the agonist towards the receptor resulting in a dissociation of the ligand.[59] After a certain amount of time the intrinsic GTPase activity of the G_{α}-unit hydrolyzes GTP to GDP and phosphate which terminates the G_{α}-unit induced signal.[56]

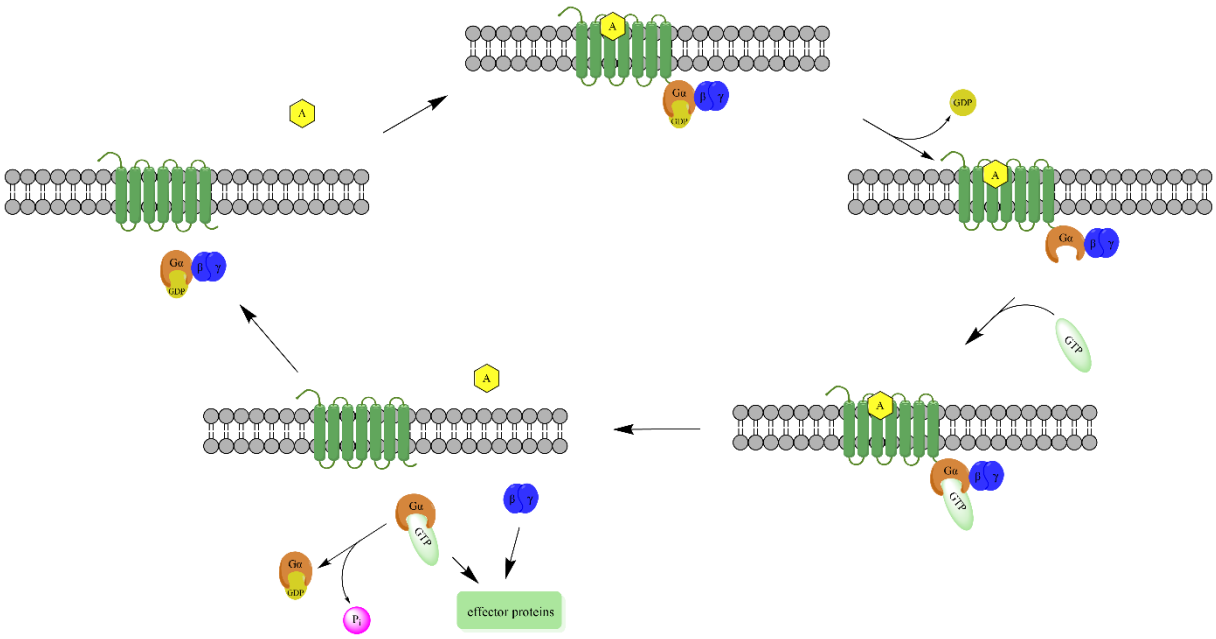

Figure 1.3: G protein cycle (adapted from [60]).

This is also necessary for the reconstruction of the initial heterotrimeric G protein with the βγ-unit.[61] The signaling cascade is now complete and can start again from the beginning.

The cellular response is continued by the aforementioned effector proteins. Upon activation these proteins produce "second messengers" like cAMP, NO, Ca^{2+}, IP_3, and cGMP (cf. **Figure 1.4**).[55] Their purpose is to transfer the original signal form the "first messenger" (agonist) to protein kinases whose stimulation leads to effects on gene expression.[55,57] The G proteins are subclassified based on the structural and pharmacological properties of their G_α-unit. Four families exist; $G\alpha_s$, $G\alpha_{i/o}$, $G\alpha_{q11}$, $G\alpha_{12/13}$. $G\alpha_s$-units activate AC 1-9 which leads to increased levels of the second messenger cAMP.[62,63] cAMP stimulates protein kinase A (PKA) as well as mitogen-activated protein kinase (MAPK) which effects gene expression in the cell.[64] This process is terminated by enzymes that hydrolyze cAMP, so called phosphodiesterases.[65]

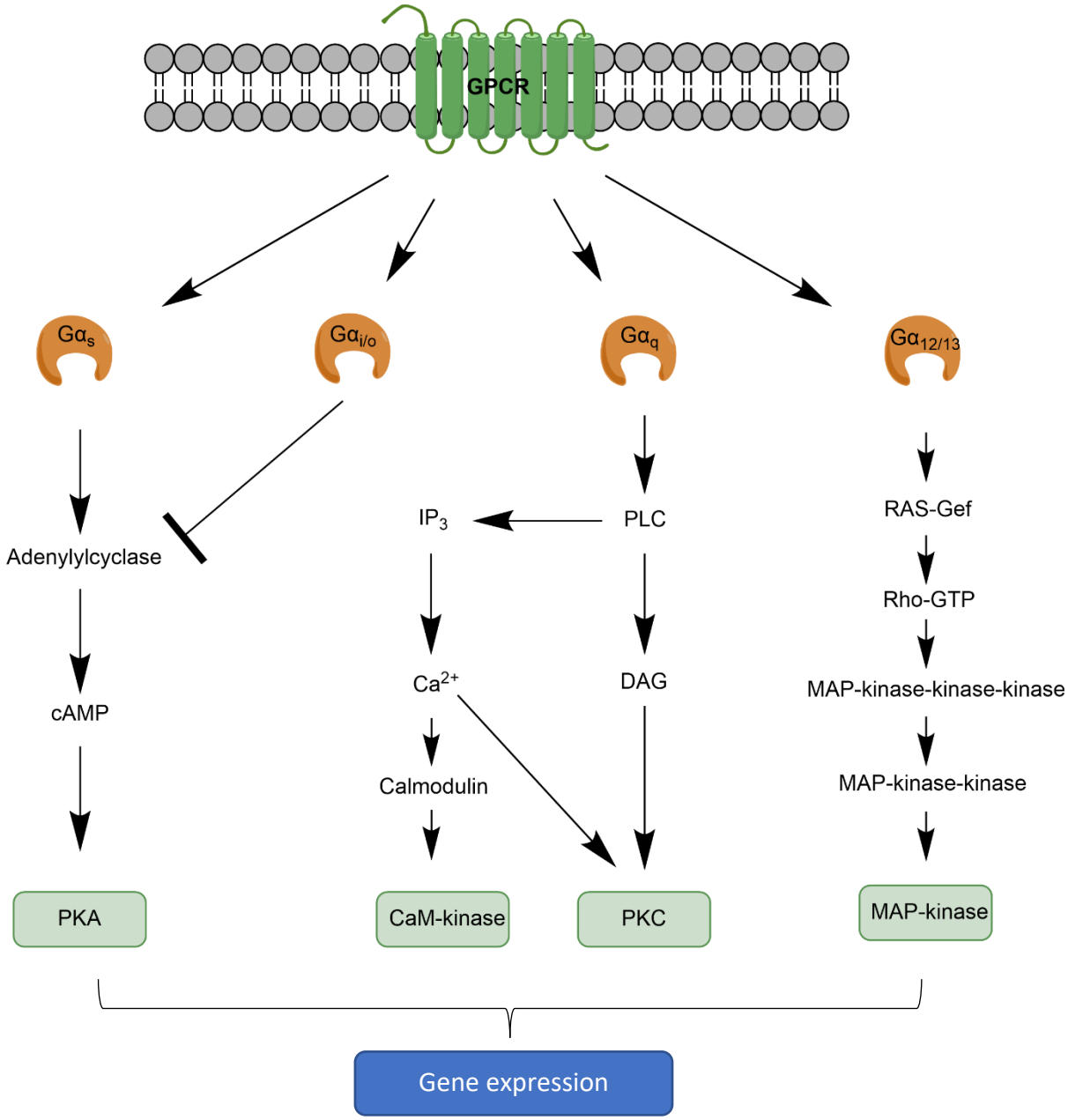

Figure 1.4: Signaling pathways of different G proteins (adapted from [66]).

In contrast, $G\alpha_{i/o}$ units inhibit AC and therefore have the contrary effect.[55] $G\alpha_{q11}$ units activate phospholipase β (PLC_β). This protein hydrolyzes phosphatidylinositol-4,5-bisphosphate (PIP_2) into inositol-1,4,5-trisphosphate (IP_3) and diacylglycerol (DAG).[67] Raised IP_3 levels increase Ca^{2+} release from the endoplasmic reticulum which together with DAG activates protein kinase C (PKC). PKC then phosphorylates further proteins in the cell.[68]

This signaling cascade is shut down by IP_3 phosphatases that metabolize IP_3 or lipases that inactivate DAG.[69] $G\alpha_{12/13}$ units interact with RhoGEFs (Ras homology guanosine nucleotide exchange factors). After GDP is replaced by GTP Rho-GTP activates the rho kinase.[70] This enzyme deactivates myosinphosphatase and phosphorylates myosin light chain (MLC) which increases contraction in smooth muscle.[71]

1.2 Dopamine

1.2.1 Dopamine as a neurotransmitter and its receptors

Dopamine (DA) represents a prominent member among the group of catecholamine neurotransmitters. This family shares a dihydroxyphenyl moiety that is linked to an amino function by an ethylene bridge as common structural composition.[72] DA and its biosynthetic pathway were discovered in 1957.[73] In a first step L-tyrosine hydroxylase (TH) converts L-tyrosine into L-DOPA. Subsequently, the aromatic amino acid decarboxylase (AADC) demerges CO_2 which leads to DA (cf. **Figure 1.5**).[72] DA targets five different GPCRs to pass on its signal. They are subclassified into D_1-like (D_1R and D_5R) and D_2-like receptors (D_2R, D_3R and D_4R) depending on sequence homology and intracellular signaling pathways.[74] D_1-like receptors are coupled to $G\alpha_s$ proteins. Their stimulation activates adenylyl cyclase (AC) and therefore leads to increased cyclic adenosine monophosphate (cAMP) levels.[75,76] In contrast, D_2-like receptors are coupled to $G\alpha_{i/o}$ proteins. In this case, activation blocks AC and thus leads to lower cAMP levels.[77] DA receptors are highly expressed in the mesocortical, tuberoinfundibular, mesolimbic, and nigrostriatal system which leads to the fact that DA is the most dominant neurotransmitter in the human brain.[78] Unsurprisingly, DA highly affects various body functions such as feeding, attention, sleep, reward, and voluntary movement.[79] Peripheral dopaminergic pathways are important for renale, cardiovascular, and gastrointestinal processes.[80] Due to the involvement of DA in all these physiological mechanisms DA receptors represent major targets for a multitude of diseases like depression,

dyskinesias, Huntington`s disease, schizophrenia, and Parkinson`s disease.[81] Especially Parkinson`s disease (PD) is mainly treated by DA receptor-targeting drugs. After realizing that PD is caused by a lack of dopamine activity due to cell death in the substantia nigra L-DOPA was the first FDA approved drug to treat PD in the 1960s.[82] Over the years more and more alternatives like D_2R agonists (pramipexole, ropinirole, rotigotine), monoamine oxidase B (MAO-B) inhibitors (rasagiline, selegiline), and acetylcholine receptor antagonists (budipine) have emerged.[83] Yet to this day, L-DOPA in combination with L-dopa decarboxylase inhibitors (carbidopa, benserazide) and catechol O-methyltransferase inhibitors (entacapone, tolcapone) remains the most effective treatment for PD.[84]

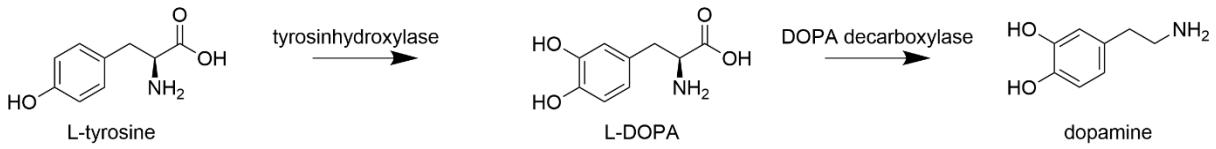

Figure 1.5: Biosynthesis of dopamine.

1.2.2 Dopamine D_2 receptor

Within the scope of research on antipsychotics for the treatment of schizophrenia scientists discovered the D_2R in 1975.[85] In search for the specific receptor which was responsible for antipsychotic effect of the drugs used at the time they successfully marked the receptor with [^{3}H]haloperidol and could inhibit binding of the radioactive probe with the then used antipsychotics.[86,87] Successful cloning of the D_2R was achieved by Grandy et al. in 1990.[88] Additionally, it was soon discovered that the D_2R exists in form of two variants caused by alternative splicing, D_2 long (D_{2L}) and D_2 short (D_{2S}). The third loop of the D_{2L} consists of 29 additional amino acids producing inherent pharmacological and physiological characteristics.[89] Due to its function as autoreceptor the D_{2S} is primarily expressed presynaptically.[89] In contrast, the D_{2L} is mostly expressed on the postsynapse.[89,90] Apart from its inhibitory effect on cAMP accumulation in the cell the D_2R can activate other G protein-dependent and also G protein-independent processes, e.g. β-arrestins, ion channels, and receptor tyrosine kinases (cf. **Figure 1.6**).[91] Especially the β-arrestin-mediated control of serine/threonine protein kinases AKT and GSK-3 has been described to effect responses *in vivo*.[92,93]

Note: From this point the abbreviation "D_2R" refers to the D_2 long receptor and the abbreviation "D_4" refers to the $D_{4.4}$ receptor. Other polymorphic variants of the receptors will be mentioned explicitly.

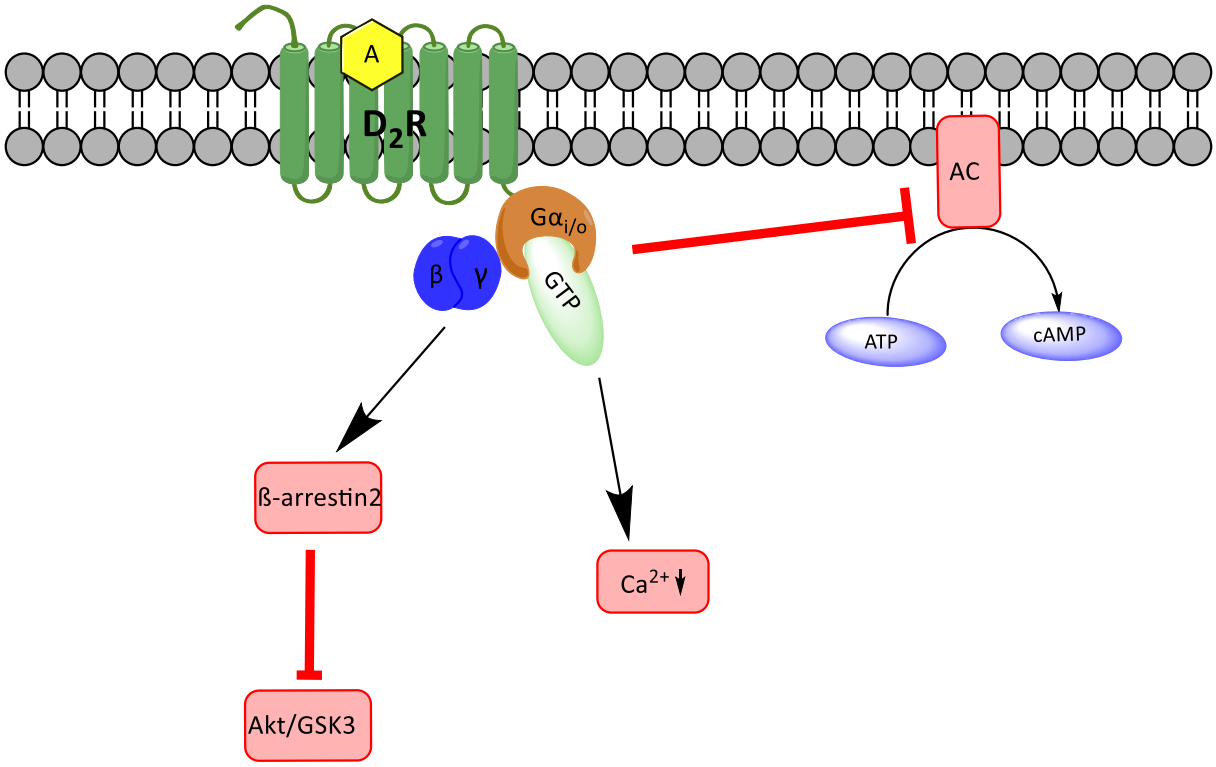

Figure 1.6: Signaling pathway of the D_2R. Upon stimulation the D_2R reduces the activity of AC leading to reduced cAMP levels.

As the D_2R represents a highly interesting target for numerous diseases due to its involvement in several physiological processes a great number of synthetic approaches have been made to target the desired receptor. Bioisosteric derivatives of dopamine, homobivalent ligands,

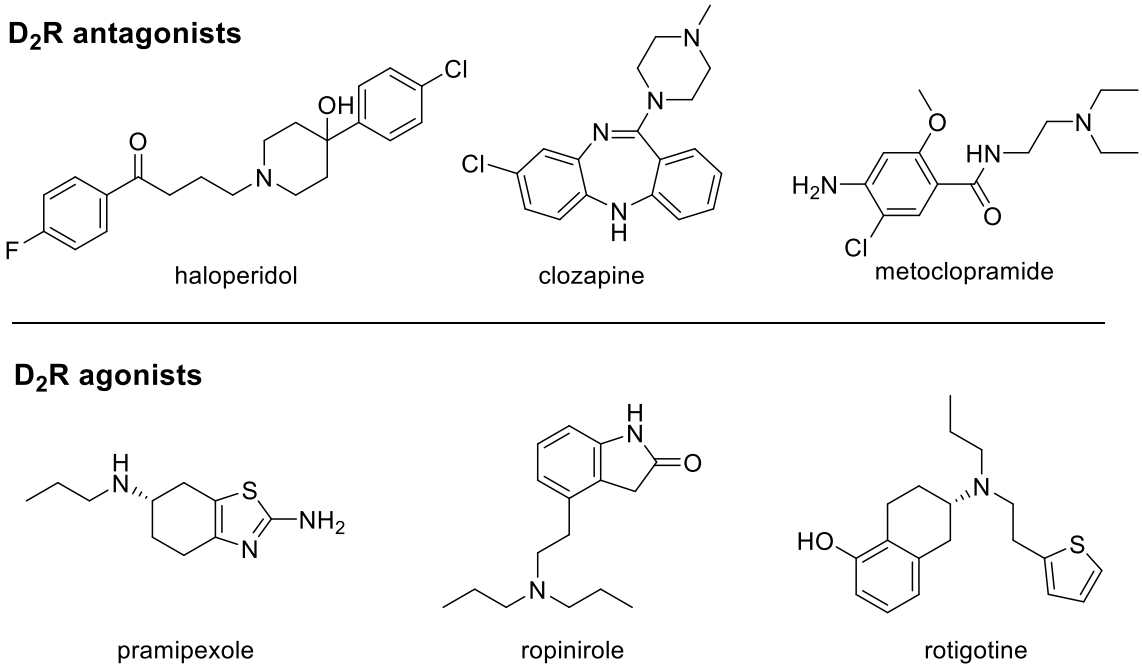

Figure 1.7: Selected D_2R antagonists and agonists.

peptidomimetic ligands, and bitopic ligands have been synthesized to further characterize the receptor.[94–97] The publication of the D_2R crystal structure bound to risperidone further supported synthetic approaches for selective D_2R ligands.[98] The great clinical relevance of the receptor is reflected by the huge number of diseases in which drugs targeting the D_2R are counted among first line medication, e.g. L-DOPA (PD), clozapine (schizophrenia), and metoclopramide (nausea) to name a few (cf. **Figure 1.7**).[99–101]

1.3 Histamine

1.3.1 Histamine as a neurotransmitter and its receptors

Histamine research dates back to the early 1910s. The first successful synthetic approach in 1907 was followed by the isolation out of ergot (Claviceps purpurea) in 1910.[102] After the H_1R, H_2R, and H_3R the H_4R was discovered as the latest member of the histamine receptor family[103–106] and the preliminary pinnacle was reached in 2011 when the first crystal structure of the H_1R was published.[107]

Histamine is a biogenic amine which is biosynthesized from the amino acid L-histidine by the enzyme histidine decarboxylase (HDC) (cf. **Figure 1.8**).[108] Looking at the structure shows that histamine possesses two basic centers, the amino moiety (pK_s = 9.4) and the imidazole cycle (pK_s =5.8).[109] The pK_s values suggest that histamine exists as mono cation under physiological conditions. Moreover, histamine can exist in form of two different tautomers, N(π)-histamine and N(τ)-histamine. Under physiological conditions the N(τ)-tautomer is the preferred form.[110] High concentrations of histamine can be found in tissues of the lungs, the gastrointestinal tract, and the skin and the neurotransmitter is stored in endothelial cells, neurons, basophil granulocytes and mast cells.[102] Due to the great dispersion of histamine and its receptors in the human body it plays an important role in a great number of physiological and pathophysiological processes like immune responses, regulation of gastrointestinal functions, and inflammatory reactions.[111]

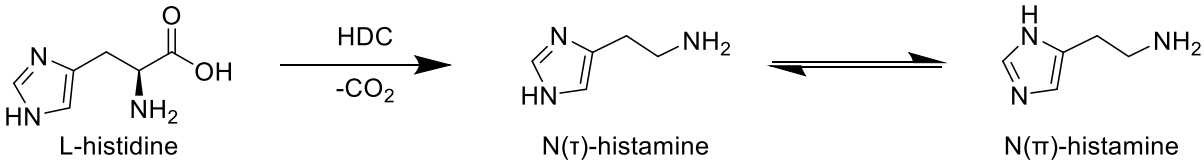

Figure 1.8: Biosynthesis of histamine.

The H_1R is $G\alpha_{q/11}$-coupled and is expressed in various tissues like smooth muscle, gastrointestinal tract, as well as lungs and mediates allergic and inflammatory processes.[112] It represents the primary target for antiallergics. The early generation of H_1-antihistamines however showed unwanted sedative side effects caused by the lipophilic structure enabling them to pass the blood-brain barrier (BBB).[113] By introduction of more hydrophilic functions (alcohols, carboxylic acids) this ability was removed which led to notably reduced levels of side effects.[114] The $G\alpha_s$-coupled H_2R is amongst others located in brain, lungs, heart, and gastric parietal cells. Activation of the H_2R causes positive inotropic and positive chronotropic effects in pericardial tissues.[115–118] As this receptor is also responsible for the transmission of histamine-induced acid secretion in parietal cells it was targeted for the treatment of gastro-oesophogal reflux disease and peptic ulcer.[116] H_2R antagonists like cimetidine and improved versions like ranitidine and famotidine were very popular in the 1970s and 1980s but have massively lost relevance since the approval of proton pump inhibitors like omeprazole and pantoprazole.[119] The H_4R receptor is mainly expressed in cells of the immune system, as well as mast cells and is $G\alpha_{i/o}$ coupled. Its primary purpose is the control of immunological and inflammatory processes in the human body.[102] Although no drugs targeting the H_4R have yet been approved, its pharmacological profile makes it a potential target for diseases such as lupus or rheumatoid arthritis.[120]

1.3.2 Histamine H_3 receptor

The H_3R was pharmacologically identified in 1983 when burimamide, a known H_2R antagonist, decreased histamine induced [^{3}H]histamine release in nanomolar range while it only possesses micromolar affinity to the H_2R.[103] The existence of the H_3R was then finally proved by the development of the selective H_3R ligands R-α-methylhistamine (RAMH) and thioperamide and the first successful cloning of the receptor in 1999.[121] Because of introns and exons in the H_3R encoding gene 20 isoforms have been identified so far. The physiologically most dominant form of the receptor, composed of 445 amino acids, exists both in the CNS and PNS.[122] It exhibits a high level of constitutive activity which was proven by lowering basal G protein activation by administration of inverse agonists.[123] Regarding the CNS, the H_3R is primarily expressed in basal ganglia, hippocampus, and cortical area while the main peripheral tissues for H_3R expression are the lungs, the gastrointestinal tract as well as

the cardiovascular system.[124] This explains why it plays a crucial role in pathophysiological processes like pain, obesity, and cognitive disorders.[124,125]

As a presynaptic autoreceptor and heteroreceptor its main function is the control of the release of histamine and non-histaminergic neurotransmitters like acetylcholine, dopamine, GABA, and serotonine.[126] The receptor couples to pertussis-toxin sensitive $G\alpha_{i/o}$ proteins which inhibits AC and leads to lower cAMP levels (cf. **Figure 1.9**).[127] In addition, the receptor also blocks the Na^+/H^+ exchanger and disables Ca^{2+} influx.[128,129] MAPK, phospholipase A2 (PLA_2) and phosphatidylinositol-3-kinase (PIK3) are activated upon H_3R stimulation.[130,131]

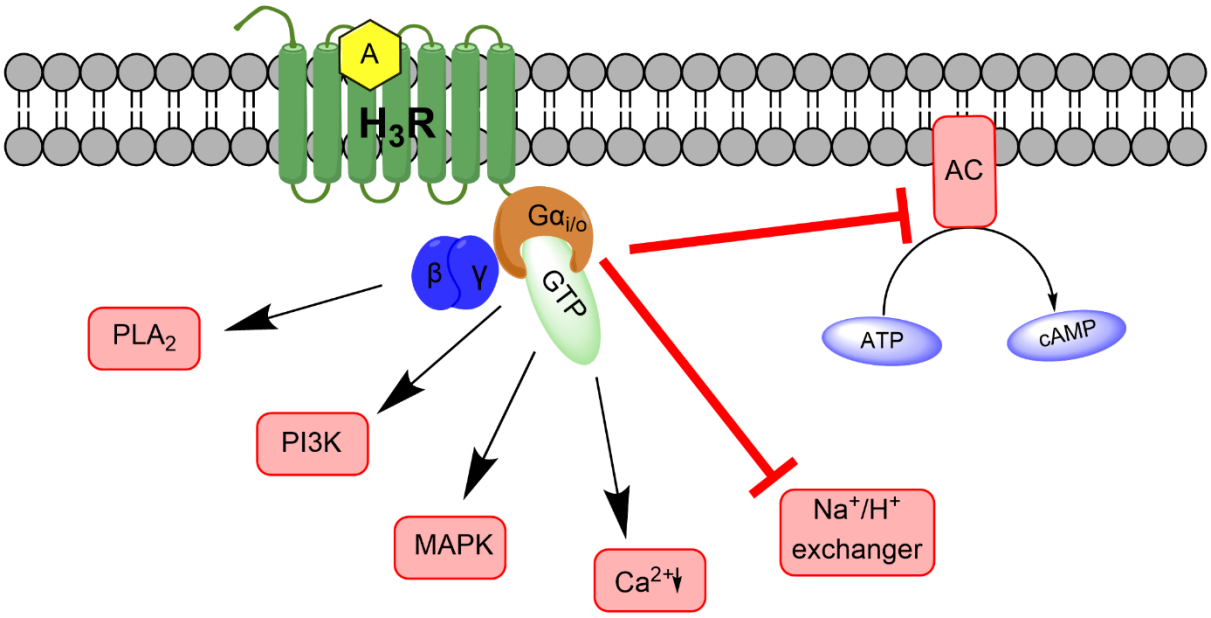

Figure 1.9: Signaling pathways of the H_3R. Upon stimulation the H_3R reduces activity of AC leading to lower cAMP levels.

All H_3R agonists share an imidazole moiety as crucial structural feature with examples like RAMH or immepip (cf. **Figure 1.10**).[132] High sequence homology between the H_3R and the H_4R caused several problems in the early stage of the development of selective H_3R agonists.[133] Structural improvement of the aforementioned compounds led to immethridine and methimmepip that displayed high selectivity towards the H_3R.[134] H_3R antagonists are classified into imidazole-like and non-imidazole-like compounds. Well known imidazole-like ligands are thioperamide and clobenpropit that have also high affinity towards the H_4R due to high homology between the two receptors.[133] The most prominent member of the non-imidazole-like ligands is the inverse agonist/antagonist pitolisant.

H_3R agonists

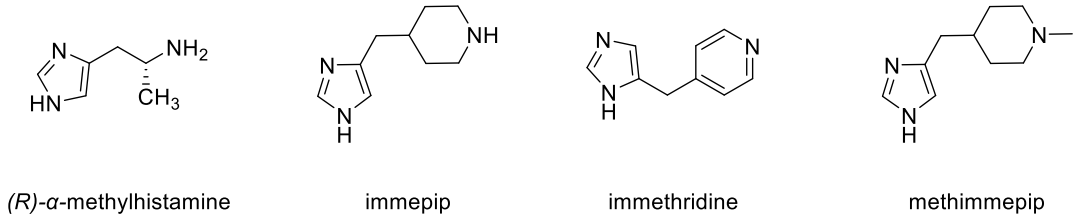

H_3R antagonists / inverse agonistis

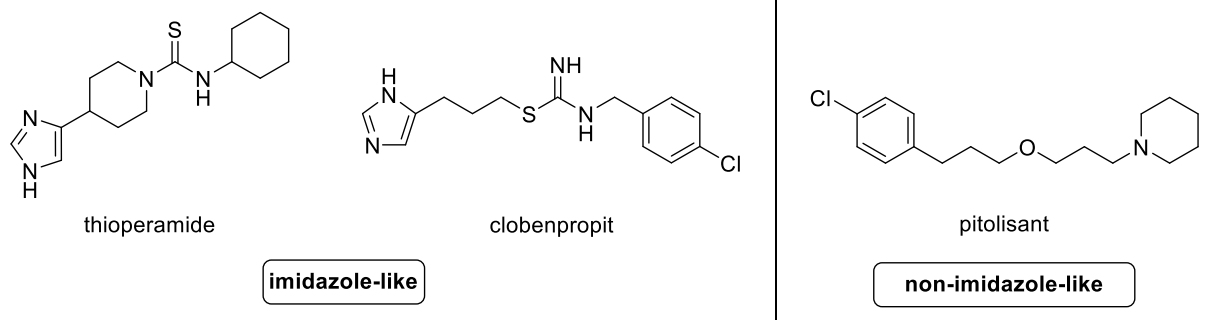

Figure 1.10: Selected H_3R agonists and antagonists.

Despite the high expression of the H_3R in the brain and the resulting relevance for CNS related diseases pitolisant is the only approved drug for this receptor. Sold under the brand name Wakix© it is used to treat narcolepsy.[135] All in all, it can be stated that the H_3R represents a very promising target for neurodegenerative diseases but due to the complexity of the receptor further research is necessary.

1.4 Receptor dimerization

The long-lasting belief that GPCRs only act single-handedly as isolated entities has been overruled in recent years. The development of new techniques such as FRET, BRET, crosslinking, Western Blot, and co-immoprecipitation has led to the identification of GPCR structures of higher order, so called dimers or oligomers.[136–139] These structures can either consist of the same GPCR which results in the formation of homodimers and -oligomers or they can be composed of different receptors resulting in newly formed heterodimers or -oligomers.[140] To this date dimerization for many class A GPCR`s has been reported, e.g. homodimerization of opioid receptors,[141] serotonin receptors,[142] histamine receptors,[143]

and dopamine receptors.[144] Heterodimerization has been proven amongst others for D_2/NTS_1, $D_2/mGLU_5$, muOP/$CXCR_4$ D_1/H_3, and D_2/H_3.[145–148] Regarding the dimerization of receptors on the membrane level three different regions are possible to interact with each other, namely the extracellular loops, transmembrane regions as well as intercellular loops with the transmembrane regions being the most common option.[149,150] With respect to dimerization within the transmembrane region two different modes of interaction have been identified (cf. **Figure 1.11**).[151] Contact dimerization describes the phenomenon when the involved helices from one receptor contact the helices from the other monomer in order to stabilize the dimer pair. Domain swapping on the other hand means that helices from each receptor are exchanged in the dimer which means that one monomer within the dimer contains helices shared by both receptors.[151]

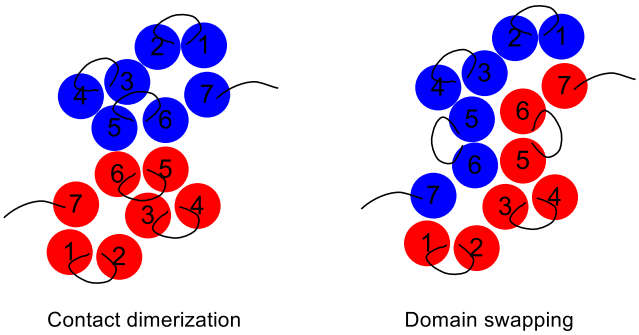

Figure 1.11: Different modes of dimerization. Regarding domain swapping the functional monomers within the complex contain proteins provided by both receptors (adapted from [151]).

Especially heterodimerization has caught more and more attention in recent years since this kind of interaction does not only expose altered ligand binding but also modified signaling pathways compared to the parent monomeric receptors.[138,140] To further characterize and standardize the topic of possible receptor heterodimerization Gomez et al. have introduced three criteria necessary for the formation of heteromers (Het).[152] First the receptors are co-localized in order to have the possibility to interact with each other. This can be verified by techniques like PLA, co-immunoprecipitation, or resonance-energy based approaches like FRET or BRET.[153–155] Second, the receptordimer possesses different properties and characteristics than the individual receptors.[152] On the one hand this includes modified binding affinity of compounds for the dimer compared to the monomeric receptors. On the other hand, functionality is highly affected by the formation of dimers.[152,156] This involves the amplification or reduction of signaling pathways or even the activation of completely different pathways.[157,158] In this context the cross-antagonism has to be mentioned. This phenomenon describes the fact that Het stimulation by an agonist of one monomeric part can be blocked

by the addition of an antagonist for the other half of the receptor dimer.[159,160] Third, these complexes and their individual signaling pathway can be stimulated selectively compared to the monomeric receptors. Possible compounds for this purpose are het-selective antibodies or bivalent ligands.[161–164] It should be stated that all three criteria should be met not only in artificial cell systems but also *in vivo* to finally proof the existence of the proposed heterodimer.[152] Since only little is known about the change in signaling caused by receptor dimerization further research on this topic is necessary to better understand its involvement in physiological and pathophysiological processes.[159]

1.4.1 Bivalent ligands

Heterobivalent ligands are defined as molecules that consist of two different pharmacophores connected by a linker which allows the ligand to simultaneously bind to the two orthosteric binding sites present in GPCR heterodimers. Compounds containing a linker of optimal length are envisioned to show higher affinity than that stemmed from the two monovalent pharmacophores.[165] Following the binding of the first pharmacophore to the receptor monomer the second pharmacophore is dragged into the proximity of the other orthosteric binding site, which results in an increased local concentration (cf. **Figure 1.12**).[165,166] This may enable the targeting of selected heteromeric subtypes, resulting in increased selectivity of drug action. This concept has been successfully demonstrated by Qian et al.[148] They described heterobivalent ligands for the $mGluR_5$–D_2R Het that showed highly increased binding affinities compared to their monovalent counterparts. Yet synthesis of such ligands is ambitious and requires a huge amount of preparation as several requirements have to be met. First, selective and very affine pharmacophores for each receptor need to be found. Second, appropriate attachment points must be selected which allow facile connection to the linker without resulting in a loss of affinity for the desired receptor. Third, a linker has to be synthesized that covers enough space for both pharmacophores to reach the orthosteric binding site without interfering with the receptor itself which would most likely result in a loss of affinity. Additional problems are caused by pharmacokinetic aspects of bivalent ligands.

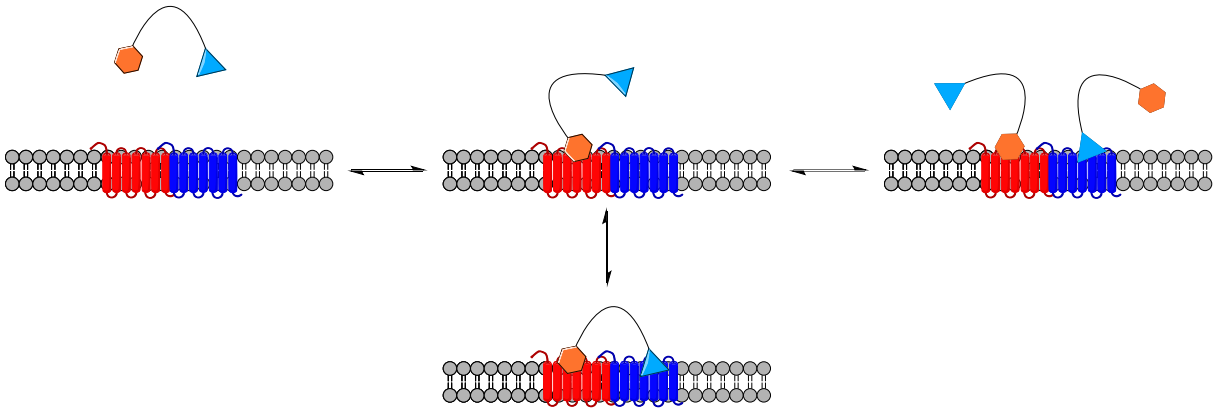

Figure 1.12: Suggested binding mode of bivalent ligands. As soon as the first pharmacophore binds to the respective receptor monomer the second pharmacophore gets dragged into the vicinity of the other orthosteric binding site, raising the local concentration (adapted from [166]).

These ligands are known for their huge size and tend to possess mostly lipophilic characteristics which is contrary to requirements for acceptable bioavailability.[167] Furthermore, these ligands would have to pass the BBB to reach their target which turns out to be very difficult due to their size.[168]

1.4.2 D_2-H_3 heteroreceptor dimer

The existence of the D_2-H_3 heterodimer has first been described by Ferrada et al. in 2008.[145] Using different techniques, they could detect interactions between the two receptors in artificial cells as well as *in vivo*. On the one hand, they performed radioligand binding assays with the D_2 receptor antagonist [^{3}H] YM-09151-2 as radioligand and increasing concentrations of the D_2R agonist quinpirole as displacer in sheep striatal membranes.[145] They could observe that competition binding curves were right shifted in the presence of H_3R agonists RAMH, immepip, or imetit.[145] This effect could be reversed by addition of the H_3R antagonist thioperamide. Furthermore, they performed BRET experiments to detect heterodimerization. Cells transiently co-transfected with constant amounts of D_2-Rluc and increasing amounts of H_3-YFP showed a saturable binding curve while cells co-transfected with D_2-Rluc and H_4-YPF, used as a negative control, showed no saturable signal.[145] Moreover, they investigated the effect of the H_3R on locomotor activation in reserpinized mice induced by quinpirole. They could observe that locomotor activation produced by 0.5 mg/kg quinpirole was highly potentiated by previous administration of H_3R antagonist thioperamide.[145] In contrast, H_3R agonist imetit reduced locomotor activation of the same dose of quinpirole.[145] According to

Ferrada et al. all these results indicate that there is a strong interaction between the two receptors which can only be explained by the formation of receptor dimerization. Because of the fact that these dimers are prominently expressed in the striatum and have a huge impact on locomotor activation they seem to play an important role in the progression of PD. Therefore, there is a need of bivalent ligands selectively targeting this receptor complex to get a better understanding of its pathophysiological significance.

1.5 Fluorescent ligands

Fluorescent ligands have emerged as powerful tools to further develop GPCR research in recent years. Their broad field of application has made them essential for numerous experimental setups. For instance, imaging experiments like total internal reflection microscopy (TIRFM) or confocal microscopy have become increasingly important to further study receptor characteristics. TIRFM has been successfully used for single molecule imaging of GPCRs at the cell membrane.[169,170] This technique is based on the principle that totally internally reflected excitation light creates an electromagnetic field at the interface between a transparent solid and liquid.[171] This so-called evanescent field has the same frequency as the excitation light and the decline of its intensity is exponential to the distance from the surface to the solid.[171] This makes TIRFM a powerful technique for single molecule imaging since solely fluorescent molecules within only hundreds of nanometers of the solid are efficiently excited.[171] Confocal microscopy is a popular method for generating high resolution pictures even of thick specimen. In contrast to a normal fluorescence microscope a confocal microscope does not take one picture of the whole specimen but uses a procedure called optical sectioning.[172] By adding a pinhole directly after the light source and a second pinhole in front of the photodetector, out-of-focus light, also called “flare”, in the specimen is eliminated by areal filtering. That way sharp pictures can be taken.[172,173]

Fluorescent ligands have also been crucial for the development of non-radioactivity-based assays to determine receptor affinities of unlabeled compounds. For the NanoBRET binding assay the NanoLuc, a genetically engineered luciferase, is attached to the N-terminus of the desired GPCR.[174] After the substrate is added an oxidation reaction is catalyzed by the fused enzyme which results in the emission of blue light.[175] When an appropriate fluorescent ligand

binds to the tagged receptor bioluminescence resonance energy transfer (BRET) makes the ligand fluoresce (cf. **Figure 1.13**).[174] Short distance between ligand and bioluminescent donor

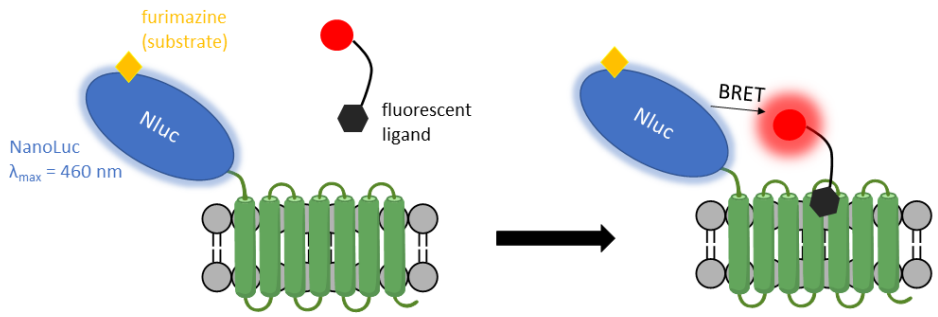

Figure 1.13: Schematic illustration of the principle of the NanoBRET binding assay. Upon binding the fluorescent ligand and the luciferase are close enough so that the fluorescent dye can be excited by BRET leading to the emission of red light.

is an indispensable requirement for BRET to take place.[176] As a result, only little unspecific binding is detected. Another positive aspect is the possibility to monitor the binding mechanism in real time which gives additional information about kinetic characteristics of tested compounds.[177] Fluorescent ligands share a common structure consisting of a pharmacophore, a linker region, and a fluorescent dye (cf. **Figure 1.14**). Each of these parts has a considerable impact on the intended use of the fluorescent probe which is why they have to be chosen carefully. The pharmacophore must have high affinity for the desired receptor since only a very small amount of the compound is usually synthesized. Additionally, a suitable attachment point for the linker has to be found. The addition of bulky structures is prone to result in a loss of affinity which is why an attachment point directing out of the binding pocket needs to be selected. Linker length is also a very important feature of a fluorescent ligand. On the one hand short linkers are desirable as the overall size of the compound should be kept as small as possible to reduce the aforementioned loss of affinity. On the other hand, certain applications require larger linkers. For a NanoBRET assay for example the linker has to enable the fluorescent ligand to reach the fused NLuc for interaction in order to generate a signal. These longer linkers are commonly based on polyethylene glycol (PEG) units as they are chemically stable, show only little interaction with cell membranes and increase water solubility.[148] The choice of the fluorescent dye depends on the intended use. For microscopy experiments the dye must be compatible with available lasers and filters. For the development of a NanoBRET assay an overlap between the emission spectrum of the used

luciferase and the excitation spectrum of the fluorescent dye is necessary to generate a detectable signal.

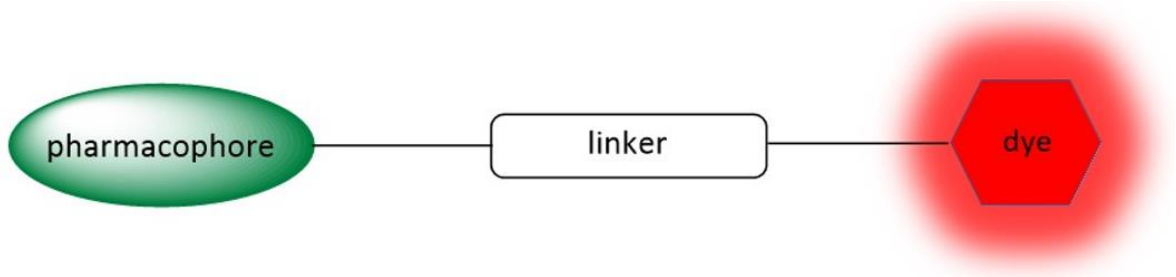

Figure 1.14: Schematic illustration of fluorescent ligands containing a pharmacophore, linker, and fluorescent dye.

1.6 Parkinson`s Disease

Parkinson`s Disease (PD) is a chronic progressive neurodegenerative disorder and affects about 2-3% of the population > 65 years of age which makes it the second most common neurodegenerative disorder in the world.[178] Mostly the elderly are affected with the mean on-set age being 55. Only in 5 % the on-set occurs under 40.[179] PD is mainly caused by dopamine deficiency as a result of a severe loss of nigrostriatal dopaminergic neurons in the substantia nigra pars compacta (SNpc) and by intracellular depositions of aggregates containing α-synuclein, so-called "Lewy-Bodies".[84,178,180] Resting tremor, postural instability, rigidity, and bradykinesia as clinical manifestations have become inglorious hallmarks for PD.[84] Yet unfortunately, symptoms exceed movement disorders and also include autonomic dysfunction, hyposmia, cognitive impairment, disorders of sleep, and depression.[178] Although the first description of PD dates back to 1817 when James Parkinson published "An Essay of the Shaking Palsy", more than 200 years of research have not yet led to a curative treatment of PD.[179] Modern therapy mainly focuses on symptom control and improving quality of live. For this purpose, a great variety of different drugs are available (cf. **Figure 1.15**). L-DOPA is the most important one and has been the gold standard for more than 50 years.[181] However, the use of L-DOPA is kind of tricky because motor complications like motor response oscillations and drug-induced dyskinesias need to be considered.[182] The mechanisms behind these phenomena are not yet fully understood. However, discontinuous drug delivery caused by the short half-life of L-DOPA and inconstant gastrointestinal absorption as well as variability of blood-brain barrier penetration are believed to play a crucial role.[181] To tackle these problems novel sustained release formulations are being developed.[183] To potentiate its

effect, L-DOPA is combined with inhibitors of AADC (carbidopa and benserazide) and/or inhibitors of catechol-O-methyltransferase (COMT, tolcapone). AADC inhibitors avert peripheral decarboxylation of L-DOPA while COMT inhibitors prevent metabolism of dopamine in the CNS.[184] Combinations of L-DOPA together with AADC inhibitors and COMT inhibitors are used to increase bioavailability and to extend the duration of effects of L-DOPA.[185,186] Another possibility to increase dopamine levels in the CNS is the use of monoamine oxidase type B-inhibitors. Substances like rasagiline or selegiline act as irreversible suicide inhibitors for MAO-B and consequently extend dopamine levels.[187] In recent years, D_2R agonists have emerged as effective alternative to the aforementioned compounds. Drugs like pramipexole, ropinirole, or rotigotine show a longer half-life time than L-DOPA which makes them ideal for adjunct therapies for patients with motor fluctuations.[188]

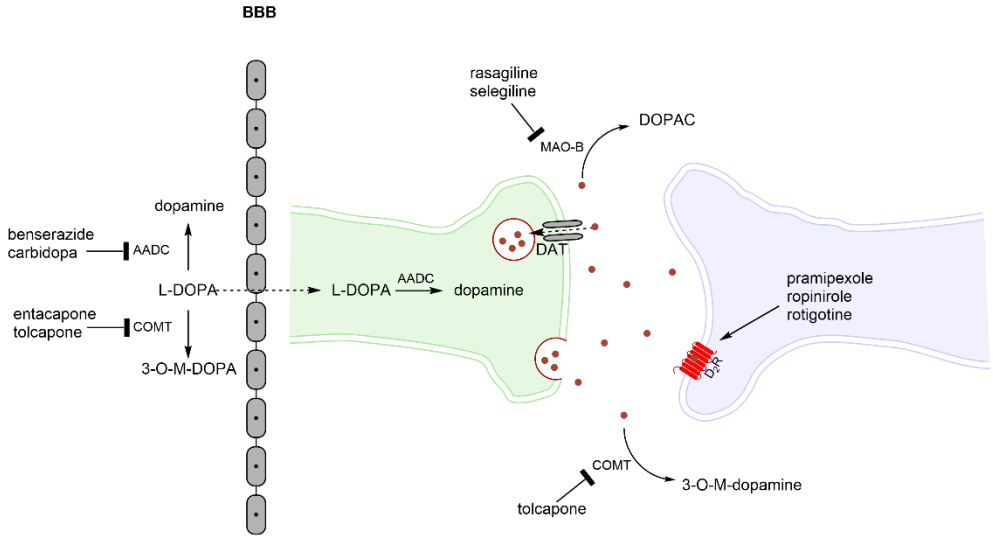

Figure 1.15: Dopaminergic drug targets in Parkinson's Disease (adapted from [84]).

It is also reported that D_2R agonists as initial monotherapy have a lesser risk for motor complications.[189] As disadvantages lower effect compared to L-DOPA and the potential to cause drowsiness and impulse dyscontrol have occurred.[190]

Although targeting the dopaminergic pathway has led to effective ways to treat the symptoms of PD, the mentioned disadvantages and side effects have made it clear that there is a need for alternative strategies and drugs. This has led to the development of compounds addressing different pharmacological systems such as glutamatergic, serotonergic, GABAergic, noradrenergic, and cholinergic pathways.[191] One example is amantadine which acts as a N-methy-d-aspartate (NMDA) antagonist and is used to treat L-DOPA induced dyskinesia.[186,189] Autonomic dysfunction which mainly occur in late-stage PD are typically treated by drugs

aiming at the autonomic nervous system. Corticoids like fludrocortisone and noradrenaline precursor droxidopa are used to treat orthostatic hypotension, anti-muscarinics such as tolterodine or trospium chloride address urinary urgency, incontinence or sialorrhea.[192,193] All in all, it can be stated that finding new ways for effective therapy of PD is one of the main challenges for the future which is highlighted by the fact that the number of patients suffering from PD is expected to reach 9.3 million in 2030 which represents a rise of about 100 % compared to 4.6 million in 2005.[178,194]

Chapter 2: Scope and objectives

2. Scope and objectives

2.1 Bivalent ligands

One goal of this thesis was the design and synthesis of selective bivalent ligands for the D_2-H_3 Het. For that purpose, pharmacophores with high affinity for the D_2R and H_3R were selected, derivatized, and then connected by an appropriate linker that should cover enough distance to enable both pharmacophores to reach both orthosteric binding pockets simultaneously. Only that way a bivalent binding mode can be achieved.

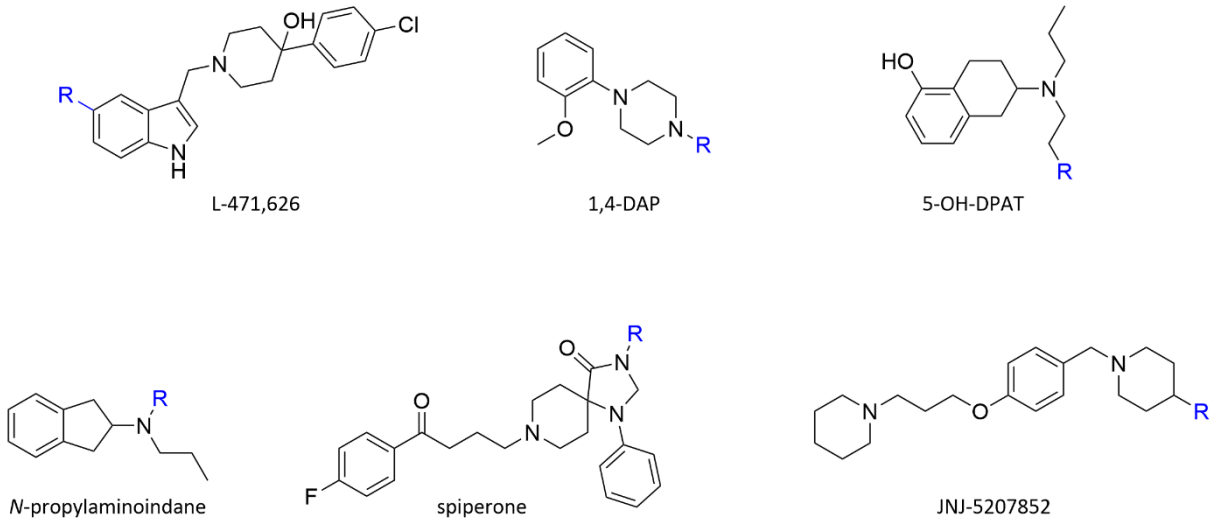

Figure 2.1: Used lead structures and selected attachment points (blue) of D_2R and H_3R pharmacophores.

To address the D_2R protomer, five different lead structures were selected. Agonists as well as antagonists were selected to find out how different functionalities might influence a possible bivalent binding mode. The first scaffold was the known D_2R antagonist L-471,626 (cf. **Figure 2.1**). Structure activity relationship studies performed by Vangvervong et al. showed that substitution of the halogen atom of the phenyl ring resulted in a huge loss of affinity while addition of alkyl ethers to position five of the indole moiety was well tolerated.[195] Therefore, this position was selected as attachment point for derivatization.

The second scaffold was a 1,4-disubstituted aromatic piperazine (1,4-DAP) (cf. **Figure 2.1**). Its antagonistic mode of action is caused by the aromatic head group and the amine moiety, which enables the compound to form a firm hydrogen bond with $Asp_{3.32}$.[148] Addition of lipophilic moieties to this amino function can ameliorate affinity which is why this part was selected as attachment point.[95] A phenyl ring was added to create a kind of spacer between

pharmacophore and linker to allow the pharmacophore to reach the orthosteric binding site while the rest of the molecule can reach out of the binding pocket.[148]

The third scaffold was the D_2R agonist 5-OH-DPAT (cf. **Figure 2.1**). Site-directed mutagenesis has shown that D_2R activation is caused by interactions between the 2-aminotetralin and an agonist binding domain connecting TM3 and TM5. The OH group and the basic amino function have also been shown to be crucial for binding affinity.[148] Therefore the same approach as mentioned before was applied for the synthesis of the precursor.

The fourth lead structure was a *N*-propylaminoindane (cf. **Figure 2.1**). It follows the common structure of D_2R ligands of an aromatic headgroup and an amino function to interact with $Asp_{3.32}$. Once again, a lipophilic appendage containing a phenyl ring was added as a spacer between the pharmacophore and the rest of the ligand.[95] The arene moiety as part of the spacer is important because it is described to interact with a hydrophobic microdomain at the extracellular end of TM2, TM3, and TM7. An interaction with parts of the extracellular loop 2 (EL2) is also reported.[196]

The fifth pharmacophore was the potent antagonist spiperone (cf. **Figure 2.1**). In a recent study Im et al. published the structure of the D_2R in complex with spiperone (cf. **Figure 2.2**).[197] It was shown that the compound is surrounded by residues of TM2, 3, 5, 6, and 7 and EL2. The triazaspiro moiety with its tertiary amine is able to form a salt bridge with $Asp_{3.32}$.[197] On the opposite side there is a hydrophobic contact between $Phe_{6.51}$ and the ligand. Additional interactions between the triazaspiro moiety and $Ile_{45.51}$, $Ile_{45.52}$, and $Cys_{45.50}$ on EL2 were detected, which seem to be essential for the antagonistic activity.[197] On the extracellular side of this salt bridge, an extended binding pocket (EBP) is formed between TM2 and TM3 which binds the phenyl ring of spiperone.[197] The amino acids $Val_{2.57}$, $Trp_{2.60}$, $Val_{2.61}$, $Leu_{2.64}$, $Trp_{23.50}$, $Phe_{3.28}$, $Val_{3.29}$, and $Cys_{45.50}$ build this EBP which is necessary for the binding of spiperone.[197] The fluorephenyl part reaches deeply into the ligand-binding pocket with its hydrophobic cleft. CH-π interactions with $Cys_{3.36}$ can be observed in this cleft.[197] Additional hydrophobic interactions with $Thr_{3.37}$, $Ile_{3.40}$, $Ser_{5.46}$, $Phe_{5.47}$, and $Phe_{6.44}$ as well as edge-to-face π interactions with $Trp_{6.48}$ and $Phe_{6.52}$ were shaped. [197] All these findings indicate that amide function within the triazaspiro ring was the most suitable attachment point for spacer and linker.

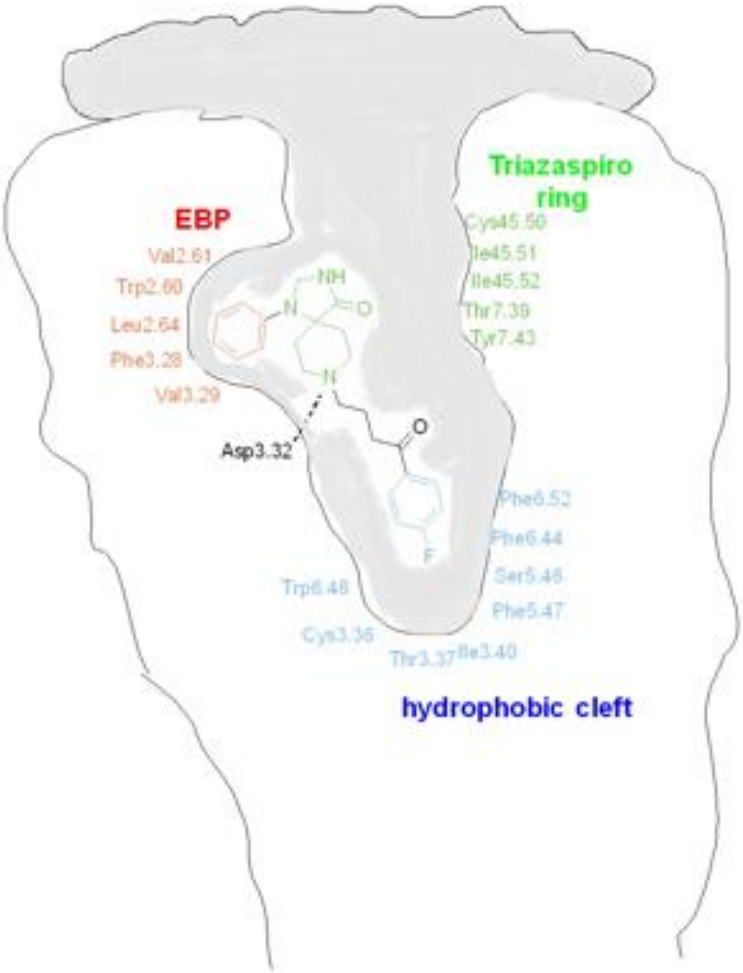

Figure 2.2: Schematic illustration of the complex of D_2R and spiperone. As shown the amide nitrogen of the imidazolidinone points out of the binding pocket making it the perfect attachment point for bulky structures. (adapted from [197]).

As mentioned before H_3R ligands can be classified into imidazole-based and non-imidazole-based subgroups. The imidazole moiety is often accompanied by pharmacological drawbacks such as potential interactions with CYP enzymes.[198] That`s why the structure JNJ-5207852 (cf. **Figure 2.2**) was selected as H_3R scaffold. Besides the fact that it does not contain an imidazole structure it shows a high affinity for the H_3R (pK_i = 9.24) and possesses an exceptional selectivity profile against the other histamine receptors.[199] The non-imidazole-based H_3R ligands share a common structure of a basic, central amino moiety and an aromatic ring surrounded by two basic amino functions. Hence, the para-position of one of the two piperazines was selected as attachment point in order to maintain the structural integrity of the scaffold.

Great importance is also attached to the design of the linkers. Not only is it crucial to cover the distance between the pharmacophores and provide enough flexibility but it also highly influences physicochemical and pharmacokinetic properties of the final compounds (cf. **Figure 2.3**). Therefore, especially the long linkers should consist of polyethylene glycol (PEG) units because they come along with several advantages. PEG linkers are known to be chemically stable, show only little interaction with cell membranes, and highly increase water solubility.[200,201] Since several different linker lengths from 22 to 80 atoms have been reported for bivalent ligands, our aim was to cover a broad spectrum of distances between the two pharmacophores.[148,196,202] Special attention was paid to the most appropriate size of about 50 atoms according to docking studies performed by our collaborator Marc Gomez under the supervision of Leonardo Pardo. Terephthalic acid, isophthalic acid and glutaric acid were used as central dicarbonic acids to find out how flexibility and rigidity influence binding affinities. All in all, it was intended to keep the overall weight of the bivalent ligands as small as possible to avoid negative size effects on bioavailability.

After selecting the scaffolds and designing the linkers an easy and efficient way to effortlessly synthesize various bivalent ligands had to be found. A one-pot copper catalyzed click reaction (CuAAC) was the most convenient approach for that purpose. The pharmacophores had to be derivatized to contain either a terminal alkyne or azide function and the linkers had to possess the respective counterpart. Equimolar amounts of the two precursors and the linker should then be mixed with catalytic amounts of ascorbic acid and $CuSO_4$ x $5{\cdot}H_2O$. After several different attempts failed to add the respective pharmacophores selectively to the linker this one-pot approach was the easiest way to synthesize a great variety of bivalent ligands by simply exchanging the precursors and delivered homobivalent compounds as side products as well as the desired heterobivalent ligands in low to moderate yields.

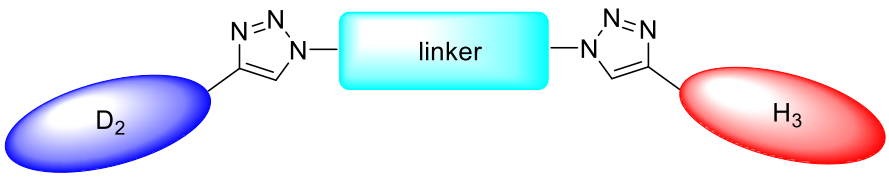

Figure 2.3: Illustration of synthesized bivalent ligands.

All final compounds should then be tested for their binding affinities towards the monomeric D_2R and H_3R. After evaluating these results, the most promising compounds should then be

chosen to be tested in assay systems with cells co-expressing both receptors which is part of the PhD thesis of co-worker Denise Mönnich in our group. That way a bivalent binding mode which is typically accompanied by a shifted and biphasic shaped binding curve should be detected. Additionally, these ligands should also be tested for their mode of action in cAMP assays.

2.2 Fluorescent ligands

Another goal of this thesis was the synthesis of fluorescent ligands that should be used for the development of NanoBRET assays for all D_2-like receptors and should also serve as powerful tracers in microscopy experiments. Spiperone was selected as a pharmacophore as it combines excellent affinity among D_2-like receptors and high selectivity compared to D_1-like receptors. Its antagonistic mode of action makes it highly appropriate for the development of a NanoBRET assay since agonists might lead to receptor internalization. Moreover, additions of bulky structures to the aniline moiety have been described to be well tolerated regarding affinity which makes this part of the molecule a perfect attachment point for the linker.[203] The choice of the attachment point has also been confirmed by computational studies performed with the pharmacophore spiperone as mentioned before. As spacers two different linkers were designed to gain more information about the necessary distance between pharmacophore and dye. A brief linker based on γ-aminobutyric acid was built to cover a rather short distance of 5 atoms to reduce the overall size of the ligand. The long linker covering a length of 18 atoms was based on polyethylene glycole (PEG) units for the same reasons as mentioned before for the bivalent ligands. Since our goal was to design a fluorescent probe for microscopy as well as for the development of a NanoBRET assay we had to choose multilaterally usable dyes. In recent publications very positive results with the 5-TAMRA dye in NanoBRET assays were obtained.[200,204] Additionally, this dye has also been reported to be suitable for confocal microscopy and TIRF microscopy for single molecule imaging.[200,205,206] As an alternative we have selected DY-549P1. Based on its excitation and emission spectrum it can be used for the NanoBRET assay and has also been used in several publications regarding single molecule imaging.[207,208] The synthesized compounds should be pharmacologically characterized in radioligand binding assays and then be checked for their capability to serve as tools for the development of NanoBRET assays. Fluorescence properties such as emission and excitation spectra or quantum yields should also be determined for

further characterization of the compounds. Finally, microscopic experiments should be performed with a selected compound to visualize binding and receptor expression.

Chapter 3: Bivalent ligands targeting the D_2-H_3 receptor dimer

3. Bivalent ligands targeting the D_2-H_3 receptor dimer

Mounting evidence for the existence of interactions between class A GPCRs has emerged in recent years. Although the formation of the D_2-H_3 Het and the resulting impact on diseases like PD was first mentioned more than 10 years ago there has been a lack of heterobivalent compounds specifically targeting the formed dimer ever since. That's why the goal of this chapter was the synthesis and biological evaluation of bivalent ligands targeting the D_2-H_3 Het. For this purpose, suitable scaffolds had to be selected and derivatized and were then connected by linkers of appropriate lengths. Biological evaluation in radioligand binding studies and in cAMP assays should identify the most promising compounds for further biological characterization.

3.1 Synthesis

In the first step precursors of the lead structures mentioned in **chapter 2.1** had to be synthesized and derivatized in a way to be suitable for the final coupling reaction. Therefore, terminal azide or alkyne functions were necessary. After that, different linkers were designed and synthesized containing the respective counterpart for a CuAAC. In a final step precursors and linkers reacted in a one-pot reaction to yield final bivalent compounds. Materials and methods for the following reactions can be found in **chapter 7**.

3.1.1 Precursors for the D_2R

3.1.1 L-471,626

Precursors of L-471,626 were synthesized from commercially available 5-(benzyloxy)indole (cf. **Scheme 3.1**). After cleavage of the benzyl-group with H_2 and Pd/C **1** was alkylated with propargyl bromide or 1-bromo-3-chloropropane to yield **2a** or **2b**. Addition of the corresponding hydroxypiperidine derivative via Mannich reaction delivered **3a-4b**. **4a** and **4b** were then converted into **5a** and **5b** by azide-exchange with NaN_3 in DMF. Additionally, monovalent compounds were synthesized in the same manner from commercially available 5-(methoxy)indole and the respective hydroxypiperidines via Mannich reaction to yield **6a** and **6b**.

Scheme 3.1: Synthesis of L-471,626 derivatives **4a, 4b, 5a**, **5b, 6a**, and **6b**[a]

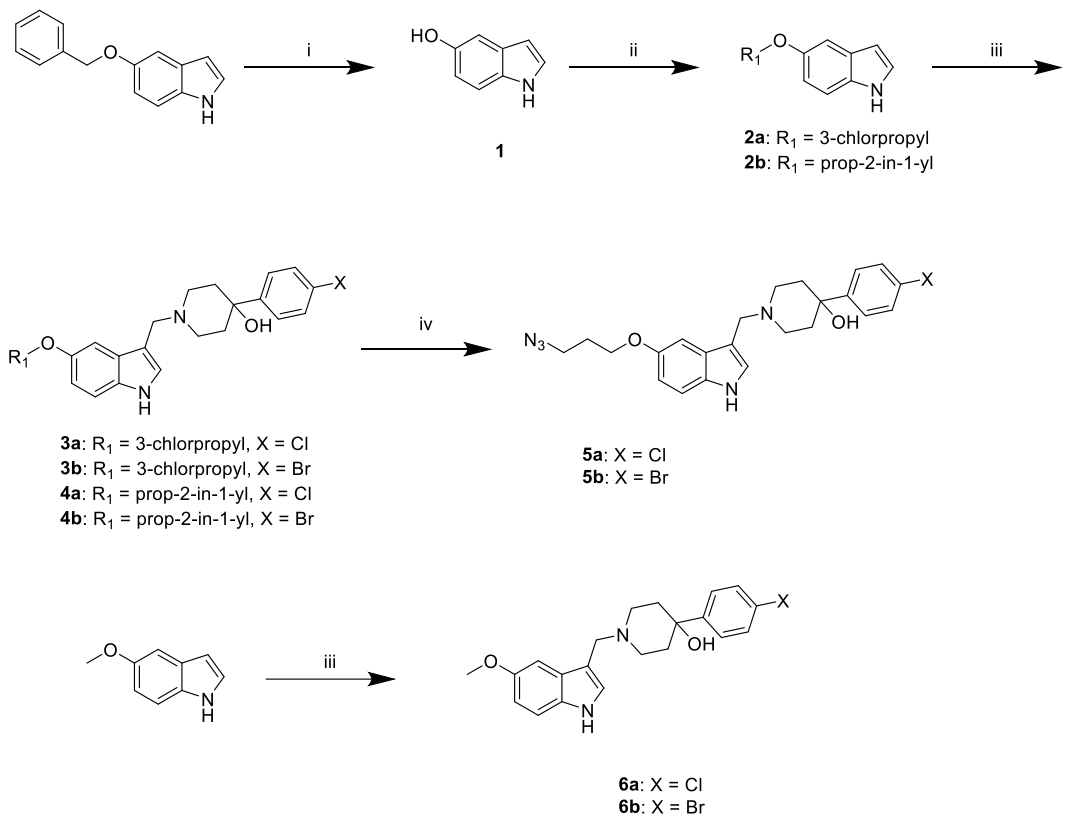

[a]Reagents and conditions: (i) ammoniumformiate, Pd/C, MeOH, 55 °C, 4 h (99%); (ii) 1-bromo-3-chloropropane or 3-bromoprop-1-yne, acetone, K_2CO_3, reflux, overnight (66-81%); (iii) 4-(4-bromophenyl)piperidin-4-ol or 4-(4-chlorophenyl)piperidin-4-ol, formaldehyde (aq. 37%), HOAc, rt, 14 h (62-65%); (iv) NaN_3, DMF, 65 °C, 10 h (87-91%).

3.1.1.2 1,4-DAP

The precursor for 1,4-DAP was synthesized according to a previously described procedure (cf. **Scheme 3.2**).[95] Starting from commercially available 2-(piperazin-1-yl)phenol the secondary amino function was protected with di-tert-butyl dicarbonate to yield **7**. In a second step the phenol group was O-methylated with CH_3I in acetonitrile overnight to obtain **8**. After cleavage of the protection group under acidic conditions **9** reacted with intermediate **10b**, which was synthesized by alkylation of vanilin with 3-bromoprop-1-yne, in a reductive amination using $NaBH(OAc)_3$ as reductive agent yielding final precursor **11b**. For the synthesis of the monovalent compound vanilin was methylated with CH_3I to yield **10a**, followed by a reductive amination with **9** using the same procedure as described before to obtain **11a**.

Scheme 3.2: Synthesis of 1,4 – DAP derivatives **11a** and **11b**[a]

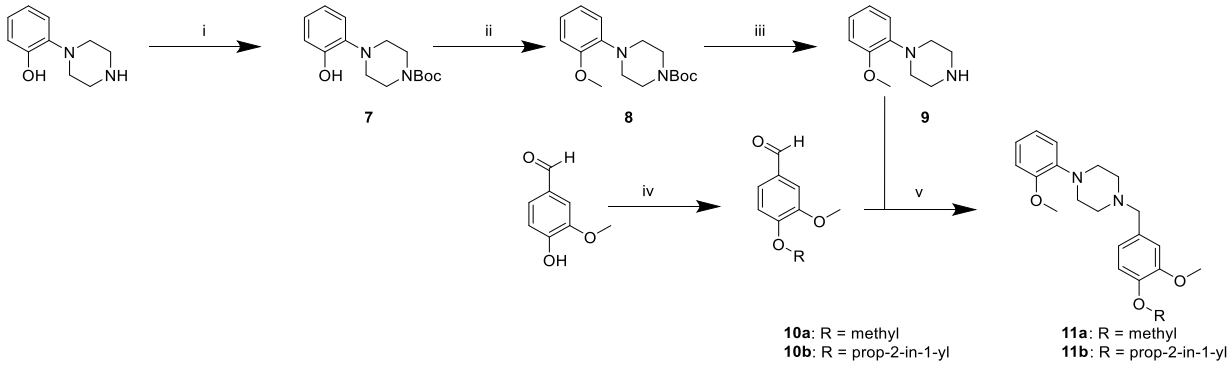

[a]Reagents and conditions: (i) di-tert-butyl dicarbonate, Et_3N, DCM, 10 h, rt (99%); (ii) CH_3I, K_2CO_3, MeCN, reflux, overnight (71%); (iii) TFA/DCM, rt, overnight (63%); (iv) CH_3I, K_2CO_3, MeCN, reflux, overnight (91%), or 3-bromoprop-1-yne, K_2CO_3, MeCN, 80 °C, 14 h (98%) (v) $NaBH(Oac)_3$, DCM, rt, 20 h (52%).

3.1.1.3 5-OH-DPAT

Synthesis of the precursor based on the scaffold of 5-OH-DPAT was carried out according to Soriano et al. with minor modifications (cf. **Scheme 3.3**).[209] In a first step naphthalene-1,6-diol was methylated with dimethyl sulfate after attempts with CH_3I failed to yield the desired intermediate **12**. A Birch reduction with Na in EtOH delivered **13** containing a ketone moiety. Reductive amination with *N*-propylamine using $NaBH(OAc)_3$ resulted in **14**. In the next step, amide coupling with 2-(4-nitrophenyl)acetic acid was carried out in the presence of EDC and HOBt to get **15**. The resulting amide function was converted into the corresponding tertiary amine with BH_3·THF to yield **16**. This step was followed by the reduction of the nitro group with N_2H_4·H_2O and Raney-Ni as catalyst to obtain **17**. Intermediate **18** was synthesized by demethylation with BBr_3 in DCM to obtain a free phenol. In a final step the aniline moiety was reacted with succinic anhydride to yield a free carboxylic acid which was then coupled to propargylamine in the presence of HATU and DIPEA for the synthesis of precursor **19**.

Scheme 3.3: Synthesis of 5-OH-DPAT derivative **19**[a]

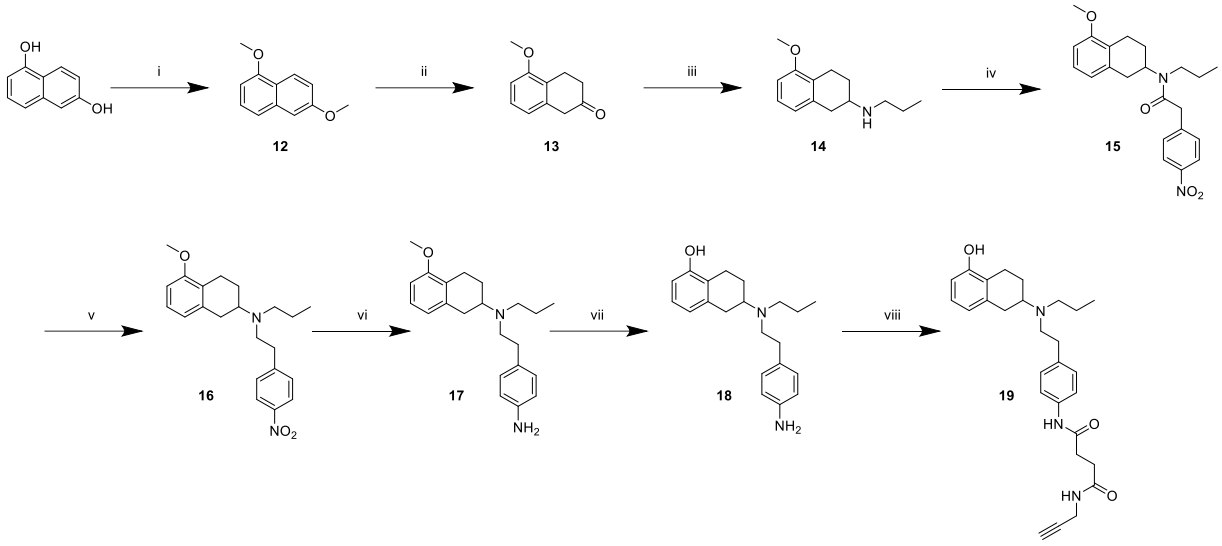

[a]Reagents and conditions: (i) dimethyl sulfate, K_2CO_3, acetone, reflux, 3 h (94%); (ii) Na, EtOH, reflux, 3 h (59%); (iii) propylamine, $NaBH(Oac)_3$, DCE, rt, overnight (63%); (iv) 2-(4-nitrophenyl)acetic acid, EDC, HOBt, DCM, rt, overnight (89%); (v) BH_3·THF, THF, reflux, 4 h (39%); (vi) N_2H_4·H_2O, Raney-Ni, EtOH, 50 °C, 3 h (95%); (vii) BBr_3, DCM, rt, overnight (47%); (viii) (1) succinic anhydride DMF, rt, overnight; (2) propargylamine, HATU, DIPEA, DMF, rt, overnight (51 %).

3.1.1.4 *N*-propylaminoindane

The synthesis of precursors based on a *N*-propylaminoindane scaffold was carried out following previous publications by Kühhorn and Tschammer (cf. **Scheme 3.4**).[196,210] First intermediate **20** was synthesized. Therefore, a reductive amination with indanone and *N*-propylamine in the presence of $NaBH_3CN$ was performed. The resulting secondary amine was alkylated with bromobutyronitrile using KI as catalyst to acquire **21**. The nitrile moiety was then reduced with $LiAlH_4$ to obtain the primary amine **22**. Simultaneously, ethyl 4-hydroxy-3-methoxybenzoate was alkylated with either CH_3I, 1-bromo-3-chloropropane, or 3-bromoprop-1-yne to get **23a-c** followed by the hydrolysis of the ester under basic conditions to yield compounds **24a-c**. Amide coupling with **22** was carried out in the presence of HATU and DIPEA in DMF to obtain **25a-c**. An azide exchange using NaN_3 was performed with **25a** to get precursor **26**.

Scheme 3.4: Synthesis of *N*-propylaminoindane derivatives **25b**, **25c** and **26**[a]

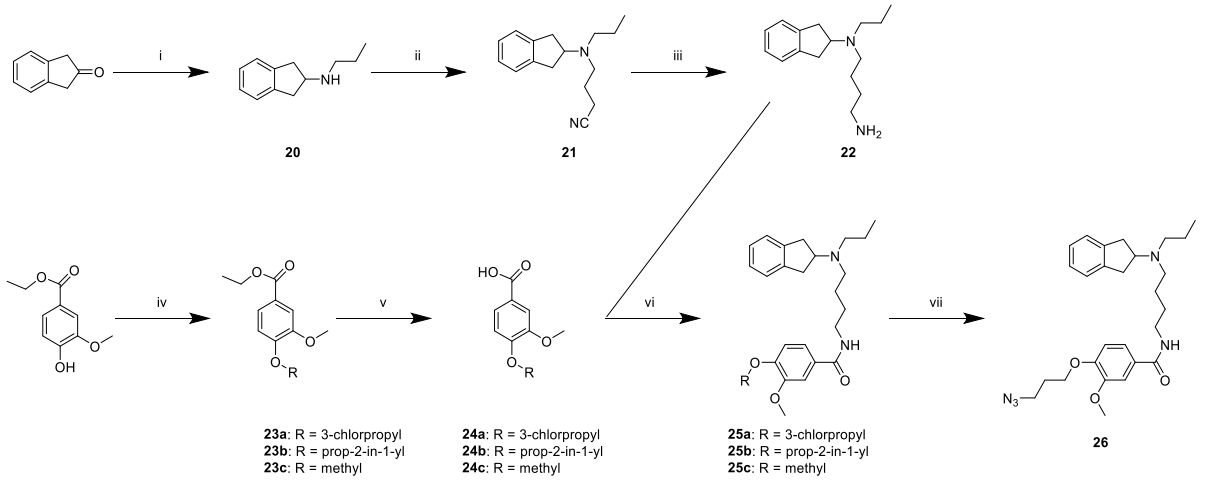

[a]Reagents and conditions: (i) propanamine, $NaBH_3CN$, HOAc, DCM, rt, overnight (80%); (ii) bromobutyronitrile, K_2CO_3, KI, MeCN, reflux, 24 h (66%); (iii) $LiAlH_4$, THF, reflux, overnight (95%); (iv) 1-bromo-3-chloropropane or 3-bromoprop-1-yne, K_2CO_3, MeCN, reflux, 14 h (94-96%); (v) KOH, H_2O, MeOH, rt, overnight (86-88%); (vi) HATU, DIPEA, DMF, rt, overnight (80-82%); (vii) NaN_3, DMF, 70 °C, 16 h (97%).

3.1.1.5 Spiperone

The synthesis of the spiperone based precursor **37** was based on a publication by Pulido et al. with minor modifications (cf. **Scheme 3.5**).[203] In a first step intermediate **27** was synthesized from commercially available aniline and *N*-benzylpiperidin-4-one in the presence of HOAc and TMSCN. Subsequently the formed nitrile moiety was converted into an amide function using concentrated sulfuric acid leading to compound **28**. Reaction with DMF·DMA in methanol resulted in cyclisation to obtain **29**. Reduction of the imidazolinone moiety with $NaBH_4$ led to **30**. Cleavage of the benzyl group with ammoniumformiate in presence of Pd/C yielded **31**. Subsequently, an alkylation with 4-chloro-1-(4-fluorophenyl)butan-1-one in the presence of KI was performed to get **32**. At the same time, 2-(4-aminophenyl)ethan-1-ol was Boc-protected to deliver **33** followed by a bromination with NBS to obtain **34**. Compound **35** was synthesized by *N*-alkylation of **32** with **34** in the presence of KOH and TBAB in toluene. TFA in DCM was used for deprotection of the aniline group to yield **36**. For the last step the resulting aniline function was reacted with succinic anhydride to generate a free carboxylic acid which was then coupled to propargylamine in the presence of HATU and DIPEA for the synthesis of precursor **37**. The monovalent compound **38** was obtained by acetylation of **36** with acetyl chloride in the presence of triethylamine.

Scheme 3.5: Synthesis of spiperone derivatives **37** and **38**[a]

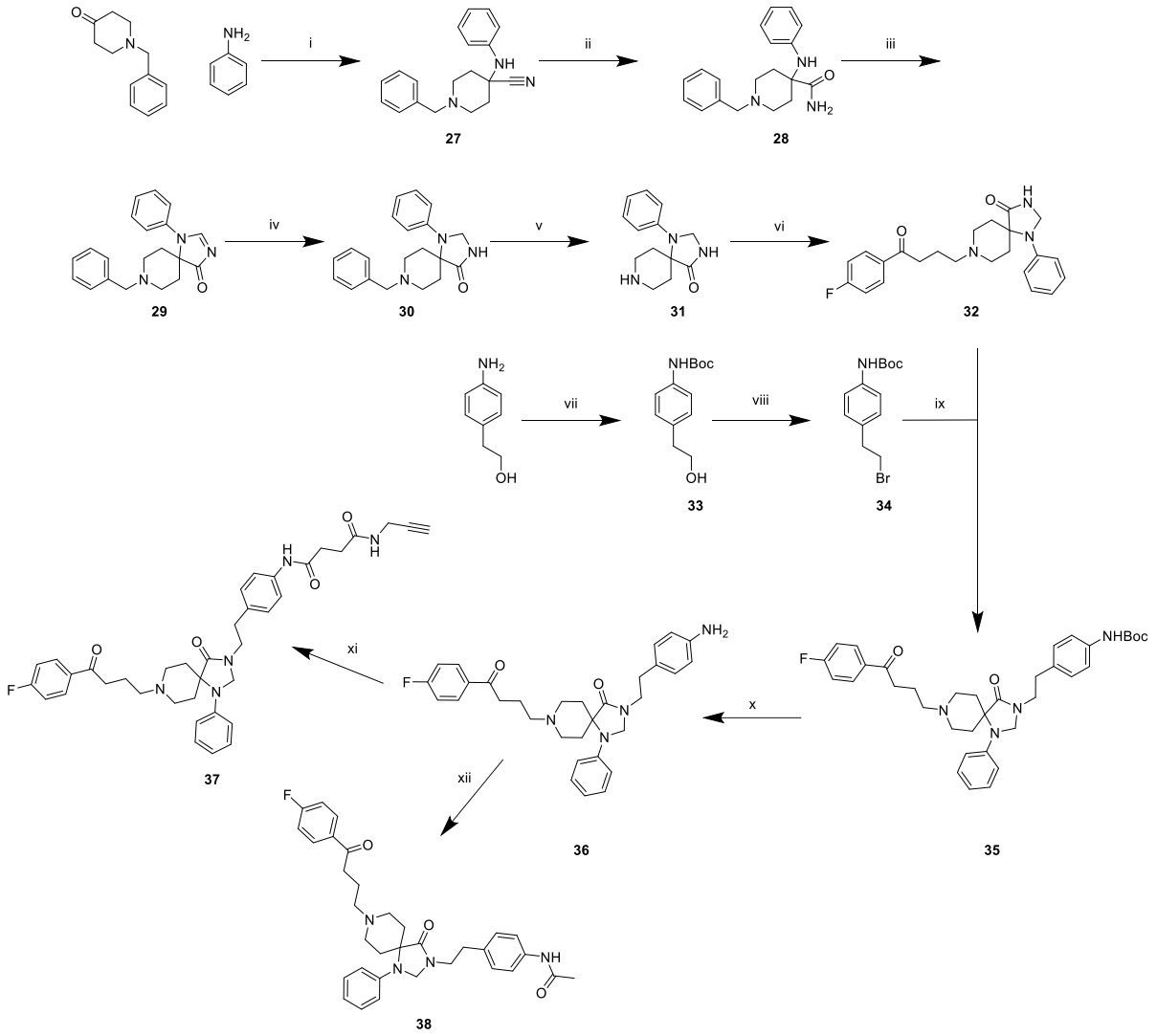

[a]Reagents and conditions: (i) TMSCN, HOAc, rt, 4 h (99%); (ii) H_2SO_4, rt, 18 h (94%); (iii) DMF-DMA, MeOH, 55 °C, 16 h (75%); (iv) $NaBH_4$, MeOH, rt, 4 h (70%); (v) ammoniumformiate, Pd/C, MeOH, 55 °C, 10 h (97%); (vi) 4-chloro-1-(4-fluorophenyl)butan-1-one, Et_3N, NaI, MeCN, reflux, 24 h (55%); (vii) di-tert-butyl dicarbonate, AcOEt, rt, 16 h (86%); (viii) NBS, PPh_3, DCM, 0 °C, 3 h (88%); (ix) KOH, TBAB, K_2CO_3, toluene, 90 °C, 48 h (35%); (x) TFA/DCM 1:4, rt, overnight (83%); (xi) succinic anhydride, propargylamine, HATU, DIPEA, DMF, rt, overnight (61%); (xii) acetyl chloride, Et_3N, DCM, rt, overnight (26%).

3.1.2 Precursors for the H_3R

The synthesis of the histamine precursor was performed according to a publication by Apodaca et al. in a slightly modified version (cf. **Scheme 3.6a**).[211] The commercially available 4-hydroxybenzaldehyde was converted into **39** in a nucleophilic substitution reaction with 1-bromo-3-chloropropane. In the next step, piperidine was introduced yielding the corresponding aldehyde **40**. Subsequently, a reductive amination with ethyl isonipecotate and $NaBH(OAc)_3$ in chloroform was performed to obtain **41**. Ester hydrolysis in aqueous HCl (2 N)

delivered the free acid **42**. In the final step **42** was coupled with propargylamine using EDC/HOBt under microwave irradiation to afford **43**.

Scheme 3.6a: Synthesis of JNJ-5207852 derivative **43**[a]

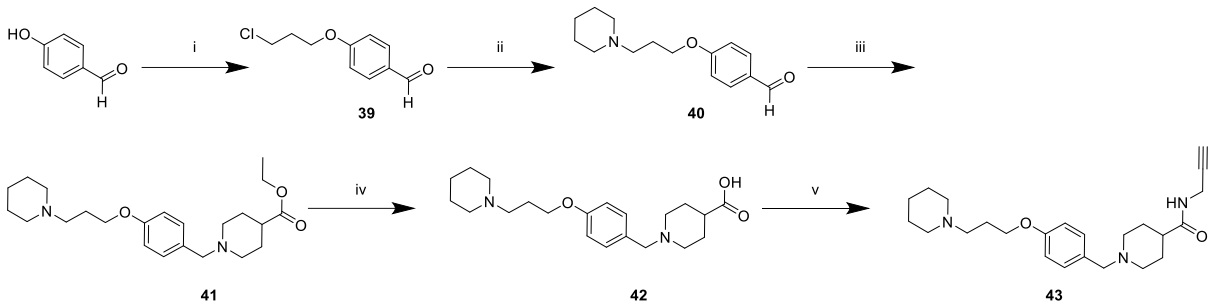

[a]Reagents and conditions: (i) 1-bromo-3-chloropropane, K_2CO_3, MeCN, reflux, 14 h (85%); (ii) piperidine, Na_2CO_3, NaI, n-butanol, 105 °C, 20 h (88%); (iii) ethyl piperidine-4-carboxylate, $NaBH(OAc)_3$, DCM, rt, 14 h (86%); (iv) 2 N HCl, THF, rt, overnight (91%); (v) propargylamine, EDC, HOBt, DIPEA, microwave 100 °C, 30 min (40%).

The histamine precursor for the smallest bivalent compounds was slightly differently synthesized as predicted in **Scheme 3.6b**. Compounds **44**-**47** were synthesized as described by Yakukhnov et al.[212] Reaction of *N*-benzylpiperidin-4-one with hydroxylamine in ethanol yielded oxime **44** which was reduced with $LiAlH_4$ to obtain the primary amine **45**.

Scheme 3.6b: Synthesis of JNJ-5207852 derivative **51**[a]

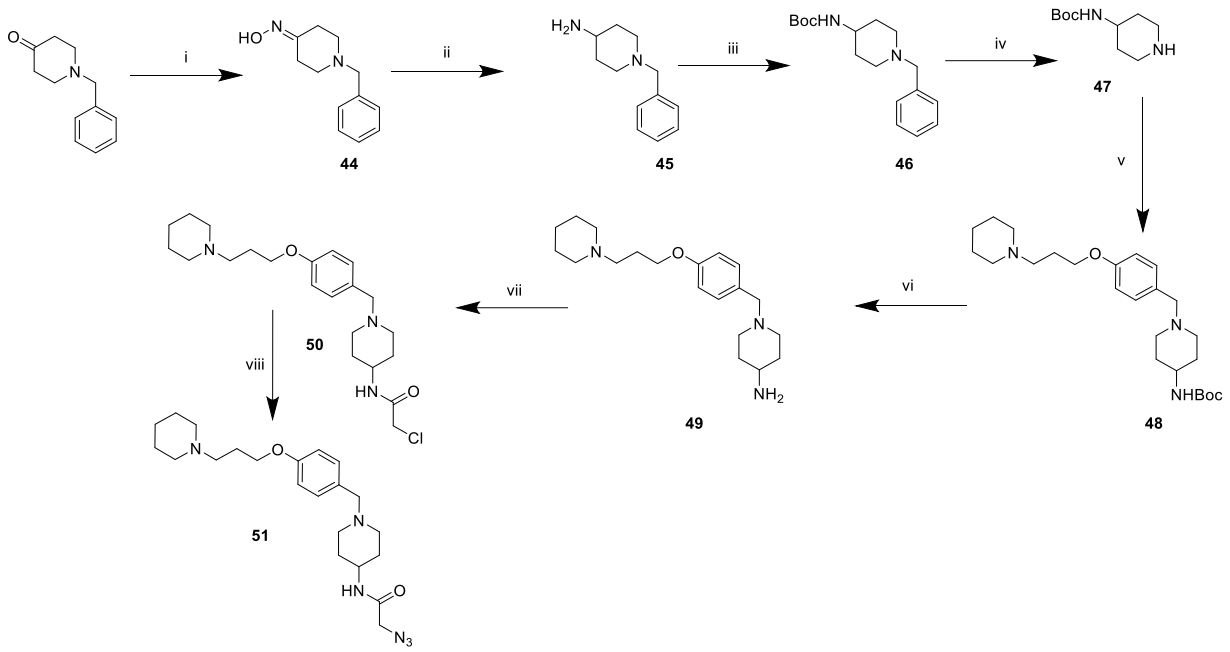

[a]Reagents and conditions: (i) hydroxylamine hydrochloride, K_2CO_3, EtOH, reflux, 3 h (86%); (ii) $LiAlH_4$, THF, reflux, 16 h (84%); (iii) di-tert-butyl dicarbonate, Et_3N, DCM, rt, 12 h (91%); (iv) H_2, Pd/C, MeOH, 70 °C, 16 h (97%); (v) **39**, $NaBH(OAc)_3$, DCM, rt, overnight (72%); (vi) TFA/DCM 1:4 (73%); (vii) 2-chloroacetyl chloride, Et_3N, DCM, rt, 5 h (82%); (viii) NaN_3, DMF, 75 °C, 15 h (quant.).

Boc protection to yield **46** was followed by cleavage of the benzylgroup in H_2 atmosphere with Pd/C as catalyst to acquire **47**. Subsequent reductive amination of **40** with **47** using $NaBH(OAc)_3$ in chloroform yielded **48**, followed by boc deprotection to obtain the primary amine **49**. Addition of 2-chloroacetly chloride delivered **50** which was converted into **51** by azide exchange in DMF.

3.1.3 Linker structures

One of the main goals of this work was to find out how different linker length and orientation can influence a possible bivalent binding mode. Hence, a great variety of linkers differing in size or central dicarbonic acid were synthesized. According to docking studies performed in the group of Prof. Pardo in Barcelona, 50 atoms was the most appropriate length which is why special focus was put on this particular size. Linkers were synthesized from commercially available diamines and dicarbonic acids. Only central dicarbonic acid **55** was synthesized separately (cf. **Scheme 3.7**). Therefore, isopthtalic acid was esterified into **52**. Alkaline hydrolysis yielded **53** which was then connected by 3,3'-((oxybis(ethane-2,1-diyl))bis(oxy))bis-propan-1-amine to deliver intermediate **54**. **55** was obtained by subsequent saponification.

Scheme 3.7: Synthesis of dicarbonic acid **55**[a]

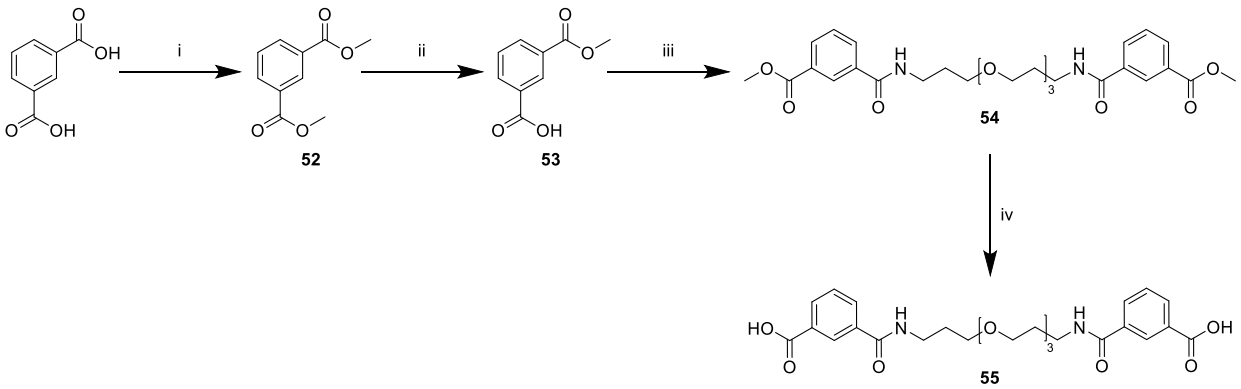

[a]Reagents and conditions: (i) MeOH, H_2SO_4, 14 h, reflux (94%); (ii) KOH, H_2O, MeOH, 10 h, rt (50%); (iii) (1) $SOCl_2$, DMF, 65 °C, 5 h (quant.); (2) 3,3'-((oxybis(ethane-2,1-diyl))bis(oxy))bis(propan-1-amine), Et_3N, DCM, 11 h, rt (99%); (iv) KOH, MeOH, 14 h, rt (95%).

Final linker synthesis is depicted in **Scheme 3.8**. Mono Boc protection of 3,3'-(ethane-1,2-diylbis(oxy))bis-propan-1-amine and 3,3'-((oxybis(ethane-2,1-diyl))bis(oxy))bis-propan-1-amine yielded **56** and **57** which were connected to the corresponding diacyl chloride or dicarbonic acid to obtain **58a-e**. Boc deprotection of **58a-e** with TFA in DCM afforded **59a-e**. Subsequently, 2-chloroacetyl chloride was added to yield intermediates **60a-e**. In the last step

azide functions were introduced using NaN_3 in DMF to obtain final linker structures **61a-e**. For the shortest, most rigid linker terephthalic acid was converted into the acyl chloride **62** and then coupled to propargylamine in the presence of triethylamine to obtain **63**.

Scheme 3.8: Synthesis of linker **61a-e** and **63**[a]

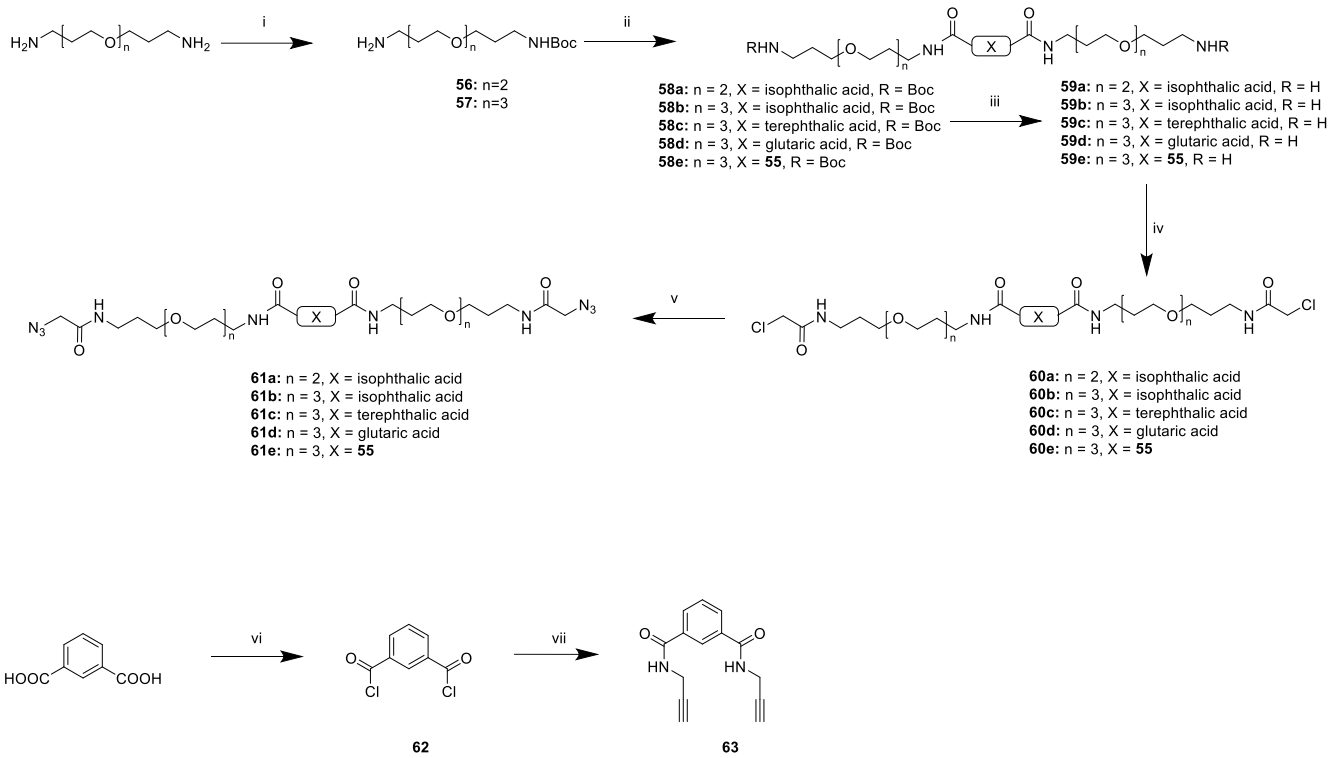

[a]Reagents and conditions: (i) di-tert-butyl dicarbonate, Et_3N, DCM, rt, 5 h; (ii) (1) respective acyl chloride, Et_3N, DCM, rt, 6 h (56-87%) or (2) **55**, HATU, DIPEA, DMF, rt, overnight (91%); (iii) TFA/DCM 1:4, 14 h, rt, (67-93%); (iv) 2-chloroacetyl chloride, Et_3N, DCM, rt, 10 h (75-91%); (v) NaN_3, DMF, 70 °C, overnight (82-91%); (vi) $SOCl_2$, DMF, 65 °C, 5 h (quant.); (vii) propargylamine, Et_3N, DCM, rt, overnight (95%).

3.1.4 Precursor for endcapped ligands

To further investigate a possible bivalent binding mode endcapped ligands containing only one pharmacophore were synthesized. These compounds should verify that the bivalent binding mode is indeed caused by the simultaneous binding of both pharmacophores and not by one pharmacophore itself. For the synthesis of these compounds propargylamine was acetylated with acetyl chloride (cf. **Scheme 3.9**).

Scheme 3.9: Synthesis of precursor **64**[a]

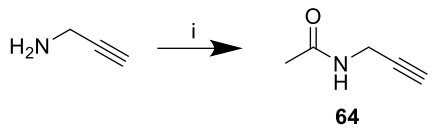

[a]Reagents and conditions: (i) acetyl chloride, Et_3N, DCM, rt, overnight (94%).

3.1.5 Final bivalent compounds

After several different attempts failed to add the respective pharmacophores selectively to the linker the final bivalent compounds were synthesized in a one-pot copper-catalyzed click reaction (CuAAC) (cf. **Scheme 3.10**). Therefore, equimolar amounts of each precursor, the linker, catalytic amounts of $CuSO_4{\cdot}5H_2O$ and ascorbic acid were stirred at room temperature for 72 h. Purification with preparative HPLC yielded homobivalent ligands as side products and the desired heterobivalent ligands as final compounds.

Scheme 3.10: Synthesis of linker structures[a]

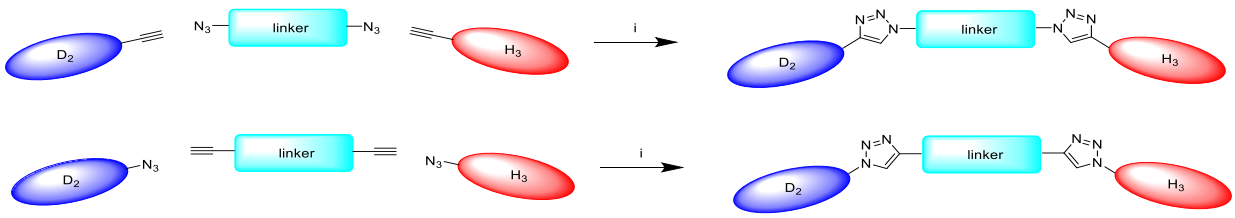

[a]Reagents and conditions: (i) $CuSO_4{\cdot}5H_2O$, ascorbic acid, DCM/MeOH 4:1, rt, 72 h.

Precursors based on L-471,626 were used for the synthesis of twelve bivalent compounds (**65-76**) and two monovalent compounds (**6a and 6b**). Because of facile synthesis and high yields of the derivatives **4a**, **4b**, **5a**, and **5b** a broad spectrum of bivalent compounds with different linker length or orientation was synthesized. Since preliminary pharmacological results were not satisfactory the synthesis of an endcapped compound to further investigate a possible bivalent binding mode was dispensed. 1,4-DAP-based precursor was used for the synthesis of three bivalent compounds (**84-86**) and the monovalent compound **11a**. As early pharmacological characterization indicated that these ligands did not show any particular increase of affinity compared to ligands **65-76** further synthesis of compounds with different lengths/orientations or monovalent compounds was neglected. *N*-propylaminoindane based precursors were used for the synthesis of six bivalent (**77–82**), one endcapped (**83**), and one

monovalent compound (**25c**). Preliminary pharmacological characterization showed improved binding affinities with this precursor which is why a broader set of compounds was synthesized. As compound **80** was the most interesting compound for further testing in co-expressing systems an endcapped ligand was also synthesized. OH-DPAT based precursor was used for the synthesis of one bivalent (**92**) and its corresponding endcapped ligand (**93**). Due to synthetic reasons and to the results form docking studies only these two compounds were synthesized. Since no pronounced improvement compared to *N*-propylaminoindane based ligands was achieved the synthesis of further compounds with shorter/longer linkers or different linker orientations was dispensed to save resources. Spiperone-based precursor was used for the synthesis of four bivalent (**87**-**90**), one monovalent (**38**), and one endcapped ligand (**91**). Since compound **90** was the most promising candidate for further testing in co-expressing systems its corresponding endcapped ligand **91** was also synthesized. Due to synthetic reasons and to the results from docking studies only these five compounds were made. Further compounds with the shortest and the longest linker were let of to save resources. Synthesized final compounds are summarized in **Figure 3.1** and **Table 3.1**.

Central parts for derivatives of linker structure L2, marked as X

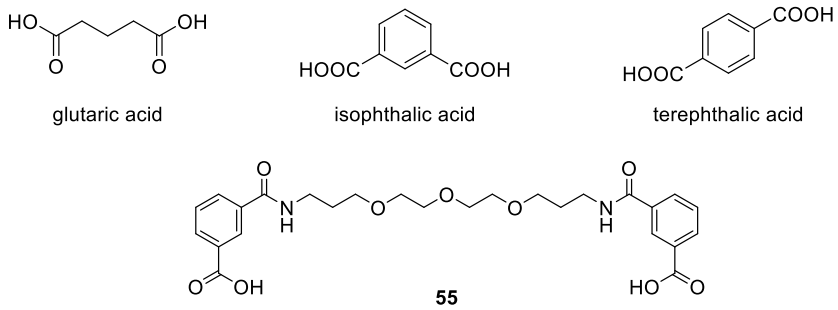

Designed linker structures

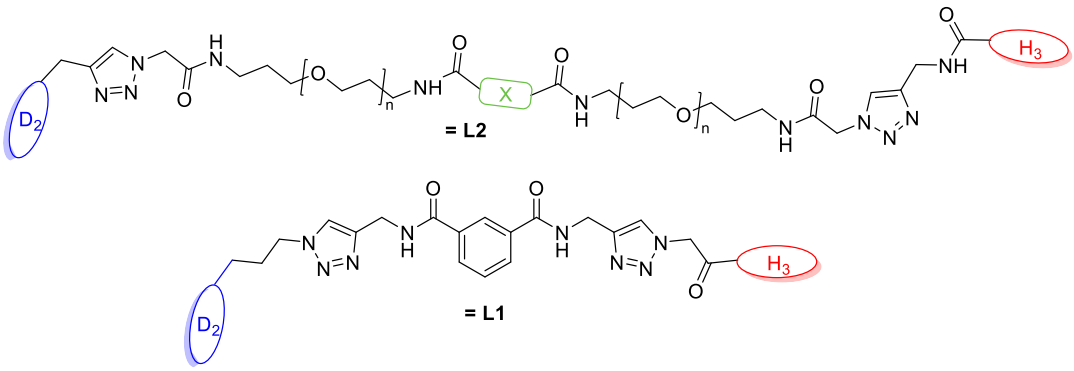

Selected pharmacophores for the D_2R (blue) or the H_3R (red)

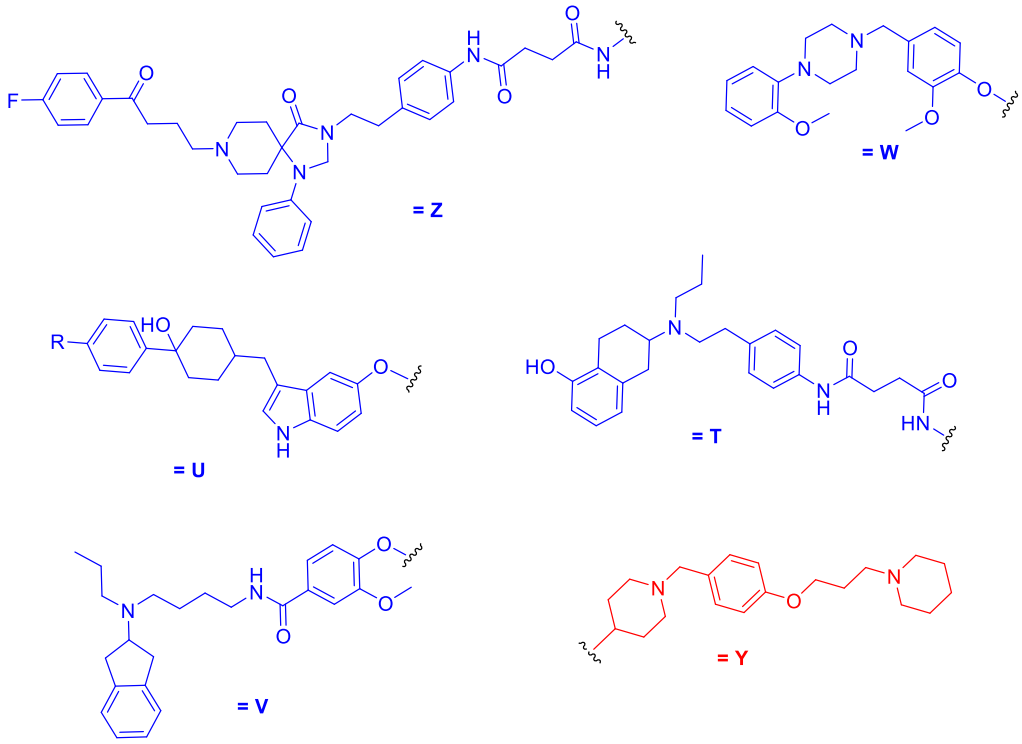

Figure 3.1: Structural design of synthesized compounds.

Table 3.1: Overview of synthesized bivalent and endcapped compounds.

No.	D_2	Linker	X	H_3	Type
65	U, R = Cl	L1		Y	bivalent
66	U, R = Cl	L2, n = 2	isopthalic acid	Y	bivalent
67	U, R = Cl	L2, n = 3	isopthalic acid	Y	bivalent
68	U, R = Cl	L2, n = 3	terephthalic acid	Y	bivalent
69	U, R = Cl	L2, n = 3	glutaric acid	Y	bivalent
70	U, R = Cl	L2, n = 3	**55**	Y	bivalent
71	U, R = Br	L1		Y	bivalent
72	U, R = Br	L2, n = 2	isopthalic acid	Y	bivalent
73	U, R = Br	L2, n = 3	isopthalic acid	Y	bivalent
74	U, R = Br	L2, n = 3	terephthalic acid	Y	bivalent
75	U, R = Br	L2, n = 3	glutaric acid	Y	bivalent
76	U, R = Br	L2, n = 3	**55**	Y	bivalent
77	V	L1		Y	bivalent
78	V	L2, n = 2	isopthalic acid	Y	bivalent
79	V	L2, n = 3	isopthalic acid	Y	bivalent
80	V	L2, n = 3	terephthalic acid	Y	bivalent
81	V	L2, n = 3	glutaric acid	Y	bivalent
82	V	L2, n = 3	**55**	Y	bivalent
83	V	L2, n = 3	terephthalic acid	CH_3	endcapped
84	W	L2, n = 3	isopthalic acid	Y	bivalent
85	W	L2, n = 3	terephthalic acid	Y	bivalent
86	W	L2, n = 3	glutaric acid	Y	bivalent
87	Z	L2, n = 2	isopthalic acid	Y	bivalent
88	Z	L2, n = 3	isopthalic acid	Y	bivalent
89	Z	L2, n = 3	terephthalic acid	Y	bivalent
90	Z	L2, n = 3	glutaric acid	Y	bivalent
91	Z	L2, n = 3	glutaric acid	CH_3	endcapped
92	T	L2, n = 3	glutaric acid	Y	bivalent
93	T	L2, n = 3	glutaric acid	CH_3	endcapped
94	CH_3	L2, n = 3	terephthalic acid	Y	endcapped
95	CH_3	L2, n = 3	glutaric acid	Y	endcapped

3.2 Biological evaluation

3.2.1 Radioligand binding assay to determine binding affinities

Binding affinities of synthesized compounds were determined in radioligand binding assays which is a well-established method in medicinal chemistry. The principle of these assays is the competition between increasing amounts of an unlabeled ligand and a constant amount of a radioactively marked tracer. Displacement of the tracer leads to lower detection of radioactivity within the cells which gives information about the affinity of the tested compound towards the desired receptor.

Evaluation of binding affinities of the final compounds for the D_2R and the H_3R was performed with competition assays. Affinities of all compounds were measured by the displacement of [^{3}H]*N*-methylspiperone from the D_2R stably expressed in homogenates of HEK293T cells or by displacement of [^{3}H]UR-PI294 in living HEK293T cells stably expressing the H_3R (cf. **Table 3.2** and **Figure 3.2**).

Ligands **65**-**76** based on L-471,626 exhibited moderate affinities for the D_2R with pK_i values from 6.47 to 7.45. It could be observed that bromine as halogen substituent in the phenyl ring was better tolerated than chlorine for all compounds. Additionally, terephthalic acid as center part of the linker structures resulted in the highest affinities with this D_2R scaffold while glutaric acid was least favorable showing that a certain amount of rigidity within the ligands was beneficial for binding to the D_2R. Unfortunately, all ligands showed a noticeable loss of affinity of one order of magnitude compared to their monovalent control compounds **6a** and **6b**. This indicates that the addition of the linker was not well tolerated and caused steric hindrance leading to lower affinities. All pK_i values for the H_3R were exceptionally high ranging from 9.05 to 10.19 indicating that the attachment point was well chosen since no loss of affinity compared to the parent structure JNJ-5207852 was observed. Concerning the choice of the central dicarbonic acid, glutaric acid delivered the best results indicating that a maximum amount of flexibility was beneficial for binding to the H_3R, followed by terephthalic acid. For both receptors it could be observed that compounds **70** and **76** containing the longest linker showed the lowest affinities.

Compounds **84**-**86** based on 1,4-DAP possessed slightly higher pK_i values for the D_2R and a better tolerance concerning the addition of the linker as monovalent ligand **11a** showed

comparable results. Affinities for all bivalent ligands and the monovalent control compound were in the range of 7.0 to 7.5 showing that the attachment point was well chosen. Once again terephthalic acid was the best choice for the synthesis of the linker as ligand **85** showed the highest affinity for the D_2R. Affinities for the H_3R were once again very high with pK_i values ranging from 9.52 to 9.73. Within this set of ligands only a marginal difference concerning the H_3R affinity was detected.

Ligands **77**–**83** based on the *N*-propylaminoindane moiety showed slight improvements concerning binding towards the D_2R. Affinities were in the range of the monovalent compound **25c** with a pK_i of 7.19 showing the suitability of the selected attachment point. Compound **77** with the shortest, most rigid linker and compound **80** with terepthtalic acid as central part showed the highest affinities with pK_i of 7.72 and 7.96, respectively. H_3R affinities were slightly lower than for the previously described compounds yet still very high ranging from 9.17 to 9.69. As described before elongation of the linker was not beneficial for binding as **82** demonstrated a pronounced loss of pK_i values for both receptors. Compound **80** showed the best results as pK_i values of 7.96 for the D_2R and 9.69 for H_3R were detected which is why this compound was selected for further testing. Additionally, the respective endcapped ligands **83** and **94** were tested and showed notably lower affinities compared to **80**, which was unexpected. A possible reason could be some kind of interaction with cell membranes.

OH-DPAT based bivalent ligand **92** showed comparable results to **80** with affinities of 7.78 for D_2R and 9.24 for the H_3R. As seen before, the endcapped ligand **93** exhibited a lower pK_i value compared to its bivalent counterpart **92** which is probably caused by the same reasons as described before.

Spiperone-based ligands **87**-**91** exhibited a pronounced increase of affinities for the D_2R with pK_i values from 9.02 to 10.03. Compared to monovalent compound **38** the bivalent compounds **87**, **88**, and **91** as well as the endcapped ligand **93** showed a loss of nearly one order of magnitude. In contrast, ligand **90** which features glutaric acid in the center tolerated the addition of the linker much better and displayed a pK_i value of 9.58 for the D_2R. Following the tendencies observed before the endcapped ligand **91** showed a lower affinity than its corresponding bivalent compound. Affinities for the H_3R were expectedly very high ranging from 9.59 to 9.83 showing once again only little influence of the selected linker structure.

All these results highlight compound **90** as the best structure with subnanomolar affinities for both receptors (pK_i D_2R: 9.58 and pK_i H_3R: 9.83).

Table 3.2: Binding affinities of tested compounds.[c]

	pK_i ± SEM			
No.	D_2R^a	N	H_3R^b	N
6a	8.01 ± 0.05	3	n.d.	-
65	7.08 ± 0.03	3	9.43 ± 0.01	3
66	6.95 ± 0.02	3	9.48 ± 0.13	3
67	6.83 ± 0.01	3	9.59 ± 0.06	3
68	7.09 ± 0.04	3	9.83 ± 0.06	3
69	6.68 ± 0.06	3	10.19 ± 0.09	3
70	6.47 ± 0.07	3	9.27 ± 0.06	3
6b	8.58 ± 0.08	3	n.d.	-
71	7.45 ± 0.05	3	9.48 ± 0.60	3
72	7.20 ± 0.07	3	9.72 ± 0.01	3
73	7.18 ± 0.04	3	9.47 ± 0.09	3
74	7.33 ± 0.05	3	9.62 ± 0.05	3
75	6.87 ± 0.03	3	9.94 ± 0.08	3
76	6.81 ± 0.08	3	9.05 ± 0.10	3
25c	7.19 ± 0.07	3	n.d.	-
77	7.72 ± 0.10	3	9.47 ± 0.06	3
78	7.30 ± 0.06	3	9.26 ± 0.04	3
79	7.33 ± 0.09	3	9.17 ± 0.12	3
80	7.96 ± 0.06	3	9.69 ± 0.07	3
81	6.87 ± 0.05	3	9.62 ± 0.05	3
82	7.14 ± 0.05	3	9.20 ± 0.12	3
83	6.43 ± 0.10	3	n.d.	-
11a	7.10 ± 0.08	3	n.d.	-
84	7.06 ± 0.05	3	9.73 ± 0.02	3
85	7.34 ± 0.08	3	9.51 ± 0.09	3
86	7.23 ± 0.09	3	9.52 ± 0.09	3

(continued)

38	10.03 ± 0.07	3	n.d.	-
87	9.12 ± 0.02	3	9.82 ± 0.01	3
88	9.15 ± 0.02	3	9.59 ± 0.04	3
89	9.15 ± 0.02	3	9.63 ± 0.02	3
90	9.58 ± 0.04	3	9.83 ± 0.05	3
91	9.02 ± 0.03	3	n.d.	-
92	7.78 ± 0.10	4	9.24 ± 0.14	3
93	7.30 ± 0.09	4	n.d.	-
JNJ-5207852	n.d.	-	9.2[211]	3
94	< 5	3	9.30 ± 0.04	3
95	< 5	3	9.62 ± 0.11	3

[a]Determined by competition binding at homogenates of HEK293T cells stably expressing the D_2R using [^{3}H]*N*-methylspiperone (K_d = 14.4 pM and c = 50 pM). [b]Determined by competition binding at HEK293-SP-FLAG-hH_3R cells using [^{3}H]UR-PI294 (K_d = 3 nM and c = 4 nM). [c]Data represent mean values ± SEM of at least three independent experiments each performed in triplicate.

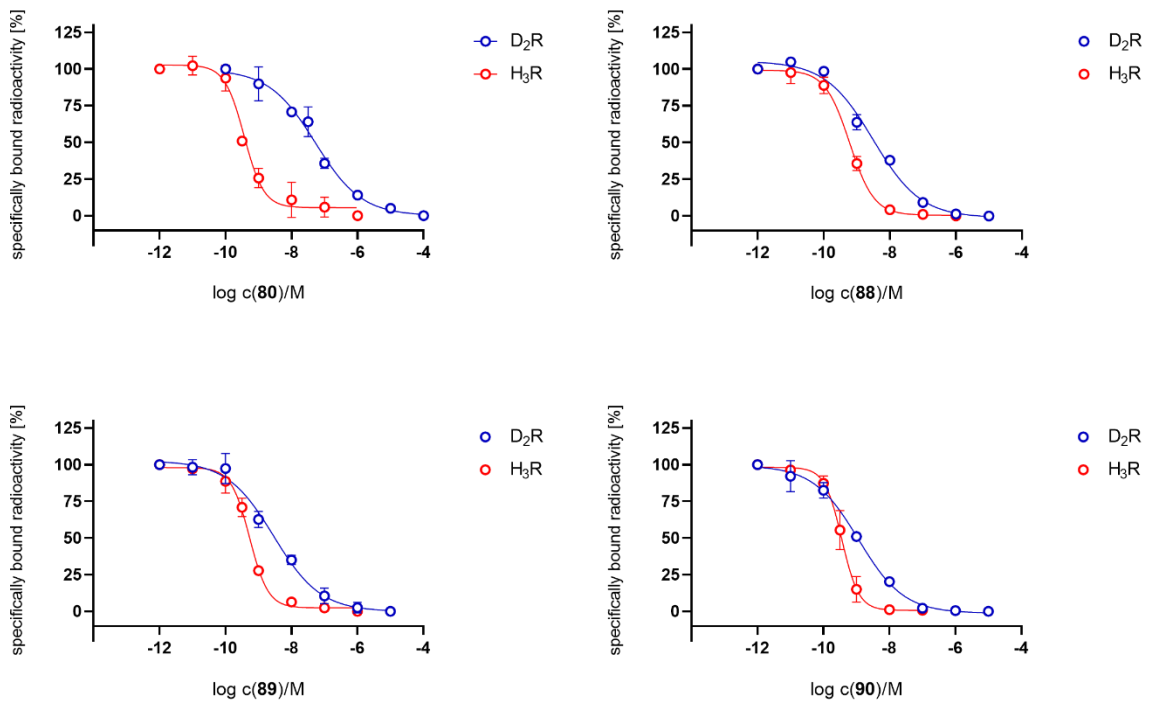

Figure 3.2: Displacement curves of selected compounds **80**, **88**, **89**, and **90** from radioligand competition binding experiments performed at the D_2R and H_3R. Data represent mean values ± SEM from at least three independent experiments, each performed in triplicate.

Additionally, selected compounds **80**, **84**, **90**, and **92** were tested for their selectivity among the histamine and dopamine receptor families to find out whether addition of the linker or the second pharmacophore changed the binding behavior among the respective receptor families.

All compounds displayed exceptional selectivity for the H_3R which was no surprise given the fact that such a pharmacological profile has also been described for the parent scaffold JNJ-5207852.[211] All compounds showed more than 10000-fold preference for the H_3R which makes them ideal candidates to target the D_2-H_3 heteromer selectively (cf. **Table 3.3**, **Figure 3.3**).

Table 3.3: Selectivity profile of bivalent ligands **90** and **92** within the histamine receptor family.[a]

	pK_i ± SEM				H_3R selectivity
No.	H_1R^b	H_2R^c	H_3R^d	H_4R^e	K_i ($H_{1,2,4}R$) / K_i (H_3R)
90	< 5	< 5	9.83 ± 0.05	< 5	> 10000
92	< 5	< 5	9.24 ± 0.14	< 5	> 10000

[a]Competition binding assay at HEK293-SP-FLAG-hH1R, HEK293-SP-FLAG-hH2R, HEK293-SP-FLAG-hH3R,or HEK293-SP-FLAG-hH4 R cells. [b]Displacement of 5 nM [^{3}H]mepyramine (K_d = 4.5 nM). [c]Displacement of 50 nM [^{3}H]UR-DE257 (K_d = 66.9 nM). [d]Displacement of 4 nM [^{3}H]UR-PI294 (K_d = 5nM). [e]Displacement of 15 nM [^{3}H]histamine (K_d = 15.88 nM). Data represent mean values ± SEM from three independent experiments each performed in triplicate.

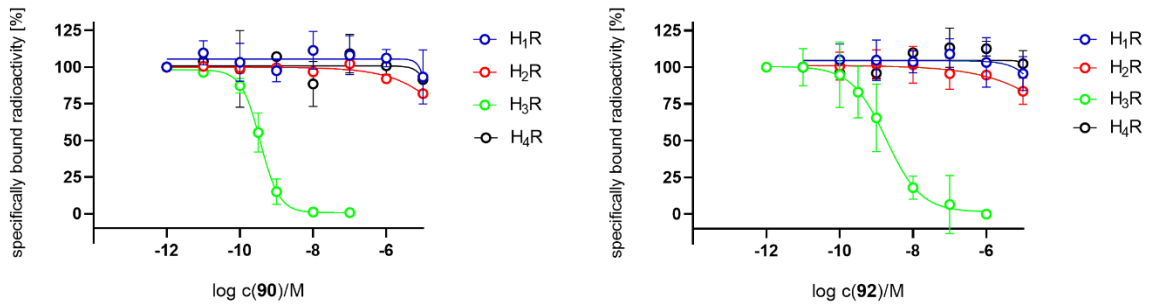

Figure 3.3: Displacement curves from radioligand competition binding experiments performed with **90** or **92** and the respective radioligand. Data represent mean values ± SEM from three independent experiments each performed in triplicate.

Among the dopamine receptors selectivities were not as distinct as for the H_3R. As expected, most of the selected compounds displayed no to little affinities for the D_1-like receptors. Only compound **90** showed moderate affinity towards the D_1R with a pK_i value of 7.17 which still results in 250-fold selectivity towards the D_2R. Concerning the D_2-like receptors compounds **90** and **92** showed a pronounced loss of affinity for the D_4R leading to approx. 10-fold preference for the D_2R. Unsurprisingly, only little to no selectivity was observed for the D_3R. Both receptors share 46% amino acid homology (overall) and 78% identity in the transmembrane region which has caused problems to target one of the receptors selectively ever since.[213] As a result none of the compounds possessed a pleasant selectivity profile for the D_2R. While compounds **84** and **90** displayed almost identical affinities for both receptors **80** and **92** even showed a slight preference for the D_3R (cf. **Table 3.4** and **Figure 3.4**).

Table 3.4: Selectivity profile of bivalent ligands **80**, **84**, **90**, and **92** within the dopamine receptor family.[a]

	pK_i ± SEM				
No.	D_1R^b	D_2R^c	D_3R^d	D_4R^e	D_5R^f
80	< 5.5	7.96 ± 0.06	8.88 ± 0.12	n.d.	< 5.5
84	< 5.5	7.06 ± 0.05	6.99 ± 0.06	n.d.	< 5.5
90	7.17 ± 0.04	9.58 ± 0.04	9.47 ± 0.07	8.47 ± 0.08	6.22 ± 0.08
92	5.94 ± 0.04	7.78 ± 0.10	8.42 ± 0.05	6.47 ± 0.23	6.46 ± 0.07

[a]Determined by competition binding at homogenates of HEK293T cells stably expressing the D_xR. [b]Displacement of 1 nM [^{3}H]SCH-23390 (K_d = 0.4 nM). [c]Displacement of 50 pM [^{3}H]*N*-methylspiperone (K_d = 14.4 pM). [d]Displacement of 50 pM [^{3}H]*N*-methylspiperone (K_d= 25 pM). [e]Displacement of 100 pM [^{3}H]*N*-methylspiperone (K_d = 77 pM). [f]Displacement of 1 nM [^{3}H]SCH-23390 (K_d = 0.4 nM). Data represent mean values ± SEM from three independent experiments each performed in triplicate.

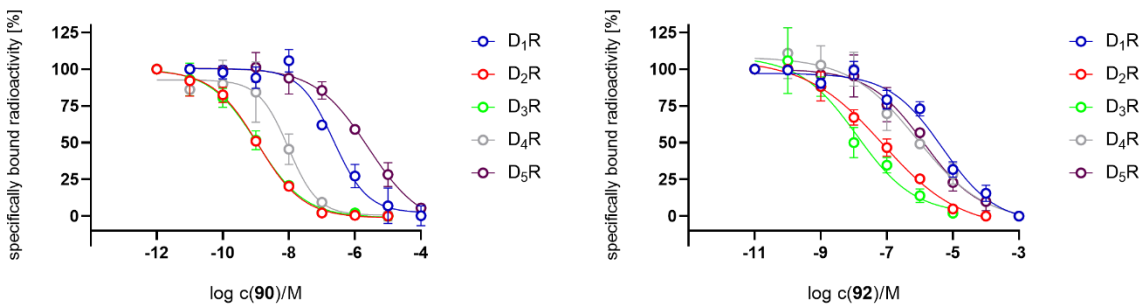

Figure 3.4: Displacement curves from radioligand competition binding experiments performed with **90** or **92** and the respective radioligand. Data represent mean values ± SEM from three independent experiments each performed in triplicate.

3.2.2 cAMP assay to determine pharmacological mode of action

Selected compounds were also tested for their functional characteristics. Sometimes the addition of large and bulky structures to certain parts of a pharmacophore can change the mode of action of the respective molecule. This phenomenon mainly affects agonists which are then turned into antagonists and has already been described, e.g for immepip at the H_3R or morphine at the μ-opioid receptor.[47,122] Based on the results obtained from radioligand binding assays the most interesting compounds were chosen and tested for their ability to inhibit or induce G protein-dependent signaling. For this purpose, the LANCE Ultra cAMP Kit from Perkin Elmer was purchased. This immunoassay uses time-resolved fluorescence resonance energy transfer (TR-FRET) and gives us the opportunity to measure cAMP produced upon modulation of adenylyl cyclase activity by GPCRs. The principle of the assay depends on the competition between a europium (Eu) chelate-labeled cAMP tracer and cellularly (endogenously) produced cAMP for binding sites on cAMP-specific monoclonal antibodies labeled with the U*Light*™ dye. Upon binding of the antibodies to the Eu-labeled cAMP tracer, light pulse at 320 or 340 nm excites the Eu chelate molecule of the tracer. FRET transfers the energy emitted by the excited Eu chelate to U*Light* molecules on the antibodies which then on their part emit light at 665 nm (cf. **Figure 3.5**).

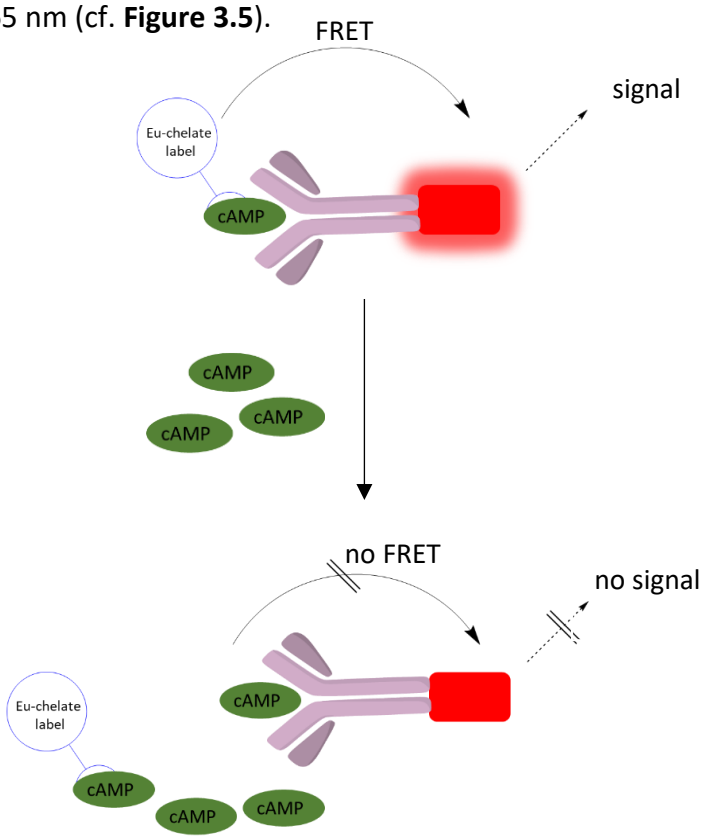

Figure 3.5: Schematic illustration of the cAMP assay principle.

3.2.2.1 Monoexpressing systems

Since both the D_2R and the H_3R are $G\alpha_{i/o}$ coupled no direct impact on G protein-dependent signaling could be measured. Instead, forskolin (0.5 µM) as activator of AC was added to induce intrinsic production of cAMP. Increasing concentrations of D_2R agonists activate the receptor which leads to the inhibition of AC resulting in lower cAMP concentrations and therefore higher detectable signals. To measure the effect of antagonists an addition of standard agonists (sumanirole 250 nM for the D_2R; imetit 500 nM for the H_3R) was necessary. As a result of displacement of the agonist by increasing concentrations of the tested antagonists the inhibition of AC is blocked resulting in higher cAMP concentrations and therefore lower detectable signals. All synthesized compounds maintained the pharmacological profile described for their respective precursor for both receptors (cf. **Table 3.5** and **Figure 3.6**). Ligands based on the *N*-propylaminoindane and 5-OH-DPAT scaffolds acted as D_2R agonists while compounds containing the spiperone structure displayed D_2R antagonism. All compounds acted as H_3R antagonists which was expected since all compounds derived from the same parent structure. For D_2R agonists, potencies (pEC_{50}) proved to be consistently slightly higher than their pK_i values but trends observed in radioligand binding assays were reflected. This phenomenon is common for cAMP assays with the D_2R and has already been described in the literature.[148] With efficacies (α) ranging from 95–99 % the tested compounds were identified as very strong partial agonists. All tested antagonists were able to fully inhibit the effect induced by sumanirole and showed pIC_{50} values that reflected trends observed in radioligand binding assays. Concerning the H_3R all compounds could entirely block the effect induced by imetit. Apart from compound **92**, which was more potent than expected, ligands **80**, **90**, and **95** confirmed tendencies observed in binding assays.

Table 3.5: Functional data of selected compounds.[a,b]

No.	pIC_{50} ± SEM or (pEC_{50} ± SEM)				
	D_2R	N	α [%] ± SEM	H_3R	N
80	(9.19 ± 0.08)	5	99 ± 7	7.80 ± 0.19	3
83	(7.38 ± 0.02)	2	99 ± 3	n.d.	-
88	6.77 ± 0.20	3	-	n.d.	-
89	6.85 ± 0.12	3	-	n.d.	-
90	7.14 ± 0.10	3	-	8.59 ± 0.08	3
91	6.50 ± 0.13	2	-	n.d.	-
92	(8.88 ± 0.27)	4	96 ± 5	8.84 ± 0.07	3
93	(8.37 ± 0.20)	4	95 ± 13	n.d.	-
95	n.d.	-	n.d.	7.97 ± 0.08	3

[a]Data represent mean values ± SEM of *N* independent experiments each performed in triplicate. α relative to the effect of the reference agonist sumanirole. [b]Tested using the experimental protocol described in the experimental section.

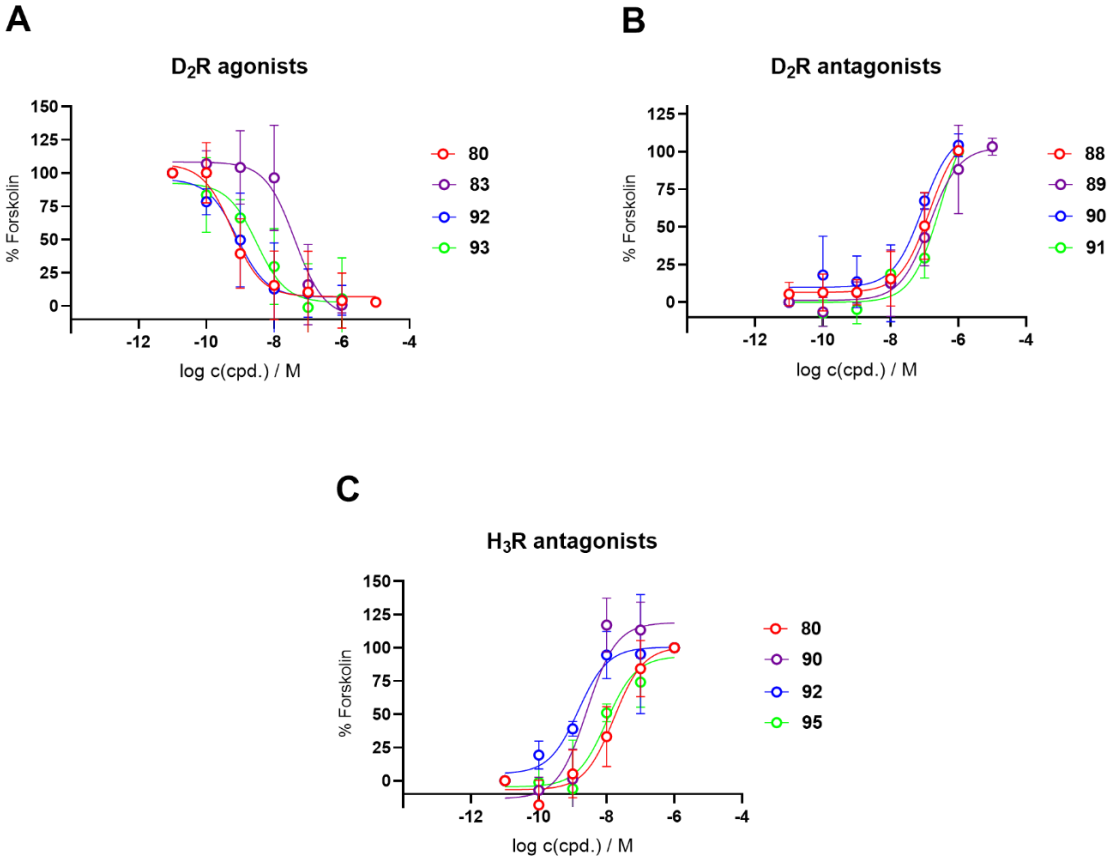

Figure 3.6: Dose response curves in HEK293T cells expressing the D_2R or H_3R. (**A**) Stimulation curves of selected D_2R agonists; (**B**) Inhibition curves of selected D_2R antagonists after activation with 250 nM sumanirole; (**C**) Inhibition curves of selected H_3R antagonistst after activation with 500 nM immetit.

3.2.2.2 Co-expressing systems

In a next step the effects of the selected agonists in cells that were transiently transfected with both receptors, the D_2R and the H_3R, should be investigated. Attempts to measure the effect induced by the dopaminergic pharmacophore were not successful since no effect was detectable, neither for selected agonistic compounds, nor for sumanirole as standard ligand (cf. **Figure 3.7**). Such a behaviour that one protomer within a dimer loses its activity has already been described.[214] According to Lohse the formation of a dimer can lead to changes in distance between the receptors and their subunits.[140] In this case, the minimal functional unit of a dimer consits of the two protomers and only one G protein which is why only one of the two receptors can be activated and signal to the G protein.[140] Accordingly, antagonists could not be tested over the dopaminergic pathway either.

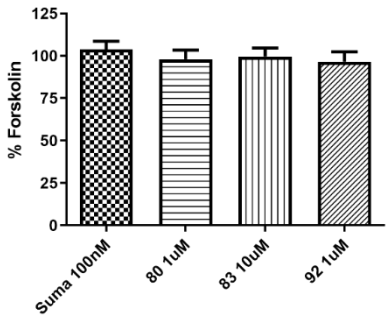

Figure 3.7: D_2R agonists in cells co-expressing the D_2R and H_3R with no detectable signal.

Therefore, we wanted to analyze the effect of our compounds on the histaminergic part of the receptor complex. All the tested ligands were able to fully block the signal induced by 500 nM imetit yet no significant difference in potencies compared to mono-expressing cells was detected (cf. **Table 3.6**).

Table 3.6: Comparison of functional data in mono- and coexpressing cells. [a,b]

	pIC_{50} ± SEM			
No.	H_3R	N	D_2-H_3	N
80	7.80 ± 0.19	3	7.88 ± 0.21	3
90	8.59 ± 0.08	3	8.31 ± 0.13	2
92	8.84 ± 0.07	3	8.63 ± 0.05	2
95	7.97 ± 0.08	3	8.28 ± 0.24	3

[a]Data represent mean values ± SEM of *N* independent experiments each performed in triplicate. [b]Tested using the experimental protocol described in the experimental section.

3.3 Conclusion

After a long-lasting belief that GPCRs only act separately as isolated entities clear evidence has emerged in recent years that they also have the ability to interact with each other by forming homo- or heteromers.[215] Ferrada et al. reported this formation of Hets between the D_2R and H_3R in striatal membranes. They could observe that this interaction influences locomotor activation which makes this Het a possible target for Parkinson`s disease.[145]

The aim of this project was to synthesize bivalent ligands which selectively target the D_2-H_3 Het. Considering the enormous synthetic effort to get to the desired final compounds a synthetic approach had to be designed which enables the easy synthesis of a broad variety of compounds. Despite the fact that purification difficulties led to low yields a one-pot CuAAC was the most effective strategy, as several different attempts to add the respective pharmacophores selectively to the linker failed. Therefore, the selected pharmacophores and designed linkers were derivatized to contain either terminal alkyne or azide functions which were then connected to each other resulting in the synthesis of 26 bivalent compounds. Constant evaluation of pharmacological results and improvement of used structures and scaffolds led to the synthesis of compound **90** which showed subnanomolar binding affinities to both receptors. This is quite remarkable considering the overall size of the molecule and has not yet been achieved so far to the best of our knowledge. Additionally, functional assays were performed to find out whether derivatization of chosen pharmacophores led to any kind of change in their mode of action. This phenomenon could not be observed and all tested compounds maintained their pharmacological profile.

Currently, co-workers in our group are working on the development of assay systems co-expressing both receptors simultaneously. Selected compounds as well as their endcapped counterparts will be tested in these systems to identify the most selective compounds for the Het and to confirm their bivalent binding mode. Preliminary results are promising.

Chapter 4: Fluorescent ligands for D_2-like receptors

4. Fluorescent ligands

The goal of this chapter was the design and synthesis of fluorescent ligands for the D_2-like receptors based on the spiperone scaffold described in **chapter 3**. A small set of fluorescent ligands differing in selected dye or attached linker length should be synthesized to find out how these variations affect binding affinities and fluorescence properties. After determination of the pharmacological characteristics of all compounds the most promising molecule should then be used for the establishment of NanoBRET assays and as tracers in microscopy experiments.

4.1 Synthesis

One of the main aims of this project was to find out how selection of the respective dye and variation of linker length between the pharmacophore and the dye influence binding characteristics and intensity of the BRET-signal. Therefore, three different fluorescent ligands (**99**, **100**, and **103**) differing in either the dye and/or linker length were designed (cf. **Scheme 4.1**). The synthesis of precursor **36** was carried out from commercially available aniline and benzylpiperidinone as described before. For fluorescent ligands **99** and **100** succinic anhydride was added to this scaffold forming a terminal carbonic acid. Coupling of **57** and **36** using HATU/DIPEA in DMF yielded intermediate **97**. Deprotection of the Boc group with TFA/DCM delivered precursor **98**. The precursor for fluorescent ligand **103** was synthesized in a slightly different manner. Boc protection of γ-aminobutyric acid yielded **96** which was directly coupled to **36** using HATU/DIPEA in DMF to obtain **101**. Cleavage of the Boc group gave scaffold **102**. In a final step, precursors **98** and **102** and the commercially available NHS-ester of 5-TAMRA or DY-549P1 were coupled in DMF in the presence of triethylamine. Purification with preparative HPLC afforded highly pure products **99**, **100**, and **103** (>98%) in good to excellent yields (60-90 %).

Scheme 4.1: Synthesis of spacers **57** and **96** (**A** and **B**) and of fluorescent ligands **99**, **100**, and **103** (**C**)[a]

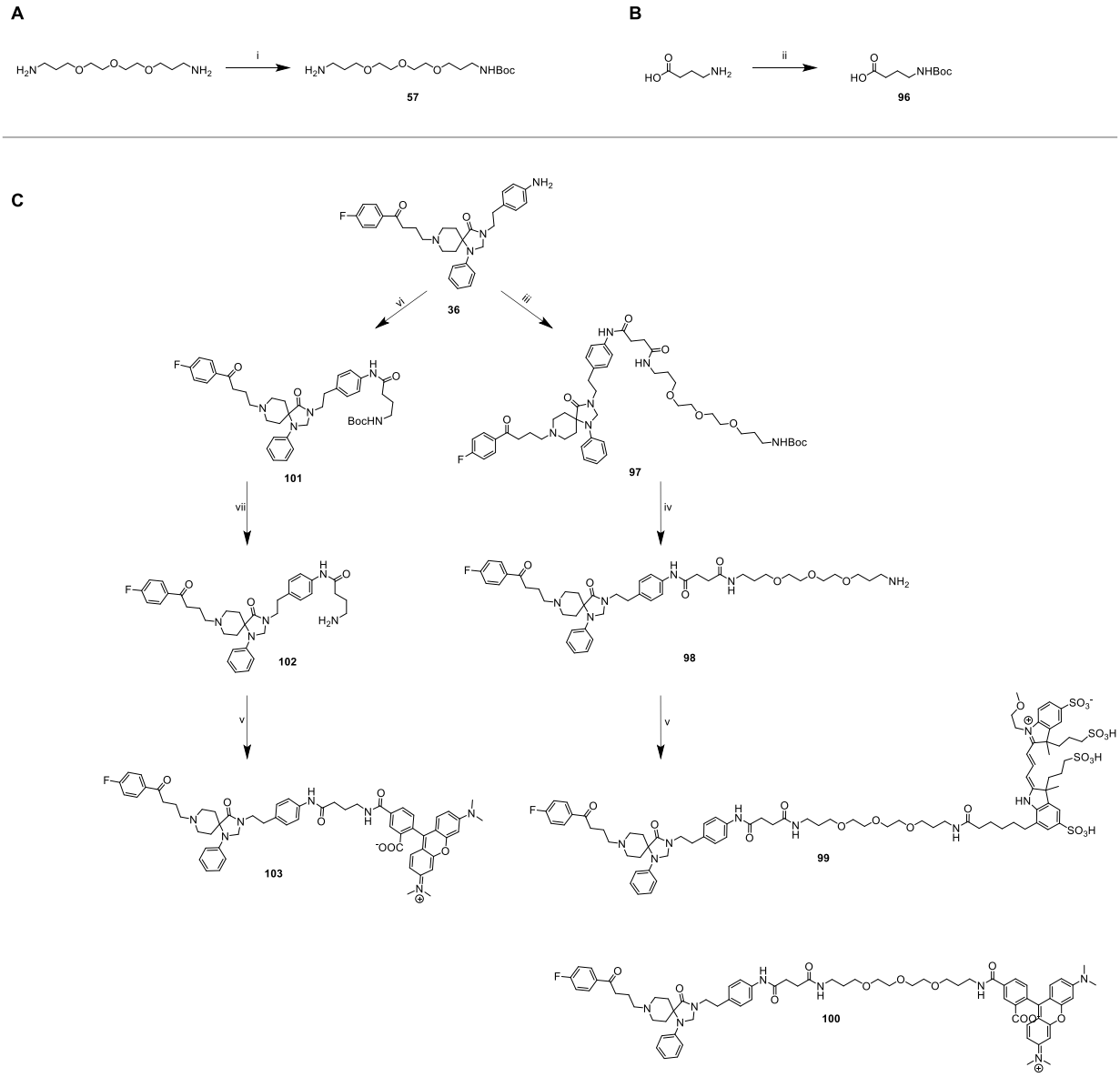

[a]Reagents and conditions: (i) di-tert-butyl dicarbonate, Et_3N, DCM, rt, 5 h; (ii) di-tert-butyl dicarbonate, Et_3N, DCM, rt, 10 h; (iii) 1) succinic anhydride, DMF, rt, 10 h; 2) **57**, HATU, DIPEA, DMF, rt, overnight; (iv) TFA/DCM 1:4, rt, 12 h; (v) 5-TAMRA NHS ester or DY-549P1 NHS ester, Et_3N, DMF, rt, 4 h; (vi) **96**, HATU, DIPEA, DMF, overnight, rt; (vii) TFA/DCM 1:4, rt, 6 h.

4.2 Biological evaluation

4.2.1 Binding affinities

In a first step synthesized compounds were tested for their binding properties for the D_2R. While 5-TAMRA labeled probes **100** and **103** showed very high affinity (pK_i = 8.25 and 8.24) towards the desired receptor in single-digit nanomolar range the addition of DY-549P1 to the pharmacophore resulted in a loss of affinity of 1.5 orders of magnitude (pK_i = 6.67) for **99**. Subsequently, selectivity of ligands **100** and **103** among the whole dopamine receptor family was determined. As expected, the selected compounds showed moderate to high affinity for the other D_2-like receptors D_3R (pK_i = 8.29 and 8.58) and D_4R (pK_i = 7.53 and 7.78) whereas only low affinity towards the D_1-like receptors was determined (cf. **Figure 4.1**; **Table 4.1**). In general, it could be observed that variations concerning the fluorescent dye had much more influence on binding affinities than different spacer lengths.

Table 4.1: Binding data of fluorescent ligands **99**, **100**, and **103** at the dopamine receptors.[a]

	pK_i ± SEM				
No.	D_1R^a	D_2R^b	D_3R^b	D_4R^b	D_5R^a
99	n.d.	6.67 ± 0.07	n.d.	n.d.	n.d.
100	6.48 ± 0.13	8.25 ± 0.03	8.29 ± 0.06	7.53 ± 0.04	< 5.5
103	7.17 ± 0.09	8.24 ± 0.05	8.58 ± 0.16	7.78 ± 0.08	6.48 ± 0.04

[a]Data represent mean values ± SEM of two[a] or three[b] independent experiments each performed in triplicate.

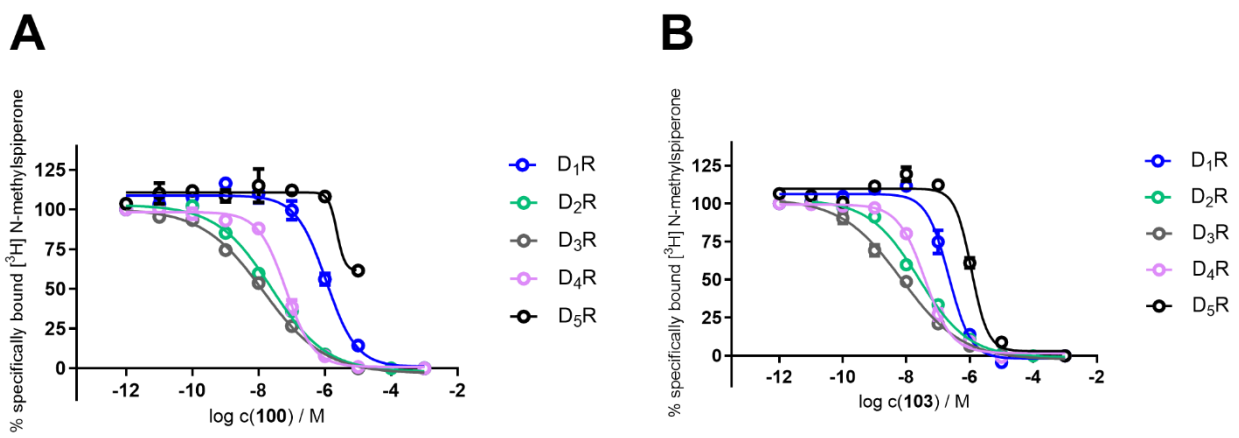

Figure 4.1: Displacement curves from radioligand competition binding experiments performed with **100** (**A**) and **103** (**B**). Data represent mean values ± SEM from at least two independent experiments each performed in triplicate.

4.2.2 Functional characterization

*experiments performed and data provided by Dr. Hannes Schihada.

As described earlier, knowing the ligand`s mode of action is very important as agonists, for example, could strain binding affinities of competitive compounds because of internalization processes as well as formation of ternary complex formation (ligand/$D_{2,3,4}$R/G Protein). That`s why it was necessary to get more information about the functional behavior of **103**. Hence, a lately employed BRET-based G_{o1} biosensor which detects G protein activation in form of a decrease in BRET between NLuc-tagged G_{o1} and cp Venus-tagged $G_{\gamma 2}$ was used to determine the ligand´s mode of action.[216] Unsurprisingly, **103** displayed neutral antagonism. No decline of the BRET signal was detected when tested in agonist mode while the signal induced by dopamine was effectively blocked (cf. **Figure 4.2**). The observed pIC_{50} values confirmed tendencies observed form radioligand binding assays with **103** showing the highest potency for the D_3R followed by the D_2R and D_4R (cf. **Table 4.2**).

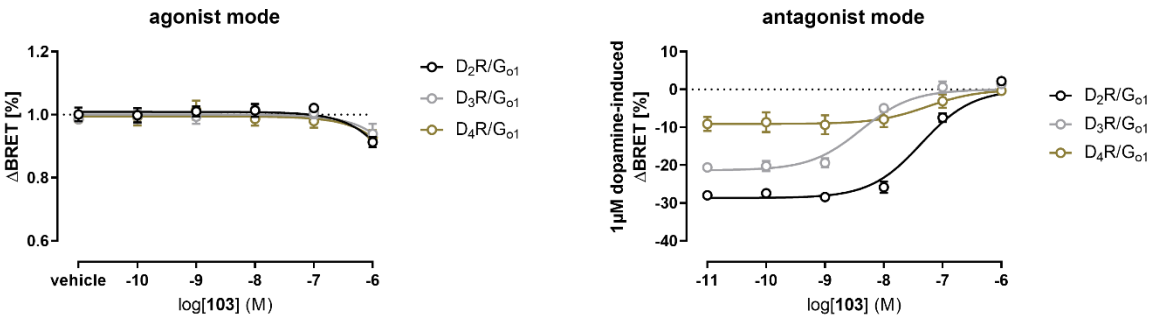

Figure 4.2: Concentration-response curves for G protein activation of **103** in the absence (agonist mode) or presence (antagonist mode) of 1 µM dopamine at HEK293A cells transiently expressing the G_{o1} BRET sensor along with the wild-type $D_{2,3,4}$R.

Table 4.2: pIC_{50} values of G protein activation at D_2-like receptors induced by dopamine.

	pIC_{50}		
No.	D_2R	D_3R	D_4R
103	7.36	8.39	7.25

4.3 Fluorescence properties

Excitation and emission spectra were recorded in order to further analyze the final compounds (in PBS containing 1% bovine serum albumin (BSA)) for their fluorescence properties. The 5-TAMRA-labeled ligands **100** and **103** showed excitation maxima at 559/562 nm and emission maxima at 583/584 nm. Excitation maximum at 562 nm and emission maximum at 576 nm were recorded for the Dyomics-labeled compound **99** (cf. **Figure 4.3**). The excitation spectra of all compounds showed an overlap with the emission spectrum of the NanoLuc making them perfectly suitable for the development of NanoBRET assays. These spectra also indicate that in microscopy experiments green lasers are best suited to excite the compounds. Nowadays green lasers belong to the standard equipment of commonly used fluorescence microscopes which makes the synthesized compounds ideal for experimental setups without upgrading the existing equipment.

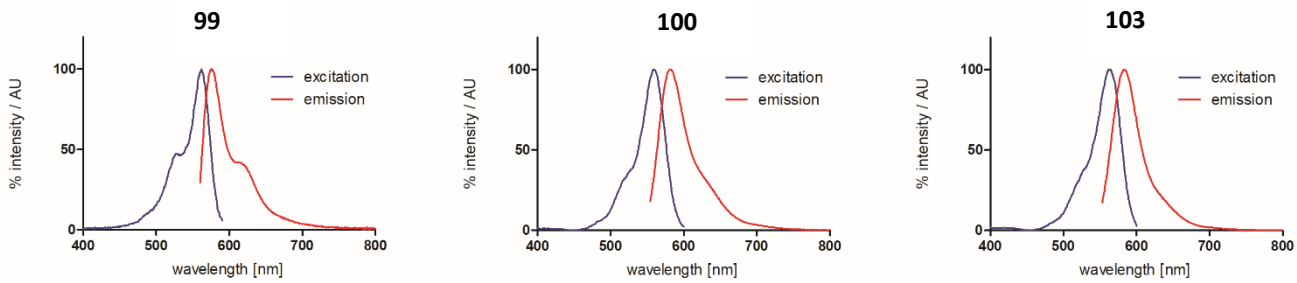

Figure 4.3: Excitation and emission spectra of fluorescent compounds **99**, **100**, and **103**.

Quantum yields were determined in PBS + 1% BSA with cresyl violet perchlorate as a red fluorescent standard according to a previously described procedure and are all in a good range at 36-39% (cf. **Table 4.3**).[217]

Table 4.3: Excitation/emission maxima and quantum yields Φ of **99**, **100**, and **103** determined in PBS + 1% BSA at 22 °C with cresyl violet perchlorate as a reference.

No.	Dye	$\lambda_{ex,\,max}/\lambda_{em,\,max}$ (nm)	Φ
99	DY-549P1	562/576	37.48%
100	5-TAMRA	559/583	38.47%
103	5-TAMRA	562/584	36.27%

Confocal microscopy imaging was used to visualize binding behavior of compound **103**. Therefore, HEK293T cells were transiently transfected with DNA of the D_2R fused to GFP_2. The receptor fused to a green fluorescent protein was used to easily identify cells expressing huge amounts of the receptor. After a suitable cell was identified, **103** (c = 50 nM) was added and pictures were taken after 3 min. The dissociation of the fluorescent ligand was induced by the addition of D_2R antagonist raclopride (c = 50 µM). Raclopride was able to entirely displace **103** as no fluorescent signal was detected after 1 min demonstrating reversible receptor binding of our probe to the D_2R (cf. **Figure 4.4**).

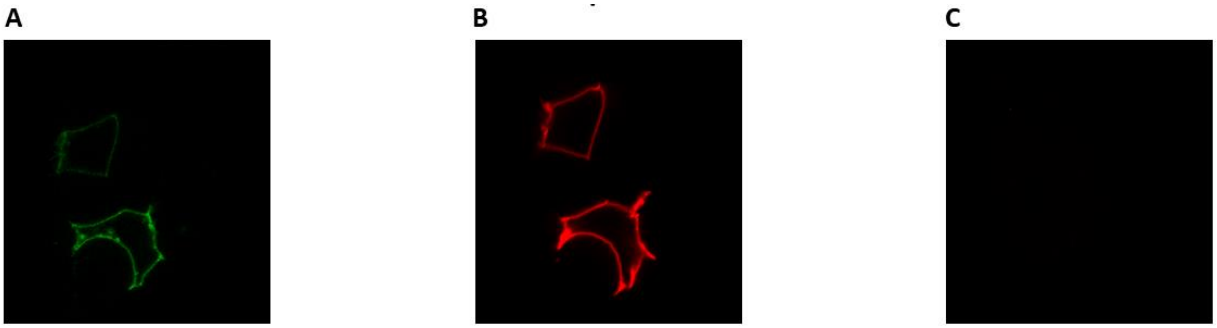

Figure 4.4: Confocal microscopy images: (**A**) Identification of cells expressing the D_2R-GFP_2 receptor; (**B**) Fluorescence observed 3 min after addition of **103**; (**C**) Displacement of **103** detected 1 min after addition of the D_2R antagonist raclopride.

4.4 Development of NanoBRET assays for D_2-like receptors

*experiments performed and data provided by Denise Mönnich as part of her PhD thesis

To test the synthesized compounds for their applicability in NanoBRET binding assays saturation binding experiments were performed at live HEK293T cells, stably expressing the NLuc-D_2R fusion protein. Saturable binding curves with very low nonspecific binding determined in the presence of haloperidole (500-fold excess) were acquired for all three ligands. For compound **100** the obtained pK_d value (8.40) was in excellent agreement with the pK_i value from the radioligand binding assay while probes **99** and **103** showed higher pK_d (8.06 and 9.34) values (cf. **Table 4.4**, **Figure 4.5**). Deviation between pK_d and pK_i have been previously reported[218–220] and can be attributed to differences between chole cells and homogenates as well as different temperatures during the respective assay (37 °C for NanoBRET, 20 °C for radioligand binding assay). In order to take advantage of the high affinity of **103** to the other D_2-like receptors the procedure was repeated for the D_3R. Saturation binding experiments performed at live HEK293T cells, stably expressing the NLuc-D_3R revealed a very high pK_d value of 8.55 for the D_3R which is in excellent agreement with obtained pK_i values from radioligand binding assays (cf. **Table 4.4** and **Table 4.1**). This proves the suitability of compound **103** for the establishment of NanoBRET assays for the D_3R besides the D_2R. Currently the experiments are performed with NLuc-hD_4R cells to characterize **103** on all D_2-like receptors.

Table 4.4: pK_d values of fluorescent ligands at NLuc-h$D_{2,3}$R.

	pK_d ± SEM			
No.	D_2R^a	N	D_3R^a	N
99	8.06 ± 0.03	3	n.d.	-
100	8.40 ± 0.06	4	n.d.	-
103	9.34 ± 0.08	4	8.55 ± 0.05	4

[a]Data represent mean values ± SEM from at least three independent experiments each performed in triplicate. NanoBRET binding experiments with live HEK293T cells stably expressing the NLuc-h$D_{2,3}$R.

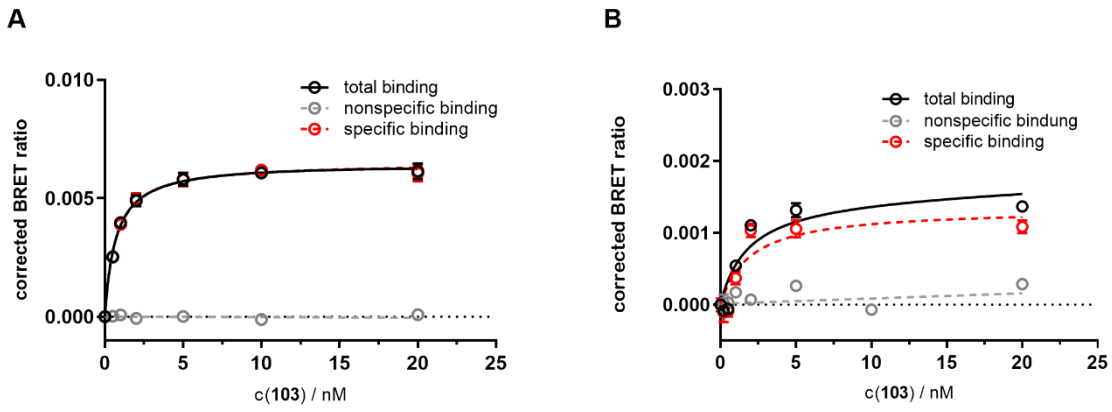

Figure 4.5: Representative isotherms form saturation binding experiments with **103** performed at NLuc-hD$_2$R (**A**) and NLuc-hD$_3$R (**B**) both stably expressed in HEK293T cells.

To confirm the established assay system competition binding experiments with different standard agonistic and antagonistic D$_2$R ligands were performed. Ligands were selected to cover a wide range of affinities (lit. pK_i from 5.7-9.7) in order to prove the suitability of the developed assay for compounds with moderate to very high affinities. Comparison with literature data showed that obtained pK_i values are in good agreement with previously reported affinities (cf. **Table 4.5**). This procedure with the same ligands was repeated for the D$_3$R with experiments revealing pK_i values which are in good agreement with literature data. These findings indicate that **103** is indeed a very useful tool for the determination of binding affinities of new ligands for D$_2$R and D$_3$R as this fluorescent ligand can be used for the two mentioned receptors in low amounts due to its excellent affinities for the D$_2$R and D$_3$R.

Table 4.5: Binding Data (pK_i values) of standard D$_{2,3}$R ligands determined at the respective receptor in the NanoBRET binding assay.

	pK_i ± SEM					
Cpd.	D$_2$R^a	N	Ref.	D$_3$R^a	N	Ref.
Pramipexole	6.51 ± 0.20	2	5.7-7.4[221,222]	6.39 ± 0.05	3	6.10[222]
Spiperone	9.83 ± 0.07	4	9.70[223]	9.64 ± 0.03	3	9.52[223]
Quinpirole	6.07 ± 0.22	2	5.97[224];6.71[223]	6.42 ± 0.06	2	7.36[225]
Dopamine	5.10	1	4.7-7.2[224,226,227]	6.08 ± 0.17	4	7.37[224]
Haloperidole	8.03 ± 0.06	4	8.20[228];8.58[226]	8.56	1	8.21[228];8.82[226]
Butaclamole	9.09 ± 0.10	4	9.15[224];9.36[226]	n.d.	-	

^{a}Data represent mean values ± SEM from N independent experiments, each performed in triplicate. NanoBRET experiments were performed at live HEK293T cells stably expressing the NLuc-hD$_{2,3}$R.

4.5 Conclusion

Fluorescent ligands have emerged as powerful instruments for investigating GPCRs. Either as tracer for microscopy experiments such as confocal microscopy or TIRFM or as a tool for the development of non-radioactive competition assays, fluorescent ligands have secured their place in modern GPCR research.

The aim of this project was the synthesis of a versatile fluorescent ligand which can be used for imaging experiments as well as for the development of NanoBRET assays for all D_2-like receptors. The antagonist spiperone was the most suitable scaffold to choose as it combines exceptional affinity towards all D_2-like receptors with high selectivity against the D_1-like receptors. Design of two linkers differing in length and coupling with different dyes (5-TAMRA or Dyomics DY-549P1) led to the synthesis of three different fluorescent dyes. Pharmacological evaluation revealed that coupling with 5-TAMRA was well tolerated while addition of the Dyomics dye led to a high decrease in affinity. Determination of emission/excitation spectra and quantum yields proved that the synthesized compounds are suitable for microscopy experiments. Excitation and emission spectra are well compatible with standard lasers and filters in microscopes and quantum yields are high enough for single-molecule imaging. Taking into account all these results **103** was selected to be used for further experiments. Microscopy experiments were successfully performed and could visualize the binding of the ligand. NanoBRET assays for the D_2R and D_3R have been successfully established and experiments with the D_4R are currently ongoing. That way **103** can serve as a powerful tool for the determination of binding affinities of new compounds for all D_2-like receptors.

Chapter 5: Bivalent fluorescent ligands

5. Bivalent fluorescent ligands

In this chapter the two previous projects were combined to synthesize a bivalent fluorescent ligand. Therefore, a promising molecule form **chapter 3** should be slightly modified to enable the attachment of fluorescent dyes. Biological evaluation of binding affinities and determination of fluorescence properties should identify the most promising molecule which could then serve as powerful tool to visualize heterodimerization.

5.1 Synthesis

Due to synthetic reasons a slightly different linker had to be designed and synthesized for a bivalent fluorescent ligand (cf. **Scheme 5.1**). Starting from commercially available 2,2'-((oxybis(ethane-2,1-diyl))bis(oxy))bis(ethan-1-ol) (PEG-4), mesyl chloride as good leaving group was introduced to obtain **104**. Azide exchange with NaN_3 in DMF yielded **105**.

Scheme 5.1: Synthesis of the linker **111**[a]

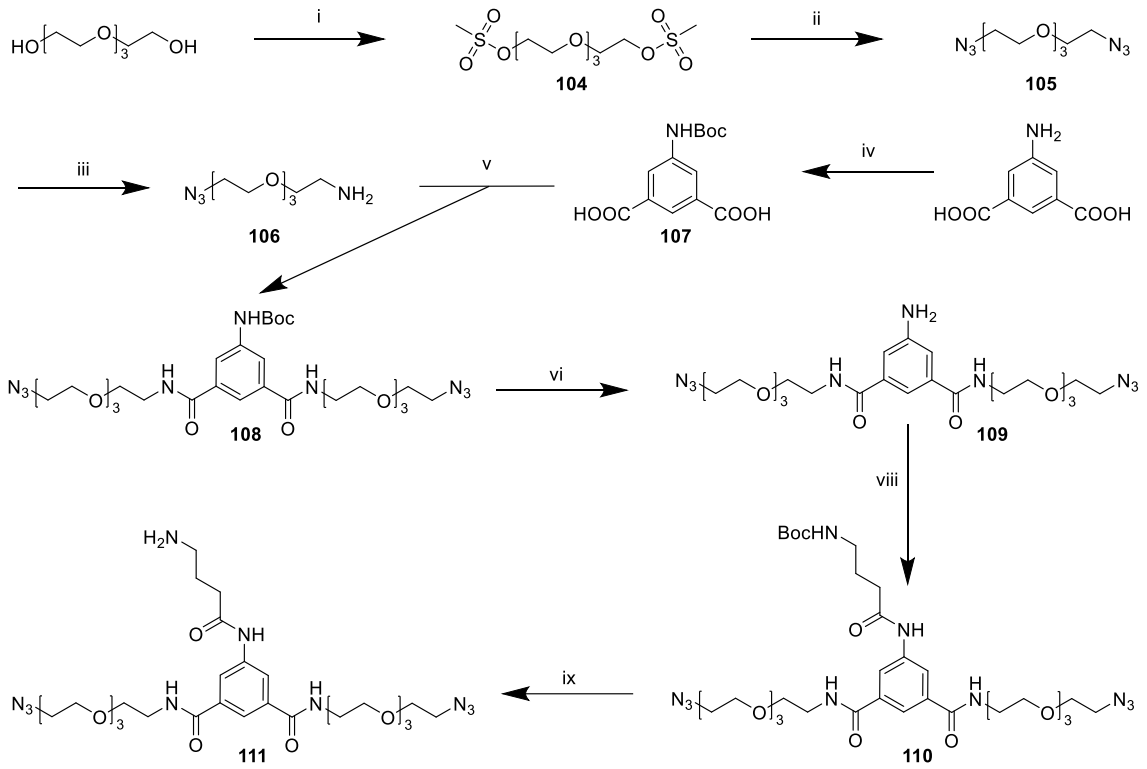

[a]Reagents and conditions: (i) MsCl, Et_3N, DCM, room temp, 15 h (99 %); (ii) NaN_3, EtOH/DMF 1:4, 80 °C, 15 h (98%); (iii) HCl (5 % aq.), PPh_3, Et_2O, room temp, 24 h (99 %); (iv) di-tert-butyl dicarbonate, dioxane/H_2O 2:1, room temp, overnight (98 %); (v) HATU, DIPEA, DMF, room temp, 14 h (87 %); (vi) TFA/DCM 1:4, room temp, 12 h (75 %); (vii) di-tert-butyl dicarbonate, NaOH, dioxane/H_2O 1:1, room temp, overnight (64 %); (viii) **96**, HATU, DIPEA, DMF, room temp, 16 h (33 %); (ix) TFA/DCM 1:4, room temp, 14 h (78 %).

In a Staudinger-type reaction one of the two azide functions was selectively reduced to get primary amine **106**. Subsequent amide coupling in the presence of HATU and DIPEA with **107**, which was obtained from Boc protection of 5-aminoisophthalic acid, delivered intermediate **108**. After cleavage with TFA the resulting aniline **109** was connected to **96** via peptide coupling leading to compound **110**. Boc deprotection yielded final linker structure **111**.

A one-pot CuAAC was performed with **37**, **43**, and the linker **111** according to the general procedure. Subsequent purification via preparative HPLC afforded final precursor **112** (cf. **Scheme 5.2**). Fluorescent compounds **113** and **114** were then synthesized and purified according to the procedure described in **chapter 4.1**.

Scheme 5.2: Synthesis of precursor **112** and final bivalent fluorescent ligands **113** and **114**[a]

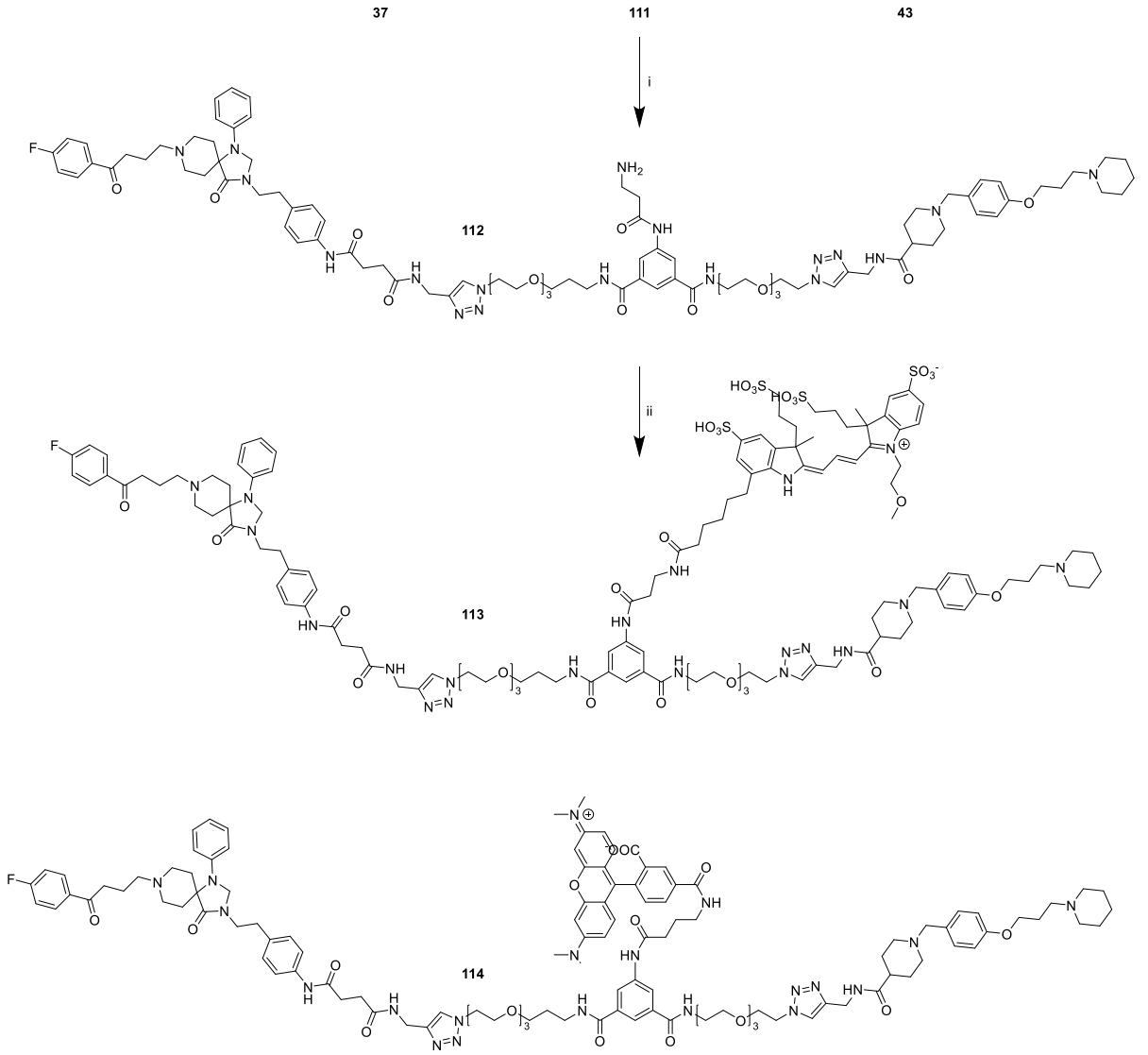

[a]Reagents and conditions: (i) $CuSO_4 \cdot 5H_2O$, ascorbic acid, DCM/MeOH 4:1, rt, 72 h; (ii) DY-549P1 NHS ester (**113**) or 5-TAMRA NHS ester (**114**), Et_3N, DMF, rt, 4 h.

5.2 Biological evaluation

As described in **chapter 3.2** binding affinities of the final compounds for the D_2R were determined with competition assays using homogenates of HEK293T cells stably expressing the D_2R (cf. **Table 5.1**). The results showed once again a high preference for 5-TAMRA as fluorescent label and were very similar to the affinities obtained for the D_2R fluorescent ligands, presented in **chapter 4.2**. Coupling with the Dyomics dye led to a huge loss in affinity for the D_2R with a pK_i value of only 6.74 for ligand **113**. In contrast, compound **114** which was labeled with 5-TAMRA showed a pK_i value of 8.41. Because of its poor affinity for the D_2R further investigation for compound **113** was discarded to save resources. Further characterization of ligand **114** revealed a very high pK_i value for the H_3R of 9.60 which was comparable to those observed for unlabeled bivalent ligands (cf. **Table 5.1**; **Figure 5.1**). These results indicate that compound **114** is highly suitable for further microscopic investigations on dimerization between the D_2R and H_3R.

Table 5.1: Binding affinities of bivalent fluorescent ligands **113** and **114**.

		pK_i ± SEM	
No.	**Dye**	D_2R	H_3R
113	DY-549P1	6.74 ± 0.04	n.d.
114	5-TAMRA	8.41 ± 0.08	9.60 ± 0.23

[a]Data represent mean values ± SEM of three independent experiments each performed in triplicate.

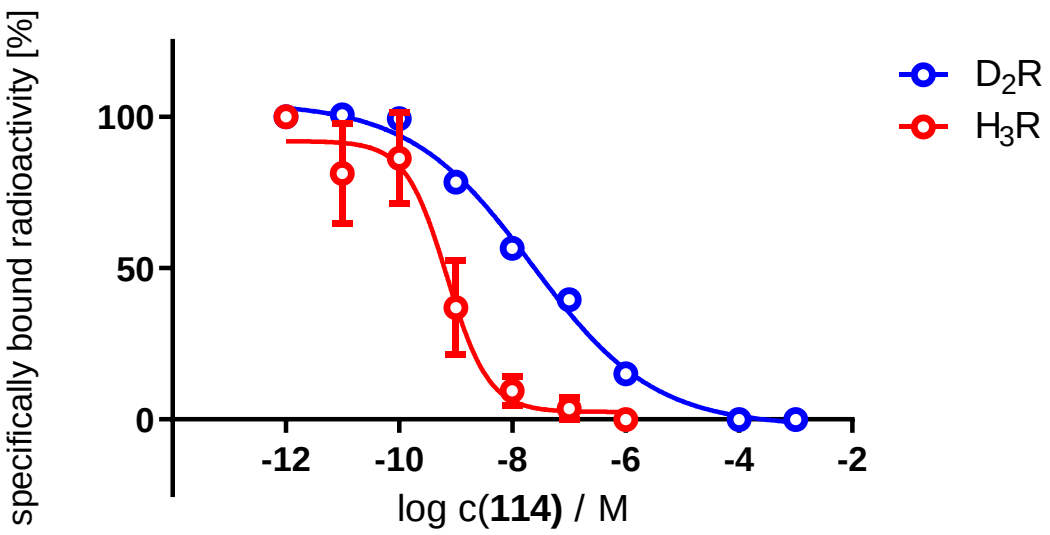

Figure 5.1: Displacement curves performed with **114** in radioligand competition binding experiments at the D_2R and H_3R. Data represent mean values ± SEM from three independent experiments each performed in triplicate.

5.3 Fluorescence properties

Excitation and emission spectra were recorded in order to further analyze the final compounds (in PBS containing 1% bovine serum albumin (BSA)) for their fluorescence properties (cf. **Figure 5.2**). The 5-TAMRA-labeled compound **114** showed an excitation maximum at 559 nm and an emission maximum at 583 nm. Excitation maximum at 562 nm and emission maximum at 576 nm were recorded for the Dyomics-labeled compound **113**. As described in **chapter 4.3** the spectra also indicate that in microscopy experiments green lasers are best suited to excite the compounds. The suitability of the dyes with commonly used fluorescence microscopes has already been mentioned in **chapter 4.3** and applies in this case as well.

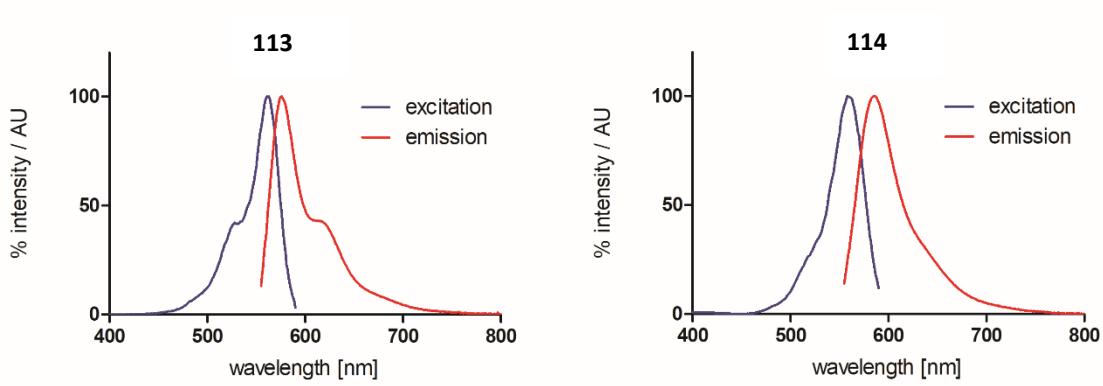

Figure 5.2: Excitation and emission spectra of bivalent fluorescent compounds **113** and **114**.

Quantum yields were determined in PBS + 1% BSA with cresyl violet perchlorate as a red fluorescent standard according to a previously described procedure and are all in a good range at 24-26%.[217]

Table 5.2: Excitation/emission maxima and quantum yields Φ of **113** and **114** determined in PBS + 1% BSA at 22 °C with cresyl violet perchlorate as a reference.

Compound	Dye	$\lambda_{ex, max}/\lambda_{em, max}$ (nm)	Φ
113	DY-549P1	562/576	24.63%
114	5-TAMRA	559/583	25.68%

5.4 Conclusion

The aim of this project was the synthesis of a bivalent fluorescent ligand. For this goal the pharmacophores **37** and **43** from **chapter 3** were used. Due to synthetic reasons the linker had to be designed alternatively which led to the synthesis of structure **111**. Pharmacological evaluation confirmed tendencies observed in **chapter 4** regarding the choice of fluorescent dyes. Compound **114** containing the 5-TAMRA dye showed very high affinities for both receptors indicating that the addition of the fluorescent dye was well tolerated. Determination of emission/excitation properties exhibited spectra that are suitable for standard lasers and filters in common microscopes. Determination of quantum yields revealed values of about 25%. All in all, it can be stated that compound **114** combines all characteristics needed for a microscopy tracer to detect and visualize receptor dimerization. Experimental setups for further tests are currently finalized and will be performed by our collaboration partners in Barcelona.

Chapter 6: Summary

6. Summary

For many years there was an established assumption that rhodopsin-like class A GPCRs could only operate discretely as independent units. However, in recent years mounting evidence has come up claiming that GPCRs also have the capability to interact with each other by forming complexes of higher order like homo- or heterodimers.[141,144,149] Ferrada et al. reported this kind of interaction for the D_2-H_3 Het.[145] According to their results the formed Het is highly involved in the regulation of motor function which makes it a very interesting target for new ways to treat PD. However, detailed physiological consequences of this heterodimerization remain unclear which is why further research on this particular target is necessary.

The aim of this thesis was to selectively target the D_2-H_3 Het by synthesizing heterobivalent ligands. For this purpose, different D_2R ligand scaffolds with high affinity and a JNJ-5207852-based H_3R pharmacophore were selected and derivatized to contain either a terminal C-C triple bond or alkyne function. Regarding linker design the goal was to cover a great variety of different distances between the two pharmacophores as varying linker lengths for bivalent ligands have been published, ranging from 20 to 80 atoms.[95,146,148] Since molecular modeling indicated that 50 atoms might be the most appropriate size a special focus was laid on linkers spanning that length. Isophthalic acid, terephthalic acid, and glutaric acid were selected as central dicarbonic structures to get more insight on how rigidity and flexibility can increase or downgrade affinities. After 26 final compounds were synthesized in a one-pot copper catalyzed CuAAC their pharmacological profile was evaluated. Binding affinities and selectivity among the respective receptor families were determined in radioligand binding assays and the pharmacological mode of action was measured in a cAMP assay. All these results identified the spiperone-based compound **90** as the most interesting ligand. Despite its huge size this molecule shows subnanomolar binding affinities for both receptors (pK_i D_2R: 9.58; pK_i H_3R: 9.83) which has not yet been achieved for any bivalent ligand to the best of my knowledge. cAMP assays revealed that **90** maintains the mode of action of its parent scaffolds and acts as antagonist for both receptors. All these findings indicate that **90** is the ideal candidate for further tests in co-expressing assays systems which are currently being developed in our group by Denise Mönnich as part of her PhD thesis. That way a possible binding mode can be detected which would make **90** a powerful tool for further research on the D_2-H_3 Het.

In a second project the spiperone pharmacophore was used for the synthesis of fluorescent ligands for D_2-like receptors. The design of different spacers and the addition of different dyes led to a final set of three different fluorescent ligands. Radioligand binding studies and saturation binding experiments revealed compound **103** as the most interesting compound. This molecule was then used for the successful establishment of NanoBRET assays for D_2-like receptors by Denise Mönnich as part of her PhD thesis. Additional microscopy experiments were performed which led to the successful visualization of the binding process of the compound.

In a final add-on project one of the spiperone-based bivalent compounds was further developed to enable the attachment of a fluorescent dye. After linker synthesis was slightly adjusted bivalent precursor **112** was obtained which was then connected to two different dyes. Pharmacological characterization and determination of fluorescence properties identified **114** as possible powerful tool to visualize the formed receptor complex. Appropriate experiments are being developed with our collaborators in Barcelona and respective experiments will be part of future PhD projects. All in all, this PhD thesis describes the successful synthesis of a broad variety of different pharmacological tools to further investigate the processes and consequences regarding the formation of the D_2-H_3 receptor heterodimer. Future scientists will hopefully benefit from this toolbox to gain new insights into the Het which might lead to new ways for the treatment of PD.

Chapter 7: Experimental section

7. Experimental section

7.1 General chemical procedures

Commercially available chemicals and solvents were purchased from standard commercial suppliers Merck (Darmstadt, Germany), Sigma-Aldrich (Munich, Germany), Acros Organics (Geel, Belgium), Alfa Aesar (Karlsruhe, Germany), abcr (Karlsruhe, Germany) or TCI Europe (Zwijndrecht, Belgium) and were used as received. All solvents were of analytical grade. The fluorescent dye 5-TAMRA NHS ester was purchased from Lumiprobe (Hannover, Germany), the fluorescent dye DY-549P1 NHS ester was purchased form Dyomics GmbH (Jena, Germany). Deuterated solvents for nuclear magnetic resonance (^{1}H NMR and ^{13}C NMR) spectra were purchased from Deutero GmbH (Kastellaun, Germany). All reactions carried out with dry solvents were accomplished in dry flasks under nitrogen or argon atmosphere. For the preparation of buffers, HPLC eluents, and stock solutions millipore water was used. Column chromatography was accomplished using Merck silica gel Geduran 60 (0.063-0.200 mm) or Merck silica gel 60 (0.040-0.063 mm) (flash column chromatography). The reactions were monitored by thin layer chromatography (TLC) on Merck silica gel 60 F254 aluminium sheets and spots were visualized under UV light at 254 nm, by potassium permanganate, or ninhydrin staining. Lyophilization was done with a Christ alpha 2-4 LD equipped with a vacuubrand RZ 6 rotary vane vacuum pump. Nuclear magnetic resonance (^{1}H NMR and ^{13}C NMR) spectra were recorded on a Bruker (Karlsruhe, Germany) Avance 300 (^{1}H: 300 MHz, ^{13}C: 75 MHz), 400 (^{1}H: 400 MHz, ^{13}C: 101 MHz) or 600 (^{1}H: 600 MHz, ^{13}C: 151 MHz) spectrometer using perdeuterated solvents. The chemical shift δ is given in parts per million (ppm). Multiplicities were specified with the following abbreviations: s (singlet), d (doublet), t (triplet), q (quartet), quin (quintet), m (multiplet), and br (broad signal) as well as combinations thereof. ^{13}C NMR-Peaks were determined by DEPT 135 and DEPT 90 (distortionless enhancement by polarization transfer). NMR spectra were processed with MestReNova 11.0 (Mestrelab Research, Compostela, Spain). High-resolution mass spectrometry (HRMS) was performed on an Agilent 6540 UHD Accurate-Mass Q-TOF LC/MS system (Agilent Technologies, Santa Clara, CA) using an ESI source. Preparative HPLC was performed with a system from Waters (Milford, Massachusetts, USA) consisting of a 2524 binary gradient module, a 2489 detector, a prep inject injector and a fraction collector III. A Phenomonex Gemini 5 µm NX-C18 column (110 Å, 250 x 21.2 mm, Phenomenex Ltd., Aschaffenburg, Germany) served as stationary phase. As mobile phase,

0.1% TFA (Method A) or 0.1% NH_3 (Method B) in millipore water and acetonitrile (MeCN) were used. The temperature was 25 °C, the flow rate 20 mL/min and UV detection was performed at 220 nm or at 560 nm for fluorescent ligands. Analytical HPLC experiments were performed on a 1100 HPLC system from Agilent Technologies equipped with Instant Pilot controller, a G1312A Bin Pump, a G1329A ALS autosampler, a G1379A vacuum degasser, a G1316A column compartment and a G1315B DAD detector. The column was a Phenomenex Gemini 5 µm NX-C18 column (110 Å, 250 x 4.6 mm, Phenomenex Ltd., Aschaffenburg, Germany), tempered at 30 °C. As mobile phase, mixtures of MeCN and aqueous TFA (Method A) or aqueous NH_3 (Method B) were used (linear gradient: MeCN/TFA or NH_3 (0.1%) (v/v) 0 min: 10:90, 25-35 min: 95:5, 36-45 min: 10:90; flow rate = 1.00 mL/min, t_0 = 3.21 min). Capacity factors were calculated according to $k = (t_R - t_0)/t_0$. Detection was performed at 220 nm or at 254 nm for fluorescent ligands. Furthermore, a filtration of the stock solutions with PTFE filters (25 mm, 0.2 µm, Phenomenex Ltd., Aschaffenburg, Germany) was carried out before testing. Compound purities determined by HPLC were calculated as the peak area of the analyzed compound in % relative to the total peak area (UV detection at 220 nm or 254 nm for fluorescent ligands). The HPLC purity of the final compounds was >95%.

7.2 Synthetic procedures and analytical data

1*H*-Indol-5-ol (1) [229]

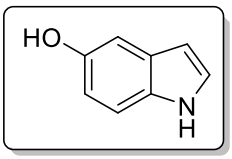

To a solution of 5-(benzyloxy)-1H-indole (5.00 g, 22.4 mmol, 1 eq) in MeOH (100 mL) ammoniumformiate (5.62 g, 89.0 mmol, 4 eq) and a catalytic amount of palladium on activated charcoal (10 % Pd basis) were added. The reaction was stirred at 55 °C for 2 h and then filtered through celite. The filtrate was concentrated under reduced pressure and dried in vacuo to give **1** (2.95 g, 99%) as a brown oil. ^{1}H NMR (300 MHz, CD_3OD) δ 7.27 – 7.15 (m, 1H), 7.13 (d, *J* = 3.1 Hz, 1H), 6.92 (dd, *J* = 2.4, 0.5 Hz, 1H), 6.65 (dd, *J* = 8.7, 2.4 Hz, 1H), 6.26 (dd, *J* = 3.1, 0.9 Hz, 1H). ^{13}C NMR (75 MHz, CD_3OD) δ 168.45, 149.85, 131.24, 128.73, 124.78, 111.05, 110.83, 103.84, 100.16. HRMS (EI-MS): m/z [$M^{\cdot+}$] calculated for $C_8H_7NO^{\cdot+}$: 133.0528, found 133.0520; C_8H_7NO (133.15).

5-(3-Chloropropoxy)-1*H*-indole (2a) [230]

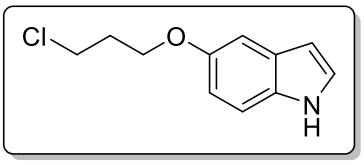

K_2CO_3 (6.22g, 45.0 mmol, 6.0 eq) and 1-bromo-3-chloropropane (3.54 g, 22.5 mmol, 3 eq) were added to a solution of **1** (1.00g, 7.5 mmol, 1 eq) in ethanol (75 mL). The reaction was heated to reflux and continued stirring overnight. After the solvent was evaporated the residue was dissolved in DCM (40 mL) and washed three times with water (3 x 30 mL). The organic phase was dried over Na_2SO_4 and concentrated under reduced pressure. The crude product was purified by column chromatography (DCM/MeOH 99/1) to yield **2a** (0.95 g, 66%) as a brown oil. ^{1}H NMR (300 MHz, $CDCl_3$) δ 8.04 (s, 1H), 7.33 – 7.23 (m, 1H), 7.18 (t, *J* = 2.8 Hz, 1H), 7.15 (d, *J* = 2.4 Hz, 1H), 6.89 (dd, *J* = 8.8, 2.4 Hz, 1H), 6.50 – 6.42 (m, 1H), 4.17 (t, *J* = 5.9 Hz, 2H), 3.80 (t, *J* = 6.4 Hz, 2H), 2.34 – 2.18 (m, 2H). ^{13}C NMR (75 MHz, $CDCl_3$) δ 153.25, 131.16, 128.33, 125.01, 112.84, 111.75, 103.74, 102.42, 65.24, 41.88, 32.55. HRMS (EI-MS): m/z [$M^{\cdot+}$] calculated for $C_8H_{15}N_2Cl_2^{\cdot+}$: 209.0607, found 209.0607; $C_8H_{15}N_2Cl_2$ (209.67).

5-(Prop-2-yn-1-yloxy)-1*H*-indole (2b) [231]

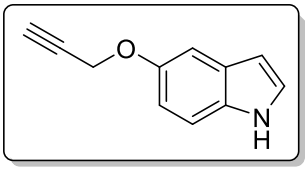

K_2CO_3 (6.00 g, 45.0 mmol, 3 eq) and 3-bromoprop-1-yne (1.96 g, 16.5 mmol, 1.1 eq) were added to a solution of **1** (2.00 g, 15.0 mmol, 1 eq) in acetone (75 mL). The reaction was stirred at room temperature overnight. After the solvent was evaporated the residue was dissolved in EtOAc (40 mL) and washed three times with water (3 x 30 mL). The organic phase was dried over Na_2SO_4 and concentrated under reduced pressure. The crude product was purified by column chromatography (DCM/MeOH 99/1) to yield **2b** (1.72 g, 66%) as a brown solid. ^{1}H NMR (300 MHz, $CDCl_3$) δ 8.09 (s, 1H), 7.30 (d, *J* = 8.8 Hz, 1H), 7.22 (d, *J* = 2.5 Hz, 1H), 7.20 (t, *J* = 2.8 Hz, 1H), 6.93 (dd, *J* = 8.8, 2.4 Hz, 1H), 6.53 – 6.47 (m, 1H), 4.73 (d, *J* = 2.4 Hz, 2H), 2.52 (t, *J* = 2.4 Hz, 1H). ^{13}C NMR (75 MHz, $CDCl_3$) δ 152.20, 131.54, 128.19, 125.10, 113.05, 111.76, 104.52, 102.59, 79.35, 75.13, 56.91. HRMS (EI-MS): m/z [$M^{\cdot+}$] calculated for $C_{11}H_9NO^{\cdot+}$: 171.0684, found 171.0676; $C_{11}H_9NO$ (171.20).

4-(4-Chlorophenyl)-1-((5-(3-chloropropoxy)-1*H*-indol-3-yl)methyl)piperidin-4-ol (3a)

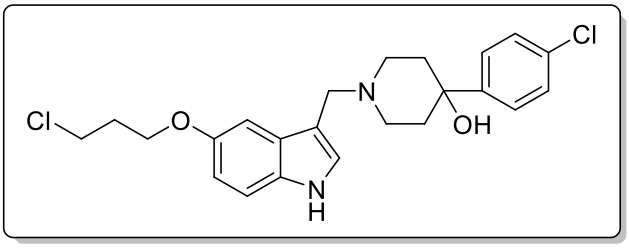

A mixture of 4-(4-chlorophenyl)piperidin-4-ol (0.38 g, 1.8 mmol, 1.3 eq) and aqueous formaldehyde (37% solution, 0.17 g, 1.43 mmol, 1.5 eq) in AcOH (15 mL) was stirred at room temperature for 15 min. Then, **2a** (0.29 g, 1.38 mmol, 1 eq) was added and the reaction was stirred overnight. The solution was basified with NaOH (1 M aqueous solution) and extracted with DCM (3 x 30 mL). The organic layer was dried over Na_2SO_4 and concentrated under reduced pressure. The crude product was purified by column chromatography (DCM/MeOH 95/5) to yield **3a** (0.23 g, 50%) as a red solid. ^{1}H NMR (300 MHz, CD_3OD) δ 7.48 – 7.42 (m, 2H), 7.33 – 7.22 (m, 4H), 7.19 (d, *J* = 2.3 Hz, 1H), 6.80 (dd, *J* = 8.8, 2.3 Hz, 1H), 4.15 (t, *J* = 5.9 Hz, 2H), 3.85 (s, 2H), 3.78 (t, *J* = 6.4 Hz, 2H), 2.95 (d, *J* = 13.1 Hz, 2H), 2.77 – 2.64 (m, 2H), 2.22 (p, *J* = 6.1 Hz, 2H), 2.09 (td, *J* = 13.5, 4.3 Hz, 2H), 1.73 (d, *J* = 12.7 Hz, 2H). ^{13}C NMR (101 MHz, CD_3OD) δ 152.97, 132.09, 131.93, 128.43, 127.76, 126.14, 125.95, 111.86, 111.61, 101.67, 69.94, 65.06, 52.52, 48.63, 41.16, 37.19, 32.41. HRMS (ESI-MS): m/z $[M+H]^+$ calculated for $C_{23}H_{27}Cl_2N_2O_2^+$: 433.1444, found 433.1449; $C_{23}H_{26}Cl_2N_2O_2$ (433.37).

4-(4-Bromophenyl)-1-((5-(3-chloropropoxy)-1*H*-indol-3-yl)methyl)piperidin-4-ol (3b)

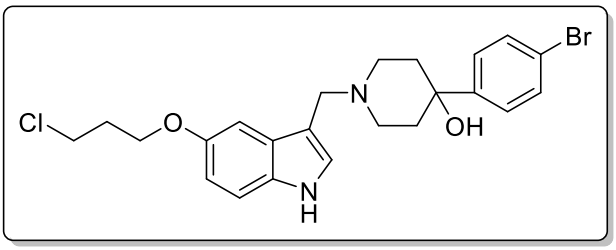

A mixture of 4-(4-bromophenyl)piperidin-4-ol (0.38 g, 1.24 mmol, 1.3 eq) and aqueous formaldehyde (37% solution, 0.12 g, 1.43 mmol, 1.5 eq) in AcOH (15 mL) was stirred at room temperature for 15 min. Then, **2a** (0.20 g, 0.95 mmol, 1 eq) was added and the reaction was stirred overnight. The solution was basified with NaOH (1 M aqueous solution) and extracted with DCM (3 x 30 mL). The organic layer was dried over Na_2SO_4 and concentrated under reduced pressure. The crude product was purified by column chromatography (DCM/MeOH 95/5) to yield **3b** (0.23 g, 50%) as a red solid. ^{1}H NMR (300 MHz, CD_3OD) δ 7.46 – 7.41 (m, 2H), 7.40 – 7.34 (m, 2H), 7.28 – 7.22 (m, 2H), 7.19 (d, *J* = 2.2 Hz, 1H), 6.80 (dd, *J* = 8.8, 2.4 Hz, 1H), 4.14 (t, *J* = 5.9 Hz, 2H), 3.84 (s, 2H), 3.77 (t, *J* = 6.4 Hz, 2H), 2.93 (d, *J* = 11.3 Hz, 2H), 2.70 (td, *J* = 12.2, 2.1 Hz, 2H), 2.27 – 2.15 (m, 2H), 2.14 – 2.00 (m, 2H), 1.71 (d, *J* = 12.6 Hz, 2H). ^{13}C NMR (75 MHz, CD_3OD) δ 153.00, 148.04, 131.89, 130.80, 128.40, 126.50, 126.13, 120.11, 111.89, 111.68, 108.57, 101.59, 69.91, 64.99, 62.90, 52.42, 41.19, 37.00, 32.40. HRMS (ESI-MS): m/z $[M+H]^+$ calculated for $C_{23}H_{27}BrClN_2O_2^+$: 477.0939, found 477.0944; $C_{23}H_{26}BrClN_2O_2$ (477.82).

4-(4-Chlorophenyl)-1-((5-(prop-2-yn-1-yloxy)-1*H*-indol-3-yl)methyl)piperidin-4-ol (4a)

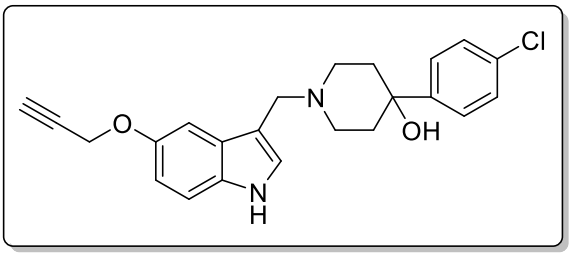

A mixture of 4-(4-chlorophenyl)piperidin-4-ol (0.64 g, 3.0 mmol, 1.3 eq) and aqueous formaldehyde (37% solution, 0.29 g, 3.5 mmol, 1.5 eq) in AcOH (15 mL) was stirred at room temperature for 15 min. Then, **2b** (0.39 g, 2.3 mmol, 1 eq) was added and the reaction was stirred overnight. The solution was basified with NaOH (1 M aqueous solution) and extracted with DCM (3 x 30 mL). The organic layer was dried over Na_2SO_4 and concentrated under reduced pressure. The crude product was purified by column chromatography (DCM/MeOH 95/5) to yield **4a** (0.57 g, 63%) as a yellow oil. ^{1}H NMR (300 MHz, CD_3OD) δ 7.49 – 7.40 (m, 2H), 7.34 – 7.20 (m, 5H), 6.82 (dd, *J* = 8.8, 2.3 Hz, 1H), 4.76 – 4.69 (m, 2H), 3.82 (s, 2H), 2.95 – 2.82 (m, 3H), 2.73 – 2.58 (m, 2H), 2.09 (td, *J* = 13.4, 4.5 Hz, 2H), 1.71 (d, *J* = 12.3 Hz, 2H). ^{13}C NMR (101 MHz, CD_3OD) δ 151.90, 142.84, 132.20, 132.07, 128.37, 127.74, 126.15, 126.01, 111.99, 111.55, 102.56, 77.85, 74.85, 70.00, 56.33, 52.45,

48.63, 37.27. HRMS (ESI-MS): m/z $[M+H]^+$ calculated for $C_{23}H_{24}ClN_2O_2^+$: 395.1521, found 395.1528; $C_{23}H_{23}ClN_2O_2$ (394.90).

4-(4-Bromophenyl)-1-((5-(prop-2-yn-1-yloxy)-1*H*-indol-3-yl)methyl)piperidin-4-ol (4b)

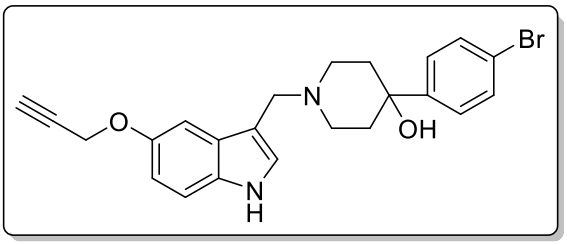

A mixture of 4-(4-bromophenyl)piperidin-4-ol (0.97 g, 3.8 mmol, 1.3 eq) and aqueous formaldehyde (37% solution, 0.36 g, 4.5 mmol, 1.5 eq) in AcOH (15 mL) was stirred at room temperature for 15 min. Then, **2b** (0.51 g, 2.92 mmol, 1 eq) was added and the reaction was stirred overnight. The solution was basified with NaOH (1 M aqueous solution) and extracted with DCM (3 x 30 mL). The organic layer was dried over Na_2SO_4 and concentrated under reduced pressure. The crude product was purified by column chromatography (DCM/MeOH 95/5) to yield **4b** (0.78 g, 62%) as a yellow oil. ^{1}H NMR (300 MHz, CD_3OD) δ 7.49 – 7.43 (m, 2H), 7.41 – 7.36 (m, 2H), 7.31 – 7.25 (m, 3H), 6.84 (dd, *J* = 8.9, 2.3 Hz, 1H), 4.74 (d, *J* = 2.4 Hz, 2H), 3.93 (s, 2H), 3.00 (d, *J* = 11.9 Hz, 2H), 2.90 (t, *J* = 2.4 Hz, 1H), 2.85 – 2.74 (m, 2H), 2.11 (td, *J* = 13.5, 4.5 Hz, 2H), 1.74 (d, *J* = 12.7 Hz, 2H). ^{13}C NMR (75 MHz, $CDCl_3$) δ 155.98, 136.12, 134.78, 132.21, 130.44, 124.14, 116.09, 115.64, 112.00, 106.36, 74.26, 73.66, 71.75, 60.22, 56.22, 52.41, 40.81. HRMS (ESI-MS): m/z $[M+H]^+$ calculated for $C_{23}H_{24}BrN_2O_2^+$: 439.1016, found 439.1019; $C_{23}H_{23}BrN_2O_2$ (439.35).

1-((5-(3-Azidopropoxy)-1*H*-indol-3-yl)methyl)-4-(4-chlorophenyl)piperidin-4-ol (5a)

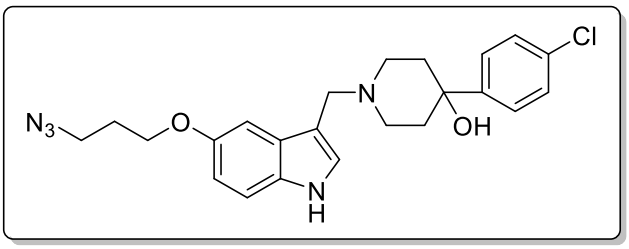

To a solution of **3a** (0.52 g, 1.1 mmol, 1 eq) in DMF (25 mL) NaN_3 (0.12 g, 1.73 mmol, 1.5 eq) was added, the reaction was heated to 80 °C and continued stirring for 8 h. After the solvent was removed under reduced pressure the resulting residue was dissolved in diethylether (35 mL) and washed three times with brine (3 x 20 mL). The organic layer was dried over Na_2SO_4 and concentrated in vacuo. The crude product was purified by column chromatography (DCM/MeOH 9/1 + 0.1% TEA) to give **5a** (0.15 g, 51%) as a brown oil. ^{1}H NMR (300 MHz, $CDCl_3$) δ 8.32 (s, 1H), 7.46 – 7.39 (m, 2H), 7.31 – 7.25 (m, 3H), 7.17 (dd, *J* = 16.4, 2.4 Hz, 2H), 6.85 (dd, *J* = 8.8, 2.4 Hz, 1H), 4.10 (t, *J* = 5.9 Hz, 2H), 3.74 (s, 2H), 3.55 (t, *J* = 6.7 Hz, 2H), 2.94 – 2.88 (m, 2H), 2.49 (td, *J* = 12.1, 2.3 Hz, 2H), 2.17 – 2.03 (m, 4H), 1.70 (d, *J* = 11.7 Hz, 2H). ^{13}C NMR (101 MHz, $CDCl_3$) δ

153.13, 146.84, 132.77, 131.54, 128.54, 128.40, 126.14, 125.02, 112.58, 111.84, 102.66, 71.10, 65.50, 53.40, 49.17, 48.46, 38.34, 29.04. HRMS (ESI-MS): m/z $[M+H]^+$ calculated for $C_{23}H_{27}ClN_5O_2^+$: 440.1848, found 440.1860; $C_{23}H_{26}ClN_5O_2$ (439.94).

1-((5-(3-Azidopropoxy)-1*H*-indol-3-yl)methyl)-4-(4-bromophenyl)piperidin-4-ol (5b)

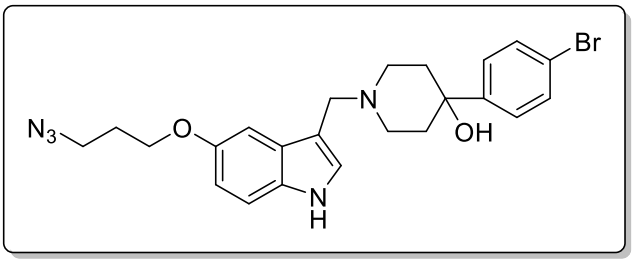

To a solution of **3b** (0.30 g, 0.6 mmol, 1 eq) in DMF (25 mL) NaN_3 (0.08 g, 1.2 mmol, 2 eq) was added, the reaction was heated to 80 °C and stirring continued for 8 h. After the solvent was removed under reduced pressure the resulting residue was dissolved in diethylether (35 mL) and washed three times with brine (3 x 20 mL). The organic layer was dried over Na_2SO_4 and concentrated in vacuo. The crude product was purified by column chromatography (DCM/MeOH 9/1 + 0.1% TEA) to give **5b** (0.15 g, 51%) as a brown oil. ^{1}H NMR (300 MHz, $CDCl_3$) δ 8.17 (s, 1H), 7.48 – 7.42 (m, 2H), 7.39 – 7.34 (m, 2H), 7.26 (d, *J* = 8.8 Hz, 1H), 7.18 (dd, *J* = 16.3, 2.4 Hz, 2H), 6.86 (dd, *J* = 8.7, 2.4 Hz, 1H), 4.11 (t, *J* = 5.9 Hz, 2H), 3.75 (s, 2H), 3.56 (t, *J* = 6.7 Hz, 2H), 2.90 (d, *J* = 9.4 Hz, 2H), 2.49 (td, *J* = 12.1, 2.4 Hz, 2H), 2.13 – 2.04 (m, 4H), 1.71 (d, *J* = 11.6 Hz, 2H). ^{13}C NMR (101 MHz, $CDCl_3$) δ 153.12, 147.41, 131.54, 131.37, 128.55, 126.53, 124.90, 120.91, 112.58, 111.82, 102.72, 71.21, 65.51, 53.48, 49.22, 48.46, 38.40, 29.05. HRMS (ESI-MS): m/z $[M+H]^+$ calculated for $C_{23}H_{27}BrN_5O_2^+$: 484.1343, found 484.1350; $C_{23}H_{26}BrN_5O_2$ (484.40).

4-(4-Chlorophenyl)-1-((5-methoxy-1*H*-indol-3-yl)methyl)piperidin-4-ol hydrotrifluoroacetate (6a) [195]

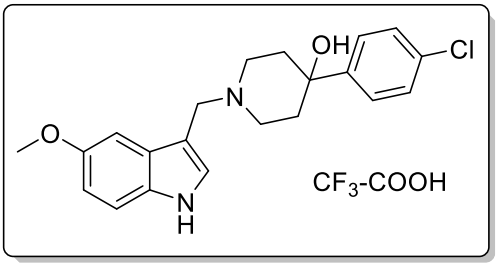

To a suspension of 5-methoxygramine (0.05 g, 0.24 mmol, 1 eq) in toluene (15 mL) 4-(4-chlorophenyl)piperidin-4-ol (0.06 g, 0.29 mmol, 1.2 eq) was added and the reaction was heated to 120 °C and stirring continued overnight. Then, the solvent was evaporated and the crude product was purified by preparative HPLC to yield **6a** (95 mg, 82%) as a red solid. ^{1}H NMR (300 MHz, CD_3OD) δ 7.51 (s, 1H), 7.48 – 7.42 (m, 2H), 7.38 – 7.31 (m, 3H), 7.26 (d, *J* = 2.2 Hz, 1H), 6.87 (dd, *J* = 8.9, 2.4 Hz, 1H), 4.56 (s, 2H), 3.86 (s, 3H), 3.52 (d, *J* = 7.0 Hz, 4H), 2.28 – 2.15 (m, 2H), 1.96 (d, *J* = 12.7 Hz, 2H). ^{13}C NMR (101 MHz, CD_3OD) δ 154.90, 145.68, 132.82, 131.68, 128.59, 128.08, 127.87, 126.00, 112.38, 112.33, 102.13, 99.68,

67.96, 54.89, 51.64, 47.69, 35.19. HRMS (ESI-MS): m/z $[M+H]^+$ calculated for $C_{21}H_{24}ClN_2^+$: 371.1521, found 371.1527. Anal. RP-HPLC (220 nm): 99% (t_R = 12.51 min, k = 3.04) $C_{21}H_{23}ClN_2$ x $C_2HF_3O_2$ (370.87 + 114.02).

4-(4-Bromophenyl)-1-((5-methoxy-1*H*-indol-3-yl)methyl)piperidin-4-ol (6b) [232]

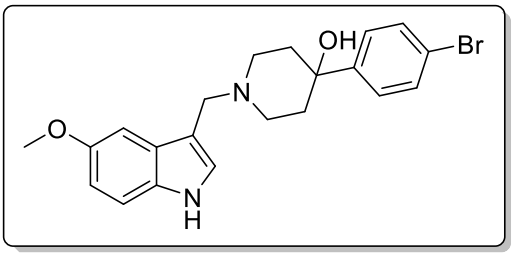

To a suspension of 5-methoxygramine (0.10 g, 0.49 mmol, 1 eq) in toluene (15 mL) 4-(4-bromophenyl)piperidin-4-ol (0.15 g, 0.59 mmol, 1.2 eq) was added and the reaction was heated to 120 °C and stirring continued overnight. Then, the solvent was evaporated and the crude product was purified by column chromatography to give **6b** (0.19 g, 95%) as a white foam. ^{1}H NMR (400 MHz, CD_3OD) δ 7.47 – 7.37 (m, 4H), 7.28 – 7.21 (m, 2H), 7.16 (d, J = 2.4 Hz, 1H), 6.78 (dd, J = 8.8, 2.4 Hz, 1H), 3.83 (s, 3H), 3.80 (s, 2H), 2.90 (d, J = 11.4 Hz, 2H), 2.65 (td, J = 12.3, 2.2 Hz, 2H), 2.08 (td, J = 13.5, 4.4 Hz, 2H), 1.72 (d, J = 12.2 Hz, 2H). ^{13}C NMR (101 MHz, CD_3OD) δ 153.83, 148.17, 131.73, 130.78, 128.44, 126.52, 125.83, 120.05, 111.60, 111.25, 109.17, 100.31, 70.14, 54.97, 52.49, 48.61, 37.20. HRMS (ESI-MS): m/z $[M+H]^+$ calculated for $C_{21}H_{24}BrN_2O_2^+$: 415.1016, found 415.1016. Anal. RP-HPLC (220 nm): 98% (t_R = 12.72 min, k = 3.06). $C_{21}H_{23}BrN_2O_2$ (415.33).

tert-Butyl 4-(2-hydroxyphenyl)piperazine-1-carboxylate (7) [233]

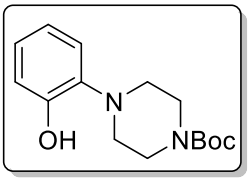

To a solution of 2-(piperazin-1-yl)phenol (1.00 g, 5.6 mmol, 1 eq) and triethylamine (0.74 g, 7.3 mmol, 1.3 eq) in DCM (30 mL) di-tert-butyl dicarbonate (1.35 g, 6.2 mmol, 1.1 eq) was added. The reaction was stirred at room temperature overnight. After the solvent was removed under reduced pressure the residue was dissolved in DCM (20 mL) and washed three times with water (3 x 20 mL). The organic phase was dried over Na_2SO_4 and concentrated under reduced pressure. Column chromatography (DCM/MeOH 99/1) yielded **7** (1.56 g, 99%) as a brown solid. ^{1}H NMR (300 MHz, DMSO-d_6) δ 8.92 (s, 1H), 6.92 – 6.68 (m, 4H), 3.51 – 3.41 (m, 4H), 2.89 – 2.82 (m, 4H), 1.42 (s, 9H). ^{13}C NMR (101 MHz, DMSO-d_6) δ 154.55, 150.56, 140.01, 123.89, 120.02, 119.56, 116.01, 79.54, 50.67 (2C), 31.11 (2C), 28.50. HRMS (ESI-MS): m/z $[M+H]^+$ calculated for $C_{15}H_{23}N_2O_3^+$: 279.1703, found 279.1710; $C_{15}H_{22}N_2O_3$ (278.35).

tert-Butyl 4-(2-methoxyphenyl)piperazine-1-carboxylate (8) [234]

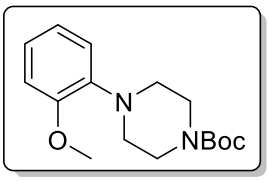

CH_3I (1.17 g, 8.25 mmol, 1.5 eq), **7** (1.5 g, 5.5 mmol, 1 eq) and $CsCO_3$ (5.36 g, 16.5 mmol, 3 eq) were suspended in DMF (30 mL) and heated at 120 °C for 10 h. Then, the solvent was evaporated and the residue was dissolved in DCM (20 mL). The organic phase was washed three times with brine (3 x 30 mL) and dried over Na_2SO_4. The solvent was removed under reduced pressure and the resulting crude product was purified by column chromatography (DCM/MeOH 98/2) to give **8** (1.14 g, 70.6%) as a yellow oil. ^{1}H NMR (300 MHz, $CDCl_3$) δ 7.08 – 6.84 (m, 4H), 3.87 (s, 3H), 3.67 – 3.55 (m, 4H), 3.09 – 2.92 (m, 4H), 1.48 (s, 9H). ^{13}C NMR (75 MHz, $CDCl_3$) δ 154.84, 152.27, 141.14, 123.34, 121.04, 118.39, 111.27, 79.73, 55.43, 53.46, 50.74, 28.48. HRMS (ESI-MS): m/z $[M+H]^+$ calculated for $C_{16}H_{25}N_2O_3^+$: 293.1860, found 293.1863; $C_{16}H_{24}N_2O_3$ (292.38).

1-(2-Methoxyphenyl)piperazine (9) [235]

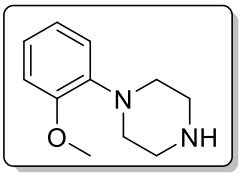

To a solution of **8** (1.15 g, 5.0 mmol) in DCM (20 mL) TFA (4 mL) was added. The mixture was stirred at room temperature until the starting material was consumed, monitored by TLC. Then, the solution was basified with aqueous KOH (20%). The organic layer was separated and dried over Na_2SO_4. The solution was concentrated under reduced pressure and purified by column chromatography (DCM/MeOH 95/5) to yield **9** as a yellow oil (0.60 g, 63%). ^{1}H NMR (300 MHz, $CDCl_3$) δ 6.98 – 6.91 (m, 1H), 6.89 – 6.84 (m, 2H), 6.82 – 6.77 (m, 1H), 3.79 (s, 3H), 3.06 – 2.95 (m, 8H). ^{13}C NMR (75 MHz, $CDCl_3$) δ 206.50, 152.27, 141.37, 123.22, 121.01, 118.34, 111.23, 55.37, 51.48, 50.42, 45.89. HRMS (ESI-MS): m/z $[M+H]^+$ calculated for $C_{11}H_{17}N_2O^+$: 193.1335, found 193.1338; $C_{11}H_{16}N_2O$ (192.26).

3,4-Dimethoxybenzaldehyde (10a) [236]

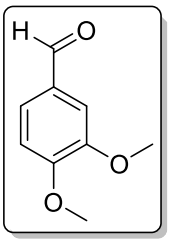

A suspension of vaniline (0.20 g, 1.3 mmol, 1 eq), CH_3I (0.20 g, 1.4 mmol, 1.1 eq) and K_2CO_3 (0.54 g, 3.9 mmol, 3 eq) in MeCN (35 mL) was heated to reflux and stirring continued overnight. After the solvent was removed under reduced pressure the residue was dissolved in water (20 mL) and extracted three times with DCM (3 x 30 mL). The organic layers were combined and dried over Na_2SO_4. The solvent was evaporated and the residue was purified by column chromatography (DCM/MeOH 99/1) to give **10a** as a white solid (0.20 g, 91%). ^{1}H NMR (300

MHz, $CDCl_3$) δ 9.81 (s, 1H), 7.42 (dd, *J* = 8.2, 1.9 Hz, 1H), 7.36 (d, *J* = 1.9 Hz, 1H), 6.94 (d, *J* = 8.2 Hz, 1H), 3.92 (s, 3H), 3.90 (s, 3H). ^{13}C NMR (75 MHz, $CDCl_3$) δ 190.91, 154.46, 149.59, 130.10, 126.89, 110.38, 108.88, 56.17, 55.98. HRMS (EI-MS): m/z [$M^{\cdot+}$] calculated for $C_9H_{10}O_3^{\cdot+}$: 166.0625, found 166.0622; $C_9H_{10}O_3$ (166.18).

3-Methoxy-4-(prop-2-yn-1-yloxy)benzaldehyde (10b) [237]

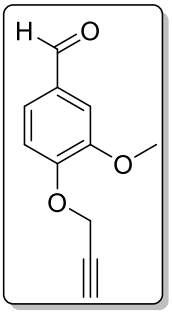

A suspension of 4-hydroxy-3-methoxybenzaldehyde (1.00 g, 6.6 mmol, 1 eq), K_2CO_3 (2.70 g, 19.7 mmol, 3 eq) and 3-bromoprop-1-yne (0.86 g, 7.2 mmol, 1.1 eq) in MeCN (50 mL) was heated to reflux and stirring continued overnight. After the solvent was evaporated the residue was diluted with water (20 mL) and extracted with DCM (30 mL). The organic layer was dried over Na_2SO_4 and concentrated under reduced pressure. The crude product was purified by column chromatography (DCM/MeOH 99/1) to give **10b** as a yellow solid (1.24 g 98%). ^1H NMR (300 MHz, $CDCl_3$) δ 9.87 (s, 1H), 7.47 (dd, *J* = 8.1, 1.9 Hz, 1H), 7.43 (d, *J* = 1.8 Hz, 1H), 4.86 (d, *J* = 2.4 Hz, 2H), 3.94 (s, 3H), 2.56 (t, *J* = 2.4 Hz, 1H). ^{13}C NMR (75 MHz, $CDCl_3$) δ 206.50, 190.95, 152.12, 150.04, 130.94, 126.33, 118.16, 112.56, 109.43, 56.62, 56.07. HRMS (EI-MS): m/z [$M^{\cdot+}$] calculated for $C_{11}H_{10}O_3^{\cdot+}$: 190.0630, found 190.0622; $C_{11}H_{10}O_3$ (190.20).

1-(3,4-Dimethoxybenzyl)-4-(2-methoxyphenyl)piperazine dihydrotrifluoroacetate (11a) [238]

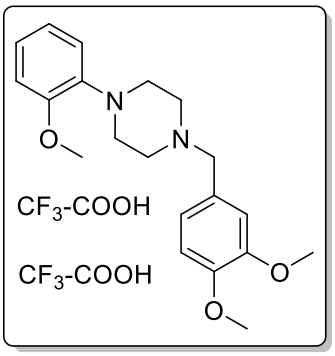

$NaBH(OAc)_3$ (0.19 g, 0.9 mmol, 2 eq) was added to a solution of **10a** (75 mg, 0.45 mmol, 1 eq) and **9** (0.13 g, 0.7 mmol, 1.5 eq) in DCM (30 mL). After the reaction was stirred at room temperature overnight the solvent was removed under reduced pressure and the residue was purified by preparative HPLC to yield **11a** (65 mg, 12%) as a white solid. ^1H NMR (400 MHz, CD_3OD) δ 7.14 (d, *J* = 2.0 Hz, 1H), 7.10 – 7.00 (m, 3H), 6.98 – 6.93 (m, 2H), 6.93 – 6.87 (m, 1H), 4.32 (s, 2H), 3.86 (s, 3H), 3.85 (s, 3H), 3.84 (s, 3H), 3.64 – 3.24 (m, 6H), 3.24 – 2.91 (m, 2H). ^{13}C NMR (101 MHz, CD_3OD) δ 152.57, 150.69, 149.55, 139.06, 124.24, 124.15, 120.95, 120.81, 118.57, 114.04, 111.56, 60.11, 55.11, 55.05, 54.61, 51.58, 47.45. HRMS (ESI-MS): m/z $[M+H]^+$ calculated for $C_{20}H_{27}N_2O_3^+$: 343.2016, found 343.2020. Anal. RP-HPLC (220 nm): 99% (t_R = 10.84 min, *k* = 2.38). $C_{20}H_{26}N_2O_3$ x $C_4H_2F_6O_4$ (342.44 + 228.05).

1-(3-Methoxy-4-(prop-2-yn-1-yloxy)benzyl)-4-(2-methoxyphenyl)piperazine (11b) [95]

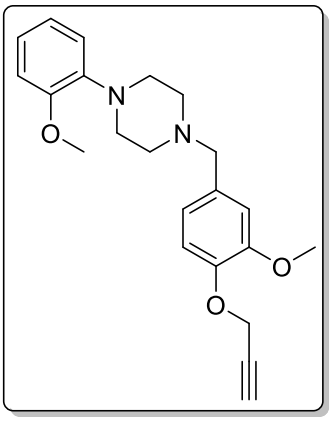

A solution of **9** (0.60 g, 3.12 mmol, 1.5 eq), **10b** (0.40 g, 2.1 mmol, 1 eq) and $NaBH(OAc)_3$ (0.89 g, 4.2 mmol, 2 eq) in DCM (35 mL) was stirred at room temperature overnight. Then, saturated $NaHCO_3$ (20 mL) was added and the aqueous phase was extracted with DCM three times (3 x 30 mL). The combined organic layers were dried over Na_2SO_4 and the solvent was removed under reduced pressure. The crude product was purified by column chromatography (DCM/MeOH 95/5) to give **11b** (0.40 g, 52%) as a yellow oil. ^{1}H NMR (300 MHz, $CDCl_3$) δ 7.02 – 6.83 (m, 7H), 4.75 (d, *J* = 2.4 Hz, 2H), 3.89 (s, 3H), 3.85 (s, 3H), 3.53 (s, 2H), 3.20 – 2.96 (m, 4H), 2.76 – 2.58 (m, 4H), 2.51 (t, *J* = 2.4 Hz, 1H).^{13}C NMR (101 MHz, $CDCl_3$) δ 152.26, 149.66, 146.01, 141.28, 122.95, 121.38, 120.99, 118.25, 114.04, 112.91, 111.17, 78.72, 75.72, 62.78, 56.84, 56.00, 55.35, 53.24, 50.48. HRMS (ESI-MS): m/z $[M+H]^+$ calculated for $C_{22}H_{27}N_2O_3^+$: 367.2016, found 367.2023; $C_{22}H_{26}N_2O_3$ (366.46).

1,6-Dimethoxynaphthalene (12) [209]

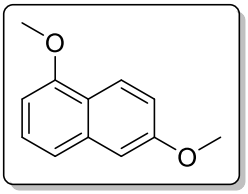

To a suspension of naphthalene-1,6-diol (1.00 g, 6.25 mmol, 1 eq) and K_2CO_3 (3.20 g, 23 mmol, 3.7 eq) in acetone (50 mL) was added dimethyl sulfate (2.77 g, 22 mmol, 3.5 eq) dropwise over 15 min. The mixture was then heated to reflux for 3 h. Afterwards the solid was removed by filtration and the filtrate was concentrated under reduced pressure. The crude product was purified by column chromatography (PE/EA 99/1 to 95/5) to yield **12** as a white solid (1.10 g, 94%). ^{1}H NMR (300 MHz, $CDCl_3$) δ 8.29 (t, *J* = 50.4 Hz, 1H), 7.41 – 7.25 (m, 2H), 7.17 – 7.11 (m, 2H), 6.70 (dd, *J* = 6.5, 2.1 Hz, 1H), 3.99 (s, 3H), 3.93 (s, 3H). ^{13}C NMR (75 MHz, $CDCl_3$) δ 158.15, 155.68, 135.93, 126.71, 123.75, 120.79, 119.28, 117.56, 105.72, 102.02, 55.46, 55.28, 29.78. HRMS (EI-MS): m/z $[M^{\cdot+}]$ calculated for $C_{12}H_{12}O_2^{\cdot+}$: 188.0832, found 188.0837; $C_{12}H_{12}O_2$ (188.26).

5-Methoxy-3,4-dihydronaphthalen-2(1*H*)-one (13) [209]

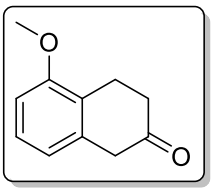

Small pieces of Na (1.10 g, 50 mmol, 8.5 eq) were added to a solution of **12** (1.10 g, 5.85 mmol, 1 eq) in EtOH (50 mL) at 50 °C over 30 min. After complete dissolution the reaction was heated to reflux for 4 h. The reaction was then quenched by the addition of conc. HCl to set pH < 1 and heated to reflux for another hour. After the solution was cooled to room temperature water (35 mL) was added and the mixture was extracted with DCM (3 x 30 mL). The organic phases were combined, dried over Na_2SO_4 and concentrated under reduced pressure. The crude product was purified by column chromatography (PE/EA 99/1 to 95/5) to obtain **13** as a yellow oil (0.62 g, 60 %). ^{1}H NMR (300 MHz, $CDCl_3$) δ 7.18 (t, *J* = 7.9 Hz, 1H), 6.76 (dd, *J* = 14.3, 7.9 Hz, 2H), 3.85 (s, 3H), 3.57 (s, 2H), 3.08 (t, *J* = 6.8 Hz, 2H), 2.57 – 2.48 (m, 2H). ^{13}C NMR (75 MHz, CDCl3) δ 211.13, 156.42, 134.99, 127.54, 125.01, 120.47, 108.48, 77.50, 77.08, 76.65, 55.49, 44.71, 37.92, 20.94. HRMS (EI-MS): m/z [$M^{\cdot+}$] calculated for $C_{11}H_{12}O_2^{\cdot+}$: 176.0832, found 176,0835: $C_{11}H_{12}O_2$ (176.21).

5-Methoxy-*N*-propyl-1,2,3,4-tetrahydronaphthalen-2-amine (14) [209]

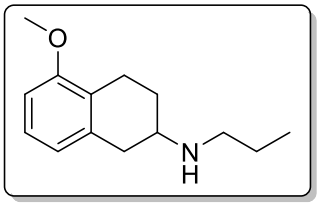

13 (0.61 g, 3.4 mmol, 1 eq) was dissolved in DCM (40 mL) and propylamine (0.30 g, 5.1 mmol, 1.5 eq) was added. After the reaction was stirred for 30 min $NaBH(OAc)_3$ (2.21 g, 10.2 mmol, 3 eq) was added in portions and the resulting mixture was stirred at room temperature overnight. After the solvent was evaporated the residue was dissolved in aqueous NaOH (1 N, 30 mL) and extracted with EtOAc (3 x 35 mL). The combined organic phases were dried over Na_2SO_4 and the solvent was removed under reduced pressure. The crude product was purified by column chromatography (DCM/MeOH 95/5 to 9/1) to afford **14** as a red oil (0.49 g, 65%). ^{1}H NMR (300 MHz, $CDCl_3$) δ 7.05 (t, *J* = 7.9 Hz, 1H), 6.64 (t, *J* = 8.3 Hz, 2H), 3.76 (s, 3H), 3.06 – 2.93 (m, 2H), 2.92 – 2.82 (m, 1H), 2.74 – 2.39 (m, 4H), 2.18 – 2.05 (m, 1H), 1.66 – 1.45 (m, 3H), 0.92 (t, *J* = 7.4 Hz, 3H). ^{13}C NMR (101 MHz, $CDCl_3$) δ 157.17, 136.11, 126.31, 124.84, 121.49, 107.16, 55.23, 53.46, 48.54, 35.83, 28.43, 22.69, 22.21, 11.81. HRMS (EI-MS): m/z [$M^{\cdot+}$] calculated for $C_{14}H_{21}NO^{\cdot+}$: 219.1618, found 219.1617; $C_{14}H_{21}NO$ (219.33).

_N_-(5-Methoxy-1,2,3,4-tetrahydronaphthalen-2-yl)-2-(4-nitrophenyl)-_N_-propylacetamide (15) [209]

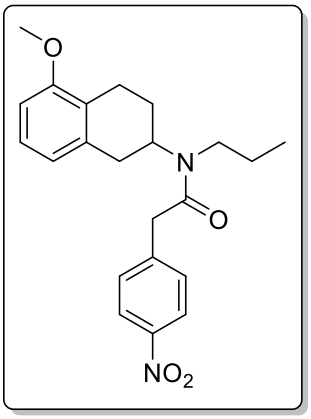

A solution of 2-(4-nitrophenyl)acetic acid (0.33 g, 1.8 mmol, 2 eq), EDC (0.52 g, 2.7 mmol, 3 eq) and HOBt (0.36 g, 2.7 mmol, 3 eq) DCM (30 mL) was stirred at room temperature for 1 h. **14** (0.21 g, 0.9 mmol, 1 eq) was added and the reaction was stirred at room temperature overnight. After the solvent was removed under reduced pressure the crude product was purified by column chromatography (DCM/MeOH 99/1) to afford **15** as a brown oil (0.35 g, 99 %). ^{1}H NMR (400 MHz, $CDCl_3$) δ 8.20 – 8.14 (m, 2H), 7.57 – 7.30 (m, 2H), 7.17 – 7.03 (m, 1H), 6.72 – 6.61 (m, 2H), 4.62 – 4.51 (m, 1H), 4.06 – 3.92 (m, 1H), 3.90 – 3.77 (m, 4H), 3.31 – 3.14 (m, 2H), 3.06 – 2.94 (m, 2H), 2.87 – 2.39 (m, 2H), 2.02 – 1.57 (m, 4H), 1.00 – 0.80 (m, 3H). ^{13}C NMR (101 MHz, $CDCl_3$) δ 170.62, 169.51, 169.09, 157.27, 157.21, 146.93, 143.22, 143.16, 141.26, 136.56, 135.67, 130.32, 130.11, 129.85, 126.83, 126.40, 124.32, 123.77, 121.31, 121.17, 107.49, 107.18, 55.28, 54.40, 53.46, 52.42, 51.94, 46.74, 44.02, 41.12, 40.80, 34.30, 33.03, 28.18, 27.23, 24.84, 23.61, 22.73, 11.66, 11.49. HRMS (ESI-MS): m/z $[M+H]^+$ calculated for $C_{22}H_{27}N_2O_4^+$: 383.1965, found 383.1972; $C_{22}H_{26}N_2O_4$ (382.46).

5-Methoxy-_N_-(4-nitrophenethyl)-_N_-propyl-1,2,3,4-tetrahydronaphthalen-2-amine (16) [209]

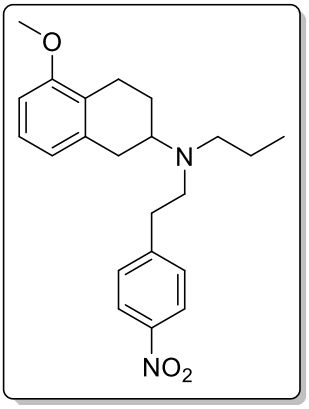

A solution of **15** (0.35 g, 0.9 mmol, 1 eq) in THF (20 mL) was added dropwise to an ice-cold solution of BH_3·THF (2.7 mL, 2.7 mmol) in THF (25 mL). The reaction was kept at 0 °C for 5 min and then heated to reflux for 4 h. The reaction was quenched by the addition of conc. HCl and subsequently basified with aqueous KOH (20 %). The mixture was extracted with DCM (3 x 30 mL) and the combined organic phases were dried over Na_2SO_4. The solvent was evaporated and the resulting residue was purified by column chromatography (DCM/MeOH 95/5) to give a brown oil for **16** (0.25 g, 75%). ^{1}H NMR (300 MHz, $CDCl_3$) δ 8.18 – 8.11 (m, 2H), 7.43 – 7.34 (m, 2H), 7.09 (t, J = 7.9 Hz, 1H), 6.67 (dd, J = 10.1, 8.0 Hz, 2H), 3.80 (s, 3H), 3.00 – 2.93 (m, 2H), 2.90 – 2.64 (m, 6H), 2.60 – 2.43 (m, 3H), 2.07 – 1.94 (m, 1H), 1.64 – 1.39 (m, 3H), 0.87 (t, J = 7.3 Hz, 3H). ^{13}C NMR (75 MHz, $CDCl_3$) δ 157.23, 148.97, 146.84, 146.41, 137.64, 129.89, 129.74,

126.28, 125.12, 123.71, 123.49, 121.60, 107.01, 62.88, 56.49, 55.26, 52.49, 52.04, 38.92, 35.74, 32.14, 25.57, 23.79, 21.98, 11.89. HRMS (ESI-MS): m/z $[M+H]^+$ calculated for $C_{22}H_{29}N_2O_3^+$: 369.2173, found 369.2177; $C_{22}H_{28}N_2O_3$ (368.48).

_N_-(4-Aminophenethyl)-5-methoxy-_N_-propyl-1,2,3,4-tetrahydronaphthalen-2-amine (17) **[209]**

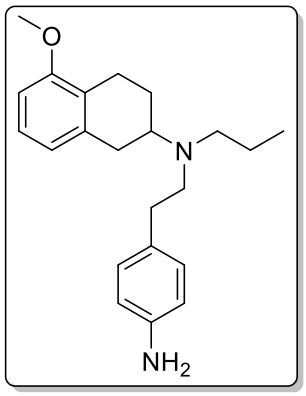

A solution of **16** (0.42 g, 1.14 mmol, 1 eq) was dissolved in EtOH (45 mL) and heated to 50 °C. Then Raney-Ni slurry (3 mL) and $N_2H_4 \cdot H_2O$ (0.86 g, 17.11 mmol, 15 eq) were added and the reaction was stirred at 50 °C for 4 h. Thereupon, the reaction was filtered over celite and the filtrate was concentrated under reduced pressure. The crude product was used without further purification. A yellow oil was obtained for **17** (0.41 g, 99%). ^{1}H NMR (300 MHz, $CDCl_3$) δ 7.09 (t, *J* = 7.9 Hz, 1H), 7.05 – 6.96 (m, 2H), 6.71 (d, *J* = 7.6 Hz, 1H), 6.68 – 6.59 (m, 3H), 3.81 (s, 3H), 3.04 – 2.45 (m, 11H), 2.12 – 2.03 (m, 1H), 1.69 – 1.44 (m, 3H), 0.87 (t, *J* = 7.3 Hz, 3H). ^{13}C NMR (101 MHz, $CDCl_3$) δ 157.20, 144.90, 144.48, 129.89, 129.54, 126.25, 121.64, 115.43, 115.29, 107.01, 63.93, 55.25, 53.19, 52.67, 38.33, 31.97, 25.54, 23.77, 11.92.HRMS (ESI-MS): m/z $[M+H]^+$ calculated for $C_{22}H_{31}N_2O^+$: 339.2431, found 339.2438; $C_{22}H_{30}N_2O$ (338.35).

6-((4-Aminophenethyl)(propyl)amino)-5,6,7,8-tetrahydronaphthalen-1-ol (18) **[209]**

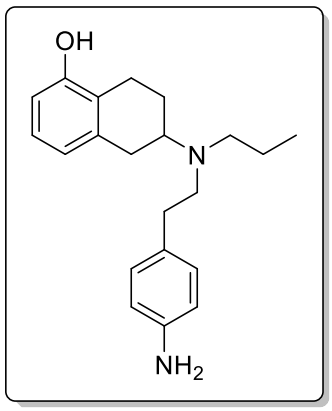

To a cold (-78 °C) solution of **17** (0.45 g, 1.33 mmol, 1 eq) in DCM (35 mL) a solution of BBr_3 (1.00 g, 4 mmol) in DCM (25 mL) was added dropwise under argon atmosphere. The reaction was allowed to warm to room temperature and stirred overnight. After the reaction was quenched by the addition of methanol (5 mL) the solvent was evaporated. The crude residue was dissolved in DCM (50 mL) and washed with saturated $NaHCO_3$ solution. The organic phase was dried over Na_2SO_4 and the solution was concentrated under reduced pressure. The crude product was purified by column chromatography (DCM/MeOH 95/5) to give a white foam for **18** (0.22 g, 51%). ^{1}H NMR (300 MHz, $CDCl_3$) δ 7.04 – 6.92 (m, 3H), 6.71 – 6.59 (m, 4H), 3.49 (s, 2H), 3.00 – 2.43 (m, 11H), 2.14 – 2.05 (m, 1H), 1.71 – 1.56 (m, 3H), 0.93 (t, *J* = 7.3 Hz,

3H). ^{13}C NMR (75 MHz, $CDCl_3$) δ 153.60, 144.58, 134.58, 129.57, 126.52, 122.70, 121.53, 115.36, 112.21, 53.08, 52.61, 50.90, 23.42, 11.89. HRMS (ESI-MS): m/z $[M+H]^+$ calculated for $C_{21}H_{29}N_2O^+$: 325.2274, found 325.2280; $C_{21}H_{28}N_2O$ (324.48).

N^1-(4-(2-((5-Hydroxy-1,2,3,4-tetrahydronaphthalen-2-yl)(propyl)amino)ethyl)phenyl)-N^4-(prop-2-yn-1-yl)succinamide (19)

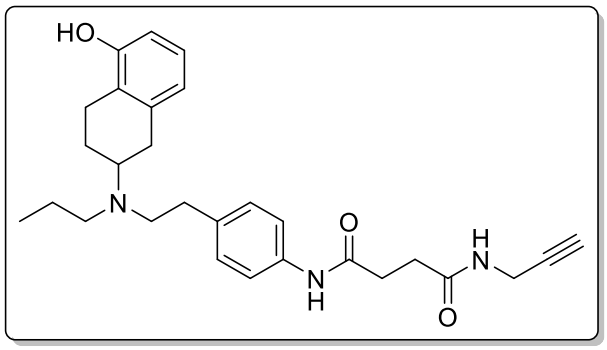

To a solution of **18** (0.22 g, 0.68 mmol, 1 eq) succinic anhydride (0.07 g, 0.68 mmol, 1 eq) was added and the reaction was stirred at room temperature overnight. After the reaction was complete, as indicated by TLC, HATU (0.39 g, 1.02 mmol, 1.5 eq), DIPEA (0.26 g, 2.04 mmol, 3 eq) and propargylamine (0.05 g, 0.89 mmol, 1.3 eq) were added. Then, the mixture was stirred for 10 h at room temperature. The solvent was evaporated and the residue was purified by column chromatography (DCM/MeOH 95/5). **19** (0.20 g, 64%) was obtained as a yellow oil. ^{1}H NMR (400 MHz, CD_3OD) δ 7.44 (d, *J* = 8.5 Hz, 2H), 7.15 (d, *J* = 8.5 Hz, 2H), 6.88 (t, *J* = 7.8 Hz, 1H), 6.54 (t, *J* = 8.6 Hz, 2H), 3.94 (d, *J* = 2.5 Hz, 2H), 2.99 – 2.90 (m, 2H), 2.88 – 2.69 (m, 6H), 2.69 – 2.59 (m, 4H), 2.58 – 2.43 (m, 4H), 2.14 – 2.04 (m, 1H), 1.62 – 1.46 (m, 3H), 0.92 (t, *J* = 7.4 Hz, 3H).^{13}C NMR (101 MHz, CD_3OD) δ 172.84, 171.50, 154.67, 137.64, 133.66, 131.94, 128.88, 126.58, 121.76, 120.26, 119.94, 112.03, 79.20, 70.78, 60.34, 52.50, 51.96, 31.28, 30.58, 30.13, 29.54, 28.10, 23.65, 22.32, 18.66, 9.91. HRMS (ESI-MS): m/z $[M+H]^+$ calculated for $C_{28}H_{36}N_3O_3^+$: 462.2751, found 462.2757; $C_{28}H_{35}N_3O_3$ (461.61).

***N*-Propyl-2,3-dihydro-1*H*-inden-2-amine (20)** [210]

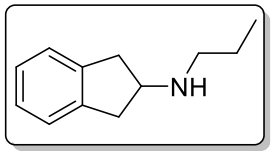

A solution of 1,3-dihydro-2H-inden-2-one (0.50 g, 3.5 mmol, 1 eq) and propan-1-amine (0.28 g, 5.0 mmol, 1.3 eq) in DCM (30 mL) and glacial acid (0.5 mL) was stirred at room temperature for 5 min. Then, $NaBH(OAc)_3$ (1.20 g, 5.6 mmol, 1.5 eq) was added and the mixture was stirred at room temperature overnight. After the solvent was removed the resulting residue was dissolved in DCM (50 mL) and washed with saturated aqueous $NaHCO_3$ (30 mL). The organic layer was dried over Na_2SO_4 and concentrated under reduced pressure. Column chromatography (DCM/MeOH 9/1 + 0.1 % NH_3) afforded **20** (0.5 g, 80%) as a red oil. ^{1}H NMR (300 MHz, $CDCl_3$) δ 7.23 – 7.09 (m, 4H), 3.69 – 3.58 (m, 1H), 3.23 – 3.11 (m, 2H), 2.82 – 2.71 (m, 2H), 2.69 – 2.61

(m, 2H), 1.57 – 1.47 (m, 2H), 0.95 (t, *J* = 7.4 Hz, 3H). ^{13}C NMR (75 MHz, $CDCl_3$) δ 141.83, 126.39, 124.71, 59.72, 50.27, 40.08, 23.49, 11.96. ^{13}C NMR (75 MHz, $CDCl_3$) δ 141.83, 126.39, 124.71, 59.72, 50.27, 40.08, 23.49, 11.96. HRMS (EI-MS): m/z [$M^{\cdot+}$] calculated for $C_{12}H_{17}N^{\cdot+}$: 175.1361, found 175.1353; $C_{12}H_{17}N$ (175.28).

4-((2,3-Dihydro-1*H*-inden-2-yl)(propyl)amino)butanenitrile (21) [210]

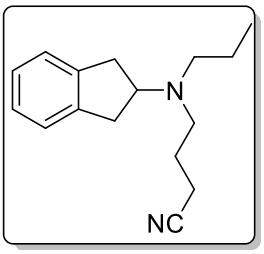

To a suspension of **20** (0.50 g, 2.9 mmol, 1 eq), K_2CO_3 (2.35 g, 17.0 mmol, 5.5 eq) and NaI (0.38 g, 2.6 mmol, 0.9 eq) in MeCN (75 mL) 4-bromobutanenitrile (1.00 g, 6.80 mmol, 2.4 eq) was added dropwise. The reaction was heated to reflux and continued stirring for 24 h. After the mixture was concentrated under reduced pressure the residue was dissolved in DCM (50 mL) and washed with NaOH (1 M, 30 mL). The organic phase was separated and dried over Na_2SO_4. The solvent was removed under reduced pressure and the crude product was purified by column chromatography (DCM/MeOH 9/1) to afford **21** (0.45 g, 66%) as a yellow oil. ^{1}H NMR (300 MHz, $CDCl_3$) δ 7.21 – 7.10 (m, 6H), 3.74 – 3.62 (m, 2H), 3.07 – 2.97 (m, 3H), 2.92 – 2.81 (m, 3H), 2.62 (t, *J* = 6.7 Hz, 3H), 2.50 – 2.40 (m, 6H), 1.81 (p, *J* = 6.9 Hz, 3H), 1.55 – 1.42 (m, 5H), 0.89 (t, *J* = 7.3 Hz, 5H). ^{13}C NMR (75 MHz, $CDCl_3$) δ 141.73, 126.40, 124.51, 120.03, 62.56, 53.24, 49.31, 36.17, 23.82, 20.38, 14.79, 11.93. HRMS (EI-MS): m/z [$M^{\cdot+}$] calculated for $C_{16}H_{22}N_2^{\cdot+}$: 242.1783, found 242. 1772; $C_{16}H_{22}N_2$ (242.36).

***N*^{1}-(2,3-Dihydro-1*H*-inden-2-yl)-*N*^{1}-propylbutane-1,4-diamine (22)** [210]

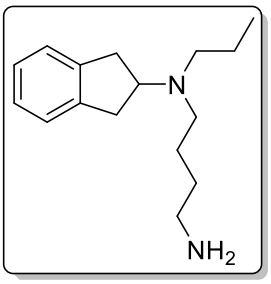

To a cooled solution of **21** (0.90 g, 3.7 mmol, 1 eq) in THF (40 mL) $LiAlH_4$ (0.42 g, 11.1 mmol, 3 eq) was added in small portions. The reaction was heated to reflux, stirring continued overnight and quenched with water (5 mL) the next morning. The mixture was filtered through celite and the filtrate was concentrated under reduced pressure. The residue was dissolved in DCM (40 mL) and washed three times with aqueous NaOH (1 M, 3 x 30 mL). The organic phase was dried over Na_2SO_4 and dried in vacuo to afford **22** (0.95 g, 95%) as a red oil. ^{1}H NMR (300 MHz, $CDCl_3$) δ 7.20 – 7.08 (m, 4H), 3.72 – 3.58 (m, 1H), 3.08 – 2.96 (m, 2H), 2.93 – 2.81 (m, 2H), 2.71 (t, *J* = 6.8 Hz, 2H), 2.59 – 2.42 (m, 4H), 1.57 – 1.41 (m, 6H), 0.88 (t, *J* = 7.3 Hz, 3H). ^{13}C NMR (75 MHz, $CDCl_3$) δ 141.99, 126.27, 124.46, 63.20, 53.43, 51.31, 42.31,

36.68, 31.98, 24.58, 20.28, 12.05. HRMS (ESI-MS): m/z $[M+H]^+$ calculated for $C_{16}H_{27}N_2^+$: 247.2169, found 247.2172; $C_{16}H_{26}N_2$ (246.40).

Ethyl 4-(3-chloropropoxy)-3-methoxybenzoate (23a) [239]

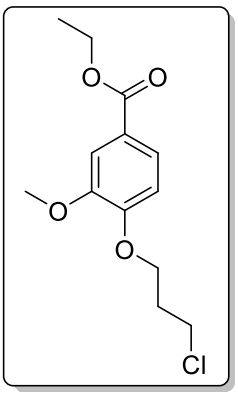

To a suspension of ethyl 4-hydroxy-3-methoxybenzoate (1.00 g, 5.1 mmol, 1 eq) and K_2CO_3 (4.30 g, 30.6 mmol, 6 eq) in MeCN (35 mL) 1-bromo-3-chloropropane (2.40 g, 15.3 mmol, 3 eq) was added, the reaction was heated to reflux and stirring continued overnight. The solvent was then removed under reduced pressure and the resulting residue was dissolved in DCM (30 mL). The organic layer was washed three times with brine (3 x 25 mL) and dried over Na_2SO_4. After the solvent was evaporated the crude product was purified by column chromatography (DCM/MeOH 99/1) to give **23a** as a yellow oil (1.3 g, 93%). ^{1}H NMR (300 MHz, $CDCl_3$) δ 7.66 (dd, *J* = 8.4, 2.0 Hz, 1H), 7.54 (d, *J* = 2.0 Hz, 1H), 6.90 (d, *J* = 8.5 Hz, 1H), 4.35 (q, *J* = 7.1 Hz, 2H), 4.22 (t, *J* = 6.0 Hz, 2H), 3.90 (s, 3H), 3.77 (t, *J* = 6.2 Hz, 2H), 2.31 (p, *J* = 6.1 Hz, 2H), 1.38 (t, *J* = 7.1 Hz, 3H). ^{13}C NMR (75 MHz, $CDCl_3$) δ 166.42, 152.12, 148.93, 123.43, 123.34, 112.45, 111.78, 65.44, 60.86, 56.05, 41.46, 32.05, 14.41. HRMS (EI-MS): m/z $[M^{\cdot+}]$ calculated for $C_{13}H_{17}O_4Cl^{\cdot+}$: 272.0810, found 272.0804; $C_{13}H_{17}O_4Cl$ (272.72).

Ethyl 3-methoxy-4-(prop-2-yn-1-yloxy)benzoate (23b)

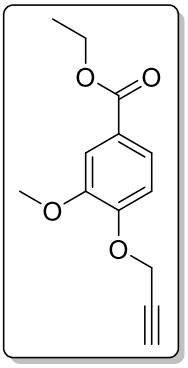

A suspension of ethyl 4-hydroxy-3-methoxybenzoate (0.50 g, 2.5 mmol, 1 eq), 3-bromoprop-1-yne (0.33 g, 2.8 mmol, 1.1 eq) and K_2CO_3 (1.05 g, 7.6 mmol, 3 eq) in MeCN (20 mL) was heated to reflux and stirring continued for 15 h. After the solvent was evaporated the residue was dissolved in DCM (25 mL) and washed with water (25 mL). The organic phase was dried over Na_2SO_4 and concentrated under reduced pressure. Column chromatography (DCM/MeOH 99/1) yielded **23b** as a yellow oil (1.3 g, 93%). ^{1}H NMR (300 MHz, $CDCl_3$) δ 7.67 (dd, *J* = 8.4, 2.0 Hz, 1H), 7.56 (d, *J* = 2.0 Hz, 1H), 7.03 (d, *J* = 8.5 Hz, 1H), 4.81 (d, *J* = 2.4 Hz, 2H), 4.35 (q, *J* = 7.1 Hz, 2H), 3.92 (s, 3H), 2.53 (t, *J* = 2.4 Hz, 1H), 1.37 (t, *J* = 7.1 Hz, 3H). ^{13}C NMR (75 MHz, $CDCl_3$) δ 166.29, 150.54, 149.07, 124.14, 123.10, 112.58, 112.42, 77.80, 76.39, 60.91, 56.53, 56.04, 14.41. HRMS (EI-MS): m/z $[M^{\cdot+}]$ calculated for $C_{13}H_{14}O_4^{\cdot+}$: 234.0892, found 234.0883; $C_{13}H_{14}O_4$ (234.25).

Ethyl 3,4-dimethoxybenzoate (23c) [240]

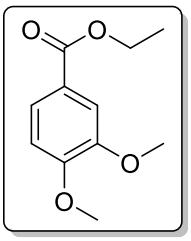

A suspension of ethyl 4-hydroxy-3-methoxybenzoate (0.50 g, 2.5 mmol, 1 eq), CH_3I (0.70 g, 5 mmol, 2 eq) and K_2CO_3 (2.10 g, 15 mmol, 6 eq) in MeCN (30 mL) was heated to reflux and stirring continued overnight. After the solvent was removed under reduced pressure the crude product was dissolved in water (30 mL) and extracted three times with DCM (3 x 30 mL). The organic layers were combined, dried over Na_2SO_4 and concentrated under reduced pressure. The residue was purified by column chromatography (DCM/MeOH 99/1) to give **23c** (0.49 g, 92%) as a yellow oil. ^{1}H NMR (300 MHz, $CDCl_3$) δ 7.67 (dd, *J* = 8.4, 2.0 Hz, 1H), 7.53 (d, *J* = 2.0 Hz, 1H), 6.89 – 6.84 (m, 1H), 4.34 (q, *J* = 7.1 Hz, 2H), 3.92 (s, 6H), 1.37 (t, *J* = 7.1 Hz, 3H). ^{13}C NMR (75 MHz, $CDCl_3$) δ 166.43, 152.86, 148.56, 123.49, 123.02, 111.91, 110.19, 60.83, 56.00, 55.99, 14.41. HRMS (EI-MS): m/z [$M^{\cdot+}$] calculated for $C_{11}H_{14}O_4^{\cdot+}$: 210.0887, found 210.0883; $C_{11}H_{14}O_4$ (210.23).

4-(3-Chloropropoxy)-3-methoxybenzoic acid (24a) [241]

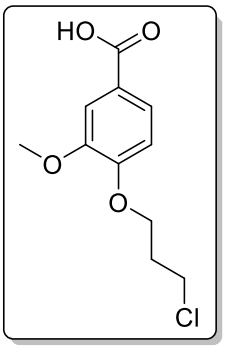

KOH (1.30 g, 23.9 mmol, 5 eq) was dissolved in water and added to a solution of **23a** (1.30 g, 4.8 mmol, 1 eq) in MeOH (40 mL). After the mixture was stirred overnight at room temperature the solvent was evaporated. The residue was diluted with water and acidified with aqueous HCl (1 N, 40 mL). The formed precipitate was filtered off and dried in vacuo to give **24a** as a white solid (1.00 g, 86%). ^{1}H NMR (300 MHz, $CDCl_3$) δ 7.76 (dd, *J* = 8.4, 1.9 Hz, 1H), 7.60 (d, *J* = 1.9 Hz, 1H), 6.95 (d, *J* = 8.5 Hz, 1H), 4.32 – 4.18 (m, 2H), 3.93 (s, 3H), 3.78 (t, *J* = 6.2 Hz, 2H), 2.33 (p, *J* = 6.0 Hz, 2H). ^{13}C NMR (75 MHz, $CDCl_3$) δ 171.40, 152.96, 149.00, 124.51, 121.90, 112.77, 111.75, 77.46, 77.04, 76.62, 65.45, 56.06, 41.43, 32.01. HRMS (ESI-MS): m/z $[M+H]^+$ calculated for $C_{11}H_{14}ClO_4^+$: 245.0575, found 245.0577; $C_{11}H_{13}ClO_4$ (244.67).

3-Methoxy-4-(prop-2-yn-1-yloxy)benzoic acid (24b) [242]

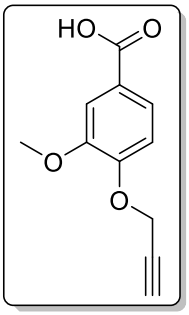

KOH (0.72 g, 12.8 mmol, 5 eq) was dissolved in water (10 mL) and added to a solution of **23b** (0.60 g, 2.5 mmol, 1 eq) in MeOH (25 mL). After the mixture was stirred overnight at room temperature the solvent was evaporated. The residue was diluted with water and acidified with aqueous HCl (1 N, 50 mL). The formed precipitate was filtered off and dried in vacuo to give **24b** as a white solid (0.46 g, 88%). ^{1}H NMR (400 MHz, CD_3OD) δ 7.64 (dd, *J* = 8.4, 2.0 Hz, 1H), 7.58 (d, *J* = 1.9 Hz, 1H), 7.10 (d, *J* = 8.4 Hz, 1H), 4.83 (d, *J* = 2.4 Hz, 2H), 3.87 (s, 3H), 2.98 (t, *J* = 2.4 Hz, 1H). ^{13}C NMR (101 MHz, CD_3OD) δ 168.22, 151.03, 149.26, 123.97, 123.15, 112.98, 112.62, 77.80, 76.01, 56.06, 55.06. HRMS (ESI-MS): m/z $[M-H]^-$ calculated for $C_{11}H_9O_4$: 205.0506, found 205.0515; $C_{11}H_{10}O_4$ (206.20).

3,4-Dimethoxybenzoic acid (24c) [243]

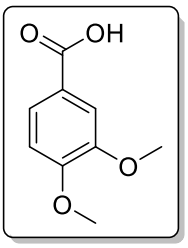

KOH (0.65 g, 11.5 mmol, 5 eq) was dissolved in water (10 mL), added to a solution of **23c** (0.49 g, 2.3 mmol, 1 eq) in MeOH (25 mL) and was then stirred at room temperature overnight. The solvent was removed under reduced pressure and the residue was dissolved in water. Aqueous HCl (2 N) was added to set pH < 2 and the mixture was extracted three times with EtOAc (3 x 30 mL). The organic layers were combined and dried in vacuo to give **24c** (0.38 g, 81%) as a white powder. ^{1}H NMR (300 MHz, $CDCl_3$) δ 7.78 (dd, *J* = 8.4, 2.0 Hz, 1H), 7.60 (d, *J* = 2.0 Hz, 1H), 6.93 (d, *J* = 8.5 Hz, 1H), 3.96 (s, 3H), 3.95 (s, 3H). ^{13}C NMR (75 MHz, $CDCl_3$) δ 171.59, 153.73, 148.69, 124.62, 121.68, 112.30, 110.33, 56.11, 56.04. HRMS (EI-MS): m/z $[M^{\cdot+}]$ calculated for $C_9H_{10}O_4^{\cdot+}$: 182.0574, found 182.0573; $C_9H_{10}O_4$ (182.18).

4-(3-Chloropropoxy)-*N*-(4-((2,3-dihydro-1H-inden-2-yl)(propyl)amino)butyl)-3-methoxybenzamide (25a)

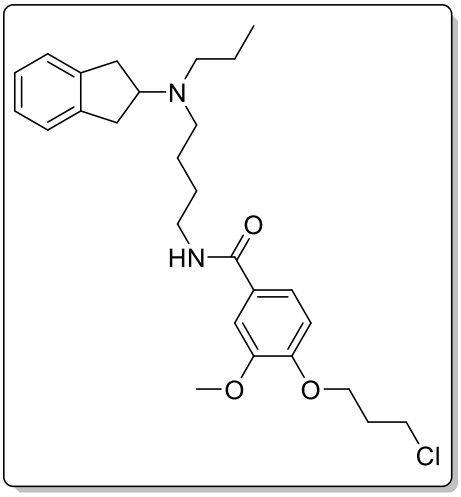

24a (0.10 g, 1.0 mmol, 0.4 eq) was dissolved in DMF (15 mL) at 0 °C and a solution of HATU (0.61 g, 1.6 mmol, 4 eq) in DMF was added. After 10 min DIPEA (0.16 g, 1.2 mmol, 3 eq) and a solution of **22** (0.25 g, 1.0 mmol, 2.5 eq) were added dropwise. The mixture was stirred at room temperature overnight. Saturated $NaHCO_3$ (15 mL) was added and the aqueous layer was extracted with DCM (30 mL). The organic layer was washed three times with brine, dried over Na_2SO_4 and concentrated under reduced pressure. Column chromatography (DCM/MeOH 95/5) afforded **25a** (0.15 g, 80%) as a sticky brown oil. ^{1}H NMR (300 MHz, $CDCl_3$) δ 7.41 – 7.34 (m, 2H), 7.17 (s, 4H), 7.03 (t, *J* = 5.4 Hz, 1H), 6.85 (d, *J* = 8.2 Hz, 1H), 4.16 (t, *J* = 6.0 Hz, 2H), 4.00 (t, *J* = 8.0 Hz, 1H), 3.87 (s, 3H), 3.75 (t, *J* = 6.3 Hz, 2H), 3.52 – 3.40 (m, 2H), 3.30 – 3.14 (m, 4H), 3.09 – 2.97 (m, 2H), 2.92 – 2.87 (m, 2H), 2.27 (p, *J* = 6.1 Hz, 2H), 1.83 – 1.61 (m, 6H), 0.94 (t, *J* = 7.3 Hz, 3H). ^{13}C NMR (75 MHz, $CDCl_3$) δ 167.68, 150.99, 149.26, 139.08, 137.11, 127.43, 124.54, 120.04, 112.11, 110.69, 65.47, 63.60, 56.06, 52.94, 51.55, 41.51, 38.97, 38.62, 35.30, 32.07, 28.00, 26.79, 11.29. HRMS (ESI-MS): m/z $[M+H]^+$ calculated for $C_{27}H_{38}ClN_2O_3^+$: 473.2565, found 473.2574; $C_{27}H_{37}ClN_2O_3$ (473.05).

_N_-(4-((2,3-Dihydro-1_H_-inden-2-yl)(propyl)amino)butyl)-3-methoxy-4-(prop-2-yn-1-yloxy)benzamide (25b)

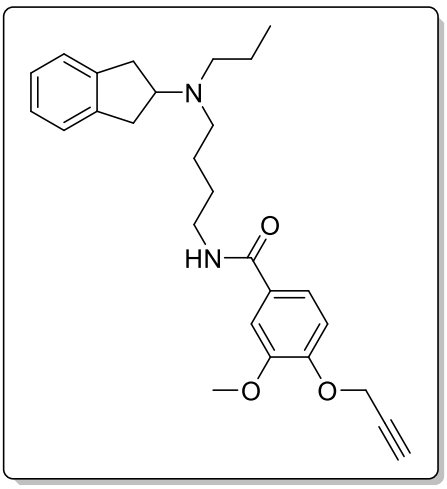

24b (0.20 g, 0.97 mmol, 1 eq) was dissolved in DMF (20 mL) at 0 °C and a solution of HATU (1.40 g, 3.9 mmol, 4 eq) in DMF was added. After 10 min DIPEA (0.37 g, 2.9 mmol, 3 eq) and a solution of **22** (0.60 g, 2.4 mmol, 2.5 eq) were added dropwise. The mixture was stirred at room temperature overnight. Saturated $NaHCO_3$ (15 mL) was added and the aqueous layer was extracted with DCM (3 x 30 mL). The organic layer was washed three times with brine (3 x 30 mL), dried over Na_2SO_4 and concentrated under reduced pressure. Column chromatography (DCM/MeOH 95/5) afforded **25b** (0.35 g, 80%) as a sticky brown oil. ^{1}H NMR (300 MHz, $CDCl_3$) δ 7.43 (d, *J* = 1.9 Hz, 1H), 7.29 – 7.21 (m, 1H), 7.18 – 7.06 (m, 4H), 6.91 (d, *J* = 8.4 Hz, 1H), 6.85 (s, 1H), 4.73 (d, *J* = 2.3 Hz, 2H), 3.85 (s, 3H), 3.63 (p, *J* = 8.2 Hz, 1H), 3.50 – 3.35 (m, 2H), 3.06 – 2.93 (m, 2H), 2.90 – 2.79 (m, 2H), 2.65 – 2.37 (m, 5H), 1.69 – 1.39 (m, 6H), 0.85 (t, *J* = 7.3 Hz, 3H). ^{13}C NMR (101 MHz, $CDCl_3$) δ 167.13, 149.47, 149.20, 141.63, 128.77, 126.38, 124.44, 119.06, 112.88, 111.16, 78.00, 76.28, 63.06, 56.60, 55.99, 53.21, 50.95, 40.05, 36.45 (2C), 27.72, 24.81, 19.70, 11.99. HRMS (ESI-MS): m/z $[M+H]^+$ calculated for $C_{27}H_{35}N_2O_3^+$: 435.2642, found 435.2652; $C_{27}H_{34}N_2O_3$ (434.58).

_N_-(4-((2,3-Dihydro-1_H_-inden-2-yl)(propyl)amino)butyl)-3,4-dimethoxybenzamide hydrotrifluoroacetate (25c)

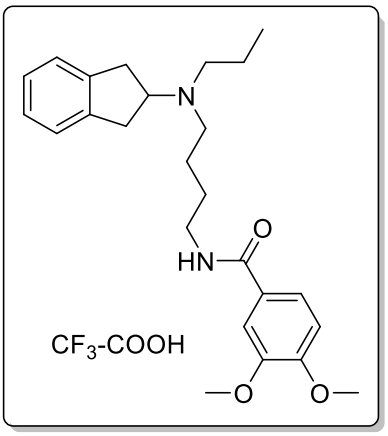

A solution of **24c** (0.07 g, 0.4 mmol, 1 eq) and HATU (0.30 g, 0.8 mmol, 2 eq) in DMF (10 mL) was stirred at 0 °C for 10 min. Then, DIPEA (0.16 g, 1.2 mmol, 3 eq) and a solution of **22** (0.25 g, 1 mmol, 2.5 eq) in DMF (10 mL) were added dropwise. The reaction was stirred at room temperature overnight. The solvent was removed under reduced pressure and the residue was purified by preparative HPLC to yield **25c** (0.10g, 48%) as a white powder. ^{1}H NMR (400 MHz, DMSO-d_6) δ 9.56 (s, 1H), 8.39 (t, *J* = 5.6 Hz, 1H), 7.47 (dd, *J* = 8.4, 2.0 Hz, 1H), 7.43 (d, *J* = 2.0 Hz, 1H), 7.26 – 7.17 (m,

4H), 7.00 (d, *J* = 8.5 Hz, 1H), 4.28 – 4.17 (m, 1H), 3.79 (s, 3H), 3.78 (s, 3H), 3.34 – 3.27 (m, 4H), 3.21 – 3.03 (m, 6H), 1.78 – 1.52 (m, 6H), 0.91 (t, *J* = 7.3 Hz, 3H). ^{13}C NMR (101 MHz, DMSO-d_6) δ 166.32, 151.68, 148.69, 139.51, 127.64, 127.23, 124.84, 120.81, 111.34, 111.07, 63.25, 56.08, 56.01, 52.52, 50.89, 38.65, 34.82, 26.82, 21.09, 17.23, 11.34. HRMS (ESI-MS): m/z $[M+H]^+$ calculated for $C_{25}H_{35}N_2O_3^+$: 411.2642, found 411.2648. Anal. RP-HPLC (220 nm): 99% (t_R = 11.97 min, *k* = 2.86). $C_{25}H_{34}N_2O_3$ x $C_2HF_3O_2$ (410.56 + 114.02).

4-(3-Azidopropoxy)-*N*-(4-((2,3-dihydro-1*H*-inden-2-yl)(propyl)amino)butyl)-3-methoxybenzamide (26)

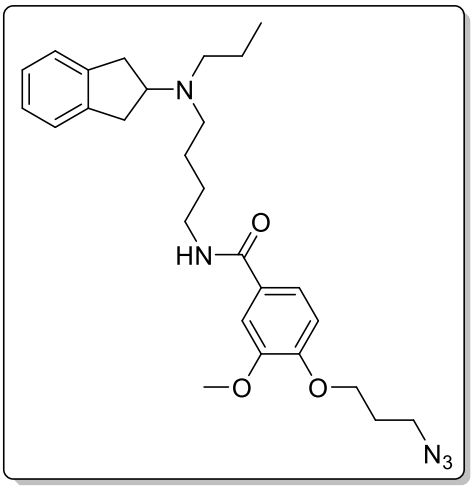

NaN_3 (0.04 g, 0.64 mmol, 2 eq) was added to a solution of **25a** (0.15 g, 0.3 mmol, 1 eq) in DMF (20 mL) and the reaction was stirred at 80 °C for 14 h. After the reaction was concentrated under reduced pressure the residue was dissolved in diethylether (25 mL) and washed three times with saturated $NaHCO_3$ (3 x 20 mL). The organic layer was then dried over Na_2SO_4 and concentrated in vacuo. The crude product was purified by column chromatography (DCM/MeOH 95/5) to give **26** as a yellow solid (0.13 g, 95%). ^{1}H NMR (300 MHz, $CDCl_3$) δ 7.42 (d, *J* = 2.0 Hz, 1H), 7.21 (dd, *J* = 8.3, 2.1 Hz, 1H), 7.18 – 7.09 (m, 4H), 6.80 (d, *J* = 8.3 Hz, 1H), 6.50 (t, *J* = 5.1 Hz, 1H), 4.10 (t, *J* = 6.1 Hz, 2H), 3.90 (s, 3H), 3.72 – 3.60 (m, 1H), 3.55 (t, *J* = 6.6 Hz, 2H), 3.50 – 3.42 (m, 2H), 3.01 – 2.92 (m, 2H), 2.86 – 2.79 (m, 2H), 2.62 – 2.45 (m, 4H), 2.10 (p, *J* = 6.3 Hz, 2H), 1.70 – 1.41 (m, 6H), 0.87 (t, *J* = 7.3 Hz, 3H). ^{13}C NMR (75 MHz, $CDCl_3$) δ 167.20, 150.73, 149.44, 141.81, 128.06, 126.34, 124.46, 119.05, 111.98, 111.19, 65.72, 63.07, 56.07, 53.28, 50.97, 48.17, 40.12, 36.56, 28.68, 27.84, 25.03, 19.73, 12.03. HRMS (ESI-MS): m/z $[M+H]^+$ calculated for $C_{27}H_{38}N_5O_3^+$: 480.2969, found 480.2972; $C_{27}H_{37}N_5O_3$ (479.62).

1-Benzyl-4-(phenylamino)piperidine-4-carbonitrile (27) [203]

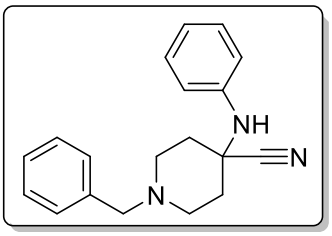

TMSCN (2.97 g, 30.0 mmol, 3 eq) was added dropwise to a solution of aniline (0.93 g, 10.0 mmol, 1 eq) and N-benzyl-piperidone (1.89 g, 10.0 mmol, 1 eq) in glacial acetic acid (15 mL) at 0 °C. The reaction was stirred at room temperature for 5 h. After the reaction was complete, monitored by TLC, the solution was basified with aqueous KOH

20% and extracted with DCM (3 x 30 mL). The combined organic phases were dried over Na_2SO_4 and the solvent was removed under reduced pressure. Column chromatography (DCM/MeOH 99/1) afforded **27** (3.01 g, 98%) as a yellow solid. ^{1}H NMR (400 MHz, $CDCl_3$) δ 7.32 – 7.24 (m, 4H), 7.25 – 7.15 (m, 3H), 6.89 – 6.82 (m, 3H), 3.62 (s, 1H), 3.50 (s, 2H), 2.82 – 2.67 (m, 2H), 2.47 – 2.36 (m, 2H), 2.32 – 2.21 (m, 2H), 1.93 – 1.81 (m, 2H). ^{13}C NMR (101 MHz, $CDCl_3$) δ 143.37, 137.92, 129.33, 129.06, 128.95, 128.40, 127.33, 120.95, 120.74, 117.82, 62.61, 53.10, 49.32, 36.10. HRMS (ESI-MS): m/z $[M+H]^+$ calculated for $C_{19}H_{22}N_3^+$: 292.1808, found 292.1813; $C_{19}H_{21}N_3$ (291.40).

1-Benzyl-4-(phenylamino)piperidine-4-carboxamide (28) [203]

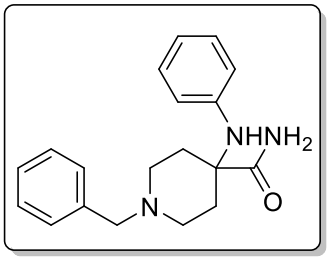

27 (3.00 g, 10.0 mmol) was dissolved in 10 mL H_2SO_4 (96% w/w) and stirred at room temperature overnight. The reaction was then carefully basified (pH > 10) by dropwise addition of aqueous NaOH (30%) while maintaining the temperature below 0 °C. The resulting mixture was extracted with DCM (3 x 30 mL). The organic phases were combined and dried over Na_2SO_4. The solvent was removed under reduced pressure to yield **28** (2.99 g, 94%) as an orange solid. ^{1}H NMR (300 MHz, DMSO-d_6) δ 7.34 – 7.17 (m, 6H), 7.11 – 7.00 (m, 3H), 6.67 – 6.53 (m, 3H), 5.49 (s, 1H), 3.43 (s, 2H), 2.59 – 2.48 (m, 2H), 2.26 (t, J = 10.5 Hz, 2H), 2.10 – 1.95 (m, 2H), 1.93 – 1.77 (m, 2H). ^{13}C NMR (101 MHz, DMSO-d_6) δ 178.14, 145.93, 139.16, 129.16, 128.94, 128.61, 127.28, 116.94, 115.17, 62.70, 57.53, 48.94, 31.84. HRMS (ESI-MS): m/z $[M+H]^+$ calculated for $C_{19}H_{24}N_3O^+$: 310.1914, found 310.1912; $C_{19}H_{23}N_3O$ (309.41).

8-Benzyl-1-phenyl-1,3,8-triazaspiro[4.5]dec-2-en-4-one (29) [203]

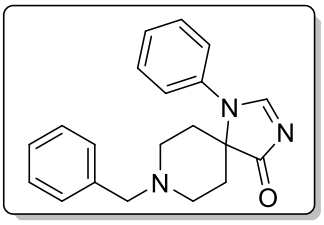

DMF-DMA (3.44 g, 29.1 mmol, 3 eq) was added to a solution of **28** (2.99 g, 9.7 mmol, 1 eq) in methanol (40 mL) and the mixture was stirred for 16 h at 55 °C. The solvent was evaporated and the crude residue was purified by column chromatography (DCM/MeOH 95/5) to yield **29** (3.01 g, 96%) as a yellow solid. ^{1}H NMR (300 MHz, $CDCl_3$) δ 8.22 (s, 1H), 7.53 – 7.43 (m, 3H), 7.32 – 7.20 (m, 5H), 7.19 – 7.14 (m, 2H), 3.56 (s, 2H), 3.08 – 2.94 (m, 2H), 2.72 – 2.59 (m, 2H), 2.05 – 1.93 (m, 2H), 1.84 – 1.71 (m, 2H). ^{13}C NMR (75 MHz, $CDCl_3$) δ 194.06, 169.16, 135.38, 130.01, 129.58, 129.16, 128.26, 128.06, 127.11, 65.05, 62.62, 46.83, 30.88.

HRMS (ESI-MS): m/z $[M+H]^+$ calculated for $C_{20}H_{22}N_3O^+$: 320.1757, found 320.1765; $C_{20}H_{21}N_3O$ (319.41).

8-Benzyl-1-phenyl-1,3,8-triazaspiro[4.5]decan-4-one (30) [203]

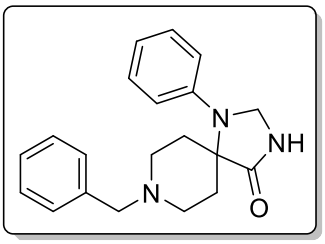

$NaBH_4$ (0.45 g, 11.8 mmol, 1.25 eq) was added to a solution of **29** (3.00 g, 9.4 mmol, 1 eq) in methanol (35 mL). The reaction was stirred at room temperature whereupon a white solid precipitated. After the reaction was complete, monitored by TLC, the solid was filtered off to obtain **30** (2.08 g, 70%) as a white powder. ^{1}H NMR (300 MHz, DMSO-d_6) δ 8.63 (s, 1H), 7.38 – 7.31 (m, 4H), 7.29 – 7.21 (m, 3H), 6.87 (d, J = 8.1 Hz, 2H), 6.76 (t, J = 7.3 Hz, 1H), 4.57 (s, 2H), 3.52 (s, 2H), 2.76 – 2.67 (m, 4H), 2.59 – 2.52 (m, 2H), 1.57 (d, J = 13.5 Hz, 2H). ^{13}C NMR (75 MHz, DMSO-d_6) δ 176.51, 143.78, 139.18, 129.53, 129.17, 128.67, 127.30, 118.16, 114.72, 62.62, 58.64, 58.61, 49.71, 28.88. HRMS (ESI-MS): m/z $[M+H]^+$ calculated for $C_{20}H_{24}N_3O^+$: 322.1914, found 322.1920; $C_{20}H_{23}N_3O$ (321.42).

1-Phenyl-1,3,8-triazaspiro[4.5]decan-4-one (31) [203]

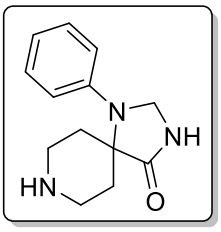

30 (2.08 g, 6.5 mmol, 1 eq) was dissolved in methanol (50 mL) and glacial acetic acid (1 mL). To the obtained solution a catalytic amount of palladium on activated charcoal (10 % Pd basis) and ammoniumformiate (1.60 g, 26.0 mmol, 4 eq) was added. The mixture was then stirred at 55 °C until the reaction was complete, indicated by TLC. The mixture was filtered through Celite, concentrated under reduced pressure, diluted with water and basified with aqueous KOH (20%). The aqueous phase was extracted with EtOAc (3 x 30 mL). The combined organic layers were dried over Na_2SO_4 and the solvent was removed under reduced pressure. **31** (1.45 g, 97%) was obtained as a white solid. ^{1}H NMR (400 MHz, DMSO-d_6) δ 8.58 (s, 1H), 7.26 – 7.15 (m, 2H), 6.88 (d, J = 8.3 Hz, 2H), 6.71 (t, J = 7.3 Hz, 1H), 4.56 (s, 2H), 3.18 – 3.07 (m, 4H), 2.83 (dd, J = 12.2, 4.9 Hz, 2H), 2.39 (td, J = 13.0, 5.5 Hz, 2H), 1.46 (d, J = 13.4 Hz, 2H). ^{13}C NMR (101 MHz, DMSO-d_6) δ 176.92, 143.89, 129.39, 117.69, 114.39, 59.24, 59.04, 49.06, 42.68, 29.76. HRMS (ESI-MS): m/z $[M+H]^+$ calculated for $C_{13}H_{18}N_3O^+$: 232.1444, found 232.1449; $C_{13}H_{17}N_3O$ (231.30).

8-(4-(4-Fluorophenyl)-4-oxobutyl)-1-phenyl-1,3,8-triazaspiro[4.5]decan-4-one (32) [203]

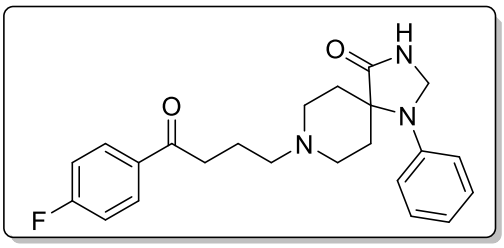

31 (1.40 g, 6.0 mmol, 1 eq), 4-chloro-1-(4-fluorophenyl)butan-1-one (1.79 g, 9.0 mmol, 1.5 eq), NaI (1.35 g, 9.0 mmol, 1.5 eq) and triethylamine (0.91 g, 9.0 mmol, 1.5 eq) were suspended in MeCN (35 mL) and refluxed under argon atmosphere overnight. After cooling to room temperature the solvent was evaporated. The resulting crude residue was dissolved in DCM (35 mL) and washed with aqueous KOH (20%, 20 mL). The organic layer was dried over Na_2SO_4 and concentrated under reduced pressure. The residue was dissolved in DCM (20 mL) and the solution was added dropwise to cold hexane (120 mL). The gray precipitate was filtered and dried in vacuo to give **32** as brown oil (1.31 g, 55%). ^{1}H NMR (400 MHz, DMSO-d_6) δ 8.58 (s, 1H), 8.10 – 8.01 (m, 2H), 7.39 – 7.29 (m, 2H), 7.24 – 7.10 (m, 3H), 6.79 – 6.68 (m, 3H), 4.54 (s, 2H), 3.02 (t, J = 6.9 Hz, 2H), 2.75 – 2.59 (m, 4H), 2.48 – 2.33 (m, 5H), 1.88 – 1.74 (m, 2H), 1.56 – 1.46 (m, 2H). ^{13}C NMR (101 MHz, DMSO-d_6) δ 199.10, 176.67, 164.8 (d, J = 251.0 Hz), 143.82, 131.29 (d, J = 9.4 Hz), 129.42, 118.05, 116.10 (d, J = 21.7 Hz), 114.71, 114.39, 59.09, 58.74, 57.63, 49.68, 36.39, 28.86, 22.05. HRMS (ESI-MS): m/z $[M+H]^+$ calculated for $C_{23}H_{27}FN_3O_2^+$: 396.2082, found 396.2087; $C_{23}H_{26}FN_3O_2$ (395.48).

tert-Butyl (4-(2-hydroxyethyl)phenyl)carbamate (33) [203]

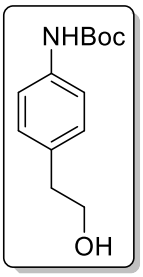

Di-tert-butyl dicarbonate (1.75 g, 8.0 mmol, 1.1 eq) was dissolved in EtOAc (20 mL) and added dropwise to a suspension of 2-(4-aminophenyl)ethan-1-ol (1.00 g, 7.3 mmol, 1 eq) in EtOAc (10 mL). After the reaction was stirred at room temperature overnight the solvent was evaporated. The resulting crude product was purified by column chromatography (DCM/MeOH 95/5) to afford **33** (1.48 g, 86%) as a white foam like solid. ^{1}H NMR (300 MHz, $CDCl_3$) δ 7.33 – 7.25 (m, 2H), 7.17 – 7.07 (m, 2H), 6.59 (bs, 1H), 3.79 (t, J = 6.6 Hz, 2H), 2.80 (t, J = 6.6 Hz, 2H), 1.51 (s, 9H). ^{13}C NMR (75 MHz, $CDCl_3$) δ 152.97, 136.80, 133.13, 129.54, 118.99, 80.50, 63.71, 38.49, 28.37. HRMS (ESI-MS): m/z $[M+H]^+$ calculated for $C_{13}H_{20}NO_3^+$: 238.1438, found 238.1437; $C_{13}H_{19}NO_3$ (237.30).

tert-Butyl (4-(2-bromoethyl)phenyl)carbamate (34) [203]

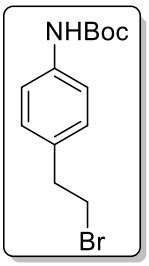

To a cooled solution of **33** (1.48 g, 6.3 mmol, 1 eq) in DCM (30 mL) triphenyl phosphine (2.50 g, 9.5 mmol, 1.5 eq) and N-bromosuccinimide (1.71 g, 9.5 mmol, 1.5 eq) were added. The mixture was stirred for 2 h while maintaining the temperature at 0 °C. Then, the solvent was evaporated and the resulting residue was purified by column chromatography (DCM/MeOH 99/1) to afford **34** (1.68 g, 88%) as a white solid. ^{1}H NMR (300 MHz, $CDCl_3$) δ 7.36 – 7.25 (m, 2H), 7.17 – 7.08 (m, 2H), 6.47 (bs, 1H), 3.52 (t, *J* = 7.6 Hz, 2H), 3.10 (t, *J* = 7.6 Hz, 2H), 1.51 (s, 9H). ^{13}C NMR (101 MHz, $CDCl_3$) δ 152.76, 137.17, 133.55, 129.84, 129.23, 124.88, 118.78, 38.77, 33.12, 28.35. HRMS (ESI-MS): m/z $[M+H]^+$ calculated for $C_{13}H_{19}BrNO_2^+$: 300.0594, found 300.0593; $C_{13}H_{18}BrNO_2$ (300.20).

tert-Butyl (4-(2-(8-(4-(4-fluorophenyl)-4-oxobutyl)-4-oxo-1-phenyl-1,3,8-triazaspiro[4.5]decan-3-yl)ethyl)phenyl)carbamate (35) [203]

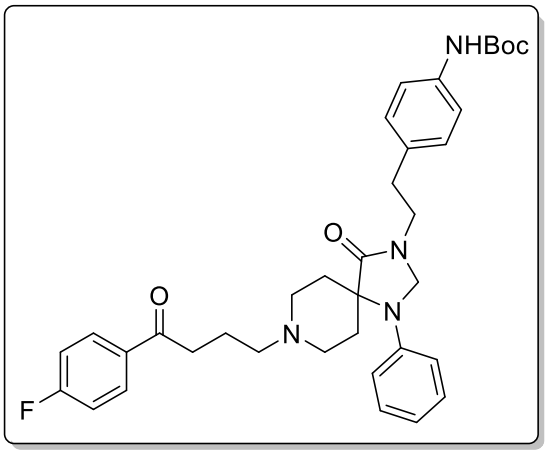

A mixture of **32** (0.79 g, 2.0 mmol, 1 eq), potassium hydroxide (0.056 g, 1.0 mmol, 0.5 eq), potassium carbonate (1.09 g, 8.0 mmol, 4 eq) and tetrabutylammonium bisulfate (0.20 g, 0.6 mmol, 0.3 eq) was suspended in anhydrous toluene (40 mL) and stirred for 30 min under argon atmosphere. Then, a solution of **34** (1.21 g, 4.0 mmol, 2 eq) in anhydrous toluene (25 mL) was added dropwise over 30 min. The reaction was stirred at 90 °C for 2 days. After that, the reaction was allowed to cool to room temperature and the solvent was evaporated. The resulting crude residue was dissolved in DCM (40 mL) and washed with aqueous KOH (20%, 20 mL). The organic layer was dried over Na_2SO_4 and concentrated under reduced pressure. The residue was purified by column chromatography (DCM/MeOH 95/5) to afford **35** (0.41 g, 35%) as a white foam. ^{1}H NMR (400 MHz, $CDCl_3$) δ 8.03 – 7.96 (m, 2H), 7.30 – 7.21 (m, 4H), 7.16 – 7.08 (m, 4H), 6.90 – 6.80 (m, 3H), 6.48 (s, 1H), 4.52 (s, 2H), 3.63 (t, *J* = 7.1 Hz, 2H), 3.15 – 2.49 (m, 12H), 2.09 – 1.96 (m, 2H), 1.54 – 1.49 (m, 2H), 1.48 (s, 9H). ^{13}C NMR (75 MHz, $CDCl_3$) δ 198.38, 174.13, 167.37, 163.99, 152.84, 142.80, 137.16, 133.51, 133.47, 132.49, 130.79, 130.67, 129.30, 129.21, 119.00, 118.86, 115.82, 115.54, 115.37, 80.48, 63.80, 60.28, 57.47,

49.43, 42.21, 36.33, 33.02, 28.92, 28.36, 21.32. HRMS (ESI-MS): m/z $[M+H]^+$ calculated for $C_{36}H_{44}FN_4O_4^+$: 615.3341, found 615.3347; $C_{36}H_{43}FN_4O_4$ (614.76).

3-(4-Aminophenethyl)-8-(4-(4-fluorophenyl)-4-oxobutyl)-1-phenyl-1,3,8-triazaspiro[4.5]decan-4-one (36) [203]

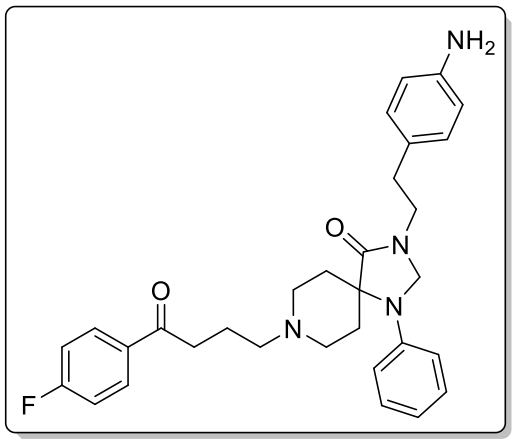

35 (0.41 g, 0.7 mmol) was dissolved in DCM (30 mL) and TFA (5 mL) was added. The mixture was stirred at room temperature overnight. After the reaction was complete, as indicated by TLC, the solution was basified with aqueous KOH (20%). The organic phase was separated, dried over Na_2SO_4 and concentrated under reduced pressure. The residue was purified by column chromatography to yield **36** (0.28 g, 83%) as a yellow oil. ^{1}H NMR (400 MHz, $CDCl_3$) δ 8.06 – 7.98 (m, 2H), 7.28 – 7.19 (m, 2H), 7.16 – 7.10 (m, 2H), 7.03 – 6.96 (m, 2H), 6.87 – 6.79 (m, 3H), 6.67 – 6.57 (m, 2H), 4.52 (s, 2H), 3.66 – 3.54 (m, 2H), 3.04 (t, *J* = 7.1 Hz, 2H), 2.97 – 2.53 (m, 10H), 2.08 – 1.97 (m, 2H), 1.55 (d, *J* = 14.1 Hz, 2H).^{13}C NMR (101 MHz, $CDCl_3$) δ 198.01, 173.84, 165.72 (d, *J* = 254.5 Hz), 145.17, 142.68, 133.39, 130.71 (d, *J* = 9.2 Hz), 129.53, 129.35, 127.62, 119.02, 115.7 (d, *J* = 21.9 Hz), 115.31, 115.14, 63.75, 59.96, 57.22, 49.26, 42.31, 36.10, 32.82, 28.56, 20.89. HRMS (ESI-MS): m/z $[M+H]^+$ calculated for $C_{31}H_{36}FN_4O_2^+$: 515.2817, found 515.2820; $C_{31}H_{35}FN_4O_2$ (514.65).

N^1-(4-(2-(8-(4-(4-Fluorophenyl)-4-oxobutyl)-4-oxo-1-phenyl-1,3,8-triazaspiro[4.5]decan-3-yl)ethyl)phenyl)-N^4-(prop-2-yn-1-yl)succinamide (37)

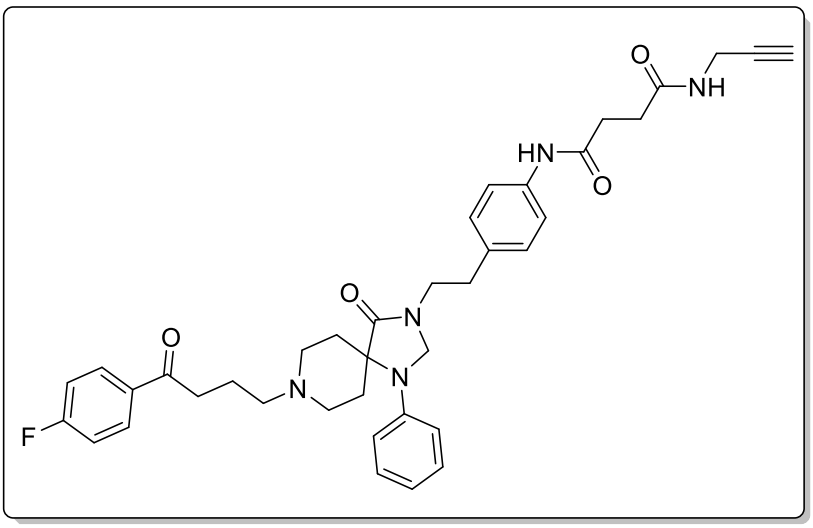

To a solution of **36** (0.14 g, 0.27 mmol, 1 eq) in DMF (20 mL) succinic anhydride (0.028 g, 0.27 mmol, 1 eq) was added and the reaction was stirred at room temperature overnight. After the reaction was complete, as indicated by TLC, HATU (0.16 g, 0.41 mmol, 1.5 eq), DIPEA (0.10 g, 0.8 mmol, 3 eq) and propargylamine (0.02 g, 0.353 mmol, 1.3 eq) were added. Then, the mixture was stirred for 10 h at room temperature. The solvent was evaporated and the residue was purified by column chromatography (DCM/MeOH 95/5). **37** (0.13 g, 73%) was obtained as a brown oil. ^{1}H NMR (400 MHz, CD_3OD) δ 8.11 – 8.01 (m, 2H), 7.45 (d, *J* = 8.5 Hz, 2H), 7.25 – 7.16 (m, 6H), 6.91 (d, *J* = 8.1 Hz, 2H), 6.84 (t, *J* = 7.3 Hz, 1H), 4.57 (s, 2H), 3.93 (d, *J* = 2.5 Hz, 2H), 3.66 (t, *J* = 7.0 Hz, 2H), 3.07 – 2.97 (m, 1H), 2.95 – 2.88 (m, 2H), 2.86 – 2.75 (m, 4H), 2.69 – 2.59 (m, 2H), 2.57 – 2.35 (m, 7H), 1.99 – 1.87 (m, 2H), 1.49 (d, *J* = 14.1 Hz, 2H). ^{13}C NMR (101 MHz, CD_3OD) δ 208.75, 198.05, 173.45, 172.82, 172.82, 171.43, 165.89 (d, J=253.3 Hz), 142.61, 137.11, 133.79, 133.29, 130.67 (d, *J* = 9.5 Hz), 129.08, 128.98, 120.60, 120.05, 117.77, 115.28 (d, *J* = 22.2 Hz), 79.24, 77.91, 70.80, 63.62, 59.37, 56.55, 49.08, 48.46, 42.39, 41.30, 32.28, 31.26, 30.33, 30.11, 29.29, 28.09, 27.75, 19.12, 18.32, 11.79. HRMS (ESI-MS): m/z $[M+H]^+$ calculated for $C_{38}H_{43}FN_5O_4^+$: 652.3294, found 652.3305; $C_{38}H_{42}FN_5O_4$ (651.78).

_N_-(4-(2-(8-(4-(4-fluorophenyl)-4-oxobutyl)-4-oxo-1-phenyl-1,3,8-triazaspiro[4.5]decan-3-yl)ethyl)phenyl)acetamide dihydrotrifluoroacetate (38)

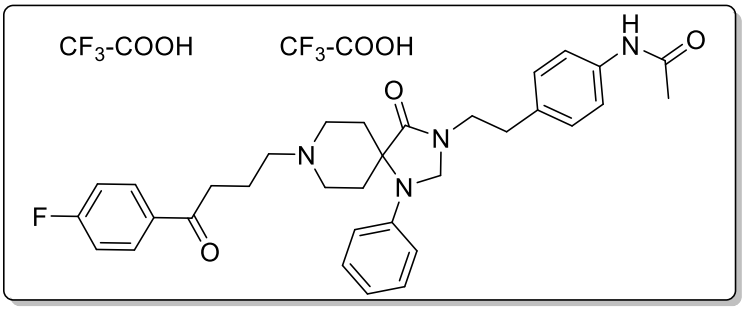

36 (15 mg, 0.03 mmol, 1 eq) and triethylamine (50 mg, 0.05 mmol, 1.7 eq) were dissolved in DCM (15 mL) and acetyl chloride (3.5 mg, 0.045 mmol, 1.5 eq), dissolved in DCM (15 mL), was added dropwise at 0 °C. After the reaction was stirred at room temperature overnight the solvent was evaporated and the crude product was purified by preparative HPLC. A yellow resin was obtained for **38** (6.24 mg, 26%). ^{1}H NMR (400 MHz, CD_3OD) δ 8.12 – 8.02 (m, 2H), 7.44 (d, *J* = 8.4 Hz, 2H), 7.33 – 7.19 (m, 6H), 7.00 – 6.89 (m, 3H), 4.67 (s, 2H), 3.77 – 3.61 (m, 4H), 3.51 – 3.42 (m, 2H), 3.23 – 3.14 (m, 4H), 2.96 (t, *J* = 6.8 Hz, 2H), 2.58 (td, *J* = 14.5, 4.7 Hz, 2H), 2.16 – 2.05 (m, 5H), 1.76 (d, *J* = 14.9 Hz, 2H). ^{13}C NMR (101 MHz, CD_3OD) δ 197.21, 172.72, 170.23, 167.24, 142.16, 137.07, 133.94, 133.07, 130.62 (d, *J* = 9.4 Hz), 129.08, 120.84, 120.24, 117.72, 115.30 (d, *J* = 22.2 Hz), 63.44, 58.43, 56.32, 49.17, 41.31, 34.46, 32.26, 27.42, 22.33, 18.20. HRMS (ESI-MS): m/z $[M+H]^+$ calculated for $C_{33}H_{38}FN_4O_3^+$: 557.2922, found 557.2937. Anal. RP-HPLC (220 nm): 98% (t_R= 13.39 min, *k* = 3.17). $C_{33}H_{37}FN_4O_3$ x $C_4H_2F_6O_4$ (556.68 + 228.05).

4-(3-Chloropropoxy)benzaldehyde (39) [211]

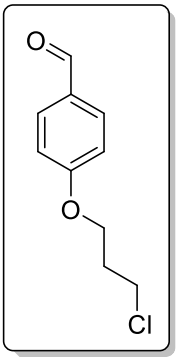

4-Hydroxybenzaldehyde (3.00 g, 24.5 mmol, 1 eq), K_2CO_3 (10.20 g, 73.1 mmol, 3 eq) and 1-bromo-3-chloropropane (6.70 g, 42.55 mmol, 1.7 eq) were suspended in MeCN (100 mL) and stirred at 85 °C overnight. After cooling to room temperature the solid was filtered off and the filtrate was concentrated under reduced pressure. The residue was dissolved in EtOAc (50 mL) and washed with water (2 x 30 mL) and brine (1 x 30 mL). The organic phase was dried over Na_2SO_4 and the solvent was evaporated. The crude product was purified by column chromatography (PE/EA 9/1) to yield **39** (4.14 g, 85%) as a yellow oil. ^{1}H NMR (300 MHz, $CDCl_3$) δ 9.89 (s, 1H), 7.88 – 7.80 (m, 2H), 7.05 – 6.98 (m, 2H), 4.21 (t, 2H), 3.76 (t, 2H), 2.32 – 2.22 (m, 2H). ^{13}C NMR (75 MHz, $CDCl_3$) δ 190.83, 163.73, 132.04, 130.11, 114.77, 64.60, 41.24, 31.99. HRMS (EI-MS): m/z $[M^{\cdot+}]$ calculated for $C_{10}H_{11}ClO_2^{\cdot+}$: 198.0448, found 198.0443; $C_{10}H_{11}ClO_2$ (198.65).

4-(3-(Piperidin-1-yl)propoxy)benzaldehyde (40) [211]

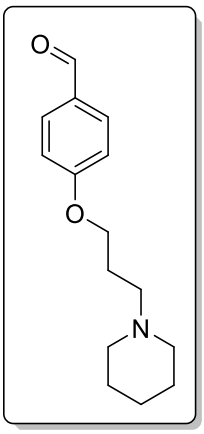

A suspension of **39** (4.00 g, 20.1 mmol, 1 eq), NaI (1.51 g, 10.1 mmol, 0.5 eq), Na_2CO_3 (3.20 g, 30.2 mmol, 1.5 eq) and piperidine (1.71 g, 20.1 mmol, 1 eq) in MeCN (50 mL) was stirred at 85 °C for 20 h. After the solvent was evaporated the residue was dissolved in DCM (40 mL) and washed with water (3 x 30 mL). The organic layer was dried over Na_2SO_4 and concentrated under reduced pressure. The crude product was purified by column chromatography (DCM/MeOH 95/5) to afford **40** (4.50 g, 88%) as a red oil. ^{1}H NMR (300 MHz, $CDCl_3$) δ 9.87 (s, 1H), 7.86 – 7.76 (m, 2H), 7.04 – 6.93 (m, 2H), 4.09 (t, *J* = 6.4 Hz, 2H), 2.57 – 2.35 (m, 6H), 2.08 – 1.97 (m, 2H), 1.65 – 1.57 (m, 4H), 1.49 – 1.40 (m, 2H). ^{13}C NMR (75 MHz, $CDCl_3$) δ 190.72, 164.19, 131.87, 129.72, 114.79, 66.84, 55.75, 54.64, 26.43, 25.76, 24.32. HRMS (ESI-MS): m/z $[M+H]^+$ calculated for $C_{15}H_{22}NO_2^+$: 248.1645, found 248.1647; $C_{15}H_{21}NO_2$ (247.34).

Ethyl 1-(4-(3-(piperidin-1-yl)propoxy)benzyl)piperidine-4-carboxylate (41) [244]

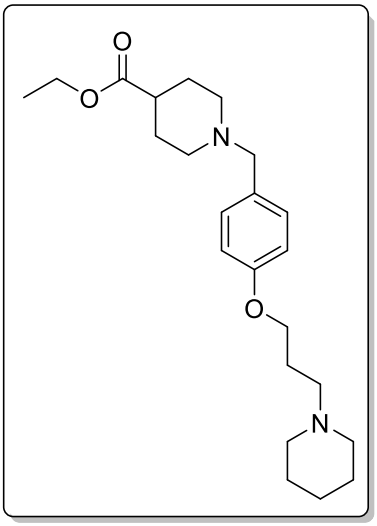

To a solution of **40** (4.00 g, 16.0 mmol, 1 eq) in DCM (75 mL) ethyl piperidine-4-carboxylate (2,71 g, 17.6 mmol, 1.1 eq) and $NaBH(OAc)_3$ (3.72 g, 17.6 mmol, 1.1 eq) were added. After the reaction was stirred at room temperature overnight aqueous KOH (20%) was added. The organic layer was separated and dried over Na_2SO_4. The solvent was removed under reduced pressure and the resulting residue was purified by column chromatography (DCM/MeOH 95/5). **41** was obtained as a yellow oil (4.21 g, 67%). ^{1}H NMR (300 MHz, $CDCl_3$) δ 7.21 – 7.13 (m, 2H), 6.86 – 6.76 (m, 2H), 4.09 (q, *J* = 7.1 Hz, 2H), 3.96 (t, *J* = 6.4 Hz, 2H), 3.39 (s, 2H), 2.87 – 2.74 (m, 2H), 2.51 – 2.31 (m, 6H), 2.29 – 2.17 (m, 1H), 2.02 – 1.90 (m, 4H), 1.88 – 1.79 (m, 2H), 1.79 – 1.68 (m, 2H), 1.61 – 1.51 (m, 4H), 1.48 – 1.36 (m, 2H), 1.21 (t, *J* = 7.1 Hz, 3H). ^{13}C NMR (75 MHz, $CDCl_3$) δ 175.25, 158.12, 130.22, 114.14, 66.43, 62.65, 60.22, 56.04, 54.62, 52.79, 41.26, 28.29, 26.82, 25.91, 24.40, 14.23. HRMS (ESI-MS): m/z $[M+H]^+$ calculated for $C_{23}H_{37}N_2O_3^+$: 389.2799, found 389.2800; $C_{23}H_{36}N_2O_3$ (388.55).

1-(4-(3-(Piperidin-1-yl)propoxy)benzyl)piperidine-4-carboxylic acid dihydrochloride (42) [244]

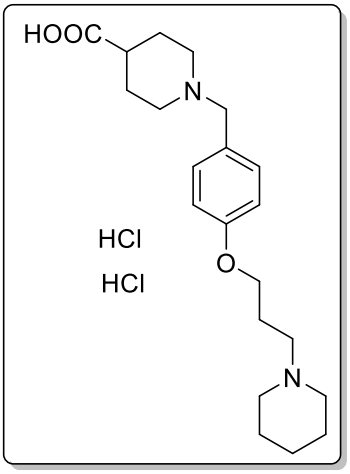

41 (2.06 g, 5.3 mmol) was dissolved in THF (40 mL) and 2 N aqueous HCl (50 mL) was added. The mixture was stirred at room temperature until the starting material was consumed. The solvent mas removed under reduced pressure and the residue was dried in vacuo. **42** (2.11 g, 91%) was obtained as a brown oil. ^{1}H NMR (300 MHz, CD_3OD) δ 7.55 – 7.46 (m, 2H), 7.09 – 6.98 (m, 2H), 4.27 (s, 2H), 4.14 (t, *J* = 5.8 Hz, 2H), 3.64 – 3.56 (m, 2H), 3.56 – 3.44 (m, 2H), 3.31 – 3.26 (m, 2H), 3.14 – 2.92 (m, 4H), 2.72 – 2.57 (m, 1H), 2.35 – 1.77 (m, 12H). ^{13}C NMR (101 MHz, CD_3OD) δ 173.56, 159.90, 132.78, 121.16, 114.77, 64.91, 59.74, 54.41, 53.05, 51.02, 38.23, 25.34, 23.76, 22.90, 21.33. HRMS (ESI-MS): m/z $[M+H]^+$ calculated for $C_{21}H_{33}N_2O_3^+$: 361.2486, found 361.2490; $C_{21}H_{32}N_2O_3$ x H_2Cl_2 (360.50 + 72.92).

1-(4-(3-(Piperidin-1-yl)propoxy)benzyl)-N-(prop-2-yn-1-yl)piperidine-4-carboxamide (43) [244]

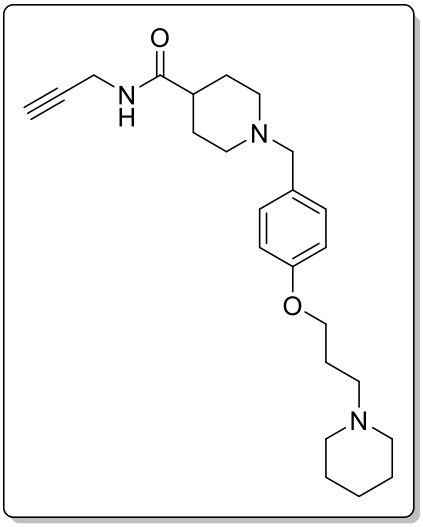

A solution of **42** (0.21 g, 0.5 mmol, 1 eq), 1-ethyl-3-(3-dimethylaminopropyl)carbodiimide (0.10 g, 0.55 mmol, 1.1 eq), 1-hydroxybenzotriazole (0.07 g, 0.55 mmol, 1.1 eq) and DIPEA (0.25 g, 2.0 mmol, 4 eq) in DMF/DCM (1/1, 20 mL) was stirred in a microwave vial at room temperature. After 25 min propargylamine (32 ul, 0.5 mmol, 1 eq) was added and the reaction was stirred in a microwave reactor (sealed vial) at 100 °C for 20 min. After the solution was cooled to room temperature water (10 mL) was added. The organic layer was separated and dried over Na_2SO_4. The solvent was removed under reduced pressure and the crude product was purified by column chromatography (DCM/MeOH 9/1 + 0.1% NH_3). **43** (80 mg, 40%) was obtained as a yellow solid. ^{1}H NMR (3ag00 MHz, $CDCl_3$) δ 7.22 – 7.16 (m, 2H), 6.87 – 6.80 (m, 2H), 5.64 (bt, *J* = 4.9 Hz, 1H), 4.04 (dd, *J* = 5.1, 2.6 Hz, 2H), 3.98 (t, *J* = 6.4 Hz, 2H), 3.42 (s, 2H), 2.96 – 2.86 (m, 2H), 2.52 – 2.32 (m, 6H), 2.22 (t, *J* = 2.6 Hz, 1H), 2.16 – 2.04 (m, 1H), 2.02 – 1.89 (m, 4H), 1.85 – 1.77 (m, 4H), 1.64 – 1.54 (m, 4H), 1.48 – 1.38 (m, 2H). ^{13}C NMR (75 MHz, $CDCl_3$) δ 174.76, 158.16, 130.24, 130.12, 114.19, 79.69, 71.63, 66.52, 62.57,

56.07, 54.66, 52.91, 43.20, 29.14, 28.80, 26.87, 25.98, 24.45. HRMS (ESI-MS): m/z $[M+H]^+$ calculated for $C_{24}H_{36}N_3O_2^+$: 398.2802, found 398.2810; $C_{24}H_{35}N_3O_2$ (397.56).

1-Benzylpiperidin-4-one oxime (44) [212]

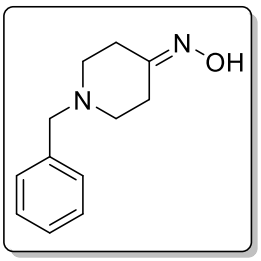

To a suspension of K_2CO_3 (14.60 g, 105.7 mmol, 2 eq) and hydroxylamine hydrochloride (7.34 g, 105.7 mmol, 105.7 eq) in EtOH (120 mL) benzylpiperidinone (10.00 g, 52.8 mmol, 1 eq) was added and the reaction was heated to reflux and continued stirring for 3 h. The solid was filtered off and the filtrate was concentrated under reduced pressure. The resulting residue was dissolved in DCM (75 mL) and washed three times with aqueous KOH (20%, 3 x 30 mL)). The organic layer was dried over Na_2SO_4 and the solvent was removed under reduced pressure. **44** (9.28 g, 86%) was obtained as a white powder. ^{1}H NMR (300 MHz, $CDCl_3$) δ 8.87 (s, 1H), 7.37 – 7.22 (m, 5H), 3.57 (s, 2H), 2.67 (t, *J* = 5.7 Hz, 2H), 2.61 – 2.49 (m, 4H), 2.37 (t, *J* = 5.8 Hz, 2H). ^{13}C NMR (75 MHz, $CDCl_3$) δ 158.14, 138.14, 129.10, 128.33, 127.21, 62.59, 53.51, 52.29, 31.50, 24.43. HRMS (EI-MS): m/z $[M^{\cdot+}]$ calculated for $C_{12}H_{16}N_2O^{\cdot+}$: 204.1257, found 204.1522; $C_{12}H_{16}N_2O$ (204.27).

1-Benzylpiperidin-4-amine (45) [212]

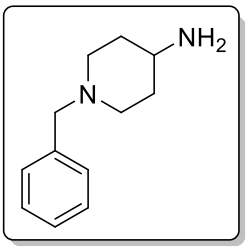

A suspension of $LiAlH_4$ (1.93 g, 51.0 mmol, 2.6 eq) in THF (20 mL) was added to a solution of **44** (4.00 g, 19.6 mmol, 1 eq) in THF (40 mL) at 0 °C. The mixture was heated to reflux and continued stirring overnight. The reaction was then quenched with 2 mL aqueous HCl (2 N) while maintaining the temperature at 0 °C. The resulting precipitate was filtered through celite and the filtrate was concentrated under reduced pressure. The residue was dissolved in DCM (40 mL) and washed three times with aqueous KOH (20%, 3 x 20 mL). The organic layer was dried over Na_2SO_4 and the solvent was removed in vacuo to give **45** (3.13 g, 86%) as a yellow oil. ^{1}H NMR (300 MHz, $CDCl_3$) δ 7.32 – 7.29 (m, 4H), 7.26 – 7.19 (m, 1H), 3.49 (s, 2H), 2.86 – 2.77 (m, 2H), 2.64 – 2.51 (m, 1H), 2.01 (td, *J* = 11.6, 2.5 Hz, 2H), 1.82 – 1.72 (m, 2H), 1.46 – 1.26 (m, 4H). ^{13}C NMR (75 MHz, $CDCl_3$) δ 138.61, 129.15, 128.18, 126.94, 63.13, 52.50, 48.84, 36.07, 32.75. HRMS (ESI-MS): m/z $[M+H]^+$ calculated for $C_{12}H_{19}N_2^+$: 191.1543, found 191.1545; $C_{12}H_{18}N_2$ (190.29).

tert-Butyl (1-benzylpiperidin-4-yl)carbamate (46)

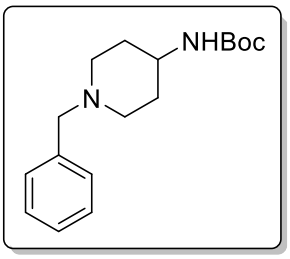

Boc_2O (4.04 g, 18.5 mmol, 1.1 eq) was added to a solution of **45** (3.20 g, 16.8 mmol, 1 eq) and TEA (2.57 g, 25.2 mmol, 1.5 eq) in DCM (75 mL). After the reaction was stirred overnight aqueous saturated $NaHCO_3$ (30 mL) was added and the organic layer was separated and washed with brine (30 mL). The organic phase was dried over Na_2SO_4 and the solvent was removed under reduced pressure. The residue was purified by column chromatography (DCM/MeOH 9/1 + 0.1% NH_3) to yield a yellow oil for **46** (4.47 g, 91%). ^{1}H NMR (300 MHz, $CDCl_3$) δ 7.35 – 7.21 (m, 5H), 4.45 (d, *J* = 6.3 Hz, 1H), 3.55 – 3.38 (m, 3H), 2.79 (d, *J* = 12.0 Hz, 2H), 2.07 (td, *J* = 11.7, 2.5 Hz, 2H), 1.95 – 1.87 (m, 2H), 1.52 (s, 2H), 1.44 (s, 9H). ^{13}C NMR (75 MHz, $CDCl_3$) δ 155.22, 138.47, 129.13, 128.23, 127.03, 79.23, 63.13, 52.38, 47.80, 32.67, 28.45. HRMS (ESI-MS): m/z $[M+H]^+$ calculated for $C_{17}H_{27}N_2O_2^+$: 291.2067, found 291.2070; $C_{17}H_{26}N_2O_2$ (290.41).

tert-Butyl piperidin-4-ylcarbamate (47) [245]

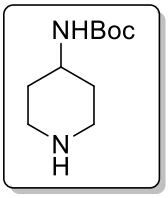

A mixture of **46** (4.47 g, 15.4 mmol, 1 eq) and a catalytic amount of palladium on activated charcoal (10% Pd basis) in MeOH (50 mL) was stirred at 55 °C for 12 h under H_2-atmosphere. The reaction was then filtered through celite and the filtrate was concentrated in vacuo to give **47** (3.00 g, 97%) as a white powder. ^{1}H NMR (300 MHz, $CDCl_3$) δ 4.48 (s, 1H), 3.56 – 3.44 (m, 1H), 3.06 (dt, *J* = 12.5, 3.2 Hz, 2H), 2.65 (td, *J* = 12.4, 2.4 Hz, 2H), 1.97 – 1.87 (m, 2H), 1.43 (s, 9H), 1.35 – 1.22 (m, 2H). ^{13}C NMR (75 MHz, $CDCl_3$) δ 155.14, 79.20, 48.12, 45.43, 33.92, 28.42. HRMS (ESI-MS): m/z $[M+H]^+$ calculated for $C_{10}H_{21}N_2O_2^+$: 201.1598, found 201.1601; $C_{10}H_{20}N_2O_2$ (200.28).

tert-Butyl (1-(4-(3-(piperidin-1-yl)propoxy)benzyl)piperidin-4-yl)carbamate (48)

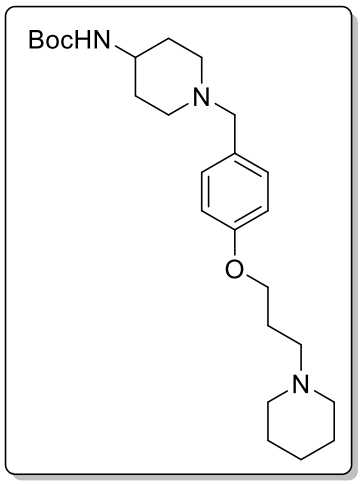

To a solution of **40** (4.50 g, 18.2 mmol, 1 eq) in DCM (50 mL) **47** (4.00 g, 20.06 mmol, 1.1 eq) and $NaBH(OAc)_3$ (5.01 g, 23.6 mmol, 1.3 eq) were added. After the reaction was stirred at room temperature overnight aqueous KOH (20%, 30 mL) was added. The organic layer was separated and dried over Na_2SO_4. The solvent was removed under reduced pressure and the resulting residue was purified by column chromatography (DCM/MeOH 95/5). **48** (5.63 g, 72%) was obtained as a yellow oil. ^{1}H NMR (300 MHz, $CDCl_3$) δ 7.21 – 7.15 (m, 2H), 6.86 – 6.80 (m, 2H), 4.42 (s, 1H), 3.98 (t, *J* = 6.4 Hz, 2H), 3.50 – 3.41 (m, 1H), 3.40 (s, 2H), 2.77 (d, *J* = 11.7 Hz, 2H), 2.51 – 2.34 (m, 6H), 2.10 – 1.93 (m, 4H), 1.93 – 1.85 (m, 2H), 1.62 – 1.54 (m, 4H), 1.46 – 1.35 (m, 13H). ^{13}C NMR (75 MHz, $CDCl_3$) δ 158.18, 155.35, 130.27, 114.20, 77.23, 73.62, 66.54, 62.51, 56.07, 54.68, 52.21, 32.67, 28.44, 26.91, 26.02, 24.47. HRMS (ESI-MS): m/z $[M+H]^+$ calculated for $C_{25}H_{42}N_3O_3^+$: 432.3221, found 432.3226; $C_{25}H_{41}N_3O_3$ (431.62).

1-(4-(3-(Piperidin-1-yl)propoxy)benzyl)piperidin-4-amine (49)

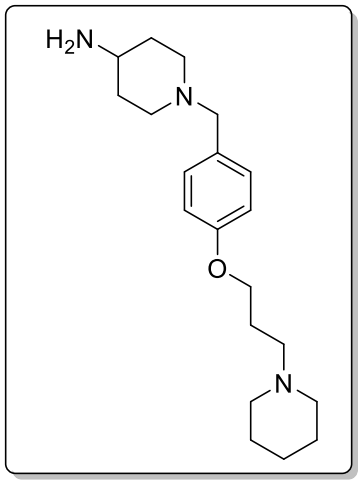

48 (5.40 g, 12.5 mmol) was dissolved in DCM (100 mL) and TFA (20 mL) was added. The reaction was stirred at room temperature until the starting material was consumed, indicated by TLC. The reaction was then poured into ice water and basified with aqueous KOH (20%). The mixture was extracted three times with DCM (3 x 30 mL). The organic layers were combined and dried over Na_2SO_4. The solvent was removed under reduced pressure and the crude product was purified by column chromatography (DCM/MeOH 9/1 + 0.1% NH_3) to give **49** as a yellow oil (3.00 g, 73%). ^{1}H NMR (300 MHz, $CDCl_3$) δ 7.22 – 7.15 (m, 2H), 6.89 – 6.78 (m, 2H), 3.98 (t, *J* = 6.4 Hz, 2H), 3.42 (s, 2H), 2.80 (dt, *J* = 5.4, 2.4 Hz, 2H), 2.69 – 2.56 (m, 1H), 2.51 – 2.29 (m, 6H), 2.04 – 1.90 (m, 4H), 1.77 (d, *J* = 12.8 Hz, 2H), 1.63 – 1.54 (m, 4H), 1.50 – 1.29 (m, 6H). ^{13}C NMR (75 MHz, $CDCl_3$) δ 158.12, 130.37, 130.32, 114.14, 66.51, 62.50, 56.08, 54.66, 52.34, 48.86, 36.06, 26.89, 25.99, 24.46. HRMS (ESI-MS): m/z $[M+H]^+$ calculated for $C_{20}H_{34}N_3O^+$: 332.2696, found 332.2700; $C_{20}H_{33}N_3O$ (331.50).

2-Chloro-*N*-(1-(4-(3-(piperidin-1-yl)propoxy)benzyl)piperidin-4-yl)acetamide (50)

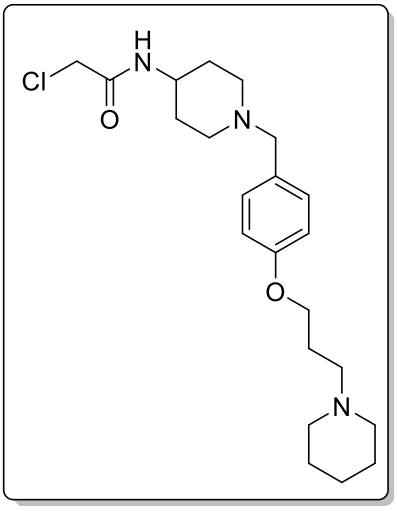

2-Chloroacetyl chloride (0.20 g, 1.8 mmol, 1.2 eq) was dissolved in DCM (20 mL) and added dropwise to a solution of **49** (0.50 g, 1.5 mmol, 1 eq) and TEA (0.20 g, 2.0 mmol, 1.3 eq) in DCM (30 mL). The reaction was stirred at room temperature for 4 h. Aqueous NaOH (1 M, 30 mL) was added and the organic layer was separated and dried over Na_2SO_4. The solution was concentrated under reduced pressure and the residue was purified by column chromatography (DCM/MeOH 9/1 + 0.1% NH_3) to give **50** as a brown solid (0.51 g, 82%). ^{1}H NMR (300 MHz, $CDCl_3$) δ 7.22 – 7.16 (m, 2H), 6.87 – 6.80 (m, 2H), 6.43 (d, *J* = 7.4 Hz, 1H), 4.03 (s, 2H), 3.99 (t, *J* = 6.3 Hz, 2H), 3.90 – 3.76 (m, 1H), 3.49 (s, 2H), 2.80 (dt, *J* = 7.1, 3.9 Hz, 2H), 2.63 – 2.38 (m, 6H), 2.15 – 1.99 (m, 4H), 1.91 – 1.80 (m, 2H), 1.68 – 1.60 (m, 4H), 1.59 – 1.39 (m, 4H). ^{13}C NMR (75 MHz, $CDCl_3$) δ 165.26, 157.94, 130.46, 129.90, 114.20, 65.78, 62.17, 55.65, 54.05, 51.79, 46.86, 42.70, 31.62, 25.44, 24.37, 23.34. HRMS (ESI-MS): m/z $[M+2H]^{2+}$ calculated for $C_{22}H_{36}ClN_3O_2^{2+}$: 204.6243, found 204.6247; $C_{22}H_{34}ClN_3O_2$ (407.98).

2-Azido-*N*-(1-(4-(3-(piperidin-1-yl)propoxy)benzyl)piperidin-4-yl)acetamide (51)

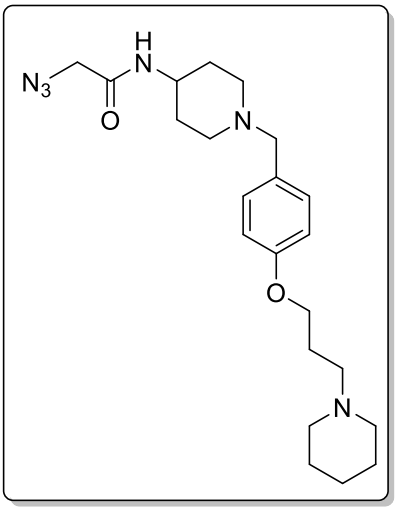

NaN_3 (0.1 g, 1.4 mmol, 2 eq) was added to a solution of **50** (0.28 g, 0.7 mmol, 1 eq) in DMF (20 mL) and the mixture was stirred at 80 °C for 14 h. The reaction was quenched with water and extracted three times with diethylether (3 x 20 mL). The organic layers were combined and dried over Na_2SO_4. The solvent was removed under reduced pressure and the residue was purified by column chromatography (DCM/MeOH 9/1 + 0.1% TEA) to afford **51** as an orange solid (0.27 g, 95%). ^{1}H NMR (300 MHz, $CDCl_3$) δ 7.23 – 7.14 (m, 2H), 6.87 – 6.80 (m, 2H), 6.15 (d, *J* = 8.0 Hz, 1H), 4.02 – 3.93 (m, 4H), 3.89 – 3.72 (m, 1H), 3.42 (s, 2H), 2.79 (d, *J* = 12.0 Hz, 2H), 2.51 – 2.31 (m, 6H), 2.09 (td, *J* = 11.7, 2.2 Hz, 2H), 2.02 – 1.75 (m, 6H), 1.63 – 1.54 (m, 4H), 1.47 – 1.41 (m, 2H). ^{13}C NMR (75 MHz, $CDCl_3$) δ 165.72, 158.23, 130.24, 130.18, 114.23, 66.55, 62.42, 56.06, 54.68, 52.77, 51.99, 46.74, 32.09, 26.92, 26.02,

24.48. HRMS (ESI-MS): m/z $[M+2H]^{2+}$ calculated for $C_{22}H_{36}N_6O_2^{2+}$: 208.1444, found 208.1450; $C_{22}H_{34}N_6O_2$ (414.55).

Dimethyl isophthalate (52) [246]

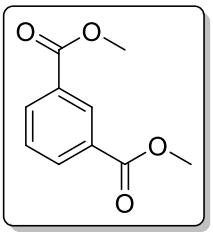

Isophthalic acid (3.00 g, 18.0 mmol) was dissolved in MeOH (50 mL) and four drops of H_2SO_4 (96% w/w) were added. The mixture was heated to reflux, continued stirring overnight and was concentrated under reduced pressure the next morning. Aqueous HCl (1 N, 30 mL) was added to the residue and the aqueous phase was extracted three times with diethylether (3 x 30 mL). The organic phase was dried over Na_2SO_4 and the solvent was removed in vacuo to give **52** as a white powder (3.29 g, 94%). ^{1}H NMR (300 MHz, $CDCl_3$) δ 8.72 – 8.64 (m, 1H), 8.23 (dd, *J* = 7.8, 1.8 Hz, 2H), 7.53 (t, *J* = 8.0 Hz, 1H), 3.95 (s, 6H). ^{13}C NMR (75 MHz, $CDCl_3$) δ 166.29, 133.84, 130.74, 130.60, 128.66, 52.41. HRMS (EI-MS): m/z $[M^{\cdot+}]$ calculated for $C_{10}H_{10}O_4^{\cdot+}$: 194.0579, found 194.0570; $C_{10}H_{10}O_4$ (194.19).

3-(Methoxycarbonyl)benzoic acid (53) [247]

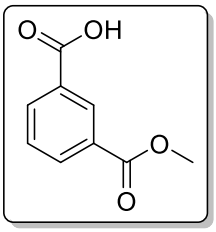

KOH (0.96 g, 17.0 mmol, 1 eq) was dissolved in water (15 mL) and added dropwise to a solution of **52** (3.30 g, 17 mmol, 1 eq) in MeOH (40 mL) at 0 °C. The mixture was then stirred at room temperature overnight. After the solvent was evaporated the residue was dissolved in water and washed three times with EtOAc (3 x 30 mL). The aqueous layer was acidified with aqueous HCl (1 N) until pH < 1 and extracted with EtOAc (3 x 30 mL). The organic layer was dried over Na_2SO_4 and the solvent was removed in vacuo to give **53** (1.51 g, 50%) as a white powder. ^{1}H NMR (300 MHz, $CDCl_3$) δ 8.79 – 8.76 (m, 1H), 8.34 – 8.27 (m, 2H), 7.59 (td, *J* = 7.8, 0.5 Hz, 1H), 3.97 (s, 3H). ^{13}C NMR (75 MHz, $CDCl_3$) δ 170.34, 166.15, 134.69, 134.37, 131.40, 130.81, 128.84, 52.49. HRMS (EI-MS): m/z $[M^{\cdot+}]$ calculated for $C_9H_8O_4^{\cdot+}$: 180.0423, found 180.0417; $C_9H_8O_4$ (180.16).

Dimethyl 3,3'-(6,9,12-trioxa-2,16-diazaheptadecanedioyl)dibenzoate (54) [248]

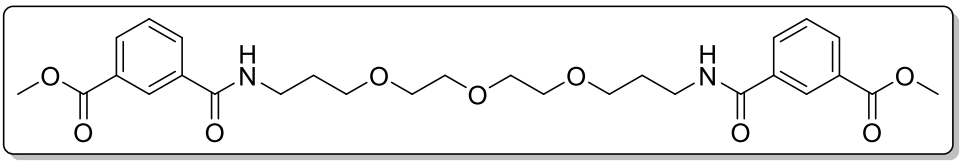

53 (1.50 g, 8.0 mmol, 2 eq) was dissolved in $SOCl_2$ (20 mL) and one drop of DMF was added. After the mixture was stirred at 80 °C for 5 h the solvent was evaporated under reduced pressure. The residue was dissolved in DCM (20 mL) and added dropwise to a solution of 3,3'-((oxybis(ethane-2,1-diyl))bis(oxy))bis(propan-1-amine) (0.88 g, 4.0 mmol, 1 eq) and triethylamine (1.60 g, 16.0 mmol, 4 eq) in DCM (30 mL) at 0 °C. The mixture was then stirred at room temperature overnight and the solvent was evaporated. The residue was purified by column chromatography (DCM/MeOH 9/1) to yield **54** (2.11 g, 99%) as a yellow oil. ^{1}H NMR (300 MHz, $CDCl_3$) δ 8.41 (t, *J* = 1.5 Hz, 2H), 8.15 – 8.10 (m, 2H), 8.08 – 8.02 (m, 2H), 7.53 – 7.46 (m, 2H), 7.32 – 7.26 (m, 2H), 3.92 (s, 6H), 3.66 – 3.45 (m, 16H), 1.90 – 1.79 (m, 4H). ^{13}C NMR (75 MHz, $CDCl_3$) δ 166.46, 166.27, 135.17, 132.16, 131.83, 130.37, 128.75, 127.83, 70.58, 70.24, 70.16, 52.35, 39.03, 28.83. HRMS (ESI-MS): m/z $[M+H]^+$ calculated for $C_{28}H_{37}N_2O_9^+$: 545.2494, found 545.2516; $C_{28}H_{36}N_2O_9$ (544.60).

3,3'-(6,9,12-Trioxa-2,16-diazaheptadecanedioyl)dibenzoic acid (55) [248]

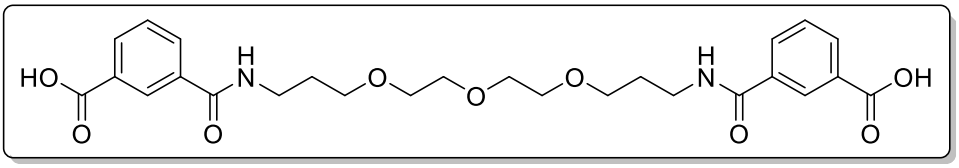

KOH (1.79 g, 32.0 mmol, 8 eq) was dissolved in MeOH (20 mL) and added to a solution of **54** (2.12 g, 4 mmol, 1 eq) in MeOH (35 mL). The reaction was then stirred at room temperature overnight. After the solvent was removed under reduced pressure the residue was diluted with water. Aqueous HCl (1 N) was added to set pH < 1 and the resulting precipitate was filtered off. The solid was dried in vacuo to give **55** as a white powder (2.04 g, 95%). ^{1}H NMR (300 MHz, DMSO-d_6) δ 8.65 (t, *J* = 5.8 Hz, 2H), 8.41 (t, *J* = 1.5 Hz, 2H), 8.06 (dd, *J* = 7.8, 1.7 Hz, 4H), 7.58 (t, *J* = 7.7 Hz, 2H), 3.55 – 3.41 (m, 16H), 1.81 – 1.71 (m, 4H). ^{13}C NMR (75 MHz, DMSO-d_6) δ 167.37, 165.87, 135.37, 132.17, 131.91, 131.33, 129.18, 128.44, 70.22, 70.00, 68.70, 55.34, 37.23, 29.69. HRMS (ESI-MS): m/z $[M+H]^+$ calculated for $C_{26}H_{33}N_2O_9^+$: 517.2181, found 517.2187; $C_{26}H_{32}N_2O_9$ (516.55).

tert-Butyl (3-(2-(3-aminopropoxy)ethoxy)propyl)carbamate (56) [249]

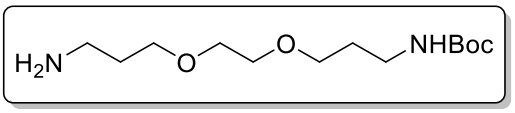

To a solution of 3,3'-(ethane-1,2-diylbis(oxy))bis(propan-1-amine) (10.00 g, 56.7 mmol, 5 eq) in DCM (100 mL) a solution of di-tert-butyl dicarbonate (2.47 g, 11.34 mmol, 1 eq) in DCM (50 mL) was added dropwise over 30 min. The mixture was stirred at room temperature for 16 h. The solvent was evaporated and the residue was purified by column chromatography (DCM/MeOH 9/1 + 0.1% NH_3) to afford **56** (3.28 g, 91%) as a yellow oil. ^{1}H NMR (300 MHz, $CDCl_3$) δ 5.04 (s, 1H), 3.55 – 3.44 (m, 8H), 3.23 – 3.08 (m, 2H), 2.77 (t, *J* = 6.6 Hz, 2H), 1.78 – 1.62 (m, 4H), 1.37 (s, 9H). ^{13}C NMR (75 MHz, $CDCl_3$) δ 156.10, 78.94, 70.23, 70.13, 69.54, 39.62, 38.53, 33.16, 29.66, 28.46. HRMS (EIS-MS): m/z $[M+H]^+$ calculated for $C_{13}H_{29}N_2O_4^+$: 277.2122, found 277.2128; $C_{13}H_{28}N_2O_4$ (276.38).

tert-Butyl (3-(2-(2-(3-aminopropoxy)ethoxy)ethoxy)propyl)carbamate (57) [250]

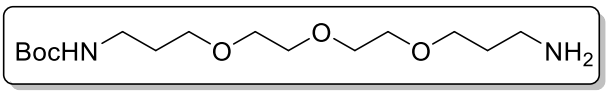

To a solution of 3,3'-((oxybis(ethane-2,1-diyl))bis(oxy))bis(propan-1-amine) (1.76 g, 8.0 mmol, 4 eq) in DCM (35 mL) a solution of di-tert-butyl dicarbonate (0.44 g, 2.0 mmol, 1 eq) in DCM (20 mL) was added dropwise over 30 min. The mixture was stirred at room temperature for 16 h. The solvent was evaporated and the residue was purified by column chromatography (DCM/MeOH 9/1 + 0.1% NH_3) to afford **57** (0.61 g, 95%) as a yellow oil. ^{1}H NMR (300 MHz, $CDCl_3$) δ 3.89 (s, 2H), 3.67 – 3.56 (m, 10H), 3.56 – 3.49 (m, 2H), 3.30 – 3.16 (m, 2H), 3.03 (t, *J* = 6.0 Hz, 2H), 1.97 – 1.84 (m, 2H), 1.82 – 1.70 (m, 2H), 1.42 (s, 9H). ^{13}C NMR (75 MHz, $CDCl_3$) δ 160.28, 81.30, 70.56, 70.38, 70.13, 70.08, 69.76, 69.40, 39.74, 38.41, 29.70, 28.48. HRMS (ESI-MS): m/z $[M+H]^+$ calculated for $C_{15}H_{33}N_2O_5^+$: 321.2384, found 321.2390; $C_{15}H_{32}N_2O_5$ (320.43).

Di-tert-butyl((((((isophthaloylbis(azanediyl))bis(propane-3,1-diyl))bis(oxy))bis(ethane-2,1-diyl))bis(oxy))bis(propane-3,1-diyl))dicarbamate (58a)

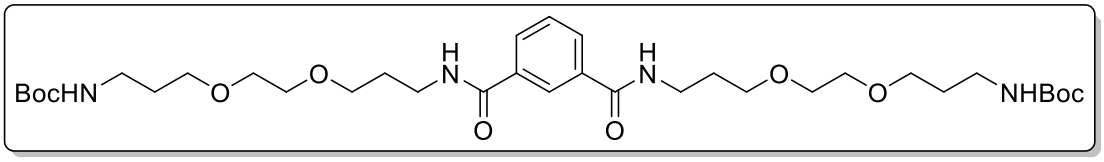

Isophthalic acid (0.25 g, 1.5 mmol, 1 eq) was dissolved in $SOCl_2$ (30 mL) and one drop of DMF was added. After the mixture was stirred at 80 °C for 5 h the solvent was evaporated under

reduced pressure. The residue was dissolved in DCM (35 mL) and added dropwise to a solution of **56** (0.86 g, 3.15 mmol, 2.1 eq) and triethylamine (0.61 g, 6.2 mmol, 4 eq) in DCM (35 mL) at 0 °C. The mixture was then stirred at room temperature overnight and the solvent was evaporated. The residue was purified by column chromatography (DCM/MeOH 9/1) to yield **58a** (0.95 g, 90%) as a red oil. ^{1}H NMR (300 MHz, $CDCl_3$) δ 8.20 – 8.10 (m, 1H), 7.93 (d, *J* = 7.2 Hz, 2H), 7.46 (t, *J* = 7.7 Hz, 1H), 7.36 (bs, 2H), 4.98 (bs, 2H), 3.68 – 3.53 (m, 16H), 3.46 (t, *J* = 5.6 Hz, 4H), 3.15 – 3.05 (m, 4H), 1.95 – 1.85 (m, 4H), 1.67 – 1.57 (m, 4H), 1.45 – 1.38 (m, 18H). ^{13}C NMR (75 MHz, $CDCl_3$) δ 166.71, 156.12, 135.08, 129.95, 128.66, 125.26, 79.00, 70.48, 70.24, 70.06, 69.35, 38.86, 38.30, 29.62, 28.92, 28.43. HRMS (ESI-MS): m/z $[M+H]^+$ calculated for $C_{34}H_{59}N_4O_{10}^+$: 683.4226, found 683.4235; $C_{34}H_{58}N_4O_{10}$ (682.86).

Di-tert-butyl (1,3-phenylenebis(1-oxo-6',9',12'-trioxa-2'-azapentadecane-1,15-diyl))dicarbamate (58b)

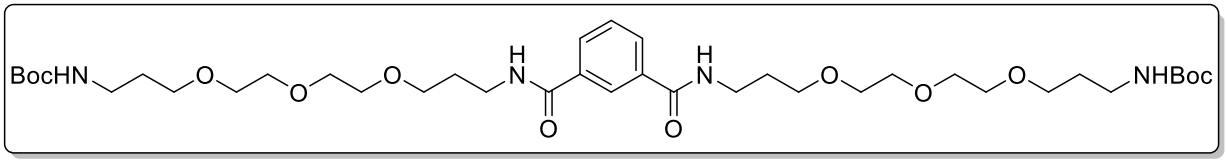

Isophthalic acid (0.21 g, 1.2 mmol, 1 eq) was dissolved in $SOCl_2$ (30 mL) and one drop of DMF was added. After the mixture was stirred at 80 °C for 5 h the solvent was evaporated under reduced pressure. The residue was dissolved in DCM (30 mL) and added dropwise to a solution of **57** (0.80 g, 2.5 mmol, 2.1 eq) and triethylamine (0.50 g, 4.8 mmol, 4 eq) in DCM (35 mL) at 0 °C. The mixture was then stirred at room temperature overnight and the solvent was evaporated. The residue was purified by column chromatography (DCM/MeOH 9/1) to yield **58b** (0.85 g, 92%) as a yellow oil. ^{1}H NMR (300 MHz, $CDCl_3$) δ 8.18 – 8.14 (m, 1H), 7.98 (dd, *J* = 7.7, 1.7 Hz, 2H), 7.48 (t, *J* = 7.4 Hz, 1H), 7.41 (bs, 2H), 4.98 (bs, 2H), 3.69 – 3.62 (m, 12H), 3.61 – 3.56 (m, 8H), 3.47 – 3.37 (m, 8H), 3.19 – 3.11 (m, 4H), 1.93 – 1.85 (m, 4H), 1.71 – 1.61 (m, 4H), 1.41 (s, 18H). ^{13}C NMR (75 MHz, $CDCl_3$) δ 166.50, 156.09, 134.91, 130.22, 128.77, 124.97, 70.45, 70.29, 70.09, 69.43, 38.89, 38.44, 29.62, 28.95, 28.47. HRMS (ESI-MS): m/z $[M+H]^+$ calculated for $C_{38}H_{67}N_4O_{12}^+$: 771.4750, found 771.4764; $C_{38}H_{66}N_4O_{12}$ (770.96).

Di-tert-butyl (1,4-phenylenebis(1-oxo-6,9,12-trioxa-2-azapentadecane-1,15-diyl))dicarbamate (58c)

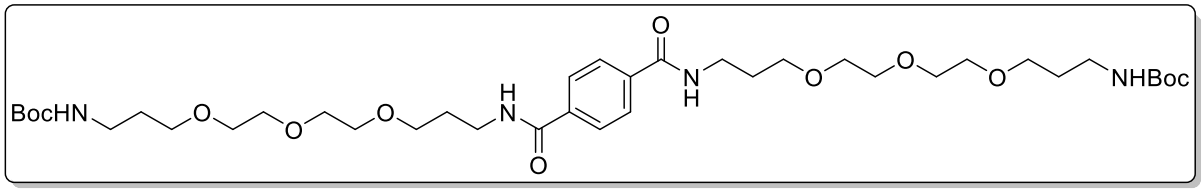

Terephthalic acid (0.16 g, 1 mmol, 1 eq) was dissolved in $SOCl_2$ (30 mL) and one drop of DMF was added. After the mixture was stirred at 80 °C for 5 h the solvent was evaporated under reduced pressure. The residue was dissolved in DCM (20 mL) and added dropwise to a solution of **57** (0.67 g, 2.1 mmol, 2.1 eq) and triethylamine (0.30 g, 3.0 mmol, 3 eq) in DCM (30 mL) at 0 °C. The mixture was then stirred at room temperature overnight and the solvent was evaporated. The residue was purified by column chromatography (DCM/MeOH 9/1) to yield **58c** (0.81 g, 99%) as a red oil. ^{1}H NMR (400 MHz, $CDCl_3$) δ 7.85 (s, 4H), 7.35 (s, 2H), 5.02 (s, 2H), 3.70 – 3.63 (m, 12H), 3.61 – 3.56 (m, 8H), 3.51 – 3.42 (m, 8H), 3.16 (t, *J* = 6.4 Hz, 4H), 1.94 – 1.87 (m, 4H), 1.74 – 1.66 (m, 4H), 1.42 (s, 18H). ^{13}C NMR (101 MHz, $CDCl_3$) δ 166.40, 156.11, 137.15, 127.19, 78.99, 70.87, 70.49, 70.46, 70.35, 70.12, 69.48, 53.42, 39.21, 38.62, 29.65, 28.74, 28.46. HRMS (ESI-MS): m/z $[M+H]^+$ calculated for $C_{38}H_{67}N_4O_{12}^+$: 771.4750, found 771.4770; $C_{38}H_{66}N_4O_{12}$ (770.96).

Di-tert-butyl (15,19-dioxo-4,7,10,24,27,30-hexaoxa-14,20-diazatritriacontane-1,33-diyl)dicarbamate (58d)

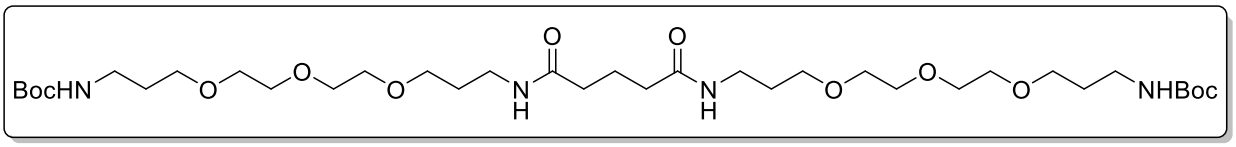

Glutaric acid (0.13 g, 1.0 mmol, 1 eq) was dissolved in $SOCl_2$ (30 mL) and one drop of DMF was added. After the mixture was stirred at 80 °C for 5 h the solvent was evaporated under reduced pressure. The residue was dissolved in DCM (20 mL) and added dropwise to a solution of **57** (0.67 g, 2.1 mmol, 2.1 eq) and triethylamine (0.30g, 3.0 mmol, 3 eq) in DCM (30 mL) at 0 °C. The mixture was then stirred at room temperature overnight and the solvent was evaporated. The residue was purified by column chromatography (DCM/MeOH 9/1) to yield **58d** (0.63 g, 82%) as a red oil. ^{1}H NMR (300 MHz, $CDCl_3$) δ 6.73 (s, 2H), 5.08 (s, 2H), 3.65 – 3.59 (m, 8H), 3.59 – 3.55 (m, 8H), 3.54 – 3.48 (m, 8H), 3.37 – 3.27 (m, 4H), 3.24 – 3.13 (m, 4H), 2.21 (t, *J* = 7.1 Hz, 4H), 1.90 (p, *J* = 6.7 Hz, 2H), 1.81 – 1.68 (m, 8H), 1.41 (s, 18H). ^{13}C NMR (75 MHz, $CDCl_3$)

δ 172.82, 156.15, 78.97, 70.50, 70.19, 70.14, 69.79, 69.46, 50.65, 38.44, 37.69, 35.42, 29.68, 28.99, 28.46, 22.09. HRMS (ESI-MS): m/z $[M+H]^+$ calculated for $C_{35}H_{69}N_4O_{12}^+$: 737.4907, found 737.4926; $C_{35}H_{68}N_4O_{12}$ (736.94).

Di-tert-butyl (((6,9,12-trioxa-2,16-diazaheptadecanedioyl)bis(3,1-phenylene))bis(1-oxo-6,9,12-trioxa-2-azapentadecane-1,15-diyl))dicarbamate (58e)

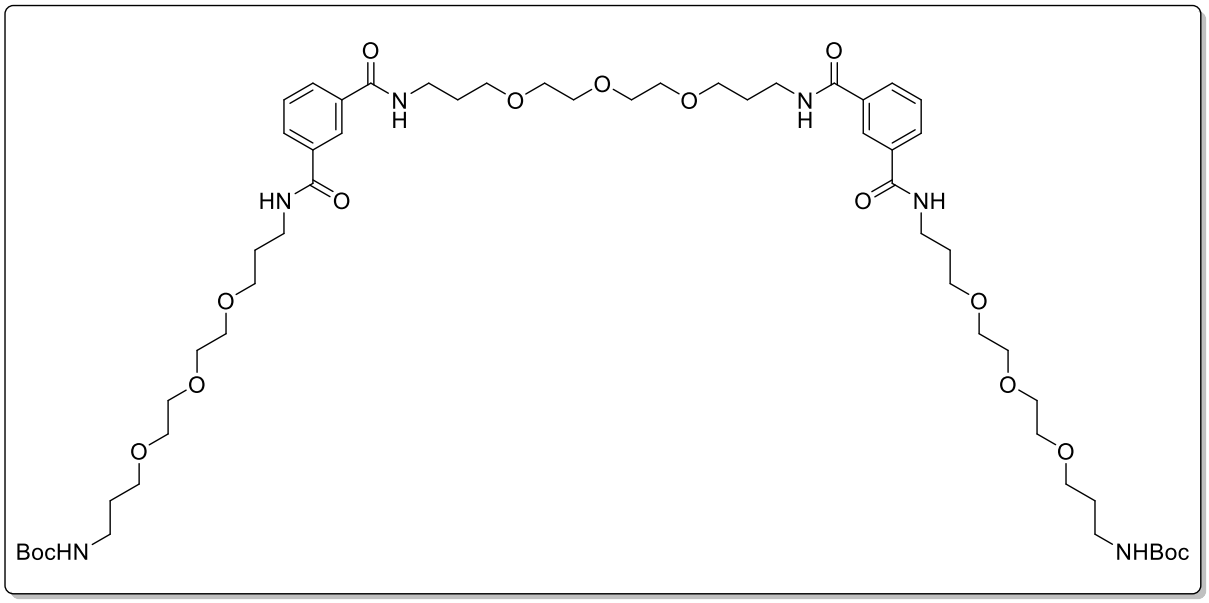

55 (0.26 g, 0.5 mmol, 1 eq) and HATU (1.14 g, 3.0 mmol, 6 eq) were dissolved in DMF (30 mL) at 0 °C. After 20 min DIPEA (0.39 g, 3.0 mmol, 6 eq) and **57** (0.80 g, 2.5 mmol, 5 eq) were added. After the reaction was stirred at room temperature overnight the solvent was removed under reduced pressure and the crude product was purified by column chromatography (DCM/MeOH 95/5) to give **58e** (0.51 g, 91%) as a brown oil. ^{1}H NMR (300 MHz, $CDCl_3$) δ 8.17 (s, 2H), 7.91 (d, *J* = 7.7 Hz, 4H), 7.58 (d, *J* = 4.7 Hz, 4H), 7.38 (t, *J* = 7.8 Hz, 2H), 5.01 (s, 2H), 3.64 – 3.31 (m, 44H), 3.08 – 2.95 (m, 4H), 1.88 – 1.70 (m, 8H), 1.66 – 1.53 (m, 4H), 1.34 (s, 18H). ^{13}C NMR (75 MHz, $CDCl_3$) δ 166.66, 156.11, 134.84, 130.33, 128.81, 125.02, 78.97, 70.35, 70.32, 70.26, 70.16, 70.10, 69.88, 38.74, 38.65, 38.41, 29.64, 29.01, 28.47. HRMS (ESI-MS): m/z $[M+H]^+$ calculated for $C_{56}H_{93}N_6O_{17}^+$: 1121.6592, found 1121.6615; $C_{56}H_{92}N_6O_{17}$ (1121.38).

N^1,N^3-bis(3-(2-(3-aminopropoxy)ethoxy)propyl)isophthalamide dihydrotrifluoroacetate (59a)

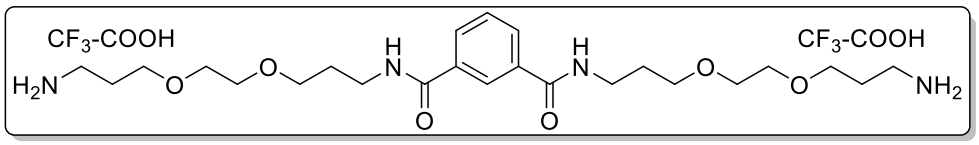

58a (0.95 g, 1.4 mmol) was dissolved in DCM (50 mL) and TFA (10 mL) was added. The mixture was stirred at room temperature until the starting material was consumed, indicated by TLC. The solution was concentrated under reduced pressure and dried in vacuo to give **59a** as a brown oil (0.64 g, 96%). The product was used without further purification. HRMS (ESI-MS): m/z $[M+H]^+$ calculated for $C_{24}H_{43}N_4O_6^+$: 483.3177, found 483.3181; $C_{24}H_{42}N_4O_6$ x $C_4H_2F_6O_4$ (482.62 + 228.05).

N^1,N^3-Bis(3-(2-(2-(3-aminopropoxy)ethoxy)ethoxy)propyl)isophthalamide (59b)

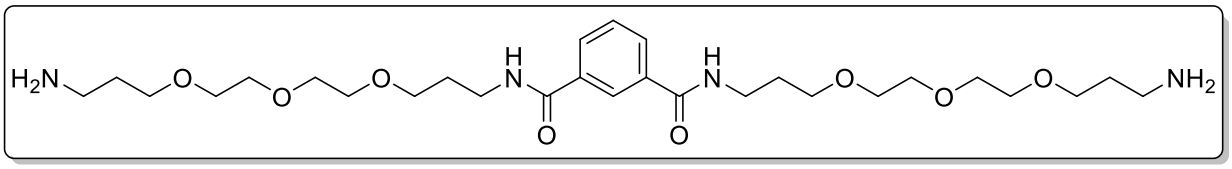

58b (0.85 g, 1.1 mmol) was dissolved in DCM (50 mL) and TFA (10 mL) was added. The mixture was stirred at room temperature until the starting material was consumed, indicated by TLC. The solution was concentrated under reduced pressure. The residue was dissolved in DCM (35 mL) and washed with 1 M NaOH three times (3 x 20 mL). The organic layer was dried over Na_2SO_4 and the solvent was removed in vacuo to give **59b** (0.62 g, 98%) as a yellow oil. ^{1}H NMR (300 MHz, CD_3OD) δ 8.30 (t, *J* = 1.6 Hz, 1H), 7.98 (dd, *J* = 7.8, 1.8 Hz, 2H), 7.57 (t, *J* = 7.8 Hz, 1H), 3.70 – 3.55 (m, 24H), 3.49 (t, *J* = 7.0 Hz, 4H), 3.10 (t, *J* = 6.5 Hz, 4H), 1.98 – 1.84 (m, 8H). ^{13}C NMR (75 MHz, $CDCl_3$) δ 160.46, 159.93, 133.44, 131.02, 129.43, 125.66, 116.99, 113.19, 70.95, 69.91, 69.61, 69.20, 68.79, 41.21, 28.63, 25.86. HRMS (ESI-MS): m/z $[M+H]^+$ calculated for $C_{28}H_{51}N_4O_8^+$: 571.3701, found 571.3708; $C_{28}H_{50}N_4O_8$ (570.72).

N^1,N^4-Bis(3-(2-(2-(3-aminopropoxy)ethoxy)ethoxy)propyl)terephthalamide (59c)

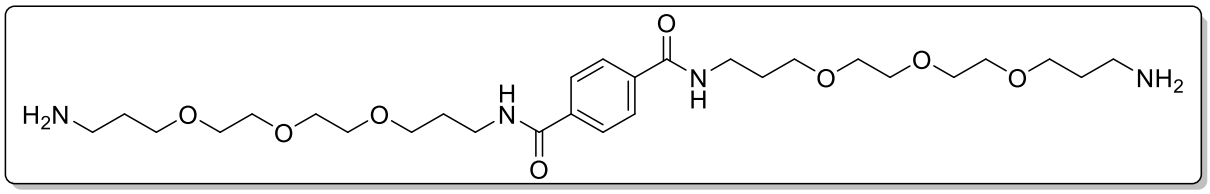

58c (0.81 g, 1.0 mmol) was dissolved in DCM (50 mL) and TFA (10 mL) was added. The mixture was stirred at room temperature until the starting material was consumed, indicated by TLC. The solution was concentrated under reduced pressure. The residue was dissolved in DCM (30 mL) and washed with 1 M NaOH three times (3 x 20 mL). The organic layer was dried over Na_2SO_4 and the solvent was removed in vacuo to give **59c** (0.57 g, 98%) as a yellow oil. ^{1}H NMR (300 MHz, CD_3OD) δ 7.89 (s, 4H), 3.67 – 3.45 (m, 30H), 2.79 – 2.70 (m, 4H), 1.96 – 1.84 (m, 4H), 1.79 – 1.68 (m, 4H). ^{13}C NMR (101 MHz, CD_3OD) δ 167.76, 137.08, 127.08, 70.11, 70.08, 69.86, 69.75, 69.02, 68.78, 38.69, 37.36, 31.45, 29.01. HRMS (ESI-MS): m/z $[M+H]^+$ calculated for $C_{28}H_{51}N_4O_8^+$: 571.3701, found 571.3705; $C_{28}H_{50}N_4O_8$ (570.73).

N^1,N^5-Bis(3-(2-(2-(3-aminopropoxy)ethoxy)ethoxy)propyl)glutaramide (59d)

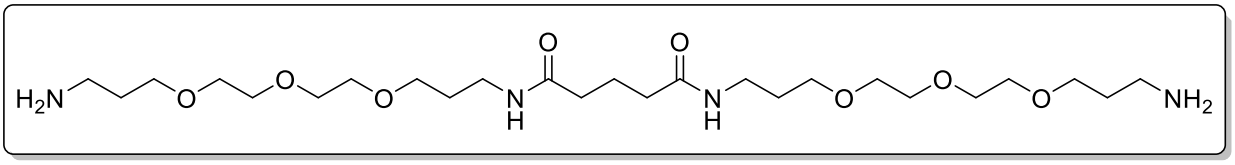

58d (0.64 g, 0.85 mmol) was dissolved in DCM (50 mL) and TFA (10 mL) was added. The mixture was stirred at room temperature until the starting material was consumed, indicated by TLC. The solution was concentrated under reduced pressure. The residue was dissolved in DCM and washed with 1 M NaOH three times (3 x 20 mL). The organic layer was dried over Na_2SO_4 and the solvent was removed in vacuo to give **59d** (0.43 g, 95%) as a yellow oil. ^{1}H NMR (300 MHz, CD_3OD) δ 3.68 – 3.56 (m, 21H), 3.51 (t, *J* = 6.1 Hz, 5H), 3.25 (t, *J* = 7.0 Hz, 4H), 2.88 – 2.81 (m, 4H), 2.20 (t, *J* = 7.4 Hz, 4H), 1.92 – 1.83 (m, 2H), 1.82 – 1.71 (m, 8H). ^{13}C NMR (75 MHz, CD_3OD) δ 206.50, 173.98, 69.98, 69.70, 69.64, 69.60, 68.94, 68.26, 38.67, 36.28, 34.90, 29.08, 26.65, 21.92. HRMS (ESI-MS): m/z $[M+H]^+$ calculated for $C_{25}H_{53}N_4O_6^+$: 537.3858, found 537.3867; $C_{25}H_{52}N_4O_6$ (536.71).

N^1,$N^{1'}$-(((Oxybis(ethane-2,1-diyl))bis(oxy))bis(propane-3,1-diyl))bis(N^3-(3-(2-(2-(3-aminopropoxy)ethoxy)ethoxy)propyl)isophthalamide dihydrotrifluoroacetate (59e)

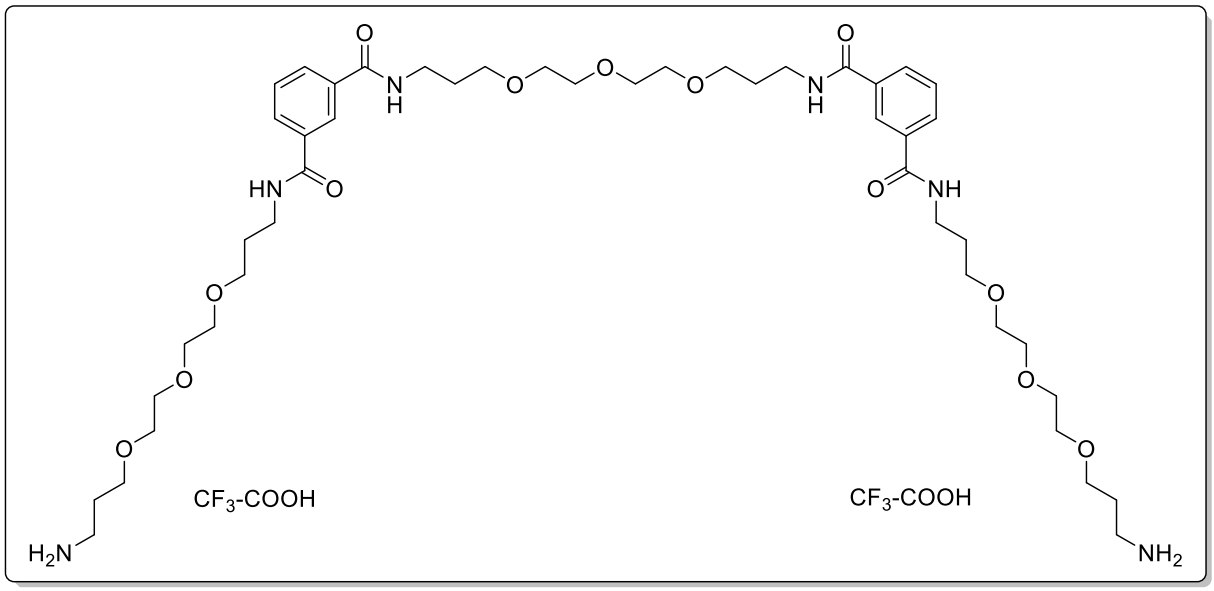

58e (0.35 g, 0.31 mmol) was dissolved in DCM (50 mL) and TFA (10 mL) was added. The mixture was stirred at room temperature until the starting material was consumed, indicated by TLC. The solution was concentrated under reduced pressure and dried in vacuo to give **59e** as a brown oil (0.28 g, 98%). The product was used without further purification. ^{1}H NMR (400 MHz, $CDCl_3$) δ 8.57 – 8.38 (m, 4H), 8.31 (s, 2H), 8.00 (d, *J* = 7.3 Hz, 4H), 7.81 (s, 4H), 7.45 (t, *J* = 6.7 Hz, 2H), 3.75 – 3.39 (m, 44H), 3.31 – 3.14 (m, 4H), 2.03 – 1.93 (m, 4H), 1.92 – 1.76 (m, 8H). ^{13}C NMR (101 MHz, $CDCl_3$) δ 167.69, 167.53, 133.81, 131.10, 128.94, 125.48, 70.46, 70.21, 69.91, 69.63, 69.54, 69.52, 69.46, 69.39, 68.72, 40.54, 37.51, 29.19, 28.87, 26.18. HRMS (ESI-MS): m/z $[M+2H]^{2+}$ calculated for $C_{46}H_{78}N_6O_{13}^{2+}$: 461.2808, found 461.2810; $C_{46}H_{76}N_6O_{13}$ x $C_4H_2F_6O_4$ (921.14 + 228.05).

N^1,N^3-Bis(3-(2-(3-(2-chloroacetamido)propoxy)ethoxy)propyl)isophthalamide (60a)

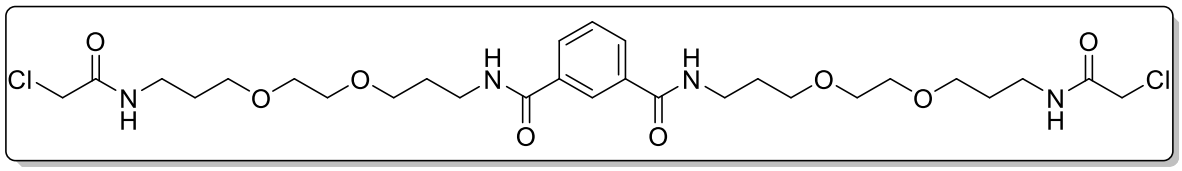

To a solution of **59a** (0.63 g, 1.3 mmol, 1 eq) and triethylamine (0.80 g, 7.8 mmol, 6 eq) in DCM (35 mL) a solution of 2-chloroacetyl chloride (0.31 g, 2.73 mmol, 2.1 eq) in DCM (20 mL) was added dropwise. The reaction was stirred at room temperature overnight. After the solvent was removed under reduced pressure the crude product was purified by column chromatography (DCM/MeOH 95/5) to yield **60a** as a red oil (0.78 g, 95%). ^{1}H NMR (300 MHz,

$CDCl_3$) δ 8.13 (t, *J* = 1.6 Hz, 1H), 7.89 (dd, *J* = 7.7, 1.8 Hz, 2H), 7.45 (t, *J* = 7.7 Hz, 1H), 7.39 (bt, *J* = 5.0 Hz, 2H), 3.99 (s, 4H), 3.66 – 3.53 (m, 16H), 3.49 (t, *J* = 5.7 Hz, 4H), 3.30 – 3.21 (m, 4H), 1.94 – 1.86 (m, 4H), 1.68 – 1.61 (m, 4H). ^{13}C NMR (75 MHz, $CDCl_3$) δ 166.81, 166.05, 135.22, 129.84, 128.69, 125.46, 70.54, 70.36, 70.32, 70.12, 50.70, 42.69, 38.99, 38.40, 28.91, 28.62. HRMS (ESI-MS): m/z $[M+H]^+$ calculated for $C_{28}H_{45}Cl_2N_4O_8^+$: 635.2609, found 635.2620; $C_{28}H_{44}Cl_2N_4O_8$ (635.58).

***N*^{1},*N*^{3}-Bis(1-chloro-2-oxo-7,10,13-trioxa-3-azahexadecan-16-yl)isophthalamide (60b)**

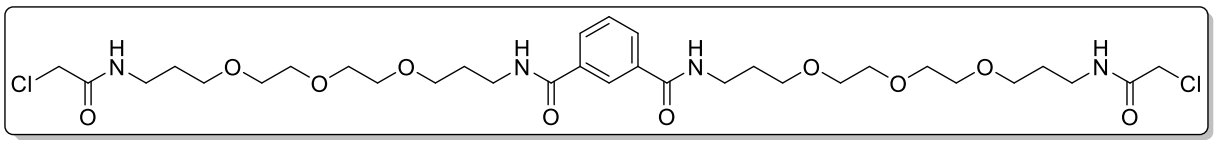

To a solution of **59b** (0.62 g, 1.1 mmol, 1 eq) and triethylamine (0.67 g, 6.6 mmol, 6 eq) in DCM (30 mL) a solution of 2-chloroacetyl chloride (0.26 g, 2.3 mmol, 2.1 eq) in DCM (20 mL) was added dropwise. The reaction was stirred at room temperature overnight. After the solvent was removed under reduced pressure the crude product was purified by column chromatography (DCM/MeOH 95/5) to yield **60b** as a red oil (0.75 g, 94%). ^{1}H NMR (300 MHz, $CDCl_3$) δ 8.18 (t, *J* = 1.5 Hz, 1H), 7.97 (dd, *J* = 7.7, 1.7 Hz, 2H), 7.48 (t, *J* = 7.8 Hz, 1H), 7.41 (t, *J* = 5.1 Hz, 2H), 7.32 – 7.26 (m, 2H), 4.01 (s, 4H), 3.68 – 3.53 (m, 21H), 3.50 – 3.43 (m, 8H), 3.40 – 3.31 (m, 4H), 1.94 – 1.84 (m, 4H), 1.77 – 1.68 (m, 4H). ^{13}C NMR (75 MHz, $CDCl_3$) δ 166.72, 166.22, 134.75, 130.25, 128.81, 125.25, 122.72, 120.65, 70.27, 70.04, 53.48, 42.69, 41.15, 38.90, 38.66, 30.97, 28.92, 28.54, 28.03. HRMS (ESI-MS): m/z $[M+H]^+$ calculated for $C_{32}H_{53}Cl_2N_4O_{10}^+$: 723.3133, found 723.3143; $C_{32}H_{52}Cl_2N_4O_{10}$ (723.68).

***N*^{1},*N*^{4}-Bis(1-chloro-2-oxo-7,10,13-trioxa-3-azahexadecan-16-yl)terephthalamide (60c)**

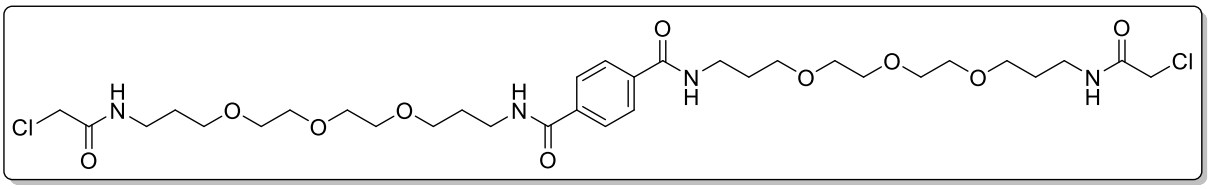

To a solution of **59c** (0.57 g, 1.0 mmol, 1 eq) and triethylamine (0.21 g, 2.1 mmol, 2.1 eq) in DCM (30 mL) a solution of 2-chloroacetyl chloride (0.24 g, 2.1 mmol, 2.1 eq) in DCM (20 mL) was added dropwise. The reaction was stirred at room temperature overnight. After the solvent was removed under reduced pressure the crude product was purified by column chromatography (DCM/MeOH 95/5) to yield a red oil for **60c** (0.64 g, 88%). ^{1}H NMR (400 MHz,

$CDCl_3$) δ 7.86 (s, 4H), 7.38 – 7.26 (m, 4H), 4.01 (s, 4H), 3.69 – 3.63 (m, 12H), 3.62 – 3.57 (m, 8H), 3.54 – 3.48 (m, 8H), 3.41 – 3.34 (m, 4H), 1.94 – 1.86 (m, 4H), 1.80 – 1.73 (m, 4H). ^{13}C NMR (101 MHz, $CDCl_3$) δ 166.36, 165.98, 137.15, 127.20, 70.93, 70.48, 70.42, 70.34, 70.31, 70.24, 42.71, 39.29, 38.57, 28.76, 28.66. HRMS (ESI-MS): m/z $[M+H]^+$ calculated for $C_{32}H_{53}Cl_2N_4O_{10}^+$: 723.3145, found 723.3145; $C_{32}H_{52}Cl_2N_4O_{10}$ (723.69).

***N*^{1},*N*^{5}-Bis(1-chloro-2-oxo-7,10,13-trioxa-3-azahexadecan-16-yl)glutaramide (60d)**

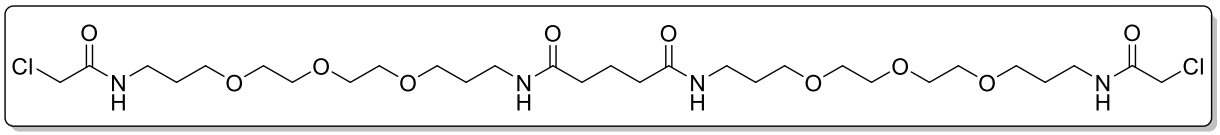

To a solution of **59d** (0.53 g, 1.0 mmol, 1 eq) and triethylamine (0.30 g, 3.0 mmol, 3 eq) in DCM (30 mL) a solution of 2-chloroacetyl chloride (0.24 g, 2.1 mmol, 2.1 eq) in DCM (20 mL) was added dropwise. The reaction was stirred at room temperature overnight. After the solvent was removed under reduced pressure the crude product was purified by column chromatography (DCM/MeOH 95/5) to yield **60d** as a brown oil (0.52 g, 75%). ^{1}H NMR (400 MHz, CD_3OD) δ 3.99 (s, 4H), 3.61 – 3.57 (m, 8H), 3.57 – 3.52 (m, 8H), 3.52 – 3.45 (m, 8H), 3.29 – 3.24 (m, 8H), 2.16 (t, *J* = 7.5 Hz, 4H), 1.83 (p, *J* = 7.5 Hz, 2H), 1.79 – 1.68 (m, 8H). ^{13}C NMR (101 MHz, $CDCl_3$) δ 177.82, 171.69, 74.10, 73.83, 73.79, 72.60, 72.44, 45.81, 41.09, 40.36, 38.87, 32.98, 32.69, 25.86. HRMS (ESI-MS): m/z $[M+H]^+$ calculated for $C_{29}H_{55}Cl_2N_4O_{10}^+$: 689.3290, found 689.3307; $C_{29}H_{54}Cl_2N_4O_{10}$ (689.67).

N^1,$N^{1'}$-(((Oxybis(ethane-2,1-diyl))bis(oxy))bis(propane-3,1-diyl))bis(*N*3-(1-chloro-2-oxo-7,10,13-trioxa-3-azahexadecan-16-yl)isophthalamide) (60e)

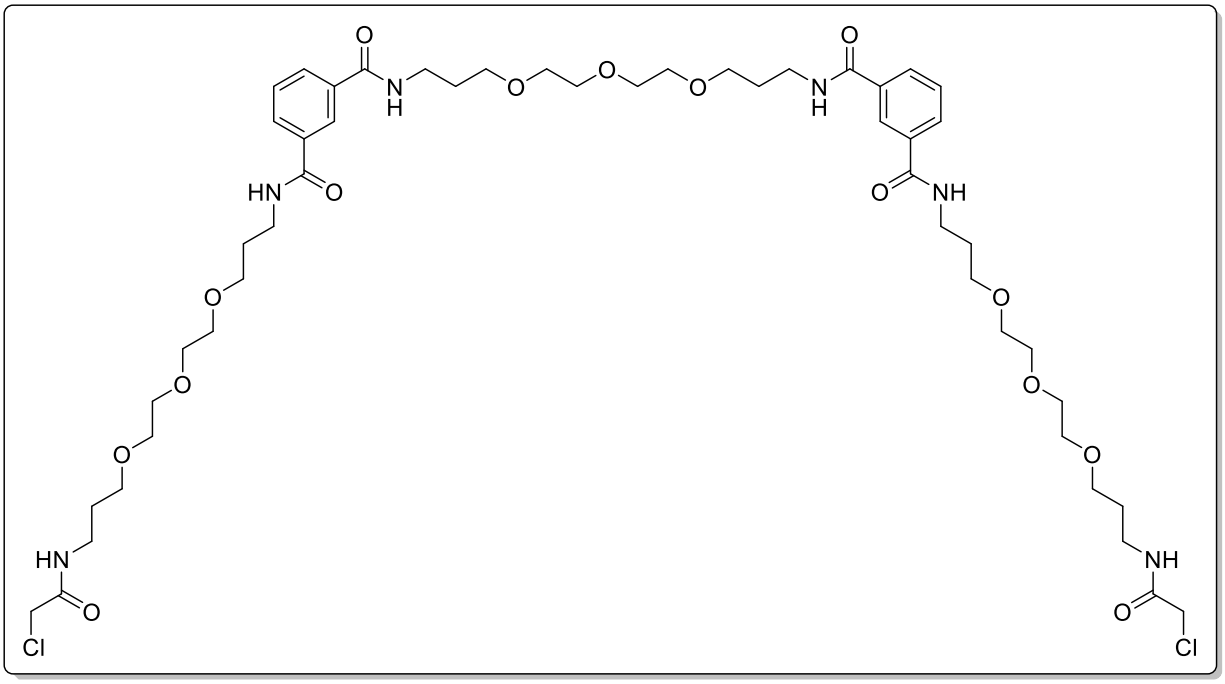

To a solution of **59e** (0.25 g, 0.27 mmol, 1 eq) and triethylamine (0.16 g, 1.6 mmol, 6 eq) in DCM (30 mL) a solution of 2-chloroacetyl chloride (0.07 g, 0.54 mmol, 2.2 eq) in DCM (20 mL) was added dropwise. The reaction was stirred at room temperature overnight. After the solvent was removed under reduced pressure the crude product was purified by column chromatography (DCM/MeOH 95/5) to yield **60e** as a red oil (0.28 g, 96%). ^{1}H NMR (300 MHz, $CDCl_3$) δ 8.20 – 8.15 (m, 2H), 7.87 (dd, *J* = 7.8, 1.2 Hz, 4H), 7.66 (dd, *J* = 12.5, 5.5 Hz, 4H), 7.40 – 7.30 (m, 4H), 3.89 (s, 4H), 3.56 – 3.46 (m, 22H), 3.43 – 3.34 (m, 22H), 3.26 – 3.21 (m, 4H), 1.80 – 1.68 (m, 8H), 1.67 – 1.59 (m, 4H). ^{13}C NMR (75 MHz, $CDCl_3$) δ 167.01, 166.46, 134.54, 134.46, 130.34, 128.76, 125.49, 70.30, 70.25, 70.20, 70.06, 70.02, 69.93, 69.84, 50.45, 45.75, 42.64, 38.51, 38.43, 28.95, 28.89, 28.53. HRMS (ESI-MS): m/z $[M+2H]^{2+}$ calculated for $C_{50}H_{80}Cl_2N_6O_{15}^{2+}$: 537.2524, found 537.2533; $C_{50}H_{78}Cl_2N_6O_{15}$ (1074.10).

N^1,N^3-Bis(3-(2-(3-(2-azidoacetamido)propoxy)ethoxy)propyl)isophthalamide (61a)

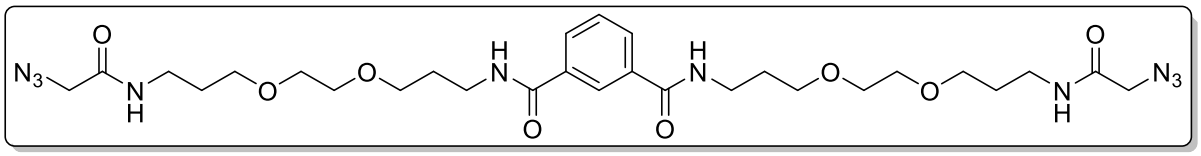

NaN_3 (0.34 g, 5.2 mmol, 4 eq) was added to a solution of **60a** (0.82 g, 1.3 mmol, 1 eq) in DMF (20 mL). The reaction was stirred at 80 °C overnight. Then, the solution was concentrated under reduced pressure and purified by column chromatography (DCM/MeOH 95/5) to give

61a (0.78 g, 92%) as a yellow oil. ^{1}H NMR (300 MHz, $CDCl_3$) δ 8.12 (t, *J* = 1.5 Hz, 1H), 7.89 (dd, *J* = 7.7, 1.7 Hz, 2H), 7.46 (t, *J* = 7.7 Hz, 1H), 7.37 (bt, *J* = 5.1 Hz, 2H), 7.00 (s, 2H), 3.90 (s, 4H), 3.69 – 3.53 (m, 16H), 3.50 – 3.44 (m, 4H), 3.25 – 3.16 (m, 4H), 1.97 – 1.83 (m, 4H), 1.69 – 1.56 (m, 4H). ^{13}C NMR (75 MHz, $CDCl_3$) δ 166.85, 166.81, 135.24, 129.88, 128.74, 125.37, 70.52, 70.33, 70.24, 69.84, 52.62, 38.98, 37.76, 28.91, 28.81. HRMS (ESI-MS): m/z $[M+H]^+$ calculated for $C_{28}H_{45}N_{10}O_8^+$: 649.3416, found 649.3419; $C_{28}H_{44}N_{10}O_8$ (648.72).

***N*^{1},*N*^{3}-Bis(1-azido-2-oxo-7,10,13-trioxa-3-azahexadecan-16-yl)isophthalamide (61b)**

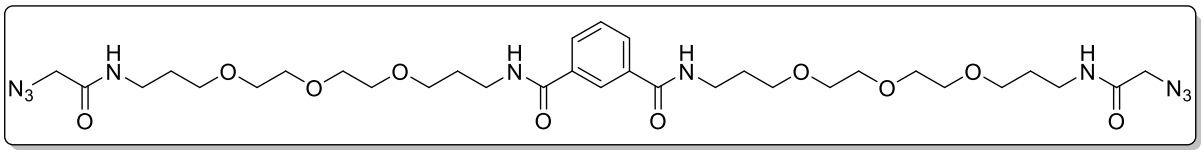

NaN_3 (0.09 g, 1.4 mmol, 4 eq) was added to a solution of **60b** (0.25 g, 0.34 mmol, 1 eq) in DMF (20 mL). The reaction was stirred at 80 °C overnight. Then, the solution was concentrated under reduced pressure and purified by column chromatography (DCM/MeOH 95/5) to give **61b** (0.78 g, 92%) as a yellow oil. ^{1}H NMR (300 MHz, $CDCl_3$) δ 8.21 – 8.14 (m, 1H), 7.96 (dd, *J* = 7.7, 1.5 Hz, 2H), 7.56 – 7.38 (m, 3H), 7.05 (bs, 2H), 3.90 (s, 4H), 3.70 – 3.50 (m, 20H), 3.50 – 3.39 (m, 8H), 3.36 – 3.27 (m, 4H), 1.95 – 1.80 (m, 4H), 1.77 – 1.63 (m, 4H). ^{13}C NMR (75 MHz, $CDCl_3$) δ 166.90, 166.67, 134.86, 130.17, 128.79, 125.15, 70.32, 70.27, 70.15, 70.12, 70.04, 69.92, 52.59, 38.64, 37.91, 28.97, 28.76. HRMS (ESI-MS): m/z $[M+H]^+$ calculated for $C_{32}H_{53}N_{10}O_{10}^+$: 737.3941, found 737.3961; $C_{32}H_{52}N_{10}O_{10}$ (736.82).

***N*^{1},*N*^{4}-Bis(1-azido-2-oxo-7,10,13-trioxa-3-azahexadecan-16-yl)terephthalamide (61c)**

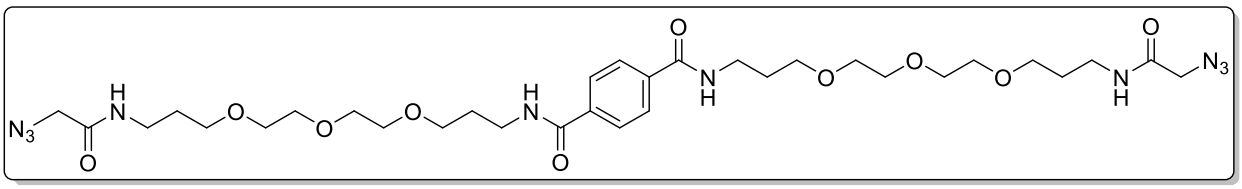

NaN_3 (0.26 g, 4.0 mmol, 4 eq) was added to a solution of **60c** (0.72 g, 1.0 mmol, 1 eq) in DMF (20 mL). The reaction was stirred at 80 °C overnight. Then, the solution was concentrated under reduced pressure and purified by column chromatography (DCM/MeOH 95/5) to give **61c** (0.67 g, 91%) as a brown oil. ^{1}H NMR (400 MHz, $CDCl_3$) δ 7.87 (s, 4H), 7.36 (bt, *J* = 4.9 Hz, 2H), 7.07 (bs, 2H), 3.91 (s, 4H), 3.71 – 3.56 (m, 20H), 3.53 – 3.46 (m, 8H), 3.40 – 3.32 (m, 4H), 1.95 – 1.86 (m, 4H), 1.79 – 1.71 (m, 4H). ^{13}C NMR (101 MHz, $CDCl_3$) δ 166.40, 137.16, 127.21, 70.93, 70.48, 70.43, 70.32, 70.17, 70.02, 52.65, 39.29, 37.97, 28.81, 28.75. HRMS (ESI-MS): m/z $[M+H]^+$ calculated for $C_{32}H_{53}N_{10}O_{10}^+$: 737.3941, found 737.3959; $C_{32}H_{52}N_{10}O_{10}$ (736.83).

N^1,N^5-Bis(1-azido-2-oxo-7,10,13-trioxa-3-azahexadecan-16-yl)glutaramide (61d)

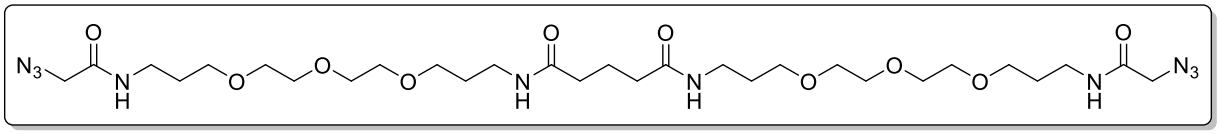

NaN_3 (0.22 g, 3.0 mmol, 4 eq) was added to a solution of **60d** (0.52 g, 0.75 mmol, 1 eq) in DMF (20 mL). The reaction was stirred at 80 °C overnight. Then, the solution was concentrated under reduced pressure and purified by column chromatography (DCM/MeOH 95/5) to give **61d** (0.44 g, 84%) as a brown oil. ^{1}H NMR (300 MHz, CD_3OD) δ 3.88 (s, 4H), 3.67 – 3.61 (m, 8H), 3.61 – 3.56 (m, 8H), 3.56 – 3.48 (m, 8H), 3.32 – 3.21 (m, 8H), 2.20 (t, *J* = 7.4 Hz, 4H), 1.93 – 1.84 (m, 2H), 1.83 – 1.70 (m, 8H). ^{13}C NMR (75 MHz, CD_3OD) δ 173.84, 168.58, 70.15, 69.86, 69.84, 68.59, 68.48, 51.63, 36.71, 36.41, 34.91, 29.03, 28.88, 21.91. HRMS (ESI-MS): m/z $[M+H]^+$ calculated for $C_{29}H_{55}N_{10}O_{10}^+$: 703.4097, found 703.4111; $C_{29}H_{54}N_{10}O_{10}$ (702.81).

N^1,$N^{1'}$-(((Oxybis(ethane-2,1-diyl))bis(oxy))bis(propane-3,1-diyl))bis(*N*3-(1-azido-2-oxo-7,10,13-trioxa-3-azahexadecan-16-yl)isophthalamide) (61e)

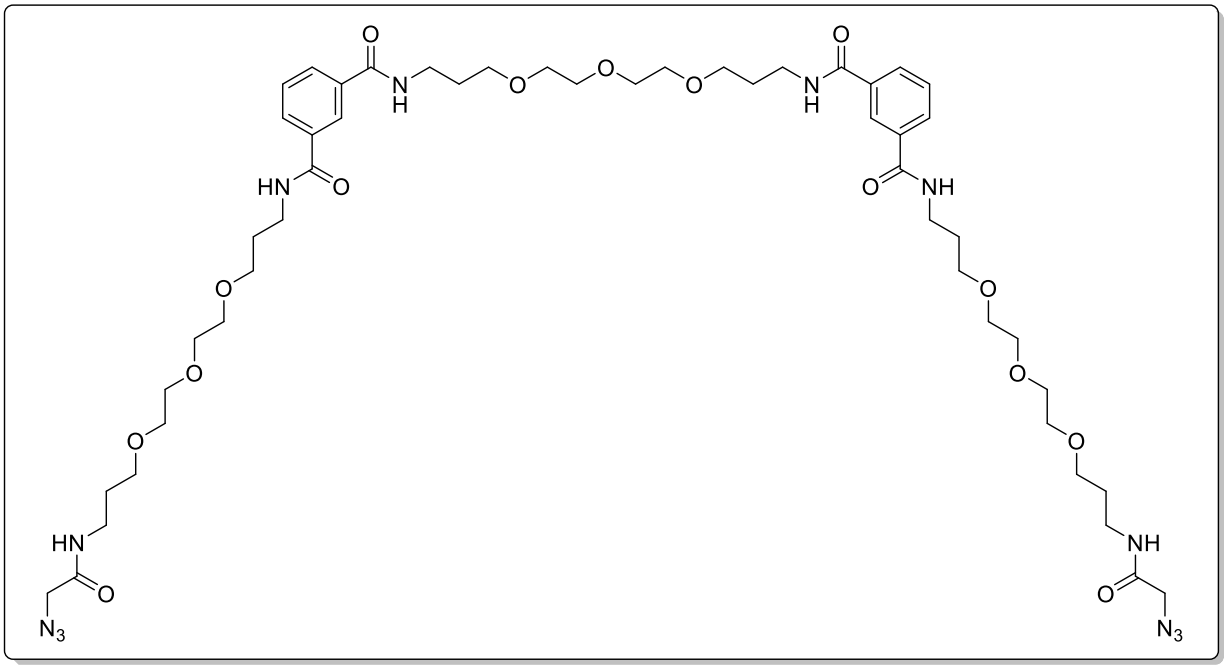

NaN_3 (0.07 g, 1.1 mmol, 4 eq) was added to a solution of **60e** (0.28 g, 0.26 mmol, 1 eq) in DMF (20 mL). The reaction was stirred at 80 °C overnight. Then, the solution was concentrated under reduced pressure and purified by column chromatography (DCM/MeOH 95/5) to give **61e** (0.27 g, 95%) as a yellow oil. ^{1}H NMR (300 MHz, $CDCl_3$) δ 8.23 – 8.17 (s, 2H), 7.94 – 7.86 (m, 4H), 7.64 (bt, *J* = 5.2 Hz, 4H), 7.39 (t, *J* = 7.7 Hz, 2H), 7.10 (bt, *J* = 5.6 Hz, 2H), 3.84 (s, 4H), 3.62 – 3.42 (m, 44H), 3.30 – 3.23 (m, 4H), 1.88 – 1.60 (m, 12H). ^{13}C NMR (101 MHz, $CDCl_3$) δ

167.19, 167.12, 134.38, 134.30, 130.56, 128.88, 125.52, 70.33, 70.28, 70.13, 70.05, 70.00, 69.87, 52.50, 38.80, 38.15, 28.97, 28.87, 28.67. HRMS (ESI-MS): m/z $[M+2H]^{2+}$ calculated for $C_{50}H_{80}N_{12}O_{15}^{2+}$: 544.2928, found 544.2934; $C_{50}H_{78}N_{12}O_{15}$ (1087.24).

N^1,N^3-Di(prop-2-yn-1-yl)isophthalamide (63) [251]

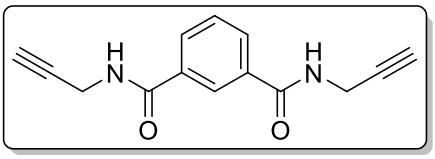

Isophthalic acid (0.50 g, 3.0 mmol, 1 eq) was dissolved in $SOCl_2$ (30 mL) and one drop of DMF was added. After the mixture was stirred at 80 °C for 5 h the solvent was then evaporated under reduced pressure to give **62**. The residue was dissolved in DCM (30 mL) and added dropwise to a solution of propargylamine (0.34 g, 6.23 mmol, 2.1 eq) and triethylamine (1.22 g, 11.9 mmol, 4 eq) in DCM (30 mL) at 0 °C. The mixture was then stirred at room temperature overnight and the solvent was evaporated. The crude product was diluted in aqueous HCl (1 N, 20 mL) and extracted three times with EtOAc (3 x 30 mL). The organic phases were combined, dried over Na_2SO_4 and concentrated under reduced pressure. The residue was dried in vacuo to give **63** (0.69 g, 95%) as an orange-brown solid. ^{1}H NMR (400 MHz, CD_3OD) δ 8.29 (t, *J* = 1.6 Hz, 1H), 7.98 (dd, *J* = 7.8, 1.8 Hz, 2H), 7.57 (t, *J* = 7.8 Hz, 1H), 4.16 (d, *J* = 2.5 Hz, 4H), 2.61 (t, *J* = 2.5 Hz, 2H). ^{13}C NMR (101 MHz, CD_3OD) δ 167.49, 134.34, 130.09, 128.58, 126.12, 79.19, 70.79, 28.62. HRMS (ESI-MS): m/z $[M+H]^+$ calculated for $C_{14}H_{13}N_2O_2^+$: 241.0972, found 241.0972; $C_{14}H_{12}N_2O_2$ (240.27).

***N*-(Prop-2-yn-1-yl)acetamide (64) [252]**

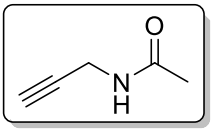

Acetyl chloride (1.8 g, 23.4 mmol, 1.3 eq) was dissolved in DCM (30 mL) and added to a solution of propargylamine (1.0 g, 18 mmol, 1 eq) and triethylamine (2.7 g, 27 mmol, 1.5 eq) in DCM (45 mL). The reaction was stirred at room temperature overnight. After the solvent was evaporated the crude product was purified by column chromatography (DCM/MeOH 95/5) to obtain **64** as a white powder (1.4 g, 80 %). ^{1}H NMR (300 MHz, $CDCl_3$) δ 5.87 (s, 1H), 4.04 (dd, *J* = 5.3, 2.6 Hz, 2H), 2.23 (t, *J* = 2.6 Hz, 1H), 2.00 (s, 3H). ^{13}C NMR (75 MHz, $CDCl_3$) δ 169.78, 79.53, 71.58, 29.28, 23.03. HRMS (EI-MS): m/z $[M^{\cdot+}]$ calculated for $C_5H_7NO^{\cdot+}$: 97.05222, found 97.05218; C_5H_7NO (97.12).

General procedure for final bivalent compounds:

Ascorbic acid (0.3 eq) and $CuSO_4 \cdot 5H_2O$ (0.1 eq) were added to a solution of the two precursors (1.1 eq each) and linker (1 eq) in DCM/MeOH (4/1, 40 mL). The reaction was stirred at room temperature for 72 h. The solvent was removed under reduced pressure and the resulting crude product was purified by preparative HPLC (MeCN/0.1% aqueous TFA) or (MeCN/10% aqueous ammonia).

N^1-((1-(3-((3-((4-(4-Chlorophenyl)-4-hydroxypiperidin-1-yl)methyl)-1*H*-indol-5-yl)oxy)propyl)-1*H*-1,2,3-triazol-4-yl)methyl)-N^3-((1-(2-oxo-2-((1-(4-(3-(piperidin-1-yl)propoxy)benzyl)piperidin-4-yl)amino)ethyl)-1*H*-1,2,3-triazol-4-yl)methyl)isophthalamide pentahydrotrifluoroacetate (65)

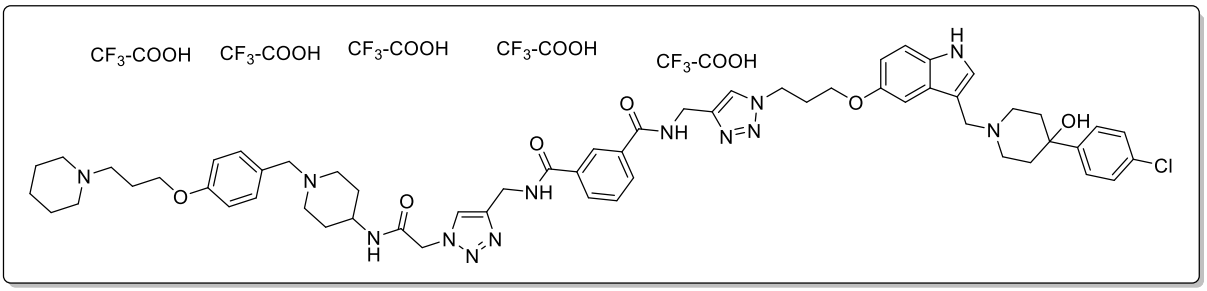

The title compound was prepared from **5a** (0.20 g, 0.45 mmol), **51** (0.19 g, 0.45 mmol) and **63** (0.10 g, 0.41 mmol) according to the general procedure. The product **65** was obtained as a red solid (59.9 mg, 8%). ^{1}H NMR (600 MHz, D_2O) δ 7.87 – 7.81 (m, 1H), 7.73 (s, 1H), 7.69 – 7.65 (m, 2H), 7.40 (d, *J* = 7.8 Hz, 1H), 7.29 – 7.22 (m, 4H), 7.21 – 7.14 (m, 5H), 7.05 – 7.00 (m, 1H), 6.93 (d, *J* = 8.6 Hz, 2H), 6.82 (d, *J* = 1.9 Hz, 1H), 6.53 (dd, *J* = 11.4, 9.5 Hz, 1H), 5.06 (s, 2H), 4.51 – 4.47 (m, 4H), 4.39 (s, 2H), 4.18 (s, 2H), 4.07 (s, 2H), 4.04 (t, *J* = 5.8 Hz, 2H), 3.76 (t, *J* = 5.3 Hz, 2H), 3.44 (d, *J* = 12.2 Hz, 2H), 3.35 (d, *J* = 12.7 Hz, 2H), 3.25 – 3.13 (m, 7H), 2.86 – 2.78 (m, 4H), 2.23 – 2.17 (m, 2H), 2.12 – 2.07 (m, 2H), 1.99 – 1.91 (m, 4H), 1.86 – 1.69 (m, 6H), 1.65 – 1.53 (m, 4H). ^{13}C NMR (151 MHz, D_2O) δ 168.70, 166.94, 159.14, 152.53, 144.62, 144.27, 133.24, 132.97, 132.75, 132.65, 131.16, 130.23, 130.01, 129.28, 128.86, 128.37, 127.23, 125.90, 125.55, 125.27, 124.51, 121.06, 117.26, 115.36, 115.13, 115.05, 112.94, 112.47, 101.81, 101.24, 68.50, 65.60, 65.23, 59.78, 54.37, 53.29, 51.91, 51.44, 50.75, 47.57, 44.78, 34.80, 34.61, 28.71, 28.17, 23.40, 22.79, 21.05. HRMS (ESI-MS): m/z $[M+H]^+$ calculated for $C_{59}H_{73}ClN_{13}O_6^+$: 1094.5490, found 1094.5486. Anal. RP-HPLC (220 nm): 97% (t_R = 10.28 min, *k* = 2.20). $C_{59}H_{72}ClN_{13}O_6$ x $C_{10}H_5F_{15}O_{10}$ (1094.76 + 570.11).

N^1-(3-(2-(3-(2-(4-(((3-((4-(4-Chlorophenyl)-4-hydroxypiperidin-1-yl)methyl)-1*H*-indol-5-yl)oxy)methyl)-1*H*-1,2,3-triazol-1-yl)acetamido)propoxy)ethoxy)propyl)-N^3-(3-(2-(3-(2-(4-((1-(4-(3-(piperidin-1-yl)propoxy)benzyl)piperidine-4-carboxamido)methyl)-1*H*-1,2,3-triazol-1-yl)acetamido)propoxy)ethoxy)propyl)isophthalamide pentahydrotrifluoroacetate (66)

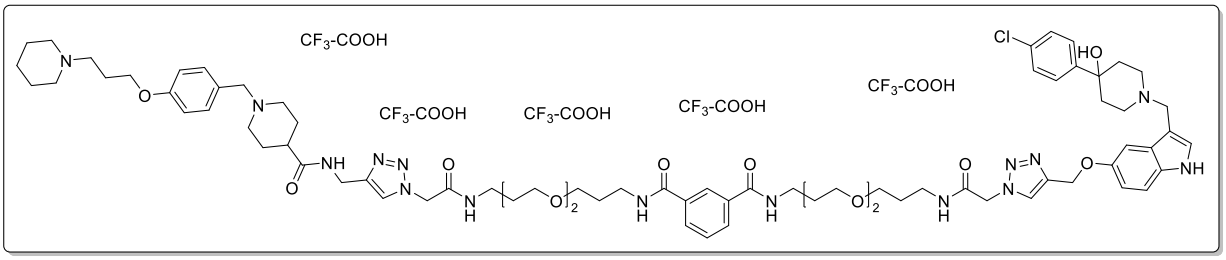

The title compound was prepared from **3a** (0.10 g, 0.25 mmol), **43** (0.10 g, 0.25 mmol) and **61a** (0.15 g, 0.23 mmol) according to the general procedure. The product **66** was obtained as a red solid (9.8 mg, 2%). ^{1}H NMR (400 MHz, D_2O) δ 7.90 (s, 1H), 7.84 (s, 1H), 7.75 (d, *J* = 12.1 Hz, 1H), 7.64 (d, *J* = 7.7 Hz, 2H), 7.41 (s, 1H), 7.30 (dd, *J* = 16.2, 8.2 Hz, 5H), 7.24 – 7.16 (m, 4H), 7.13 (s, 1H), 6.91 (t, *J* = 10.9 Hz, 2H), 6.79 (d, *J* = 8.7 Hz, 1H), 5.09 (s, 2H), 5.02 (d, *J* = 6.9 Hz, 4H), 4.30 (d, *J* = 14.4 Hz, 4H), 4.09 (s, 2H), 4.03 – 3.95 (m, 2H), 3.42 (s, 16H), 3.33 (t, *J* = 6.2 Hz, 2H), 3.24 – 3.20 (m, 10H), 3.19 – 3.14 (m, 2H), 3.08 (t, *J* = 6.6 Hz, 2H), 3.03 (t, *J* = 6.7 Hz, 2H), 2.90 – 2.77 (m, 4H), 2.43 (tt, *J* = 12.2, 3.0 Hz, 1H), 2.15 – 2.06 (m, 2H), 2.04 – 1.90 (m, 2H), 1.94 – 1.46 (m, 20H). ^{13}C NMR (101 MHz, D_2O) δ 175.69, 168.95, 167.34, 167.02, 159.21, 152.01, 144.50, 143.86, 134.06, 132.84, 132.76, 131.77, 130.07, 129.81, 129.13, 129.02, 128.47, 127.49, 126.25, 126.02, 125.65, 125.10, 121.13, 120.71, 117.81, 115.11, 114.91, 113.28, 112.01, 102.79, 102.11, 69.33, 68.70, 68.55, 68.21, 68.17, 65.29, 62.01, 60.11, 54.41, 53.34, 52.17, 52.05, 51.53, 51.06, 47.64, 39.64, 37.41, 37.36, 36.72, 34.73, 34.31, 28.26, 28.06, 27.99, 25.68, 23.42, 22.83, 21.10. HRMS (ESI-MS): m/z $[M+2H]^{2+}$ calculated for $C_{75}H_{104}ClN_{15}O_{12}^{2+}$: 720.883, found 720.8844. Anal. RP-HPLC (220 nm): 99% (t_R = 10.51 min, *k* = 2.27). $C_{75}H_{102}ClN_{15}O_{12}$ x $C_{10}H_5F_{15}O_{10}$ (1441.18 + 570.11).

N^1-(1-(4-(((3-((4-(4-Chlorophenyl)-4-hydroxypiperidin-1-yl)methyl)-1*H*-indol-5-yl)oxy)methyl)-1*H*-1,2,3-triazol-1-yl)-2-oxo-7,10,13-trioxa-3-azahexadecan-16-yl)-N^3-(2-oxo-1-(4-((1-(4-(3-(piperidin-1-yl)propoxy)benzyl)piperidine-4-carboxamido)methyl)-1*H*-1,2,3-triazol-1-yl)-7,10,13-trioxa-3-azahexadecan-16-yl)isophthalamide pentahydrotrifluoroacetate (67)

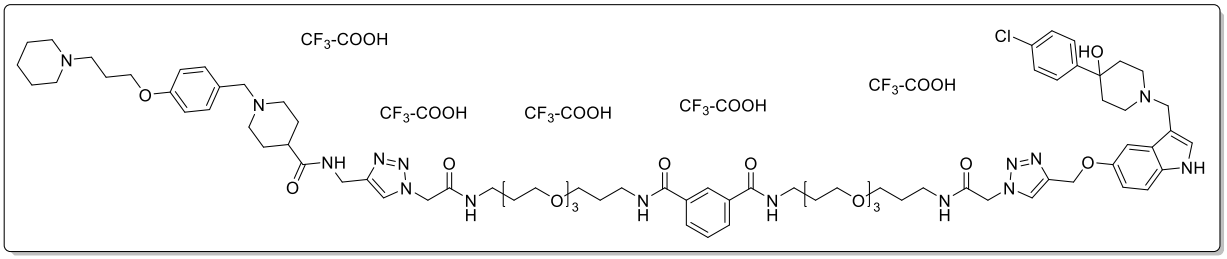

The title compound was prepared from **3a** (0.04 g, 0.11 mmol), **43** (0.05 g, 0.11 mmol) and **61b** (0.07 g, 0.1 mmol) according to the general procedure. The product **67** was obtained as a red solid (29.0 mg). ^{1}H NMR (600 MHz, D_2O) δ 7.89 – 7.80 (m, 2H), 7.74 – 7.69 (m, 1H), 7.61 (d, *J* = 6.1 Hz, 2H), 7.37 – 7.31 (m, 1H), 7.28 – 7.19 (m, 4H), 7.16 – 7.00 (m, 5H), 6.88 (d, *J* = 8.4 Hz, 2H), 6.68 (d, *J* = 7.9 Hz, 1H), 4.98 (s, 6H), 4.33 – 4.18 (m, 4H), 4.04 (s, 2H), 3.98 (t, *J* = 5.4 Hz, 2H), 3.48 – 3.33 (m, 24H), 3.29 – 3.26 (m, 4H), 3.25 – 3.15 (m, 10H), 3.14 – 3.11 (m, 2H), 3.06 (t, *J* = 6.7 Hz, 2H), 3.01 – 2.94 (m, 2H), 2.86 – 2.72 (m, 4H), 2.40 (t, *J* = 12.0 Hz, 1H), 2.09 – 2.02 (m, 2H), 1.87 (d, *J* = 13.5 Hz, 2H), 1.79 (d, *J* = 14.7 Hz, 2H), 1.72 – 1.52 (m, 14H), 1.50 – 1.44 (m, 2H). ^{13}C NMR (151 MHz, D_2O) δ 175.55, 168.52, 167.20, 166.78, 159.14, 152.17, 144.46, 143.72, 133.96, 132.76, 132.44, 130.02, 129.03, 128.30, 125.95, 125.64, 125.02, 121.02, 119.25, 117.31, 115.38, 115.02, 113.45, 113.05, 102.35, 102.03, 69.50, 69.46, 69.30, 69.20, 68.62, 68.43, 68.17, 65.17, 60.03, 54.33, 53.26, 51.96, 50.99, 47.57, 39.58, 37.30, 36.66, 34.70, 34.27, 30.18, 28.30, 28.05, 25.63, 23.36, 22.76, 21.05. HRMS (ESI-MS): m/z $[M+2H]^{2+}$ calculated for $C_{79}H_{112}ClN_{15}O_{14}^{2+}$: 764.9095, found 764.9099. Anal. RP-HPLC (220 nm): 95% (t_R = 10.79 min, *k* = 2.36). $C_{79}H_{110}ClN_{15}O_{14}$ x $C_{10}H_5F_{15}O_{10}$ (1529.29 + 570.11).

N^1-(1-(4-(((3-((4-(4-Chlorophenyl)-4-hydroxypiperidin-1-yl)methyl)-1*H*-indol-5-yl)oxy)methyl)-1*H*-1,2,3-triazol-1-yl)-2-oxo-7,10,13-trioxa-3-azahexadecan-16-yl)-N^4-(2-oxo-1-(4-((1-(4-(3-(piperidin-1-yl)propoxy)benzyl)piperidine-4-carboxamido)methyl)-1*H*-1,2,3-triazol-1-yl)-7,10,13-trioxa-3-azahexadecan-16-yl)terephthalamide pentahydrotrifluoroacetate (68)

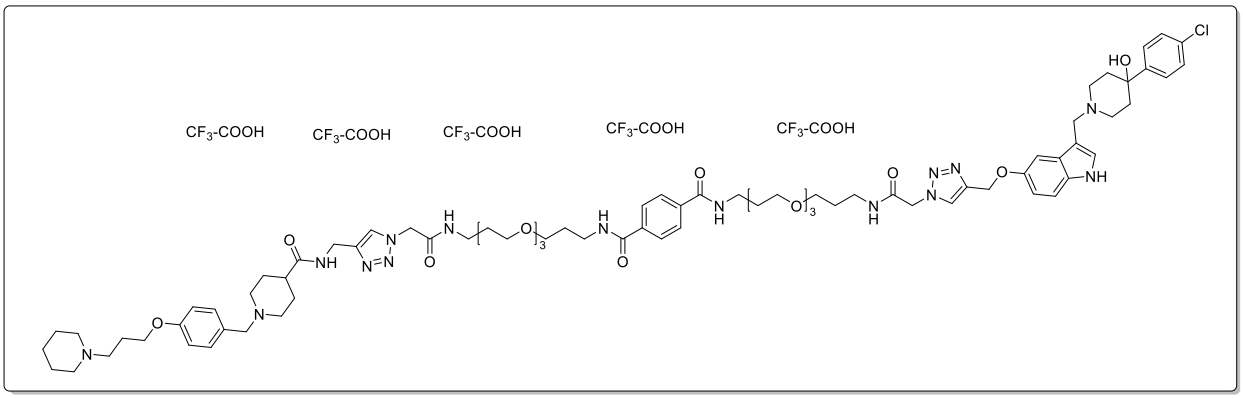

The title compound was prepared from **3a** (0.07 g, 0.17 mmol), **43** (0.07 g, 0.17 mmol) and **61c** (0.11 g, 0.15 mmol) according to the general procedure. The product **68** was obtained as a red solid (30.1 mg, 10%). ^{1}H NMR (400 MHz, D_2O) δ 7.79 (s, 1H), 7.68 (s, 1H), 7.51 (s, 4H), 7.29 (s, 1H), 7.22 (d, *J* = 8.6 Hz, 2H), 7.16 (d, *J* = 10.5 Hz, 1H), 7.10 – 7.02 (m, 3H), 6.97 (d, *J* = 7.7 Hz, 2H), 6.85 (d, *J* = 8.7 Hz, 2H), 6.63 (d, *J* = 7.9 Hz, 1H), 4.95 (s, 6H), 4.27 – 4.20 (m, 2H), 4.02 (s, 2H), 3.95 (t, *J* = 5.3 Hz, 2H), 3.42 – 3.22 (m, 30H), 3.21 – 3.13 (m, 8H), 3.12 – 3.02 (m, 6H), 2.99 – 2.91 (m, 2H), 2.84 – 2.69 (m, 4H), 2.37 (t, *J* = 11.9 Hz, 1H), 2.07 – 1.98 (m, 2H), 1.85 (d, *J* = 12.9 Hz, 2H), 1.77 (d, *J* = 14.7 Hz, 2H), 1.69 – 1.49 (m, 14H), 1.48 – 1.40 (m, 2H). ^{13}C NMR (101 MHz, D_2O) δ 175.60, 168.57, 167.25, 166.80, 159.23, 152.36, 144.51, 143.80, 136.48, 132.83, 132.51, 131.69, 128.32, 127.30, 126.04, 125.10, 121.08, 120.77, 117.87, 115.09, 114.96, 112.06, 102.09, 69.55, 69.39, 69.29, 68.66, 68.49, 68.25, 65.23, 60.11, 54.41, 53.33, 52.04, 51.07, 39.66, 37.31, 36.74, 34.32, 28.39, 28.14, 25.71, 23.44, 22.84, 21.13. HRMS (ESI-MS): m/z $[M+2H]^{2+}$ calculated for $C_{79}H_{112}ClN_{15}O_{14}^{2+}$: 764.9095, found 764.9103. Anal. RP-HPLC (220 nm): 96% (t_R = 10.30 min, *k* = 2.21). $C_{79}H_{110}ClN_{15}O_{14}$ x $C_{10}H_5F_{15}O_{10}$ (1529.29 + 570.11).

N^1-(1-(4-(((3-((4-(4-Chlorophenyl)-4-hydroxypiperidin-1-yl)methyl)-1*H*-indol-5-yl)oxy)methyl)-1*H*-1,2,3-triazol-1-yl)-2-oxo-7,10,13-trioxa-3-azahexadecan-16-yl)-N^5-(2-oxo-1-(4-((1-(4-(3-(piperidin-1-yl)propoxy)benzyl)piperidine-4-carboxamido)methyl)-1*H*-1,2,3-triazol-1-yl)-7,10,13-trioxa-3-azahexadecan-16-yl)glutaramide pentahydrotrifluoroacetate (69)

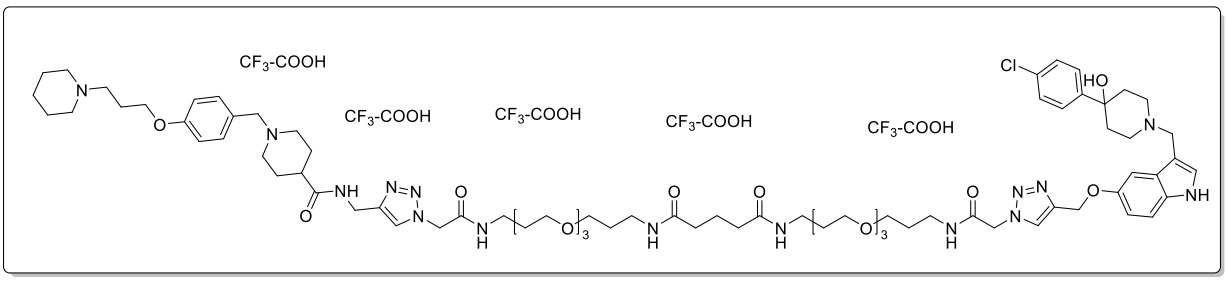

The title compound was prepared from **3a** (0.05 g, 0.13 mmol), **43** (0.05 g, 0.13 mmol) and **61d** (0.09 g, 0.13 mmol) according to the general procedure. The product **69** was obtained as a red solid (29.9 mg, 12%). ^{1}H NMR (400 MHz, D_2O) δ 7.89 (d, *J* = 17.0 Hz, 1H), 7.76 (d, *J* = 11.5 Hz, 1H), 7.41 (s, 1H), 7.30 – 7.14 (m, 8H), 6.91 (d, *J* = 8.7 Hz, 2H), 6.79 (dd, *J* = 8.9, 2.2 Hz, 1H), 5.10 (s, 2H), 5.01 (d, *J* = 10.9 Hz, 4H), 4.30 (d, *J* = 9.6 Hz, 4H), 4.09 (d, *J* = 8.2 Hz, 2H), 4.02 (t, *J* = 5.7 Hz, 2H), 3.48 – 3.23 (m, 32H), 3.14 – 3.10 (m, 4H), 3.08 – 3.00 (m, 6H), 2.91 – 2.74 (m, 4H), 2.43 – 2.31 (m, 1H), 2.13 – 1.97 (m, 8H), 1.96 – 1.87 (m, 2H), 1.82 (d, *J* = 15.7 Hz, 2H), 1.79 – 1.52 (m, 18H). ^{13}C NMR (101 MHz, D_2O) δ 175.77, 175.42, 167.46, 167.13, 159.25, 152.11, 144.58, 143.86, 132.88, 132.81, 131.83, 129.87, 128.54, 127.59, 126.37, 126.11, 125.17, 121.17, 117.86, 115.14, 114.96, 113.36, 102.84, 102.18, 69.57, 69.34, 68.60, 68.38, 68.30, 65.30, 62.08, 60.15, 54.45, 53.37, 52.16, 52.08, 51.52, 51.10, 47.66, 39.70, 36.76, 36.39, 34.96, 34.78, 34.37, 28.28, 28.14, 28.10, 25.72, 23.46, 22.87, 21.88, 21.14. HRMS (ESI-MS): m/z $[M+2H]^{2+}$ calculated for $C_{76}H_{114}ClN_{15}O_{14}^{2+}$: 747.9174, found 747.9180. Anal. RP-HPLC (220 nm): 98% (t_R = 9.50 min, *k* = 1.96). $C_{76}H_{112}ClN_{15}O_{14}$ x $C_{10}H_5F_{15}O_{10}$ (1495.27 + 570.11).

N^1-(1-(3-((1-(4-(((3-((4-(4-Chlorophenyl)-4-hydroxypiperidin-1-yl)methyl)-1*H*-indol-5-yl)oxy)methyl)-1*H*-1,2,3-triazol-1-yl)-2-oxo-7,10,13-trioxa-3-azahexadecan-16-yl)carbamoyl)phenyl)-1-oxo-6,9,12-trioxa-2-azapentadecan-15-yl)-N^3-(2-oxo-1-(4-((1-(4-(3-(piperidin-1-yl)propoxy)benzyl)piperidine-4-carboxamido)methyl)-1*H*-1,2,3-triazol-1-yl)-7,10,13-trioxa-3-azahexadecan-16-yl)isophthalamide pentahydrotrifluoroacetat (70)

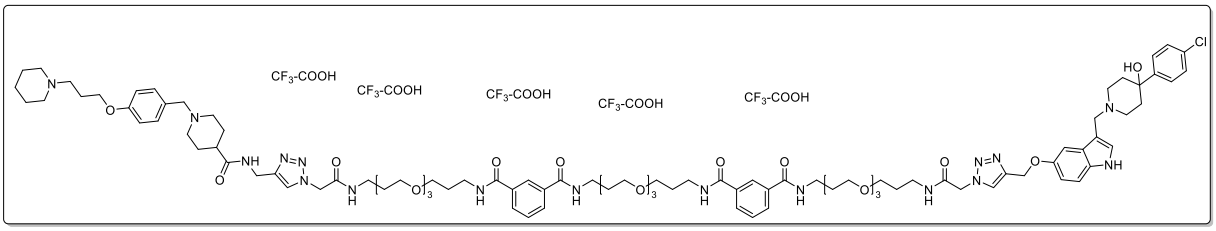

The title compound was prepared from **3a** (0.13 g, 0.32 mmol), **43** (0.13 g, 0.32 mmol) and **61e** (0.29 g, 0.27 mmol) according to the general procedure. The product **70** was obtained as a red solid (33.3 mg, 5%). ^{1}H NMR (600 MHz, D_2O) δ 7.86 (s, 2H), 7.80 (s, 1H), 7.73 – 7.68 (m, 1H), 7.63 – 7.55 (m, 4H), 7.28 (s, 1H), 7.23 – 7.12 (m, 5H), 7.10 – 6.97 (m, 3H), 6.95 – 6.85 (m, 2H), 6.82 (d, *J* = 8.1 Hz, 2H), 6.60 (s, 1H), 4.96 (s, 6H), 4.26 – 4.21 (m, 2H), 4.05 – 3.99 (m, 2H), 3.93 (s, 2H), 3.40 – 3.23 (m, 41H), 3.19 – 3.08 (m, 14H), 3.07 – 2.95 (m, 7H), 2.94 (s, 2H), 2.82 – 2.74 (m, 2H), 2.71 – 2.61 (m, 2H), 2.44 – 2.34 (m, 1H), 2.04 – 2.00 (m, 2H), 1.86 (d, *J* = 9.2 Hz, 2H), 1.75 (d, *J* = 14.0 Hz, 2H), 1.70 – 1.50 (m, 18H), 1.45 – 1.38 (m, 2H). ^{13}C NMR (151 MHz, D_2O) δ 175.40, 168.22, 168.00, 167.07, 162.96, 162.72, 162.49, 162.26, 159.12, 144.45, 133.94, 132.70, 129.97, 125.94, 124.98, 120.97, 119.28, 117.34, 115.40, 114.96, 113.47, 69.49, 69.30, 69.20, 68.57, 68.34, 68.16, 65.09, 59.99, 54.28, 53.21, 51.93, 50.98, 39.56, 37.26, 36.64, 34.25, 28.41, 28.09, 25.63, 23.35, 22.74, 21.05. HRMS (ESI-MS): m/z $[M+2H]^{2+}$ calculated for $C_{97}H_{138}ClN_{17}O_{19}^{2+}$: 940.0016, found 940.0022. Anal. RP-HPLC (220 nm): 98% (t_R = 12.19 min, *k* = 2.80). $C_{97}H_{136}ClN_{17}O_{19}$ x $C_{10}H_5F_{15}O_{10}$ (1879.71 + 570.11).

N^1-((1-(3-((3-((4-(4-Bromophenyl)-4-hydroxypiperidin-1-yl)methyl)-1*H*-indol-5-yl)oxy)propyl)-1*H*-1,2,3-triazol-4-yl)methyl)-N^3-((1-(2-oxo-2-((1-(4-(3-(piperidin-1-yl)propoxy)benzyl)piperidin-4-yl)amino)ethyl)-1*H*-1,2,3-triazol-4-yl)methyl)isophthalamide pentahydrotrifluoroacetate (71)

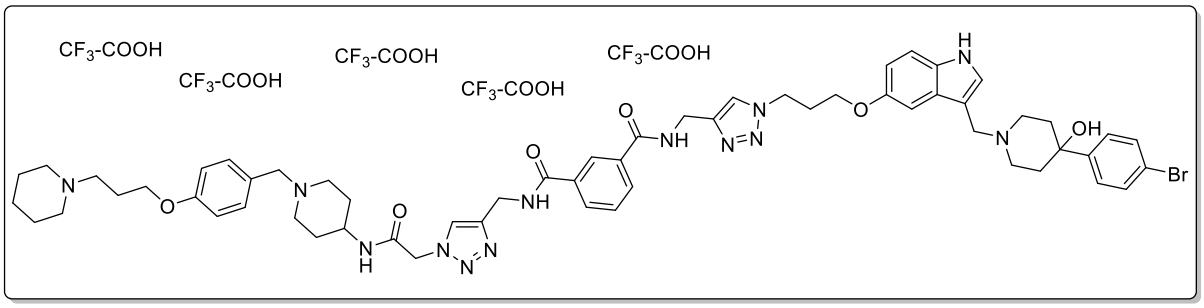

The title compound was prepared from **5b** (0.22 g, 0.45 mmol), **51** (0.19 g, 0.45 mmol) and **63** (0.10 g, 0.41 mmol) according to the general procedure. The product **71** was obtained as a red solid (52.4 mg, 7%). ^{1}H NMR (400 MHz, D_2O) δ 7.78 (s, 2H), 7.60 (d, *J* = 23.8 Hz, 2H), 7.42 (s, 1H), 7.23 – 6.71 (m, 12H), 6.42 (s, 1H), 4.99 (s, 2H), 4.48 – 4.14 (m, 6H), 4.10 – 3.77 (m, 6H), 3.74 – 3.49 (m, 3H), 3.48 – 3.17 (m, 6H), 3.16 – 2.93 (m, 7H), 2.80 – 2.61 (m, 4H), 2.15 – 1.69 (m, 10H), 1.68 – 1.42 (m, 6H). ^{13}C NMR (101 MHz, D_2O) δ 168.10, 166.66, 159.15, 152.73, 144.56, 133.11, 132.70, 131.22, 127.40, 126.23, 125.29, 120.99, 120.74, 117.83, 115.03, 114.93, 112.02, 101.87, 68.45, 65.18, 59.71, 54.29, 53.23, 50.70, 47.46, 46.67, 44.76, 34.73, 28.16, 24.29, 23.36, 22.74, 21.05, 17.70, 16.23. HRMS (ESI-MS): m/z $[M+H]^+$ calculated for $C_{59}H_{73}BrN_{13}O_6^+$: 1138.4985, found 1138.4971. Anal. RP-HPLC (220 nm): 98% (t_R = 10.42 min, *k* = 2.24). $C_{59}H_{72}BrN_{13}O_6$ x $C_{10}H_5F_{15}O_{10}$ (1139.21 + 570.11).

N^1-(3-(2-(3-(2-(4-(((3-((4-(4-Bromophenyl)-4-hydroxypiperidin-1-yl)methyl)-1*H*-indol-5-yl)oxy)methyl)-1*H*-1,2,3-triazol-1-yl)acetamido)propoxy)ethoxy)propyl)-N^3-(3-(2-(3-(2-(4-((1-(4-(3-(piperidin-1-yl)propoxy)benzyl)piperidine-4-carboxamido)methyl)-1*H*-1,2,3-triazol-1-yl)acetamido)propoxy)ethoxy)propyl)isophthalamide pentahydrotrifluoroacetate (72)

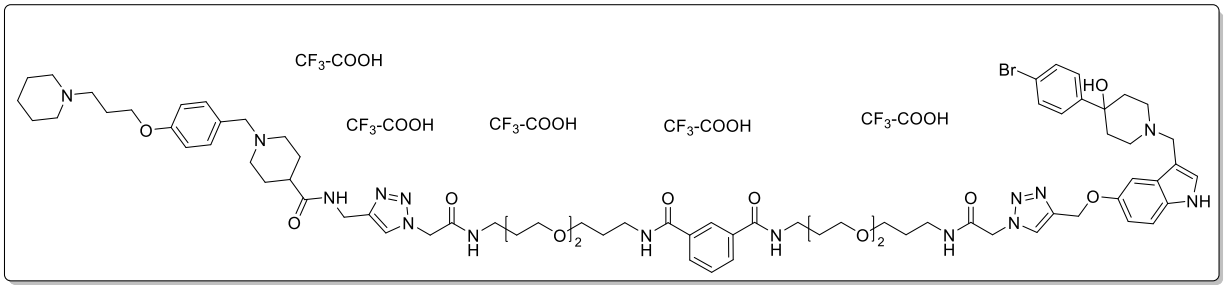

The title compound was prepared from **3b** (0.11 g, 0.25 mmol), **43** (0.10 g, 0.25 mmol) and **61a** (0.15 g, 0.23 mmol) according to the general procedure. The product **72** was obtained as a red solid (33,1 mg, 7%). ^{1}H NMR (600 MHz, D_2O) δ 7.87 (s, 1H), 7.85 – 7.80 (m, 1H), 7.71 (s, 1H), 7.63 – 7.59 (m, 2H), 7.38 (s, 1H), 7.33 – 7.21 (m, 7H), 7.14 – 7.08 (m, 3H), 6.93 – 6.86 (m, 2H), 6.75 (dd, *J* = 8.8, 2.1 Hz, 1H), 5.04 (s, 2H), 5.02 – 4.98 (m, 4H), 4.29 (s, 2H), 4.26 (s, 2H), 4.07 (s, 2H), 4.01 (t, *J* = 5.7 Hz, 2H), 3.45 – 3.35 (m, 17H), 3.32 – 3.29 (m, 2H), 3.27 – 3.20 (m, 11H), 3.17 – 3.13 (m, 2H), 3.06 (t, *J* = 6.9 Hz, 2H), 3.00 (t, *J* = 6.7 Hz, 2H), 2.86 – 2.76 (m, 4H), 2.40 (tt, *J* = 12.2, 3.4 Hz, 1H), 2.12 – 2.05 (m, 2H), 2.00 – 1.92 (m, 2H), 1.88 (d, *J* = 14.2 Hz, 2H), 1.82 (d, *J* = 14.9 Hz, 2H), 1.75 – 1.62 (m, 9H), 1.62 – 1.53 (m, 4H), 1.48 – 1.34 (m, 2H). ^{13}C NMR (151 MHz, D_2O) δ 175.61, 168.82, 167.26, 166.91, 159.14, 151.96, 144.94, 144.42, 143.77, 133.96, 132.76, 131.68, 131.35, 130.00, 129.72, 129.05, 127.42, 126.26, 126.16, 125.60, 125.02, 121.04, 120.88, 119.20, 117.27, 115.33, 115.03, 113.40, 113.20, 102.62, 102.04, 69.27, 68.63, 68.52, 68.15, 68.11, 65.20, 61.88, 60.04, 54.35, 53.28, 52.08, 51.97, 51.45, 50.99, 47.56, 39.58, 37.35, 37.29, 36.65, 34.62, 34.25, 28.21, 28.01, 27.94, 25.62, 23.36, 22.78, 21.04. HRMS (ESI-MS): m/z $[M+2H]^{2+}$ calculated for $C_{75}H_{104}BrN_{15}O_{12}^{2+}$: 742.8581, found 742.8592. Anal. RP-HPLC (220 nm): 98% (t_R = 10.71 min, *k* = 2.34). $C_{75}H_{102}BrN_{15}O_{12}$ x $C_{10}H_5F_{15}O_{10}$ (1485.64 + 570.11).

N^1-(1-(4-(((3-((4-(4-Bromophenyl)-4-hydroxypiperidin-1-yl)methyl)-1*H*-indol-5-yl)oxy)methyl)-1*H*-1,2,3-triazol-1-yl)-2-oxo-7,10,13-trioxa-3-azahexadecan-16-yl)-N^3-(2-oxo-1-(4-((1-(4-(3-(piperidin-1-yl)propoxy)benzyl)piperidine-4-carboxamido)methyl)-1*H*-1,2,3-triazol-1-yl)-7,10,13-trioxa-3-azahexadecan-16-yl)isophthalamide pentahydrotrifluoroacetate (73)

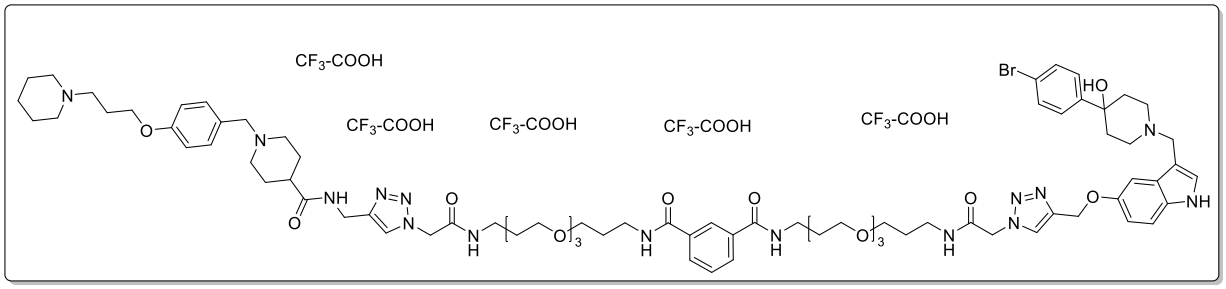

The title compound was prepared from **3b** (0.05 g, 0.11 mmol), **43** (0.05 g, 0.11 mmol) and **61b** (0.07 g, 0.1 mmol) according to the general procedure. The product **73** was obtained as a red solid (34.2 mg, 16%). ^{1}H NMR (400 MHz, D_2O) δ 7.88 (s, 1H), 7.82 (s, 1H), 7.73 (d, *J* = 12.8 Hz, 1H), 7.67 – 7.57 (m, 2H), 7.33 (s, 1H), 7.29 – 7.22 (m, 3H), 7.22 – 7.17 (m, 1H), 7.17 – 6.93 (m, 5H), 6.87 (t, *J* = 9.0 Hz, 2H), 6.66 (s, 1H), 4.98 (s, 6H), 4.26 (s, 4H), 4.02 (d, *J* = 25.7 Hz, 4H), 3.69 – 2.88 (m, 44H), 2.87 – 2.72 (m, 4H), 2.41 (t, *J* = 11.6 Hz, 1H), 2.11 – 1.99 (m, 2H), 1.99 – 1.82 (m, 4H), 1.80 (d, *J* = 14.1 Hz, 2H), 1.72 – 1.41 (m, 14H). ^{13}C NMR (101 MHz, D_2O) δ 175.51, 168.39, 167.16, 166.70, 159.17, 152.31, 145.27, 144.47, 143.76, 134.00, 132.76, 132.49, 131.65, 131.24, 130.03, 129.06, 127.55, 126.33, 125.70, 125.04, 121.03, 120.72, 117.82, 115.05, 114.92, 113.05, 112.01, 102.05, 69.48, 69.32, 69.23, 68.65, 68.46, 68.20, 65.19, 61.76, 60.06, 54.33, 53.27, 51.99, 51.02, 47.54, 39.60, 37.32, 36.69, 34.28, 28.36, 28.09, 25.65, 23.38, 22.77, 21.07. HRMS (ESI-MS): m/z $[M+2H]^{2+}$ calculated for $C_{79}H_{112}BrN_{15}O_{14}^{2+}$: 786.8843, found 786.8850. Anal. RP-HPLC (220 nm): 96% (t_R = 10.91 min, *k* = 2.40). $C_{79}H_{110}BrN_{15}O_{14}$ x $C_{10}H_5F_{15}O_{10}$ (1573.44 + 570.11).

N^1-(1-(4-(((3-((4-(4-Bromophenyl)-4-hydroxypiperidin-1-yl)methyl)-1*H*-indol-5-yl)oxy)methyl)-1*H*-1,2,3-triazol-1-yl)-2-oxo-7,10,13-trioxa-3-azahexadecan-16-yl)-N^4-(2-oxo-1-(4-((1-(4-(3-(piperidin-1-yl)propoxy)benzyl)piperidine-4-carboxamido)methyl)-1*H*-1,2,3-triazol-1-yl)-7,10,13-trioxa-3-azahexadecan-16-yl)terephthalamide pentahydrotrifluoroacetate (74)

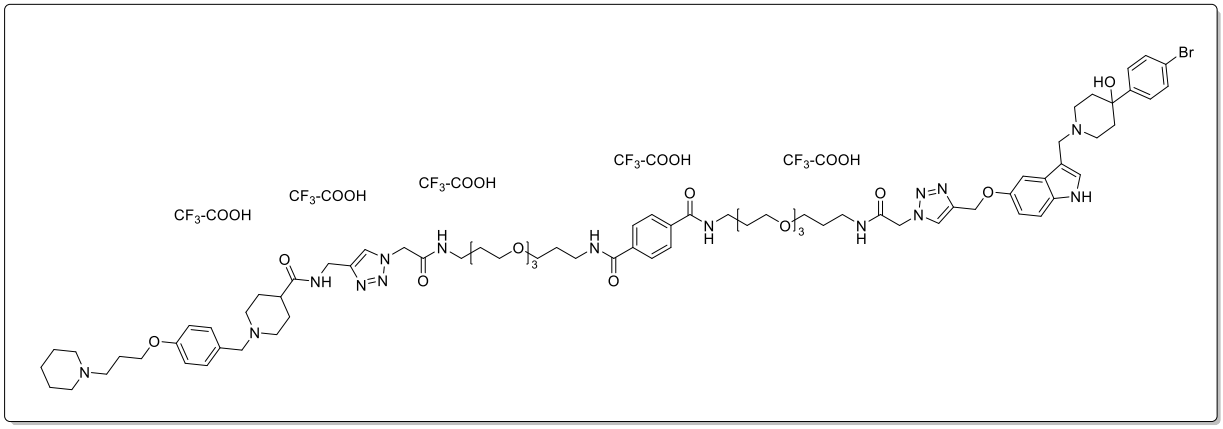

The title compound was prepared from **3b** (0.07 g, 0.17 mmol), **43** (0.07 g, 0.17 mmol) and **61c** (0.11 g, 0.15 mmol) according to the general procedure. The product **74** was obtained as a red solid (47.6 mg, 15%). ^{1}H NMR (400 MHz, D_2O) δ 7.78 (s, 1H), 7.71 (d, *J* = 12.8 Hz, 1H), 7.52 (s, 4H), 7.29 (s, 1H), 7.22 (d, *J* = 8.5 Hz, 2H), 7.14 (s, 1H), 7.08 – 6.93 (m, 5H), 6.86 (d, *J* = 8.5 Hz, 2H), 6.61 (s, 1H), 4.96 (s, 6H), 4.24 (s, 2H), 4.02 (s, 2H), 3.96 (s, 2H), 3.39 – 3.23 (m, 30H), 3.19 – 3.02 (m, 14H), 2.98 – 2.90 (m, 2H), 2.81 – 2.69 (m, 4H), 2.37 – 2.30 (m, 1H), 2.08 – 1.97 (m, 2H), 1.86 (d, *J* = 12.0 Hz, 2H), 1.78 (d, *J* = 14.7 Hz, 2H), 1.68 – 1.49 (m, 14H), 1.44 (s, 2H). ^{13}C NMR (101 MHz, D_2O) δ 175.58, 168.48, 167.24, 166.73, 159.23, 152.42, 144.54, 136.49, 132.83, 131.25, 127.31, 126.40, 125.09, 121.08, 120.85, 117.94, 115.10, 115.04, 112.13, 102.11, 69.57, 69.40, 69.30, 68.67, 68.52, 68.27, 65.23, 60.14, 54.41, 53.33, 52.03, 51.08, 39.67, 37.34, 36.75, 34.36, 28.44, 28.17, 25.72, 23.45, 22.85, 21.14. HRMS (ESI-MS): m/z $[M+2H]^{2+}$ calculated for $C_{79}H_{112}BrN_{15}O_{14}^{2+}$: 786.8843, found 786.8845. Anal. RP-HPLC (220 nm): 96% (t_R = 10.54 min, *k* = 2.28). $C_{79}H_{110}BrN_{15}O_{14}$ x $C_{10}H_5F_{15}O_{10}$ (1573.74 + 570.11).

N^1-(1-(4-(((3-((4-(4-Bromophenyl)-4-hydroxypiperidin-1-yl)methyl)-1*H*-indol-5-yl)oxy)methyl)-1*H*-1,2,3-triazol-1-yl)-2-oxo-7,10,13-trioxa-3-azahexadecan-16-yl)-N^5-(2-oxo-1-(4-((1-(4-(3-(piperidin-1-yl)propoxy)benzyl)piperidine-4-carboxamido)methyl)-1*H*-1,2,3-triazol-1-yl)-7,10,13-trioxa-3-azahexadecan-16-yl)glutaramide pentahydrotrifluoroacetate (75)

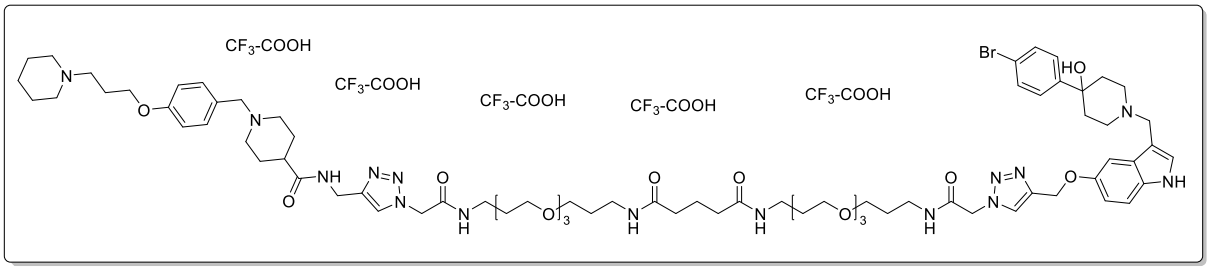

The title compound was prepared from **3b** (0.05 g, 0.13 mmol), **43** (0.05 g, 0.13 mmol) and **61d** (0.09 g, 0.13 mmol) according to the general procedure. The product **75** was obtained as a red solid (29.3 mg, 11%). ^{1}H NMR (400 MHz, D_2O) δ 7.87 (s, 1H), 7.77 – 7.71 (m, 1H), 7.37 (s, 1H), 7.27 – 7.22 (m, 5H), 7.15 – 7.07 (m, 3H), 6.90 (d, *J* = 8.6 Hz, 2H), 6.74 (d, *J* = 9.1 Hz, 1H), 5.06 – 4.96 (m, 6H), 4.33 – 4.21 (m, 4H), 4.06 (s, 2H), 4.00 (t, *J* = 5.7 Hz, 2H), 3.49 – 3.26 (m, 30H), 3.25 – 3.15 (m, 4H), 3.14 – 3.07 (m, 4H), 3.05 – 2.97 (m, 6H), 2.87 – 2.71 (m, 4H), 2.41 (t, *J* = 12.2 Hz, 1H), 2.09 – 2.00 (m, 6H), 1.89 (d, *J* = 15.1 Hz, 2H), 1.80 (d, *J* = 14.8 Hz, 2H), 1.74 – 1.48 (m, 18H). ^{13}C NMR (101 MHz, D_2O) δ 175.71, 175.34, 167.39, 167.00, 159.24, 152.24, 145.22, 144.54, 143.82, 132.88, 131.79, 131.45, 127.62, 126.44, 125.18, 121.14, 117.85, 115.14, 114.95, 102.17, 69.57, 69.34, 68.63, 68.39, 68.30, 65.29, 61.98, 60.11, 54.44, 53.36, 52.10, 51.10, 39.68, 36.77, 36.40, 34.97, 34.37, 28.31, 28.15, 25.72, 23.46, 22.87, 21.90, 21.14. HRMS (ESI-MS): m/z $[M+2H]^{2+}$ calculated for $C_{76}H_{114}BrN_{15}O_{14}^{2+}$: 769.8921, found 769.8929. Anal. RP-HPLC (220 nm): 98% (t_R = 9.87 min, *k* = 2.07). $C_{76}H_{112}BrN_{15}O_{14}$ x $C_{10}H_5F_{15}O_{10}$ (1539.73 + 570.11).

N^1-(1-(3-((1-(4-(((3-((4-(4-Bromophenyl)-4-hydroxypiperidin-1-yl)methyl)-1*H*-indol-5-yl)oxy)methyl)-1*H*-1,2,3-triazol-1-yl)-2-oxo-7,10,13-trioxa-3-azahexadecan-16-yl)carbamoyl)phenyl)-1-oxo-6,9,12-trioxa-2-azapentadecan-15-yl)-N^3-(2-oxo-1-(4-((1-(4-(3-(piperidin-1-yl)propoxy)benzyl)piperidine-4-carboxamido)methyl)-1*H*-1,2,3-triazol-1-yl)-7,10,13-trioxa-3-azahexadecan-16-yl)isophthalamide pentahydrotrifluoroacetate (76)

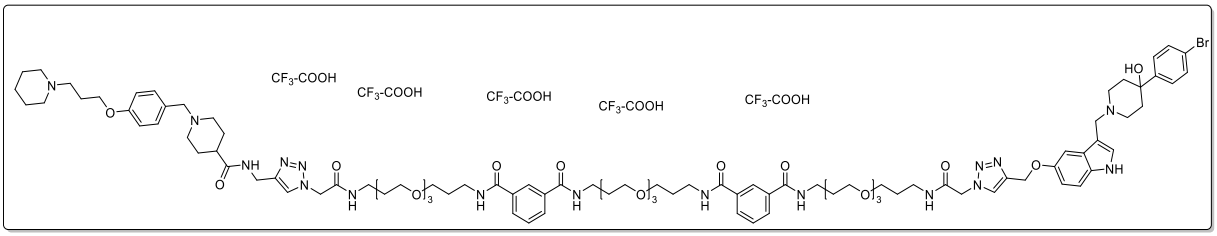

The title compound was prepared from **3b** (0.07 g, 0.17 mmol), **43** (0.07g, 0.17 mmol) and **61e** (0.16 g, 0.15 mmol) according to the general procedure. The product **76** was obtained as a red solid (38.8 mg, 10%). ^{1}H NMR (400 MHz, D_2O) δ 7.93 – 7.85 (m, 2H), 7.82 (s, 1H), 7.73 (d, *J* = 13.4 Hz, 1H), 7.68 – 7.55 (m, 4H), 7.30 (s, 1H), 7.26 – 7.10 (m, 6H), 7.10 – 6.94 (m, 4H), 6.85 (d, *J* = 7.0 Hz, 2H), 6.62 (s, 1H), 4.98 (s, 6H), 4.32 – 4.22 (m, 2H), 3.99 (d, *J* = 31.6 Hz, 4H), 3.46 – 3.03 (m, 60H), 2.99 – 2.89 (m, 2H), 2.83 – 2.67 (m, 4H), 2.43 (t, *J* = 17.4 Hz, 1H), 2.09 – 2.01 (m, 2H), 1.88 (d, *J* = 9.7 Hz, 2H), 1.78 (d, *J* = 13.7 Hz, 2H), 1.75 – 1.48 (m, 18H), 1.48 – 1.38 (m, 2H). ^{13}C NMR (101 MHz, D_2O) δ 175.45, 168.23, 168.01, 167.12, 166.56, 159.19, 152.50, 144.52, 134.01, 132.77, 131.63, 131.21, 130.04, 128.95, 125.78, 125.03, 121.02, 120.82, 117.91, 115.01, 112.10, 102.05, 69.54, 69.36, 68.65, 68.24, 65.16, 60.07, 54.34, 53.27, 52.00, 51.05, 39.61, 37.34, 36.72, 34.33, 28.49, 28.17, 25.70, 23.41, 22.79, 21.10. HRMS (ESI-MS): m/z $[M+2H]^{2+}$ calculated for $C_{97}H_{138}BrN_{17}O_{19}^{2+}$: 961.9764, found 961.9777. Anal. RP-HPLC (220 nm): 97% (t_R = 12.03 min, *k* = 2.75). $C_{97}H_{136}BrN_{17}O_{19}$ x $C_{10}H_5F_{15}O_{10}$ (1924.16 + 570.11).

N^1-((1-(3-(4-((4-((2,3-Dihydro-1*H*-inden-2-yl)(propyl)amino)butyl)carbamoyl)-2-methoxyphenoxy)propyl)-1*H*-1,2,3-triazol-4-yl)methyl)-N^3-((1-(2-oxo-2-((1-(4-(3-(piperidin-1-yl)propoxy)benzyl)piperidin-4-yl)amino)ethyl)-1*H*-1,2,3-triazol-4-yl)methyl)isophthalamide pentahydrotrifluoroacetate (77)

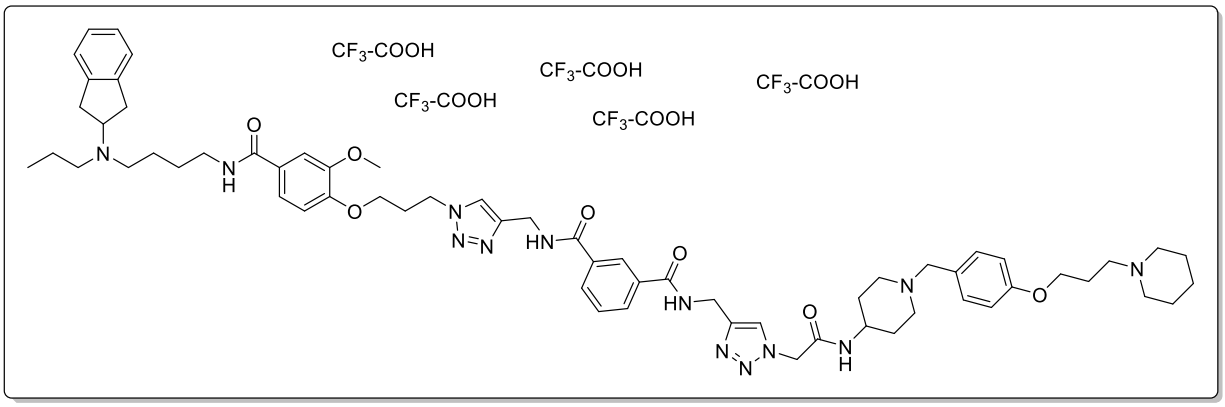

The title compound was prepared from **26** (0.17 g, 0.36 mmol), **51** (0.15 g, 0.36 mmol) and **63** (0.08g, 0.32 mmol) according to the general procedure. The product **77** was obtained as a yellow solid (43,0 mg, 7%). ^{1}H NMR (600 MHz, D_2O) δ 7.89 – 7.83 (m, 1H), 7.78 (s, 1H), 7.72 (d, *J* = 7.8 Hz, 1H), 7.68 (s, 1H), 7.53 (d, *J* = 7.8 Hz, 1H), 7.32 (t, *J* = 7.8 Hz, 1H), 7.29 – 7.25 (m, 2H), 7.02 – 6.97 (m, 4H), 6.97 – 6.89 (m, 4H), 6.55 (d, *J* = 8.3 Hz, 1H), 5.05 (s, 2H), 4.53 – 4.51 (m, 2H), 4.47 (t, *J* = 6.1 Hz, 2H), 4.40 (s, 2H), 4.12 – 4.08 (m, 2H), 4.03 (t, *J* = 5.7 Hz, 2H), 3.95 – 3.88 (m, 1H), 3.73 – 3.70 (m, 2H), 3.60 (s, 3H), 3.45 (d, *J* = 12.2 Hz, 2H), 3.36 (d, *J* = 12.8 Hz, 2H), 3.25 – 3.21 (m, 2H), 3.19 – 3.14 (m, 2H), 3.13 – 3.00 (m, 7H), 2.99 – 2.90 (m, 4H), 2.90 – 2.78 (m, 4H), 2.24 – 2.18 (m, 2H), 2.14 – 2.07 (m, 2H), 1.97 (d, *J* = 13.8 Hz, 2H), 1.83 (d, *J* = 15.2 Hz, 2H), 1.67 – 1.47 (m, 10H), 0.78 (t, *J* = 7.3 Hz, 3H). ^{13}C NMR (151 MHz, D_2O) δ 168.97, 168.75, 166.91, 162.97, 162.74, 159.16, 150.11, 147.82, 144.63, 138.52, 138.45, 133.42, 133.30, 132.76, 130.27, 129.06, 127.34, 127.30, 125.84, 125.72, 125.29, 124.33, 124.26, 121.07, 120.58, 117.24, 115.31, 115.03, 111.77, 110.12, 65.22, 65.05, 63.07, 59.78, 55.48, 54.37, 53.29, 52.92, 51.91, 50.75, 50.43, 47.17, 46.63, 44.80, 38.75, 34.82, 34.76, 34.22, 33.99, 28.32, 28.16, 25.50, 23.37, 22.78, 21.05, 20.56, 17.23, 10.08, 8.17.HRMS (ESI-MS): m/z $[M+2H]^{2+}$ calculated for $C_{63}H_{85}N_{13}O_7^{2+}$: 567.8342, found 567.8352. Anal. RP-HPLC (220 nm): 97% (t_R = 10.00 min, *k* = 2.11). $C_{63}H_{83}N_{13}O_7$ x $C_{10}H_5F_{15}O_{10}$ (1134.44 + 570.11).

N^1-(3-(2-(3-(2-(4-((4-((4-((2,3-Dihydro-1*H*-inden-2-yl)(propyl)amino)butyl)carbamoyl)-2-methoxyphenoxy)methyl)-1*H*-1,2,3-triazol-1-yl)acetamido)propoxy)ethoxy)propyl)-N^3-(3-(2-(3-(2-(4-((1-(4-(3-(piperidin-1-yl)propoxy)benzyl)piperidine-4-carboxamido)methyl)-1*H*-1,2,3-triazol-1-yl)acetamido)propoxy)ethoxy)propyl)isophthalamide pentahydrotrifluoroacetate (78)

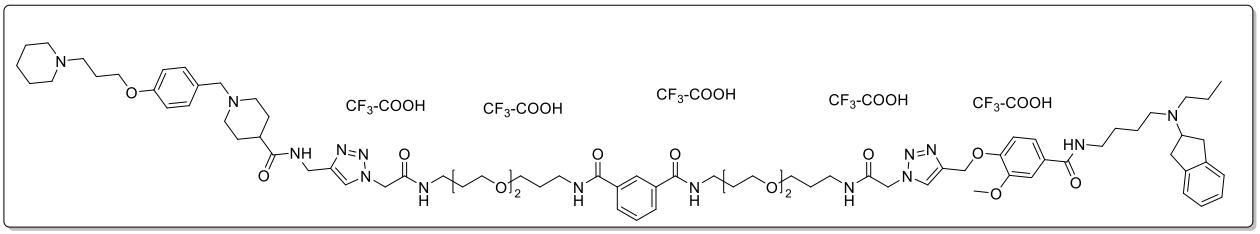

The title compound was prepared from **25b** (0.11 g, 0.25 mmol), **43** (0.10 g, 0.25 mmol) and **61a** (0.15 g, 0.23 mmol) according to the general procedure. The product **78** was obtained as a yellow solid (28,0 mg, 6%). ^{1}H NMR (600 MHz, D_2O) δ 7.98 (s, 1H), 7.87 (s, 1H), 7.76 (d, *J* = 17.7 Hz, 1H), 7.67 (dd, *J* = 7.8, 1.4 Hz, 2H), 7.35 (t, *J* = 7.8 Hz, 1H), 7.28 (d, *J* = 8.7 Hz, 2H), 7.22 (dd, *J* = 8.4, 1.9 Hz, 1H), 7.16 (d, *J* = 1.9 Hz, 1H), 7.10 – 7.05 (m, 3H), 7.02 (d, *J* = 6.8 Hz, 1H), 6.98 (d, *J* = 8.5 Hz, 1H), 6.94 – 6.90 (m, 2H), 5.12 (s, 2H), 5.05 (s, 2H), 5.02 (s, 2H), 4.31 (d, *J* = 13.6 Hz, 2H), 4.12 – 4.05 (m, 3H), 4.03 (t, *J* = 5.8 Hz, 2H), 3.65 (s, 3H), 3.50 – 3.38 (m, 17H), 3.36 – 3.32 (m, 4H), 3.31 – 3.27 (m, 6H), 3.25 – 3.12 (m, 6H), 3.12 – 3.08 (m, 6H), 3.07 – 2.97 (m, 6H), 2.90 – 2.79 (m, 4H), 2.45 (tt, *J* = 12.2, 3.5 Hz, 1H), 2.14 – 2.08 (m, 2H), 1.93 (d, *J* = 14.2 Hz, 2H), 1.84 (d, *J* = 14.9 Hz, 2H), 1.76 – 1.52 (m, 21H), 0.81 (t, *J* = 7.3 Hz, 3H). ^{13}C NMR (151 MHz, D_2O) δ 175.68, 169.25, 169.03, 169.01, 167.34, 167.07, 159.14, 149.52, 148.42, 144.46, 142.91, 138.64, 134.05, 132.77, 132.51, 130.04, 129.10, 127.41, 127.39, 126.85, 126.50, 125.60, 125.03, 124.41, 124.33, 121.07, 120.56, 119.19, 117.26, 115.33, 115.08, 115.02, 113.40, 113.09, 110.53, 69.31, 68.66, 68.18, 68.15, 65.22, 63.16, 61.38, 60.06, 55.58, 54.37, 53.29, 52.94, 52.20, 51.99, 51.01, 50.49, 46.63, 39.60, 38.74, 37.36, 37.33, 36.69, 36.66, 34.31, 34.29, 34.09, 28.22, 28.01, 27.94, 25.64, 25.55, 23.38, 22.79, 21.05, 20.65, 17.24, 10.10. HRMS (ESI-MS): m/z $[M+2H]^{2+}$ calculated for $C_{79}H_{115}N_{15}O_{13}^{2+}$: 740.9394, found 740.9404. Anal. RP-HPLC (220 nm): 98% (t_R = 10.48 min, *k* = 2.26). $C_{79}H_{113}N_{15}O_{13}$ x $C_{10}H_5F_{15}O_{10}$ (1480.87 + 570.11).

N^1-(1-(4-((4-((4-((2,3-Dihydro-1*H*-inden-2-yl)(propyl)amino)butyl)carbamoyl)-2-methoxyphenoxy)methyl)-1*H*-1,2,3-triazol-1-yl)-2-oxo-7,10,13-trioxa-3-azahexadecan-16-yl)-N^3-(2-oxo-1-(4-((1-(4-(3-(piperidin-1-yl)propoxy)benzyl)piperidine-4-carboxamido)methyl)-1*H*-1,2,3-triazol-1-yl)-7,10,13-trioxa-3-azahexadecan-16-yl)isophthalamide pentahydrotrifluoroacetate (79)

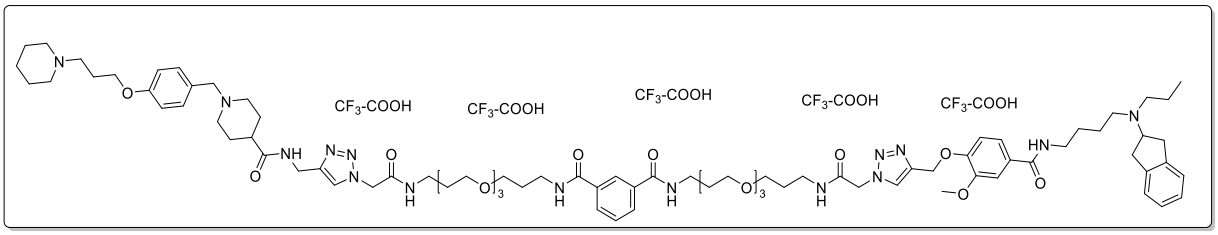

The title compound was prepared from **25b** (0.07g, 0.17 mmol), **43** (0.07g, 0.17 mmol) and **61b** (0.11 g, 0.15 mmol) according to the general procedure. The product **79** was obtained as a yellow solid (56.7 mg). ^{1}H NMR (400 MHz, D_2O) δ 7.93 (s, 1H), 7.88 (s, 1H), 7.74 (d, *J* = 13.0 Hz, 1H), 7.65 (dd, *J* = 7.8, 1.5 Hz, 2H), 7.32 (t, *J* = 7.8 Hz, 1H), 7.24 (d, *J* = 8.2 Hz, 2H), 7.18 (dd, *J* = 8.4, 1.6 Hz, 1H), 7.11 (d, *J* = 1.4 Hz, 1H), 7.00 (s, 3H), 6.95 (s, 1H), 6.87 (d, *J* = 7.3 Hz, 3H), 4.99 (s, 6H), 4.28 (d, *J* = 10.8 Hz, 2H), 4.07 (d, *J* = 12.4 Hz, 2H), 3.98 (t, *J* = 5.0 Hz, 2H), 3.91 (d, *J* = 6.3 Hz, 1H), 3.57 (s, 3H), 3.46 – 3.35 (m, 24H), 3.30 – 3.28 (m, 4H), 3.27 – 3.20 (m, 6H), 3.17 – 2.89 (m, 15H), 2.88 – 2.74 (m, 4H), 2.49 – 2.35 (m, 1H), 2.12 – 2.01 (m, 2H), 1.90 (d, *J* = 13.8 Hz, 2H), 1.80 (d, *J* = 14.5 Hz, 2H), 1.74 – 1.47 (m, 19H), 0.76 (t, *J* = 7.1 Hz, 3H). ^{13}C NMR (101 MHz, D_2O) δ 175.64, 168.76, 168.70, 167.29, 166.94, 159.23, 149.71, 148.42, 144.54, 142.86, 138.61, 134.11, 132.84, 130.15, 129.20, 127.48, 126.81, 126.59, 125.74, 125.13, 124.48, 124.40, 121.10, 120.65, 117.85, 115.10, 114.95, 112.75, 112.06, 110.50, 69.62, 69.58, 69.42, 69.32, 68.72, 68.28, 65.25, 63.22, 61.41, 60.12, 55.58, 54.42, 53.35, 52.91, 52.16, 52.08, 51.09, 50.59, 39.68, 38.85, 37.38, 36.83, 36.76, 34.36, 34.20, 28.41, 28.14, 25.73, 23.45, 22.86, 21.14, 20.72, 17.22, 10.23. HRMS (ESI-MS): m/z $[M+2H]^{2+}$ calculated for $C_{83}H_{123}N_{15}O_{15}^{2+}$: 784.9656, found 784.9668. Anal. RP-HPLC (220 nm): 96% (t_R = 10.65 min, *k* = 2.32). $C_{83}H_{121}N_{15}O_{15}$ x $C_{10}H_5F_{15}O_{10}$ (1568.97 + 570.11).

N^1-(1-(4-((4-((4-((2,3-Dihydro-1*H*-inden-2-yl)(propyl)amino)butyl)carbamoyl)-2-methoxyphenoxy)methyl)-1*H*-1,2,3-triazol-1-yl)-2-oxo-7,10,13-trioxa-3-azahexadecan-16-yl)-N^4-(2-oxo-1-(4-((1-(4-(3-(piperidin-1-yl)propoxy)benzyl)piperidine-4-carboxamido)methyl)-1*H*-1,2,3-triazol-1-yl)-7,10,13-trioxa-3-azahexadecan-16-yl)terephthalamide pentahydrotrifluoroacetate (80)

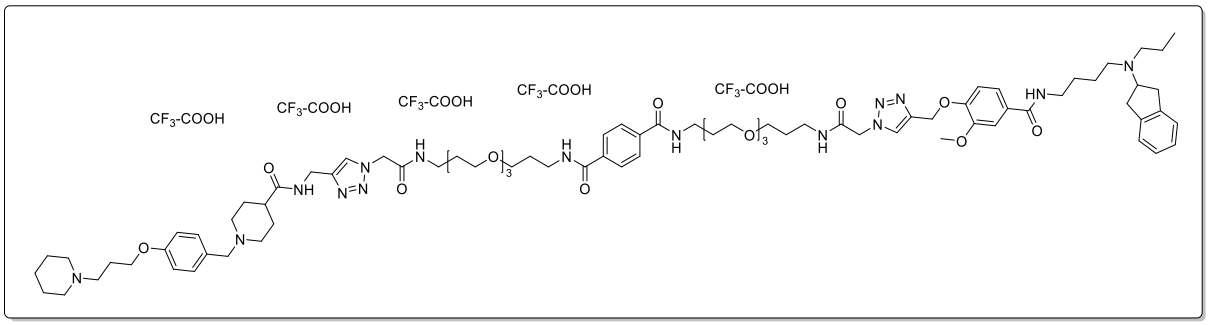

The title compound was prepared from **25b** (0.07 g, 0.17 mmol), **43** (0.07 g, 0.17 mmol) and **61c** (0.11 g, 0.15 mmol) according to the general procedure. The product **80** was obtained as a yellow solid (31.3 mg, 10%). ^{1}H NMR (400 MHz, D_2O) δ 7.95 (s, 1H), 7.77 – 7.70 (m, 1H), 7.57 (s, 4H), 7.27 – 7.23 (m, 2H), 7.19 (dd, *J* = 8.4, 2.0 Hz, 1H), 7.12 (d, *J* = 2.0 Hz, 1H), 7.07 – 7.01 (m, 3H), 6.99 – 6.96 (m, 1H), 6.94 – 6.86 (m, 3H), 5.07 – 4.97 (m, 6H), 4.30 (d, *J* = 10.1 Hz, 2H), 4.09 (d, *J* = 12.8 Hz, 2H), 4.03 – 3.94 (m, 3H), 3.60 (s, 3H), 3.50 – 3.36 (m, 24H), 3.36 – 3.31 (m, 4H), 3.29 – 3.21 (m, 6H), 3.17 – 3.08 (m, 8H), 3.05 – 2.91 (m, 6H), 2.89 – 2.74 (m, 4H), 2.43 (tt, *J* = 12.1, 3.4 Hz, 1H), 2.14 – 2.03 (m, 2H), 1.91 (d, *J* = 16.2 Hz, 2H), 1.82 (d, *J* = 14.8 Hz, 2H), 1.76 – 1.47 (m, 20H), 0.78 (t, *J* = 7.3 Hz, 3H). ^{13}C NMR (101 MHz, D_2O) δ 175.75, 169.07, 168.93, 167.41, 167.09, 159.24, 149.67, 148.44, 144.54, 142.92, 138.67, 138.61, 136.56, 132.86, 127.48, 127.34, 126.83, 126.61, 125.14, 124.50, 124.42, 121.14, 120.63, 117.85, 115.11, 114.95, 112.92, 112.05, 110.52, 69.63, 69.59, 69.43, 69.33, 68.70, 68.33, 68.29, 65.28, 63.23, 61.42, 60.14, 55.61, 54.45, 53.37, 52.96, 52.20, 52.07, 51.10, 50.57, 48.65, 39.69, 38.85, 37.34, 36.85, 36.76, 34.37, 34.19, 28.36, 28.13, 25.73, 23.46, 22.87, 21.14, 20.72, 17.27, 10.20. HRMS (ESI-MS): m/z $[M+2H]^{2+}$ calculated for $C_{83}H_{123}N_{15}O_{15}^{2+}$: 784.8656, found 784.9665. Anal. RP-HPLC (220 nm): 99% (t_R = 9.97 min, *k* = 2.11). $C_{83}H_{121}N_{15}O_{15}$ x $C_{10}H_5F_{15}O_{10}$ (1568.97 + 570.11).

N^1-(1-(4-((4-((4-((2,3-Dihydro-1*H*-inden-2-yl)(propyl)amino)butyl)carbamoyl)-2-methoxyphenoxy)methyl)-1*H*-1,2,3-triazol-1-yl)-2-oxo-7,10,13-trioxa-3-azahexadecan-16-yl)-N^5-(2-oxo-1-(4-((1-(4-(3-(piperidin-1-yl)propoxy)benzyl)piperidine-4-carboxamido)methyl)-1*H*-1,2,3-triazol-1-yl)-7,10,13-trioxa-3-azahexadecan-16-yl)glutaramide pentahydrotrifluoroacetate (81)

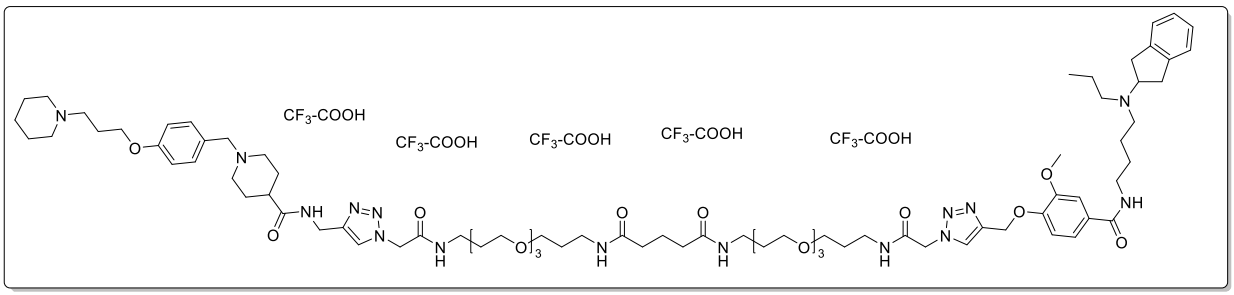

The title compound was prepared from **25b** (0.06 g, 0.14 mmol), **43** (0.06 g, 0.14 mmol) and **61d** (0.09 g, 0.13 mmol) according to the general procedure. The product **81** was obtained as a yellow solid (34.3 mg, 13%). ^{1}H NMR (400 MHz, D_2O) δ 7.99 (s, 1H), 7.80 – 7.74 (m, 1H), 7.30 – 7.23 (m, 3H), 7.19 (d, *J* = 2.0 Hz, 1H), 7.09 – 6.99 (m, 5H), 6.93 – 6.88 (m, 2H), 5.13 (s, 2H), 5.07 – 5.02 (m, 4H), 4.35 – 4.29 (m, 2H), 4.14 – 3.99 (m, 5H), 3.65 (s, 3H), 3.57 – 3.28 (m, 32H), 3.28 – 2.90 (m, 22H), 2.90 – 2.75 (m, 4H), 2.45 (tt, *J* = 12.2, 3.5 Hz, 1H), 2.13 – 2.02 (m, 6H), 1.98 – 1.89 (m, 2H), 1.87 – 1.77 (m, 2H), 1.76 – 1.51 (m, 22H), 0.79 (t, *J* = 7.3 Hz, 3H). ^{13}C NMR (101 MHz, D_2O) δ 175.81, 175.48, 169.25, 167.48, 167.21, 163.02, 159.25, 154.55, 149.70, 148.56, 142.95, 138.75, 132.88, 127.50, 126.71, 125.19, 124.52, 121.16, 117.83, 115.13, 113.17, 110.64, 69.60, 69.37, 68.40, 68.32, 65.30, 63.27, 55.70, 54.46, 53.38, 52.23, 52.11, 51.11, 39.71, 38.86, 36.81, 36.40, 34.97, 34.41, 28.30, 28.14, 25.74, 23.47, 22.88, 21.89, 21.15, 20.77, 17.29, 10.20. HRMS (ESI-MS): m/z $[M+2H]^{2+}$ calculated for $C_{80}H_{125}N_{15}O_{15}^{2+}$: 767.9734, found 767.9741. Anal. RP-HPLC (220 nm): 97% (t_R = 9.69 min, *k* = 2.02). $C_{80}H_{123}N_{15}O_{15}$ x $C_{10}H_5F_{15}O_{10}$ (1534.95 + 570.11).

N^1-(1-(3-((1-(4-((4-((4-((2,3-Dihydro-1*H*-inden-2-yl)(propyl)amino)butyl)carbamoyl)-2-methoxyphenoxy)methyl)-1*H*-1,2,3-triazol-1-yl)-2-oxo-7,10,13-trioxa-3-azahexadecan-16-yl)carbamoyl)phenyl)-1-oxo-6,9,12-trioxa-2-azapentadecan-15-yl)-N^3-(2-oxo-1-(4-((1-(4-(3-(piperidin-1-yl)propoxy)benzyl)piperidine-4-carboxamido)methyl)-1*H*-1,2,3-triazol-1-yl)-7,10,13-trioxa-3-azahexadecan-16-yl)isophthalamide pentahydrotrifluoroacetate (82)

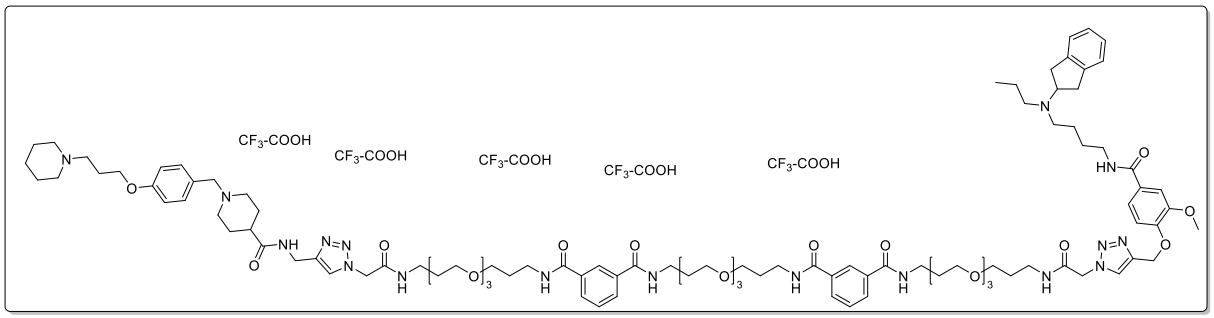

The title compound was prepared from **25b** (0.07 g, 0.17 mmol), **43** (0.07g, 0.17 mmol) and **61e** (0.16 g, 0.15 mmol) according to the general procedure. The product **82** was obtained as a yellow solid (32.4 mg, 9%). ^{1}H NMR (400 MHz, D_2O) δ 7.93 – 7.88 (m, 1H), 7.87 – 7.83 (m, 2H), 7.75 – 7.69 (m, 1H), 7.65 – 7.58 (m, 4H), 7.30 – 7.13 (m, 5H), 7.09 (s, 1H), 6.97 – 6.80 (m, 7H), 4.97 (s, 5H), 4.32 – 4.21 (m, 2H), 4.09 – 3.91 (m, 4H), 3.84 (s, 1H), 3.53 (s, 3H), 3.47 – 3.28 (m, 40H), 3.28 – 3.16 (m, 13H), 3.15 – 2.99 (m, 10H), 2.95 – 2.70 (m, 9H), 2.41 (t, *J* = 11.7 Hz, 1H), 2.10 – 1.99 (m, 2H), 1.93 – 1.84 (m, 2H), 1.77 (d, *J* = 12.1 Hz, 2H), 1.71 – 1.44 (m, 23H), 0.73 (t, *J* = 6.2 Hz, 3H). ^{13}C NMR (101 MHz, D_2O) δ 175.59, 168.48, 167.22, 166.84, 162.80, 162.45, 159.22, 158.85, 149.73, 148.39, 144.51, 142.83, 134.06, 134.01, 132.82, 130.12, 129.14, 126.77, 126.58, 125.75, 125.13, 124.42, 121.08, 120.75, 117.85, 115.08, 114.95, 112.05, 69.62, 69.58, 69.41, 69.32, 68.70, 68.28, 65.22, 63.22, 60.12, 55.54, 54.40, 53.33, 52.07, 51.09, 39.67, 37.36, 36.82, 36.75, 34.35, 28.47, 28.17, 25.72, 23.45, 22.85, 21.14, 10.27. HRMS (ESI-MS): m/z $[M+2H]^{2+}$ calculated for $C_{101}H_{149}N_{17}O_{20}^{2+}$: 960.0577, found 960.0584. Anal. RP-HPLC (220 nm): 97% (t_R = 10.91 min, *k* = 2.40). $C_{101}H_{147}N_{17}O_{20}$ x $C_{10}H_5F_{15}O_{10}$ (1919.39 + 570.11).

N^1-(1-(4-(Acetamidomethyl)-1*H*-1,2,3-triazol-1-yl)-2-oxo-7,10,13-trioxa-3-azahexadecan-16-yl)-N^4-(1-(4-((4-((4-((2,3-dihydro-1*H*-inden-2-yl)(propyl)amino)butyl)carbamoyl)-2-methoxyphenoxy)methyl)-1*H*-1,2,3-triazol-1-yl)-2-oxo-7,10,13-trioxa-3-azahexadecan-16-yl)terephthalamide (83)

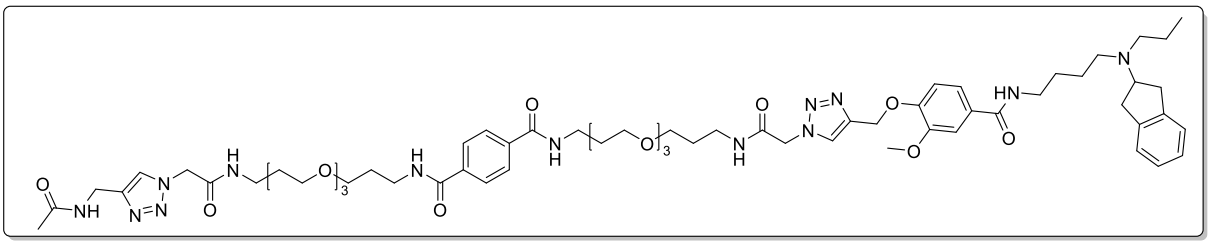

The title compound was prepared form **64** (9.7 mg, 0.1 mmol, 1 eq), **25b** (47.8 mg, 0.11 mmol, 1.1 eq) and **61c** (73.6 mg, 0.1 mmol, 1 eq) according to the general procedure. Purification was performed under basic conditions (Method B). The product **83** was obtained as a white solid (13.9 mg, 11 %). ^{1}H NMR (400 MHz, CD_3OD) δ 8.10 (s, 1H), 7.86 (s, 5H), 7.42 (dd, *J* = 10.9, 2.0 Hz, 2H), 7.19 – 7.09 (m, 5H), 5.23 (s, 2H), 5.14 (s, 2H), 5.09 (s, 2H), 4.57 (s, 1H), 4.41 (s, 2H), 3.83 (s, 3H), 3.66 – 3.39 (m, 32H), 3.27 (d, *J* = 6.7 Hz, 2H), 3.17 – 3.04 (m, 2H), 2.97 – 2.91 (m, 2H), 2.90 – 2.83 (m, 2H), 2.80 – 2.73 (m, 2H), 1.94 (s, 3H), 1.89 – 1.82 (m, 4H), 1.78 – 1.71 (m, 4H), 1.69 – 1.58 (m, 6H), 0.92 (t, *J* = 7.3 Hz, 3H). ^{13}C NMR (101 MHz, CD_3OD) δ 168.30, 167.71, 166.31, 166.23, 165.94, 150.59, 149.46, 144.78, 143.22, 140.16, 137.06, 127.58, 127.09, 126.56, 125.85, 124.03, 120.13, 113.14, 110.90, 70.12, 69.86, 69.77, 68.83, 68.42, 63.22, 61.92, 55.08, 52.84, 51.85, 51.77, 50.70, 38.96, 37.41, 36.92, 36.86, 35.63, 34.29, 28.96, 28.75, 26.90, 22.28, 21.06, 20.65, 18.24, 10.48. HRMS (ESI-MS): m/z $[M+3H]^{3+}$ calculated for $C_{64}H_{96}N_{13}O_{14}^{3+}$: 423.5728, found 423.5740; Anal. RP-HPLC (220 nm) 99% (t_R = 11.10 min, *k* = 2,7). $C_{64}H_{93}N_{13}O_{14}$ (1268.53).

N^1-(1-(4-((2-Methoxy-4-((4-(2-methoxyphenyl)piperazin-1-yl)methyl)phenoxy)methyl)-1*H*-1,2,3-triazol-1-yl)-2-oxo-7,10,13-trioxa-3-azahexadecan-16-yl)-N^3-(2-oxo-1-(4-((1-(4-(3-(piperidin-1-yl)propoxy)benzyl)piperidine-4-carboxamido)methyl)-1*H*-1,2,3-triazol-1-yl)-7,10,13-trioxa-3-azahexadecan-16-yl)isophthalamide hexahydrotrifluoroacetate (84)

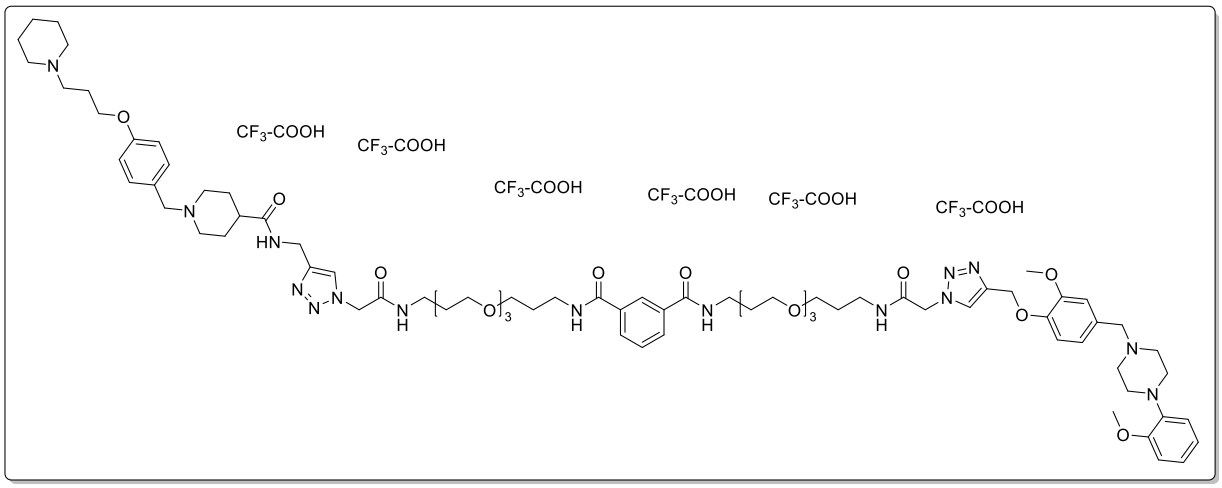

The title compound was prepared from **11b** (0.05 g, 0.14 mmol) **43** (0.06 g, 0.14 mmol) and **61b** (0.09 g, 0.13 mmol) according to the general procedure. The product **84** was obtained as a yellow solid (35.66 mg, 14%). ^{1}H NMR (400 MHz, D_2O) δ 7.95 (s, 1H), 7.90 – 7.85 (m, 1H), 7.76 – 7.71 (m, 1H), 7.67 (dd, *J* = 7.8, 1.7 Hz, 2H), 7.35 (t, *J* = 7.8 Hz, 1H), 7.28 – 7.21 (m, 2H), 7.11 – 7.06 (m, 1H), 6.99 (d, *J* = 8.3 Hz, 2H), 6.94 – 6.82 (m, 6H), 5.06 (s, 2H), 5.03 (s, 2H), 5.00 (s, 2H), 4.31 – 4.25 (m, 2H), 4.18 (s, 2H), 4.10 – 4.04 (m, 2H), 3.99 (t, *J* = 5.7 Hz, 2H), 3.70 (s, 3H), 3.64 (s, 3H), 3.49 – 3.21 (m, 40H), 3.15 – 3.07 (m, 6H), 2.87 – 2.73 (m, 4H), 2.42 (tt, *J* = 12.2, 3.4 Hz, 1H), 2.06 – 1.97 (m, 2H), 1.90 (d, *J* = 14.7 Hz, 2H), 1.80 (d, *J* = 14.8 Hz, 2H), 1.74 – 1.51 (m, 14H). ^{13}C NMR (101 MHz, D_2O) δ 175.73, 168.95, 167.35, 167.14, 159.23, 151.75, 149.08, 148.01, 144.51, 143.02, 135.02, 134.16, 132.86, 130.19, 129.25, 127.34, 126.66, 125.74, 125.18, 124.45, 121.71, 121.36, 121.13, 120.70, 119.41, 117.81, 115.11, 114.91, 114.53, 114.19, 112.36, 112.01, 69.62, 69.57, 69.41, 69.31, 68.74, 68.29, 65.27, 61.57, 60.13, 55.70, 55.47, 54.43, 53.36, 52.10, 51.09, 50.39, 48.31, 39.68, 37.39, 36.82, 36.75, 34.33, 28.36, 28.11, 25.72, 23.45, 22.86, 21.13. HRMS (ESI-MS): m/z $[M+2H]^{2+}$ calculated for $C_{78}H_{115}N_{15}O_{15}^{2+}$: 750.9343, found 750.9348. Anal. RP-HPLC (220 nm): 99% (t_R = 9.44 min, *k* = 1.94). $C_{78}H_{113}N_{15}O_{15}$ x $C_{12}H_6F_{18}O_{12}$ (1500.82 + 684.14).

N^1-(1-(4-((2-Methoxy-4-((4-(2-methoxyphenyl)piperazin-1-yl)methyl)phenoxy)methyl)-1*H*-1,2,3-triazol-1-yl)-2-oxo-7,10,13-trioxa-3-azahexadecan-16-yl)-N^4-(2-oxo-1-(4-((1-(4-(3-(piperidin-1-yl)propoxy)benzyl)piperidine-4-carboxamido)methyl)-1*H*-1,2,3-triazol-1-yl)-7,10,13-trioxa-3-azahexadecan-16-yl)terephthalamide hexahydrotrifluoroacetate (85)

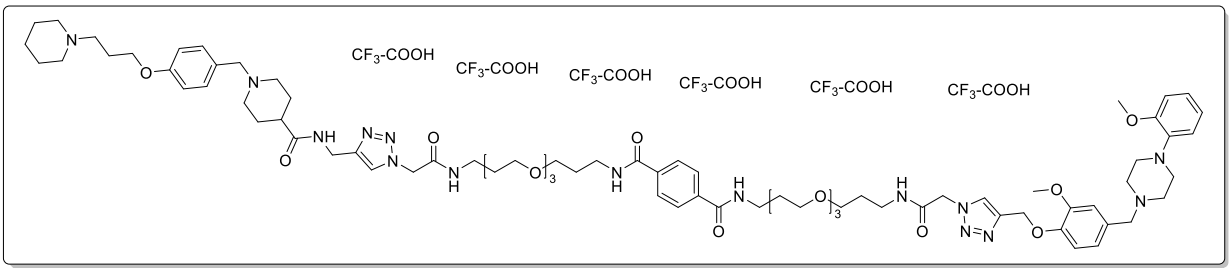

The title compound was prepared from **11b** (0.05 g, 0.14 mmol) **43** (0.06 g, 0.14 mmol) and **61c** (0.09 g, 0.13 mmol) according to the general procedure. The product **85** was obtained as a yellow solid (42.3 mg, 16%). ^{1}H NMR (400 MHz, D_2O) δ 7.97 (d, *J* = 12.0 Hz, 1H), 7.77 – 7.71 (m, 1H), 7.60 (s, 4H), 7.26 (q, *J* = 3.2 Hz, 2H), 7.07 – 6.98 (m, 2H), 6.95 – 6.87 (m, 6H), 6.83 (t, *J* = 7.6 Hz, 1H), 5.07 (d, *J* = 10.9 Hz, 2H), 5.04 (s, 2H), 5.01 (s, 2H), 4.32 – 4.26 (m, 2H), 4.17 (s, 2H), 4.09 (d, *J* = 13.8 Hz, 2H), 4.01 – 3.91 (m, 2H), 3.70 (s, 3H), 3.66 (s, 3H), 3.51 – 3.37 (m, 28H), 3.36 – 3.31 (m, 6H), 3.27 – 3.21 (m, 6H), 3.17 – 3.07 (m, 8H), 2.89 – 2.75 (m, 4H), 2.49 – 2.39 (m, 1H), 2.08 – 1.97 (m, 2H), 1.91 (d, *J* = 14.6 Hz, 2H), 1.86 – 1.79 (m, 2H), 1.76 – 1.55 (m, 14H). ^{13}C NMR (101 MHz, D_2O) δ 175.75, 169.05, 167.41, 167.18, 159.24, 151.86, 149.08, 147.95, 144.55, 143.05, 136.87, 136.62, 132.87, 127.37, 126.67, 126.20, 125.15, 124.43, 121.91, 121.30, 121.15, 119.08, 117.84, 115.12, 114.94, 114.56, 114.25, 112.09, 69.63, 69.58, 69.43, 69.33, 68.71, 68.31, 65.28, 61.61, 60.14, 55.71, 55.33, 54.44, 53.37, 52.08, 51.10, 50.89, 47.90, 39.69, 37.34, 36.83, 36.76, 34.36, 28.35, 28.12, 25.73, 23.46, 22.87, 21.14. HRMS (ESI-MS): m/z $[M+2H]^{2+}$ calculated for $C_{78}H_{115}N_{15}O_{15}^{2+}$: 750.9343, found 750.9350. Anal. RP-HPLC (220 nm): 99% (t_R = 9.69 min, *k* = 2.02). $C_{78}H_{113}N_{15}O_{15}$ x $C_{12}H_6F_{18}O_{12}$ (1500.82 + 684.14).

N^1-(1-(4-((2-Methoxy-4-((4-(2-methoxyphenyl)piperazin-1-yl)methyl)phenoxy)methyl)-1*H*-1,2,3-triazol-1-yl)-2-oxo-7,10,13-trioxa-3-azahexadecan-16-yl)-N^5-(2-oxo-1-(4-((1-(4-(3-(piperidin-1-yl)propoxy)benzyl)piperidine-4-carboxamido)methyl)-1*H*-1,2,3-triazol-1-yl)-7,10,13-trioxa-3-azahexadecan-16-yl)glutaramide hexahydrotrifluoroacetate (86)

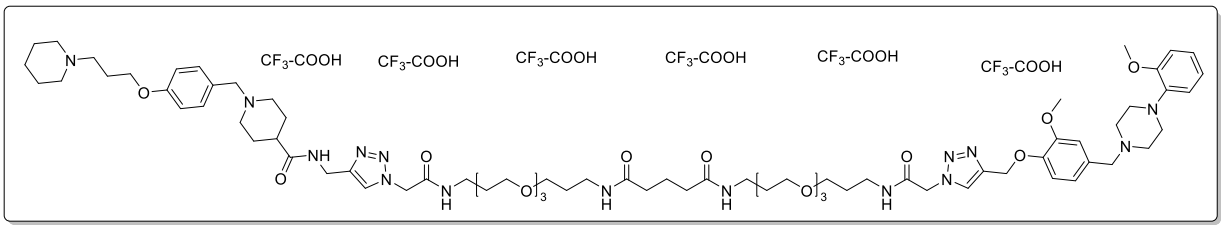

The title compound was prepared from **11b** (0.05 g, 0.13 mmol), **43** (0.06 g, 0.14 mmol) and **61d** (0.09 g, 0.13 mmol) according to the general procedure. The product **86** was obtained as a yellow solid (41.5 mg, 16%). ^{1}H NMR (400 MHz, D_2O) δ 8.01 (s, 1H), 7.81 – 7.76 (m, 1H), 7.30 (d, *J* = 8.7 Hz, 2H), 7.09 (d, *J* = 8.3 Hz, 1H), 7.06 – 6.95 (m, 3H), 6.96 – 6.91 (m, 4H), 6.89 – 6.83 (m, 1H), 5.18 (s, 2H), 5.08 (s, 2H), 5.06 (s, 2H), 4.36 – 4.31 (m, 2H), 4.22 (s, 2H), 4.11 (s, 2H), 4.05 (t, *J* = 5.7 Hz, 2H), 3.73 (s, 3H), 3.72 (s, 3H), 3.56 – 3.35 (m, 32H), 3.34 – 3.22 (m, 2H), 3.21 – 3.11 (m, 8H), 3.08 – 3.00 (m, 4H), 2.84 – 2.74 (m, 4H), 2.47 (tt, *J* = 12.2, 3.5 Hz, 1H), 2.11 – 2.02 (m, 6H), 1.95 (d, *J* = 14.3 Hz, 2H), 1.84 (d, *J* = 14.8 Hz, 2H), 1.78 – 1.53 (m, 16H). ^{13}C NMR (101 MHz, D_2O) δ 175.83, 175.52, 167.53, 167.33, 159.27, 151.97, 149.18, 147.92, 144.59, 143.10, 138.23, 132.91, 126.75, 125.42, 125.18, 124.49, 122.19, 121.29, 121.20, 118.91, 117.87, 115.15, 114.97, 114.72, 114.54, 111.94, 69.60, 69.37, 68.41, 68.32, 65.32, 61.74, 60.17, 55.81, 55.26, 54.47, 53.39, 52.21, 52.10, 51.28, 51.12, 47.65, 39.72, 36.81, 36.77, 36.40, 34.98, 34.40, 28.30, 28.15, 25.75, 23.48, 22.89, 21.90, 21.15. HRMS (ESI-MS): m/z $[M+2H]^{2+}$ calculated for $C_{75}H_{117}N_{15}O_{15}^{2+}$: 733.9421, found 733.9433. Anal. RP-HPLC (220 nm): 98% (t_R = 9.14 min, *k* = 1.85). $C_{75}H_{115}N_{15}O_{15}$ x $C_{12}H_6F_{18}O_{12}$ (1466.84 + 684.14).

N^1-(3-(2-(3-(2-(4-((4-((4-(2-(8-(4-(4-Fluorophenyl)-4-oxobutyl)-4-oxo-1-phenyl-1,3,8-triazaspiro[4.5]decan-3-yl)ethyl)phenyl)amino)-4-oxobutanamido)methyl)-1*H*-1,2,3-triazol-1-yl)acetamido)propoxy)ethoxy)propyl)-N^3-(3-(2-(3-(2-(4-((1-(4-(3-(piperidin-1-yl)propoxy)benzyl)piperidine-4-carboxamido)methyl)-1*H*-1,2,3-triazol-1-yl)acetamido)propoxy)ethoxy)propyl)isophthalamide hexahydrotrifluoroacetate (87)

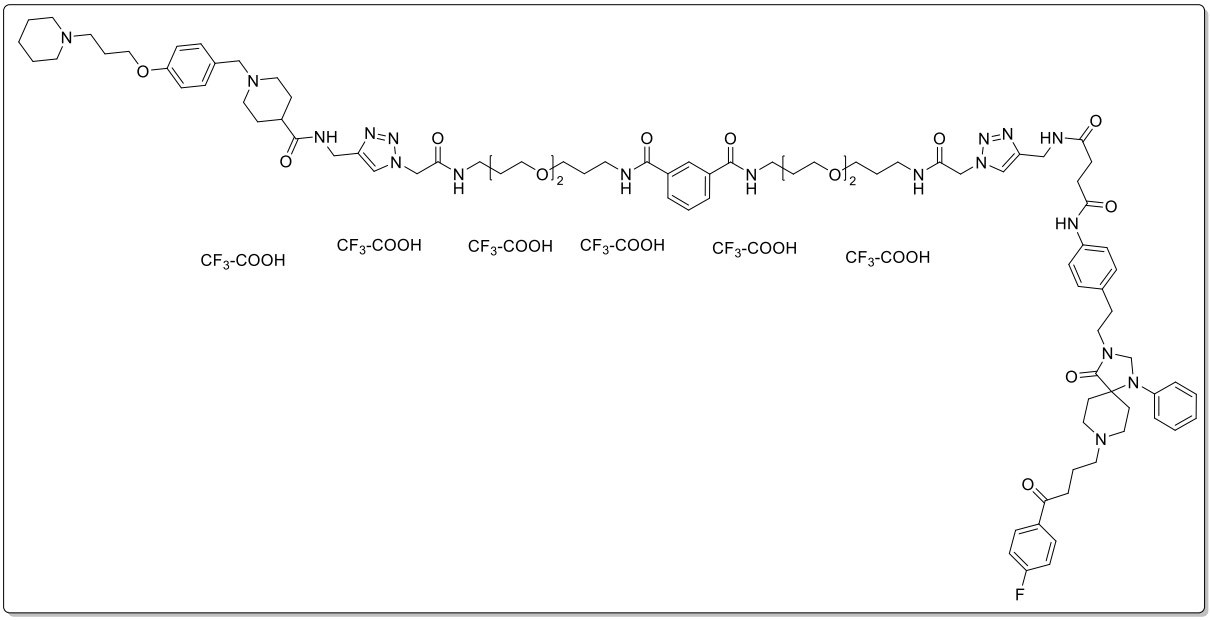

The title compound was prepared from **37** (0.07 g, 0.11 mmol), **43** (0.04 g, 0.11 mmol) and **61a** (0.06 g, 0.1 mmol) according to the general procedure. The product **87** was obtained as a yellow solid (22.4 mg, 9%). ^{1}H NMR (400 MHz, CD_3OD) δ 8.24 (t, *J* = 1.6 Hz, 1H), 8.09 – 8.01 (m, 2H), 7.93 (dd, *J* = 7.8, 1.8 Hz, 2H), 7.88 (d, *J* = 3.9 Hz, 2H), 7.53 (t, *J* = 7.8 Hz, 1H), 7.42 (dd, *J* = 8.5, 1.7 Hz, 4H), 7.31 – 7.17 (m, 6H), 7.02 (d, *J* = 8.6 Hz, 2H), 6.98 – 6.88 (m, 3H), 5.13 – 5.02 (m, 4H), 4.66 (s, 2H), 4.41 (s, 4H), 4.24 (s, 2H), 4.12 (t, *J* = 5.7 Hz, 2H), 3.73 (t, *J* = 6.7 Hz, 2H), 3.66 – 3.54 (m, 18H), 3.53 – 3.43 (m, 12H), 3.33 – 3.28 (m, 6H), 3.27 – 3.23 (m, 4H), 3.20 – 3.13 (m, 4H), 2.99 – 2.92 (m, 6H), 2.70 – 2.47 (m, 7H), 2.29 – 2.19 (m, 2H), 2.15 – 2.06 (m, 2H), 2.03 – 1.61 (m, 20H) ^{13}C NMR (101 MHz, CD_3OD) δ 197.30, 167.85, 166.29, 142.20, 137.14, 134.94, 133.69, 132.60, 130.70, 129.67, 129.21, 129.07, 128.52, 125.92, 124.46, 120.12, 117.55, 115.41, 115.19, 114.76, 69.89, 69.85, 68.82, 68.33, 64.76, 58.43, 54.37, 53.07, 51.72, 51.13, 49.12, 48.24, 48.03, 47.89, 47.81, 47.60, 47.39, 47.18, 46.96, 37.40, 36.74, 34.52, 34.33, 30.20, 29.03, 28.84, 27.33, 25.88, 23.78, 22.93, 21.28, 18.17. HRMS (ESI-MS): m/z $[M+2H]^{2+}$ calculated for $C_{90}H_{123}FN_{18}O_{14}^{2+}$: 849.472, found 849.4728. Anal. RP-HPLC (220 nm): 99% (t_R = 10.82 min, *k* = 2.37). $C_{90}H_{121}FN_{18}O_{14}$ x $C_{12}H_6F_{18}O_{12}$ (1698.07 + 684.14).

N^1-(1-(4-((4-((4-(2-(8-(4-(4-Fluorophenyl)-4-oxobutyl)-4-oxo-1-phenyl-1,3,8-triazaspiro[4.5]decan-3-yl)ethyl)phenyl)amino)-4-oxobutanamido)methyl)-1*H*-1,2,3-triazol-1-yl)-2-oxo-7,10,13-trioxa-3-azahexadecan-16-yl)-N^3-(2-oxo-1-(4-((1-(4-(3-(piperidin-1-yl)propoxy)benzyl)piperidine-4-carboxamido)methyl)-1*H*-1,2,3-triazol-1-yl)-7,10,13-trioxa-3-azahexadecan-16-yl)isophthalamide hexahydrotrifluoroacetate (88)

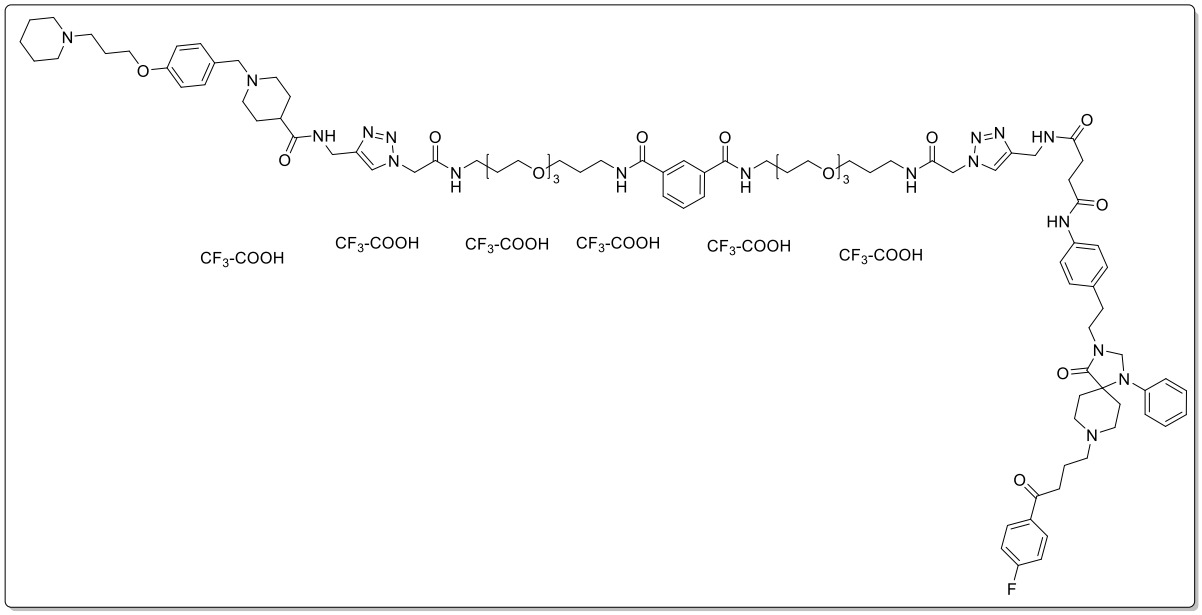

The title compound was prepared from **37** (0.07 g, 0.11 mmol), **43** (0.04 g, 0.11 mmol) and **61b** (0.07 g, 0.1 mmol) according to the general procedure. The product **88** was obtained as a yellow solid (10.1 mg, 4%). ^{1}H NMR (600 MHz, D_2O) δ 7.90 (s, 1H), 7.84 (dd, *J* = 8.6, 5.4 Hz, 2H), 7.76 – 7.71 (m, 3H), 7.66 (d, *J* = 14.1 Hz, 1H), 7.42 (t, *J* = 7.8 Hz, 1H), 7.28 (t, *J* = 8.3 Hz, 2H), 7.23 (dd, *J* = 14.7, 6.8 Hz, 2H), 7.18 (d, *J* = 8.3 Hz, 2H), 7.14 (d, *J* = 8.4 Hz, 2H), 7.09 (t, *J* = 8.8 Hz, 2H), 6.96 – 6.90 (m, 3H), 6.84 (d, *J* = 8.2 Hz, 2H), 5.07 – 5.01 (m, 2H), 4.88 (s, 2H), 4.54 (s, 2H), 4.34 – 4.30 (m, 2H), 4.29 – 4.24 (m, 2H), 4.14 – 4.09 (m, 2H), 4.04 (t, *J* = 5.7 Hz, 2H), 3.61 (t, *J* = 6.2 Hz, 2H), 3.54 – 3.50 (m, 8H), 3.49 – 3.46 (m, 8H), 3.44 – 3.39 (m, 6H), 3.37 – 3.33 (m, 4H), 3.31 (t, *J* = 6.0 Hz, 6H), 3.19 – 3.16 (m, 2H), 3.13 (t, *J* = 6.9 Hz, 2H), 3.10 (t, *J* = 6.8 Hz, 2H), 3.07 – 2.98 (m, 8H), 2.90 – 2.79 (m, 6H), 2.53 – 2.47 (m, 4H), 2.46 – 2.42 (m, 2H), 2.27 – 2.20 (m, 2H), 2.14 – 2.07 (m, 2H), 1.96 – 1.88 (m, 4H), 1.84 (d, *J* = 14.8 Hz, 2H), 1.78 – 1.70 (m, 6H), 1.70 – 1.64 (m, 6H), 1.63 – 1.59 (m, 4H), 1.51 (d, *J* = 14.4 Hz, 2H). ^{13}C NMR (151 MHz, D_2O) δ 200.66, 175.68, 174.40, 173.21, 172.67, 169.02, 169.01, 167.36, 167.14, 165.07, 159.15, 144.91, 144.46, 141.60, 135.74, 134.82, 134.13, 132.79, 132.33, 130.94, 130.88, 130.14, 129.67, 129.55, 129.21, 125.67, 125.05, 124.84, 122.11, 121.11, 119.19, 118.74, 117.26, 115.81, 115.66, 115.33, 115.04, 113.39, 69.56, 69.50, 69.36, 69.26, 68.70, 68.21, 65.23, 63.37,

60.06, 59.16, 56.00, 54.37, 53.30, 52.00, 51.91, 51.02, 48.80, 44.50, 41.36, 39.61, 37.35, 36.69, 34.80, 34.34, 34.29, 31.94, 31.60, 30.71, 28.27, 28.04, 27.10, 25.65, 23.38, 22.79, 22.16, 21.43, 21.06, 18.04. HRMS (ESI-MS): m/z $[M+3H]^{3+}$ calculated for $C_{94}H_{132}FN_{18}O_{18}^{3+}$: 596.0012, found 596.0025. Anal. RP-HPLC (220 nm): 96% (t_R = 11.81 min, k = 2.68). $C_{94}H_{129}FN_{18}O_{18}$ x $C_{12}H_6F_{18}O_{12}$ (1786.17 + 684.14).

N^1-(1-(4-((4-((4-(2-(8-(4-(4-Fluorophenyl)-4-oxobutyl)-4-oxo-1-phenyl-1,3,8-triazaspiro[4.5]decan-3-yl)ethyl)phenyl)amino)-4-oxobutanamido)methyl)-1*H*-1,2,3-triazol-1-yl)-2-oxo-7,10,13-trioxa-3-azahexadecan-16-yl)-N^4-(2-oxo-1-(4-((1-(4-(3-(piperidin-1-yl)propoxy)benzyl)piperidine-4-carboxamido)methyl)-1*H*-1,2,3-triazol-1-yl)-7,10,13-trioxa-3-azahexadecan-16-yl)terephthalamide hexahydrotrifluoroacetate (89)

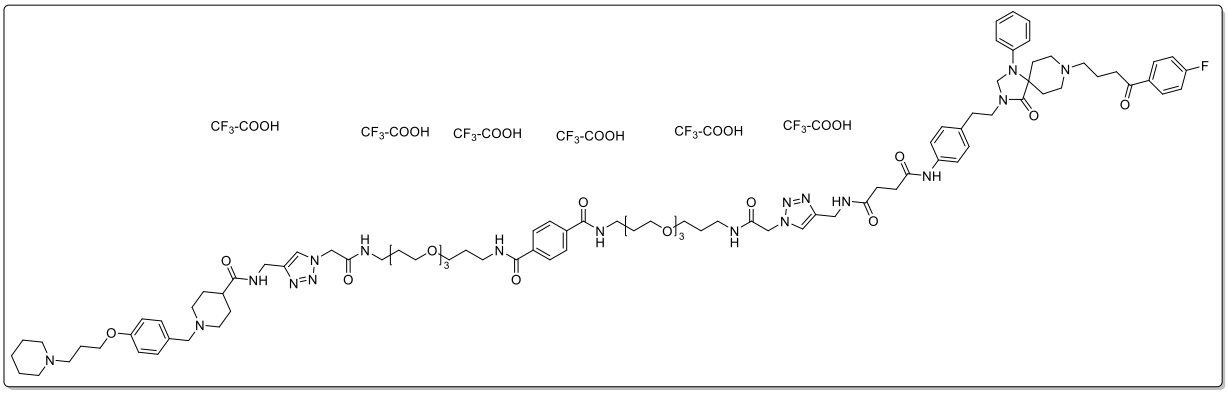

The title compound was prepared from **37** (0.07 g, 0.11 mmol), **43** (0.04 g, 0.11 mmol) and **61c** (0.07 g, 0.1 mmol) according to the general procedure. The product **89** was obtained as a yellow solid (23.2 mg, 9%). ^{1}H NMR (400 MHz, D_2O) δ 7.86 – 7.56 (m, 8H), 7.27 (d, J = 8.6 Hz, 2H), 7.18 (s, 2H), 7.13 – 7.03 (m, 2H), 7.03 – 6.86 (m, 6H), 6.84 – 6.54 (m, 3H), 5.01 (s, 2H), 4.88 (s, 2H), 4.45 – 4.16 (m, 5H), 4.08 (s, 2H), 4.01 (t, J = 5.5 Hz, 2H), 3.51 – 3.31 (m, 30H), 3.30 – 3.23 (m, 6H), 3.19 – 3.01 (m, 8H), 2.99 – 2.91 (m, 2H), 2.90 – 2.75 (m, 6H), 2.73 – 2.56 (m, 2H), 2.54 – 2.29 (m, 6H), 2.14 – 2.04 (m, 2H), 1.92 (d, J = 13.7 Hz, 2H), 1.82 (d, J = 14.1 Hz, 2H), 1.79 – 1.64 (m, 8H), 1.63 – 1.49 (m, 6H), 1.44 – 1.27 (m, 2H). ^{13}C NMR (101 MHz, D_2O) δ 175.61, 174.05, 168.62, 167.27, 166.94, 164.47, 159.22, 144.88, 144.53, 136.57, 132.82, 130.86, 129.43, 127.36, 125.09, 121.11, 120.76, 117.86, 115.09, 114.95, 112.05, 69.56, 69.40, 69.30, 68.66, 68.26, 65.24, 60.10, 58.68, 54.38, 53.31, 52.04, 51.08, 39.64, 37.31, 36.73, 34.35, 28.41, 28.14, 25.70, 23.43, 22.82, 21.11. HRMS (ESI-MS): m/z $[M+2H^{2+}]$ calculated for $C_{94}H_{131}FN_{18}O_{16}^{2+}$: 893.4982, found 893.4989. Anal. RP-HPLC (220 nm): 99% (t_R = 10.54 min, k = 2.28). $C_{94}H_{129}FN_{18}O_{16}$ x $C_{12}H_6F_{18}O_{12}$ (1786.17 + 684.14).

N^1-(1-(4-((4-((4-(2-(8-(4-(4-Fluorophenyl)-4-oxobutyl)-4-oxo-1-phenyl-1,3,8-triazaspiro[4.5]decan-3-yl)ethyl)phenyl)amino)-4-oxobutanamido)methyl)-1*H*-1,2,3-triazol-1-yl)-2-oxo-7,10,13-trioxa-3-azahexadecan-16-yl)-N^5-(2-oxo-1-(4-((1-(4-(3-(piperidin-1-yl)propoxy)benzyl)piperidine-4-carboxamido)methyl)-1*H*-1,2,3-triazol-1-yl)-7,10,13-trioxa-3-azahexadecan-16-yl)glutaramide hexahydrotrifluoroacetate (90)

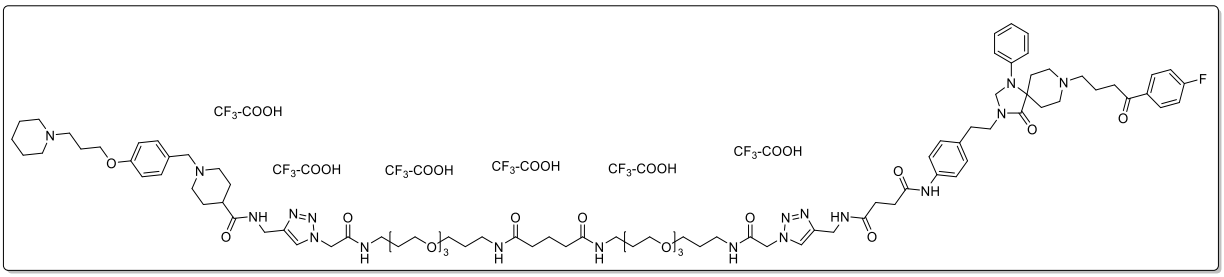

The title compound was prepared from **37** (0.07 g, 0.11 mmol) **43** (0.04 g, 0.11 mmol) and **61d** (0.07 g, 0.1 mmol) according to the general procedure. The product **90** was obtained as a yellow solid (22.0 mg, 9%). ^{1}H NMR (400 MHz, D_2O) δ 7.89 – 7.75 (m, 3H), 7.71 (d, *J* = 9.2 Hz, 1H), 7.31 (d, *J* = 8.6 Hz, 2H), 7.27 – 7.13 (m, 4H), 7.06 – 6.97 (m, 4H), 6.94 (d, *J* = 8.7 Hz, 2H), 6.80 (d, *J* = 20.8 Hz, 3H), 5.08 (d, *J* = 8.0 Hz, 2H), 4.93 (s, 2H), 4.47 (s, 2H), 4.38 – 4.21 (m, 4H), 4.13 (d, *J* = 15.6 Hz, 2H), 4.05 (t, *J* = 5.6 Hz, 2H), 3.58 – 3.36 (m, 32H), 3.31 (s, 2H), 3.24 – 3.05 (m, 12H), 3.03 – 2.69 (m, 10H), 2.48 – 2.37 (m, 6H), 2.09 (t, *J* = 7.5 Hz, 6H), 1.95 (d, *J* = 10.8 Hz, 3H), 1.84 (d, *J* = 14.9 Hz, 3H), 1.77 – 1.54 (m, 16H), 1.52 – 1.30 (m, 2H). ^{13}C NMR (101 MHz, D_2O) δ 200.00, 175.73, 175.38, 174.27, 173.08, 172.50, 167.40, 167.13, 164.59, 159.23, 144.87, 144.53, 141.92, 136.11, 134.55, 132.86, 132.43, 130.96, 130.88, 129.59, 125.16, 124.98, 121.16, 120.91, 120.72, 117.82, 115.83, 115.63, 115.12, 114.91, 112.01, 69.57, 69.34, 68.38, 68.29, 65.29, 60.12, 58.93, 56.07, 54.40, 53.34, 52.09, 51.09, 48.70, 41.64, 39.67, 36.75, 36.38, 34.96, 34.35, 31.97, 31.64, 30.72, 28.30, 28.16, 28.14, 27.06, 25.71, 23.44, 22.83, 21.87, 21.11, 18.06. HRMS (ESI-MS): m/z $[M+2H]^{2+}$ calculated for $C_{91}H_{133}FN_{18}O_{16}^{2+}$: 876.5060, found 876.5072. Anal. RP-HPLC (220 nm): 97% (t_R = 10.49 min, *k* = 2.28). $C_{91}H_{131}FN_{18}O_{16}$ x $C_{12}H_6F_{18}O_{12}$ (1752.16 + 684.14).

N^1-(1-(4-(Acetamidomethyl)-1*H*-1,2,3-triazol-1-yl)-2-oxo-7,10,13-trioxa-3-azahexadecan-16-yl)-N^5-(1-(4-((4-((4-(2-(8-(4-(4-fluorophenyl)-4-oxobutyl)-4-oxo-1-phenyl-1,3,8-triazaspiro[4.5]decan-3-yl)ethyl)phenyl)amino)-4-oxobutanamido)methyl)-1*H*-1,2,3-triazol-1-yl)-2-oxo-7,10,13-trioxa-3-azahexadecan-16-yl)glutaramide tetrahydrotrifluoroacetate (91)

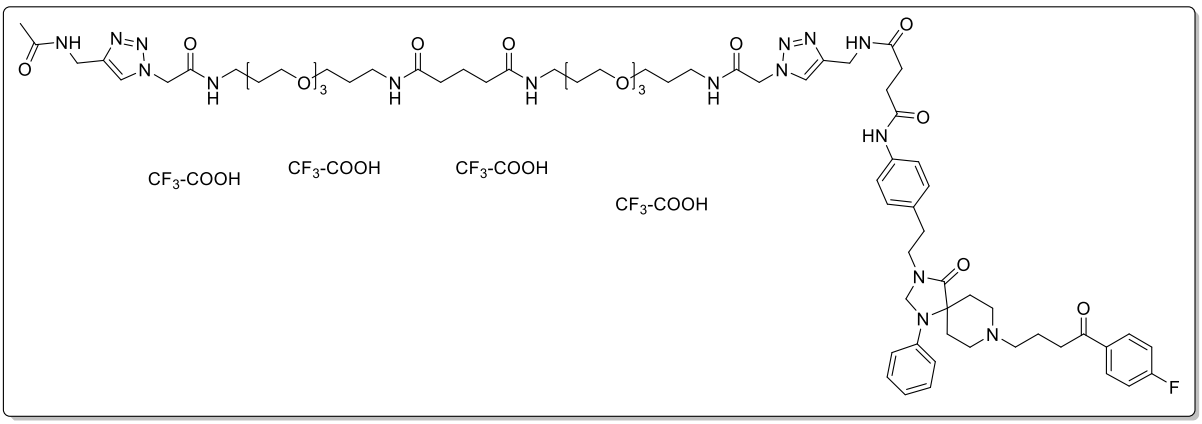

The title compound was prepared from **64** (2.4 mg, 0.025 mmol, 1 eq), **37** (17.8 mg, 0.0275 mmol, 1.1 eq) and **61d** (18.4 mg, 0.025 mmol, 1 eq) according to the general procedure. The product **91** was obtained as a white solid (4.97 mg, 10 %). ^{1}H NMR (600 MHz, CD_3OD) δ 8.07 – 8.04 – 7.97 (m, 2H), 7.88 (s, 2H), 7.43 (d, *J* = 8.4 Hz, 2H), 7.30 – 7.26 (m, 2H), 7.26 – 7.21 (m, 4H), 6.97 – 6.92 (m, 3H), 5.11 (s, 2H), 5.07 (s, 2H), 4.68 (s, 2H), 4.42 (d, *J* = 2.3 Hz, 4H), 3.76 (t, *J* = 6.7 Hz, 2H), 3.63 – 3.60 (m, 10H), 3.58 – 3.54 (m, 10H), 3.53 – 3.45 (m, 12H), 3.25 – 3.18 (m, 4H), 3.17 – 3.09 (m, 4H), 2.96 (t, *J* = 6.7 Hz, 2H), 2.64 (t, *J* = 6.7 Hz, 2H), 2.59 – 2.50 (m, 4H), 2.18 (t, *J* = 7.5 Hz, 4H), 2.10 – 2.04 (m, 2H), 1.95 (s, 3H), 1.89 – 1.83 (m, 2H), 1.79 – 1.75 (m, 4H), 1.73 – 1.69 (m, 4H), 1.65 (d, *J* = 14.8 Hz, 2H). ^{13}C NMR (151 MHz, CD_3OD) δ 197.29, 173.84, 173.16, 172.66, 171.77, 171.50, 166.31, 166.29, 165.93 (d, *J* = 253.3 Hz), 145.02, 144.79, 142.18, 137.12, 133.62, 133.07, 133.05, 130.64 (d, *J* = 9.4 Hz), 129.23, 129.07, 124.46, 124.44, 120.91, 120.12, 117.89, 115.30 (d, *J* = 22.2 Hz), 70.12, 69.80, 69.79, 68.46, 68.43, 63.26, 58.42, 56.29, 51.77, 49.17, 40.93, 36.93, 36.88, 36.41, 34.92, 34.50, 34.29, 32.19, 31.24, 30.16, 29.01, 28.79, 27.40, 21.91, 21.08, 18.19. HRMS (ESI-MS): m/z $[M+3H]^{3+}$ calculated for $C_{72}H_{106}FN_{16}O_{15}^{3+}$: 484.5997, found 484.6005; Anal. RP-HPLC (220 nm) 99% (t_R = 12.01 min, *k* = 2.74). $C_{72}H_{103}FN_{16}O_{15}$ x $C_8H_4F_{12}O_8$ (1451.72 + 456.01).

N^1-(1-(4-((4-((4-(2-((5-Hydroxy-1,2,3,4-tetrahydronaphthalen-2-yl)(propyl)amino)ethyl)phenyl)amino)-4-oxobutanamido)methyl)-1*H*-1,2,3-triazol-1-yl)-2-oxo-7,10,13-trioxa-3-azahexadecan-16-yl)-N^5-(2-oxo-1-(4-((1-(4-(3-(piperidin-1-yl)propoxy)benzyl)piperidine-4-carboxamido)methyl)-1*H*-1,2,3-triazol-1-yl)-7,10,13-trioxa-3-azahexadecan-16-yl)glutaramide pentahydrotrifluoroacetate (92)

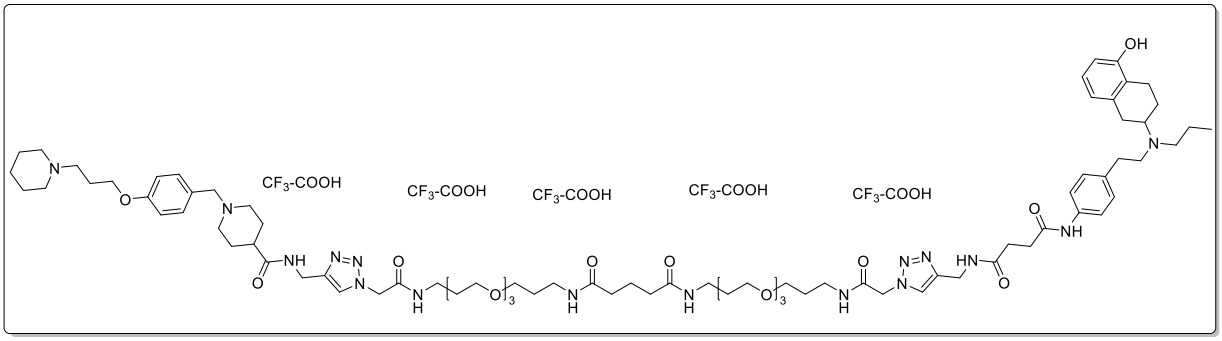

The title compound was prepared from **19** (0.05 g, 0.11 mmol), **43** (0.04 g, 0.11 mmol) and **61d** (0.07 g, 0.1 mmol) according to the general procedure. The product **92** was obtained as a yellow solid (17.4 mg, 8 %). ^{1}H NMR (400 MHz, D_2O) δ 7.75 (d, *J* = 21.7 Hz, 2H), 7.32 – 7.21 (m, 4H), 7.17 (dd, *J* = 8.5, 2.9 Hz, 2H), 6.98 – 6.91 (m, 3H), 6.66 – 6.59 (m, 2H), 5.09 – 5.04 (m, 2H), 4.92 (s, 2H), 4.36 – 4.30 (m, 4H), 4.16 – 4.09 (m, 2H), 4.05 (t, *J* = 5.7 Hz, 2H), 3.63 – 3.28 (m, 32H), 3.26 – 2.99 (m, 14H), 2.98 – 2.78 (m, 8H), 2.63 – 2.55 (m, 2H), 2.54 – 2.38 (m, 4H), 2.23 – 2.04 (m, 7H), 2.00 – 1.90 (m, 2H), 1.84 (d, *J* = 14.8 Hz, 2H), 1.77 – 1.58 (m, 18H), 0.88 (t, *J* = 1.6 Hz, 3H). ^{13}C NMR (101 MHz, D_2O) δ 175.85, 175.85, 175.54, 174.73, 173.10, 167.55, 167.42, 167.42, 163.11, 162.76, 159.26, 153.28, 144.57, 136.26, 134.24, 132.93, 129.44, 127.38, 125.20, 125.09, 122.18, 121.77, 121.70, 121.29, 121.20, 115.17, 112.90, 69.61, 69.38, 68.42, 68.31, 65.35, 60.16, 59.79, 54.48, 53.40, 52.10, 51.13, 39.71, 36.76, 36.41, 34.98, 34.52, 31.79, 30.90, 30.12, 28.31, 28.16, 25.75, 23.49, 22.90, 22.22, 21.91, 21.16, 10.32. HRMS (ESI-MS): m/z $[M+3H]^{3+}$ calculated for $C_{81}H_{127}N_{16}O_{15}^{3+}$: 521.3217, found 521.3230; Anal. RP-HPLC (220 nm) 99% (t_R = 8.61 min, *k* = 1.69). $C_{81}H_{124}N_{16}O_{15}$ x $C_{10}H_5F_{15}O_{10}$ (1561.90 + 570.12).

N^1-(1-(4-(Acetamidomethyl)-1*H*-1,2,3-triazol-1-yl)-2-oxo-7,10,13-trioxa-3-azahexadecan-16-yl)-N^5-(1-(4-((4-((4-(2-((5-hydroxy-1,2,3,4-tetrahydronaphthalen-2-yl)(propyl)amino)ethyl)phenyl)amino)-4-oxobutanamido)methyl)-1*H*-1,2,3-triazol-1-yl)-2-oxo-7,10,13-trioxa-3-azahexadecan-16-yl)glutaramide trihydrotrifluoroacetate (93)

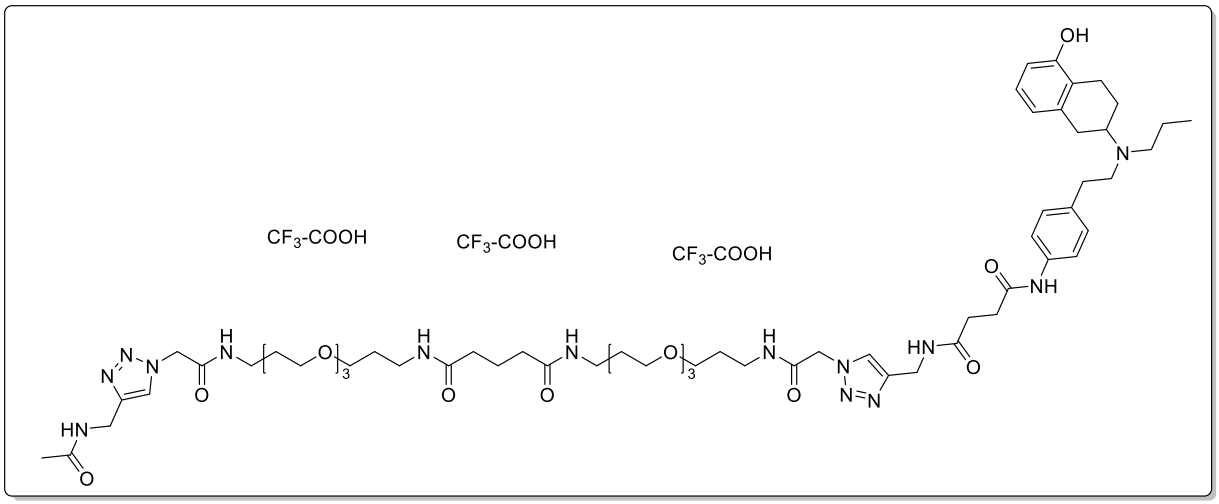

The title compound was prepared from **64** (9.7 mg, 0.1 mmol, 1 eq), **19** (50.8 mg, 0.11 mmol, 1.1 eq) and **61d** (70.2 mg, 0.1 mmol, 1 eq) according to the general procedure. The product **93** was obtained as a yellow solid (11.4 mg, 7%). ^{1}H NMR (400 MHz, CD_3OD) δ 7.88 (d, *J* = 3.8 Hz, 2H), 7.53 (d, *J* = 7.0 Hz, 2H), 7.26 (d, *J* = 8.3 Hz, 2H), 6.97 (t, *J* = 7.8 Hz, 1H), 6.66 – 6.57 (m, 2H), 5.10 (s, 2H), 5.07 (s, 2H), 4.43 (d, *J* = 12.4 Hz, 4H), 3.78 (s, 1H), 3.66 – 3.58 (m, 10H), 3.58 – 3.55 (m, 8H), 3.54 – 3.46 (m, 10H), 3.35 – 3.25 (m, 12H), 3.24 – 3.17 (m, 5H), 3.13 – 3.04 (m, 4H), 2.70 – 2.61 (m, 2H), 2.58 (t, *J* = 6.6 Hz, 2H), 2.34 (d, *J* = 7.1 Hz, 1H), 2.18 (t, *J* = 7.4 Hz, 4H), 1.94 (d, *J* = 8.7 Hz, 3H), 1.86 – 1.83 (m, 4H), 1.82 – 1.68 (m, 10H), 1.05 (t, *J* = 7.3 Hz, 3H). ^{13}C NMR (151 MHz, CD_3OD) δ 173.84, 173.23, 171.76, 171.52, 168.58, 166.30, 166.29, 160.28, 160.03, 154.74, 145.02, 144.78, 137.84, 133.33, 131.52, 128.87, 126.64, 124.47, 124.43, 121.64, 120.17, 119.83, 112.07, 70.14, 70.12, 69.85, 69.83, 69.80, 69.79, 68.59, 68.48, 68.46, 68.44, 68.43, 60.60, 60.57, 52.35, 52.09, 51.82, 51.78, 51.65, 36.90, 36.88, 36.72, 36.41, 34.92, 34.38, 34.29, 31.37, 30.41, 30.26, 29.39, 29.32, 29.01, 28.87, 28.78, 23.55, 23.45, 22.29, 21.91, 21.09, 18.55, 18.38, 9.91, 9.89. HRMS (ESI-MS): m/z $[M+3H]^{3+}$ calculated for $C_{62}H_{99}N_{14}O_{14}^{3+}$: 421.2496; found 421,2483; Anal. RP-HPLC (220 nm) 99% (t_R = 10.11 min, *k* = 2.15). $C_{62}H_{96}N_{14}O_{14}$ x $C_6H_3F_9O_6$ (1603.60).

N^1-(1-(4-(Acetamidomethyl)-1*H*-1,2,3-triazol-1-yl)-2-oxo-7,10,13-trioxa-3-azahexadecan-16-yl)-N^4-(2-oxo-1-(4-((1-(4-(3-(piperidin-1-yl)propoxy)benzyl)piperidine-4-carboxamido)methyl)-1*H*-1,2,3-triazol-1-yl)-7,10,13-trioxa-3-azahexadecan-16-yl)terephthalamide tetrahydrotrifluoroacetate (94)

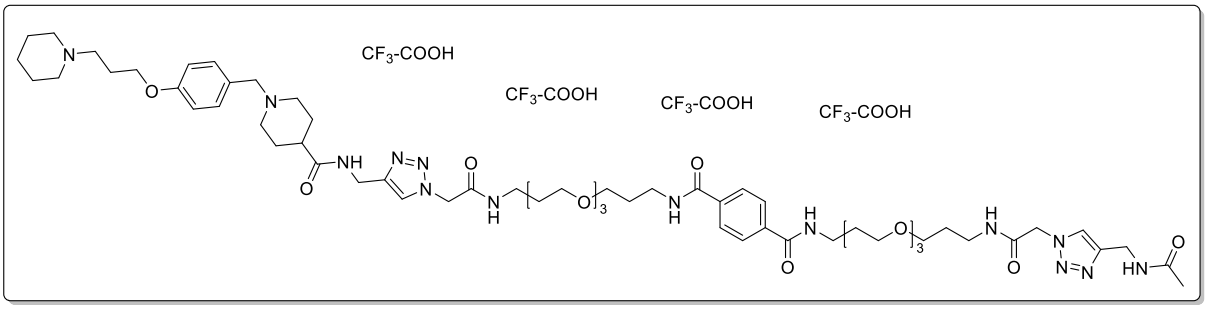

The title compound was prepared from **64** (9.7 mg, 0.1 mmol, 1 eq), **43** (43.0 mg, 0.11 mmol, 1.1 eq) and **61c** (73.6 mg, 0.1 mmol, 1 eq) according to the general procedure. The product **94** was obtained as a yellow solid (25.1 mg, 14.8 %). ^{1}H NMR (400 MHz, CD_3OD) δ 7.90 – 7.82 (m, 6H), 7.41 (d, *J* = 8.6 Hz, 2H), 7.02 (d, *J* = 8.6 Hz, 2H), 5.13 – 5.06 (m, 4H), 4.46 – 4.40 (m, 4H), 4.29 – 4.20 (m, 2H), 4.12 (t, *J* = 5.7 Hz, 2H), 3.66 – 3.55 (m, 18H), 3.54 – 3.42 (m, 14H), 3.30 – 3.25 (m, 8H), 3.04 – 2.88 (m, 4H), 2.55 – 2.44 (m, 1H), 2.29 – 2.19 (m, 2H), 2.18 – 1.62 (m, 21H). ^{13}C NMR (101 MHz, CD_3OD) δ 173.89, 171.77, 167.71, 166.32, 166.28, 159.95, 137.09, 132.60, 127.10, 124.48, 121.13, 114.76, 70.12, 69.86, 69.77, 68.82, 68.42, 64.76, 59.89, 54.37, 53.07, 51.77, 51.73, 51.14, 39.67, 37.42, 36.87, 34.30, 34.19, 28.97, 28.78, 25.88, 23.78, 22.93, 21.29, 21.10. HRMS (ESI-MS): m/z $[M+3H]^{3+}$ calculated for $C_{61}H_{97}N_{14}O_{13}^{3+}$: 411.2448, found 411.2458; Anal. RP-HPLC (220 nm) 99% (t_R = 8.36 min, *k* = 1.60). $C_{61}H_{94}N_{14}O_{13}$ x $C_8H_4F_{12}O_8$ (1231.51 + 456.10).

N^1-(1-(4-(Acetamidomethyl)-1*H*-1,2,3-triazol-1-yl)-2-oxo-7,10,13-trioxa-3-azahexadecan-16-yl)-*N*5-(2-oxo-1-(4-((1-(4-(3-(piperidin-1-yl)propoxy)benzyl)piperidine-4-carboxamido)methyl)-1*H*-1,2,3-triazol-1-yl)-7,10,13-trioxa-3-azahexadecan-16-yl)glutaramide tetrahydrotrifluoroacetate (95)

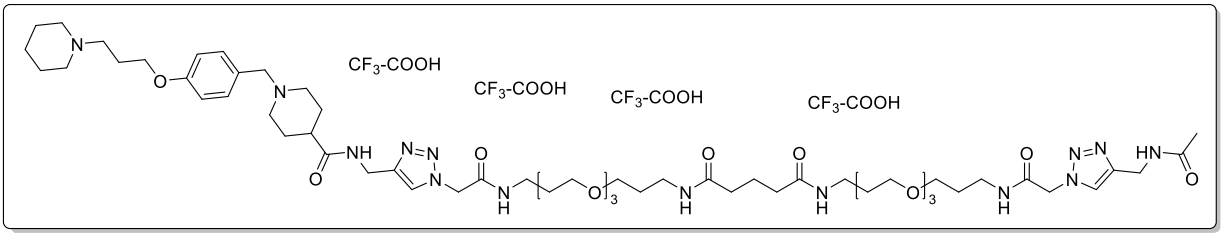

The title compound was prepared from **64** (2.4 mg, 0.025 mmol, 1 eq), **43** (17.6 mg, 0.0275 mmol, 1.1 eq) and **61c** (17.6 mg, 0.025 mmol, 1 eq) according to the general procedure. The product **95** was obtained as a yellow solid (6.4 mg, 21%). ^{1}H NMR (600 MHz, DMSO-d_6) δ 8.34 (t, *J* = 5.6 Hz, 1H), 8.30 – 8.23 (m, 3H), 7.81 (d, *J* = 30.3 Hz, 2H), 7.74 (t, *J* = 5.5 Hz, 2H), 7.16 (d, *J* = 8.5 Hz, 2H), 6.84 (d, *J* = 8.6 Hz, 2H), 5.01 (d, *J* = 3.9 Hz, 4H), 4.26 (d, *J* = 5.7 Hz, 4H), 3.95 (t, *J* = 6.3 Hz, 2H), 3.55 – 3.43 (m, 20H), 3.41 – 3.39 (m, 8H), 3.15 – 3.10 (m, 4H), 3.05 – 2.95 (m, 4H), 2.78 (d, *J* = 10.9 Hz, 2H), 2.49 – 2.37 (m, 6H), 2.13 – 2.07 (m, 1H), 2.01 (t, *J* = 7.5 Hz, 4H), 1.91 – 1.83 (m, 4H), 1.82 (s, 3H), 1.69 – 1.48 (m, 18H). ^{13}C NMR (151 MHz, DMSO-d_6) δ 174.88, 172.12, 169.61, 165.76, 165.75, 158.02, 145.36, 145.14, 130.49, 124.69, 124.53, 114.51, 70.21, 70.20, 69.98, 68.55, 68.32, 66.11, 62.14, 55.36, 54.25, 52.92, 52.00, 40.47, 36.55, 36.21, 35.26, 34.56, 29.83, 29.53, 28.90, 22.91, 22.03. HRMS (ESI-MS): m/z $[M+3H]^{3+}$ calculated for $C_{58}H_{99}N_{14}O_{13}^{3+}$: 399.9167, found 399.9174; Anal. RP-HPLC (220 nm) 99% (t_R = 7.64 min, *k* = 1.38). $C_{58}H_{96}N_{14}O_{13}$ x $C_8H_4F_{12}O_8$ (1197.49 + 456.10).

4-((tert-Butoxycarbonyl)amino)butanoic acid (96) [253]

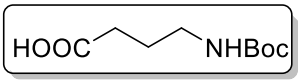

To a mixture of 4-aminobutryric acid (0.30 g, 2.9 mmol, 1 eq) and NaOH (0.12 g, 2.9 mmol, 1 eq) in dioxane/water (1/1, 30 mL) a solution of Boc_2O (0.70 g, 3.2 mmol, 1.1 eq) was added in dioxane (30 mL). After the reaction was stirred at room temperature overnight aqueous HCl (1 N) was added to set pH < 1. The mixture was extracted three times with EtOAc (3 x 30 mL) and the organic layer was dried over Na_2SO_4. The solvent was removed under reduced pressure and the crude product was purified by column chromatography (DCM/MeOH 95/5 to 9/1) to afford **96** as a colorless oil (0.38 g, 64%). ^{1}H NMR (400 MHz, $CDCl_3$) δ 3.17 (t, *J* = 6.7 Hz, 2H), 2.39 (t, *J* = 7.2 Hz, 2H), 1.81 (p, *J* = 7.0 Hz, 2H), 1.44 (s, 9H). ^{13}C NMR (101 MHz, $CDCl_3$) δ 178.05, 156.20, 79.53, 39.93, 31.27, 28.37, 25.17. HRMS (ESI-MS): m/z $[M+H]^+$ calculated for $C_9H_{18}NO_4^+$: 204.1230, found 204.1231; $C_9H_{17}NO_4$ (203.24).

tert-Butyl (18-((4-(2-(8-(4-(4-fluorophenyl)-4-oxobutyl)-4-oxo-1-phenyl-1,3,8-triazaspiro[4.5]decan-3-yl)ethyl)phenyl)amino)-15,18-dioxo-4,7,10-trioxa-14-azaoctadecyl)carbamate (97) [203]

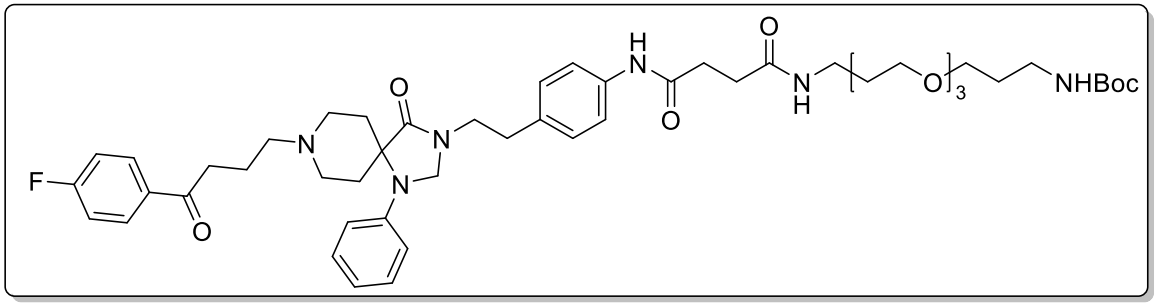

To a solution of **36** (0.28 g, 0.54 mmol, 1 eq) in DMF (30 mL) succinic anhydride (0.054 g, 0.54 mmol, 1 eq) was added and the reaction was stirred at room temperature overnight. After the reaction was complete, as indicated by TLC, HATU (0.31 g, 0.82 mmol, 1.5 eq), DIPEA (0.21 g, 1.62 mmol, 3 eq) and **57** (0.17 g, 0.54 mmol, 1 eq) were added. Then, the mixture was stirred for 10 h at room temperature. The solvent was evaporated and the residue was purified by column chromatography (DCM/MeOH 95/5). **97** (0.25 g, 47%) was obtained as a brown oil. ^{1}H NMR (400 MHz, $CDCl_3$) δ 8.02 – 7.96 (m, 2H), 7.45 (d, *J* = 8.3 Hz, 2H), 7.30 (t, *J* = 8.0 Hz, 2H), 7.18 – 7.10 (m, 4H), 6.97 (d, *J* = 8.3 Hz, 2H), 6.93 – 6.83 (m, 2H), 5.00 (s, 1H), 4.59 (s, 2H), 4.40 (s, 1H), 3.76 – 3.64 (m, 4H), 3.64 – 3.59 (m, 4H), 3.59 – 3.42 (m, 10H), 3.39 – 3.30 (m, 2H), 3.28 – 3.08 (m, 8H), 2.97 – 2.88 (m, 2H), 2.70 – 2.63 (m, 2H), 2.62 – 2.54 (m, 2H), 2.35 – 2.23 (m, 2H), 1.80 – 1.67 (m, 4H), 1.52 (d, *J* = 14.1 Hz, 2H), 1.42 (s, 9H). ^{13}C NMR (101 MHz, $CDCl_3$) δ

196.67, 172.80, 171.00, 165.98 (d, *J* = 255.5 Hz), 156.19, 141.80, 137.20, 132.79, 132.75, 130.78 (d, *J* = 9.4 Hz)129.75, 129.18, 120.24, 119.62, 115.89 (d, *J* = 21.9 Hz), 114.80, 79.10, 70.49, 70.17, 70.04, 69.42, 63.47, 58.48, 56.57, 48.67, 41.58, 38.42, 35.51, 33.02, 32.92, 31.60, 29.70, 28.64, 28.45, 26.81, 18.21. HRMS (ESI-MS): m/z $[M+H]^+$ calculated for $C_{50}H_{70}FN_6O_6^+$: 917.5183, found 917.5194; $C_{50}H_{69}FN_6O_6$ (917.13).

N^1-(3-(2-(2-(3-Aminopropoxy)ethoxy)ethoxy)propyl)-N^4-(4-(2-(8-(4-(4-fluorophenyl)-4-oxobutyl)-4-oxo-1-phenyl-1,3,8-triazaspiro[4.5]decan-3-yl)ethyl)phenyl)succinamide trihydrotrifluoroacetate (98) [203]

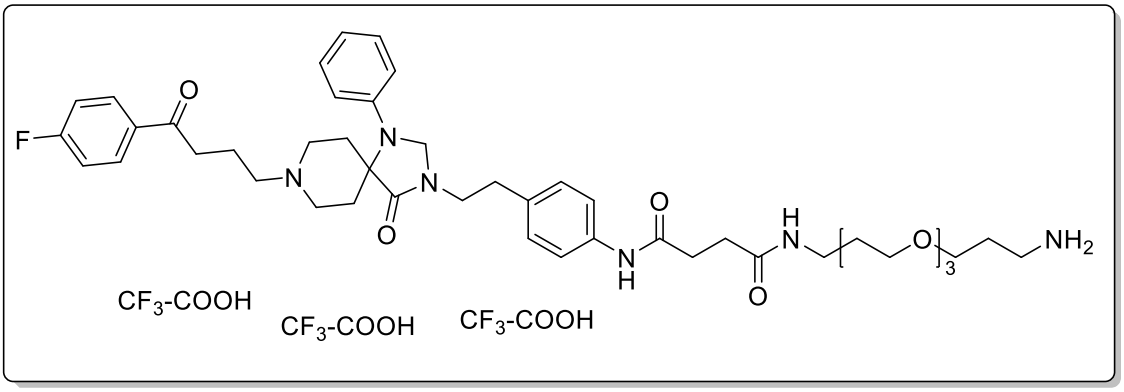

97 (0.05 g, 0.07 mmol) was dissolved in DCM (30 mL) and TFA (5 mL) was added. The mixture was stirred at room temperature overnight. After the reaction was complete, as indicated by TLC, the solvent was evaporated. The resulting crude product was purified by preparative HPLC. **98** (18.1 mg, 22%) was obtained as a yellow solid. ^{1}H NMR (400 MHz, D_2O) δ 8.04 – 7.95 (m, 2H), 7.43 – 7.33 (m, 4H), 7.32 – 7.19 (m, 4H), 7.13 – 6.92 (m, 3H), 4.63 (s, 2H), 3.77 – 3.68 (m, 2H), 3.66 – 3.55 (m, 8H), 3.54 – 3.50 (m, 2H), 3.50 – 3.03 (m, 14H), 3.00 – 2.88 (m, 2H), 2.75 – 2.58 (m, 2H), 2.58 – 2.48 (m, 2H), 2.48 – 2.33 (m, 2H), 2.12 – 1.99 (m, 2H), 1.99 – 1.88 (m, 2H), 1.85 – 1.62 (m, 4H). ^{13}C NMR (101 MHz, D_2O) δ 200.77, 174.41, 173.34, 172.89, 165.98 (d, *J* = 255.2 Hz), 141.75, 135.86, 135.02, 132.50, 131.05 (d, *J* = 9.8 Hz), 129.75, 129.66, 122.13, 121.36, 118.72, 117.86, 115.86 (d, *J* = 22.2 Hz), 69.52, 69.43, 69.28, 68.31, 63.55, 59.29, 56.08, 48.88, 41.60, 37.69, 36.29, 34.90, 32.08, 31.91, 31.07, 28.31, 27.17, 26.52, 18.14. HRMS (ESI-MS): m/z $[M+H]^+$ calculated for $C_{45}H_{62}FN_6O_7^+$: 817.4659, found 817.4654; $C_{45}H_{61}FN_6O_7$ x $C_6H_3F_9O_6$ (817.02 + 342.07).

Triammonium 2-((E)-3-((E)-7-(1-((4-(2-(8-(4-(4-fluorophenyl)-4-oxobutyl)-4-oxo-1-phenyl-1,3,8-triazaspiro[4.5]decan-3-yl)ethyl)phenyl)amino)-1,4,20-trioxo-9,12,15-trioxa-5,19-diazapentacosan-25-yl)-3-methyl-5-sulfonato-3-(3-sulfonatopropyl)indolin-2-ylidene)prop-1-en-1-yl)-1-(2-methoxyethyl)-3-methyl-3-(3-sulfonatopropyl)-3*H*-indol-1-ium-5-sulfonate (99)

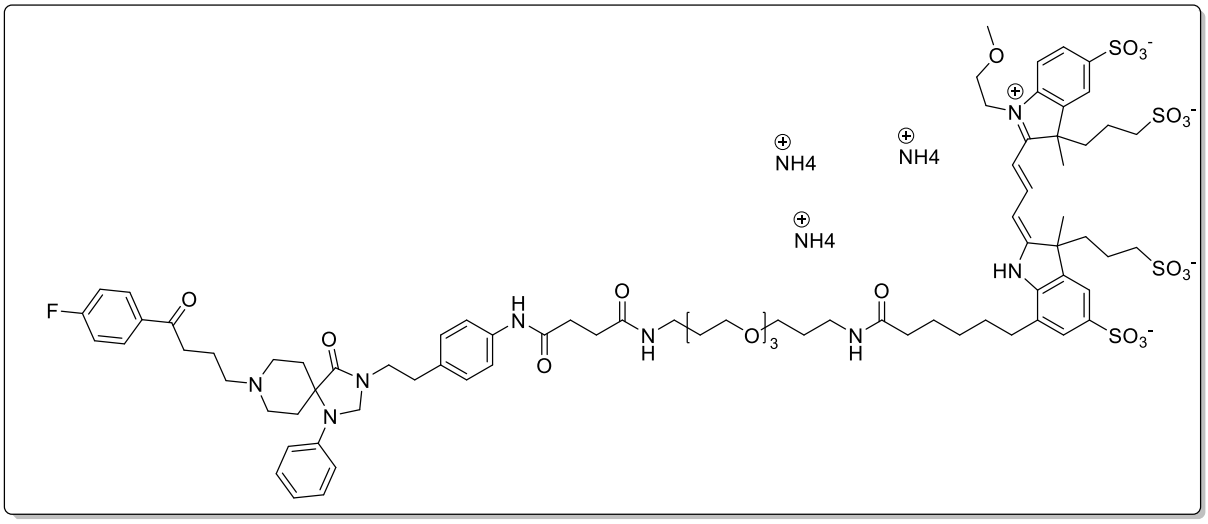

98 (0.333 mg, 0.288 µmol, 1.5 eq) was dissolved in DMF (30 µL). Triethylamine (0.20 mg, 1.92 µmol, 10 eq) and Dyomics Dye DY-549P1 NHS ester (0.2 mg, 0.192 µmol, 1 eq) in DMF (60 µL) were added and the reaction was shaken for 2.5 h in the dark at room temperature. The reaction was quenched with 10% aqueous TFA (20 µL) and the crude product was purified by preparative HPLC (Method B). **99** (0.3 mg, 89%) was obtained as a pink solid. Anal. RP-HPLC (220 nm) (Method B): 99% (t_R = 7.22 min, k = 1.25). HRMS (ESI-MS): m/z $[M+3H]^{3+}$ calculated for $C_{81}H_{110}FN_8O_{21}S_4^{3+}$: 559.2212, found 559.2226; $C_{81}H_{107}FN_8O_{21}S_4$ x N_3H_9 (1673.00 + 54.12).

2-(6-(Dimethylamino)-3-(dimethyliminio)-3*H*-xanthen-9-yl)-5-((18-((4-(2-(8-(4-(4-fluorophenyl)-4-oxobutyl)-4-oxo-1-phenyl-1,3,8-triazaspiro[4.5]decan-3-yl)ethyl)phenyl)amino)-15,18-dioxo-4,7,10-trioxa-14-azaoctadecyl)carbamoyl)benzoate dihydrotrifluoroacetate (100)

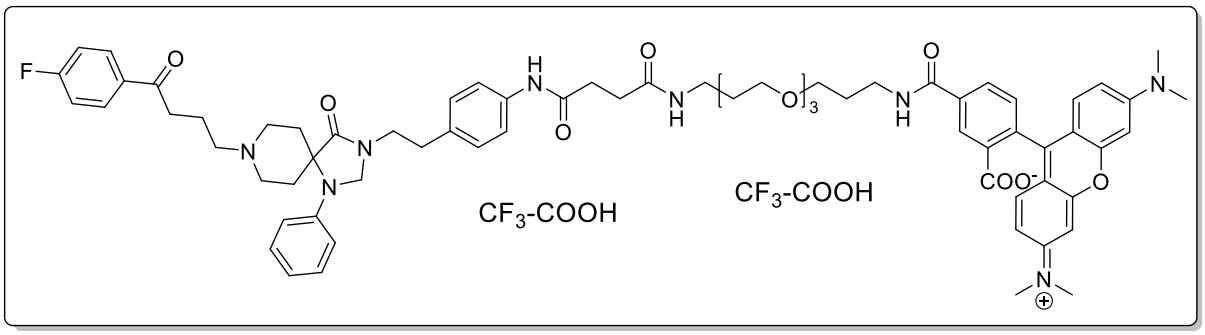

98 (1.8 mg, 1.56 µmol, 1.2 eq) was dissolved in DMF (30 µL). Triethylamine (1.1 mg, 10.4 µmol, 10 eq) and 5-carboxytetramethylrhodamine succinimidyl ester (5-TAMRA NHS ester) (0.65 mg, 1.28 µmol, 1 eq) in DMF (60 µL) were added and the reaction was shaken for 2.5 h in the dark at room temperature. The reaction was quenched with 10% aqueous TFA (20 µL) and the crude product was purified by preparative HPLC. A pink solid was obtained for **100** (1.58 mg, 1.08 µmol, 84%). Anal. RP-HPLC (254 nm): 99% (t_R = 13.38 min, k = 3.17). HRMS (ESI-MS): m/z $[M+H]^+$ calculated for $C_{70}H_{82}FN_8O_{11}^+$: 1229.6082, found 1229.6092; $C_{70}H_{81}FN_8O_{11}$ x $C_4H_2F_6O_4$ (1229.46 + 228.05).

tert-Butyl (4-((4-(2-(8-(4-(4-fluorophenyl)-4-oxobutyl)-4-oxo-1-phenyl-1,3,8-triazaspiro[4.5]decan-3-yl)ethyl)phenyl)amino)-4-oxobutyl)carbamate (101)

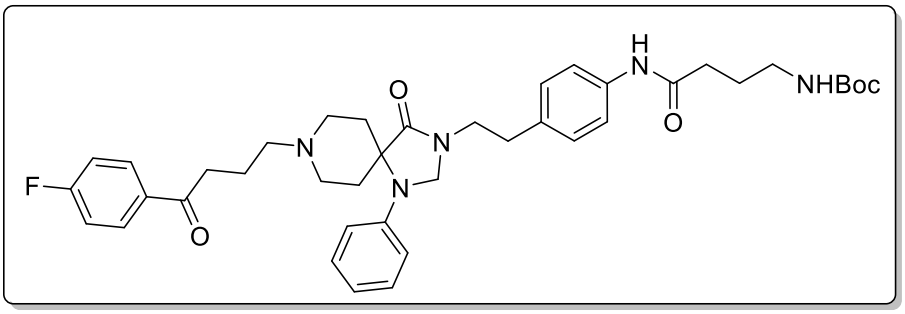

A mixture of **96** (23 mg, 0.11 mmol, 1.1 eq) and HATU (57 mg, 0.15 mmol, 1.5 eq) in DMF (15 mL) was stirred at 0 °C for 10 min. Then, DIPEA (40 mg, 0.3 mmol, 3 eq) and **36** (50 mg, 0.1 mmol, 1 eq) were added slowly and the reaction was stirred at room temperature overnight. After the solvent was removed under reduced pressure the residue was dissolved in DCM (10 mL) and washed three times with aqueous KOH (20%, 3 x 10 mL). The organic layer was dried over Na_2SO_4 and the solution was concentrated in vacuo. The crude product was purified by column

chromatography (DCM/MeOH 99/1 to 95/5) to give **101** as a yellow oil (63 mg, 90%). ^{1}H NMR (400 MHz, $CDCl_3$) δ 9.01 (d, *J* = 17.7 Hz, 1H), 8.17 – 8.08 (m, 2H), 7.67 – 7.62 (m, 2H), 7.35 (dd, *J* = 8.4, 7.6 Hz, 2H), 7.28 – 7.20 (m, 4H), 7.04 – 6.90 (m, 3H), 5.11 (t, *J* = 5.7 Hz, 1H), 4.66 (s, 2H), 3.77 (t, *J* = 7.1 Hz, 2H), 3.32 (d, *J* = 5.3 Hz, 2H), 3.20 – 2.63 (m, 12H), 2.50 – 2.46 (m, 2H), 2.10 (d, *J* = 26.2 Hz, 2H), 2.01 – 1.93 (m, 3H), 1.66 (d, *J* = 14.0 Hz, 2H), 1.55 (s, 9H). ^{13}C NMR (101 MHz, $CDCl_3$) δ 198.23, 173.98, 171.32, 165.7 (d, *J* = 254.5 Hz), 157.15, 142.73, 137.28, 136.83, 134.28, 133.41, 133.31, 130.72 (d, *J* = 9.2 Hz), 129.40, 129.32, 129.09, 120.19, 120.06, 119.16, 115.69 (d, *J* = 21.8 Hz), 115.49, 79.68, 63.77, 63.58, 60.10, 57.35, 53.47, 49.37, 42.09, 39.39, 38.66, 36.20, 34.56, 33.10, 28.41, 27.09. HRMS (ESI-MS): m/z $[M+H]^+$ calculated for $C_{40}H_{51}FN_5O_5^+$: 700.3869, found 700.3875; $C_{40}H_{50}FN_5O_5$ (699.87).

4-Amino-*N*-(4-(2-(8-(4-(4-fluorophenyl)-4-oxobutyl)-4-oxo-1-phenyl-1,3,8-triazaspiro[4.5]decan-3-yl)ethyl)phenyl)butanamide trihydrotrifluoroacetate (102)

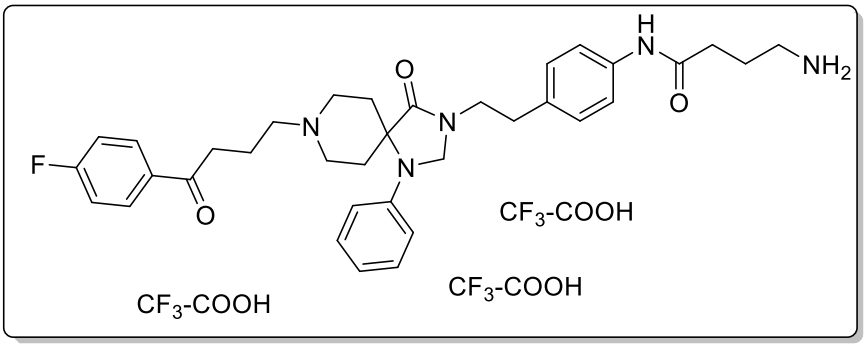

101 (63 mg, 0.09 mmol) was dissolved in DCM (30 mL) and TFA (5 mL) was added. The mixture was stirred at room temperature overnight. After the reaction was complete, as indicated by TLC, the solvent was evaporated. The resulting crude product was purified by preparative HPLC. **102** (32.1 mg, 60%) was obtained as a white solid. ^{1}H NMR (400 MHz, CD_3OD) δ 8.10 – 8.04 (m, 2H), 7.47 (d, *J* = 8.4 Hz, 2H), 7.28 – 7.18 (m, 6H), 6.97 – 6.86 (m, 3H), 4.65 (s, 2H), 3.79 – 3.64 (m, 4H), 3.54 (d, *J* = 8.8 Hz, 2H), 3.25 – 3.14 (m, 4H), 3.06 – 2.92 (m, 4H), 2.76 – 2.63 (m, 2H), 2.51 (t, *J* = 7.0 Hz, 2H), 2.18 – 2.07 (m, 2H), 2.05 – 1.94 (m, 2H), 1.74 (d, *J* = 14.7 Hz, 2H). ^{13}C NMR (101 MHz, CD_3OD) δ 197.32, 172.82, 165.95 (d, *J* = 253.4 Hz)171.37, 142.18, 136.94, 134.07, 133.07, 130.64 (d, *J* = 9.5 Hz) 129.10, 129.06, 120.34, 120.18, 116.90, 115.29 (d, *J* = 22.2 Hz) 63.45, 58.44, 56.25, 49.04, 41.40, 39.00, 34.53, 32.96, 32.27, 27.21, 22.86, 18.17. HRMS (ESI-MS): m/z $[M+H]^+$ calculated for $C_{35}H_{43}FN_5O_3^+$: 600.3344, found 600.3345; $C_{35}H_{42}FN_5O_3$ x $C_6H_3F_9O_6$ (599.75 + 342.07).

2-(6-(Dimethylamino)-3-(dimethyliminio)-3*H*-xanthen-9-yl)-5-((4-((4-(2-(8-(4-(4-fluorophenyl)-4-oxobutyl)-4-oxo-1-phenyl-1,3,8-triazaspiro[4.5]decan-3-yl)ethyl)phenyl)amino)-4-oxobutyl)carbamoyl)benzoate dihydrotrifluoroacetate (103)

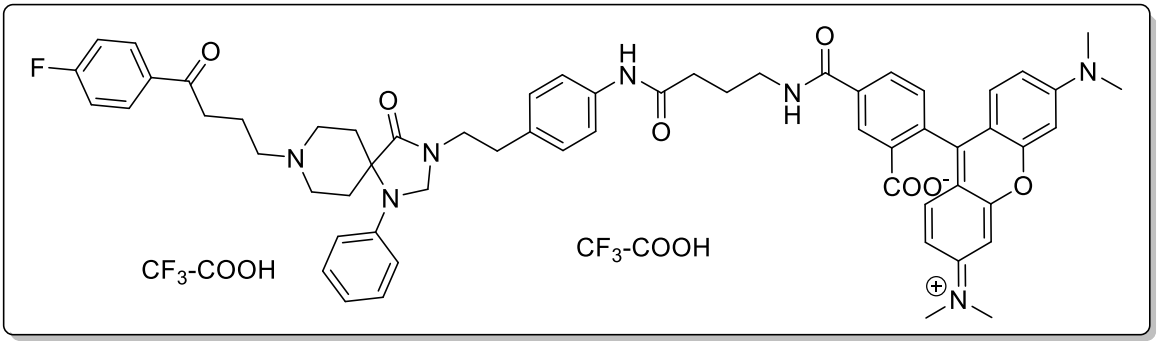

102 (1.8 mg, 1.92 µmol, 1.5 eq) was dissolved in DMF (30 µL). Triethylamine (1.1 mg, 10.4 µmol, 10 eq) and 5-carboxytetramethylrhodamine succinimidyl ester (5-TAMRA NHS ester) (0.65 mg, 1.28 µmol, 1 eq) in DMF (60 µL) were added and the reaction was shaken for 2.5 h in the dark at room temperature. The reaction was quenched with 10% aqueous TFA (20 µL) and the crude product was purified by preparative HPLC. A pink solid was obtained for **103** (0.84 mg, 0.75 µmol, 59%). Anal. RP-HPLC (254 nm): 99% (t_R = 13.20 min, k = 3.15). HRMS (ESI-MS): m/z $[M+H]^+$ calculated for $C_{60}H_{63}FN_7O_7^+$: 10212.4768, found 1012.4764; $C_{60}H_{62}FN_7O_7$ x $C_4H_2F_6O_4$ (1012.19 + 228.05).

((Oxybis(ethane-2,1-diyl))bis(oxy))bis(ethane-2,1-diyl) dimethanesulfonate (104) [254]

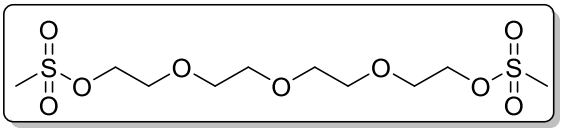

To a solution of 2,2'-((oxybis(ethane-2,1-diyl))bis(oxy))bis(ethan-1-ol) (3.00 g, 15.0 mmol, 1 eq) and triethylamine (3.73 g, 37.0 mmol, 2.4 eq) in DCM (50 mL) MsCl (4.20 g, 37.0 mmol, 2.4 eq) was added and the reaction was stirred at room temperature for 15 h. Water (35 mL) was added and the organic phase was separated, dried over Na_2SO_4 and the solvent was removed under reduced pressure. The resulting residue was purified by column chromatography (DCM/MeOH 9/1) to give **104** (5.42 g, 99%) as a yellow oil. ^{1}H NMR (300 MHz, $CDCl_3$) δ 4.36 – 4.31 (m, 4H), 3.75 – 3.71 (m, 4H), 3.65 – 3.58 (m, 8H), 3.04 (s, 6H). ^{13}C NMR (75 MHz, $CDCl_3$) δ 70.61, 70.49, 69.34, 69.00, 52.62, 37.65. HRMS (ESI-MS): m/z $[M+H]^+$ calculated for $C_{10}H_{23}O_9S_2^+$: 351.0778, found 351.0779; $C_{10}H_{22}O_9S_2$ (350.40).

1-Azido-2-(2-(2-(2-azidoethoxy)ethoxy)ethoxy)ethane (105) [255]

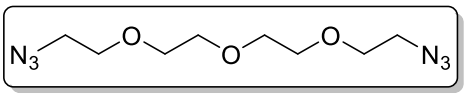

NaN_3 (3.90 g, 60.0 mmol, 4 eq) was added to a solution of **104** (5.42 g, 15.0 mmol, 1 eq) in EtOH/DMF (4/1, 40 mL) and the reaction was heated to 80 °C and stirring was continued overnight. The solvent was removed under reduced pressure and the crude product was dissolved in DCM (40 mL). The organic layer was washed with water three times and dried over Na_2SO_4. The solvent was evaporated and the residue dried in vacuo to give **105** (3.60 g, 98%) as colorless oil. ^{1}H NMR (300 MHz, $CDCl_3$) δ 3.69 – 3.60 (m, 12H), 3.40 – 3.32 (m, 4H). ^{13}C NMR (101 MHz, $CDCl_3$) δ 70.68, 70.01, 50.67. HRMS (ESI-MS): m/z $[M+H]^+$ calculated for $C_8H_{17}N_6O_3^+$: 245.1357, found 245.1358; $C_8H_{16}N_6O_3$ (244.26).

2-(2-(2-(2-Azidoethoxy)ethoxy)ethoxy)ethan-1-amine (106) [255]

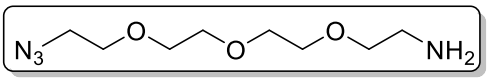

105 (3.50 g, 14.3 mmol, 1eq) was dissolved in aqueous HCl (5%, 45 mL) and a solution of triphenylphosphine (3.70g, 14.3 mmol, 1eq) in diethylether (50 mL) was added dropwise. Then the reaction was stirred at room temperature overnight. The aqueous phase was separated and washed with DCM three times (3 x 30 mL). The aqueous layer was then basified with aqueous KOH (20%) and extracted with DCM three times (3 x 30 mL). The organic layer was dried over Na_2SO_4 and concentrated in vacuo to yield **106** (3.50 g, 99%) as colorless oil. ^{1}H NMR (300 MHz, $CDCl_3$) δ 3.65 – 3.58 (m, 10H), 3.47 (t, *J* = 5.2 Hz, 2H), 3.38 – 3.32 (m, 2H), 2.82 (t, *J* = 5.2 Hz, 2H), 1.45 (s, 2H). ^{13}C NMR (75 MHz, $CDCl_3$) δ 73.26, 70.70, 70.66, 70.63, 70.27, 70.04, 50.68, 41.71. HRMS (ESI-MS): m/z $[M+H]^+$ calculated for $C_8H_{19}N_4O_3^+$: 219.1452, found 219.1455; $C_8H_{18}N_4O_3$ (218.26).

5-((tert-Butoxycarbonyl)amino)isophthalic acid (107) [256]

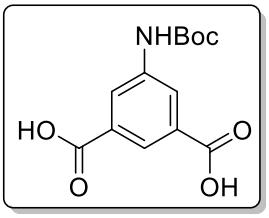

A solution of Boc_2O (0.72 g, 3.3 mmol, 1.2 eq) in dioxane (30 mL) was added dropwise to a mixture of 5-aminoisophthalic acid (0.50 g, 2.8 mmol, 1 eq) and triethylamine (0.58 g, 5.5 mmol, 2.1 eq) in dioxane/water (2/1, 30 mL) at 0 °C. After stirring at room temperature for 10 h the reaction was carefully acidified by dropwise addition of aqueous HCl (1 N) to set pH < 1. A red solid precipitated and was filtered off. The product was dried in vacuo to give **107** as a red powder (0.76 g, 98%). ^{1}H NMR (300 MHz, DMSO-d_6) δ 9.76 (s, 1H), 8.27 (s, 2H),

8.07 (s, 1H), 1.47 (s, 9H). ^{13}C NMR (101 MHz, DMSO-d_6) δ 167.03, 153.23, 140.74, 132.12, 123.96, 122.99, 80.19, 28.52. HRMS (ESI-MS): m/z $[M-H]^-$ calculated for $C_{13}H_{14}NO_6^-$: 280.0830, found 280.0827; $C_{13}H_{15}NO_6$ (281.26).

tert-Butyl (3,5-bis((2-(2-(2-(2-azidoethoxy)ethoxy)ethoxy)ethyl)carbamoyl)phenyl)carbamate (108)

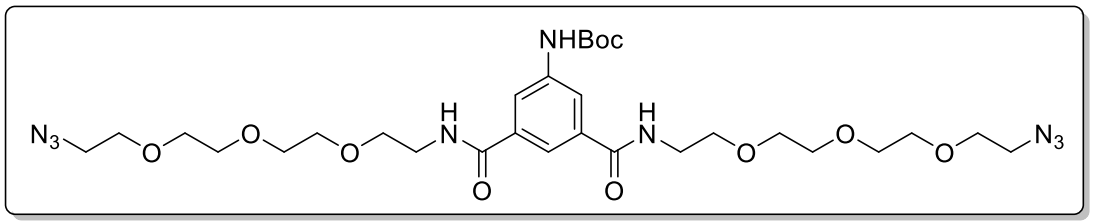

A mixture of **107** (0.10 g, 0.33 mmol, 1 eq) and HATU (0.34 g, 0.89 mmol, 2.5 eq) in DMF (20 mL) was stirred at 0 °C for 10 min. DIPEA (0.18 g, 1.4 mmol, 4 eq) and **106** (0.17 g, 0.8 mmol, 2.2 eq) were added slowly and the reaction was stirred at room temperature overnight. The solvent was removed under reduced pressure and the residue was purified by column chromatography to afford **108** as a yellow solid (0.21 g, 87%). ^{1}H NMR (300 MHz, $CDCl_3$) δ 8.07 (d, *J* = 1.2 Hz, 2H), 7.87 (s, 1H), 7.55 (s, 1H), 7.17 (s, 2H), 3.72 – 3.55 (m, 28H), 3.40 – 3.27 (m, 4H), 1.52 (s, 9H). ^{13}C NMR (75 MHz, $CDCl_3$) δ 166.70, 152.90, 139.58, 135.49, 119.92, 119.80, 80.95, 70.62, 70.54, 70.33, 69.97, 69.80, 50.64, 40.03, 28.36. HRMS (ESI-MS): m/z $[M+H]^+$ calculated for $C_{29}H_{48}N_9O_{10}^+$: 682.3519, found 682.3531; $C_{29}H_{47}N_9O_{10}$ (681.75).

5-Amino-N^1,N^3-bis(2-(2-(2-(2-azidoethoxy)ethoxy)ethoxy)ethyl)isophthalamide hydrotrifluoroacetate (109)

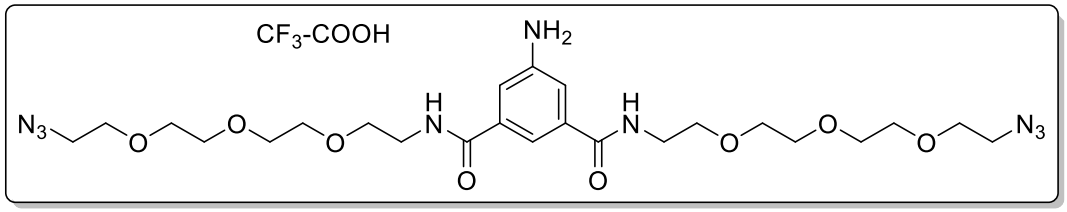

To a solution of **108** (0.21 g, 0.3 mmol) in DCM (50 mL) TFA (10 mL) was added and the reaction was stirred at room temperature. After the starting material was consumed, indicated by TLC, aqueous KOH (20%) was added and the organic layer was separated. The organic phase was dried over Na_2SO_4 and the solvent was removed under reduced pressure to give **109** (0.13 g, 75%) as a yellow oil. The product was used without further purification. ^{1}H NMR (400 MHz, $CDCl_3$) δ 7.58 (s, 1H), 7.31 (s, 2H), 7.19 – 7.07 (m, 2H), 3.76 – 3.58 (m, 28H), 3.37 – 3.29 (m,

4H). ^{13}C NMR (101 MHz, $CDCl_3$) δ 166.98, 146.14, 135.86, 119.33, 117.07, 70.59, 70.51, 70.24, 69.94, 69.83, 50.64, 39.94. HRMS (ESI-MS): m/z $[M+H]^+$ calculated for $C_{24}H_{40}N_9O_8^+$: 582.2994, found 582.3004; $C_{24}H_{39}N_9O_8$ x $C_2H_1F_3O_2$ (581.63 + 114.02).

tert-Butyl (4-((3,5-bis((2-(2-(2-(2-azidoethoxy)ethoxy)ethoxy)ethyl)carbamoyl)phenyl)amino)-4-oxobutyl)carbamate (110)

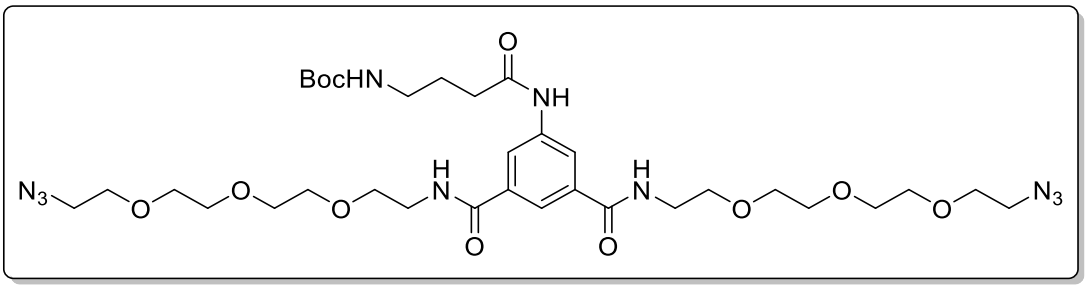

A mixture of **96** (0.07 g, 0.35 mmol, 1 eq) and HATU (0.20 g, 0.53 mmol, 1.5 eq) in DMF (20 mL) was stirred at 0 °C for 10min. DIPEA (0.14 g, 1.1 mmol, 3 eq) and **109** (0.20 g, 0.35 mmol, 2.2 eq) were added slowly and the reaction was stirred at room temperature overnight. The solvent was removed under reduced pressure and the residue was purified by column chromatography (DCM/MeOH 95/5) to afford **110** as a yellow solid (0.09 g, 33%). ^{1}H NMR (400 MHz, $CDCl_3$) δ 9.37 (s, 1H), 8.13 (s, 2H), 7.85 (s, 1H), 7.26 (s, 2H), 3.69 – 3.58 (m, 28H), 3.34 – 3.30 (m, 4H), 3.21 (t, *J* = 6.3 Hz, 2H), 2.43 (t, *J* = 6.8 Hz, 2H), 1.87 (p, *J* = 6.6 Hz, 2H), 1.43 (s, 9H). ^{13}C NMR (101 MHz, $CDCl_3$) δ 171.92, 166.79, 156.88, 139.21, 135.40, 121.19, 120.86, 79.66, 70.65, 70.61, 70.56, 70.33, 69.95, 69.70, 50.63, 40.09, 34.34, 28.44. HRMS (ESI-MS): m/z $[M+H]^+$ calculated for $C_{33}H_{55}N_{10}O_{11}^+$: 767.4046, found 767.4063; $C_{33}H_{54}N_{10}O_{11}$ (766.85).

5-(4-Aminobutanamido)-*N*^{1},*N*^{3}-bis(2-(2-(2-(2-azidoethoxy)ethoxy)ethoxy)ethyl)isophthalamide hydrotrifluoroacetate (111)

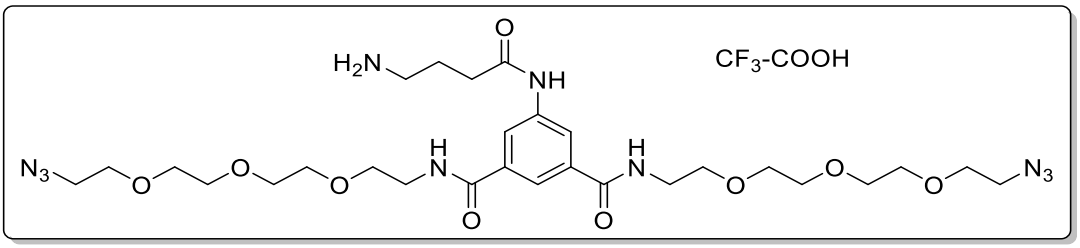

To a solution of **110** (0.09 g, 0.12 mmol) in DCM (50 mL) TFA (10 mL) was added and the reaction was stirred at room temperature. After the starting material was consumed, indicated by TLC, aqueous KOH (20%) was added and the organic layer was separated. The

organic phase was dried over Na_2SO_4 and the solvent was removed under reduced pressure to give **111** (0.06 g, 78%) as a yellow oil. The product was used without further purification. ^{1}H NMR (300 MHz, CD_3OD) δ 8.17 (d, *J* = 1.5 Hz, 2H), 7.96 (t, *J* = 1.5 Hz, 1H), 3.71 – 3.54 (m, 28H), 3.35 – 3.30 (m, 4H), 3.04 (t, *J* = 7.5 Hz, 2H), 2.59 (t, *J* = 7.0 Hz, 2H), 2.10 – 1.95 (m, 2H). ^{13}C NMR (75 MHz, CD_3OD) δ 171.62, 167.86, 139.09, 135.55, 121.39, 120.77, 70.22, 70.19, 70.05, 69.90, 69.66, 69.08, 50.32, 39.71, 38.97, 32.92, 22.65. HRMS (ESI-MS): m/z $[M+Na]^+$ calculated for $C_{28}H_{46}N_{10}O_9Na^+$: 689.3341, found 689.3347; $C_{28}H_{46}N_{10}O_9$ x $C_2HF_3O_2$ (666.73 + 114.02).

5-(4-Aminobutanamido)-*N*^{1}-(2-(2-(2-(2-(4-((4-((4-(2-(8-(4-(4-fluorophenyl)-4-oxobutyl)-4-oxo-1-phenyl-1,3,8-triazaspiro[4.5]decan-3-yl)ethyl)phenyl)amino)-4-oxobutanamido)methyl)-1*H*-1,2,3-triazol-1-yl)ethoxy)ethoxy)ethoxy)ethyl)-N^3-(2-(2-(2-(2-(4-((1-(4-(3-(piperidin-1-yl)propoxy)benzyl)piperidine-4-carboxamido)methyl)-1*H*-1,2,3-triazol-1-yl)ethoxy)ethoxy)ethoxy)ethyl)isophthalamide heptahydrotrifluoroacetate (112)

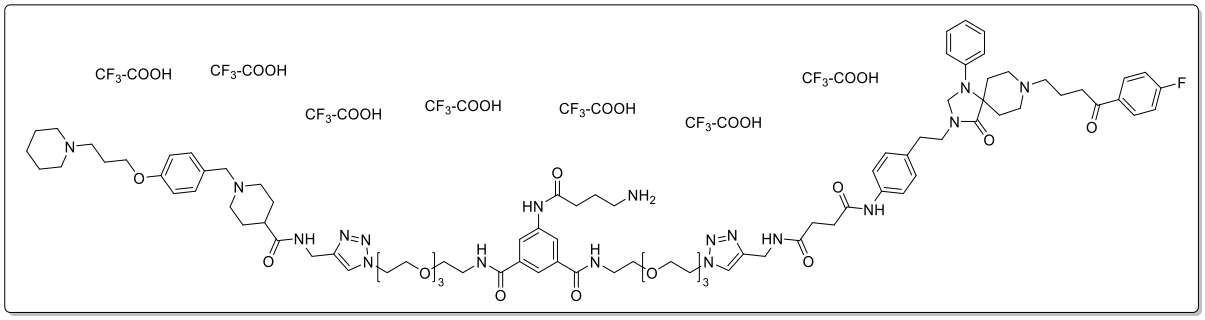

To a solution of **37** (53.0 mg, 0.082 mmol, 1.1 eq), **43** (32.3 mg, 0.082 mmol 1.1 eq) and linker **111** (50.0 mg, 0.075 mmol, 1 eq) in DCM/MeOH (4/1, 40 mL) ascorbic acid (4.0 mg, 0.0225 mmol, 0.3 eq) and $CuSO_4{\cdot}5H_2O$ (1.9 mg, 0.0075 mmol, 0.1 eq) were added. The reaction was stirred at room temperature for 72 h. The solvent was removed under reduced pressure and the resulting crude product was purified by preparative HPLC (MeCN/0.1% aqueous TFA) to give **112** (TFA salt, 20.0 mg, 10%) as a yellow shiny solid. ^{1}H NMR (400 MHz, D_2O) δ 7.88 – 7.60 (m, 7H), 7.54 – 7.34 (m, 2H), 7.33 – 7.26 (m, 2H), 7.23 – 7.13 (m, 3H), 7.11 – 6.94 (m, 4H), 6.94 – 6.86 (m, 2H), 6.86 – 6.68 (m, 2H), 4.54 – 4.46 (m, 2H), 4.39 – 4.14 (m, 8H), 4.14 – 3.95 (m, 4H), 3.75 – 3.25 (m, 36H), 3.25 – 3.10 (m, 4H), 3.06 – 2.89 (m, 6H), 2.88 – 2.69 (m, 6H), 2.52 – 2.27 (m, 9H), 2.14 – 2.05 (m, 2H), 2.01 – 1.76 (m, 8H), 1.74 – 1.31 (m, 8H).^{13}C NMR (101 MHz, D_2O) δ 175.67, 168.51, 163.16, 162.81, 138.20, 134.81, 132.91, 130.98, 130.92, 130.13, 129.67, 122.89, 118.38, 117.83, 115.89, 115.66, 115.14, 114.93, 69.57, 69.46, 68.75, 67.74, 65.35, 64.29, 59.22, 54.39, 53.34, 53.06, 51.06, 49.89, 48.81, 39.70, 38.90, 34.92, 34.56, 34.40,

33.18, 31.97, 31.62, 25.74, 23.43, 23.36, 22.83. HRMS (ESI-MS): m/z $[M+3H]^{3+}$ calculated for $C_{90}H_{126}FN_{18}O_{15}^{3+}$: 572.6539, found 572.6553; $C_{90}H_{123}FN_{18}O_{15}$ x $C_{14}H_7F_{21}O_{14}$ (1716.08 + 798.16).

Triammonium 2-((E)-3-((E)-7-(6-((4-((3-((2-(2-(2-(2-(4-((4-((4-(2-(8-(4-(4-fluorophenyl)-4-oxobutyl)-4-oxo-1-phenyl-1,3,8-triazaspiro[4.5]decan-3-yl)ethyl)phenyl)amino)-4-oxobutanamido)methyl)-1*H*-1,2,3-triazol-1-yl)ethoxy)ethoxy)ethoxy)ethyl)carbamoyl)-5-((2-(2-(2-(2-(4-((1-(4-(3-(piperidin-1-yl)propoxy)benzyl)piperidine-4-carboxamido)methyl)-1*H*-1,2,3-triazol-1-yl)ethoxy)ethoxy)ethoxy)ethyl)carbamoyl)phenyl)amino)-4-oxobutyl)amino)-6-oxohexyl)-3-methyl-5-sulfonato-3-(3-sulfonatopropyl)indolin-2-ylidene)prop-1-en-1-yl)-1-(2-methoxyethyl)-3-methyl-3-(3-sulfonatopropyl)-3H-indol-1-ium-5-sulfonate (113)

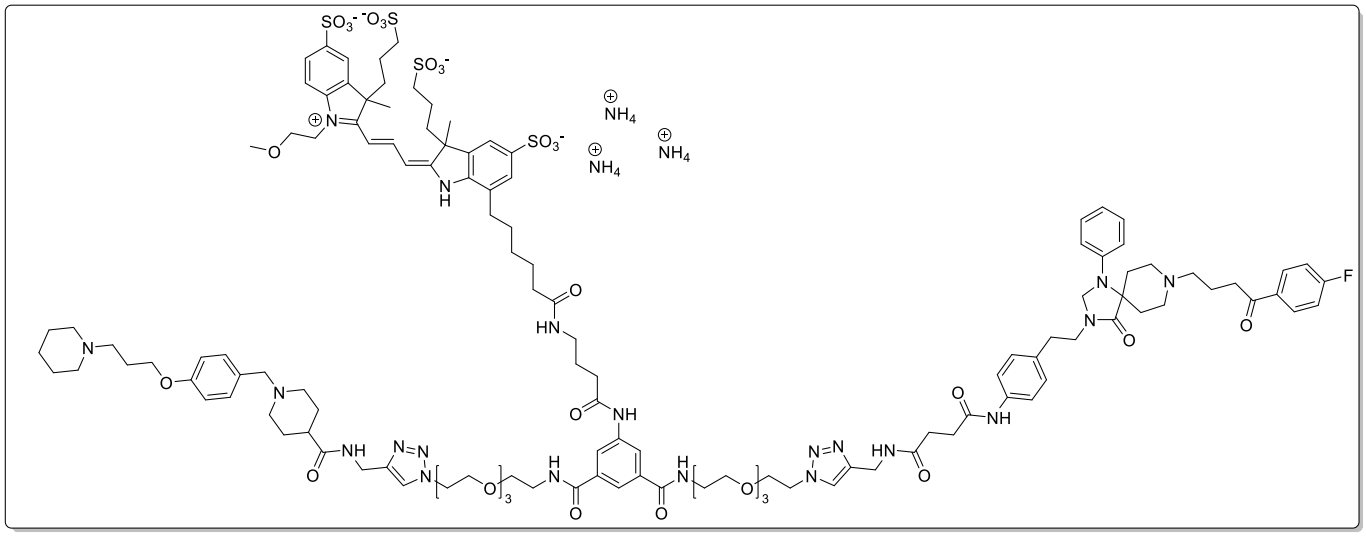

112 (0.70 mg, 0.288 µmol, 1.5 eq) was dissolved in DMF (30 µL). Triethylamine (0.19 mg, 2.11 µmol, 11 eq) and Dyomics Dye DY-549P1 NHS ester (0.2 mg, 0.192 µmol, 1 eq) in DMF (60 µL) were added and the reaction was shaken for 2.5 h in the dark at room temperature. The reaction was quenched with 10% aqueous NH_3 (20 µL) and the crude product was purified by preparative HPLC. **113** (0.45 mg, 89%) was obtained as a pink solid. Anal. RP-HPLC (220 nm): 99% (t_R = 9,09 min, k = 1.83). HRMS (ESI-MS): m/z $[M+3H]^{3+}$ calculated for $C_{126}H_{172}FN_{20}O_{29}S_4^{3+}$: 858.7150, found 858.7159; $C_{126}H_{169}FN_{20}O_{29}S_4$ x 3 NH_3 (2575.09 + 51.09).

2-(6-(Dimethylamino)-3-(dimethyliminio)-3H-xanthen-9-yl)-5-((4-((3-((2-(2-(2-(2-(4-((4-((4-(2-(8-(4-(4-fluorophenyl)-4-oxobutyl)-4-oxo-1-phenyl-1,3,8-triazaspiro[4.5]decan-3-yl)ethyl)phenyl)amino)-4-oxobutanamido)methyl)-1H-1,2,3-triazol-1-yl)ethoxy)ethoxy)ethoxy)ethyl)carbamoyl)-5-((2-(2-(2-(2-(4-((1-(4-(3-(piperidin-1-yl)propoxy)benzyl)piperidine-4-carboxamido)methyl)-1H-1,2,3-triazol-1-yl)ethoxy)ethoxy)ethoxy)ethyl)carbamoyl)phenyl)amino)-4-oxobutyl)carbamoyl)benzoate hexahydrotrifluoroacetate (114)

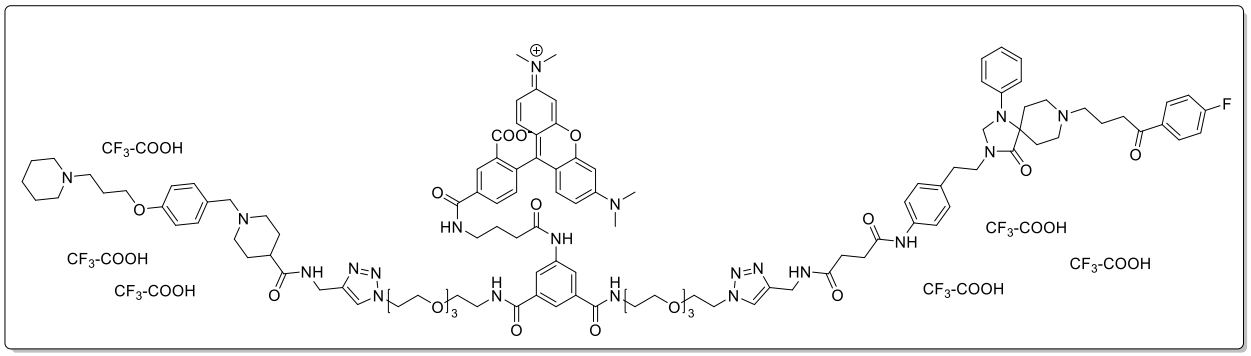

112 (8.1 mg, 3.3 µmol, 1.5 eq) was dissolved in DMF (30 µL). Triethylamine (2.2 mg, 22 µmol, 11 eq) and 5-TAMRA NHS ester (1.2 mg, 2.2 µmol, 1 eq) in DMF (60 µL) were added and the reaction was shaken for 2.5 h in the dark at room temperature. The reaction was quenched with 10% aqueous TFA (20 µL) and the crude product was purified by preparative HPLC. **114** (2 mg, 32%) was obtained as a pink solid. Anal. RP-HPLC (220 nm): 99% (t_R = 11.46 min, k = 2.57). HRMS (ESI-MS): m/z $[M+2H]^{2+}$ calculated for $C_{115}H_{145}FN_{20}O_{19}^{2+}$: 1064.5484, found 1064.5486; $C_{115}H_{143}FN_{20}O_{19}$ x $C_{12}H_6F_{18}O_{12}$ (2128.53 + 684.14).

7.3 Fluorescence properties

Excitation and emission spectra of fluorescent ligands were recorded in PBS (137 mM NaCl, 2.7 mM KCl, 10 mM Na_2HPO_4, 1.8 mM KH_2PO_4, pH 7.4) containing 1% BSA (Sigma- Aldrich, Munich, Germany) using a Cary Eclipse spectrofluorometer (Varian Inc., Mulgrave, Victoria, Australia) at 22 °C, in acryl cuvettes (10 ×10 mm, Sarstedt, Nümbrecht, Germany). The slit adjustments (excitation/emission) were 5/10 nm for excitation spectra and 10/5 nm for emission spectra. Net spectra were calculated by subtracting the respective vehicle reference spectrum, and corrected emission spectra were calculated by multiplying the net emission spectra with the respective lamp correction spectrum. The quantum yields of fluorescent ligands were determined according to a previously described procedure with minor modifications using a Cary Eclipse spectrofluorometer (Varian Inc., Mulgrave, Victoria, Australia) at 22 °C, using acryl cuvettes (10 ×10 mm, Sarstedt, Nümbrecht, Germany) and cresyl violet perchlorate (Biomol GmbH −Life Science Shop, Hamburg, Germany) as a red fluorescent standard.[203] Absorption spectra were recorded by UV/Vis spectroscopy (350−850 nm, scan rate: 300 nm/min, slits: fixed 2 nm) at a concentration of 2 µM for cresyl violet (in EtOH, $\lambda_{abs,max}$ = 575 nm) and fluorescent ligands (in PBS + 1% BSA, $\lambda_{abs,max}$ = 550 nm). The quantum yields were calculated for three different slit adjustments (exc./em.): 5/5, 10/5, and 10/10 nm. The means of the quantum yields, absorption and emission maxima, and absorbance are presented in the respective chapters.

7.4 Radioligand binding assays

7.4.1 Dopamine receptors

Radioligand binding experiments with homogenates were performed as previously described with minor modifications.[257] In brief, ligand dilutions of tested compounds were prepared 10-fold concentrated in binding buffer (50 mM Tris·HCl, 1 mM EDTA, 5 mM $MgCl_2$ and 100 µg/mL bacitracin, pH = 7.4), and 20 µL/well was transferred to a flat-bottom polypropylene 96-well microtiter plate (Greiner Bio-One, Frickenhausen, Germany), as well as 20 µL/well of the respective radioligand ([^{3}H]N-methylspiperone was applied at a final concentration of 0.05 nM for the D_{2long}R and the D_3R or 0.1 nM for the $D_{4.4}$R; [^{3}H]SCH-23390 was applied at a final concentration of 1 nM for the D_1R and the D_5R). Homogenates of HEK cells containing the respective dopamine receptor were resuspended in binding buffer and 160 µL/well was added to obtain a final concentration of 0.3 µg (D_2longR), 0.7 µg (D_3R), 0.5–1.0 µg ($D_{4.4}$R), or 80 µL/well was added to obtain a final concentration of 0.3 µg (D_1R) and 0.5–1.0 µg (D_5R) protein/well . Incubation time was 60 min for all receptors. Unspecific binding was determined in the presence of (+)-butaclamol (2000-fold excess). All data were analyzed using GraphPad Prism9 software (San Diego, CA, USA). The normalized competition binding curves were then fitted with a four-parameter logistic fit yielding pIC_{50}-values. These were transformed into pK_i-values using the Cheng–Prusoff equation.[258]

7.4.2 Histamine receptors

Radioligand competition binding experiments were performed as previously described by Pockes et al. with minor modifications.[259] All experiments were carried out on whole HEK cells instead of Sf9 membranes. Generation of the stable HEK293-SP-FLAG-hH_1R and HEK293-SP-FLAG-hH_2R cell lines was conducted as described for the HEK293-SP-FLAG-hH_3R and HEK293-SP-FLAG-hH_4R.[260] Ligand dilutions of compounds were prepared 10-fold concentrated in L-15 with 1% BSA, and 10 µL/well was transferred to a fiat-bottom polypropylene 96-well microtiter plate (Greiner Bio-One, Frickenhausen, Germany), as well as 10 µL/well of the radioligand. The cells were adjusted to a density of 1.25 x 10^6 cells/mL, and 80 µL of the cell suspension was added to each well (total volume of 100 µL). All data were analyzed using GraphPad Prism9 software (San Diego, CA, USA). The normalized competition binding curves were then fitted with a four-parameter logistic fit yielding pIC_{50} valued. These were transformed into pK_i values using the Cheng-Prusoff equation.[258]

7.5 Functional assays

HEK293T cells were grown in Dulbecco`s modified medium (DMEM) (Gibcro, Paisley, Scotland, UK) supplemented with 2 mM L-glutamine, 100 U/mL penicillin/streptomycin, MEM non-essential amino acids solution (1/100), and 5% (v/v) heat-inactivated fetal bovine serum (FBS) (Invitrogen, Paisley, Scotland, UK). Cells were maintained in a humid atmosphere of 5% CO_2 at 37 °C. Cells were transiently transfected with the PEI (polythyleneimine, Sigma-Aldrich) method as previously described.[261] For cAMP determination, HEK293T cells were transiently transfected with 2 µg of cDNA for H_3R, D_2R or both with the PEI method. Two hours before initiating the experiment, the cell medium was exchanged to the non-supplemented DMEM medium. The cells were then detached and suspended in the medium containing 50 µM zardaverine. Cells were placed in 384-well plates (2500 cells/well), pretreated with antagonists or vehicle (15 min) and stimulated with agonists (15 min) before adding 0.5 µM forskolin or vehicle (15 min). Readings were performed after 1 h of incubation at 25 °C. Homogenous time-resolved fluorescence energy transfer (HTRF) measurements were carried out using the Lance Ultra cAMP kit (Perkin Elmer, Waltham, MA, USA). Fluorescence at 665 nm was analyzed on a PHERstar Flagship plate reader equipped with an HTRF optical module (BMG Lab Technologies, Offenburg, Germany). The reference value (100%) was that achieved by 0.5 µM forskolin treatment, 0% was the effect induced by 250 nM sumanirole or 500 nM imetit. The effect of ligands is given as a percentage with respect to the reference values. All data were analyzed using GraphPad Prism9 software (San Diego, CA, USA). The normalized competition binding curves were then fitted with a three-parameter logistic fit yielding pEC_{50} -or pIC_{50}-values.

Chapter 8: References

8. References

[1] M.A. Hanson, R.C. Stevens, Discovery of new GPCR biology: one receptor structure at a time, Structure 17 (2009) 8-14. https://doi.org/10.1016/j.str.2008.12.003.

[2] M.C. Lagerström, H.B. Schiöth, Structural diversity of G protein-coupled receptors and significance for drug discovery, Nat. Rev. Drug Discov. 7 (2008) 339–357. https://doi.org/10.1038/nrd2518.

[3] S.-M. Lee, J.M. Booe, A.A. Pioszak, Structural insights into ligand recognition and selectivity for classes A, B, and C GPCRs, European Journal of Pharmacology 763 (2015) 196–205. https://doi.org/10.1016/j.ejphar.2015.05.013.

[4] D.K. Vassilatis, J.G. Hohmann, H. Zeng, F. Li, J.E. Ranchalis, M.T. Mortrud, A. Brown, S.S. Rodriguez, J.R. Weller, A.C. Wright, J.E. Bergmann, G.A. Gaitanaris, The G protein-coupled receptor repertoires of human and mouse, Proceedings of the National Academy of Sciences 100 (2003) 4903–4908. https://doi.org/10.1073/pnas.0230374100.

[5] D.E. Felsing, J. Zamora, S. Raval, J.A. Allen, Striatal specific orphan GPCRs crosstalk with Dopamine D2 receptors to regulate cAMP signaling, FASEB j. 34 (2020) 1. https://doi.org/10.1096/fasebj.2020.34.s1.09769.

[6] K. Lundstrom, An Overview on GPCRs and Drug Discovery: Structure-Based Drug Design and Structural Biology on GPCRs, in: W.R. Leifert (Ed.), G Protein-Coupled Receptors in Drug Discovery, Humana Press, Totowa, NJ, 2009, pp. 51–66.

[7] A.S. Hauser, S. Chavali, I. Masuho, L.J. Jahn, K.A. Martemyanov, D.E. Gloriam, M.M. Babu, Pharmacogenomics of GPCR Drug Targets, Cell 172 (2018) 41-54. https://doi.org/10.1016/j.cell.2017.11.033.

[8] D.A. Fonseca, I. Amaral, A.C. Pinto, M.D. Cotrim, Orphan drugs: major development challenges at the clinical stage, Drug Discovery Today 24 (2019) 867–872. https://doi.org/10.1016/j.drudis.2019.01.005.

[9] V. Giannuzzi, R. Conte, A. Landi, S.A. Ottomano, D. Bonifazi, P. Baiardi, F. Bonifazi, A. Ceci, Orphan medicinal products in Europe and United States to cover needs of patients with rare diseases: an increased common effort is to be foreseen, Orphanet J Rare Dis 12 (2017) 64. https://doi.org/10.1186/s13023-017-0617-1.

[10] G. Lebon, T. Warne, P.C. Edwards, K. Bennett, C.J. Langmead, A.G.W. Leslie, C.G. Tate, Agonist-bound adenosine A2A receptor structures reveal common features of GPCR activation, Nature 474 (2011) 521–525. https://doi.org/10.1038/nature10136.

[11] D.A. Goldfeld, K. Zhu, T. Beuming, R.A. Friesner, Loop prediction for a GPCR homology model: algorithms and results, Proteins 81 (2013) 214–228. https://doi.org/10.1002/prot.24178.

[12] T.H. Ji, M. Grossmann, I. Ji, G protein-coupled receptors. I. Diversity of receptor-ligand interactions, J. Biol. Chem. 273 (1998) 17299–17302. https://doi.org/10.1074/jbc.273.28.17299.

[13] A.C. Magalhaes, H. Dunn, S.S. Ferguson, Regulation of GPCR activity, trafficking and localization by GPCR-interacting proteins, British Journal of Pharmacology 165 (2012) 1717–1736. https://doi.org/10.1111/j.1476-5381.2011.01552.x.

[14] A. Koehl, H. Hu, D. Feng, B. Sun, Y. Zhang, M.J. Robertson, M. Chu, T.S. Kobilka, T. Laeremans, J. Steyaert, J. Tarrasch, S. Dutta, R. Fonseca, W.I. Weis, J.M. Mathiesen, G. Skiniotis, B.K. Kobilka, Structural insights into the activation of metabotropic glutamate receptors, Nature 566 (2019) 79–84. https://doi.org/10.1038/s41586-019-0881-4.

[15] D. Hilger, M. Masureel, B.K. Kobilka, Structure and dynamics of GPCR signaling complexes, Nat. Struct. Mol. Biol. 25 (2018) 4–12. https://doi.org/10.1038/s41594-017-0011-7.

[16] M.E. Huber, L. Toy, M.F. Schmidt, H. Vogt, J. Budzinski, M.F.J. Wiefhoff, N. Merten, E. Kostenis, D. Weikert, M. Schiedel, A Chemical Biology Toolbox Targeting the Intracellular Binding Site of CCR9: Fluorescent Ligands, New Drug Leads and PROTACs, Angew. Chem. Int. Ed. Engl. 61 (2022) e202116782. https://doi.org/10.1002/anie.202116782.

[17] A.J.M. Zweemer, J. Bunnik, M. Veenhuizen, F. Miraglia, E.B. Lenselink, M. Vilums, H. de Vries, A. Gibert, S. Thiele, M.M. Rosenkilde, A.P. IJzerman, L.H. Heitman, Discovery and mapping of an intracellular antagonist binding site at the chemokine receptor CCR2, Mol. Pharmacol. 86 (2014) 358–368. https://doi.org/10.1124/mol.114.093328.

[18] N.V. Ortiz Zacarías, E.B. Lenselink, A.P. IJzerman, T.M. Handel, L.H. Heitman, Intracellular Receptor Modulation: Novel Approach to Target GPCRs, Trends Pharmacol. Sci. 39 (2018) 547–559. https://doi.org/10.1016/j.tips.2018.03.002.

[19] K. Palczewski, T. Kumasaka, T. Hori, C.A. Behnke, H. Motoshima, B.A. Fox, I. Le Trong, D.C. Teller, T. Okada, R.E. Stenkamp, M. Yamamoto, M. Miyano, Crystal structure of

rhodopsin: A G protein-coupled receptor, Science 289 (2000) 739–745. https://doi.org/10.1126/science.289.5480.739.

[20] S.G.F. Rasmussen, H.-J. Choi, D.M. Rosenbaum, T.S. Kobilka, F.S. Thian, P.C. Edwards, M. Burghammer, V.R.P. Ratnala, R. Sanishvili, R.F. Fischetti, G.F.X. Schertler, W.I. Weis, B.K. Kobilka, Crystal structure of the human beta2 adrenergic G-protein-coupled receptor, Nature 450 (2007) 383–387. https://doi.org/10.1038/nature06325.

[21] T. Warne, M.J. Serrano-Vega, J.G. Baker, R. Moukhametzianov, P.C. Edwards, R. Henderson, A.G.W. Leslie, C.G. Tate, G.F.X. Schertler, Structure of a beta1-adrenergic G-protein-coupled receptor, Nature 454 (2008) 486–491. https://doi.org/10.1038/nature07101.

[22] R.B. Clark, Profile of Brian K. Kobilka and Robert J. Lefkowitz, 2012 Nobel laureates in chemistry, PNAS 110 (2013) 5274–5275. https://doi.org/10.1073/pnas.1221820110.

[23] S.P.H. Alexander, H.E. Benson, E. Faccenda, A.J. Pawson, J.L. Sharman, M. Spedding, J.A. Peters, A.J. Harmar, The Concise Guide to PHARMACOLOGY 2013/14: G protein-coupled receptors, British Journal of Pharmacology 170 (2013) 1459–1581. https://doi.org/10.1111/bph.12445.

[24] Ranganathan, A., Rodríguez, D., Carlsson, J. (2017). Structure-Based Discovery of GPCR Ligands from Crystal Structures and Homology Models. In: Lebon, G. (eds) Structure and Function of GPCRs. Topics in Medicinal Chemistry, vol 30. Springer, Cham. https://doi.org/10.1007/7355_2016_25.

[25] M.N. Davies, D.E. Gloriam, A. Secker, A.A. Freitas, M. Mendao, J. Timmis, D.R. Flower, Proteomic applications of automated GPCR classification, Proteomics 7 (2007) 2800–2814. https://doi.org/10.1002/pmic.200700093.

[26] T.K. Attwood, J.B. Findlay, Fingerprinting G-protein-coupled receptors, Protein Eng. 7 (1994) 195–203. https://doi.org/10.1093/protein/7.2.195.

[27] L.F. Kolakowski, GCRDb: a G-protein-coupled receptor database, Recept. Channels 2 (1994) 1–7.

[28] R. Fredriksson, M.C. Lagerström, L.-G. Lundin, H.B. Schiöth, The G-protein-coupled receptors in the human genome form five main families. Phylogenetic analysis, paralogon groups, and fingerprints, Mol. Pharmacol. 63 (2003) 1256–1272. https://doi.org/10.1124/mol.63.6.1256.

[29] D. Fridmanis, R. Fredriksson, I. Kapa, H.B. Schiöth, J. Klovins, Formation of new genes explains lower intron density in mammalian Rhodopsin G protein-coupled receptors, Mol. Phylogenet. Evol. 43 (2007) 864–880. https://doi.org/10.1016/j.ympev.2006.11.007.

[30] J. Chandrashekar, K.L. Mueller, M.A. Hoon, E. Adler, L. Feng, W. Guo, C.S. Zuker, N.J. Ryba, T2Rs Function as Bitter Taste Receptors, Cell 100 (2000) 703–711. https://doi.org/10.1016/S0092-8674(00)80706-0.

[31] D.C. Slusarski, V.G. Corces, R.T. Moon, Interaction of Wnt and a Frizzled homologue triggers G-protein-linked phosphatidylinositol signalling, Nature 390 (1997) 410–413. https://doi.org/10.1038/37138.

[32] T.K. Bjarnadóttir, R. Fredriksson, P.J. Höglund, D.E. Gloriam, M.C. Lagerström, H.B. Schiöth, The human and mouse repertoire of the adhesion family of G-protein-coupled receptors, Genomics 84 (2004) 23–33. https://doi.org/10.1016/j.ygeno.2003.12.004.

[33] M.C. Peeters, M. Fokkelman, B. Boogaard, K.L. Egerod, B. van de Water, A.P. IJzerman, T.W. Schwartz, The adhesion G protein-coupled receptor G2 (ADGRG2/GPR64) constitutively activates SRE and NFκB and is involved in cell adhesion and migration, Cellular Signalling 27 (2015) 2579–2588. https://doi.org/10.1016/j.cellsig.2015.08.015.

[34] J. Kniazeff, A.-S. Bessis, D. Maurel, H. Ansanay, L. Prézeau, J.-P. Pin, Closed state of both binding domains of homodimeric mGlu receptors is required for full activity, Nat. Struct. Mol. Biol. 11 (2004) 706–713. https://doi.org/10.1038/nsmb794.

[35] N. Kunishima, Y. Shimada, Y. Tsuji, T. Sato, M. Yamamoto, T. Kumasaka, S. Nakanishi, H. Jingami, K. Morikawa, Structural basis of glutamate recognition by a dimeric metabotropic glutamate receptor, Nature 407 (2000) 971–977. https://doi.org/10.1038/35039564.

[36] J.C.R. Cardoso, V.C. Pinto, F.A. Vieira, M.S. Clark, D.M. Power, Evolution of secretin family GPCR members in the metazoa, BMC Evol. Biol. 6 (2006) 108. https://doi.org/10.1186/1471-2148-6-108.

[37] A. de Lean, J.M. Stadel, R.J. Lefkowitz, A ternary complex model explains the agonist-specific binding properties of the adenylate cyclase-coupled beta-adrenergic receptor, J. Biol. Chem. 255 (1980) 7108–7117. https://doi.org/10.1016/S0021-9258(20)79672-9.

[38] J.M. Weiss, P.H. Morgan, M.W. Lutz, T.P. Kenakin, The Cubic Ternary Complex Receptor–Occupancy Model I. Model Description, Journal of Theoretical Biology 178 (1996) 151–167. https://doi.org/10.1006/jtbi.1996.0014.

[39] F.J. Meye, G.M.J. Ramakers, R.A.H. Adan, The vital role of constitutive GPCR activity in the mesolimbic dopamine system, Transl. Psychiatry 4 (2014) e361. https://doi.org/10.1038/tp.2013.130.

[40] J.M. Weiss, P.H. Morgan, M.W. Lutz, T.P. Kenakin, The cubic ternary complex receptor-occupancy model. III. resurrecting efficacy, Journal of Theoretical Biology 181 (1996) 381–397. https://doi.org/10.1006/jtbi.1996.0139.

[41] P. Samama, S. Cotecchia, T. Costa, R.J. Lefkowitz, A mutation-induced activated state of the beta 2-adrenergic receptor. Extending the ternary complex model, J. Biol. Chem. 268 (1993) 4625–4636. https://doi.org/10.1016/S0021-9258(18)53442-6.

[42] G. Milligan, Constitutive activity and inverse agonists of G protein-coupled receptors: a current perspective, Mol. Pharmacol. 64 (2003) 1271–1276. https://doi.org/10.1124/mol.64.6.1271.

[43] J.M. Weiss, P.H. Morgan, M.W. Lutz, T.P. Kenakin, The Cubic Ternary Complex Receptor–Occupancy Model II. Understanding Apparent Affinity, Journal of Theoretical Biology 178 (1996) 169–182. https://doi.org/10.1006/jtbi.1996.0015.

[44] D. Wacker, R.C. Stevens, B.L. Roth, How Ligands Illuminate GPCR Molecular Pharmacology, Cell 170 (2017) 414–427. https://doi.org/10.1016/j.cell.2017.07.009.

[45] P.S.-H. Park, D.T. Lodowski, K. Palczewski, Activation of G protein-coupled receptors: beyond two-state models and tertiary conformational changes, Annu. Rev. Pharmacol. Toxicol. 48 (2008) 107–141. https://doi.org/10.1146/annurev.pharmtox.48.113006.094630.

[46] D.A. Hall, Modeling the functional effects of allosteric modulators at pharmacological receptors: an extension of the two-state model of receptor activation, Mol. Pharmacol. 58 (2000) 1412–1423. https://doi.org/10.1124/mol.58.6.1412.

[47] P.I. Dosa, E.A. Amin, Tactical Approaches to Interconverting GPCR Agonists and Antagonists, J. Med. Chem. 59 (2016) 810–840. https://doi.org/10.1021/acs.jmedchem.5b00982.

[48] R. Seifert, K. Wenzel-Seifert, Constitutive activity of G-protein-coupled receptors: cause of disease and common property of wild-type receptors, Naunyn Schmiedebergs. Arch. Pharmacol. 366 (2002) 381–416. https://doi.org/10.1007/s00210-002-0588-0.

[49] R.A. Bond, E.Y. Lucero Garcia-Rojas, A. Hegde, J.K.L. Walker, Therapeutic Potential of Targeting ß-Arrestin, Front. Pharmacol. 10 (2019) 124. https://doi.org/10.3389/fphar.2019.00124.

[50] D.L. Hay, D.R. Poyner, P.M. Sexton, GPCR modulation by RAMPs, Pharmacology & Therapeutics 109 (2006) 173–197. https://doi.org/10.1016/j.pharmthera.2005.06.015.

[51] J.D. Violin, A.L. Crombie, D.G. Soergel, M.W. Lark, Biased ligands at G-protein-coupled receptors: promise and progress, Trends Pharmacol. Sci. 35 (2014) 308–316. https://doi.org/10.1016/j.tips.2014.04.007.

[52] M. Bermudez, T.N. Nguyen, C. Omieczynski, G. Wolber, Strategies for the discovery of biased GPCR ligands, Drug Discovery Today 24 (2019) 1031–1037. https://doi.org/10.1016/j.drudis.2019.02.010.

[53] S. Rajagopal, K. Rajagopal, R.J. Lefkowitz, Teaching old receptors new tricks: biasing seven-transmembrane receptors, Nat. Rev. Drug Discov. 9 (2010) 373–386. https://doi.org/10.1038/nrd3024.

[54] D. Wacker, C. Wang, V. Katritch, G.W. Han, X.-P. Huang, E. Vardy, J.D. McCorvy, Y. Jiang, M. Chu, F.Y. Siu, W. Liu, H.E. Xu, V. Cherezov, B.L. Roth, R.C. Stevens, Structural features for functional selectivity at serotonin receptors, Science 340 (2013) 615–619. https://doi.org/10.1126/science.1232808.

[55] T. Gudermann, T. Schöneberg, G. Schultz, Functional and structural complexity of signal transduction via G-protein-coupled receptors, Annu. Rev. Neurosci. 20 (1997) 399–427. https://doi.org/10.1146/annurev.neuro.20.1.399.

[56] L. Birnbaumer, M. Birnbaumer, Signal transduction by G proteins: 1994 edition, J. Recept. Signal Transduct. Res. 15 (1995) 213–252. https://doi.org/10.3109/10799899509045218.

[57] D.E. Clapham, E.J. Neer, New roles for G-protein beta gamma-dimers in transmembrane signalling, Nature 365 (1993) 403–406. https://doi.org/10.1038/365403a0.

[58] A.V. Smrcka, G protein βγ subunits: central mediators of G protein-coupled receptor signaling, Cell. Mol. Life Sci. 65 (2008) 2191–2214. https://doi.org/10.1007/s00018-008-8006-5.

[59] S. Offermanns, G-proteins as transducers in transmembrane signalling, Progress in Biophysics and Molecular Biology 83 (2003) 101–130. https://doi.org/10.1016/s0079-6107(03)00052-x.

[60] E.H. Schneider, R. Seifert, Sf9 cells: a versatile model system to investigate the pharmacological properties of G protein-coupled receptors, Pharmacology & Therapeutics 128 (2010) 387–418. https://doi.org/10.1016/j.pharmthera.2010.07.005.

[61] E.M. Ross, T.M. Wilkie, GTPase-activating proteins for heterotrimeric G proteins: regulators of G protein signaling (RGS) and RGS-like proteins, Annu. Rev. Biochem. 69 (2000) 795–827. https://doi.org/10.1146/annurev.biochem.69.1.795.

[62] T.A. Baldwin, C.W. Dessauer, Function of Adenylyl Cyclase in Heart: the AKAP Connection, J. Cardiovasc. Dev. Dis. 5 (2018). https://doi.org/10.3390/jcdd5010002.

[63] M.I. Simon, M.P. Strathmann, N. Gautam, Diversity of G proteins in signal transduction, Science 252 (1991) 802–808. https://doi.org/10.1126/science.1902986.

[64] M. Ferrer-Alcón, M.J. García-Fuster, R. La Harpe, J.A. García-Sevilla, Long-term regulation of signalling components of adenylyl cyclase and mitogen-activated protein kinase in the pre-frontal cortex of human opiate addicts, J. Neurochem. 90 (2004) 220–230. https://doi.org/10.1111/j.1471-4159.2004.02473.x.

[65] T. Sasaki, J. Kotera, K. Yuasa, K. Omori, Identification of human PDE7B, a cAMP-specific phosphodiesterase, Biochem. Biophys. Res. Commun. 271 (2000) 575–583. https://doi.org/10.1006/bbrc.2000.2661.

[66] S. Pockes, Synthese und pharmakologische Charakterisierung von Heteroarylpropylguanidin-Derivaten an Histamin-Rezeptorsubtypen: Struktur-Wirkungsbeziehungen mono- und bivalenter Liganden, PhD thesis (2018).

[67] S.G. Rhee, Regulation of phosphoinositide-specific phospholipase C, Annu. Rev. Biochem. 70 (2001) 281–312. https://doi.org/10.1146/annurev.biochem.70.1.281.

[68] E.J. Dickson, B.H. Falkenburger, B. Hille, Quantitative properties and receptor reserve of the IP(3) and calcium branch of G(q)-coupled receptor signaling, J. Gen. Physiol. 141 (2013) 521–535. https://doi.org/10.1085/jgp.201210886.

[69] S. Qazi, B.A. Trimmer, The role of inositol 1,4,5-trisphosphate 5-phosphatase in inositol signaling in the CNS of larval Manduca sexta, Insect Biochemistry and Molecular Biology 29 (1999) 161–175. https://doi.org/10.1016/s0965-1748(98)00120-9.

[70] J. Gambardella, M.B. Morelli, X. Wang, V. Castellanos, P. Mone, G. Santulli, The discovery and development of IP3 receptor modulators: an update, Expert Opin. Drug Discov. 16 (2021) 709–718. https://doi.org/10.1080/17460441.2021.1858792.

[71] M. Sato, E. Tani, H. Fujikawa, K. Kaibuchi, Involvement of Rho-kinase-mediated phosphorylation of myosin light chain in enhancement of cerebral vasospasm, Circulation Research 87 (2000) 195–200. https://doi.org/10.1161/01.RES.87.3.195.

[72] K. Yamamoto, P. Vernier, The evolution of dopamine systems in chordates, Front. Neuroanat. 5 (2011) 21. https://doi.org/10.3389/fnana.2011.00021.

[73] A. CARLSSON, M. LINDQVIST, T. MAGNUSSON, B. WALDECK, On the presence of 3-hydroxytyramine in brain, Science 127 (1958) 471. https://doi.org/10.1126/science.127.3296.471.

[74] D. Vallone, R. Picetti, E. Borrelli, Structure and function of dopamine receptors, Neuroscience & Biobehavioral Reviews 24 (2000) 125–132. https://doi.org/10.1016/S0149-7634(99)00063-9.

[75] D.M. Jackson, A. Westlind-Danielsson, Dopamine receptors: Molecular biology, biochemistry and behavioural aspects, Pharmacology & Therapeutics 64 (1994) 291–370. https://doi.org/10.1016/0163-7258(94)90041-8.

[76] A.S. Undieh, Pharmacology of signaling induced by dopamine D(1)-like receptor activation, Pharmacology & Therapeutics 128 (2010) 37–60. https://doi.org/10.1016/j.pharmthera.2010.05.003.

[77] D.J. Surmeier, J. Ding, M. Day, Z. Wang, W. Shen, D1 and D2 dopamine-receptor modulation of striatal glutamatergic signaling in striatal medium spiny neurons, Trends Neurosci. 30 (2007) 228–235. https://doi.org/10.1016/j.tins.2007.03.008.

[78] J.H. Ko, A.P. Strafella, Dopaminergic neurotransmission in the human brain: new lessons from perturbation and imaging, Neuroscientist 18 (2012) 149–168. https://doi.org/10.1177/1073858411401413.

[79] M.O. Klein, D.S. Battagello, A.R. Cardoso, D.N. Hauser, J.C. Bittencourt, R.G. Correa, Dopamine: Functions, Signaling, and Association with Neurological Diseases, Cell. Mol. Neurobiol. 39 (2019) 31–59. https://doi.org/10.1007/s10571-018-0632-3.

[80] C. Missale, S.R. Nash, S.W. Robinson, M. Jaber, M.G. Caron, Dopamine receptors: from structure to function, Physiological Reviews 78 (1998) 189–225. https://doi.org/10.1152/physrev.1998.78.1.189.

[81] K.D. Alex, E.A. Pehek, Pharmacologic mechanisms of serotonergic regulation of dopamine neurotransmission, Pharmacology & Therapeutics 113 (2007) 296–320. https://doi.org/10.1016/j.pharmthera.2006.08.004.

[82] A.J. Lees, E. Tolosa, C.W. Olanow, Four pioneers of L-dopa treatment: Arvid Carlsson, Oleh Hornykiewicz, George Cotzias, and Melvin Yahr, Mov. Disord. 30 (2015) 19–36. https://doi.org/10.1002/mds.26120.

[83] C.A. Davie, A review of Parkinson's disease, British Medical Bulletin 86 (2008) 109–127. https://doi.org/10.1093/bmb/ldn013.

[84] W. Poewe, K. Seppi, C.M. Tanner, G.M. Halliday, P. Brundin, J. Volkmann, A.-E. Schrag, A.E. Lang, Parkinson disease, Nat. Rev. Dis. Primers 3 (2017) 17013. https://doi.org/10.1038/nrdp.2017.13.

[85] P. Seeman, Targeting the dopamine D2 receptor in schizophrenia, Expert Opinion on Therapeutic Targets 10 (2006) 515–531. https://doi.org/10.1517/14728222.10.4.515.

[86] P. Seeman, M. Chau-Wong, J. Tedesco, K. Wong, Brain receptors for antipsychotic drugs and dopamine: direct binding assays, Proceedings of the National Academy of Sciences 72 (1975) 4376–4380. https://doi.org/10.1073/pnas.72.11.4376.

[87] P. Seeman, T. LEE, M. Chau-Wong, K. Wong, Antipsychotic drug doses and neuroleptic/dopamine receptors, Nature 261 (1976) 717–719. https://doi.org/10.1038/261717a0.

[88] D.K. Grandy, M.A. Marchionni, H. Makam, R.E. Stofko, M. Alfano, L. Frothingham, J.B. Fischer, K.J. Burke-Howie, J.R. Bunzow, A.C. Server, Cloning of the cDNA and gene for a human D2 dopamine receptor, Proc. Natl. Acad. Sci. U.S.A. 86 (1989) 9762–9766. https://doi.org/10.1073/pnas.86.24.9762.

[89] J.-M. Beaulieu, S. Espinoza, R.R. Gainetdinov, Dopamine receptors - IUPHAR Review 13, British Journal of Pharmacology 172 (2015) 1–23. https://doi.org/10.1111/bph.12906.

[90] R. Dal Toso, B. Sommer, M. Ewert, A. Herb, D.B. Pritchett, A. Bach, B.D. Shivers, P.H. Seeburg, The dopamine D2 receptor: two molecular forms generated by alternative splicing, The EMBO Journal 8 (1989) 4025–4034. https://doi.org/10.1002/j.1460-2075.1989.tb08585.x.

[91] A. Usiello, J.H. Baik, F. Rougé-Pont, R. Picetti, A. Dierich, M. LeMeur, P.V. Piazza, E. Borrelli, Distinct functions of the two isoforms of dopamine D2 receptors, Nature 408 (2000) 199–203. https://doi.org/10.1038/35041572.

[92] J.-M. Beaulieu, T.D. Sotnikova, S. Marion, R.J. Lefkowitz, R.R. Gainetdinov, M.G. Caron, An Akt/beta-arrestin 2/PP2A signaling complex mediates dopaminergic neurotransmission and behavior, Cell 122 (2005) 261–273. https://doi.org/10.1016/j.cell.2005.05.012.

[93] J.-M. Beaulieu, T.D. Sotnikova, W.-D. Yao, L. Kockeritz, J.R. Woodgett, R.R. Gainetdinov, M.G. Caron, Lithium antagonizes dopamine-dependent behaviors mediated by an AKT/glycogen synthase kinase 3 signaling cascade, Proc. Natl. Acad. Sci. U.S.A. 101 (2004) 5099–5104. https://doi.org/10.1073/pnas.0307921101.

[94] S. Bhagwanth, R.K. Mishra, R.L. Johnson, Development of peptidomimetic ligands of Pro-Leu-Gly-NH(2) as allosteric modulators of the dopamine D(2) receptor, Beilstein J. Org. Chem. 9 (2013) 204–214. https://doi.org/10.3762/bjoc.9.24.

[95] J. Kühhorn, H. Hübner, P. Gmeiner, Bivalent dopamine D2 receptor ligands: synthesis and binding properties, J. Med. Chem. 54 (2011) 4896–4903. https://doi.org/10.1021/jm2004859.

[96] A.B. Shaik, C.A. Boateng, F.O. Battiti, A. Bonifazi, J. Cao, L. Chen, R. Chitsazi, S. Ravi, K.H. Lee, L. Shi, A.H. Newman, Structure Activity Relationships for a Series of Eticlopride-Based Dopamine D2/D3 Receptor Bitopic Ligands, J. Med. Chem. 64 (2021) 15313–15333. https://doi.org/10.1021/acs.jmedchem.1c01353.

[97] B.S. Publishers, Current Medicinal Chemistry, Bentham Science Publishers, 1998.

[98] S. Wang, T. Che, A. Levit, B.K. Shoichet, D. Wacker, B.L. Roth, Structure of the D2 dopamine receptor bound to the atypical antipsychotic drug risperidone, Nature 555 (2018) 269–273. https://doi.org/10.1038/nature25758.

[99] N. Malek, S. Kanavou, M.A. Lawton, V. Pitz, K.A. Grosset, N. Bajaj, R.A. Barker, Y. Ben-Shlomo, D.J. Burn, T. Foltynie, J. Hardy, N.M. Williams, N. Wood, H.R. Morris, D.G. Grosset, L-dopa responsiveness in early Parkinson's disease is associated with the rate of motor progression, Parkinsonism Relat. Disord. 65 (2019) 55–61. https://doi.org/10.1016/j.parkreldis.2019.05.022.

[100] D. Singha, A. Thakur, M.F. Nazar, J. Singh, S. Bhandari, P. Sood, Comparative study of palonosetron with metoclopramide and ondansetron in prevention of PONV in laparoscopic cholecystectomy a randomized controlled trial, Int. J. Med. Anesthesiology 4 (2021) 122–127. https://doi.org/10.33545/26643766.2021.v4.i3b.292.

[101] D.J. Siskind, M. Lee, A. Ravindran, Q. Zhang, E. Ma, B. Motamarri, S. Kisely, Augmentation strategies for clozapine refractory schizophrenia: A systematic review and meta-analysis, Aust. N. Z. J. Psychiatry 52 (2018) 751–767. https://doi.org/10.1177/0004867418772351.

[102] K. Figueroa, N. Shankley, One hundred years of histamine research, Adv. Exp. Med. Biol. 709 (2010) 1–9. https://doi.org/10.1007/978-1-4419-8056-4_1.

[103] J.M. Arrang, M. Garbarg, J.C. Schwartz, Auto-inhibition of brain histamine release mediated by a novel class (H3) of histamine receptor, Nature 302 (1983) 832–837. https://doi.org/10.1038/302832a0.

[104] J.W. BLACK, W.A. Duncan, C.J. DURANT, C.R. GANELLIN, E.M. PARSONS, Definition and antagonism of histamine H 2 -receptors, Nature 236 (1972) 385–390. https://doi.org/10.1038/236385a0.

[105] D.G. Raible, T. Lenahan, Y. Fayvilevich, R. Kosinski, E.S. Schulman, Pharmacologic characterization of a novel histamine receptor on human eosinophils, Am. J. Respir. Crit. Care Med. 149 (1994) 1506–1511. https://doi.org/10.1164/ajrccm.149.6.8004306.

[106] U. Trendelenburg, The action of histamine and 5-hydroxytryptamine on isolated mammalian atria, J Pharmacol Exp Ther 130 (1960) 450–460.

[107] T. Shimamura, M. Shiroishi, S. Weyand, H. Tsujimoto, G. Winter, V. Katritch, R. Abagyan, V. Cherezov, W. Liu, G.W. Han, T. Kobayashi, R.C. Stevens, S. Iwata, Structure of the human histamine H1 receptor complex with doxepin, Nature 475 (2011) 65–70. https://doi.org/10.1038/nature10236.

[108] J.C. Schwartz, H. Pollard, T.T. Quach, Histamine as a neurotransmitter in mammalian brain: neurochemical evidence, J. Neurochem. 35 (1980) 26–33. https://doi.org/10.1111/j.1471-4159.1980.tb12485.x.

[109] T.B. Paiva, M. Tominaga, A.C. Paiva, Ionization of histamine, N-acetylhistamine, and their iodinated derivatives, J. Med. Chem. 13 (1970) 689–692. https://doi.org/10.1021/jm00298a025.

[110] Ganellin, C.R. (1974). Imidazole Tautomerism of Histamine Derivatives. In: Bergmann, E.D., Pullman, B. (eds) Molecular and Quantum Pharmacology. The Jerusalem Symposia on Quantum Chemistry and Biochemistry, vol 7. Springer, Dordrecht. https://doi.org/10.1007/978-94-010-1758-9_4.

[111] D. MacGlashan, Histamine, Journal of Allergy and Clinical Immunology 112 (2003) S53-S59. https://doi.org/10.1016/S0091-6749(03)01877-3.

[112] S.J. Hill, Distribution, properties, and functional characteristics of three classes of histamine receptor, Pharmacological Reviews 42 (1990) 45–83.

[113] I. Hindmarch, Z. Shamsi, Antihistamines: models to assess sedative properties, assessment of sedation, safety and other side-effects, Clin. Exp. Allergy 29 Suppl 3 (1999) 133–142. https://doi.org/10.1046/j.1365-2222.1999.0290s3133.x.

[114] F.E. Simons, The therapeutic index of newer H1-receptor antagonists, Clin. Exp. Allergy 24 (1994) 707–723. https://doi.org/10.1111/j.1365-2222.1994.tb00981.x.

[115] S. BRAUDE, HISTAMINE INCREASES LUNG PERMEABILITY BY AN H2-RECEPTOR MECHANISM, The Lancet 324 (1984) 372–374. https://doi.org/10.1016/S0140-6736(84)90542-7.

[116] R.W. Brimblecombe, W. Duncan, G.J. Durant, J.C. Emmett, C.R. GANELLIN, G.B. Leslie, M.E. Parsons, Characterization and development of cimetidine as a histamine H2-receptor antagonist, Gastroenterology 74 (1978) 339–347. https://doi.org/10.1016/0016-5085(78)90758-8.

[117] J. Del Valle, I. Gantz, Novel insights into histamine H2 receptor biology, Am. J. Physiol. 273 (1997) G987-96. https://doi.org/10.1152/ajpgi.1997.273.5.G987.

[118] R. Ginsburg, M.R. Bristow, E.B. Stinson, D.C. Harrison, Histamine receptors in the human heart, Life Sciences 26 (1980) 2245–2249. https://doi.org/10.1016/0024-3205(80)90209-X.

[119] L.S. Welage, R.R. Berardi, Evaluation of Omeprazole, Lansoprazole, Pantoprazole, and Rabeprazole in the Treatment of Acid-Related Diseases, Journal of the American Pharmaceutical Association 40 (2000) 52–62. https://doi.org/10.1016/S1086-5802(16)31036-1.

[120] R.L. Thurmond, E.W. Gelfand, P.J. Dunford, The role of histamine H1 and H4 receptors in allergic inflammation: the search for new antihistamines, Nat. Rev. Drug Discov. 7 (2008) 41–53. https://doi.org/10.1038/nrd2465.

[121] T.W. Lovenberg, B.L. Roland, S.J. Wilson, X. Jiang, J. Pyati, A. Huvar, M.R. Jackson, M.G. Erlander, Cloning and Functional Expression of the Human Histamine H 3 Receptor, Mol. Pharmacol. 55 (1999) 1101–1107. https://doi.org/10.1124/mol.55.6.1101.

[122] R. Leurs, R.A. Bakker, H. Timmerman, I.J.P. de Esch, The histamine H3 receptor: from gene cloning to H3 receptor drugs, Nat. Rev. Drug Discov. 4 (2005) 107–120. https://doi.org/10.1038/nrd1631.

[123] S. Morisset, A. Rouleau, X. Ligneau, F. Gbahou, J. Tardivel-Lacombe, H. Stark, W. Schunack, C.R. Ganellin, J.C. Schwartz, J.M. Arrang, High constitutive activity of native H3

receptors regulates histamine neurons in brain, Nature 408 (2000) 860–864. https://doi.org/10.1038/35048583.

[124] P.L. Chazot, V. Hann, C. Wilson, G. Lees, C.L. Thompson, Immunological identification of the mammalian H3 histamine receptor in the mouse brain, NeuroReport 12 (2001) 259-262. https://doi.org/10.1097/00001756-200102120-00016.

[125] H. Pollard, J. Moreau, J.M. Arrang, J.C. Schwartz, A detailed autoradiographic mapping of histamine H3 receptors in rat brain areas, Neuroscience 52 (1993) 169–189. https://doi.org/10.1016/0306-4522(93)90191-H.

[126] M.B. Passani, P. Blandina, Histamine receptors in the CNS as targets for therapeutic intervention, Trends Pharmacol. Sci. 32 (2011) 242–249. https://doi.org/10.1016/j.tips.2011.01.003.

[127] G. Drutel, N. Peitsaro, K. Karlstedt, K. Wieland, M.J. Smit, H. Timmerman, P. Panula, R. Leurs, Identification of Rat H 3 Receptor Isoforms with Different Brain Expression and Signaling Properties, Mol. Pharmacol. 59 (2001) 1–8. https://doi.org/10.1124/mol.59.1.1.

[128] R.B. Silver, C.J. Mackins, N.C. Smith, I.L. Koritchneva, K. Lefkowitz, T.W. Lovenberg, R. Levi, Coupling of histamine H3 receptors to neuronal Na+/H+ exchange: a novel protective mechanism in myocardial ischemia, Proceedings of the National Academy of Sciences 98 (2001) 2855–2859. https://doi.org/10.1073/pnas.051599198.

[129] R.B. Silver, K.S. Poonwasi, N. Seyedi, S.J. Wilson, T.W. Lovenberg, R. Levi, Decreased intracellular calcium mediates the histamine H3-receptor-induced attenuation of norepinephrine exocytosis from cardiac sympathetic nerve endings, Proceedings of the National Academy of Sciences 99 (2002) 501–506. https://doi.org/10.1073/pnas.012506099.

[130] A. Molina-Hernández, A. Nuñez, J.-J. Sierra, J.-A. Arias-Montaño, Histamine H3 receptor activation inhibits glutamate release from rat striatal synaptosomes, Neuropharmacology 41 (2001) 928–934. https://doi.org/10.1016/S0028-3908(01)00144-7.

[131] A. Rouleau, X. Ligneau, J. Tardivel-Lacombe, S. Morisset, F. Gbahou, J.-C. Schwartz, J.-M. Arrang, Histamine H3-receptor-mediated 35SGTP gammaS binding: evidence for constitutive activity of the recombinant and native rat and human H3 receptors, British Journal of Pharmacology 135 (2002) 383–392. https://doi.org/10.1038/sj.bjp.0704490.

[132] H. Stark, J.-M. Arrang, X. Ligneau, M. Garbarg, C.R. Ganellin, J.-C. Schwartz, W. Schunack, 6 The Histamine H3 Receptor and its Ligands, Progress in Medicinal Chemistry 38 (2001) 279–308. https://doi.org/10.1016/S0079-6468(08)70096-1.

[133] H. Stark, Recent advances in histamine H 3 /H 4 receptor ligands, Expert Opinion on Therapeutic Patents 13 (2003) 851–865. https://doi.org/10.1517/13543776.13.6.851.

[134] R. Kitbunnadaj, O.P. Zuiderveld, B. Christophe, S. Hulscher, W.M.P.B. Menge, E. Gelens, E. Snip, R.A. Bakker, S. Celanire, M. Gillard, P. Talaga, H. Timmerman, R. Leurs, Identification of 4-(1H-imidazol-4(5)-ylmethyl)pyridine (immethridine) as a novel, potent, and highly selective histamine H(3) receptor agonist, J. Med. Chem. 47 (2004) 2414–2417. https://doi.org/10.1021/jm049932u.

[135] Y.Y. Syed, Pitolisant: First Global Approval, Drugs 76 (2016) 1313–1318. https://doi.org/10.1007/s40265-016-0620-1.

[136] L. Albizu, M. Cottet, M. Kralikova, S. Stoev, R. Seyer, I. Brabet, T. Roux, H. Bazin, E. Bourrier, L. Lamarque, C. Breton, M.-L. Rives, A. Newman, J. Javitch, E. Trinquet, M. Manning, J.-P. Pin, B. Mouillac, T. Durroux, Time-resolved FRET between GPCR ligands reveals oligomers in native tissues, Nat. Chem. Biol. 6 (2010) 587–594. https://doi.org/10.1038/nchembio.396.

[137] R.S. Kasai, A. Kusumi, Single-molecule imaging revealed dynamic GPCR dimerization, Current Opinion in Cell Biology 27 (2014) 78–86. https://doi.org/10.1016/j.ceb.2013.11.008.

[138] G. Milligan, M. Canals, J.D. Pediani, J. Ellis, J.F. Lopez-Gimenez, The role of GPCR dimerisation/oligomerisation in receptor signalling, Ernst Schering Found. Symp. Proc. (2006) 145–161. https://doi.org/10.1007/2789_2006_007.

[139] K. Skieterska, J. Duchou, B. Lintermans, K. van Craenenbroeck, Detection of G protein-coupled receptor (GPCR) dimerization by coimmunoprecipitation, Methods Cell Biol. 117 (2013) 323–340. https://doi.org/10.1016/B978-0-12-408143-7.00017-7.

[140] M.J. Lohse, Dimerization in GPCR mobility and signaling, Curr. Opin. Pharmacol. 10 (2010) 53–58. https://doi.org/10.1016/j.coph.2009.10.007.

[141] M. Filizola, H. Weinstein, Structural models for dimerization of G-protein coupled receptors: the opioid receptor homodimers, Biopolymers 66 (2002) 317–325. https://doi.org/10.1002/bip.10311.

[142] K. Herrick-Davis, Functional significance of serotonin receptor dimerization, Exp Brain Res 230 (2013) 375–386. https://doi.org/10.1007/s00221-013-3622-1.

[143] P. Panula, P.L. Chazot, M. Cowart, R. Gutzmer, R. Leurs, W.L.S. Liu, H. Stark, R.L. Thurmond, H.L. Haas, International Union of Basic and Clinical Pharmacology. XCVIII. Histamine Receptors, Pharmacological Reviews 67 (2015) 601–655. https://doi.org/10.1124/pr.114.010249.

[144] S.P. Lee, B.F. O'Dowd, R.D. Rajaram, T. Nguyen, S.R. George, D2 dopamine receptor homodimerization is mediated by multiple sites of interaction, including an intermolecular interaction involving transmembrane domain 4, Biochemistry 42 (2003) 11023–11031. https://doi.org/10.1021/bi0345539.

[145] C. Ferrada, S. Ferré, V. Casadó, A. Cortés, Z. Justinova, C. Barnes, E.I. Canela, S.R. Goldberg, R. Leurs, C. Lluis, R. Franco, Interactions between histamine H3 and dopamine D2 receptors and the implications for striatal function, Neuropharmacology 55 (2008) 190–197. https://doi.org/10.1016/j.neuropharm.2008.05.008.

[146] H. Hübner, T. Schellhorn, M. Gienger, C. Schaab, J. Kaindl, L. Leeb, T. Clark, D. Möller, P. Gmeiner, Structure-guided development of heterodimer-selective GPCR ligands, Nat Commun 7 (2016) 12298. https://doi.org/10.1038/ncomms12298.

[147] E. Moreno, H. Hoffmann, M. Gonzalez-Sepúlveda, G. Navarro, V. Casadó, A. Cortés, J. Mallol, M. Vignes, P.J. McCormick, E.I. Canela, C. Lluís, R. Moratalla, S. Ferré, J. Ortiz, R. Franco, Dopamine D1-histamine H3 receptor heteromers provide a selective link to MAPK signaling in GABAergic neurons of the direct striatal pathway, Journal of Biological Chemistry 286 (2011) 5846–5854. https://doi.org/10.1074/jbc.M110.161489.

[148] M. Qian, E. Wouters, J.A.R. Dalton, M.D.P. Risseeuw, R.A.J. Crans, C. Stove, J. Giraldo, K. van Craenenbroeck, S. van Calenbergh, Synthesis toward Bivalent Ligands for the Dopamine D2 and Metabotropic Glutamate 5 Receptors, J. Med. Chem. 61 (2018) 8212–8225. https://doi.org/10.1021/acs.jmedchem.8b00671.

[149] G. Milligan, D. Ramsay, G. Pascal, J.J. Carrillo, GPCR dimerisation, Life Sciences 74 (2003) 181–188. https://doi.org/10.1016/j.lfs.2003.09.005.

[150] S.R. George, B.F. O'Dowd, S.P. Lee, G-protein-coupled receptor oligomerization and its potential for drug discovery, Nat. Rev. Drug Discov. 1 (2002) 808–820. https://doi.org/10.1038/nrd913.

[151] G.E. Breitwieser, G protein-coupled receptor oligomerization: implications for G protein activation and cell signaling, Circulation Research 94 (2004) 17–27. https://doi.org/10.1161/01.RES.0000110420.68526.19.

[152] I. Gomes, M.A. Ayoub, W. Fujita, W.C. Jaeger, K.D.G. Pfleger, L.A. Devi, G Protein-Coupled Receptor Heteromers, Annu. Rev. Pharmacol. Toxicol. 56 (2016) 403–425. https://doi.org/10.1146/annurev-pharmtox-011613-135952.

[153] W.C. Jaeger, S.P. Armstrong, S.J. Hill, K.D.G. Pfleger, Biophysical Detection of Diversity and Bias in GPCR Function, Front. Endocrinol. (Lausanne) 5 (2014) 26. https://doi.org/10.3389/fendo.2014.00026.

[154] K.C. Jonas, F. Fanelli, I.T. Huhtaniemi, A.C. Hanyaloglu, Single molecule analysis of functionally asymmetric G protein-coupled receptor (GPCR) oligomers reveals diverse spatial and structural assemblies, Journal of Biological Chemistry 290 (2015) 3875–3892. https://doi.org/10.1074/jbc.M114.622498.

[155] I. Weibrecht, K.-J. Leuchowius, C.-M. Clausson, T. Conze, M. Jarvius, W.M. Howell, M. Kamali-Moghaddam, O. Söderberg, Proximity ligation assays: a recent addition to the proteomics toolbox, Expert Review of Proteomics 7 (2010) 401–409. https://doi.org/10.1586/epr.10.10.

[156] S. Ferré, R. Baler, M. Bouvier, M.G. Caron, L.A. Devi, T. Durroux, K. Fuxe, S.R. George, J.A. Javitch, M.J. Lohse, K. Mackie, G. Milligan, K.D.G. Pfleger, J.-P. Pin, N.D. Volkow, M. Waldhoer, A.S. Woods, R. Franco, Building a new conceptual framework for receptor heteromers, Nat Chem Biol 5 (2009) 131–134. https://doi.org/10.1038/nchembio0309-131.

[157] J. González-Maeso, R.L. Ang, T. Yuen, P. Chan, N.V. Weisstaub, J.F. López-Giménez, M. Zhou, Y. Okawa, L.F. Callado, G. Milligan, J.A. Gingrich, M. Filizola, J.J. Meana, S.C. Sealfon, Identification of a serotonin/glutamate receptor complex implicated in psychosis, Nature 452 (2008) 93–97. https://doi.org/10.1038/nature06612.

[158] R. Rozenfeld, I. Bushlin, I. Gomes, N. Tzavaras, A. Gupta, S. Neves, L. Battini, G.L. Gusella, A. Lachmann, A. Ma'ayan, R.D. Blitzer, L.A. Devi, Receptor heteromerization expands the repertoire of cannabinoid signaling in rodent neurons, PLoS One 7 (2012) e29239. https://doi.org/10.1371/journal.pone.0029239.

[159] K. Bourque, J. Jones-Tabah, D. Devost, P.B.S. Clarke, T.E. Hébert, Exploring functional consequences of GPCR oligomerization requires a different lens, Prog. Mol. Biol. Transl. Sci. 169 (2020) 181–211. https://doi.org/10.1016/bs.pmbts.2019.11.001.

[160] X.-Y. Liu, Z.-C. Liu, Y.-G. Sun, M. Ross, S. Kim, F.-F. Tsai, Q.-F. Li, J. Jeffry, J.-Y. Kim, H.H. Loh, Z.-F. Chen, Unidirectional cross-activation of GRPR by MOR1D uncouples itch and analgesia induced by opioids, Cell 147 (2011) 447–458. https://doi.org/10.1016/j.cell.2011.08.043.

[161] E. Akgün, M.I. Javed, M.M. Lunzer, B.A. Smeester, A.J. Beitz, P.S. Portoghese, Ligands that interact with putative MOR-mGluR5 heteromer in mice with inflammatory pain produce potent antinociception, PNAS 110 (2013) 11595–11599. https://doi.org/10.1073/pnas.1305461110.

[162] I. Bushlin, A. Gupta, S.D. Stockton, L.K. Miller, L.A. Devi, Dimerization with cannabinoid receptors allosterically modulates delta opioid receptor activity during neuropathic pain, PLOS ONE 7 (2012) e49789. https://doi.org/10.1371/journal.pone.0049789.

[163] R. Rozenfeld, A. Gupta, K. Gagnidze, M.P. Lim, I. Gomes, D. Lee-Ramos, N. Nieto, L.A. Devi, AT1R-CB_1R heteromerization reveals a new mechanism for the pathogenic properties of angiotensin II, The EMBO Journal 30 (2011) 2350–2363. https://doi.org/10.1038/emboj.2011.139.

[164] Y. Yuan, C.K. Arnatt, N. El-Hage, S.M. Dever, J.C. Jacob, D.E. Selley, K.F. Hauser, Y. Zhang, A Bivalent Ligand Targeting the Putative Mu Opioid Receptor and Chemokine Receptor CCR5 Heterodimers: Binding Affinity versus Functional Activities, Medchemcomm 4 (2013) 847–851. https://doi.org/10.1039/C3MD00080J.

[165] P.S. Portoghese, From models to molecules: opioid receptor dimers, bivalent ligands, and selective opioid receptor probes, J. Med. Chem. 44 (2001) 2259–2269. https://doi.org/10.1021/jm010158.

[166] P.S. Portoghese, Bivalent ligands and the message-address concept in the design of selective opioid receptor antagonists, Trends Pharmacol. Sci. 10 (1989) 230–235. https://doi.org/10.1016/0165-6147(89)90267-8.

[167] C.A. Lipinski, Lead- and drug-like compounds: the rule-of-five revolution, Drug Discov. Today Technol. 1 (2004) 337–341. https://doi.org/10.1016/j.ddtec.2004.11.007.

[168] B.S. Desai, A.J. Monahan, P.M. Carvey, B. Hendey, Blood-brain barrier pathology in Alzheimer's and Parkinson's disease: implications for drug therapy, Cell Transplant. 16 (2007) 285–299. https://doi.org/10.3727/000000007783464731.

[169] Y. Sun, N. Li, M. Zhang, W. Zhou, J. Yuan, R. Zhao, J. Wu, Z. Li, Y. Zhang, X. Fang, Single-molecule imaging reveals the stoichiometry change of β2-adrenergic receptors by a pharmacological biased ligand, Chem. Commun. (Camb) 52 (2016) 7086–7089. https://doi.org/10.1039/C6CC00628K.

[170] B.E. Snaar-Jagalska, A. Cambi, T. Schmidt, S. de Keijzer, Single-Molecule Imaging Technique to Study the Dynamic Regulation of GPCR Function at the Plasma Membrane, in: Methods in Enzymology, Elsevier, 521 (2013) 47–67. https://doi.org/10.1016/B978-0-12-391862-8.00003-X.

[171] K.N. Fish, Total internal reflection fluorescence (TIRF) microscopy, Curr. Protoc. Cytom. Chapter 12 (2009) Unit12.18. https://doi.org/10.1002/0471142956.cy1218s50.

[172] S.W. Paddock, Principles and Practices of Laser Scanning Confocal Microscopy, MB 16 (2000) 127–150. https://doi.org/10.1385/MB:16:2:127.

[173] J. Robinson, Chapter 4 Principles of confocal microscopy, in: Cytometry, Methods in Cell Biology 63 (2001) 89–106. https://doi.org/10.1016/S0091-679X(01)63008-5.

[174] N.C. Dale, E.K.M. Johnstone, C.W. White, K.D.G. Pfleger, NanoBRET: The Bright Future of Proximity-Based Assays, Front. Bioeng. Biotechnol. 7 (2019) 56. https://doi.org/10.3389/fbioe.2019.00056.

[175] M. Soave, S.J. Briddon, S.J. Hill, L.A. Stoddart, Fluorescent ligands: Bringing light to emerging GPCR paradigms, British Journal of Pharmacology 177 (2020) 978–991. https://doi.org/10.1111/bph.14953.

[176] L.A. Stoddart, L.E. Kilpatrick, S.J. Hill, NanoBRET Approaches to Study Ligand Binding to GPCRs and RTKs, Trends Pharmacol. Sci. 39 (2018) 136–147. https://doi.org/10.1016/j.tips.2017.10.006.

[177] L. Grätz, K. Tropmann, M. Bresinsky, C. Müller, G. Bernhardt, S. Pockes, NanoBRET binding assay for histamine H2 receptor ligands using live recombinant HEK293T cells, Sci. Rep. 10 (2020) 13288. https://doi.org/10.1038/s41598-020-70332-3.

[178] B. Thomas, M.F. Beal, Parkinson's disease, Hum. Mol. Genet. 16 Spec No. 2 (2007) R183-94. https://doi.org/10.1093/hmg/ddm159.

[179] O.-B. Tysnes, A. Storstein, Epidemiology of Parkinson's disease, J Neural Transm 124 (2017) 901–905. https://doi.org/10.1007/s00702-017-1686-y.

[180] L.V. Kalia, A.E. Lang, Parkinson's disease, The Lancet 386 (2015) 896–912. https://doi.org/10.1016/S0140-6736(14)61393-3.

[181] P.A. LeWitt, S. Fahn, Levodopa therapy for Parkinson disease: A look backward and forward, Neurology 86 (2016) S3-12. https://doi.org/10.1212/WNL.0000000000002509.

[182] M.A. Cenci, Presynaptic Mechanisms of l-DOPA-Induced Dyskinesia: The Findings, the Debate, and the Therapeutic Implications, Front. Neurol. 5 (2014) 242. https://doi.org/10.3389/fneur.2014.00242.

[183] W. Poewe, A. Antonini, Novel formulations and modes of delivery of levodopa, Mov. Disord. 30 (2015) 114–120. https://doi.org/10.1002/mds.26078.

[184] T. Müller, Catechol-O-methyltransferase inhibitors in Parkinson's disease, Drugs 75 (2015) 157–174. https://doi.org/10.1007/s40265-014-0343-0.

[185] J.J. Ferreira, A. Lees, J.-F. Rocha, W. Poewe, O. Rascol, P. Soares-da-Silva, Opicapone as an adjunct to levodopa in patients with Parkinson's disease and end-of-dose motor fluctuations: a randomised, double-blind, controlled trial, The Lancet Neurology 15 (2016) 154–165. https://doi.org/10.1016/S1474-4422(15)00336-1.

[186] S.H. Fox, R. Katzenschlager, S.-Y. Lim, B. Ravina, K. Seppi, M. Coelho, W. Poewe, O. Rascol, C.G. Goetz, C. Sampaio, The Movement Disorder Society Evidence-Based Medicine Review Update: Treatments for the motor symptoms of Parkinson's disease, Movement Disorders 26 Suppl 3 (2011) S2-41. https://doi.org/10.1002/mds.23829.

[187] A.H.V. Schapira, Monoamine oxidase B inhibitors for the treatment of Parkinson's disease: a review of symptomatic and potential disease-modifying effects, CNS Drugs 25 (2011) 1061–1071. https://doi.org/10.2165/11596310-000000000-00000.

[188] I. Zahoor, A. Shafi, E. Haq, Parkinson's disease: Pathogenesis and clinical aspects, Codon Publications, Brisbane, Australia, 2018. https://doi.org/10.15586/codonpublications.parkinsonsdisease.2018.ch7.

[189] J. Jankovic, W. Poewe, Therapies in Parkinson's disease, Current Opinion in Neurology 25 (2012) 433–447. https://doi.org/10.1097/WCO.0b013e3283542fc2.

[190] D. Vilas, C. Pont-Sunyer, E. Tolosa, Impulse control disorders in Parkinson's disease, Parkinsonism & Related Disorders 18 (2012) S80-S84. https://doi.org/10.1016/s1353-8020(11)70026-8.

[191] L.V. Kalia, J.M. Brotchie, S.H. Fox, Novel nondopaminergic targets for motor features of Parkinson's disease: review of recent trials, Movement Disorders 28 (2013) 131–144. https://doi.org/10.1002/mds.25273.

[192] S. Perez-Lloret, M.V. Rey, A. Pavy-Le Traon, O. Rascol, Emerging drugs for autonomic dysfunction in Parkinson's disease, Expert Opin. Emerg. Drugs 18 (2013) 39–53. https://doi.org/10.1517/14728214.2013.766168.

[193] K. Seppi, D. Weintraub, M. Coelho, S. Perez-Lloret, S.H. Fox, R. Katzenschlager, E.-M. Hametner, W. Poewe, O. Rascol, C.G. Goetz, C. Sampaio, The Movement Disorder Society Evidence-Based Medicine Review Update: Treatments for the non-motor symptoms of Parkinson's disease, Movement Disorders 26 Suppl 3 (2011) S42-80. https://doi.org/10.1002/mds.23884.

[194] E.R. Dorsey, R. Constantinescu, J.P. Thompson, K.M. Biglan, R.G. Holloway, K. Kieburtz, F.J. Marshall, B.M. Ravina, G. Schifitto, A. Siderowf, C.M. Tanner, Projected number of people with Parkinson disease in the most populous nations, 2005 through 2030, Neurology 68 (2007) 384–386. https://doi.org/10.1212/01.wnl.0000247740.47667.03.

[195] S. Vangveravong, M. Taylor, J. Xu, J. Cui, W. Calvin, S. Babic, R.R. Luedtke, R.H. Mach, Synthesis and characterization of selective dopamine D2 receptor antagonists. 2. Azaindole, benzofuran, and benzothiophene analogs of L-741,626, Bioorg. Med. Chem. 18 (2010) 5291–5300. https://doi.org/10.1016/j.bmc.2010.05.052.

[196] J. Kühhorn, A. Götz, H. Hübner, D. Thompson, J. Whistler, P. Gmeiner, Development of a bivalent dopamine D_2 receptor agonist, J. Med. Chem. 54 (2011) 7911–7919. https://doi.org/10.1021/jm2009919.

[197] D. Im, A. Inoue, T. Fujiwara, T. Nakane, Y. Yamanaka, T. Uemura, C. Mori, Y. Shiimura, K.T. Kimura, H. Asada, N. Nomura, T. Tanaka, A. Yamashita, E. Nango, K. Tono, F.M.N. Kadji, J. Aoki, S. Iwata, T. Shimamura, Structure of the dopamine D2 receptor in complex with the antipsychotic drug spiperone, Nat Commun 11 (2020) 6442. https://doi.org/10.1038/s41467-020-20221-0.

[198] T. Nakamura, H. Kakinuma, H. Umemiya, H. Amada, N. Miyata, K. Taniguchi, K. Bando, M. Sato, Imidazole derivatives as new potent and selective 20-HETE synthase inhibitors, Bioorganic and Medicinal Chemistry Letters 14 (2004) 333-336. https://doi.org/10.1016/j.bmcl.2003.11.005.

[199] A.J. Barbier, C. Berridge, C. Dugovic, A.D. Laposky, S.J. Wilson, J. Boggs, L. Aluisio, B. Lord, C. Mazur, C.M. Pudiak, X. Langlois, W. Xiao, R. Apodaca, N.I. Carruthers, T.W. Lovenberg, Acute wake-promoting actions of JNJ-5207852, a novel, diamine-based H3 antagonist, British Journal of Pharmacology 143 (2004) 649–661. https://doi.org/10.1038/sj.bjp.0705964.

[200] N. Rosier, L. Grätz, H. Schihada, J. Möller, A. Işbilir, L.J. Humphrys, M. Nagl, U. Seibel, M.J. Lohse, S. Pockes, A Versatile Sub-Nanomolar Fluorescent Ligand Enables NanoBRET Binding Studies and Single-Molecule Microscopy at the Histamine H3 Receptor, J. Med. Chem. 64 (2021) 11695–11708. https://doi.org/10.1021/acs.jmedchem.1c01089.

[201] Z. Zhang, J.C. Pickens, W.G.J. Hol, E. Fan, Solution- and solid-phase syntheses of guanidine-bridged, water-soluble linkers for multivalent ligand design, Org. Lett. 6 (2004) 1377–1380. https://doi.org/10.1021/ol049835v.

[202] H. Hübner, T. Schellhorn, M. Gienger, C. Schaab, J. Kaindl, L. Leeb, T. Clark, D. Möller, P. Gmeiner, Structure-guided development of heterodimer-selective GPCR ligands, Nat Commun 7 (2016) 12298. https://doi.org/10.1038/ncomms12298.

[203] D. Pulido, V. Casadó-Anguera, L. Pérez-Benito, E. Moreno, A. Cordomí, L. López, A. Cortés, S. Ferré, L. Pardo, V. Casadó, M. Royo, Design of a True Bivalent Ligand with Picomolar Binding Affinity for a G Protein-Coupled Receptor Homodimer, J. Med. Chem. 61 (2018) 9335–9346. https://doi.org/10.1021/acs.jmedchem.8b01249.

[204] M.M. Sakyiamah, W. Nomura, T. Kobayakawa, H. Tamamura, Development of a NanoBRET-Based Sensitive Screening Method for CXCR4 Ligands, Bioconjug. Chem. 30 (2019) 1442–1450. https://doi.org/10.1021/acs.bioconjchem.9b00182.

[205] T. Laasfeld, R. Ehrminger, M.-J. Tahk, S. Veiksina, K.R. Kõlvart, M. Min, S. Kopanchuk, A. Rinken, Budded baculoviruses as a receptor display system to quantify ligand binding with TIRF microscopy, Nanoscale 13 (2021) 2436–2447. https://doi.org/10.1039/D0NR06737G.

[206] S. Rüttinger, B. Lamarre, A.E. Knight, Single molecule genotyping by TIRF microscopy, J Fluoresc 18 (2008) 1021–1026. https://doi.org/10.1007/s10895-008-0386-2.

[207] S. Gupta, L.J. Friedman, J. Gelles, S.P. Bell, A helicase-tethered ORC flip enables bidirectional helicase loading, Elife 10 (2021). https://doi.org/10.7554/eLife.74282.

[208] M. Hirsch, R. Wareham, J.W. Yoon, D.J. Rolfe, L.C. Zanetti-Domingues, M.P. Hobson, P.J. Parker, M.L. Martin-Fernandez, S.S. Singh, A global sampler of single particle tracking

solutions for single molecule microscopy, PLOS ONE 14 (2019) e0221865. https://doi.org/10.1371/journal.pone.0221865.

[209] A. Soriano, R. Ventura, A. Molero, R. Hoen, V. Casadó, A. Cortés, F. Fanelli, F. Albericio, C. Lluís, R. Franco, M. Royo, Adenosine A2A receptor-antagonist/dopamine D2 receptor-agonist bivalent ligands as pharmacological tools to detect A2A-D2 receptor heteromers, J. Med. Chem. 52 (2009) 5590–5602. https://doi.org/10.1021/jm900298c.

[210] N. Tschammer, M. Dörfler, H. Hübner, P. Gmeiner, Engineering a GPCR-ligand pair that simulates the activation of D(2L) by Dopamine, ACS Chem. Neurosci. 1 (2010) 25–35. https://doi.org/10.1021/cn900001b.

[211] R. Apodaca, C.A. Dvorak, W. Xiao, A.J. Barbier, J.D. Boggs, S.J. Wilson, T.W. Lovenberg, N.I. Carruthers, A new class of diamine-based human histamine H3 receptor antagonists: 4-(aminoalkoxy)benzylamines, J. Med. Chem. 46 (2003) 3938–3944. https://doi.org/10.1021/jm030185v.

[212] S.A. Yakukhnov, V.P. Ananikov, Catalytic Transfer Hydrodebenzylation with Low Palladium Loading, Adv. Synth. Catal. 361 (2019) 4781–4789. https://doi.org/10.1002/adsc.201900686.

[213] D. Im Cho, M. Zheng, K.-M. Kim, Current perspectives on the selective regulation of dopamine D_2 and D_3 receptors, Arch. Pharm. Res. 33 (2010) 1521–1538. https://doi.org/10.1007/s12272-010-1005-8.

[214] Y. Han, I.S. Moreira, E. Urizar, H. Weinstein, J.A. Javitch, Allosteric communication between protomers of dopamine class A GPCR dimers modulates activation, Nat Chem Biol 5 (2009) 688–695. https://doi.org/10.1038/nchembio.199.

[215] A.J. Rico, I.G. Dopeso-Reyes, E. Martínez-Pinilla, D. Sucunza, D. Pignataro, E. Roda, D. Marín-Ramos, J.L. Labandeira-García, S.R. George, R. Franco, J.L. Lanciego, Neurochemical evidence supporting dopamine D1-D2 receptor heteromers in the striatum of the long-tailed macaque: changes following dopaminergic manipulation, Brain Struct Funct 222 (2017) 1767–1784. https://doi.org/10.1007/s00429-016-1306-x.

[216] H. Schihada, R. Shekhani, G. Schulte, Quantitative assessment of constitutive G protein-coupled receptor activity with BRET-based G protein biosensors, Sci. Signal. 14 (2021) eabf1653. https://doi.org/10.1126/scisignal.abf1653.

[217] M. Keller, D. Erdmann, N. Pop, N. Pluym, S. Teng, G. Bernhardt, A. Buschauer, Red-fluorescent argininamide-type NPY Y1 receptor antagonists as pharmacological tools, Bioorg. Med. Chem. 19 (2011) 2859–2878. https://doi.org/10.1016/j.bmc.2011.03.045.

[218] A. Allikalt, N. Purkayastha, K. Flad, M.F. Schmidt, A. Tabor, P. Gmeiner, H. Hübner, D. Weikert, Fluorescent ligands for dopamine D2/D3 receptors, Sci Rep 10 (2020) 21842. https://doi.org/10.1038/s41598-020-78827-9.

[219] M. Bouzo-Lorenzo, L.A. Stoddart, L. Xia, A.P. IJzerman, L.H. Heitman, S.J. Briddon, S.J. Hill, A live cell NanoBRET binding assay allows the study of ligand-binding kinetics to the adenosine A3 receptor, Purinergic Signal. 15 (2019) 139–153. https://doi.org/10.1007/s11302-019-09650-9.

[220] L.A. Stoddart, A.J. Vernall, M. Bouzo-Lorenzo, R. Bosma, A.J. Kooistra, C. de Graaf, H.F. Vischer, R. Leurs, S.J. Briddon, B. Kellam, S.J. Hill, Development of novel fluorescent histamine H1-receptor antagonists to study ligand-binding kinetics in living cells, Sci Rep 8 (2018) 1572. https://doi.org/10.1038/s41598-018-19714-2.

[221] J. Mierau, F.J. Schneider, H.A. Ensinger, C.L. Chio, M.E. Lajiness, R.M. Huff, Pramipexole binding and activation of cloned and expressed dopamine D2, D3 and D4 receptors, European Journal of Pharmacology: Molecular Pharmacology 290 (1995) 29–36. https://doi.org/10.1016/0922-4106(95)90013-6.

[222] F. Sautel, N. Griffon, D. Lévesque, C. Pilon, J.C. Schwartz, P. Sokoloff, A functional test identifies dopamine agonists selective for D3 versus D2 receptors, NeuroReport 6 (1995) 329–332. https://doi.org/10.1097/00001756-199501000-00026.

[223] R.G. MacKenzie, D. VanLeeuwen, T.A. Pugsley, Y.-H. Shih, S. Demattos, L. Tang, R.D. Todd, K.L. O'Malley, Characterization of the human dopamine D3 receptor expressed in transfected cell lines, European Journal of Pharmacology: Molecular Pharmacology 266 (1994) 79–85. https://doi.org/10.1016/0922-4106(94)90212-7.

[224] K. Burris, Lack of Discrimination by Agonists for D2 and D3 Dopamine Receptors, Neuropsychopharmacology 12 (1995) 335–345. https://doi.org/10.1016/0893-133X(94)00099-L.

[225] M.J. Millan, J.L. Peglion, J. Vian, J.M. Rivet, M. Brocco, A. Gobert, A. Newman-Tancredi, C. Dacquet, K. Bervoets, S. Girardon, Functional correlates of dopamine D3 receptor activation in the rat in vivo and their modulation by the selective antagonist, (+)-S 14297: 1. Activation of postsynaptic D3 receptors mediates hypothermia, whereas blockade of

D2 receptors elicits prolactin secretion and catalepsy, J Pharmacol Exp Ther 275 (1995) 885–898.

[226] S.B. Freedman, S. Patel, R. Marwood, F. Emms, G.R. Seabrook, M.R. Knowles, G. McAllister, Expression and pharmacological characterization of the human D3 dopamine receptor, J Pharmacol Exp Ther 268 (1994) 417–426.

[227] F. Sautel, N. Griffon, D. Lévesque, C. Pilon, J.C. Schwartz, P. Sokoloff, A functional test identifies dopamine agonists selective for D3 versus D2 receptors, Neuroreport: A Journal of Rapid Communication of Research in Neuroscience 6 (1995) 329-332. https://10.1097/00001756-199501000-00026.

[228] M. Tice, T. Hashemi, L.A. Taylor, R.A. Duffy, R.D. McQuade, Characterization of the binding of SCH 39166 to the five cloned dopamine receptor subtypes, Pharmacology Biochemistry and Behavior 49 (1994) 567–571. https://doi.org/10.1016/0091-3057(94)90070-1.

[229] E.D. Cox, H. Diaz-Arauzo, Q. Huang, M.S. Reddy, C. Ma, B. Harris, R. McKernan, P. Skolnick, J.M. Cook, Synthesis and evaluation of analogues of the partial agonist 6-(propyloxy)-4-(methoxymethyl)-beta-carboline-3-carboxylic acid ethyl ester (6-PBC) and the full agonist 6-(benzyloxy)-4-(methoxymethyl)-beta-carboline-3-carboxylic acid ethyl ester (Zk 93423) at wild type and recombinant GABAA receptors, J. Med. Chem. 41 (1998) 2537–2552. https://doi.org/10.1021/jm970460b.

[230] N. Mahindroo, C.-F. Huang, Y.-H. Peng, C.-C. Wang, C.-C. Liao, T.-W. Lien, S.K. Chittimalla, W.-J. Huang, C.-H. Chai, E. Prakash, C.-P. Chen, T.-A. Hsu, C.-H. Peng, I.-L. Lu, L.-H. Lee, Y.-W. Chang, W.-C. Chen, Y.-C. Chou, C.-T. Chen, C.M.V. Goparaju, Y.-S. Chen, S.-J. Lan, M.-C. Yu, X. Chen, Y.-S. Chao, S.-Y. Wu, H.-P. Hsieh, Novel indole-based peroxisome proliferator-activated receptor agonists: design, SAR, structural biology, and biological activities, J. Med. Chem. 48 (2005) 8194–8208. https://doi.org/10.1021/jm0506930.

[231] G.N. Karageorge, J.E. Macor, Synthesis of dihydropyrano[3,2-e]indoles as rotationally restricted phenolic analogs of 5-hydroxyindole—thermal Claisen approach versus gold catalysis, Tetrahedron Letters 52 (2011) 1011–1013. https://doi.org/10.1016/j.tetlet.2010.12.084.

[232] S. Vangveravong, E. McElveen, M. Taylor, J. Xu, Z. Tu, R.R. Luedtke, R.H. Mach, Synthesis and characterization of selective dopamine D2 receptor antagonists, Bioorg. Med. Chem. 14 (2006) 815–825. https://doi.org/10.1016/j.bmc.2005.09.008.

[233] R. Tietze, C. Hocke, S. Löber, H. Hübner, T. Kuwert, P. Gmeiner, O. Prante, Syntheses and radiofluorination of two derivatives of 5-cyano-indole as selective ligands for the dopamine subtype-4 receptor, J Label Compd Radiopharm 49 (2006) 55–70. https://doi.org/10.1002/jlcr.1026.

[234] S.W. Reilly, S. Griffin, M. Taylor, K. Sahlholm, C.-C. Weng, K. Xu, D.A. Jacome, R.R. Luedtke, R.H. Mach, Highly Selective Dopamine D3 Receptor Antagonists with Arylated Diazaspiro Alkane Cores, J. Med. Chem. 60 (2017) 9905–9910. https://doi.org/10.1021/acs.jmedchem.7b01248.

[235] A. Hackling, R. Ghosh, S. Perachon, A. Mann, H.-D. Höltje, C.G. Wermuth, J.-C. Schwartz, W. Sippl, P. Sokoloff, H. Stark, N-(omega-(4-(2-methoxyphenyl)piperazin-1-yl)alkyl)carboxamides as dopamine D2 and D3 receptor ligands, J. Med. Chem. 46 (2003) 3883–3899. https://doi.org/10.1021/jm030836n.

[236] W. Kemnitzer, J. Drewe, S. Jiang, H. Zhang, Y. Wang, J. Zhao, S. Jia, J. Herich, D. Labreque, R. Storer, K. Meerovitch, D. Bouffard, R. Rej, R. Denis, C. Blais, S. Lamothe, G. Attardo, H. Gourdeau, B. Tseng, S. Kasibhatla, S.X. Cai, Discovery of 4-aryl-4H-chromenes as a new series of apoptosis inducers using a cell- and caspase-based high-throughput screening assay. 1. Structure-activity relationships of the 4-aryl group, J. Med. Chem. 47 (2004) 6299–6310. https://doi.org/10.1021/jm049640t.

[237] S. Löber, P. Rodriguez-Loaiza, P. Gmeiner, Click linker: efficient and high-yielding synthesis of a new family of SPOS resins by 1,3-dipolar cycloaddition, Org. Lett. 5 (2003) 1753–1755. https://doi.org/10.1021/ol034520l.

[238] J.R. Boissier, R. Ratouis, C. Dumont, Synthesis and pharmacological study of new piperazine derivatives. I. benzylpiperazines, J. Med. Chem. 6 (1963) 541–544. https://doi.org/10.1021/jm00341a016.

[239] A. Pandey, D.L. Volkots, J.M. Seroogy, J.W. Rose, J.-C. Yu, J.L. Lambing, A. Hutchaleelaha, S.J. Hollenbach, K. Abe, N.A. Giese, R.M. Scarborough, Identification of orally active, potent, and selective 4-piperazinylquinazolines as antagonists of the platelet-derived growth factor receptor tyrosine kinase family, J. Med. Chem. 45 (2002) 3772–3793. https://doi.org/10.1021/jm020143r.

[240] Q.-Z. Zheng, X.-M. Zhang, Y. Xu, K. Cheng, Q.-C. Jiao, H.-L. Zhu, Synthesis, biological evaluation, and molecular docking studies of 2-chloropyridine derivatives possessing 1,3,4-oxadiazole moiety as potential antitumor agents, Bioorg. Med. Chem. 18 (2010) 7836–7841. https://doi.org/10.1016/j.bmc.2010.09.051.

[241] H. Wang, Y. Mao, J. Qin, H. He, G. Liu, B. Gao, A New and Practical Synthesis of 7-(3-Chloropropoxy)-6-methoxy-4-oxo-1,4-dihydroquinoline-3-carbonitrile, Heterocycles 89 (2014) 1885. https://doi.org/10.3987/COM-14-13023.

[242] Y. Qu, H. Wen, R. Ge, Y. Xu, H. Gao, X. Shi, J. Wang, W. Cui, W. Su, H. Yang, L. Kuai, A.L. Satz, X. Peng, Copper-Mediated DNA-Compatible One-Pot Click Reactions of Alkynes with Aryl Borates and TMS-N3, Org. Lett. 22 (2020) 4146–4150. https://doi.org/10.1021/acs.orglett.0c01219.

[243] P. Khare, R.C. Gupta, NMR study of 3,4-dimethoxy benzoic acid, Journal of Molecular Structure 70 (1981) 213–217. https://doi.org/10.1016/0022-2860(81)80108-1.

[244] K. Wingen, J.S. Schwed, K. Isensee, L. Weizel, A. Zivković, D. Odadzic, D. Odazic, H. Stark, Benzylpiperidine variations on histamine H3 receptor ligands for improved drug-likeness, Bioorganic and Medicinal Chemistry Letters 24 (2014) 2236-2239. https://doi.org/10.1016/j.bmcl.2014.03.098.

[245] T. Mase, I.N. Houpis, A. Akao, I. Dorziotis, K. Emerson, T. Hoang, T. Iida, T. Itoh, K. Kamei, S. Kato, Y. Kato, M. Kawasaki, F. Lang, J. Lee, J. Lynch, P. Maligres, A. Molina, T. Nemoto, S. Okada, R. Reamer, J.Z. Song, D. Tschaen, T. Wada, D. Zewge, R.P. Volante, P.J. Reider, K. Tomimoto, Synthesis of a muscarinic receptor antagonist via a diastereoselective Michael reaction, selective deoxyfluorination and aromatic metal-halogen exchange reaction, J. Org. Chem. 66 (2001) 6775–6786. https://doi.org/10.1021/jo0157425.

[246] L. Finelli, M. Fiorini, V. Siracusa, N. Lotti, A. Munari, Synthesis and characterization of poly(ethylene isophthalate-co-ethylene terephthalate) copolyesters, J. Appl. Polym. Sci. 92 (2004) 186–193. https://doi.org/10.1002/app.13430.

[247] M.H. Chen, J.G. Davidson, J.T. Freisler, E. Iakovleva, J. Magano, AN EFFICIENT AND SCALABLE SYNTHESIS OF METHYL 3-HYDROXYMETHYLBENZOATE, Organic Preparations and Procedures International 32 (2000) 381–384. https://doi.org/10.1080/00304940009355940.

[248] F. Vögtle, T. Dünnwald, M. Händel, R. Jäger, S. Meier, G. Harder, A [3]Rotaxane of the Amide Type, Chem. Eur. J. 2 (1996) 640–643. https://doi.org/10.1002/chem.19960020607.

[249] J. Gravier, R. Schneider, C. Frochot, T. Bastogne, F. Schmitt, J. Didelon, F. Guillemin, M. Barberi-Heyob, Improvement of meta-tetra(hydroxyphenyl)chlorin-like photosensitizer selectivity with folate-based targeted delivery. synthesis and in vivo delivery studies, J. Med. Chem. 51 (2008) 3867–3877. https://doi.org/10.1021/jm800125a.

[250] T.L. Schmidt, C.K. Nandi, G. Rasched, P.P. Parui, B. Brutschy, M. Famulok, A. Heckel, Polyamide struts for DNA architectures, Angew. Chem. Int. Ed Engl. 46 (2007) 4382–4384. https://doi.org/10.1002/anie.200700469.

[251] Y.-J. Zhang, X.-P. He, C. Li, Z. Li, D.-T. Shi, L.-X. Gao, B.-Y. Qiu, X.-X. Shi, Y. Tang, J. Li, G.-R. Chen, Triazole-linked Benzylated Glucosyl, Galactosyl, and Mannosyl Monomers and Dimers as Novel Sugar Scaffold-based PTP1B Inhibitors, Chem. Lett. 39 (2010) 1261–1263. https://doi.org/10.1246/cl.2010.1261.

[252] G. Amiet, H.M. Hügel, F. Nurlawis, The Synthesis of the Kynurenamines K1 and K2, Metabolites of Melatonin, Synlett 2002 (2002) 495–497. https://doi.org/10.1055/s-2002-20476.

[253] I.L. Karle, A. Pramanik, A. Banerjee, S. Bhattacharjya, P. Balaram, ω-Amino Acids in Peptide Design. Crystal Structures and Solution Conformations of Peptide Helices Containing a β-Alanyl-γ-Aminobutyryl Segment, J. Am. Chem. Soc. 119 (1997) 9087–9095. https://doi.org/10.1021/ja970566w.

[254] A. Merz, O. Schneider, L. Parkanyi, Side-Arm Participation in a Four-Component Template Synthesis of a[30]Crown-10 Derivative, Angew. Chem. Int. Ed. Engl. 35 (1996) 2369–2372. https://doi.org/10.1002/anie.199623691.

[255] A.W. Schwabacher, J.W. Lane, M.W. Schiesher, K.M. Leigh, C.W. Johnson, Desymmetrization Reactions: Efficient Preparation of Unsymmetrically Substituted Linker Molecules, J. Org. Chem. 63 (1998) 1727–1729. https://doi.org/10.1021/jo971802o.

[256] J. Bitta, S. Kubik, Cyclic hexapeptides with free carboxylate groups as new receptors for monosaccharides, Org. Lett. 3 (2001) 2637–2640. https://doi.org/10.1021/ol016158l.

[257] L. Forster, L. Grätz, D. Mönnich, G. Bernhardt, S. Pockes, A Split Luciferase Complementation Assay for the Quantification of β-Arrestin2 Recruitment to Dopamine D2-Like Receptors, Int. J. Mol. Sci. 21 (2020). https://doi.org/10.3390/ijms21176103.

[258] C. Yung-Chi, W.H. Prusoff, Relationship between the inhibition constant (KI) and the concentration of inhibitor which causes 50 per cent inhibition (I50) of an enzymatic reaction, Biochemical Pharmacology 22 (1973) 3099–3108. https://doi.org/10.1016/0006-2952(73)90196-2.

[259] S. Pockes, D. Wifling, M. Keller, A. Buschauer, S. Elz, Highly Potent, Stable, and Selective Dimeric Hetarylpropylguanidine-Type Histamine H2 Receptor Agonists, ACS Omega 3 (2018) 2865–2882. https://doi.org/10.1021/acsomega.8b00128.

[260] E. Bartole, L. Grätz, T. Littmann, D. Wifling, U. Seibel, A. Buschauer, G. Bernhardt, UR-DEBa242: A Py-5-Labeled Fluorescent Multipurpose Probe for Investigations on the Histamine H3 and H4 Receptors, J. Med. Chem. 63 (2020) 5297–5311. https://doi.org/10.1021/acs.jmedchem.0c00160.

[261] G. Navarro, J. Hradsky, C. Lluís, V. Casadó, P.J. McCormick, M.R. Kreutz, M. Mikhaylova, NCS-1 associates with adenosine A(2A) receptors and modulates receptor function, Front. Mol. Neurosci. 5 (2012) 53. https://doi.org/10.3389/fnmol.2012.00053.

Chapter 9: Appendix

9. Appendix

^{1}H and ^{13}C-NMR spectra of compounds **6a**, **6b**, **11a**, **25c**, **38** and **65-95**

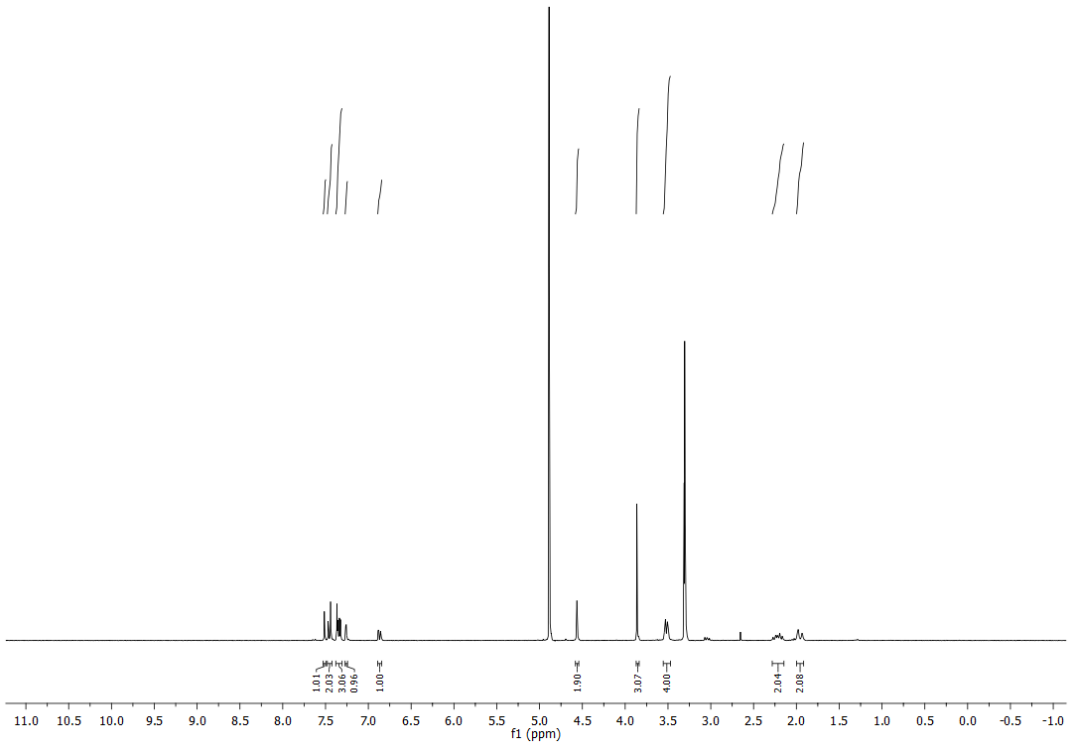

Figure 9.1: ^{1}H-NMR spectrum (300 MHz, CD_3OD) of compound **6a**.

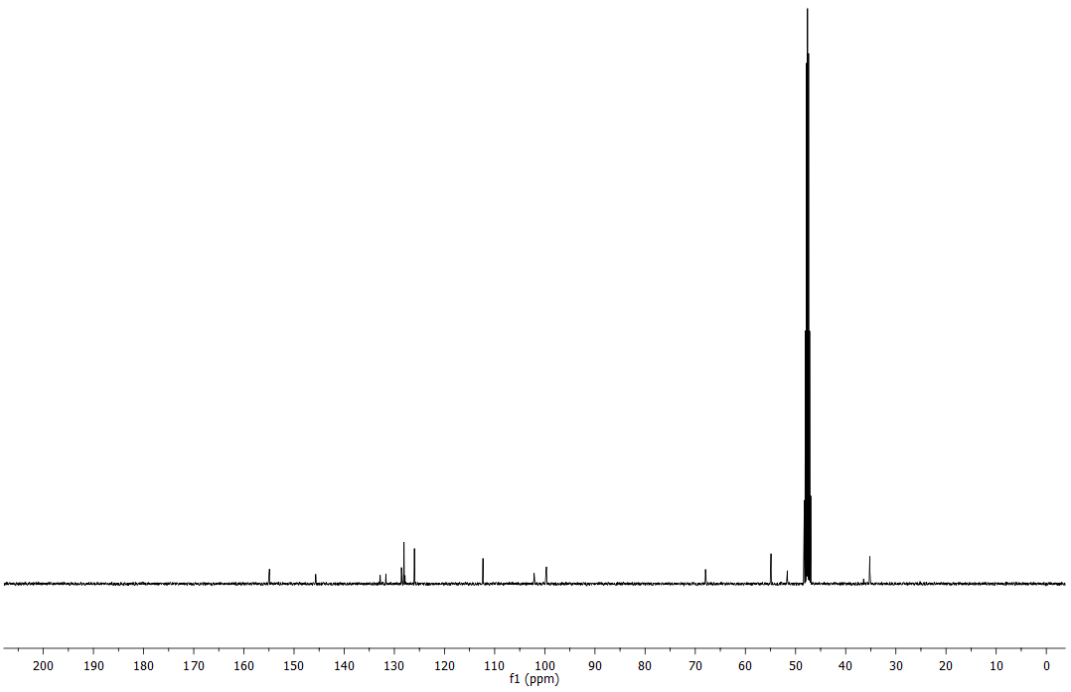

Figure 9.2: ^{13}C-NMR spectrum (101 MHz, CD_3OD) of compound **6a**.

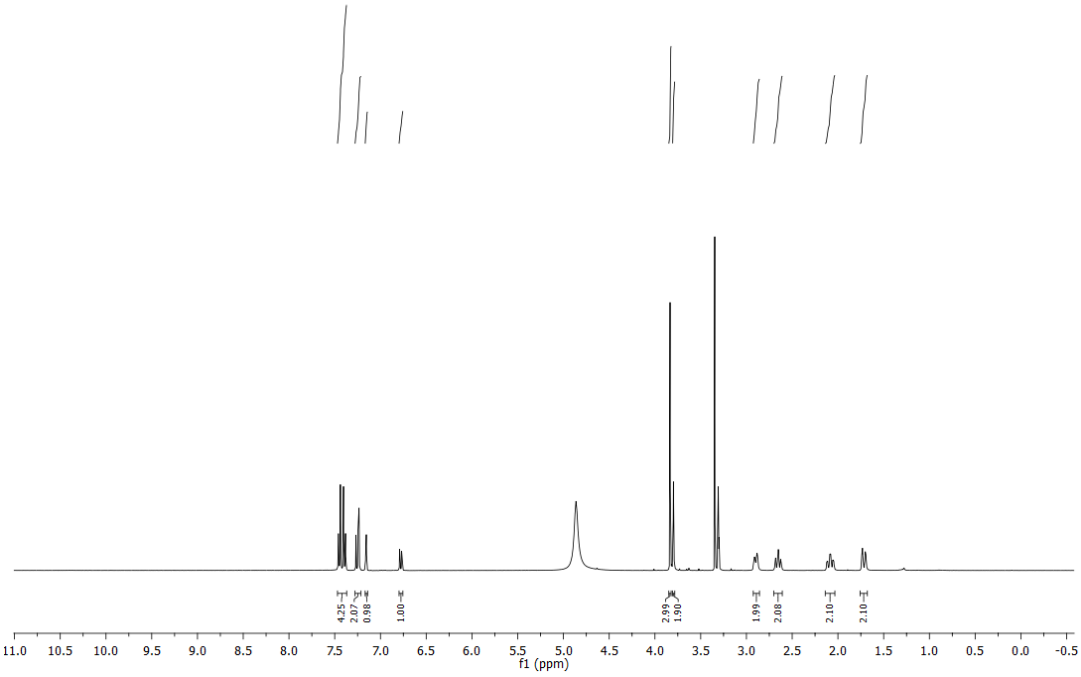

Figure 9.3: ^{1}H-NMR spectrum (400 MHz, CD_3OD) of compound **6b**.

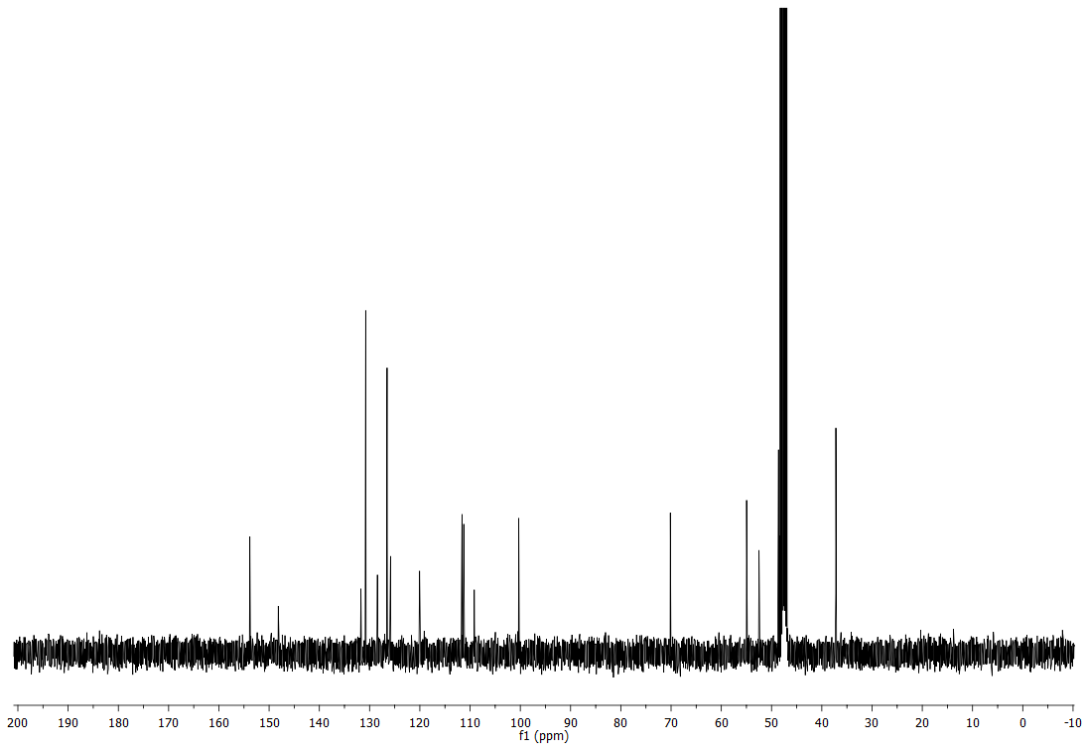

Figure 9.4: ^{13}C-NMR spectrum (101 MHz, CD_3OD) of compound **6b**.

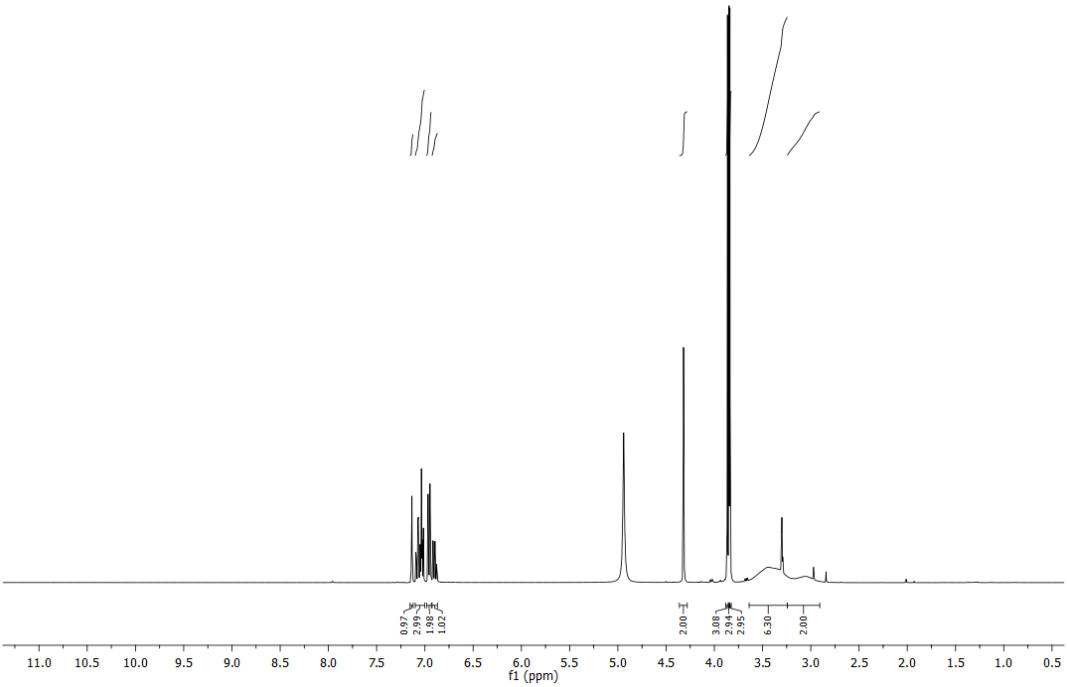

Figure 9.5: ^{1}H-NMR spectrum (400 MHz, CD_3OD) of compound **11a**.

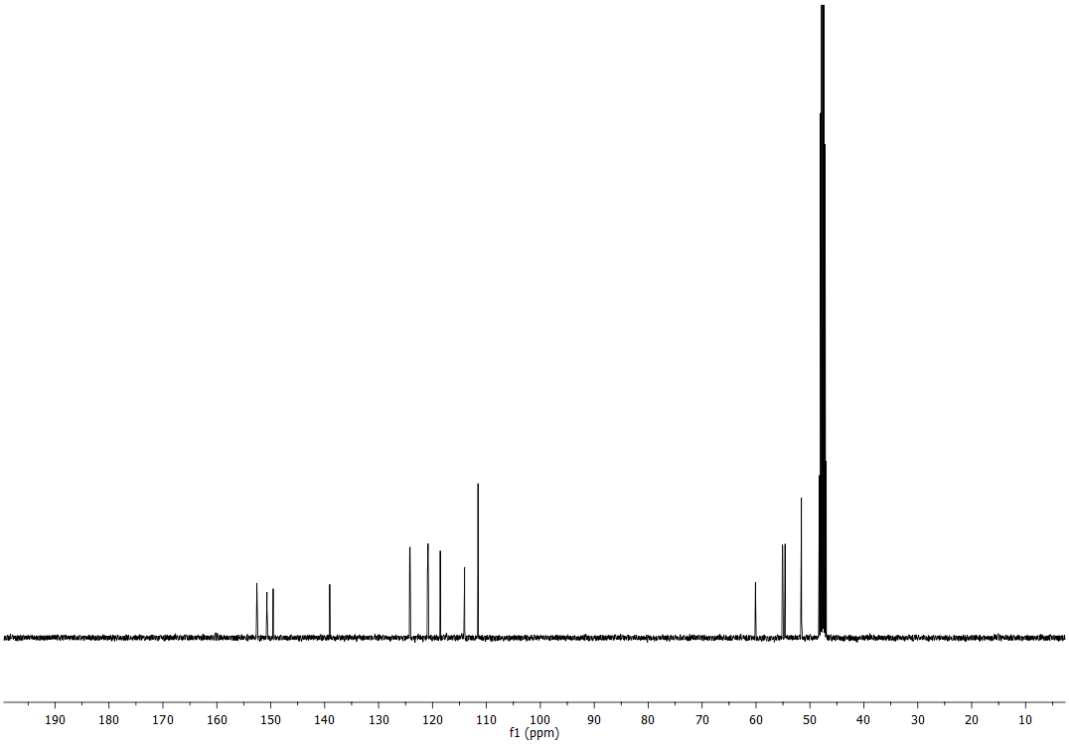

Figure 9.6: ^{13}C-NMR spectrum (101 MHz, CD_3OD) of compound **11a**.

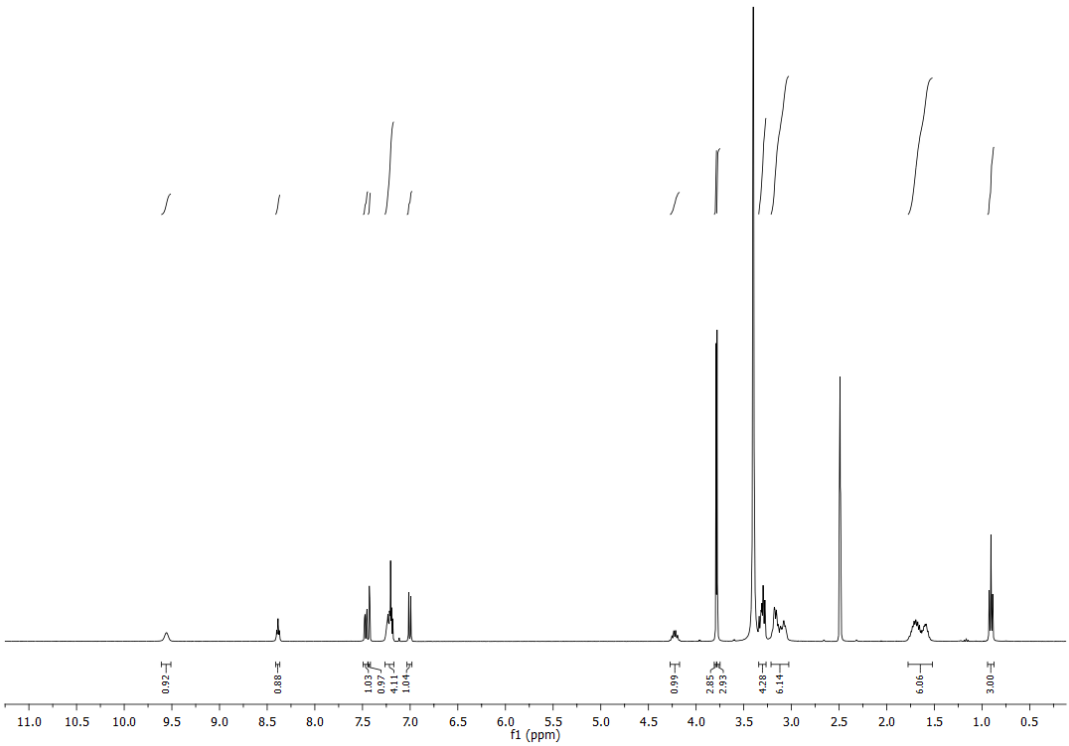

Figure 9.7: ^{1}H-NMR spectrum (400 MHz, DMSO-d_6) of compound **25c**.

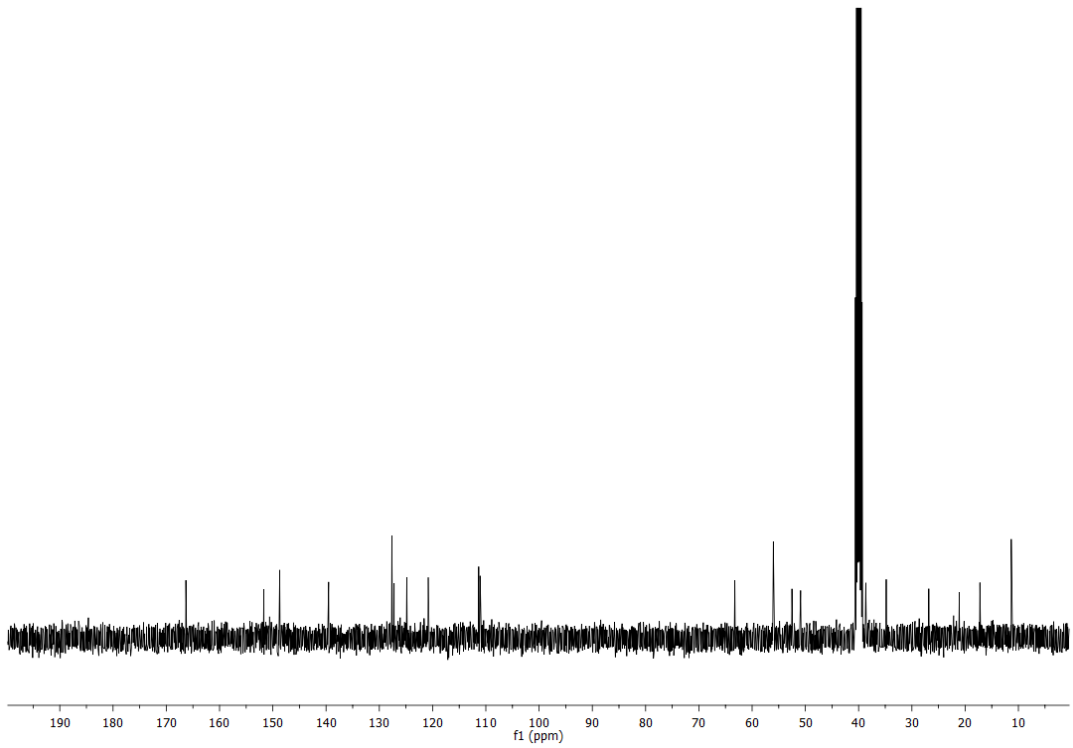

Figure 9.8: ^{13}C-NMR spectrum (101 MHz, DMSO-d_6) of compound **25c**.

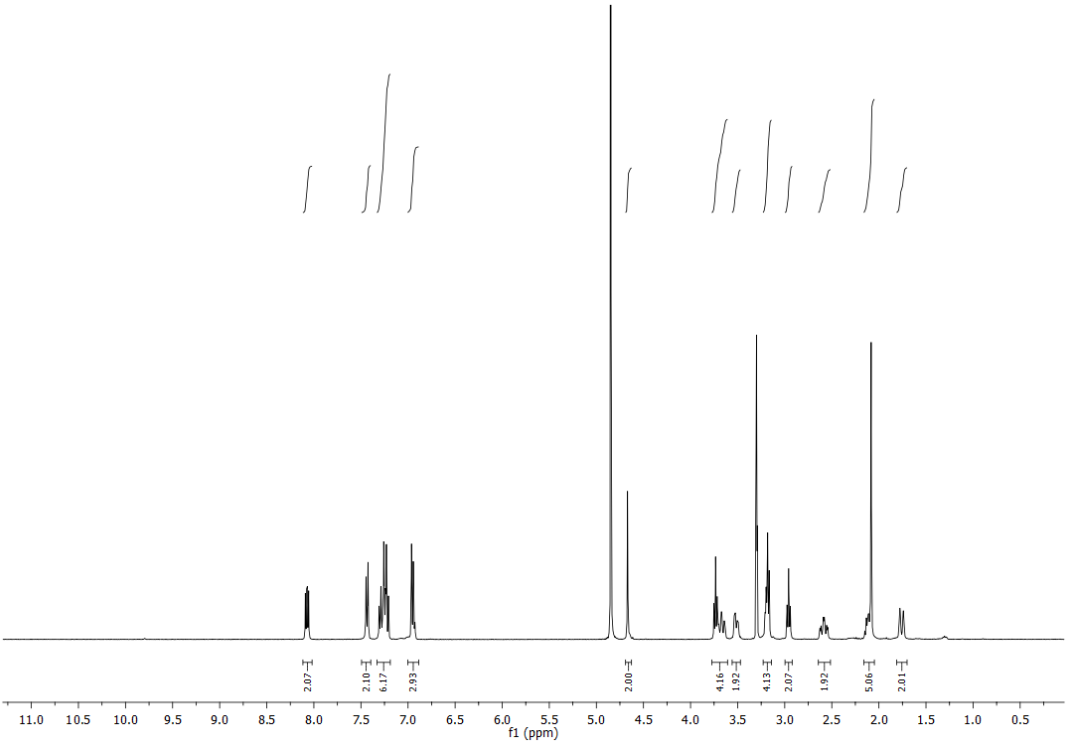

Figure 9.10: ^{1}H-NMR spectrum (400 MHz, CD_3OD) of compound **38**.

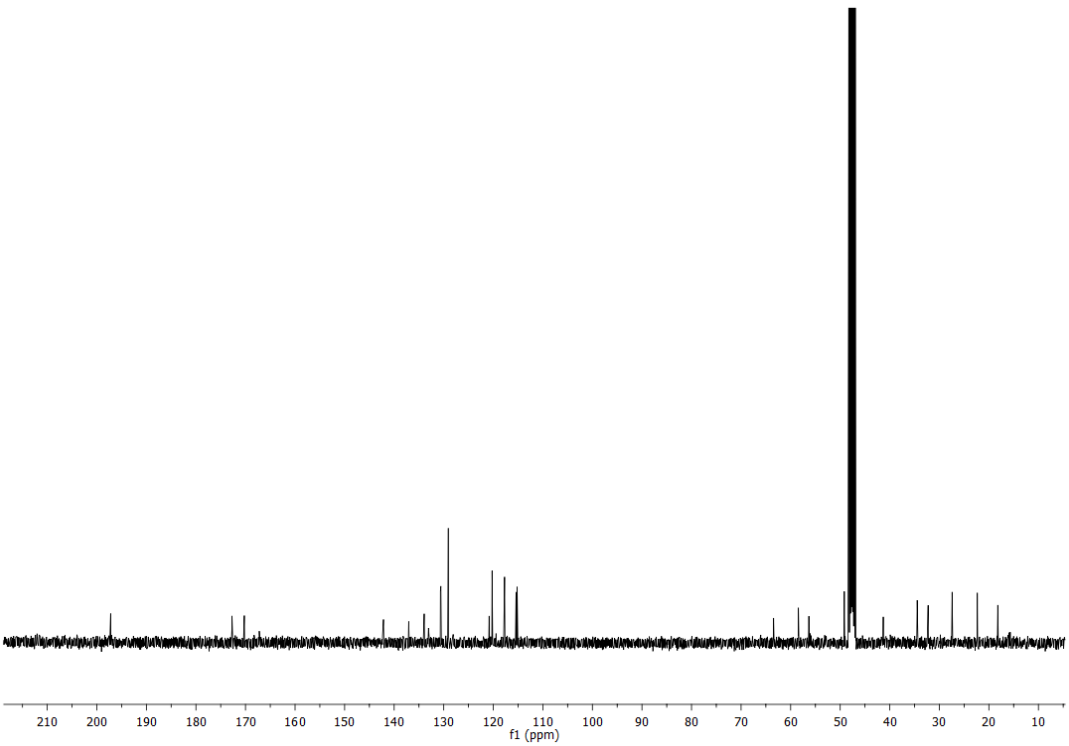

Figure 9.11: ^{13}C-NMR spectrum (101 MHz, CD_3OD) of compound **38**.

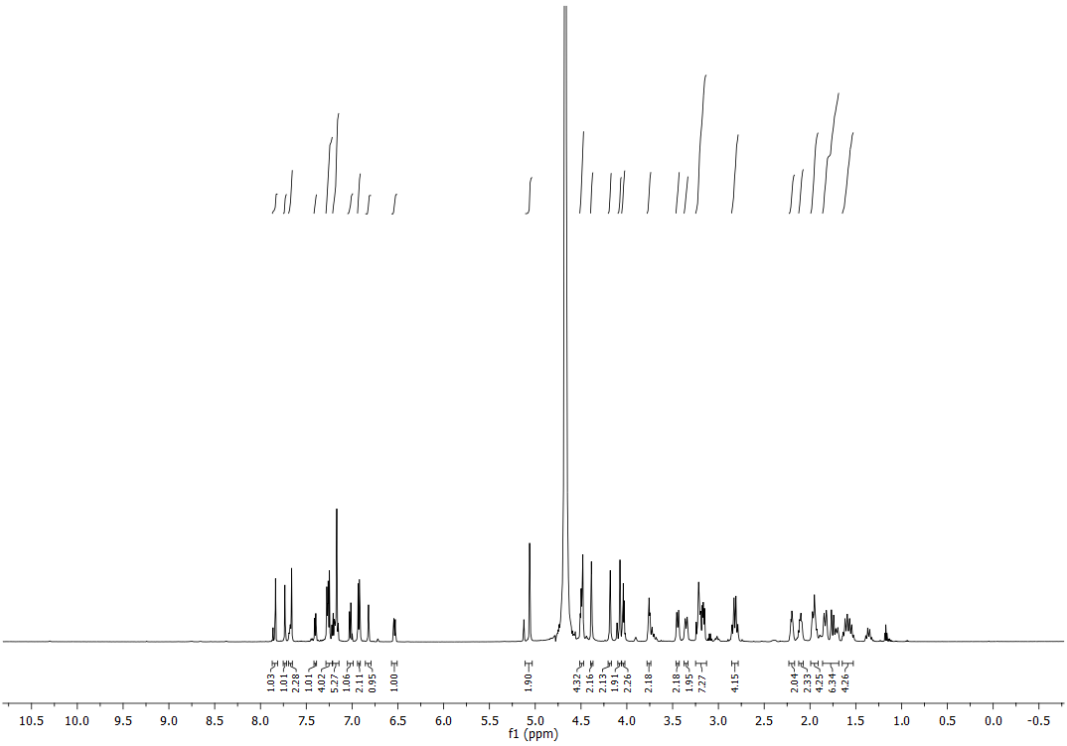

Figure 9.12: ^{1}H-NMR spectrum (600 MHz, D_2O) of compound **65**.

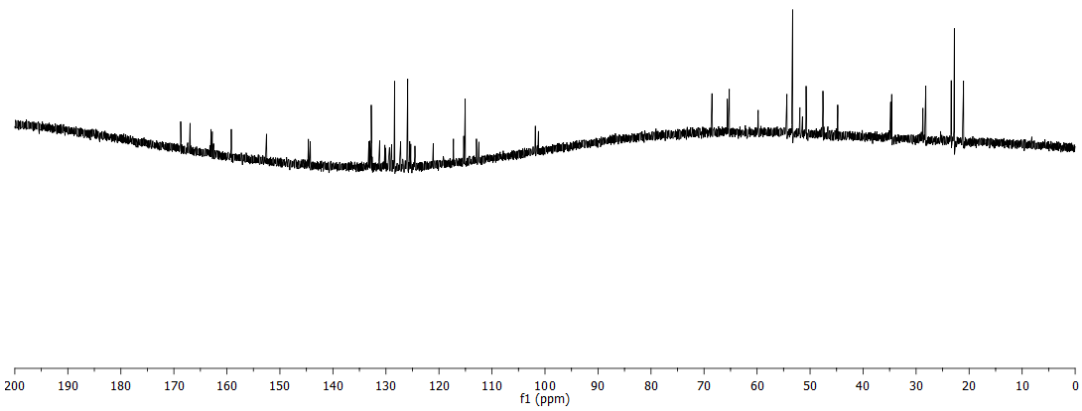

Figure 9.13: ^{13}C-NMR spectrum (151 MHz, D_2O) of compound **65**.

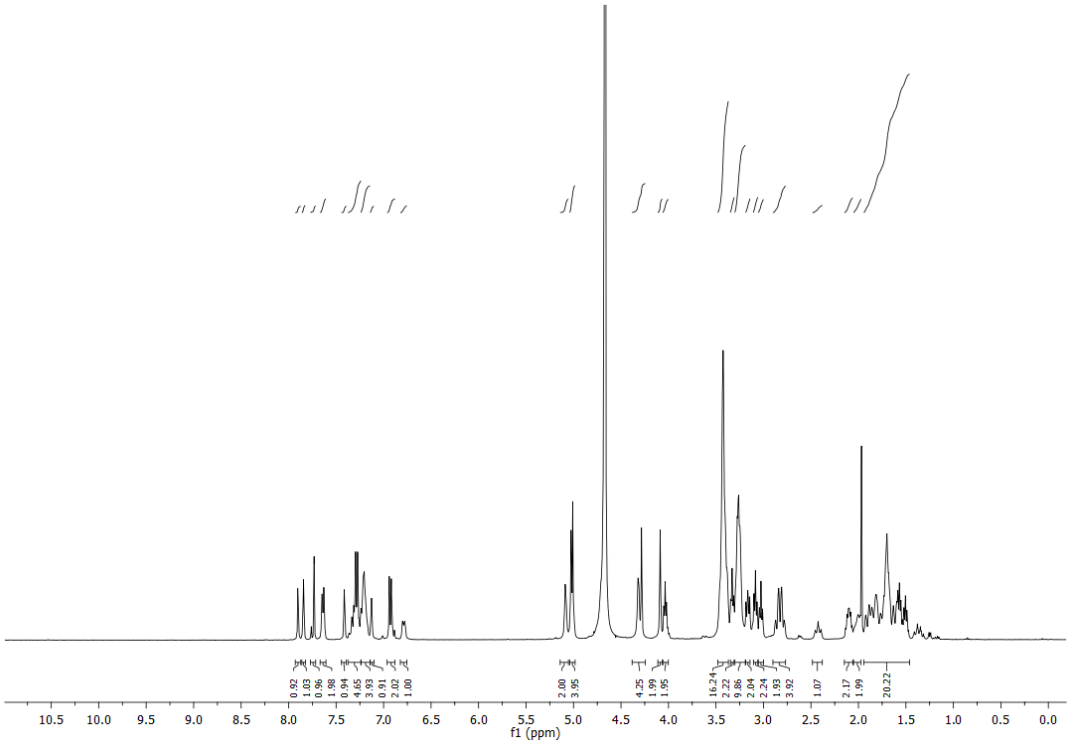

Figure 9.14: ^{1}H-NMR spectrum (600 MHz, D_2O) of compound **66**.

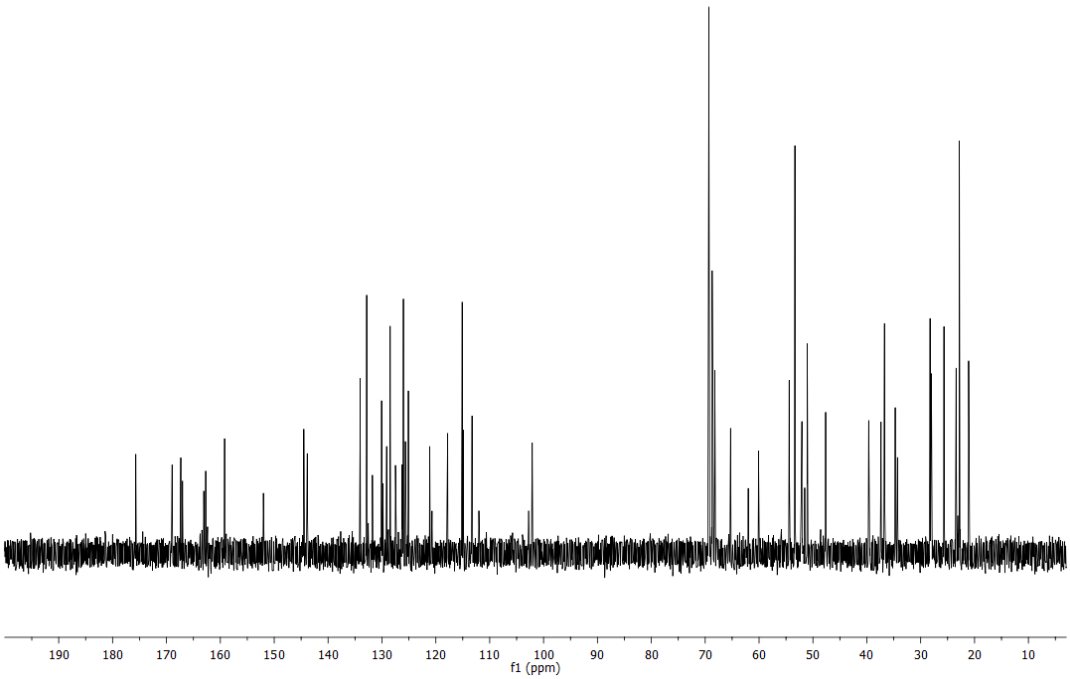

Figure 9.15: ^{13}C-NMR spectrum (151 MHz, D_2O) of compound **66**.

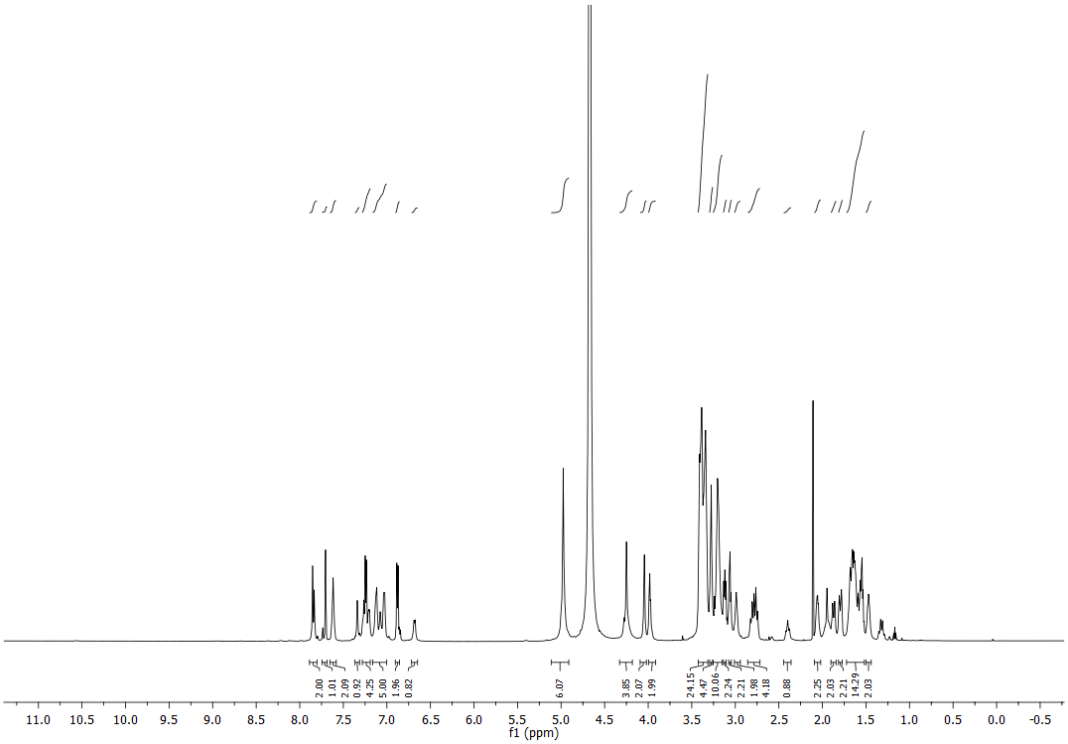

Figure 9.16: ^{1}H-NMR spectrum (600 MHz, D_2O) of compound **67**.

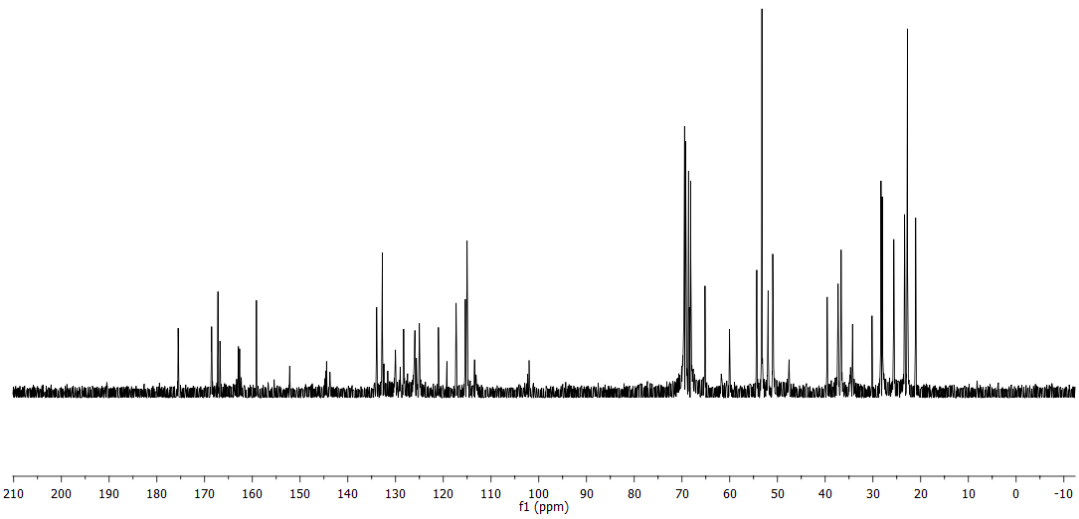

Figure 9.17: ^{13}C-NMR spectrum (151 MHz, D_2O) of compound **67**.

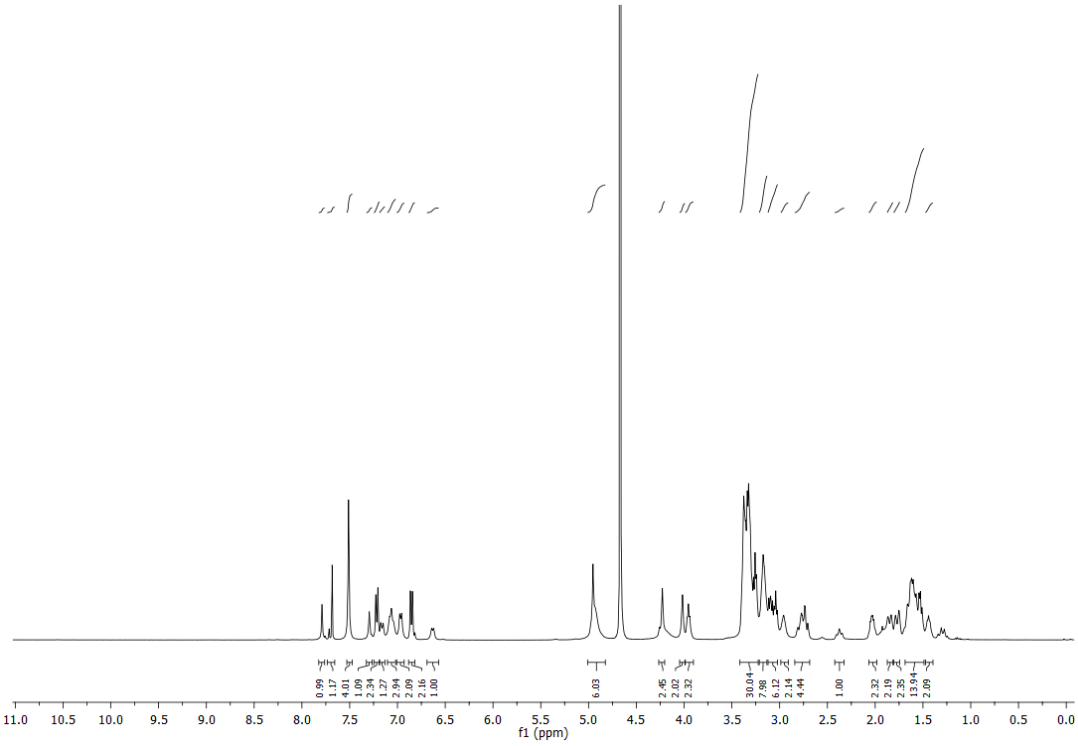

Figure 9.18: ^{1}H-NMR spectrum (400 MHz, D_2O) of compound **68**.

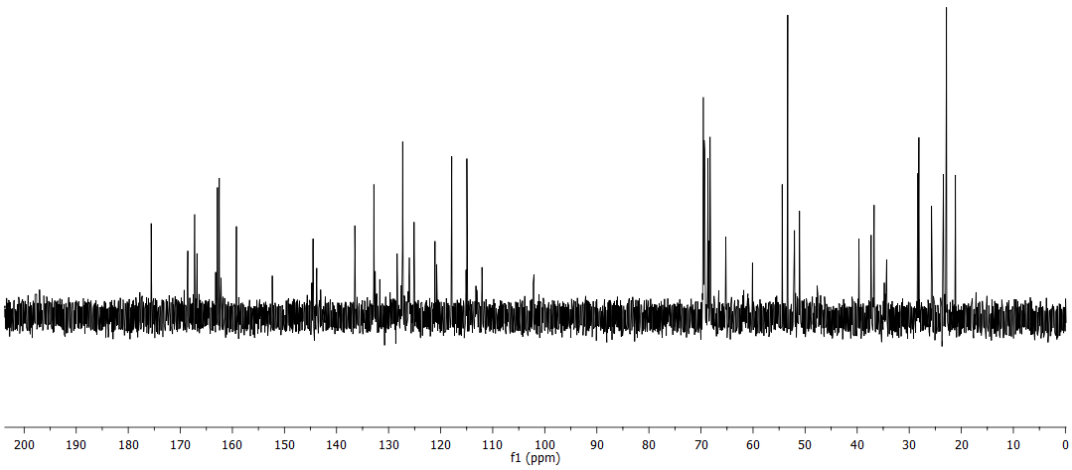

Figure 9.19: ^{13}C-NMR spectrum (101 MHz, D_2O) of compound **68**.

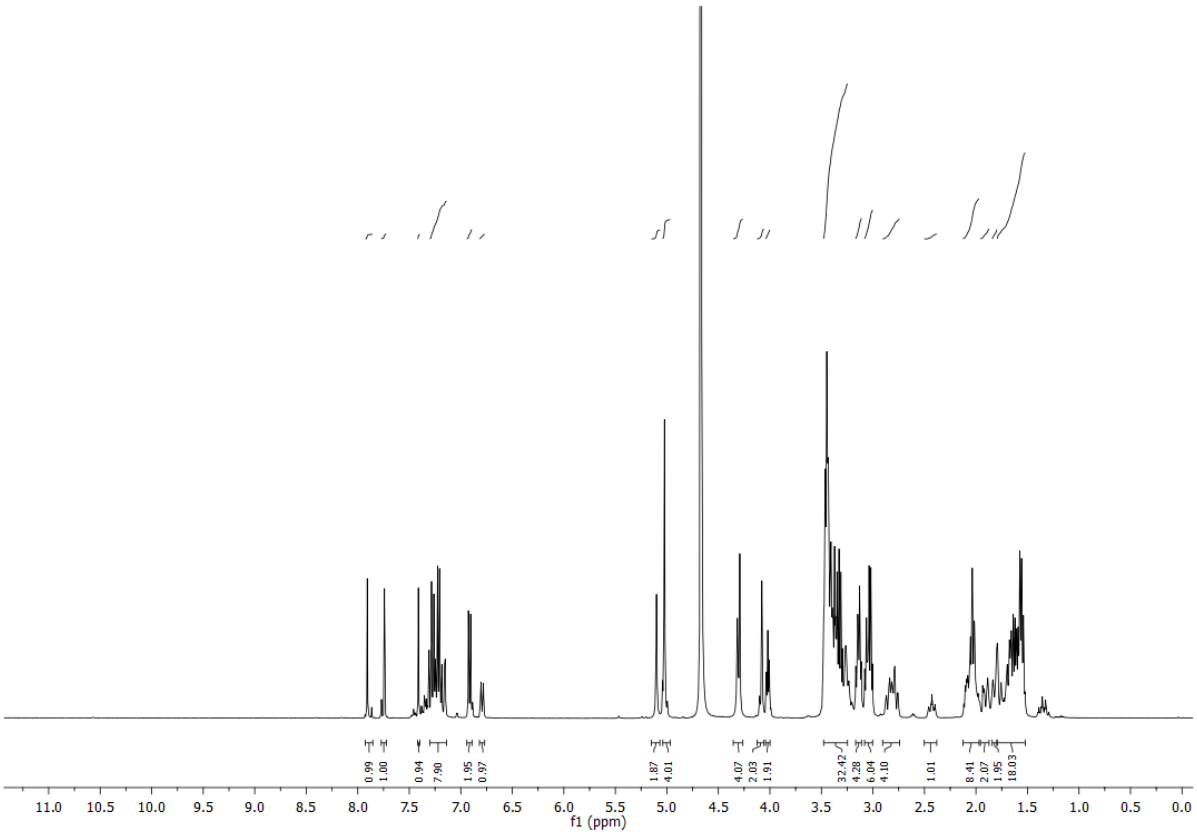

Figure 9.20: ^{1}H-NMR spectrum (400 MHz, D_2O) of compound **69**.

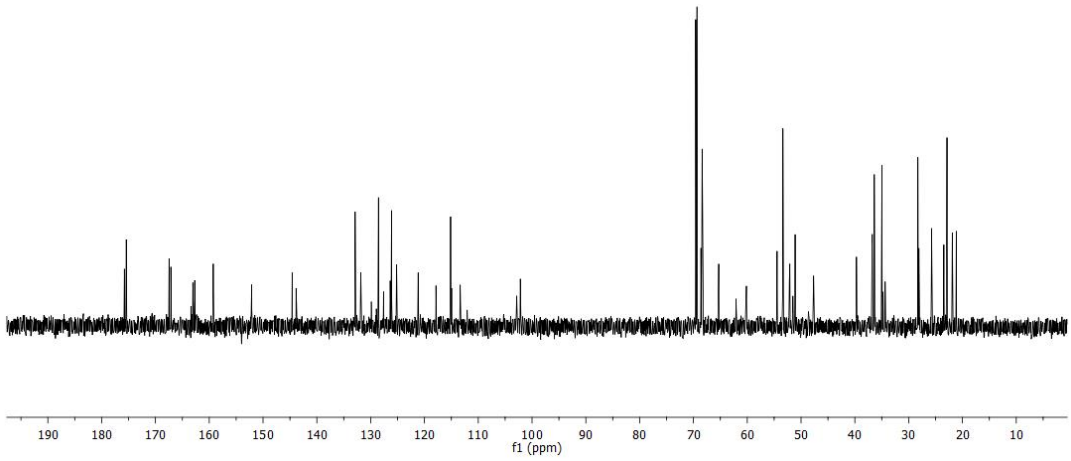

Figure 9.21: ^{13}C-NMR spectrum (101 MHz, D_2O) of compound **69**.

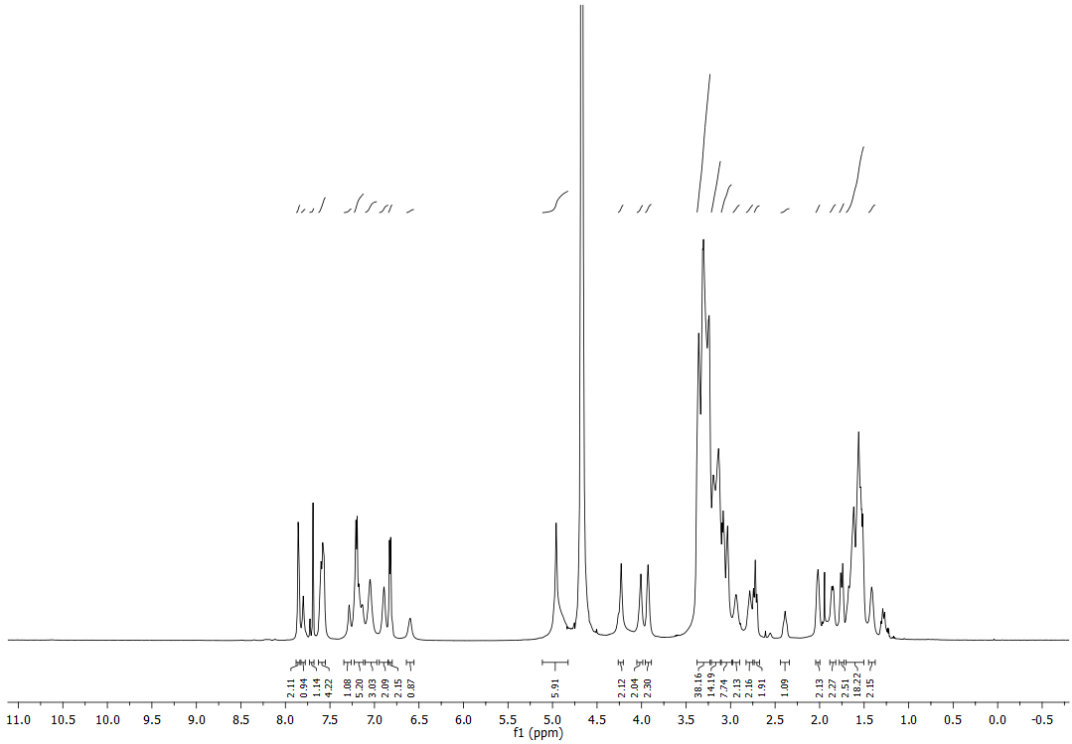

Figure 9.22: ^{1}H-NMR spectrum (400 MHz, D_2O) of compound **70**.

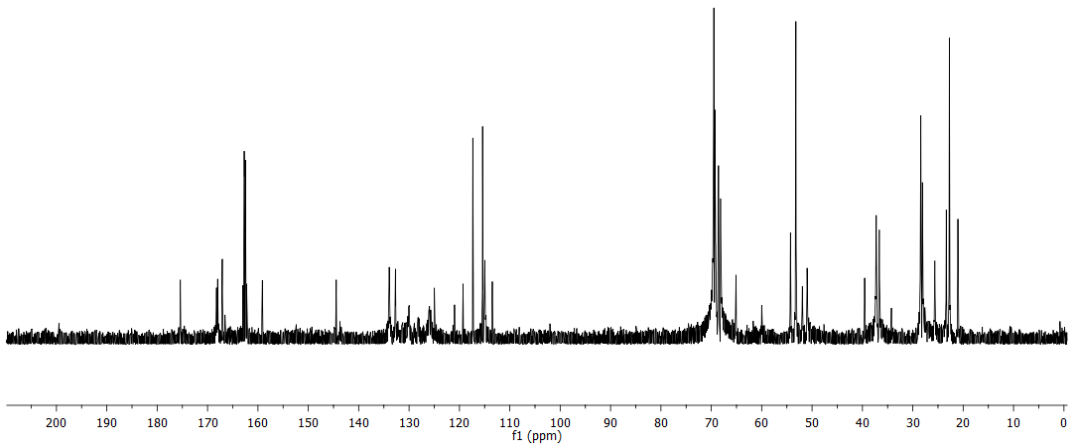

Figure 9.23: ^{13}C-NMR spectrum (101 MHz, D_2O) of compound **70**.

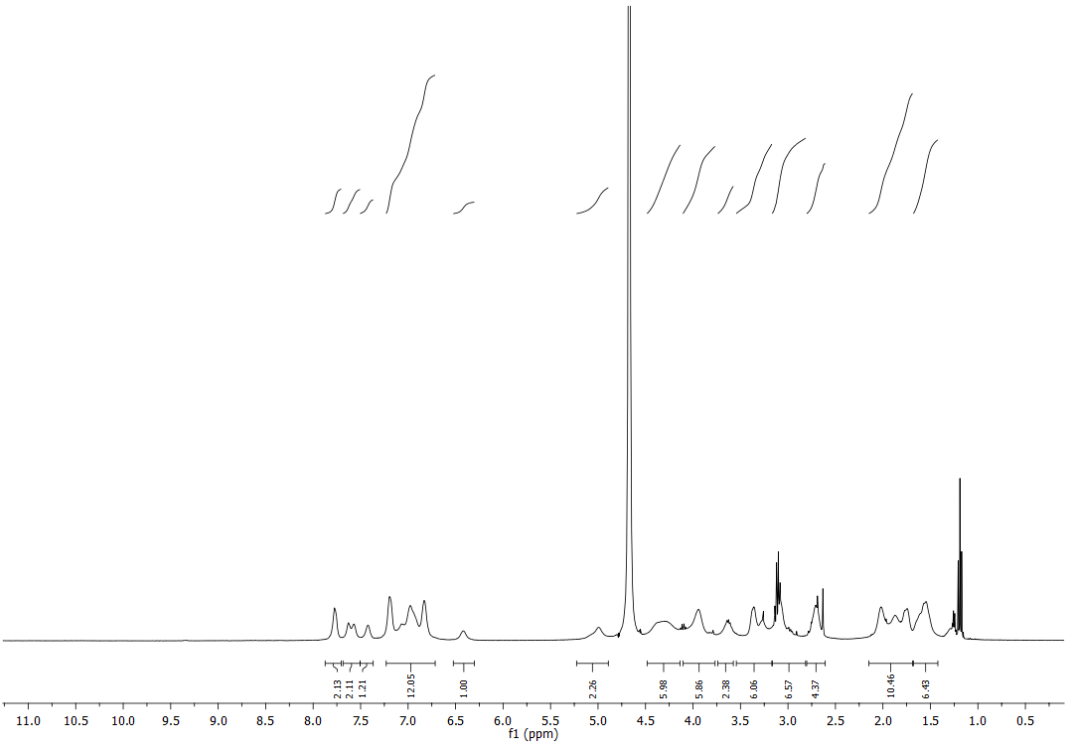

Figure 9.24: ^{1}H-NMR spectrum (400 MHz, D_2O) of compound **71**.

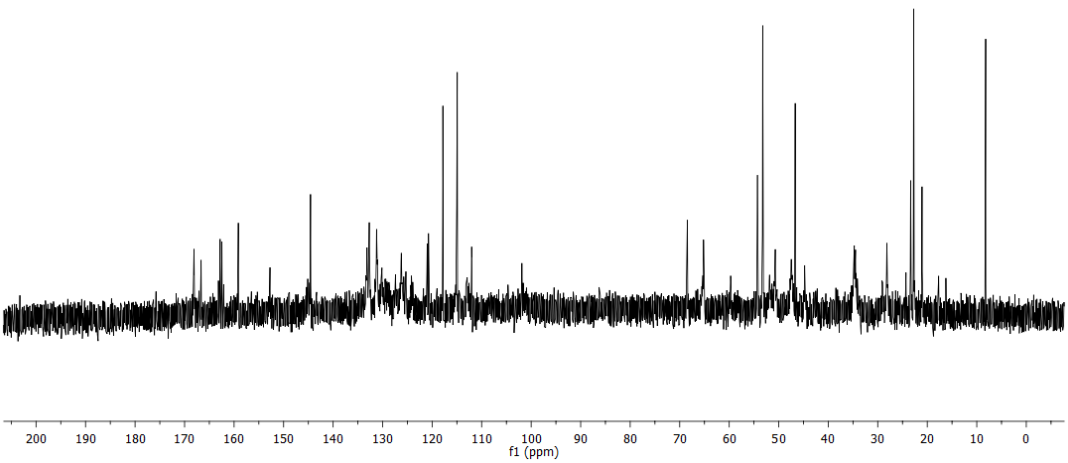

Figure 9.25: ^{13}C-NMR spectrum (101 MHz, D_2O) of compound **71**.

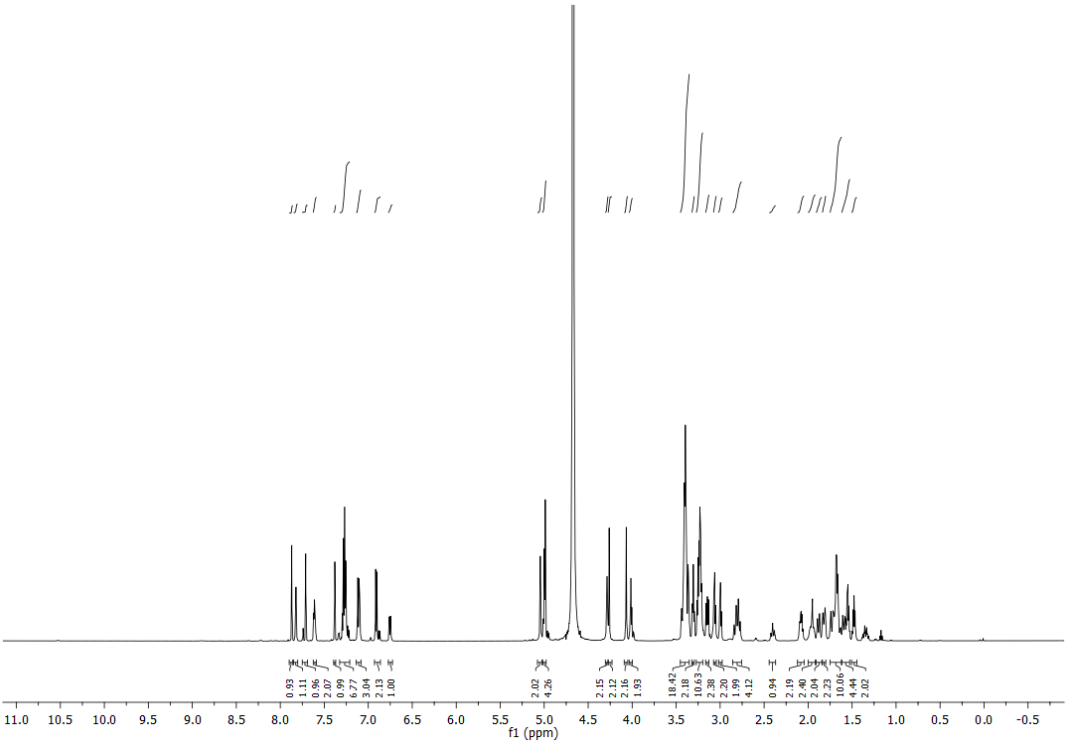

Figure 9.26: ^{1}H-NMR spectrum (600 MHz, D_2O) of compound **72**.

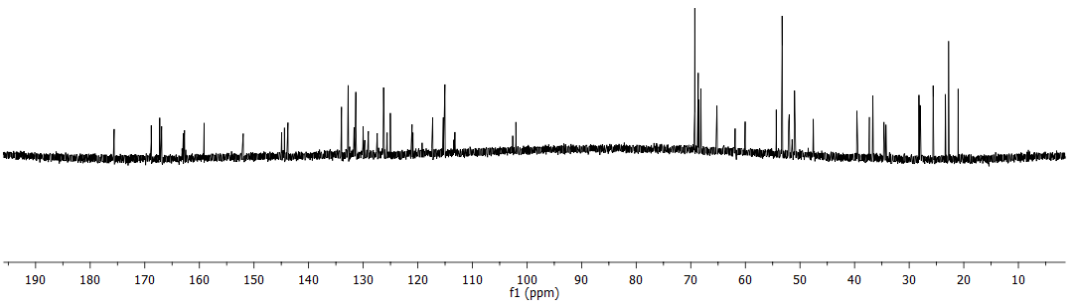

Figure 9.27: ^{13}C-NMR spectrum (151 MHz, D_2O) of compound **72**.

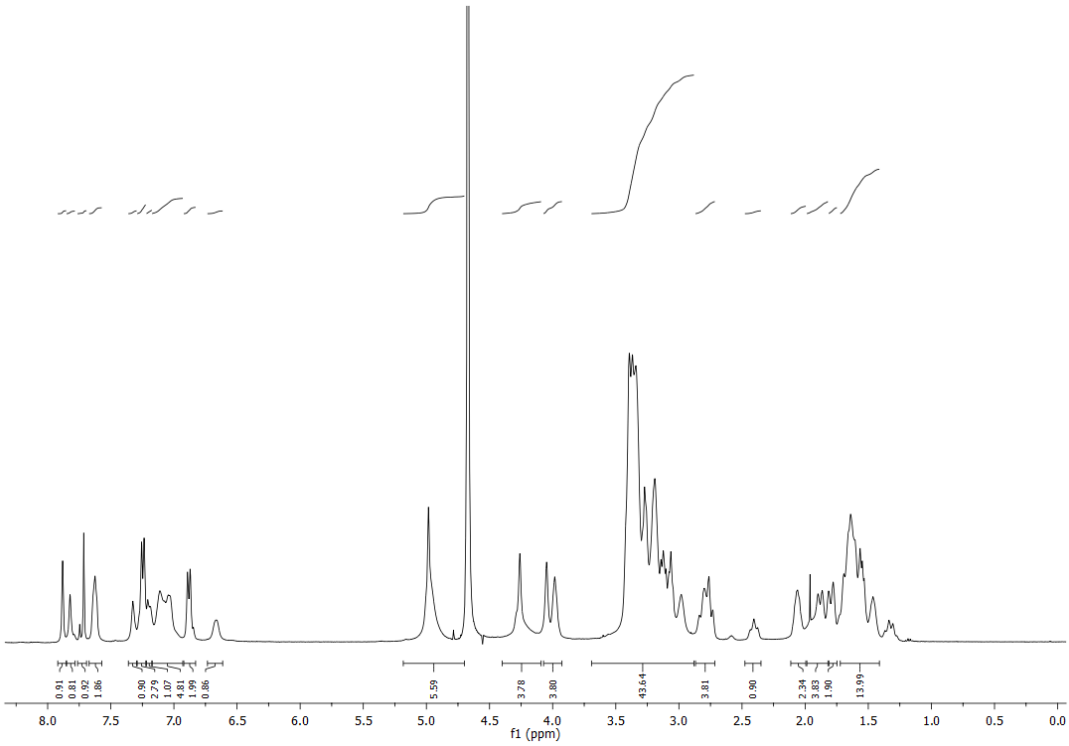

Figure 9.28: ^{1}H-NMR spectrum (400 MHz, D_2O) of compound **73**.

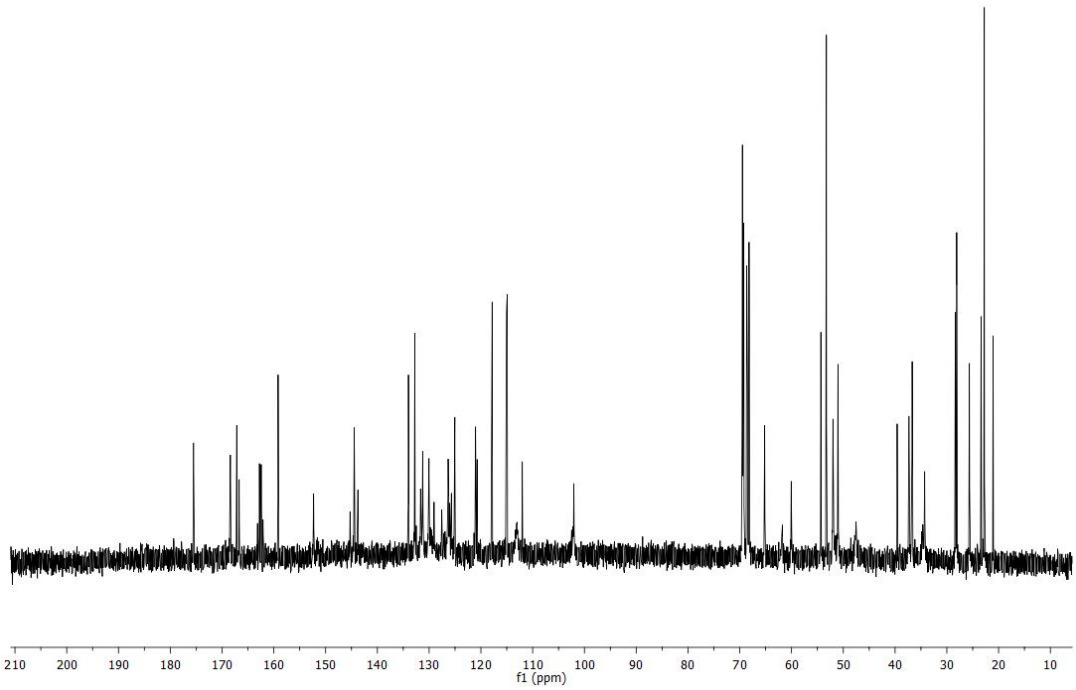

Figure 9.29: ^{13}C-NMR spectrum (101 MHz, D_2O) of compound **73**.

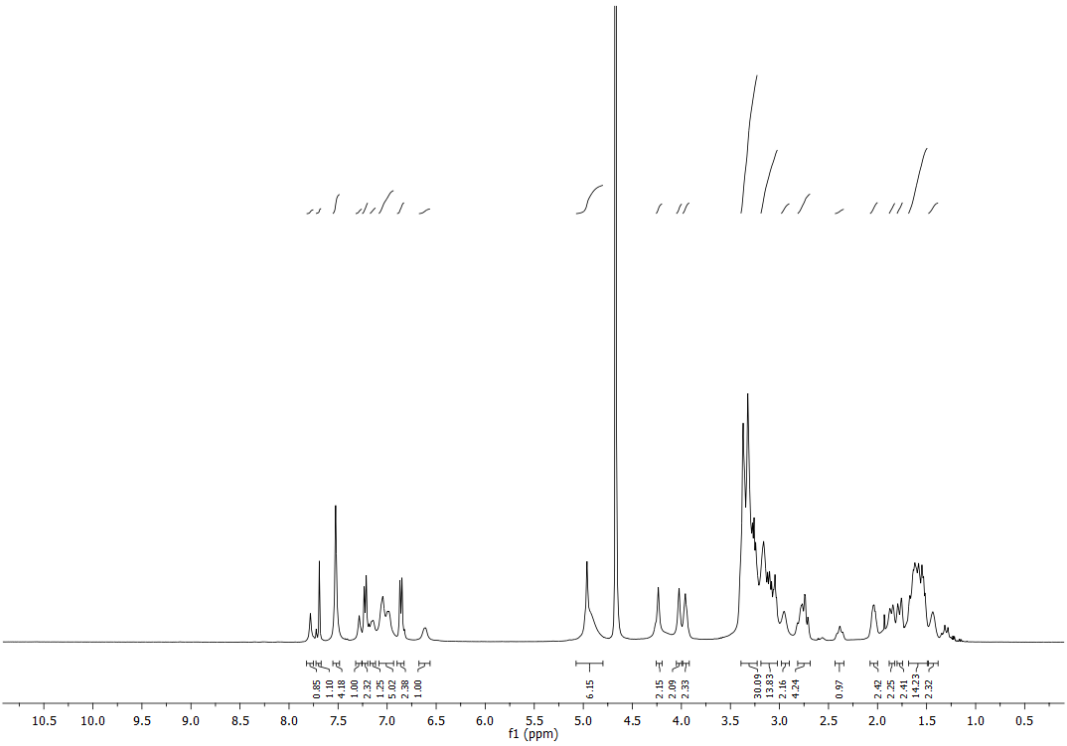

Figure 9.30: ^{1}H-NMR spectrum (400 MHz, D_2O) of compound **74**.

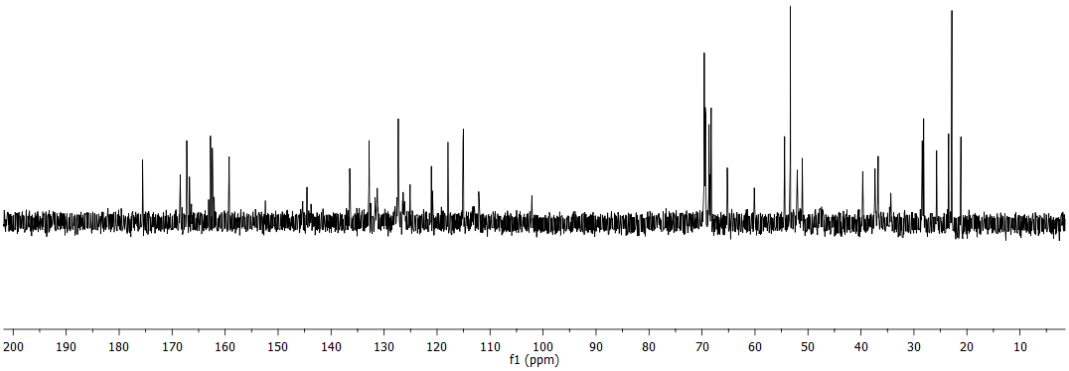

Figure 9.31: ^{13}C-NMR spectrum (101 MHz, D_2O) of compound **74**.

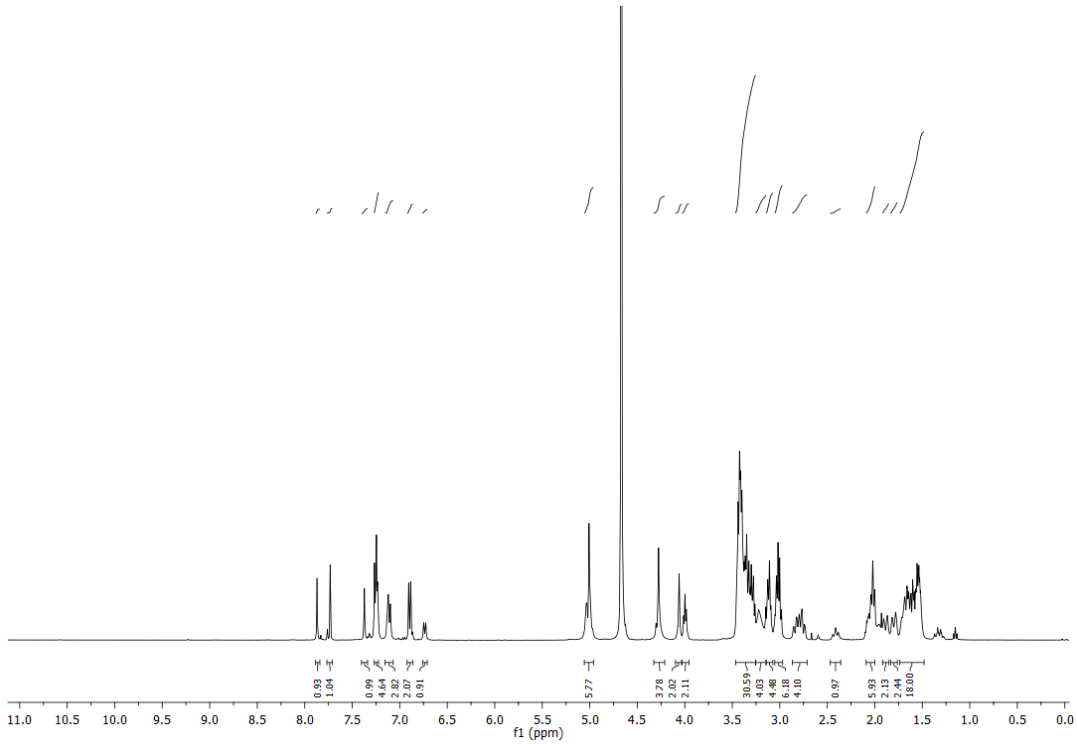

Figure 9.32: ^{1}H-NMR spectrum (400 MHz, D_2O) of compound **75**.

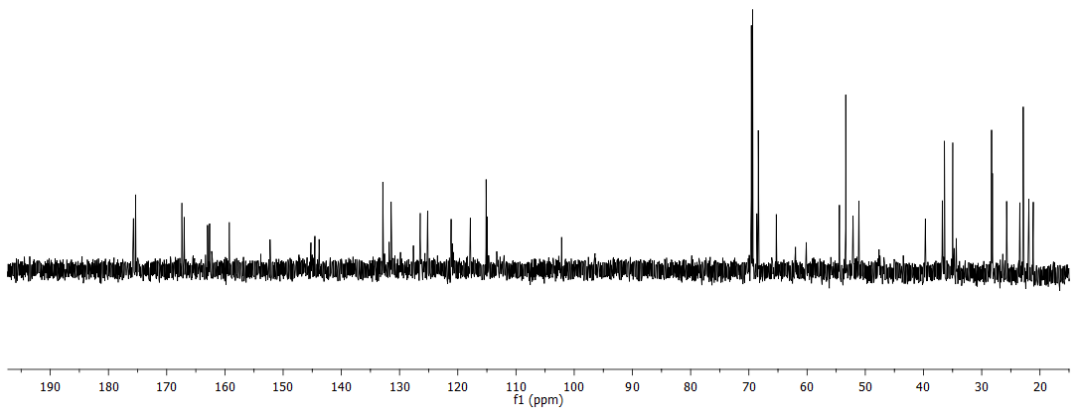

Figure 9.33: ^{13}C-NMR spectrum (101 MHz, D_2O) of compound **75**.

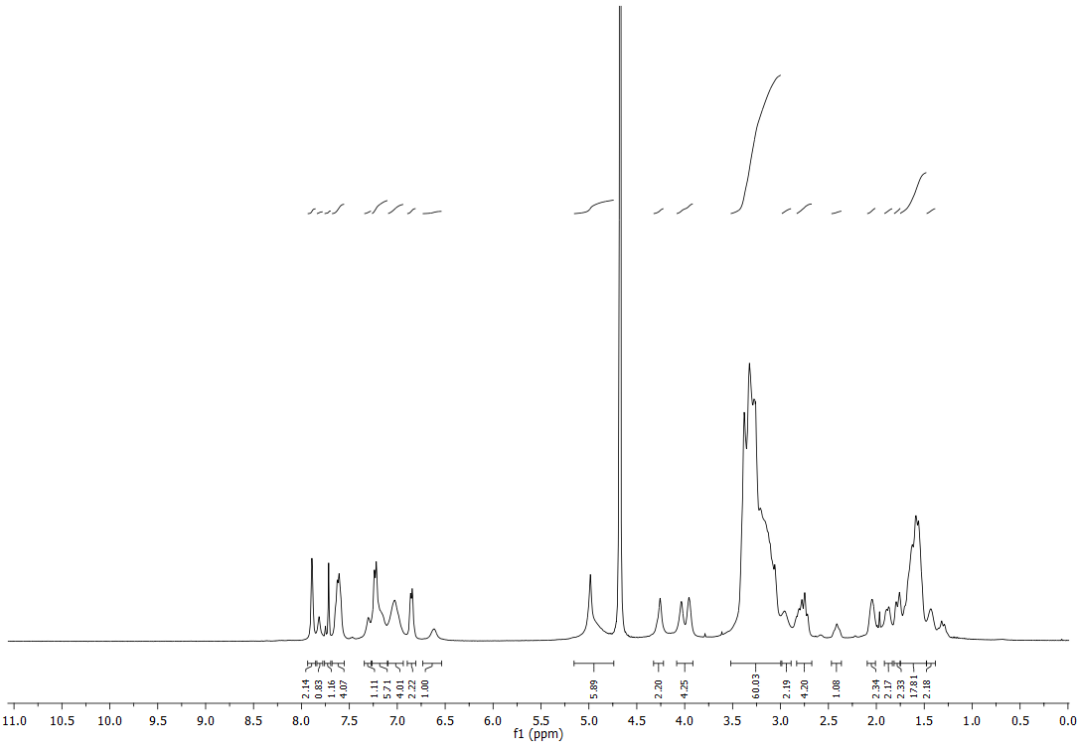

Figure 9.34: ^{1}H-NMR spectrum (400 MHz, D_2O) of compound **76**.

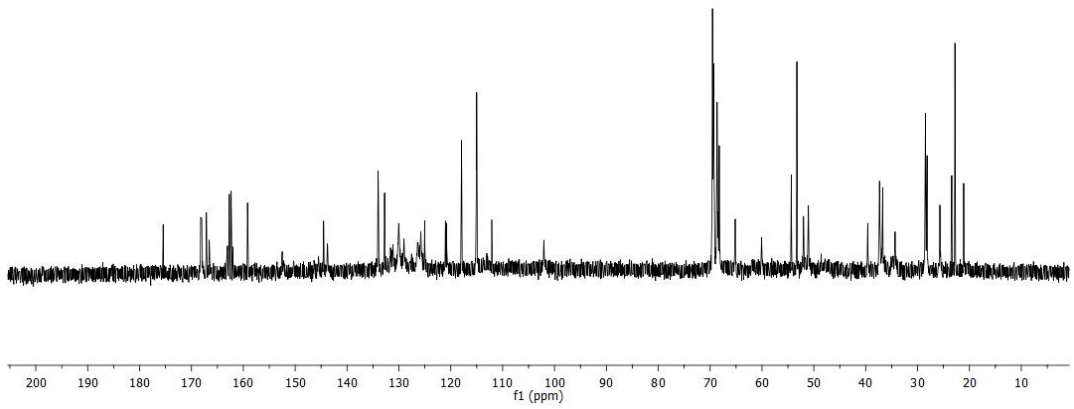

Figure 9.35: ^{13}C-NMR spectrum (101 MHz, D_2O) of compound **76**.

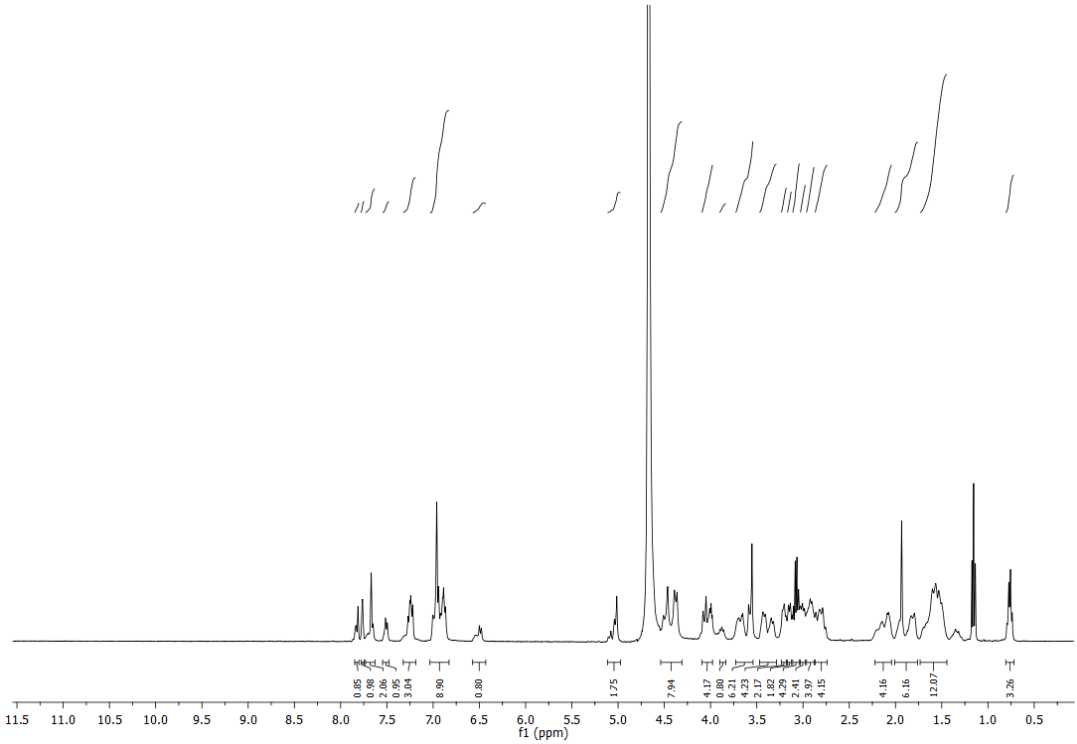

Figure 9.36: ^{1}H-NMR spectrum (600 MHz, D_2O) of compound **77**.

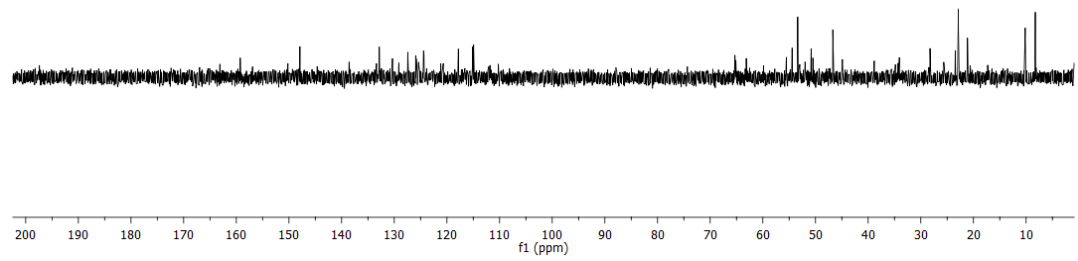

Figure 9.37: ^{13}C-NMR spectrum (151 MHz, D_2O) of compound **77**.

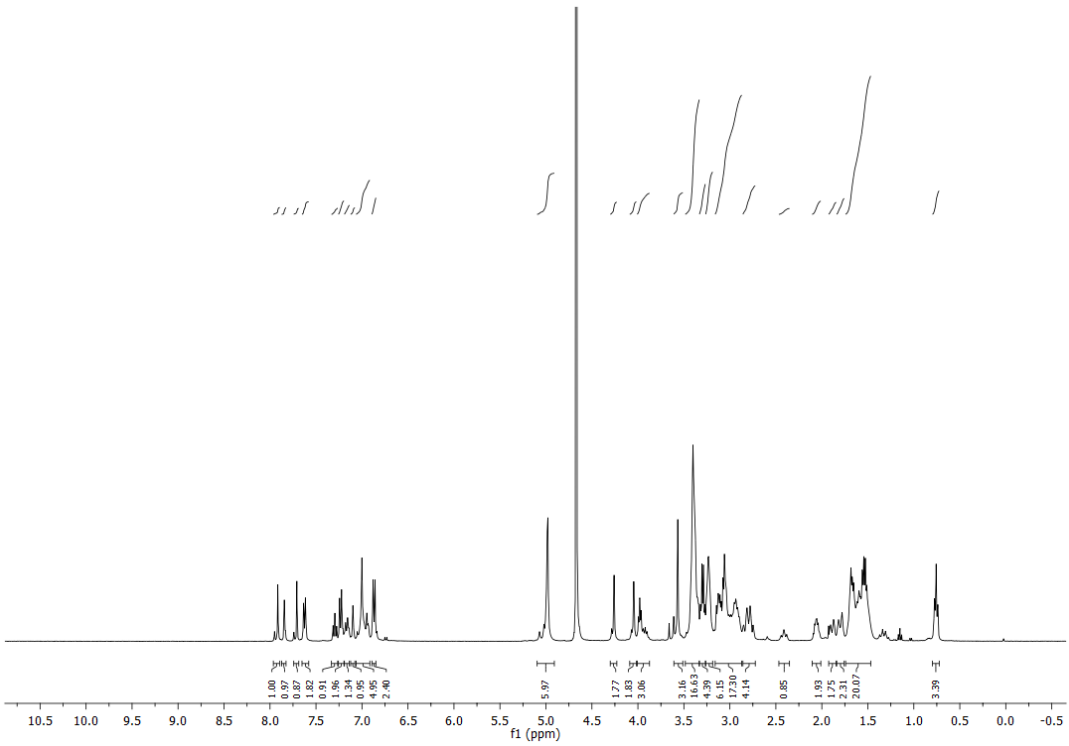

Figure 9.38: ^{1}H-NMR spectrum (400 MHz, D_2O) of compound **78**.

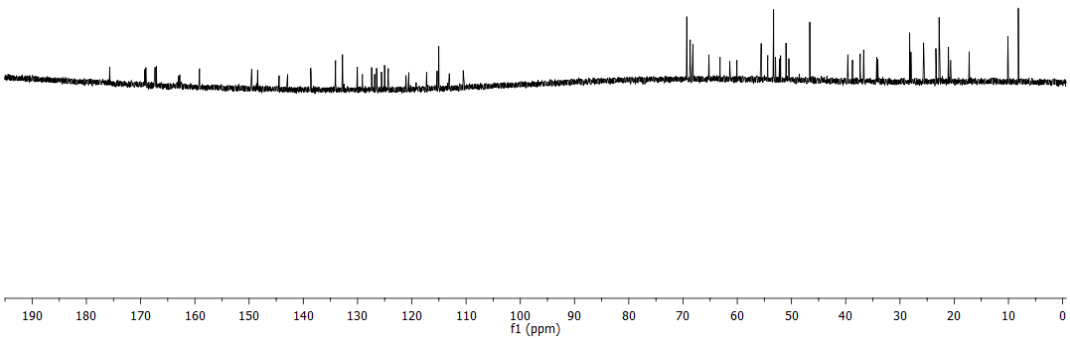

Figure 9.39: ^{13}C-NMR spectrum (151 MHz, D_2O) of compound **78**.

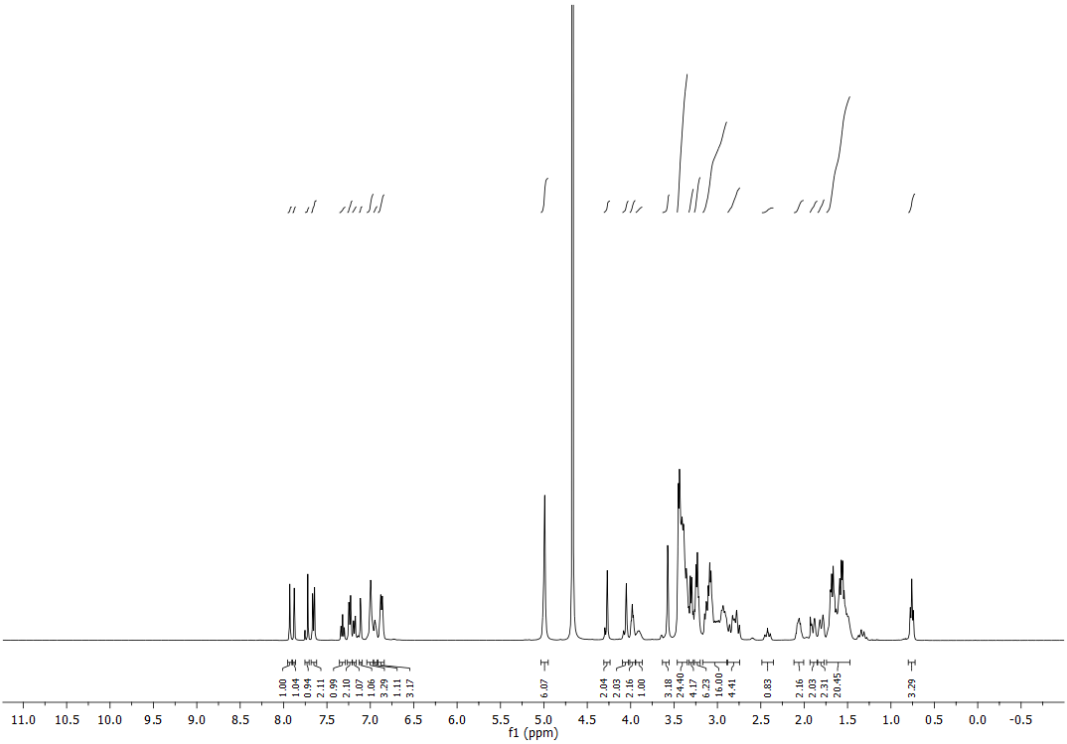

Figure 9.40: ^{1}H-NMR spectrum (400 MHz, D_2O) of compound **79**.

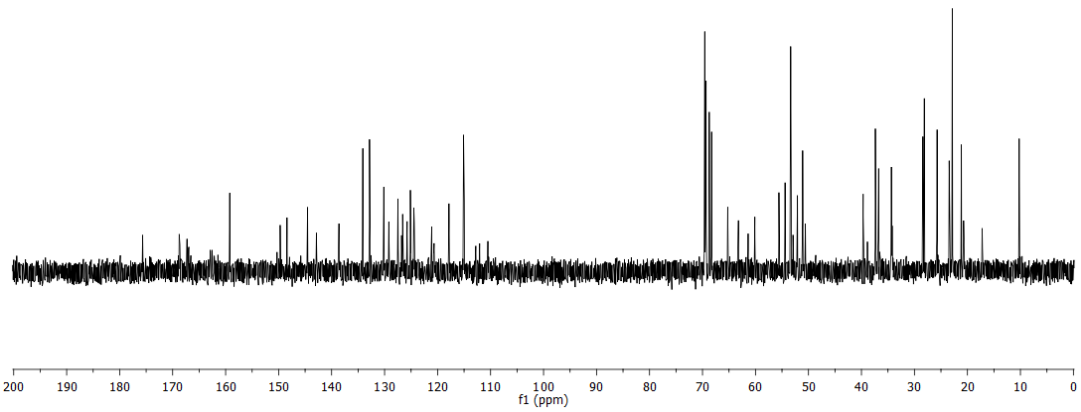

Figure 9.41: ^{13}C-NMR spectrum (101 MHz, D_2O) of compound **79**.

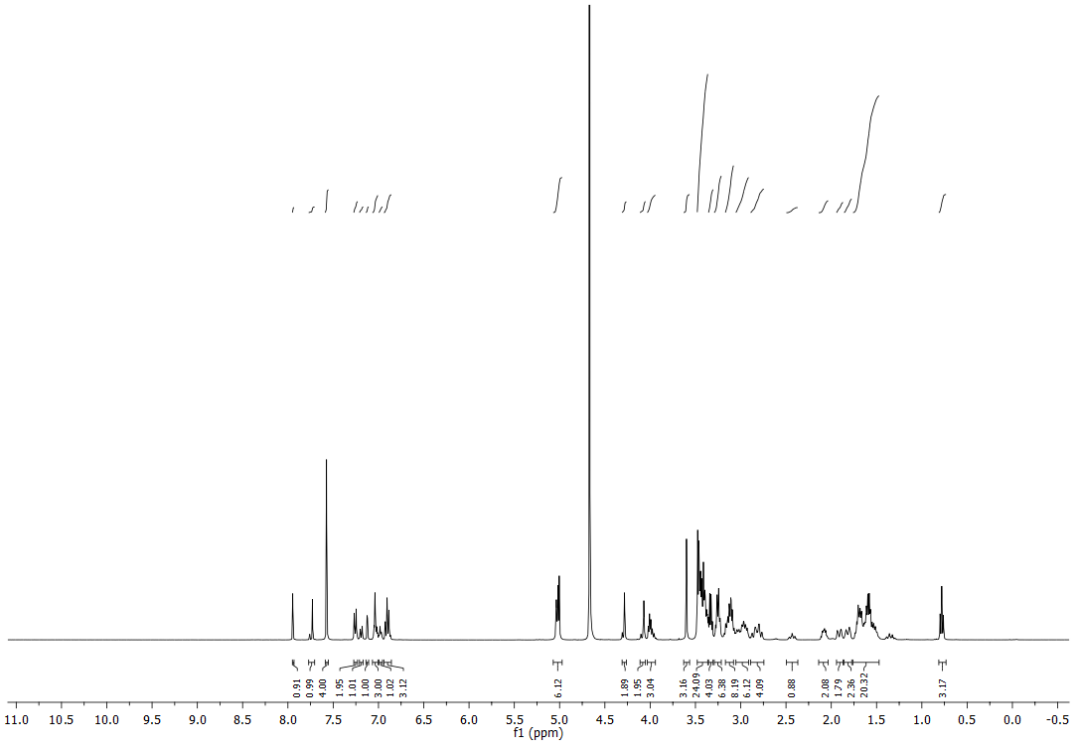

Figure 9.42: ^{1}H-NMR spectrum (400 MHz, D_2O) of compound **80**.

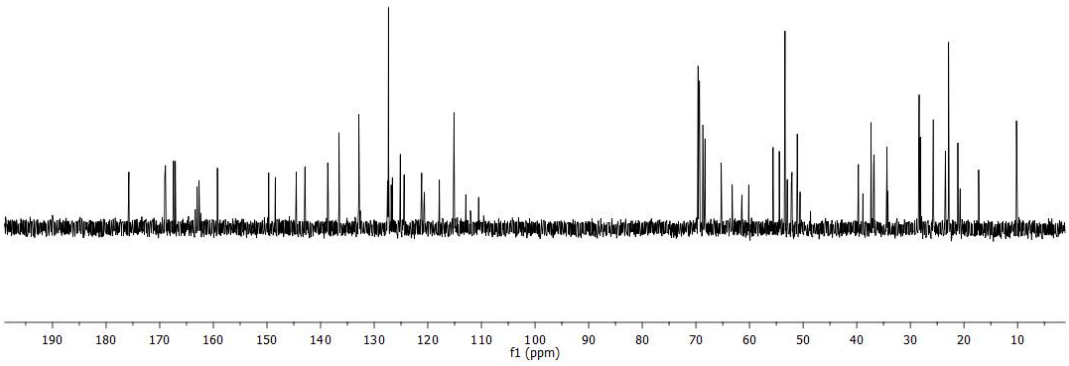

Figure 9.43: ^{13}C-NMR spectrum (101 MHz, D_2O) of compound **80**.

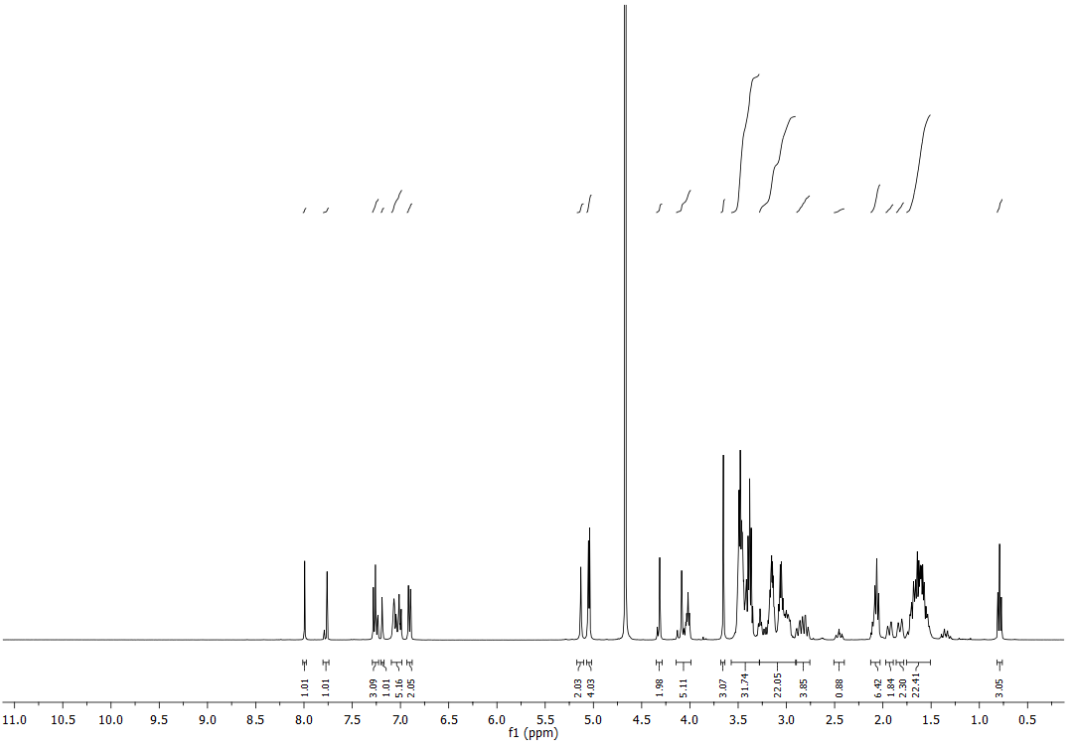

Figure 9.44: ^{1}H-NMR spectrum (400 MHz, D_2O) of compound **81**.

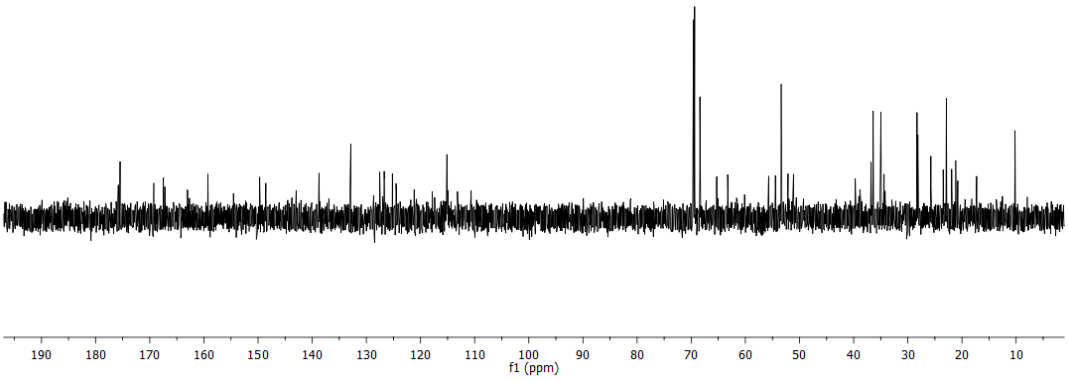

Figure 9.45: ^{13}C-NMR spectrum (101 MHz, D_2O) of compound **81**.

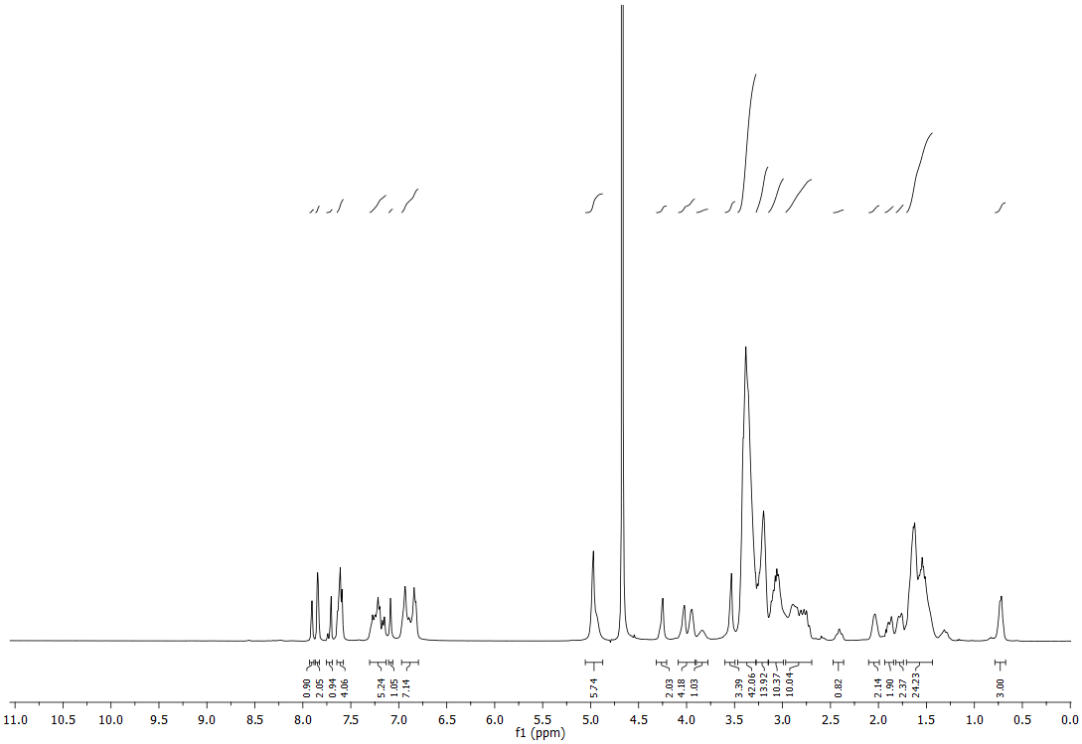

Figure 9.46: ^{1}H-NMR spectrum (400 MHz, D_2O) of compound **82**.

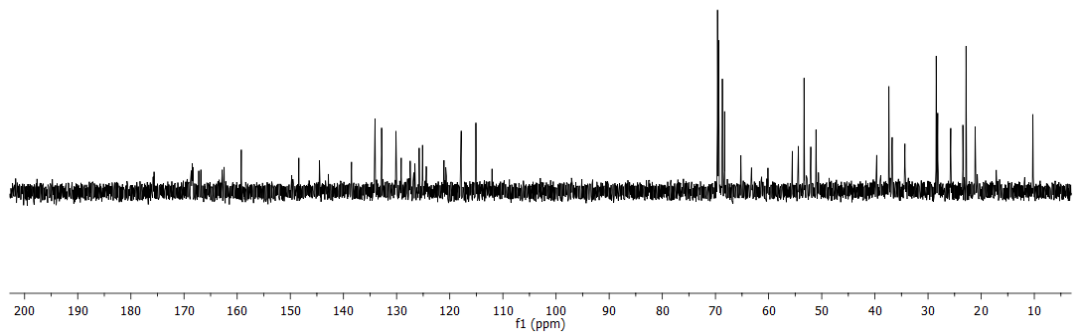

Figure 9.47: ^{13}C-NMR spectrum (101 MHz, D_2O) of compound **82**.

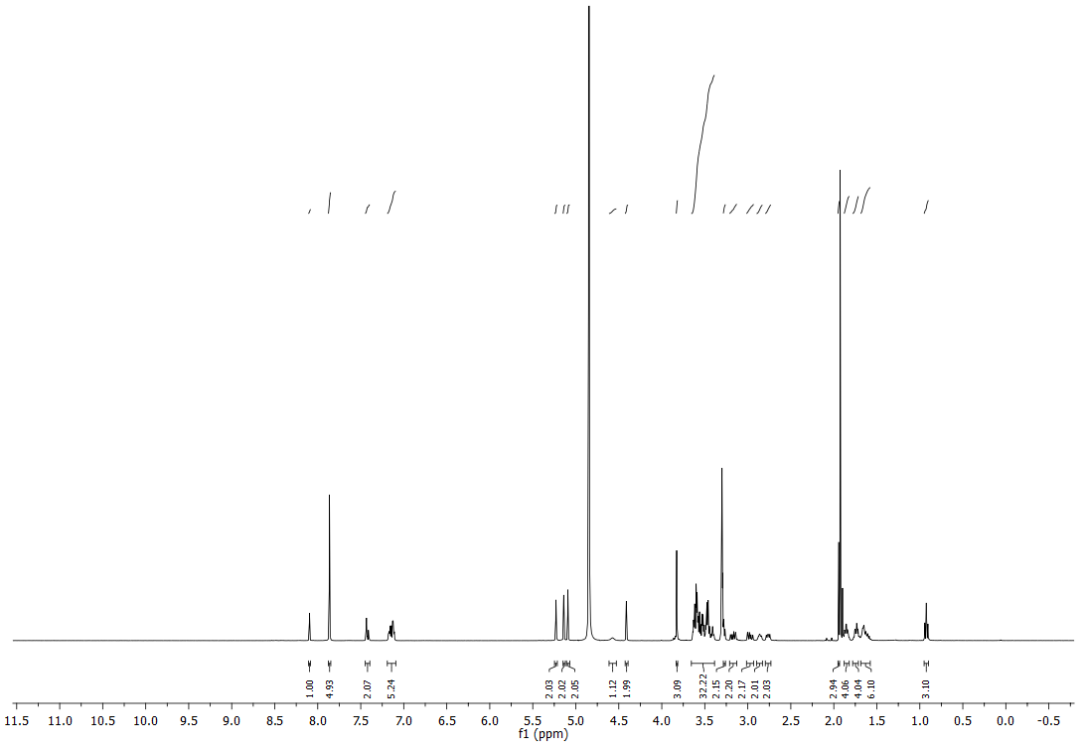

Figure 9.48: ^{1}H-NMR spectrum (400 MHz, CD_3OD) of compound **83**.

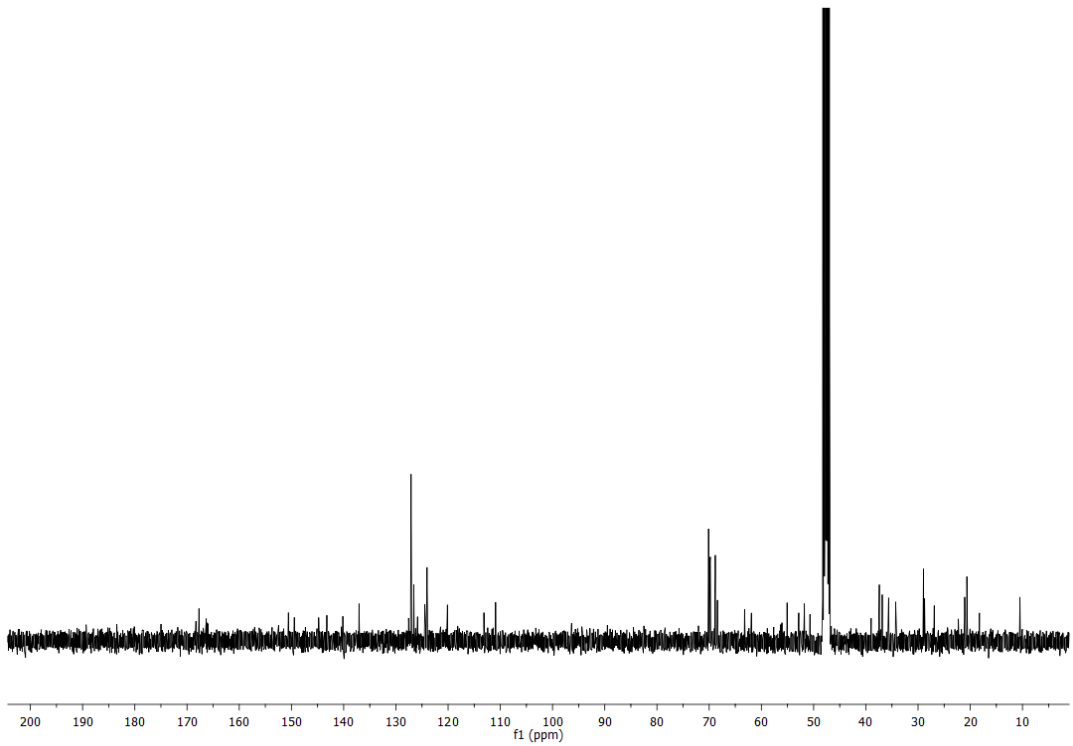

Figure 9.49: ^{13}C-NMR spectrum (101 MHz, CD_3OD) of compound **83**.

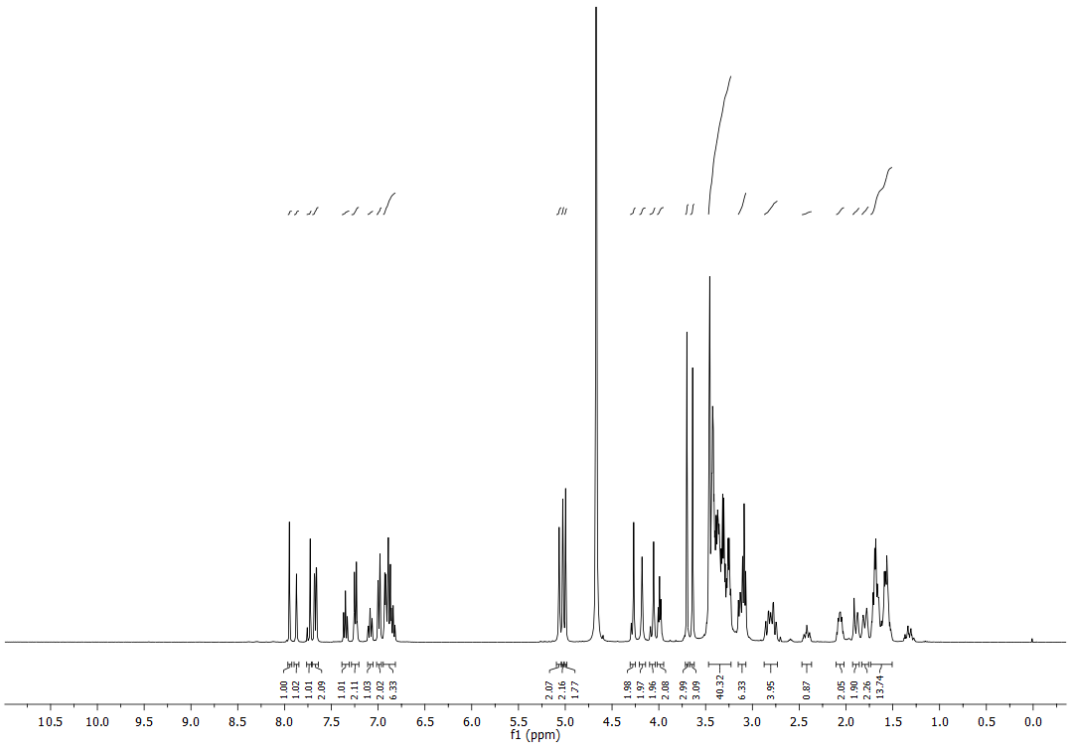

Figure 9.50: ^{1}H-NMR spectrum (400 MHz, D_2O) of compound **84**.

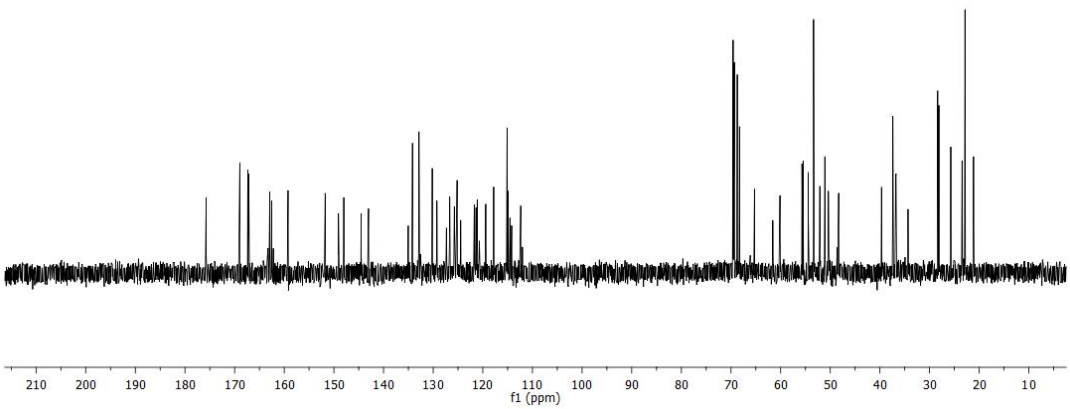

Figure 9.51: ^{13}C-NMR spectrum (101 MHz, D_2O) of compound **84**.

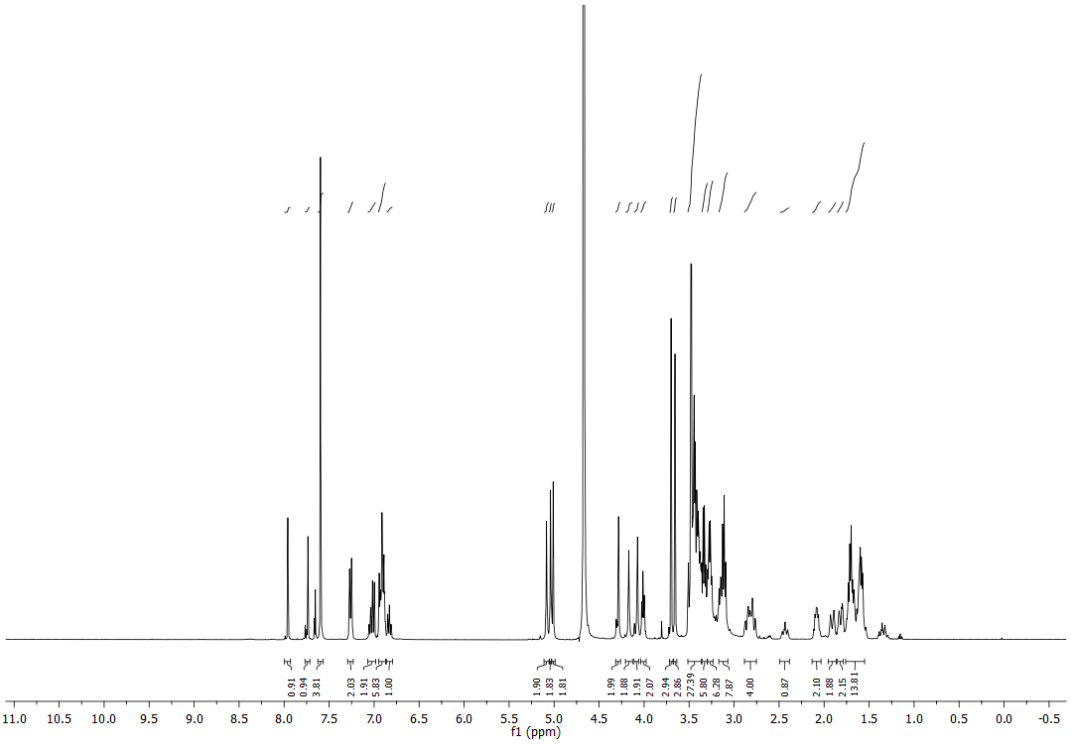

Figure 9.52: ^{1}H-NMR spectrum (400 MHz, D_2O) of compound **85**.

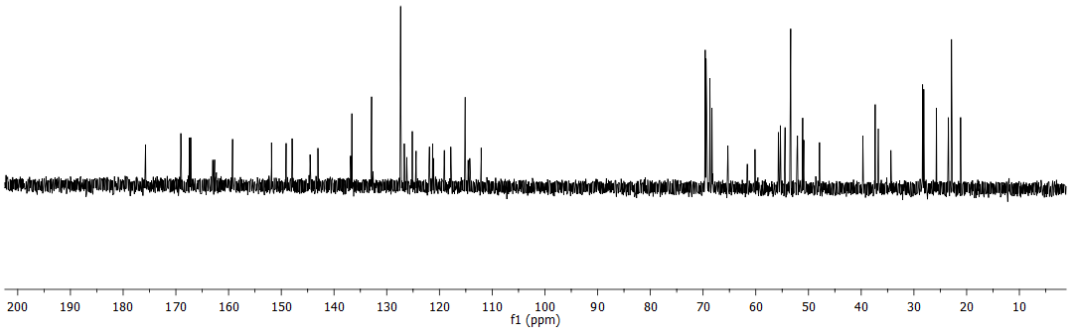

Figure 9.53: ^{13}C-NMR spectrum (101 MHz, D_2O) of compound **85**.

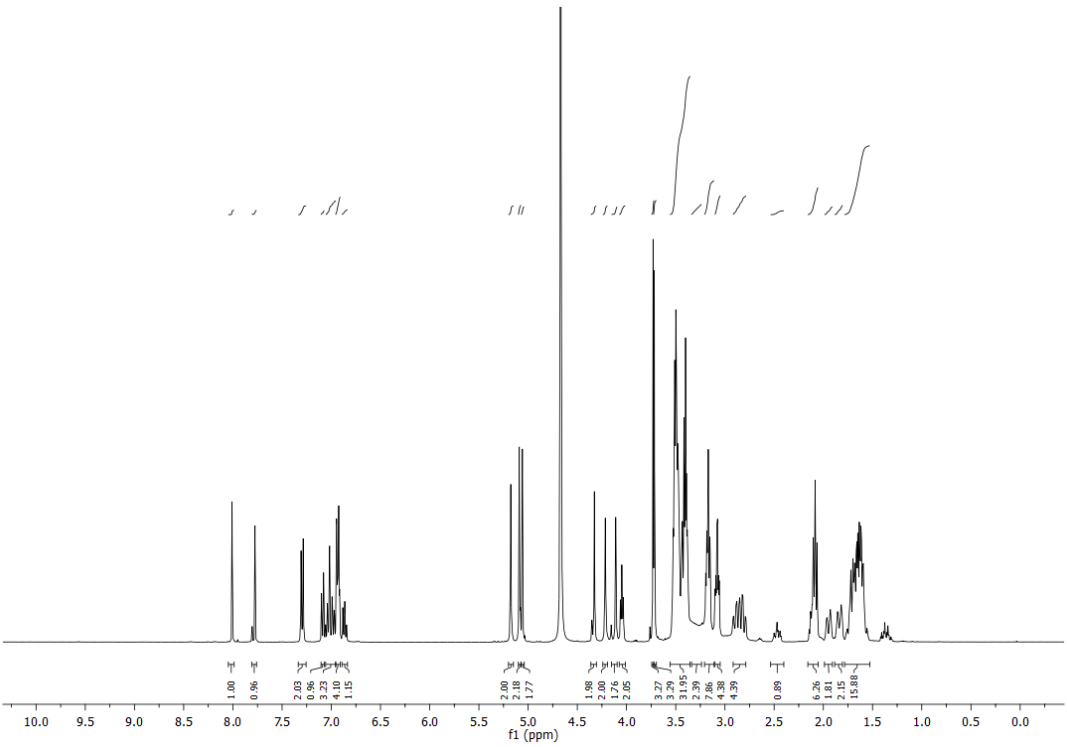

Figure 9.54: ^{1}H-NMR spectrum (400 MHz, D_2O) of compound **86**.

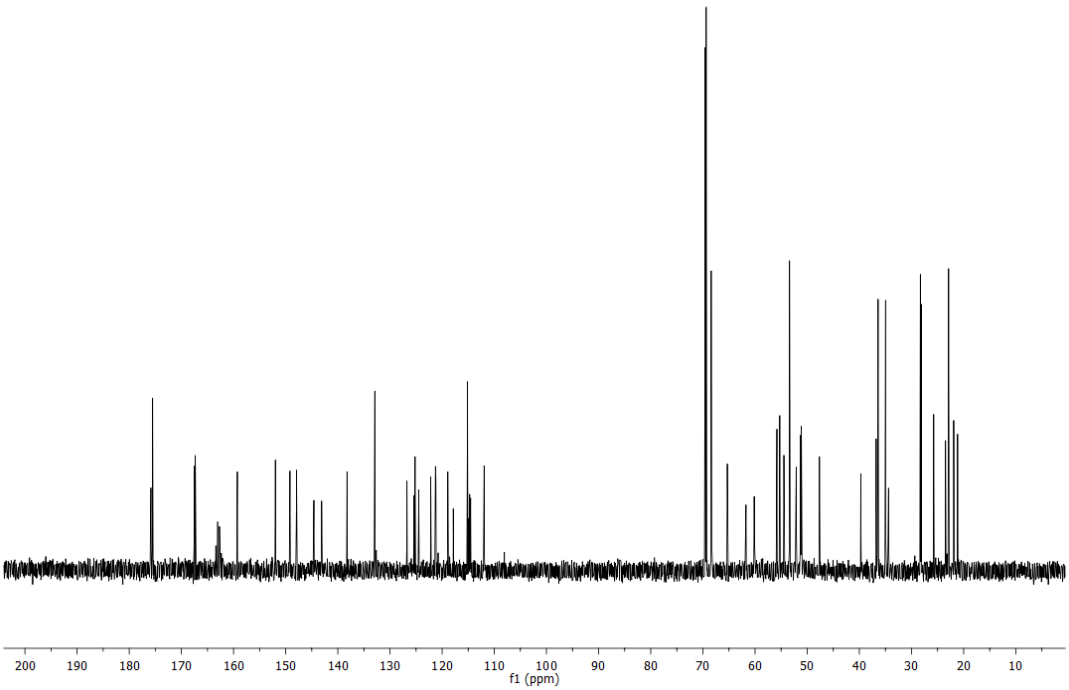

Figure 9.55: ^{13}C-NMR spectrum (101 MHz, D_2O) of compound **86**.

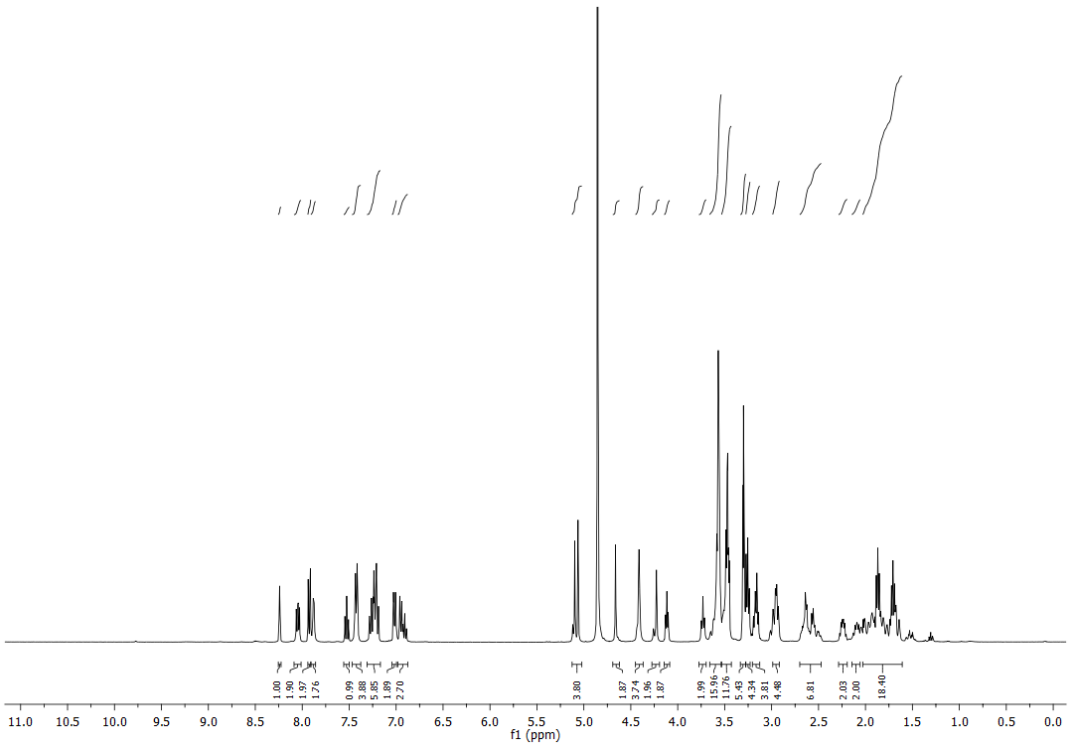

Figure 9.56: ^{1}H-NMR spectrum (400 MHz, D_2O) of compound **87**.

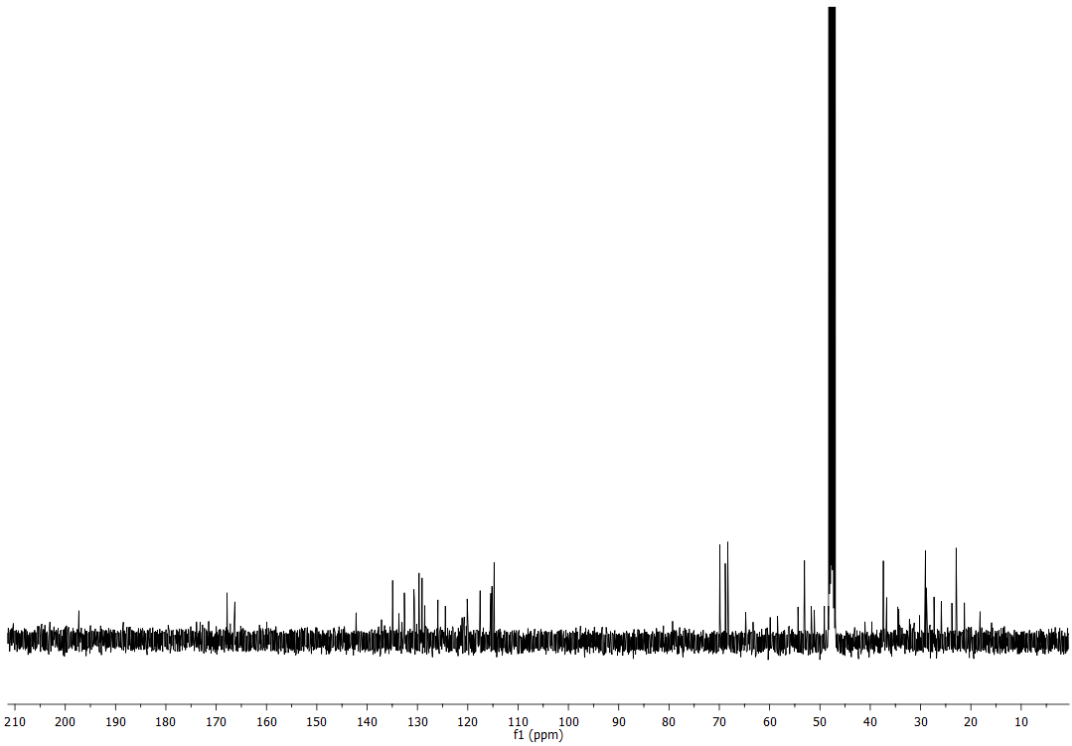

Figure 9.57: ^{13}C-NMR spectrum (101 MHz, D_2O) of compound **87**.

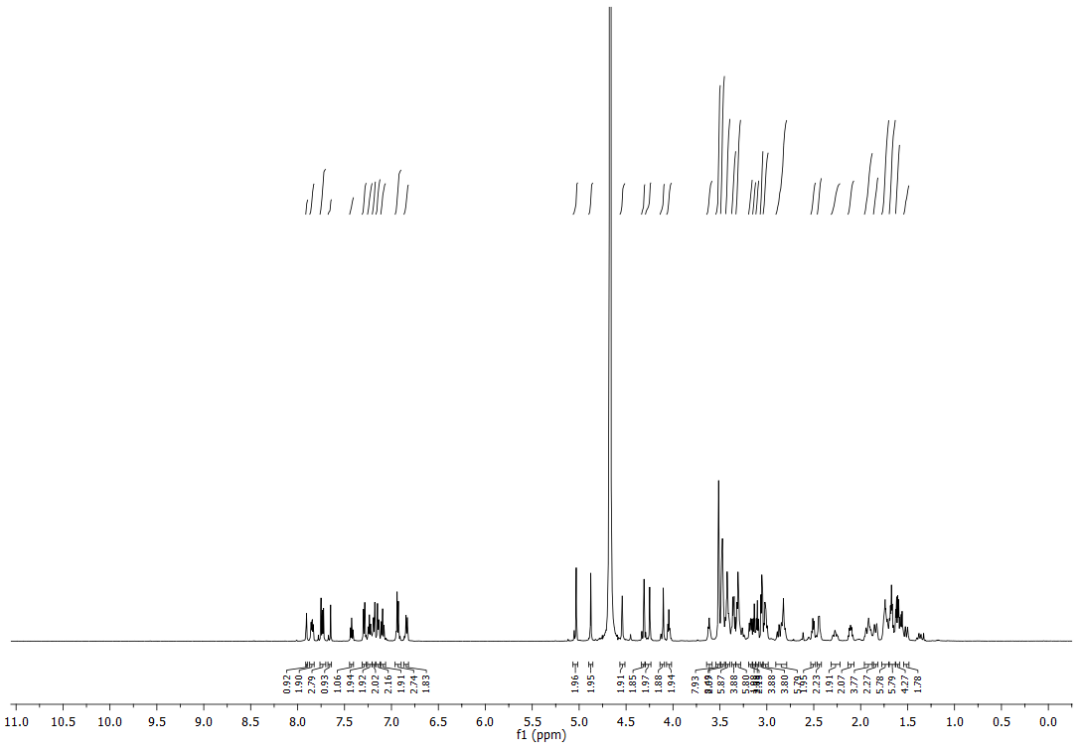

Figure 9.58: ^{1}H-NMR spectrum (600 MHz, D_2O) of compound **88**.

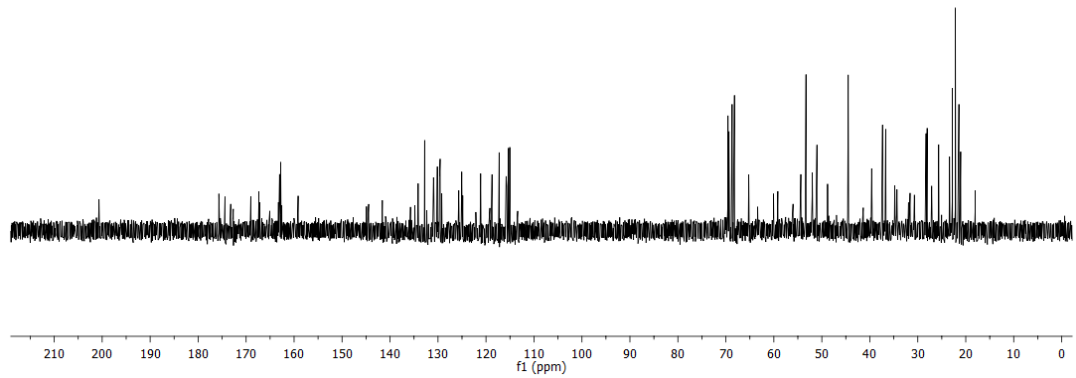

Figure 9.59: ^{13}C-NMR spectrum (151 MHz, D_2O) of compound **88**.

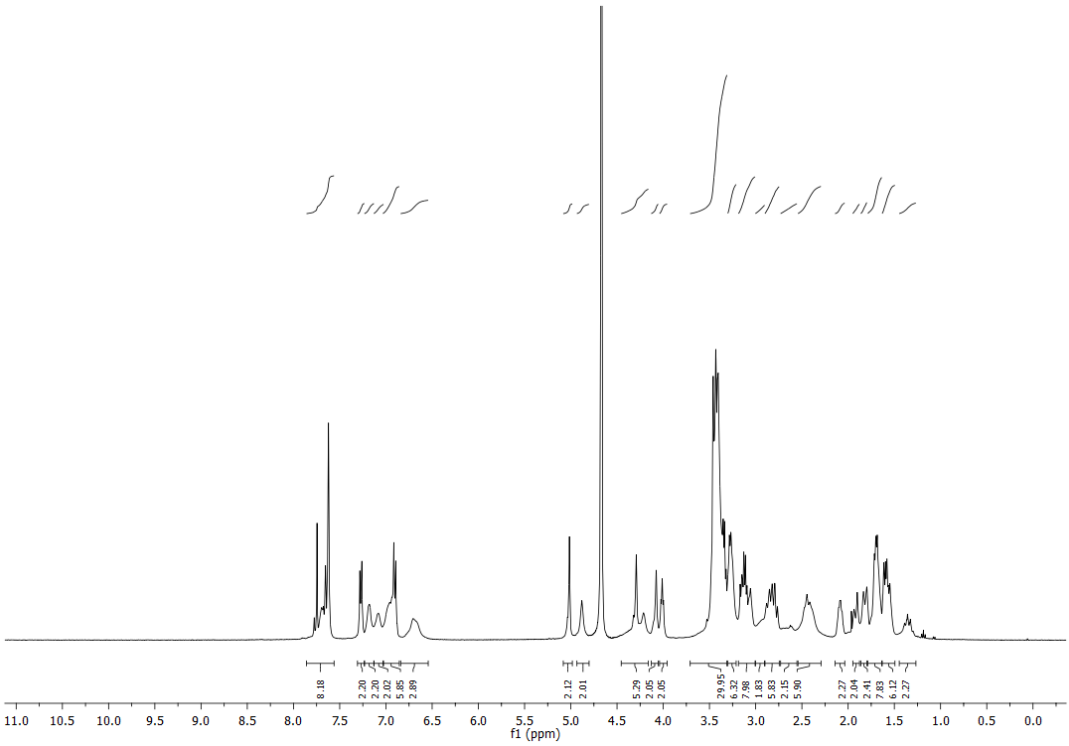

Figure 9.60: ^{1}H-NMR spectrum (400 MHz, D_2O) of compound **89**.

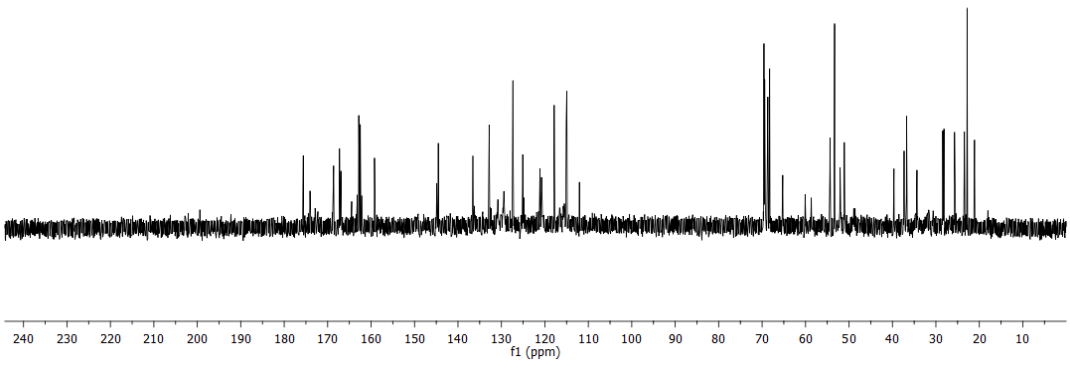

Figure 9.61: ^{13}C-NMR spectrum (101 MHz, D_2O) of compound **89**.

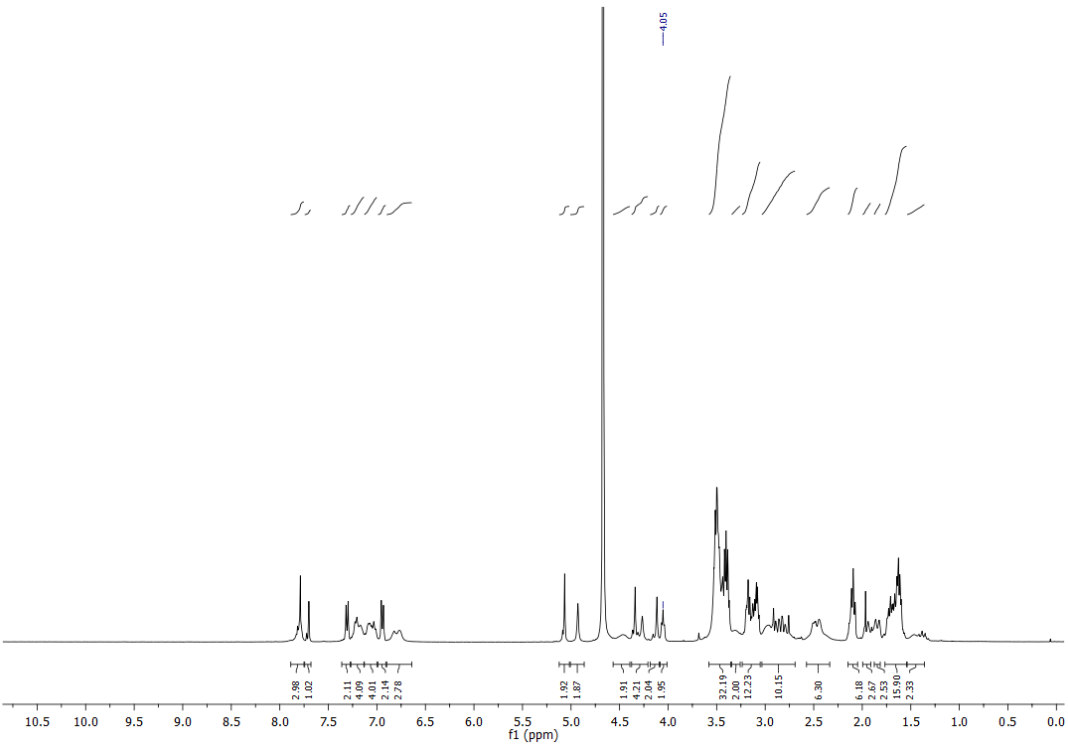

Figure 9.62: ^{1}H-NMR spectrum (400 MHz, D_2O) of compound **90**.

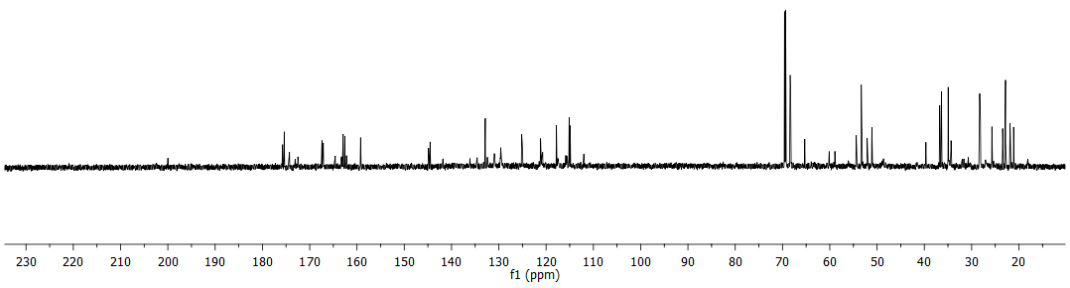

Figure 9.63: ^{13}C-NMR spectrum (101 MHz, D_2O) of compound **90**.

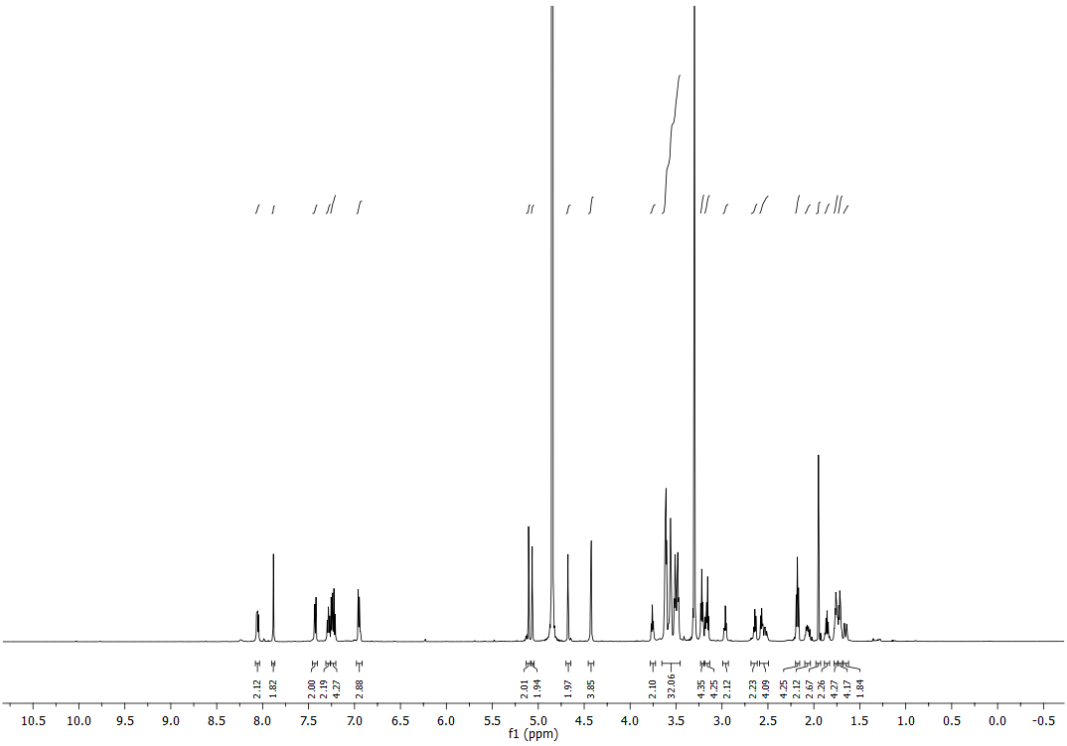

Figure 9.64: ^{1}H-NMR spectrum (400 MHz, CD_3OD) of compound **91**.

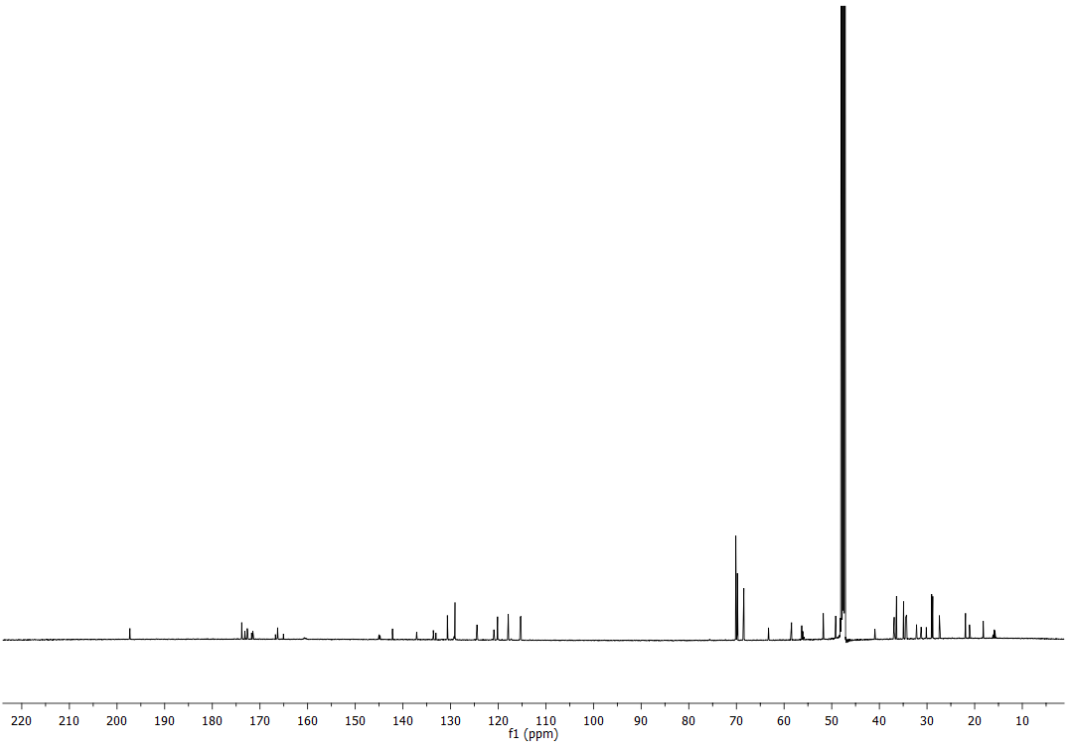

Figure 9.65: ^{13}C-NMR spectrum (101 MHz, CD_3OD) of compound **91**.

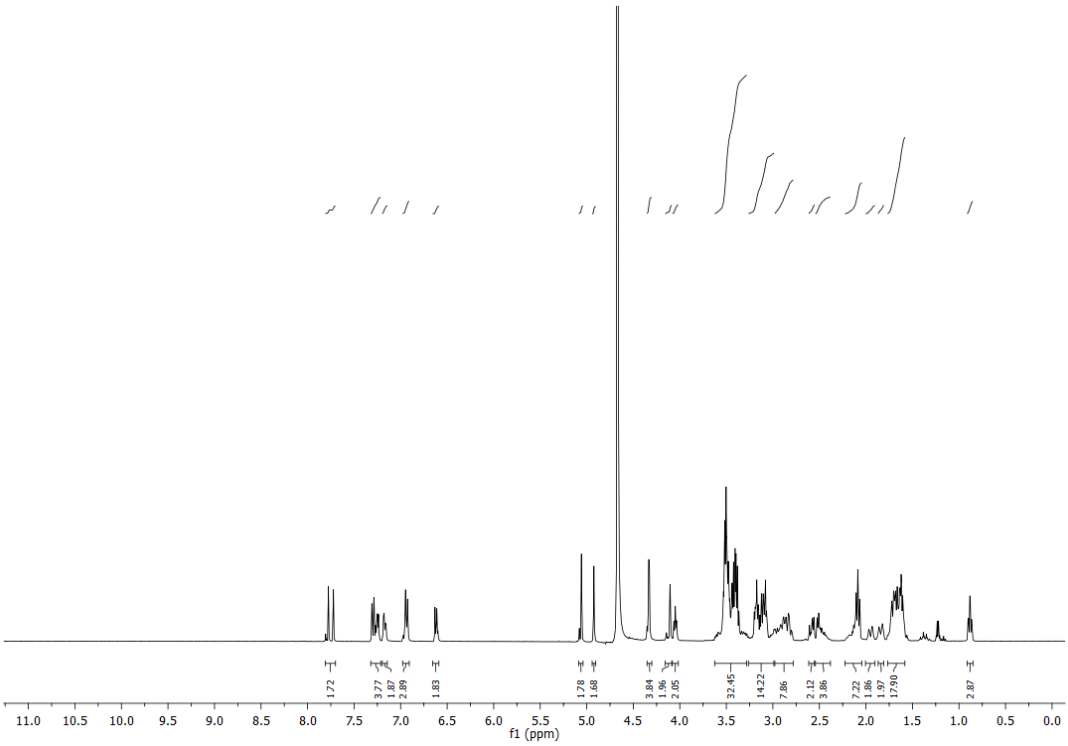

Figure 9.66: ^{1}H-NMR spectrum (400 MHz, D_2O) of compound **92**.

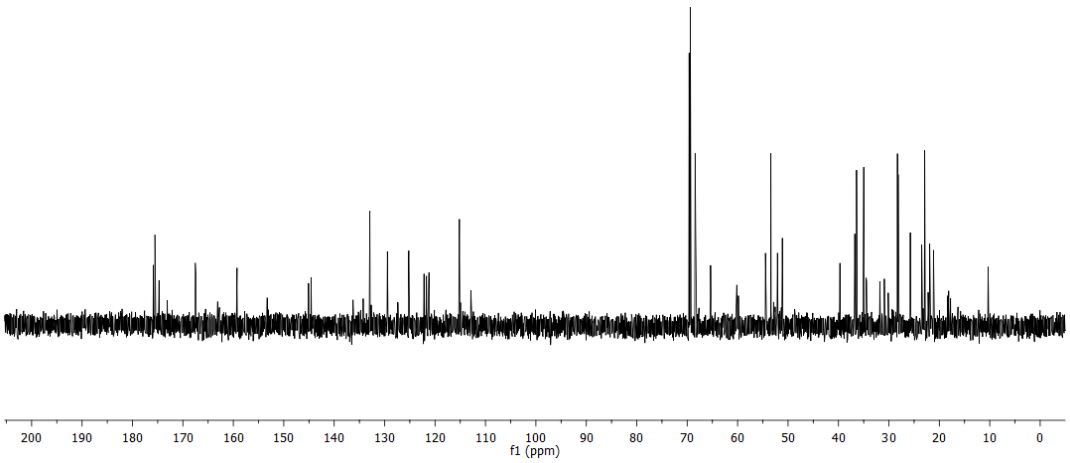

Figure 9.67: ^{13}C-NMR spectrum (101 MHz, D_2O) of compound **92**.

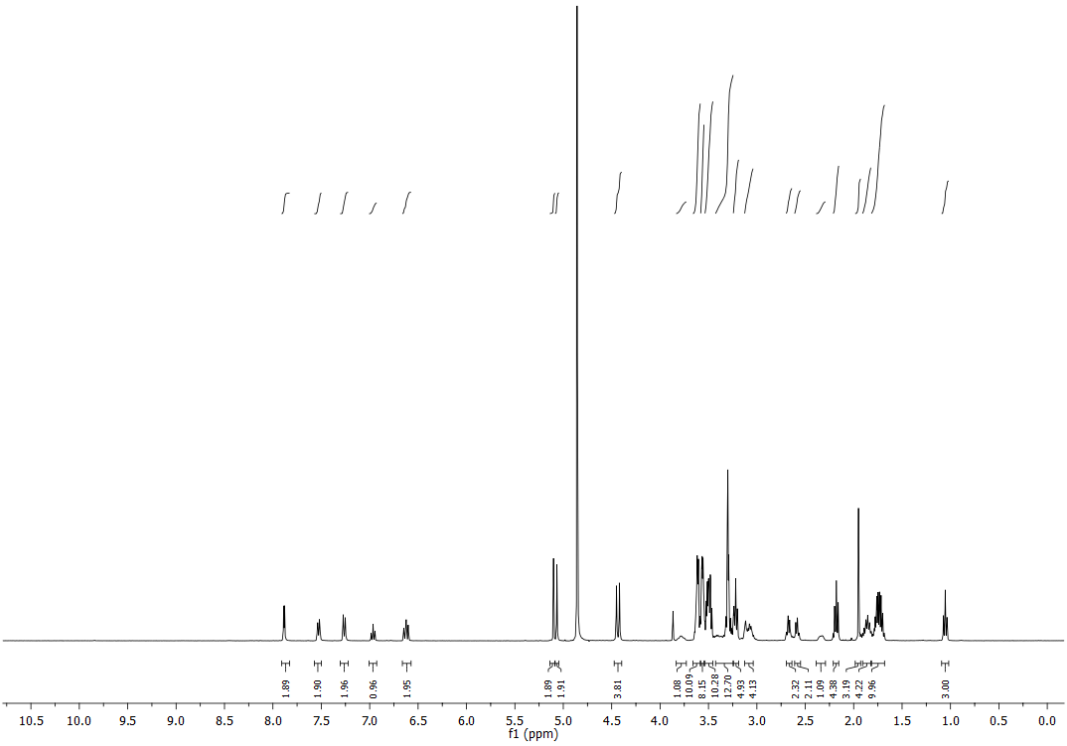

Figure 9.68: ^{1}H-NMR spectrum (400 MHz, CD_3OD) of compound **93**.

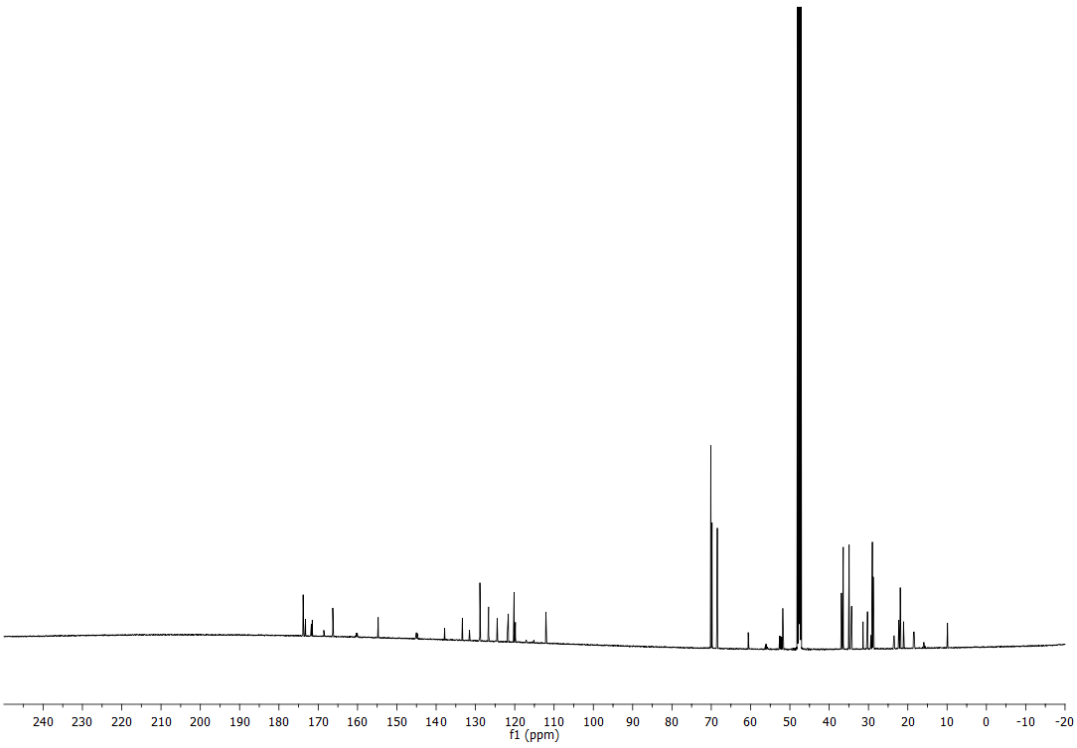

Figure 9.69: ^{13}C-NMR spectrum (151 MHz, CD_3OD) of compound **93**.

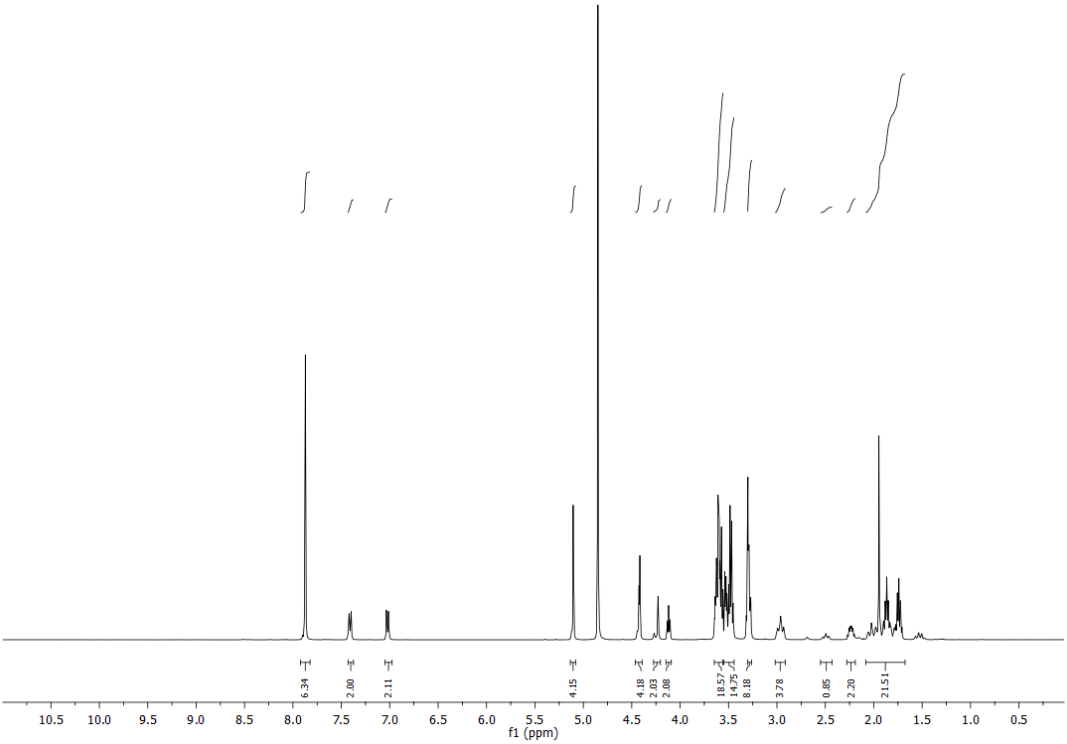

Figure 9.70: ^{1}H-NMR spectrum (400 MHz, CD_3OD) of compound **94**.

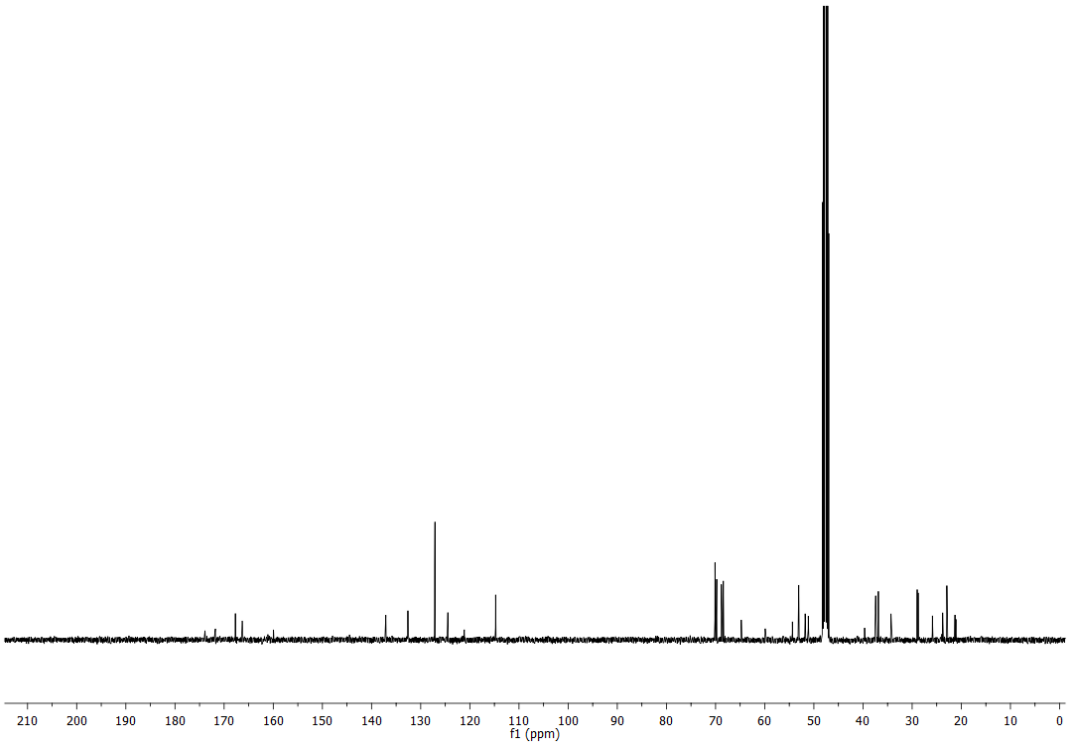

Figure 9.71: ^{13}C-NMR spectrum (101 MHz, CD_3OD) of compound **94**.

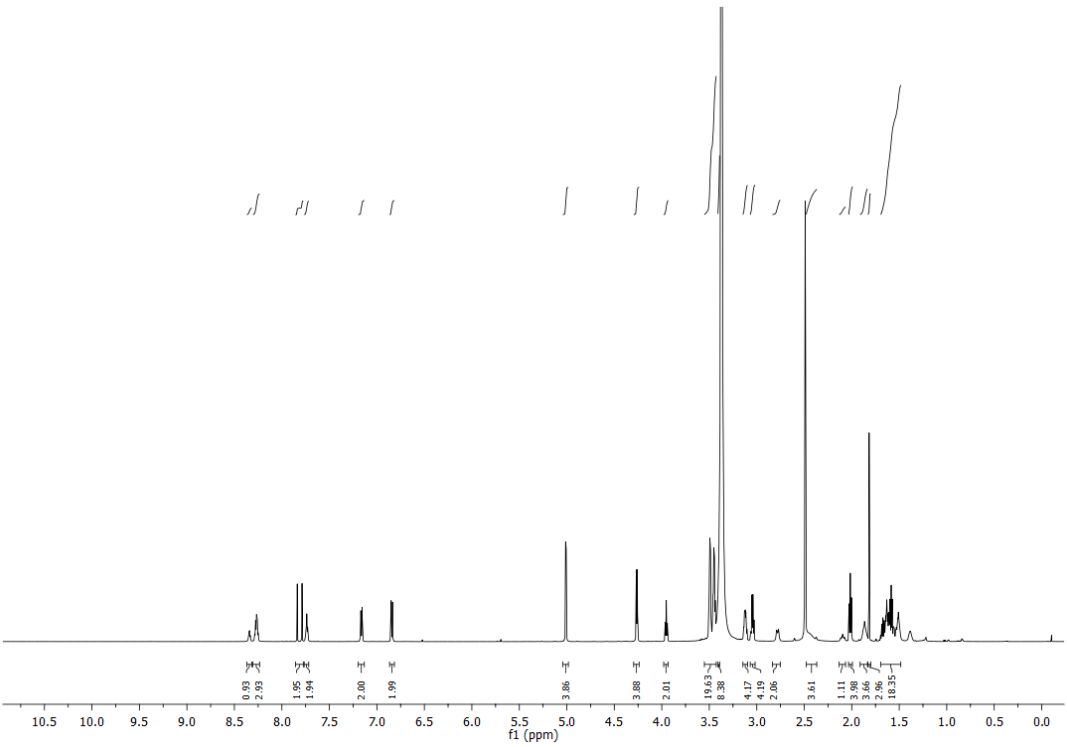

Figure 9.72: ^{1}H-NMR spectrum (600 MHz, DMSO-d_6) of compound **95**.

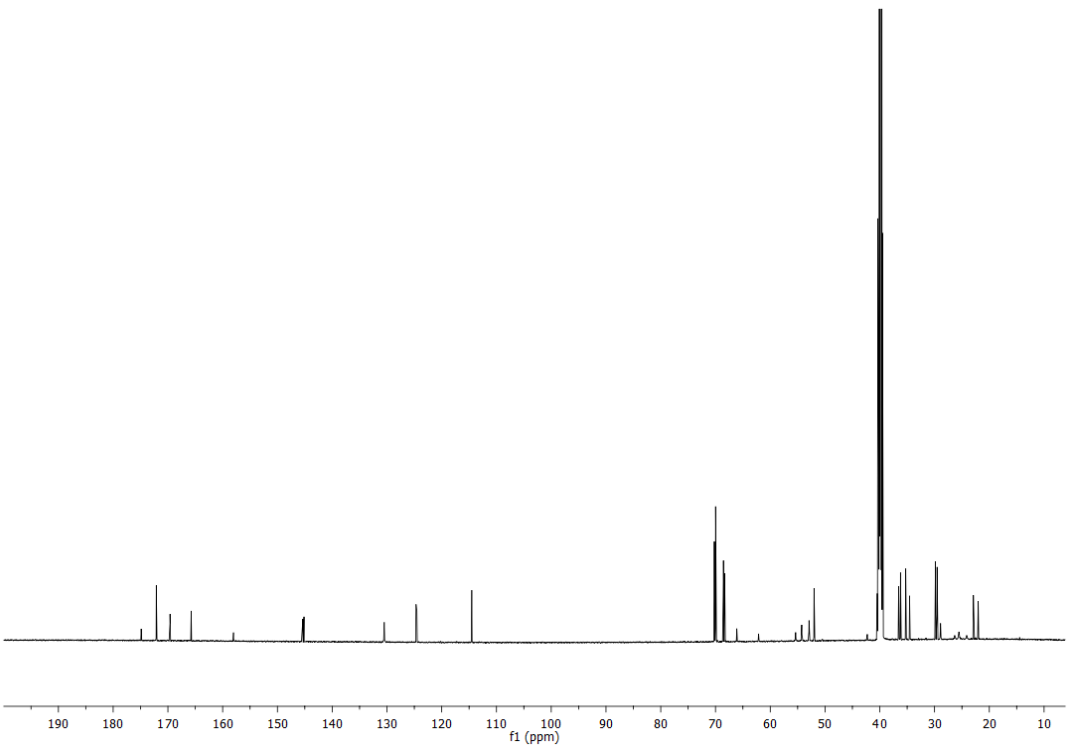

Figure 9.73: ^{13}C-NMR spectrum (151 MHz, DMSO-d_6) of compound **95**.

RP-HPLC chromatograms of tested compounds

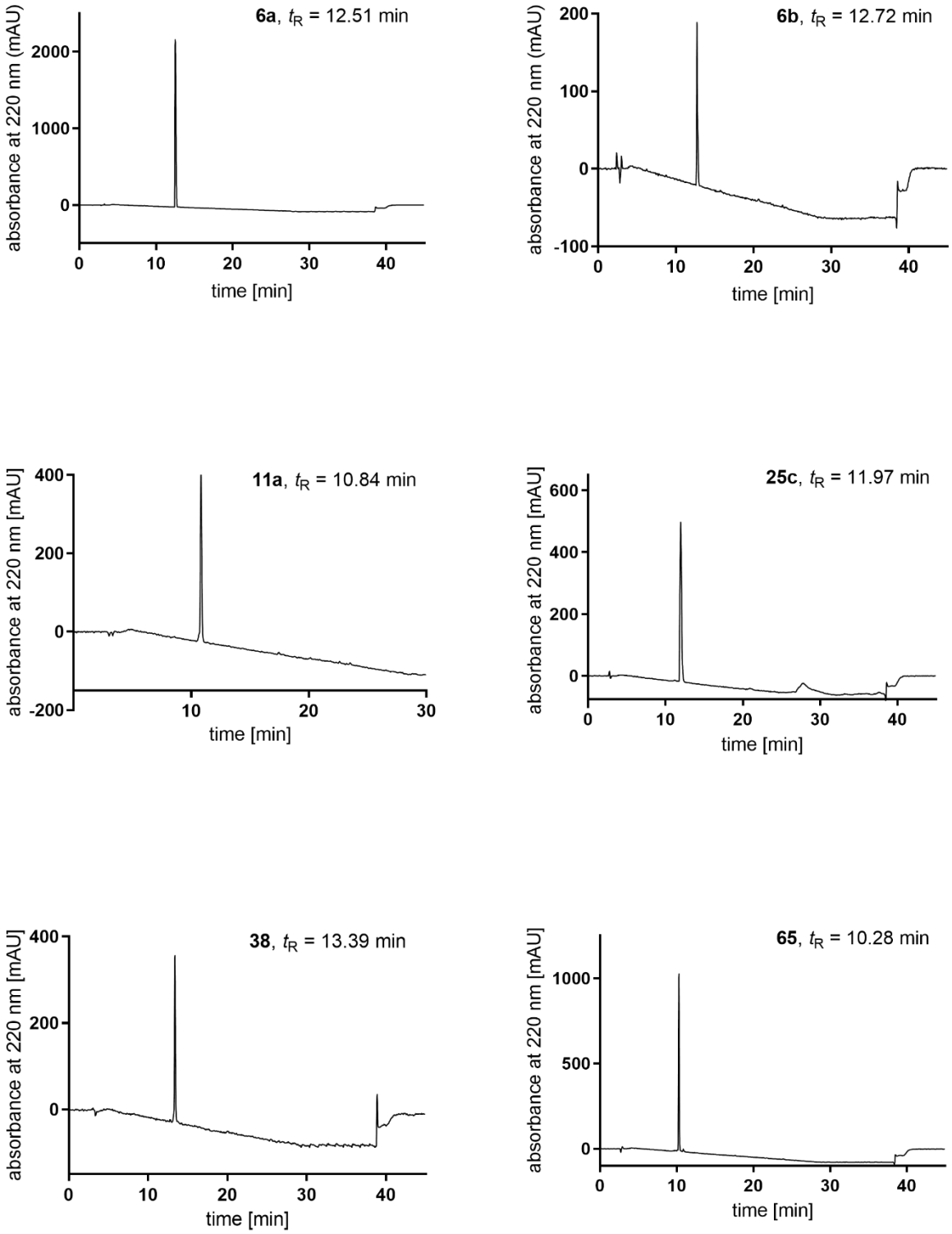

Figure 9.74: HPLC purity controls of compounds **6a**, **6b**, **11a**, **25c**, **38**, and **65**.

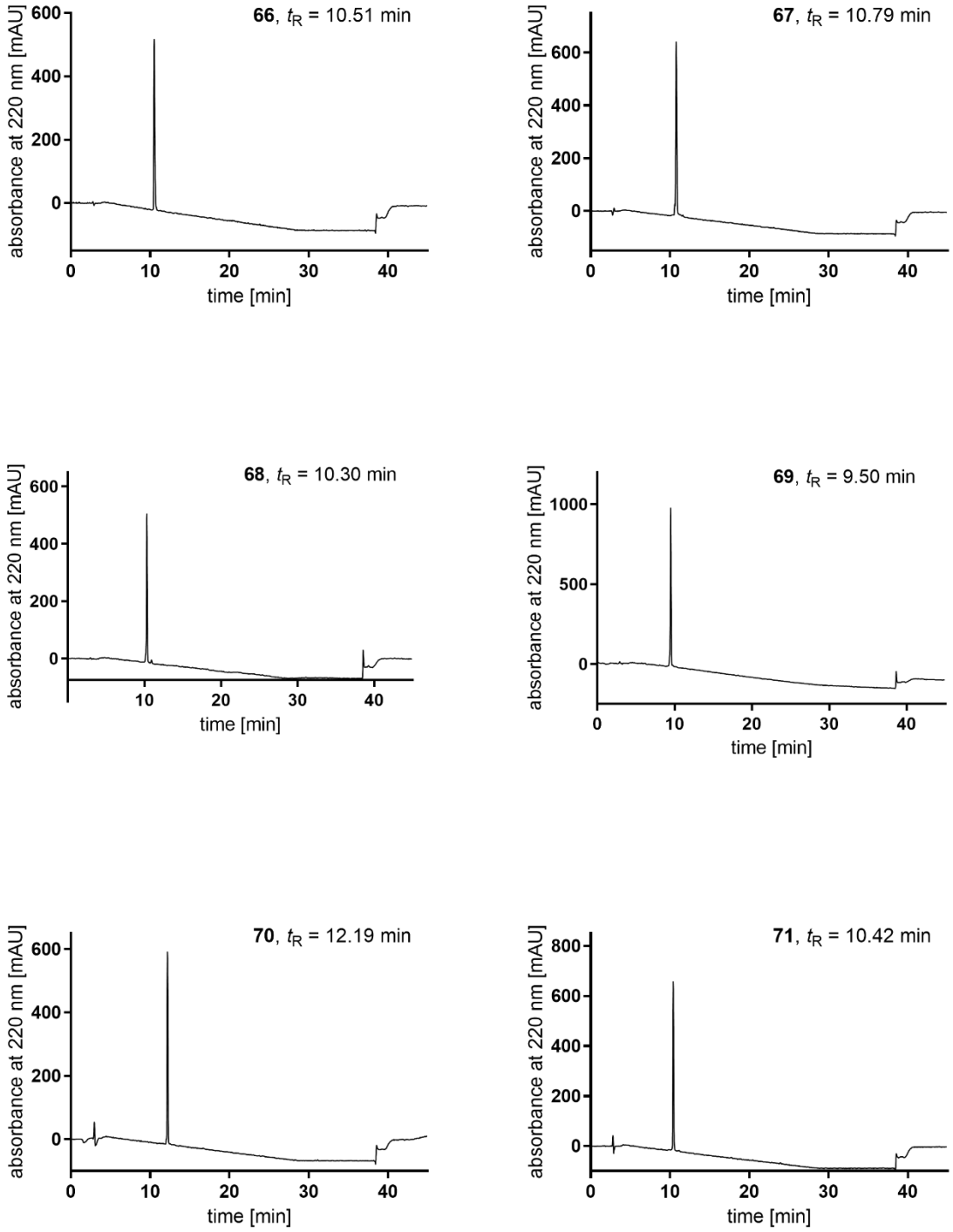

Figure 9.75: HPLC purity controls of compounds **66**-**71**.

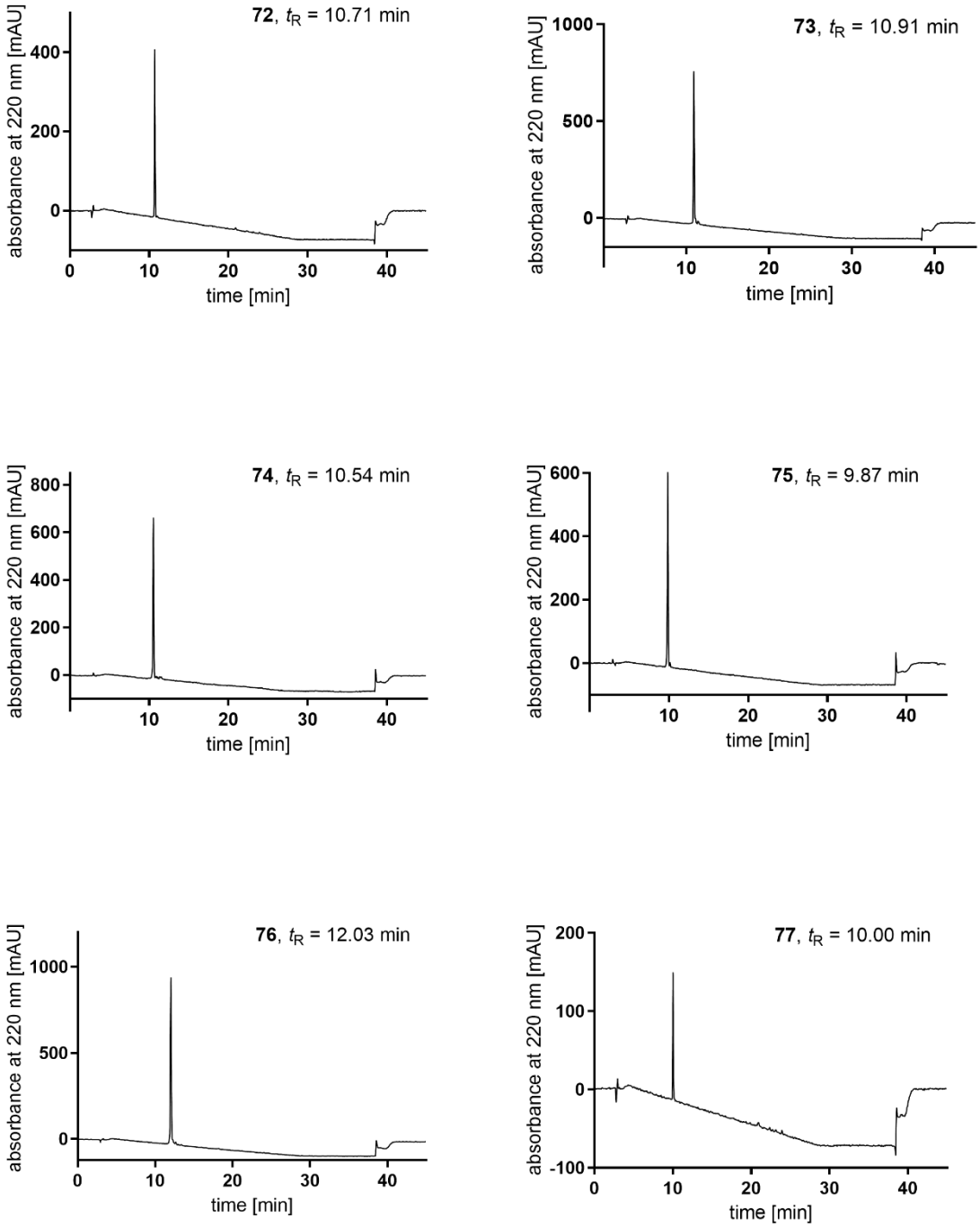

Figure 9.76: HPLC purity controls of compounds **72**-**77**.

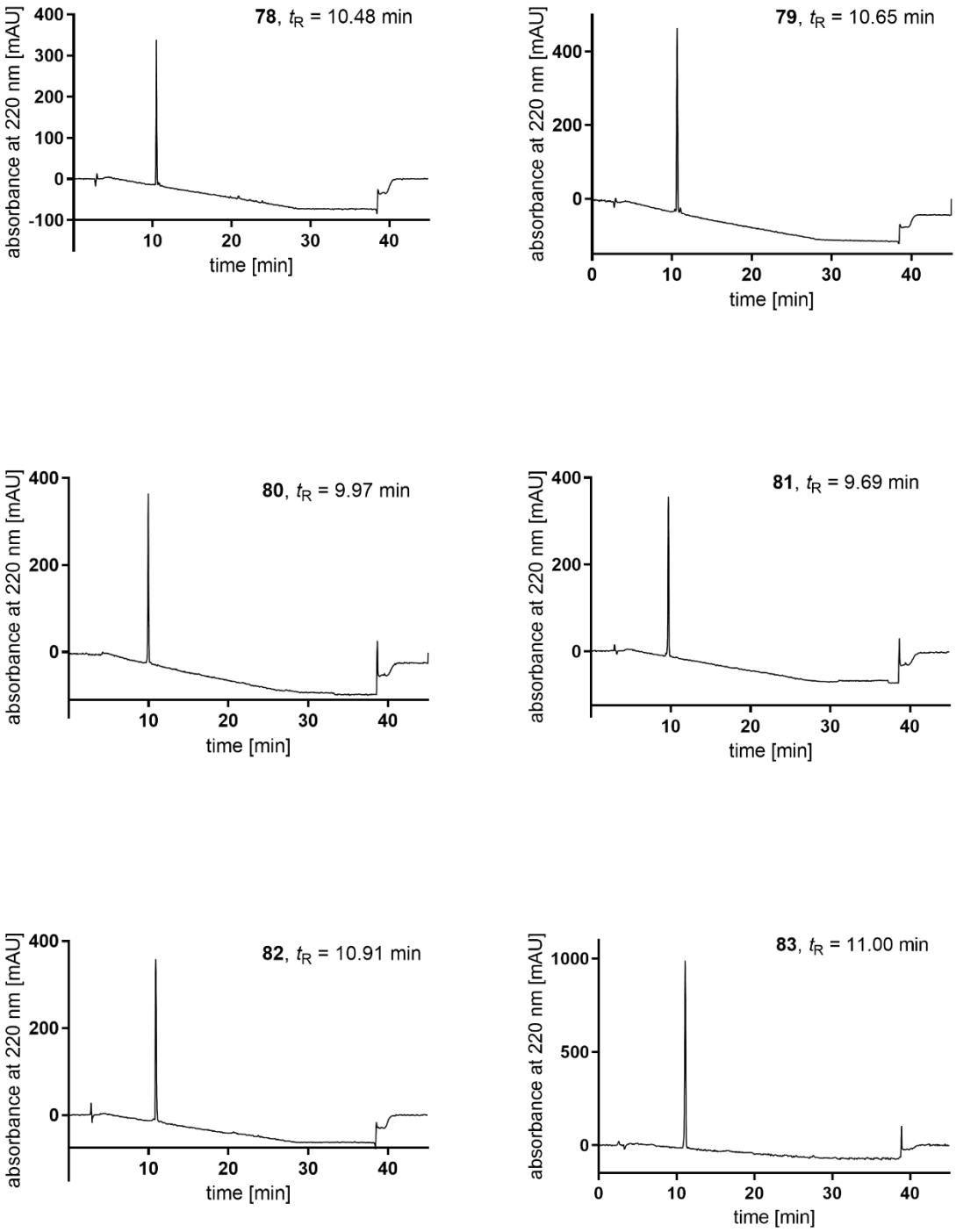

Figure 9.77: HPLC purity controls of compounds **78**-**83**.

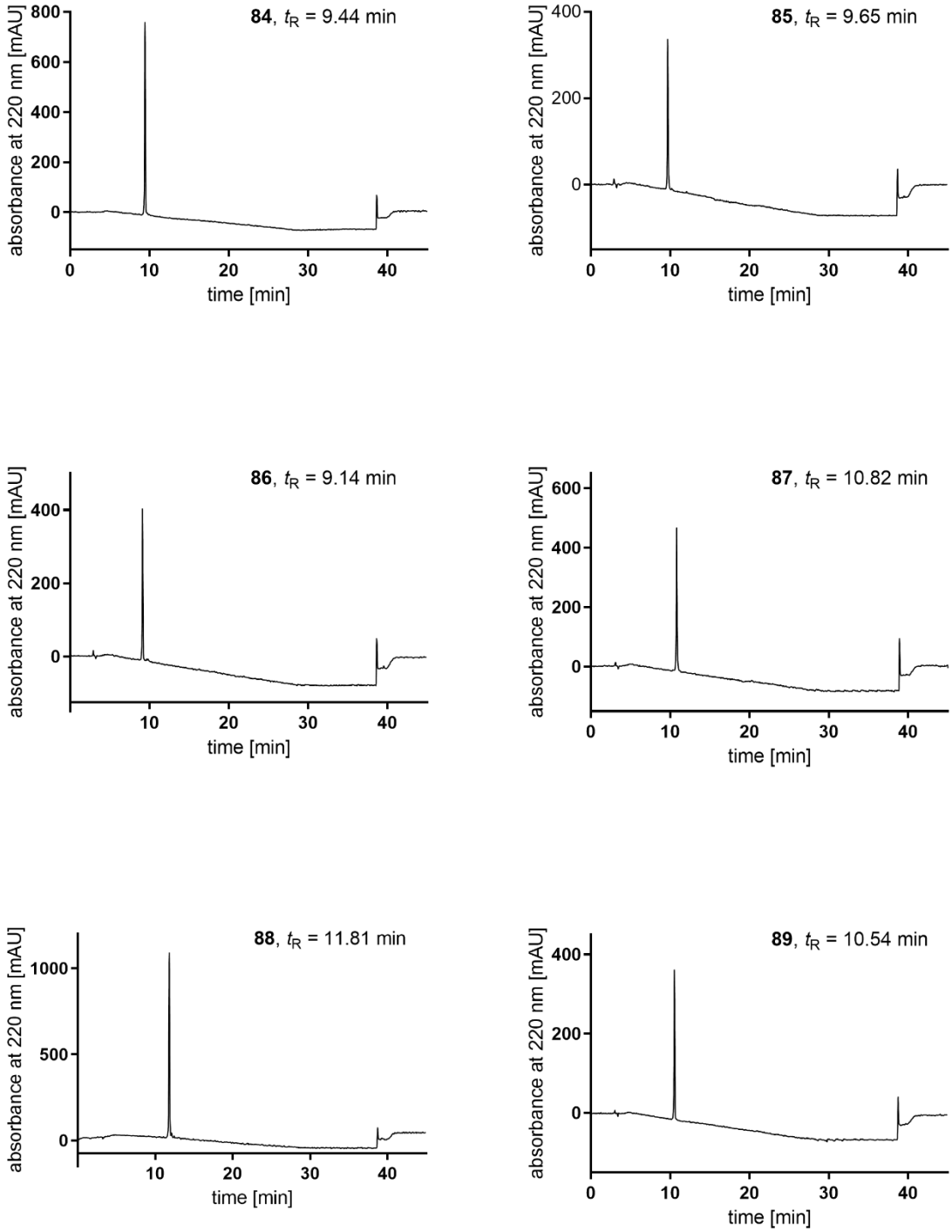

Figure 9.78: HPLC purity controls of compounds **84**-**89**.

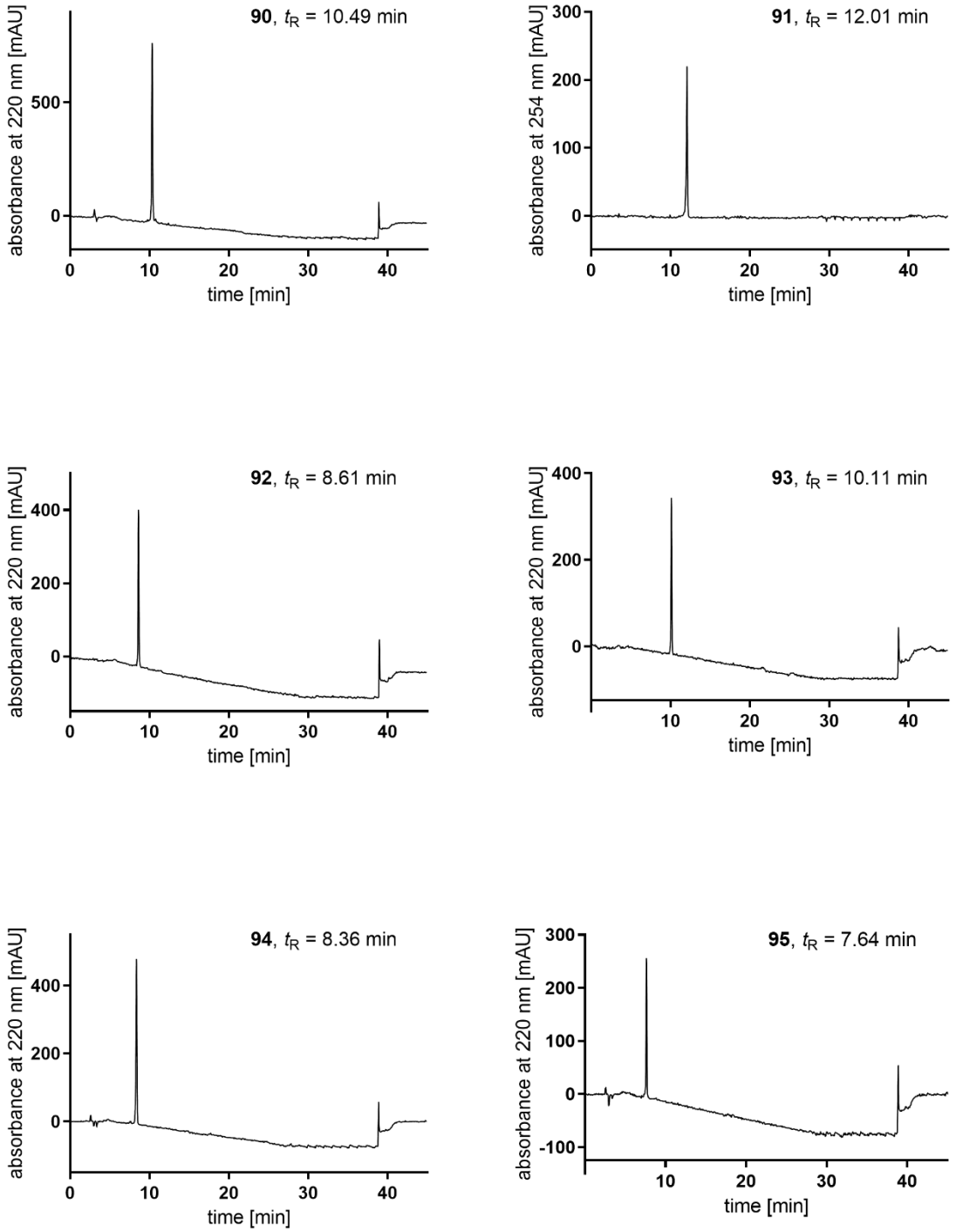

Figure 9.79: HPLC purity controls of compounds **90**-**95**.

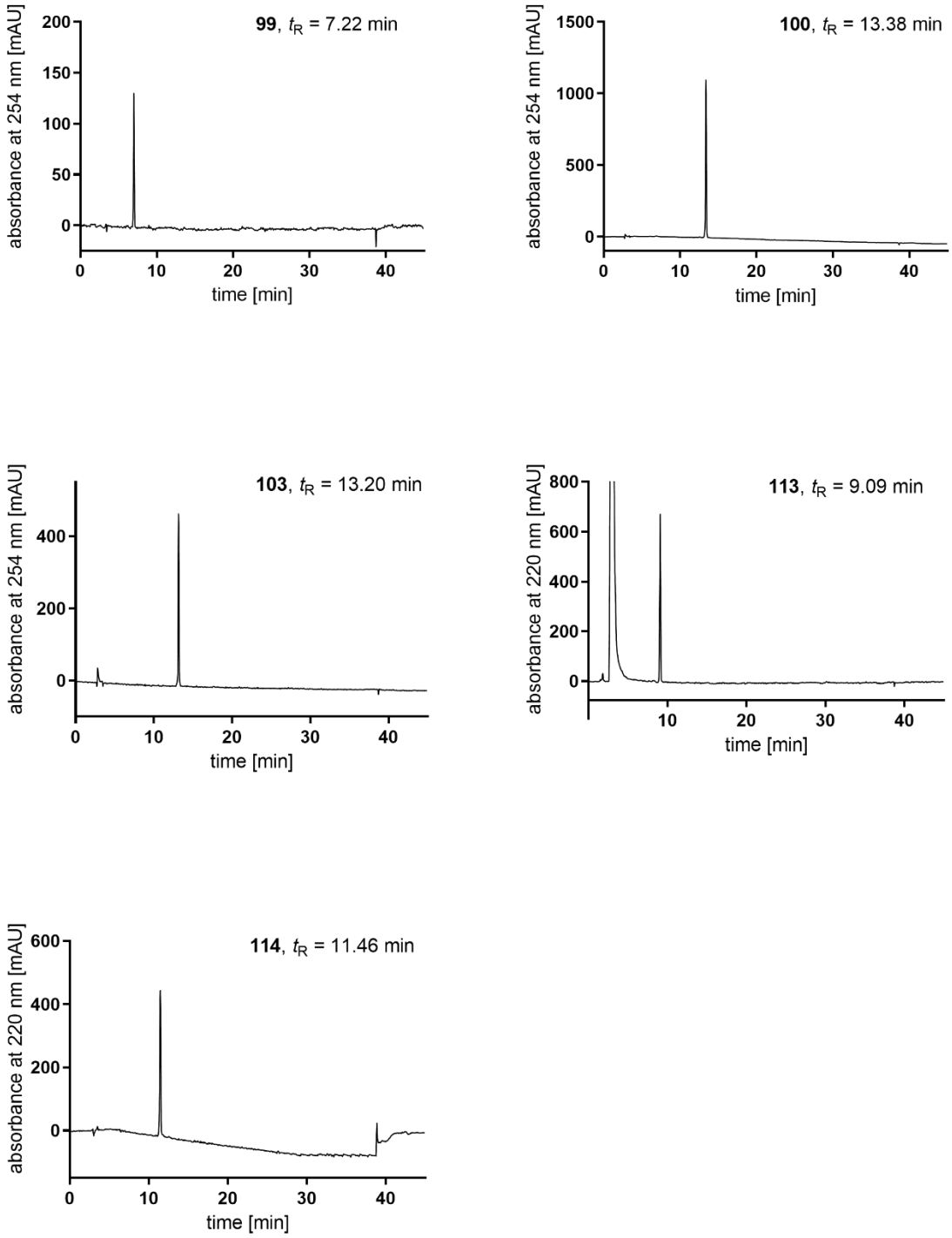

Figure 9.80: HPLC purity controls of compounds **99**, **100**, **103**, **113**, and **114.**

Stability of **103** in water/DMSO (1:1) was observed over a period of 24 h after incubation at room temperature (cf. **Figure 9.81**).

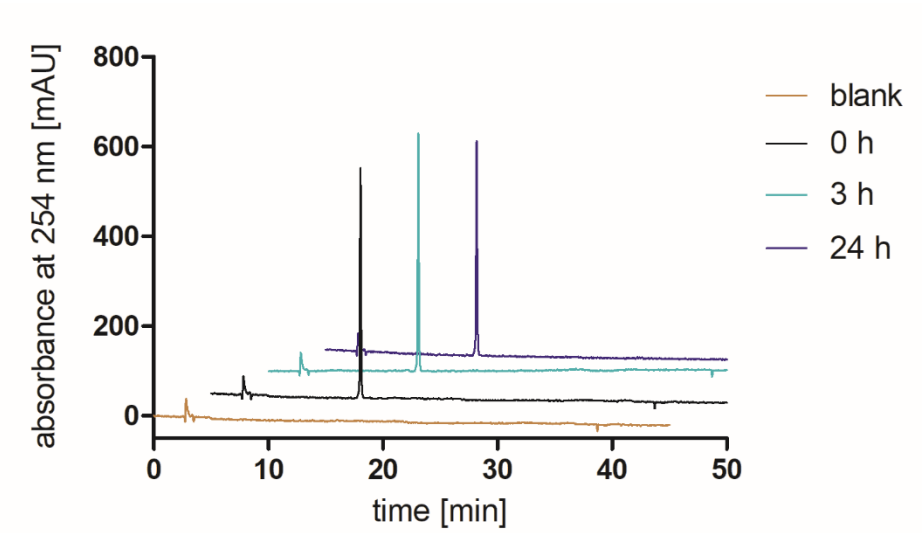

Figure 9.81: RP-HPLC analysis (stability control) of **103** after incubation in water/DMSO 1:1 at rt for up to 24 h. Exemplary compound **103** showed no decomposition.

Eidesstattliche Erklärung

Ich erkläre hiermit an Eides statt, dass ich die vorliegende Arbeit ohne unzulässige Hilfe Dritter und ohne Benutzung anderer als der angegebenen Hilfsmittel angefertigt habe; die aus anderen Quellen direkt oder indirekt übernommenen Daten und Konzepte sind unter Angabe des Literaturzitats gekennzeichnet.
Weitere Personen waren an der inhaltlich-materiellen Herstellung der vorliegenden Arbeit nicht beteiligt. Insbesondere habe ich hierfür nicht die entgeltliche Hilfe eines Promotionsberaters oder anderer Personen in Anspruch genommen. Niemand hat von mir weder unmittelbar noch mittelbar geldwerte Leistungen für Arbeiten erhalten, die im Zusammenhang mit dem Inhalt der vorgelegten Dissertation stehen.
Die Arbeit wurde bisher weder im In- noch im Ausland in gleicher oder ähnlicher Form einer anderen Prüfungsbehörde vorgelegt

Regensburg, im November 2022

_____

(Martin Nagl)